UNITED STATES DEPARTMENT OF THE INTERIOR

GEOLOGICAL SURVEY

SUMMARIES OF TECHNICAL REPORTS, VOLUME XIX

Prepared by Participants in

NATIONAL EARTHQUAKE HAZARDS REDUCTION PROGRAM

December 1984

OPEN-FILE REPORT 85-22

Menlo Park, California

1985

The research results described in the following summaries were submitted by the investigators on October 10, 1984 and cover the 6-months period from May 1, 1984 through October 1, 1984. These reports include both work performed under contracts administered by the Geological Survey and work by members of the Geological Survey. The report summaries are grouped into the three major elements of the National Earthquake Hazards Reduction Program.

Open File Report No. 85-22

The data and interpretations in these progress reports may be reevaluated by the investigators upon completion of the research. Readers who wish to cite findings described herein should confirm their accuracy with the author.

UNITED STATES
DEPARTMENT OF THE INTERIOR
GEOLOGICAL SURVEY

SUMMARIES OF TECHNICAL REPORTS, VOLUME XIX

Prepared by Participants in

NATIONAL EARTHQUAKE HAZARDS REDUCTION PROGRAM

Compiled by

Muriel L. Jacobson

Thelma R. Rodriguez

CONTENTS

Earthquake Hazards Reduction Program

Page

Develop, operate and evaluate instrumentation for monitoring potential earthquake precursors.
Analyze and evaluate seismicity data collected prior to medium and large earthquakes.
Obtain and analyze data from seismically active regions of foreign countries through cooperative projects with the host countries.
Systematically evaluate data and develop statistics that relate observations of specific phenomena to earthquake occurrence.
Develop, study and test prediction methods that can be used to proceed from estimates of long-range earthquake potential to specific short-term predictions............... 158

Objective P-2. Earthquake Prediction Experiments

Conduct data collection and analysis experiments in areas of California capable of great earthquakes, where large populations are at risk. The experiments will emphasize improved coordination of data collection, data reporting, review and analysis according to set schedules and standards.

Collect and analyze data for an earthquake prediction experiment in southern California, concentrating on the southern San Andreas fault from Parkfield, California to the Salton Sea.
Collect and analyze data for an earthquake prediction experiment in central California, concentrating on the San Andreas fault north of Parkfield, California......... 283

Objective P-3. Theoretical, Laboratory and Fault Zone Studies

Improve our understanding of the physics of earthquake processes through theoretical and laboratory studies to guide and test earthquake prediction observations and data analysis. Measure physical properties of those zones selected for earthquake experiments, including stress, temperature, elastic and anelastic characteristics, pore pressure, and material properties.

Conduct theoretical investigations of failure and pre-failure processes and the nature of large-scale earthquake instability.
Conduct experimental studies of the dynamics of faulting and the constitutive properties of fault zone materials. Through the use of drilled holes and appropriate down hole instruments, determine the physical state of the fault zone in regions of earthquake prediction experiments..................... 422

Most of the technical summaries contained in this volume are for research contracts solicited by RFP-1284. The description in the previous table of contents corresponds to respective Elements and Objectives of that RFP. Additionally some of the summaries are for research objectives that were initiated in earlier years. These objectives are covered in the descriptions found in the following table of contents.

Initiated before FY83

Page

I. Earthquake Hazards and Risk Assessment (H)

II. Earthquake Prediction (P)

III. Global Seismicity (G)

Southern California Seismic Arrays

Contract No. 14-08-0001-21854

Clarence R. Allen
Seismological Laboratory, California Institute of Technology
Pasadena, California 91125 (818-356-6904)

Investigations

This semi-annual Technical Report Summary covers the six-month period from 1 April 1984 to 30 September 1984. The contract's purpose is the partial support of the joint USGS-Caltech Southern California Seismographic Network, which is also supported by other groups, as well as by direct USGS funding of its own employees at Caltech. According to the contract, the primary visible product will be a joint Caltech-USGS catalog of earthquakes in the southern California region; quarterly epicenter maps and preliminary catalogs are also required and have been submitted as due during the contract period. About 250 preliminary catalogs are routinely distributed to interested parties.

Results

Figure 1 shows the epicenters of all cataloged shocks that were located during the period from 1 April to 22 September 1984--8 days short of the end of the reporting period. Some of the seismic highlights during the period are as follows:

Number of earthquakes entered into the catalog: 8516
Number of earthquakes of M = 3.0 and greater: 151
Number of earthquakes of M = 4.0 and greater: 16
Number of shocks reported felt: 31
Largest shock within network area: M = 4.3 (7 September, 68 km northwest of San Diego)
Smallest felt earthquake: M = 2.5 (20 April, Brea)
Number of earthquakes for which systematic telephone notification to agencies was made: 10

This was a period of fairly usual seismic activity in southern California, and the seismicity map (Fig. 1) looks remarkably similar to that of the previous six months. Activity continued high in the Coso area, along the general alignment of Kern Canyon fault, along the San Jacinto fault zone, and in the San Gorgonio Pass area. Outside of the network area, activity also remained high in the Coalinga and Mammoth areas

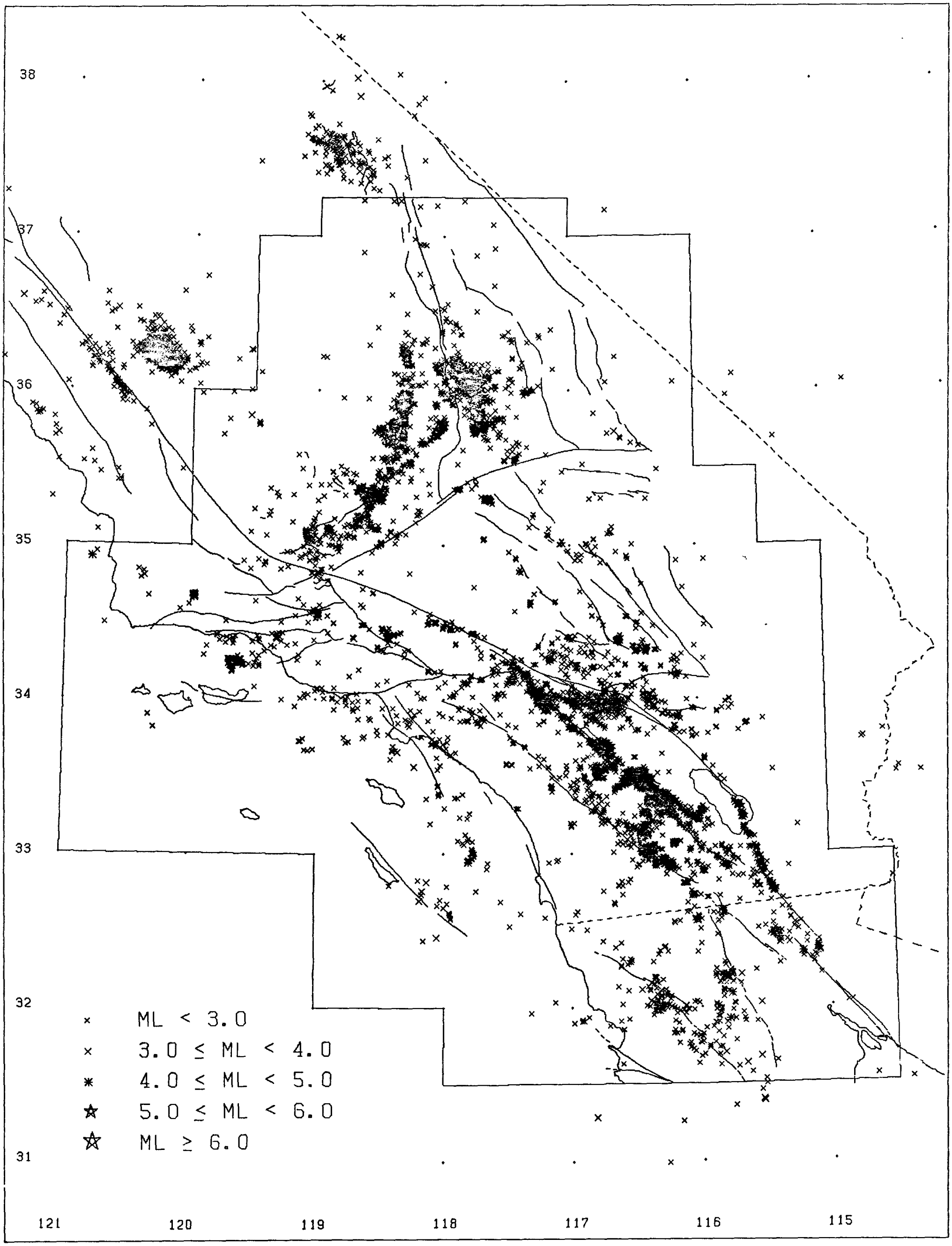

Fig. 1.--Epicenters of larger earthquakes in the southern California region, 1 April 1984 to 22 September 1984.

REGIONAL SEISMIC MONITORING ALONG THE WASATCH FRONT URBAN CORRIDOR AND ADJACENT INTERMOUNTAIN SEISMIC BELT

14-08-0001-21857

W. J. ARABASZ, R.B. SMITH, J.C. PECHMANN, and W.D. RICHINS
Department of Geology and Geophysics
University of Utah
Salt Lake City, Utah 84112
(801)581-6274

Investigations

This contract supports "network operations" (including a computerized central recording laboratory) associated with the University of Utah 80-station regional seismic telemetry network. USGS support focuses on the seismically hazardous Wasatch Front urban corridor of north-central Utah but also encompasses neighboring areas of the Intermountain seismic belt (ISB). The University of Utah maintains de facto responsibility for earthquake surveillance, including emergency response and direct public interface, for an 800-km-long segment of the ISB between Yellowstone Park and southernmost Utah. The State of Utah, the U.S. Bureau of Reclamation, the National Park Service and the U.S. Geological Survey (Geothermal Research Program) also contributed support to operation of the University of Utah network during the report period.

Primary products of this USGS contract are quarterly earthquake catalogs and a semi-annual data submission, in magnetic-tape form, to the USGS Data Archive. Supplemental funds were received from the USGS during FY84 for aftershock recording and special network analysis related to the Borah Peak, Idaho, earthquake of October 1983.

Results

Figure 1 shows the epicenters of 521 earthquakes located in the Utah region (lat. 36.75°-42.5°N, long. 108.73°-114.25°W) during the one-year period October 1, 1983, to September 30, 1984. The largest local earthquake during this period was one of magnitude (M_L) 4.3 on October 8, 1983, located 3 km south of the Salt Lake International Airport. The seismicity sample includes nine earthquakes of magnitude 3.0 or greater and a total of ten felt earthquakes ($2.5 \leqslant M \leqslant 4.3$). A seismographic bulletin published in August 1984 by the University of Utah (Richins and others, 1984a) summarizes earthquake data and information for the Utah region through 1983.

A local network of portable seismographs (Richins and others, 1984b) was established surrounding the surface rupture of the October 28, 1983 Borah Peak, Idaho earthquake within several hours after the main shock. At least 75 sites were occupied from October 28 to November 19, 1983 in a cooperative effort to examine the aftershock activity in detail by the University of Utah, U.S. Geological Survey, Boise State University, Idaho National Engineering Laboratory, University of Washington and the Montana Bureau of Mines and Geology.

Figure 2 summarizes the distribution of 374 aftershocks located using the temporary network. The aftershock zone is approximately 75 km x 15 km--elongate parallel to the surface rupture and displaced laterally to the southwest by 5 to 10 km. There was intense clustering near the western splay of the surface rupture. Few aftershocks were located within 6 to 10 km of the mainshock. Vertical cross sections are generally consistent with a moderately dipping (near 45°) fault zone except to the northwest (A-A') where a complex distribution with depth is apparent.

A 25-station regional network (Δ<600 km) was calibrated using six master events located with the dense temporary network and used to locate the main shock and first 24 hours of aftershock activity. Forty-eight earthquakes during this time period show an epicenter pattern similar to that defined by the activity shown in Figure 2.

The same regional network, augmented somewhat by up to 5 USGS temporary telemetry stations was used by Zollweg and Richins (1984 see companion USGS research contract)) to locate activity during the period November 20, 1983, to August 22, 1984. Preliminary results define an intense cluster of aftershocks, including a magnitude 5.8 shock on August 22, 1984, 10-15 km north of the aftershock zone defined for the first 3 weeks of aftershock activity in October-November 1983.

Reports and Publications

Richins, W. D., 1984, Utah earthquake activity, October 1983 to March 1984: Survey Notes, Utah Geological and Mineral Survey, v. 18, no. 1, p. 9.

Richins, W.D., Arabasz, W.J., Hathaway, G.M., McPherson, E., Oehmich, P.J., and Sells, L.L., 1984a, Earthquake Data for the Utah Region: January 1, 1981 to December 31, 1983: Special Publication, University of Utah Seismograph Stations, Salt Lake City, 111 p.

Richins, W.D., Smith, R.B., Langer, C.J., Zollweg, J.E., King, J.J., and Pechmann, J.C., 1984b, The 1983 Borah Peak, Idaho, earthquake: Relationship of aftershocks to the mainshock, surface faulting, and regional tectonics: Proceedings of USGS Workshop on "The Borah Peak Earthquake," Sun Valley, Idaho, October 1984 (includes summary of aftershock recording and related network analysis funded by this contract).

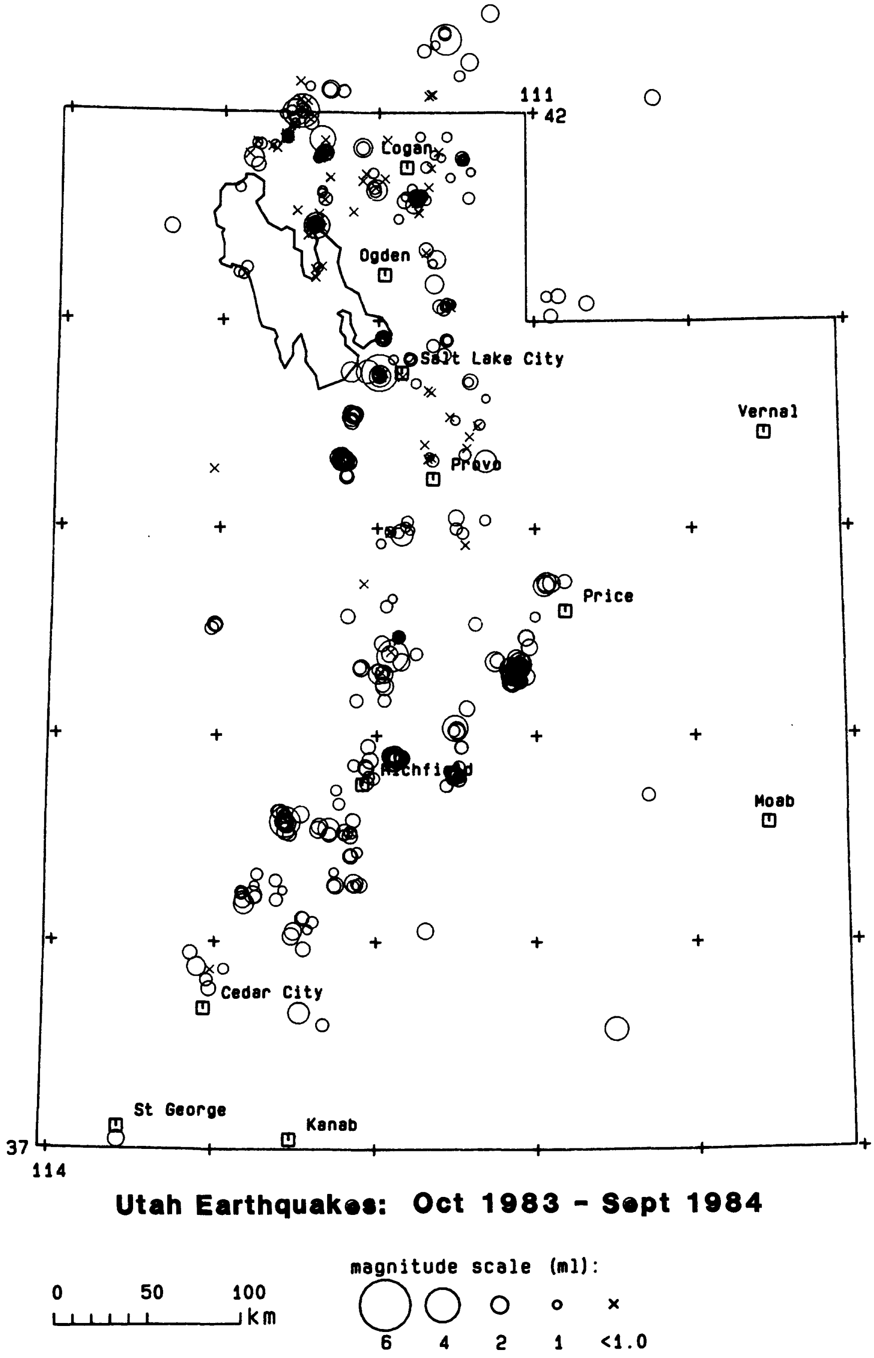
111
42
Logan
Ogden
Salt Lake City
Vernal
Provo
Price
Richfield
Moab
Cedar City
St George
Kanab
37
114
Utah Earthquakes: Oct 1983 - Sept 1984
magnitude scale (ml):
0
50
100
km
6
4
2
1
<1.0

Figure 1.

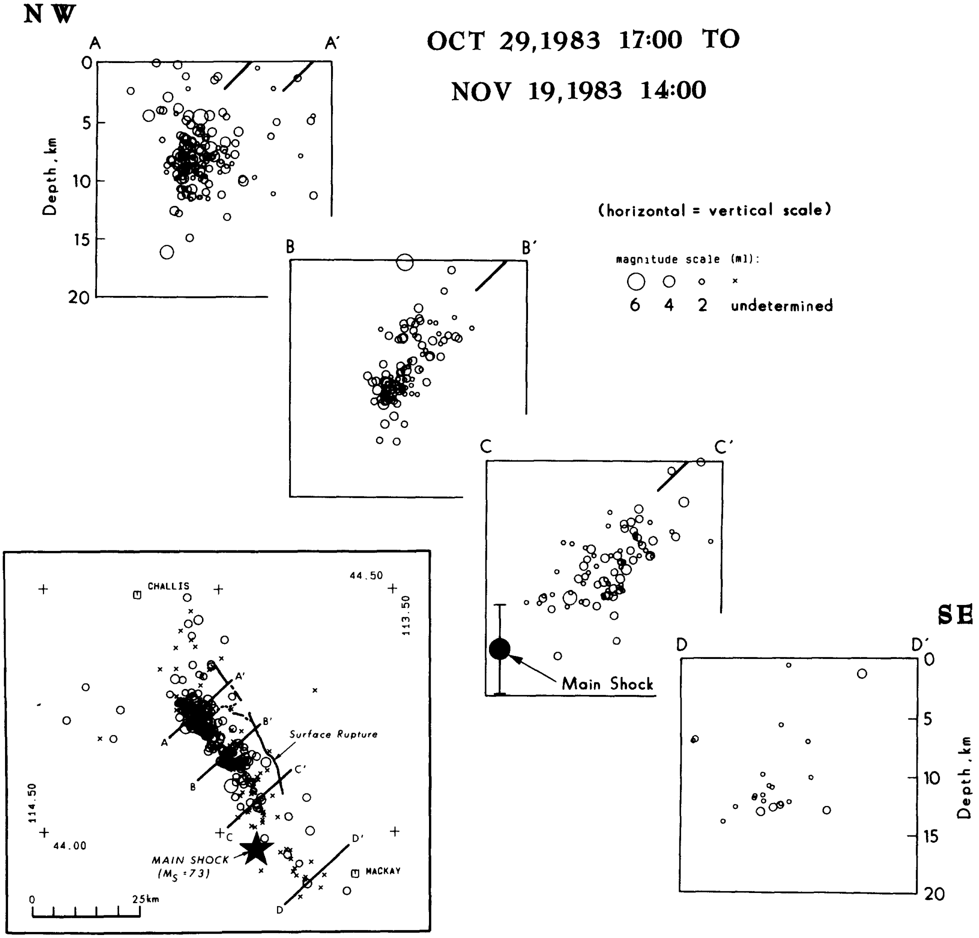
NW
OCT 29,1983 17:00 TO
NOV 19,1983 14:00
A
A′
Depth, km
0
5
10
15
20
B
B′
C
C′
Main Shock
(horizontal = vertical scale)
magnitude scale (ml):
6
4
2
undetermined
SE
D
D′
CHALLIS
44.50
113.50
Surface Rupture
114.50
44.00
MAIN SHOCK
(M_S =7.3)
MACKAY
0
25km

Figure 2.

Seismic Source Mechanism Studies In the Anza-Coyote Seismic Gap

14-08-0001-21893

Jonathan Berger and James N. Brune
Institute of Geophysics and Planetary Physics
Scripps Institution of Oceanography
University of California, San Diego
La Jolla, CA 92093

Investigations

This report covers the progress of the research investigating the Anza-Coyote Canyon seismic gap for the period of the first half of 1984. The objectives of this research are: 1) To study the mechanisms and seismic characteristics of small and moderate earthquakes, and 2) To determine if there are premonitory changes in seismic observables preceeding small and moderate earthquakes. This work is carried out in cooperation with Tom Hanks, Joe Fletcher and Linda Haar, of the U.S. Geological Survey, Menlo Park.

Network Status

During the period of this report, ten stations of the Anza Seismic Network were telemetering three component data. The network was set at a low gain to try to record earthquakes up to magnitude 4 occurring inside the array.

The winter and spring of 1984 were very mild, which allowed access to all sites for thorough testing of the VHF telemetry. The telemetry is still sensitive to temperature variations in the transmitters and receivers. They require retuning at periodic intervals. There were no weather related equipment failures in the winter of 1984. The only significant modification to the data acquisition equipment was the change of the anti-alias filter corner frequency from 100 Hz down to 62.5 Hz.

Seismicity

In the six months of winter and spring, the Anza network recorded over 50 events which were large enough to locate and determine source parameters. These events had moments ranging from 1×10^{18} to 1.4×10^{20} dyne-cm, and stress drops ranging from about 1 to 100 bars (Brune model). The seismicity pattern seems unchanged from what has been observed before (Figure 1). The seismicity does not appear to be associated with the main trace of the San Jacinto fault on the north-west end of the array. These events in this area tend to be between the Hot Springs fault at depths of 12 to 19 km. The events on the south-east end of the array near the trifurcation of the San Jacinto fault also do not have any obvious associations with the identified fault traces. These earthquakes are occurring at depths between 8 and 12 km. The shallowest events are still occurring in the Coahuilla area.

Velocity Structure

We have constructed an improved estimate of the velocity structure in the Anza area based on a joint hypocentral-velocity inversion originally written by Robert Crosson. The inversion used 79 well-recorded events with no initial station corrections. The result of the inversion was the six layer model below:

Depth (km)	V_p (km/sec)	V_s (km/sec)
0-1	2.57	1.62
1-3	4.97	2.22
3-5	5.67	3.21
5-9.5	5.89	3.51
9.5-14	5.89	3.50
14-18.5	5.97	3.41

The inversion also produced station corrections which correlate very strongly with surface geology. The stations which are associated with granitic rocks had negative station corrections, and the stations which are associated with sedimentary or metamorphic rocks have positive station corrections.

Attenuation

A preliminary attempt to determine the shear wave attenuation properties in the Anza area used the spectral ratio method. Values of Q for over 100 station pairs from 20 events were determined. The spectral ratios were averaged at 20 frequencies and a value of Q was estimated for each frequency. The apparent values ranged from Q = 100 at 5 Hz to Q = 850 at 80 Hz. A more thorough study of this data is currently in progress to see if these seemingly low values are consistent with other data reduction methods.

U.S. Seismic Network

9920-01899

Marvin A. Carlson
Branch of Global Seismology and Geomagnetism
U.S. Geological Survey
Denver Federal Center, MS 967
Denver, Colorado 80225
(303) 236-1506

Investigations

U.S. Seismicity. Data from the U.S. Seismic Network are used to obtain a preliminary location and magnitude of significant earthquakes throughout the United States and the world.

Results

As an operational program, the U.S. Seismic Network operated normally throughout the report period. Data were recorded continuously in real time at the NEIS main office in Golden, Colorado. At the present time, 100 channels of SPZ data are being recorded at Golden on develocorder film. This includes data telemetered to Golden via satellite from both the Alaska Tsunami Warning Center, Palmer, Alaska, and the Pacific Tsunami Warning Center, Ewa Beach, Hawaii. A representative number of SPZ channels are also recorded on Helicorders to give NEIS real time monitoring capability of the more active seismic areas of the United States. In addition, 15 channels of LPZ data are recorded in real time on multiple pen Helicorders.

Data from the U.S. Seismic Network are interpreted by record analysts and the seismic readings are entered into the NEIS data base. The data are also used by NEIS standby personnel to monitor seismic activity in the United States and worldwide on a real time basis. Additionally, the data are used to support the Alaska Tsunami Warning Center and the Pacific Tsunami Warning Service. At the present time, all earthquakes large enough to be recorded on several stations are worked up using the "Quick Quake" program to obtain a provisional solution as rapidly as possible. Finally, the data are used in such NEIS publications as the "Preliminary Determination of Epicenters" and the "Earthquake Data Report."

Recently the National Earthquake Information Center received approval for access to three channels of seismic data from the Southern United States Station (SUSS) in West Texas. The data is being telemetered to Golden over an existing data link at no additional cost to the USGS. At the present time, data from two short period vertical channels and one long period vertical channel are being recorded in Golden.

Objectives

The U.S. Seismic Network is an operational program as the data generated are routinely used to support the NEIS operational requirement of timely location and publication of earthquakes worldwide. Also, the network data directly support the NEIS standby personnel who are responsible for locating and reporting to the media, disaster agencies and other organizations, all significant earthquakes worldwide. Thirdly, support is given to the Alaska Tsunami Warning Center and the Pacific Tsunami Warning Service as network data are exchanged with both organizations.

Seismic Hazard Investigations in the Pacific Northwest

14-08-0001-21861
14-08-0001-21862

R.S. Crosson & S.D. Malone
Geophysics Program
University of Washington
Seattle, WA 98195
(202) 543-8020

Investigations

1. Operation of the western Washington regional seismograph network, and routine preliminary analysis of seismic events in western Washington

2. Analysis and interpretation of Pn observations for both eastern and western Washington

3. Development and implementation of automated processing of seismic events using digital network data

4. Crustal structure determination in the vicinity of Mt. St. Helens and in the greater Puget Sound region from earthquakes and explosions recorded digitally on the local and regional networks

5. Locations, focal mechanisms and occurrence characteristics of crustal and subcrustal earthquakes beneath western Washington and their relationship to subduction processes

6. Automated spectral analysis of digital seismic data for determination of source parameters for local earthquakes in the Pacific Northwest

Results

1. Network operation for stations in western Washington, eastern Washington, and northern Oregon continued normally. No unusual regional earthquake activity was recorded outside of the Mt. St. Helens region. A new station (OSD) which provides critical data for depth determination in the subduction complex beneath the Olympic Peninsula was established in the central Olympic Mts. Reconfiguration of the telemetry routes and the installation and reinstallation of stations in the northeast part of the Puget Sound basin is underway and scheduled for completion for autumn 1984. An analysis of magnitude thresholds for catalog completeness was done for the network, and will be utilized henceforth in report and catalog presentations. Efforts are underway to establish a uniform data base of earthquake phase data for the greater western Washington region, from 1970 through the transition to digital data acquisition in 1980 to the present. Eventually, pre-network instrumental and historic data will be merged into

a uniform data base with appropriate quality indicators.

2. Results from Pn analysis reinforce the existence of significant differences in structure between eastern and western Washington. East of the Cascade Range, Pn velocity averages 8.18 +/- 0.02 km/sec, whereas the average for western Washington is 7.77 +/- 0.02 km/sec. Anisotropy appears to be significant east, but relatively unimportant west, of the Cascades. Calculated Moho dip east of the Cascades, assuming no lateral change in crustal velocity, is about 0.7 degree whereas the calculated regional dip for the west is about 2.1 degrees in a southeasterly direction. There is little direct evidence in the regional Pn data for Moho dip associated with a dipping slab beneath western Washington.

3. A new algorithm for phase picking has been developed and incorporated into an automated processing program for digital network data. In the current configuration, feedback is provided between phase picking and location processing to reduce the number of blunders due to noise spikes and poor signal-to-noise ratio. An important aspect of automated processing is making quantitative and consistent estimates of phase picking errors for both P and S phases and coda length estimates. We are undertaking a complete recalibration of our auto-processed coda duration measurements for the purpose of improving the consistency and accuracy of local magnitude determinations. The current version of our program is being run in a test mode and is also being used for special studies. Use of automatic processing in our routine network data analysis is feasible based on results to date. We view these efforts as being important in the long range to improve the quantity, quality and consistency of network data analysis. In recently completed work on structure inversion, for example, we exclusively utilized auto-picked phase data.

4. A joint P/S layered structure inversion program was developed to use earthquake and explosion arrival times, providing additional constraint on structure determination where high quality S arrivals are measured. The method uses coupled P and S models, and makes use of an an independently determined VP/VS ratio. Using the joint P/S inversion program, crustal structure at Mt. St. Helens was inverted from both earthquake and explosion arrival times. The incorporation of S phases offers significantly greater stability to the modeling process than the use of P phases alone. Our final model indicates that the P velocity in the vicinity of St. Helens rises rapidly to about 6.1 km/sec at 1 km depth (very high shallow velocity) and then increases slowly in approximately a linear fashion to about 6.5 km/sec at 20 km depth. In comparison with the Puget Sound region, higher velocities are reached at shallower depths but mid-crustal values are somewhat lower. Using auto-picked digital data for 58 seismic events (48 earthquakes, 10 explosions), we inverted for a coupled P and S velocity model for the greater Puget Sound region. The final model, although similar to our previous model in the depth range from about 12 km to 30 km, has a thinner surface layer of velocity 5.4 km/sec and a slight velocity reversal in the interval 30-40 km. km. The constraint on the velocity in the 30-40 km depth range, an earthquake free zone, with our new model appears to be better than that previously obtained. This structure inversion

effort is preliminary to undertaking a careful analysis of deep earthquake seismicity.

5. Focal mechanisms for small earthquakes are commonly utilized to infer tectonic stress directions and trajectories. In the Puget Sound region, the volumetric distribution of earthquakes offers an excellent opportunity to study stresses associated with subduction. Such studies provide one of the most reliable methods to assess the degree of coupling between the overlying North American and the subducted Juan de Fuca plates. McKenzie (1969) has shown quantitatively how preexisting faults or fractures can distort the interpretation of stress directions when these are based on the common assumption of fracture of previously unbroken rock. Since there are probably no regions of the earth's crust or upper mantle that behave as unfractured rock, caution is required. With reasonable assumptions as to the effect of the earth's free surface and the relative magnitudes of the principal stresses, we can use McKenzie's results to show that substantial error may be introduced if strike-slip earthquakes are used to determine the P axis for the Pacific Northwest. By contrast, thrust or normal earthquakes should provide better estimates of the azimuth of P or T axes. We are studying a data base of well recorded regional earthquakes in order to test this hypothesis, and possibly reconcile varying values of P axis azimuth estimated from northwest earthquakes. These studies of regional tectonics are critically dependent on the data base efforts discussed in (1) above.

6. Routines for determining seismic moment, corner frequency, and stress drop from digital seismic data are being tested. A synthetic source spectrum is fit to the amplitude density spectrum for P, S, and coda waves corrected for instrument response and Q. All events located by the routine processing will ultimately have source parameters determined by this process. Periodic testing of the process is underway. Calibration of amplitude-frequency responses of network stations is crucial to this effort, and is ongoing.

Reports

Crosson, R.S. and D.A. Bame, 1984, A Spherical Source Model for Volcanic Earthquakes (abs), EOS, (in press).

Ludwin, R.S. and R.S. Crosson, 1984, The Azimuth of Regional Tectonic Compression in the Pacific Northwest from Shallow Thrust Earthquakes (abs), EOS, (in press).

Noson, Linda Lawrance, R.S. Ludwin, and R.S. Crosson, 1984, Compilation of Earthquake Hypocenters in western Washington, 1979, Washington Division of Geology and Earth Resources Information Circular, (in press).

Univ. of Wash. Geophysics Program, 1984, Earthquake Hazard Evaluation in the Pacific Northwest, 1981-1982 Final Technical Report U.S.G.S.

Contract 14-08-0001-19274.

Univ. of Wash. Geophysics Program, 1984, Earthquake Hazard Evaluation in the Pacific Northwest, 1982-1983 Final Technical Report U.S.G.S. Contract 14-08-0001-21192.

Univ. of Wash. Geophysics Program, 1984, Quarterly Network Report 84-A on Seismicity of Washington and Northern Oregon Jan 1 through March 31, 1984,27p.

Univ. of Wash. Geophysics Program, 1984, Quarterly Network Report 84-B on Seismicity of Washington and Northern Oregon April 1 through June 30, 1984,26p.

Zervas, C., 1984, A Time-Term analysis of Pn Velocities in Washington, M.S. Thesis, Univ. of Washington.

Reanalysis of Instrumentally-Recorded U.S. Earthquakes

9920-01901

J. W. Dewey
Branch of Global Seismology and Geomagnetism
U.S. Geological Survey
Denver Federal Center,MS 967
Denver, Colorado 80225
(303)236-1506

Investigations

1. Relocate instrumentally recorded U.S. earthquakes using the method of joint hypocenter determination (JHD) or the master event method, using subsidiary phases (Pg, S, Lg) in addition to first arriving P-waves, using regional travel-time tables, and expressing the uncertainty of the computed hypocenter in terms of confidence ellipsoids on the hypocentral coordinates.

2. Evaluate the implications of the revised hypocenters on regional tectonics and seismic risk.

Results

1. Relocated hypocenters for instrumentally recorded, magnitude 3.0 or greater, earthquakes in Eastern and Central United States and adjacent Canada have been published in a Miscellaneous Field Studies Map and accompanying pamphlet (Dewey and Gordon, 1984). The map is at the scale and projection of the USGS, 1:2,500,000, geologic and tectonic maps of the United States. Professional Papers covering the Eastern United States and adjacent Canada (J. Dewey and D. Gordon) and the central United States (D. Gordon) are in review; these discuss in detail the relocations published in the Miscellaneous Field Studies Map.

2. Epicenters published by Dewey and Gordon (1984) are shown in figure 1, plotted without their confidence ellipses because of the small scale of the figure. The epicenters show a view of the seismicity of eastern North America at a time scale and spatial resolution that are intermediate between the long time-scale and low resolution provided by catalogs of macroseismic epicenters and the short time-scale and high resolution provided by catalogs from regional microearthquake networks. Several elongated belts of epicenters are suggested by earthquakes occurring in the time and magnitude windows of the Dewey and Gordon catalog. A belt of epicenters extending from western Alabama through the Panhandle of Texas (shown in fig. 1), and into southern Colorado and northern New Mexico (not shown in fig. 1) is spatially associated with the Amarillo-Wichita uplift, the Anadarko basin, and the Ouachita foldbelt (Gordon, 1984). A prominent linear trend of epicenters follows the southern Appalachians from western Alabama to western Virginia. A trend of epicenters parallels the Ohio River Valley from western Kentucky to eastern Ohio. The controversial "Boston-Ottawa trend" (the NW trend extending in figure 1 from coastal New Hampshire through northeast New York into Canada), for which

little evidence can be seen in detailed geologic and seismologic studies of northern New England, northern New York and southern Canada, appears prominently at the broad scale of figure 1.

Reports

(M) Dewey, James W., and Gordon, David W., 1984, Map showing recomputed hypocenters of earthquakes in the eastern and central United States and adjacent Canada, 1925-1980: U.S. Geological Survey Miscellaneous Field Studies Map MF-1699, scale 1:2,500,000, with pamphlet, 39 p.

(A) Gordon, D. W., 1984, The Wichita-Ouachita Seismic Lineament -- a preferred seismic direction in a uniform compressive stress field: presented at the 56th annual meeting of the Eastern Section of the Seismological Society of America, October 10-12, 1984, Earthquake Notes, in press.

(P) Viret, Marc, Bollinger, G. A., Snoke, J. A., and Dewey, J. W., 1984, Joint hypocenter relocation studies with sparse data sets -- a case history: Virginia earthquakes: Bull. Seism. Soc. Am., in press.

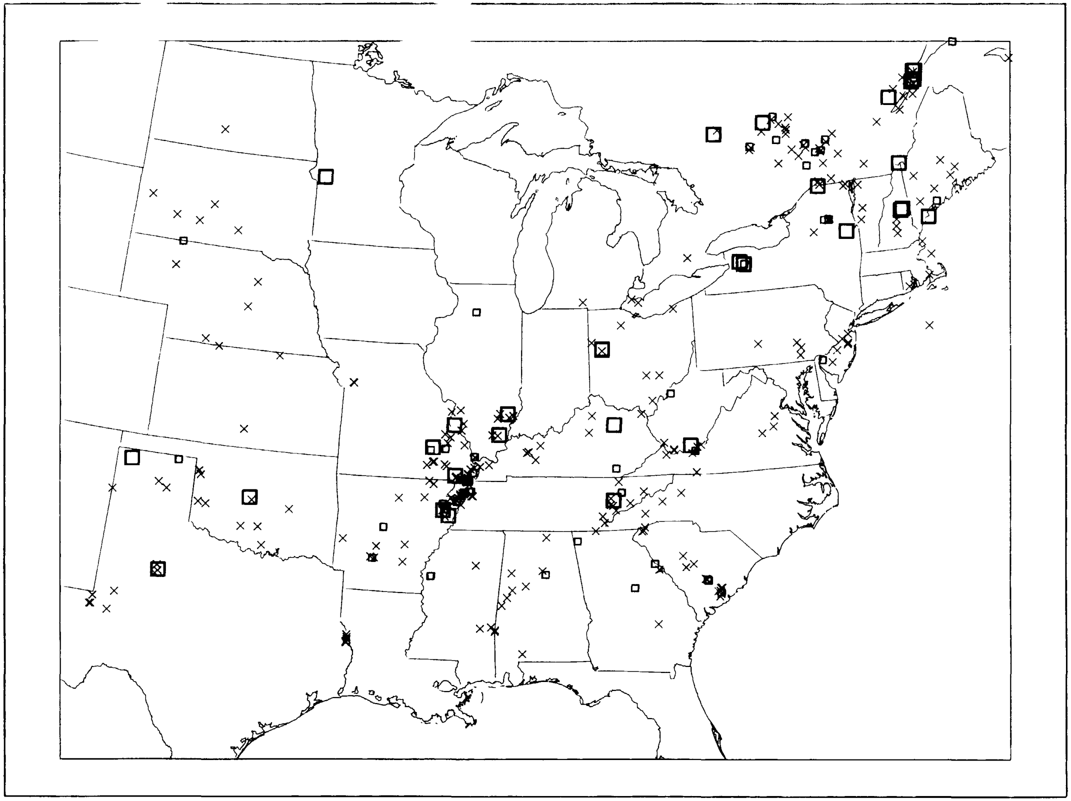

Figure 1. Epicenters of instrumentally recorded earthquakes from 1925 to 1980, from the catalog of Dewey and Gordon (1984). Large square -- magnitude (mbLg) 4.6 and greater, 1925-1980. Small square -- magnitude (mbLg) 3.8 and greater, 1964-1980. X -- magnitude (mbLg) 3.0 and greater, but falling outside the time-magnitude windows of the squares; the catalog is not complete for this class of earthquakes. The catalog does not cover the Rocky Mountain states.

Central Aleutian Islands Seismic Network
and
Prediction Methodology for Subduction Zone Earthquakes, Central Aleutian Islands

Contract No. 14-08-0001-21896 and Grant No. 14-01-0001-G-881

Carl Kisslinger and Selena Billington
Cooperative Institute for Research in Environmental Sciences
Campus Box 449, University of Colorado
Boulder, Colorado 80309
(303) 492-8028

Network Operations

The primary objectives of the network contract are the operation of the Adak Seismic Network and the production of a catalogue of earthquakes in the Adak seismic zone from the data acquired by this network. The Adak seismic zone is defined as that portion of the Aleutian arc within which the network is capable of providing hypocenter locations with adequate precision and accuracy. This zone extends from approximately 50.25°-52.25°N latitude and 175°-178.5°W longitude. The network consists of 14 stations deployed on Adak and nearby islands. Thirteen of these are two-component, short-period, high-gain stations, connected by radio telemetry to the Adak Observatory; the other is a conventional six-component earthquake station, ADK.

Network Maintenance. Maintenance of this network requires the solutions of difficult problems of the natural environment, remoteness from our headquarters and difficulty of access to the individual stations even after reaching Adak Island. After ten years of experience S.T. Morrissey, the project engineer, has developed stations capable of operating unattended for two years, if no extreme natural catastrophes strike. A successful maintenance trip was carried out in July-August, 1984, during which all of the stations except one were reached and serviced with the aid of a rented small craft. The station that could not be reached by surface transport is inoperative and will remain so until we can once again get to it by helicopter. This trip did restore some of the coverage of the western part of the seismic zone that had been lost during 1982 through the first part of 1984.

Seismicity in the Adak zone. Earthquake locations are complete through July, 1984. The location task has fallen behind the normal lag of three to four weeks because of disruptions in data flow during the summer maintenance trip and the diversion of personnel to other essential tasks. Temporary experienced staff has been added and we expect the backlog to be eliminated by the end of November.

The seismicity patterns in terms of the locations of concentrations of earthquakes are not unusual during the past six months, but the continuation of the low rate of occurrence of events in all magnitude bands is still an important feature. We consider this seismic quiescence, which has been in progress since September, 1982, to be a possible precursor to a major earthquake, as discussed in the Research section of this summary.

Research on Prediction Methodology

The research program has had two long-term goals since its inception in 1974: improved understanding of the relation of the seismic activity to local and regional tectonics, through seismotectonic investigations; and the discovery, documentation and explanation of phenomena indicative of the approach of the occurrence of a large earthquake in order to make possible the prediction of earthquakes in this subduction zone. Data provided by the Adak network are the primary basis of these studies, but teleseismic data and theoretical approaches have also been incorporated. This work is currently supported under Grant G-881, but research under other, non-USGS support is an integral part of the program and some of the results obtained from these other efforts are included for completeness.

Forecast of the Location of the 6May1984 Earthquake. An earthquake, m_b 5.8 (NEIS), occurred in sub-region SW2 of the Adak seismic zone on May 6, 1984. This earthquake, the largest to occur in this part of the Adak zone since we started work here in 1974, was located at the place which we had selected and announced as the likely site of a strong earthquake in the indefinite but near future. This forecast may be found, among other places, in our entry in Volume XVII of these Technical Summaries, December, 1983, and in a letter to the Chief, Office of Earthquakes, Volcanoes, and Engineering, U.S.G.S., January 4, 1984. The forecast was based on our conclusion that sub-region SW2 enclosed an asperity on the main thrust plane that had become activated in July 1980, as evidenced by a cluster of moderate earthquakes between that time and the end of 1983, Fig. 1 (Bowman and Kisslinger, 1985). The occurrence of the May 6 event is taken as confirmation of this interpretation, but leaves open the other part of our forecast, that a major earthquake will occur in the Adak zone soon.

In a related study based on Adak network data but carried out with other support, the state of stress (apparent stresses and stress drops from microearthquakes) in SW2 and adjacent parts of the main seismic zone was examined on the basis of the spectra of S-waves (Scherbaum and Kisslinger, 1984.) They found that the higher stress microearthquakes occurred in the same place as the cluster of moderate events mentioned above, Fig. 2a, and the stresses associated with these stronger microearthquakes have been increasing steadily since the latter part of 1982, Fig. 2b. We do not yet have comparable results for earthquakes after May 6. The gradual increase in these seismically determined stresses began at about the same time as the overall quiescence in the Adak seismic zone.

Quiescence in the Adak Seismic Zone. We have reported previously that a pronounced decrease in the rate of occurrence of earthquake located by our network started in mid-September, 1982. The decrease in the rate for the year before and the year after this time was about 60 percent in all magnitude bands, as given by our Adak catalogue. In view of Habermann's discovery of a clear quiescence that lasted for three years prior to the strong event of February 7 and May 2, 1971, we were led to the conclusion that this quiescence had to be considered as a possible precursor to the next major earthquake in this zone. The fact that no event of magnitude 7 or greater has occurred in the neighborhood of Adak for more than 13 years lends credence to this expectation. If the 1971 scenario is followed, an event of magnitude 7 or larger should occur within the next 12 months.

After the May 6 event, we hypothesized that another feature of 1971 might be observed again. In that case a smaller earthquake, magnitude 6.7, occurred east of Adak Canyon three months before (Feb. 7) the large event in Adak Canyon (May 2). We, therefore, announced the highly speculative outlook that a major event would occur in August, 1984. This did not happen, and we conclude that the May 6 event is not related directly to the occurrence of a larger event. However, the May 6 event did not change the observed rate of occurrence of local earthquakes, so whatever is responsible for the quiescence had not ceased operating.

An independent check on the reality of the quiescence indicated by the local network catalogue has been made by an examination of the rate of occurrence of events reported in the Preliminary Determinations of Epicenters by NEIS. The results for earthquakes with m_b 4.5 and greater are the most reliable, because the catalogue of these events is more likely to be complete than a listing including smaller events. The average rate of occurrence during the 247 months was 0.891 events per month, or just under 11 per year. The teleseismic data show a strong decrease in activity during October 1982 through March 1983, with an increase after that. Further analysis confirmed that much of the teleseismic activity during the supposed quiescence occurred within SW2, the activated sub-region. The rate of occurrence of earthquakes in the region of study, with SW2 eliminated, with m_b greater than or equal to 4.5 during the two year period prior to September, 1982 was about 0.9 per month, during 1983 was 0.67 per month, and during 1984 has been 0.17 per month, one of the lowest rates seen in the 20 years covered, and about the same as 1969. It is, however, not the lowest rate ever seen, as 1975 was marked by extremely low rate of 0.1 per month. The 1975 drop in teleseisms lasted only one year and was not followed by a large event.

The teleseismic data do not contradict the data from the local network, but they do not provide strong confirmation. They do indicate that sharp drops in rates of activity can last as long as one year without being precursors to strong events. Only continued observations will tell if they can last two years or longer and still not be followed by a major event.

Research on local and regional tectonics

Work has been completed and manuscripts are being prepared on two seismotectonic studies: (1) the study of shallow-focus earthquakes seaward of the main thrust zone; and (2) the search for possible precursors to the m_b 5.8 June 4, 1982, Adak Canyon earthquake. No precursors to this earthquake were found in an examination of the time-space patterns of seismicity or in the focal mechanisms of preceding earthquakes. Spectral analyses of small events occurring in the vicinity prior to the 1982 event are in progress.

The shallow-focus earthquakes trenchward of the main thrust zone are infrequent, occur in both spatial and temporal clusters, have thrust mechanisms in which the probable fault plane dips with a very shallow angle to the northwest, and occur at depths near 17 km under a prominent bathymethric forward rise called "Hawley Ridge". The "Hawley Ridge earthquakes" are particularly interesting in light of the seismicity pattern associated with the 1971 earthquakes discussed above: the February event occurred under Hawley Ridge, the larger May event occurred north of the western edge of the February aftershock zone. The 1982 Adak Canyon event was followed five days later by events under Hawley Ridge at the same longitude. These sequences suggest a correlation between events on the plate interface under Hawley Ridge and those occurring farther north within the main thrust zone. The further interpretation of this observation in terms of the details of failure along the plate interface must wait for more examples, either at Adak or in other subduction zones.

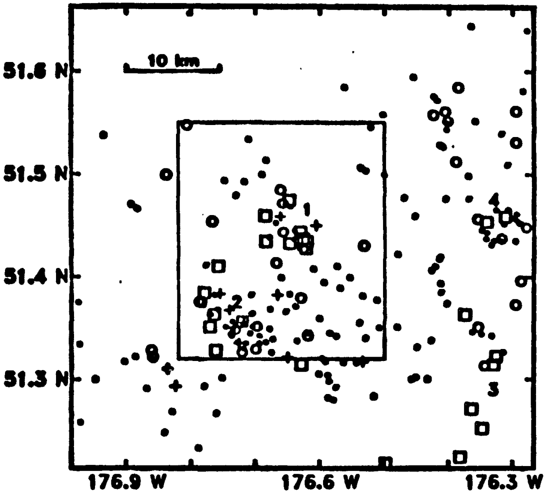

1.

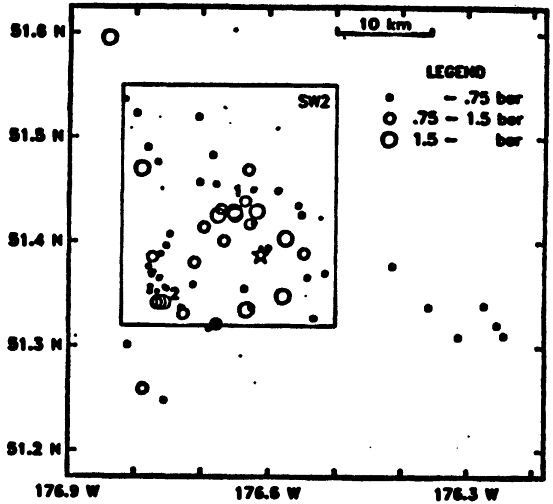

2a.

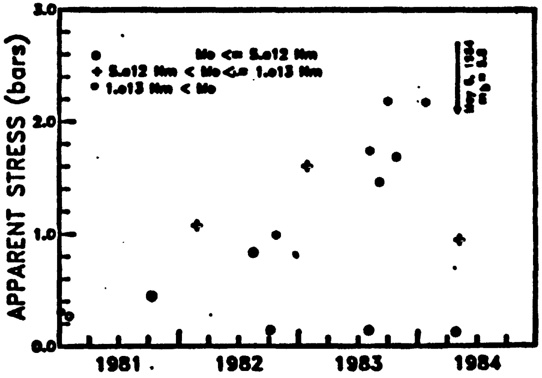

2b.

Figure 1. Shallow (<70 km) seismicity in and around SW2, August 1974-June 1983. The squares are local network locations of events on the PDE, circles are microearthquakes. Clusters 1 and 2 are associated with the asperity.

Figure 2a. Apparent stresses of SW2 earthquakes. The higher stresses concentrate at the clusters in Fig. 1. The star is the 6May1984 earthquake.

Figure 2b. Apparent stress as a function of time for earthquakes within 7.5 km of the 6May1984 earthquake.

References

Bowman, J.R. and C. Kisslinger, 1985, Seismicity associated with a cluster of m_b>4.5 earthquakes near Adak, Alaska: evidence for an asperity, *Bull. Seis. Soc. Amer.*, *75*(1): in press.

Scherbaum, F. and C. Kisslinger, 1984, Variations of apparent stresses and stress drops prior to the earthquake of 6May1984 (m_b 5.8) in the Adak Seismic Zone, *Bull. Seis. Soc. Amer.*, *74*(6): in press.

Publications and Abstracts, April-September, 1984

Toth, T. and C. Kisslinger, 1984, Revised focal depths and velocity model for local earthquakes in the Adak Seismic Zone, *Bull. Seis. Soc. Amer.*, *74*(4): 1349-1360.

Billington, S., C. Kisslinger and E.R. Engdahl, 1984, Features of locally-recorded seismicity in the central Aleutian islands (abstract), *Abstracts with Program*, G.S.A. Cordilleran Section Meeting, volume 16, number 5, p. 270.

Engdahl, E.R., J. Dewey and S. Billington, 1984, Redefined spatial distribution of teleseismically recorded earthquakes in the central Aleutian islands (abstract), *Abstracts with Program*, G.S.A. Cordilleran Section Meeting, volume 16, number 5, p. 282.

Scherbaum, F. and C. Kisslinger, 1984, Stress monitoring, source parameters and scaling laws in the Adak region, Aleutian Islands (abstract), *Earthquake Notes*, S.S.A. Eastern Section, volume 55, number 1, p. 16.

WESTERN GREAT BASIN-EASTERN SIERRA NEVADA SEISMIC NETWORK

Contract 14-08-0001-21867

A.S. Ryall, W.F. Nicks, and E.J. Corbett
Seismological Laboratory
University of Nevada
Reno, NV 89557
(702) 784-4975

Investigations

This program supports continued operation of a seismic network in the western Great Basin of Nevada and eastern California, with the purpose of recording and location of earthquakes occurring in the western Great Basin; and acquiring a data base of phase times and analog and digital seismograms from these earthquakes. These data are used for research on: (1) ongoing seismicity in the western Great Basin with emphasis on the Long Valley caldera; (2) source mechanism studies of these earthquakes; (3) possible precursory seismicity patterns in the White Mountains gap; (4) seismicity near reservoirs in the Lake Tahoe region; and (5) evaluation of the contribution that high-quality digital broad-band seismic stations can make to regional network-seismic studies.

Results

A. *Seismic Network Operation*

One of the areas of highest seismic activity since 1978 has been the area south of the Long Valley caldera. Since this is an area inaccessible by road and by helicopter due to its wilderness status, it has always had poor station coverage. One station was installed at Red Slate Mountain by the USGS in July, 1983, but it has been out of commission for most of its existence. This summer, RSM was repaired and five additional stations were installed in the mountain block on foot and horseback by UNR personnel. The new UNR stations are: MGC, HTC, PRB, STR, and HOP (see map). These stations should provide excellent horizontal and vertical control for High Sierra earthquakes as well as provide the basis from which to derive station corrections to better locate past activity. Stations PRB, STR, and HOP were installed as temporary stations and are expected to be de-commissioned by the coming winter snows.

At the request of John Rundle, of Sandia National Labs, we are taking over recording of a seismometer located at the bottom of a drill hole in the northern Long Valley caldera (DHL on map). By mid-November we will be telemetering 3-component short-period seismic signals to our central recording facility in Reno.

We have also deployed five new seismic stations at the north end of the Owens Valley along the western flank of the White Mountains: BHP, CWC, MLN, BCK, and POC (see map). These stations should provide data on possible attenuation effects observed for earthquakes in the Long Valley region as well as begin to give us data on the seismicity in the northern Owens Valley - White Mountains region.

In the Lake Tahoe region, station SIE has been removed and two new stations have been installed. Station GBK has been deployed on the east shore of Lake Tahoe and EMB at Emerald Bay on the southwest shore of Lake Tahoe.

In summary, the University of Nevada is currently operating 55 short-period analog seismographic stations, four of which are multi-component. In addition we are recording signals from 11 USGS stations, 2 U.C. Berkeley stations, and 1 from the California Division of Water Resources. All 69 of these stations are being recorded on analog magnetic tape at Reno as well as digitally by our on-line system.

In addition to the analog stations, the University of Nevada operates 3 remote digital seismographic stations. The digital stations provide broad-band (0.05-30 Hz), wide dynamic-range (96 dB) digitization of signals from a 3-component set of seismometers, and telemeter the data to the Reno facility where it is continuously recorded. The three stations are now operating in mine-tunnels at Mina, Bodie, and Washoe Lake. A fourth station is to be installed in the Las Vegas area in the near future.

We are in the process of acquiring a microwave system to replace some of our major VHF radio links. Although the initial investment is substantial, the savings in telephone line costs will offset the expense in about 2 years. The principal advantages of the microwave system are increased reliability, especially during the winter months, less susceptibility to nearby lightning ground strikes, reduced radio interference, and a substantial increase in the number of signals we can transmit.

B. *On-line System*

A computer-based earthquake recording system has been installed that provides on-line event detection and digitization of the analog seismic signals transmitted to the Reno data facility. This system facilitates analysis of large numbers of earthquakes and will allow waveform analysis of the network data. The on-line system commenced operation on May 11 and is triggering successfully on local events, regional earthquakes, teleseisms, and explosions. The triggering algorithm has been tuned sufficiently so that false triggers are now reduced to about 10%. We are still plagued by noise triggers during lightning storms, due to our dependence on VHF radio telemetry, but we expect this problem to be alleviated by the installation of the microwave system. We are currently recording 79 seismic signals and 4 time signals on the 96-channel on-line system. For the period May 11 to August 7, 1984, we have recorded and archived digital seismograms for 1516 seismic events. Of this number 1230 (81%) are local earthquakes. Since June 8, we have adopted a policy of locating only earthquakes with a minimum duration of 10 seconds (which corresponds roughly to magnitude > 1.5 M_L). Consequently, the number of earthquakes located with the on-line system so far has been 801.

C. *Data Analysis*

Our earthquake data have been timed and located through August 7, 1984. Compared to past years, 1984 has so far been relatively quiescent. A few short-duration swarms have occured in the Mammoth Lakes region, but none have approached the intensity of swarms observed in 1979-1983. Still, Mammoth activity continues at a high level compared to the rest of the western Great Basin. Of all the local earthquakes recorded by the on-line system: 83% are located in the Mammoth Lakes region; 14% in the western Nevada region; and 3% in the northern Sierra Nevada.

T-1

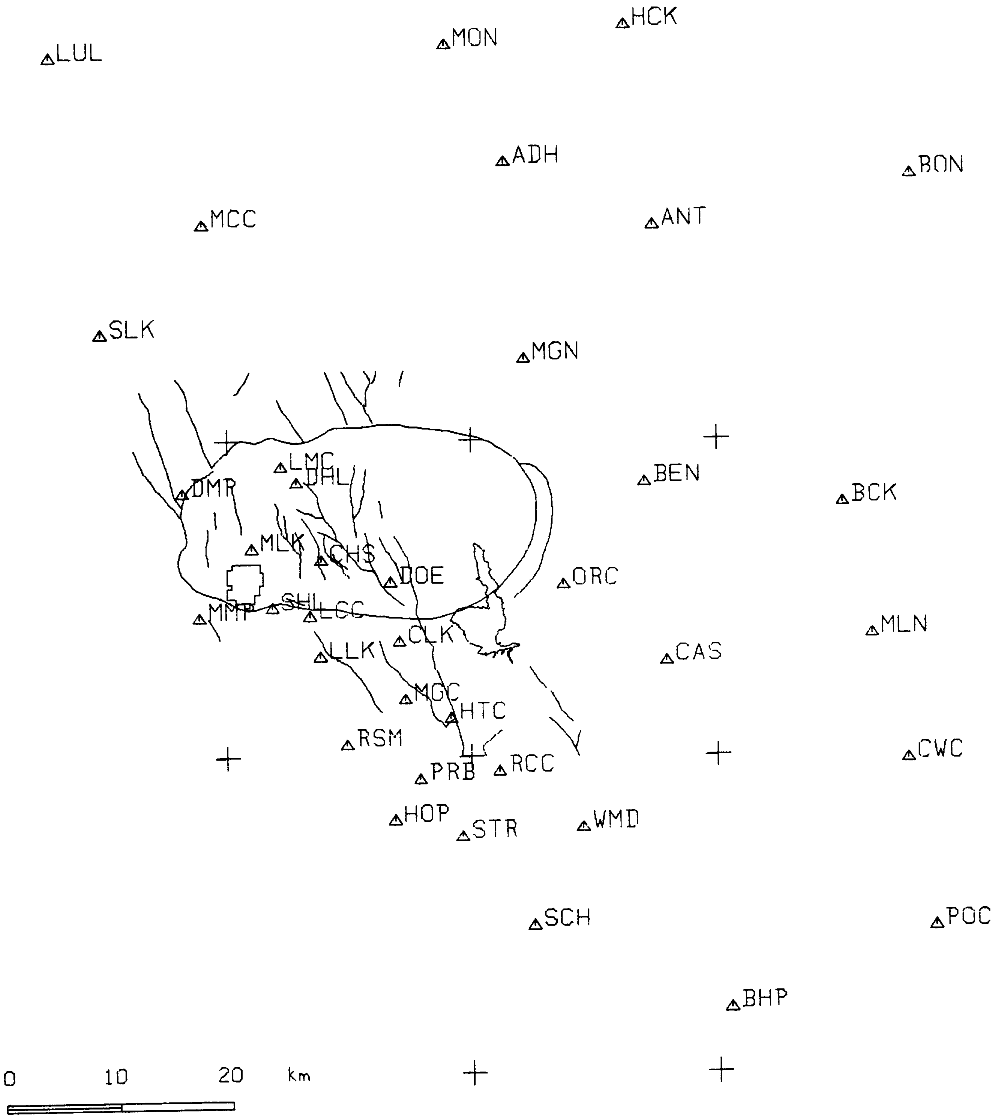

Mammoth stations recorded by UNR Nov 84

Intraplate Neotectonics from Seismic Network and Pre-instrumental Earthquake Data in New York-New Jersey and Surrounding Areas

USGS 14-08-0001-21876

Leonardo Seeber and Lynn R. Sykes
Lamont-Doherty Geological Observatory of Columbia University
Palisades, New York 10964
(914) 359-2900

Objectives: It has recently become apparent that reliable estimates of earthquake hazard in eastern North America can only be based on an improved understanding of the mechanism responsible for neotectonic activity in this intraplate environment. One of the main objectives in this project is to gather earthquake data on recent seismicity from networks and on pre-instrumental earthquakes from archival sources which are particularly significant for constraining models of neotectonics in the northeastern U.S.

The local seismic network operated by L-DGO covers a wide region across the Appalachians, from the platform/shield of western and northern N.Y., through the foldbelt and to the crystalline overthrust terrane of southern N.Y./N.J. It also samples prominent Mesozoic rift structures and the Cretaceous-Cenozoic passive margin. Seismic zones have been recognized in each of these structural provinces, except the foldbelt. The L-DGO local network offers the unique opportunity to compare in one data set seismicity from most of the structural environments in the eastern U.S. This opportunity is exploited in a number of detailed studies directed at decifering active fault kinematics, source characteristics (stress-drop), space-time seismicity patterns, and at comparing these characteristics with characteristics of preexisting structures. This approach is inspired by the hypothesis that fundamental characteristics of intraplate neotectonics and seismicity are controlled to a large extent by preexisting structural features.

Methods: The strategy adopted in this project is to focus the effort in selected areas for intense studies combining earthquake and structural analysis. The data from the telemetered network is augmented with data from portable seismographs for studies of recent seismicity. Archival sources such as newspapers are searched for felt reports on pre-instrumental events. The relatively short data base from the reliable instrumental period can be substantially lengthened by systematic studies of felt reports from newspapers, particularly along the Atlantic seaboard. Archival data is analyzed in this project to study events of particular interest, such as the 1884 New York City earthquake, and for decifering the long-term pattern of seismicity in areas of particular interest, such as Lancaster County, Pa.

Results: The topics discussed in this report reflect only the major topics of concern during the last year, namely the seismicity in the central Adirondacks and in the crystalline Appalachians of southeastern Pennsylvania, the sites of the largest earthquakes in these areas in many decades.

The 7 October, 1983 Goodnow earthquake in the Central Adirondack seismic zone was the largest earthquake (M_b = 5.2) in New York State in the last forty years. The fault plane solution shows reverse faulting with P axes oriented NE-SW, similar to the source mechanism of previous microearthquakes in the area. A focal depth of 12 km was determined by the permanent New York State Network, of which the nearest station was 20 km away. However, a preliminary analysis of teleseismic data indicates a focal depth of 6 to 8 km. At this shallower depth, the main shock lies within the well defined, quasi circular zone of aftershock activity. The seismic moment determined from a few long-period Rayleigh wave seismograms recorded at Canadian stations yields a value of 2.5 x 10^{23} dyne-cm. Using this value of seismic moment and a source radius of 0.75 km, determined from the planar fault surface defined by the aftershock distribution, a stress drop of 140 bars is obtained. This value of static stress drop probably represents a lower bound since the fault area determined from the aftershock distribution is usually over-estimated. Determination of stress drop for other recent earthquakes of similar size in eastern North America range from a few bars for the 1980 Sharpsburg earthquake to hundreds of bars for the 1982 New Brunswick event. A common problem in these estimates is the uncertainty in the size of the rupture area. The accurate location of the Goodnow aftershocks provides a reliable estimate of the fault area which is unprecedented for other eastern North American events.

The Easter Sunday, 1984 Martic earthquake, centered about 10 km south of Lancaster, Penn., was felt from NY City to Washington, DC, had a maximum intensity MM V-VI and was characterized by M_{b1g} = 4.1. A 10 day deployment of portable instruments detected many aftershocks. Reliable source parameters were obtained for 10 of these. The vertical scatter of hypocenters about a depth of 4.5 km is insignificant (300 meters). Horizontally, however, the aftershocks are distributed over a 3 km long NNE zone significantly larger than the location error. The strongest effects for a foreshock and for the main shock are reported from the southern and northern end of that aftershock zone, respectively, and may reflect the NNE length of the source. 37 first motions from main shock and aftershocks narrowly constrain the two planes of a composite double couple solution with a nearly horizontal ENE P-axis. One of these planes strike NNE, parallel to the aftershock alignment, dips ≈ 60° east with reverse and right lateral slip. Previous seismicity in eastern Pennsylvania include a few recent earthquakes well constrained instrumentally and about 10 pre-instrumental earthquakes, only half of which were previously known. We found the rest and improved constraints on all of them by compiling reports from contemporary newspapers. The Lancaster area stands out as a persistent source of seismicity. The new data indicate that the April 1984 and March 1889 earthquakes are of similar size and are the largest known for eastern Pennsylvania. Structure associated with multiphase ductile Paleozoic deformation is at a high angle with the surface extrapolation of the inferred April 22 fault zone, although, on a larger scale, Paleozoic structural features seem to control the regional distributions of seismicity. Mesozoic structural features, on the other hand, include a Mid-Jurassic basic dike and a possibly related brittle fault zone which are adjacent and parallel to the April 1984 aftershock zone and may be associated with some of the previous earthquakes. The Lancaster Co. and the Moodus, Connecticut sources are similar in their relationship to Mesozoic structures and their persistency through time.

Reports

Seeber, L., E. Cranswick, J. Armbruster and N. Barstow, The Oct. 1983 Goodnow Aftershock Sequence, Regional Seismicity and Structural Features in the Adirondacks, EOS, 65, pp. 240, April 17, 1984.

Seeber, L., J. Armbruster and G. Suarez, The April 1984 Martic, Lancaster Co. Earthquake, Historic Seismicity and Tectonic Setting in Eastern Pennsylvania, Seismol. Soc. Am., Eastern Section, 56th Annual Meeting, Saint Louis University, October 10-12, 1984.

Seeber, L. and K. Coles, Seismicity in the Central Adirondacks with emphasis on the Goodnow, October 7, 1984 Epicentral Zone and its Geology, in Field Trip Guidebook, N.Y. State Geol. Assoc., 56th Annual Meeting, D. Potter, editor, 1984.

Seeber, L., N. Barstow, E. Cranswick, J.G. Armbruster, G. Suarez, K. Coles and C. Aviles, Grenville Structure and the Central Adirondack Seismic Zone including the October 7, 1983 Main Shock - Aftershock Sequence, Joint Programme with Abstracts, Canadian Geophysical Union, 11th Annual Meeting., Halifax, pp. 66, 29 May - 1 June, 1984.

Suarez, G., L. Seeber, C. Aviles and E. Schlesinger-Miller, The Goodnow, N.Y. Earthquake: Results of a broadband teleseismic analysis, EOS, Am. Geophys. Union Trans., 65, 239-240, 1984.

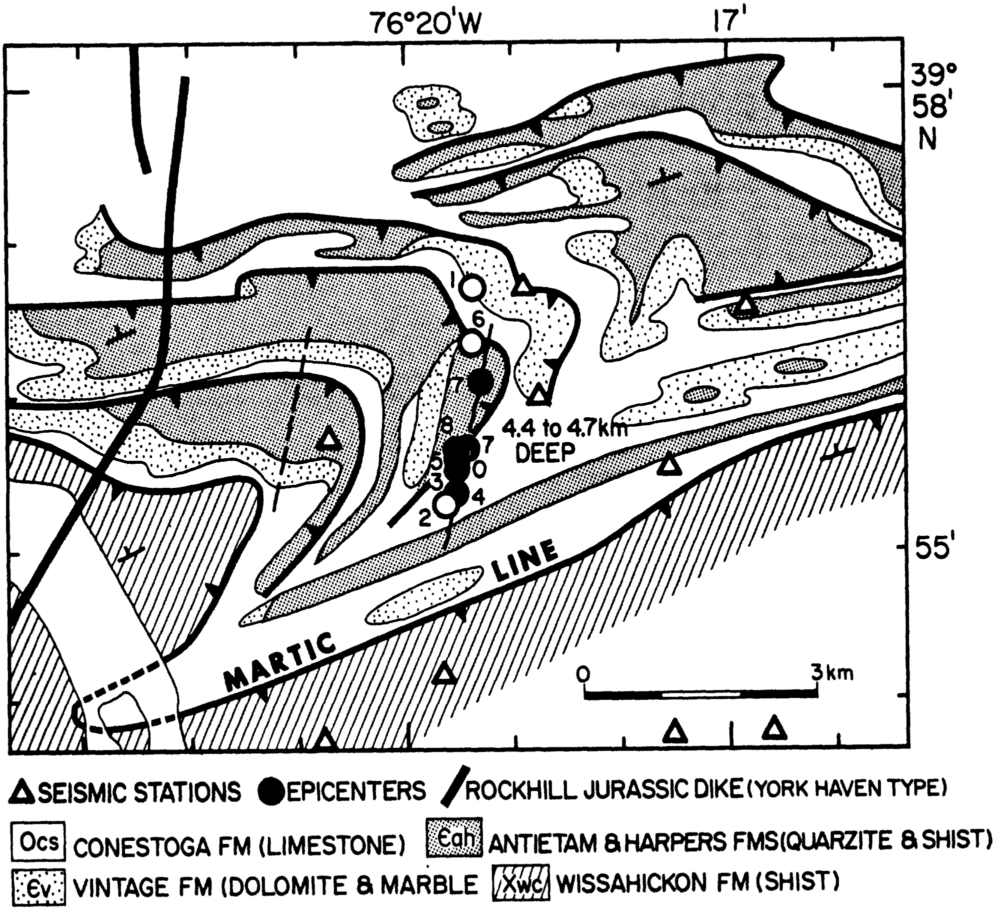

Figure 1. Aftershock hypocenters of the Martic, April 23, 1984 earthquake in eastern Pennsylvania were determined from a temporary network. They scatter over a narrow depth range at about 4 km below the surface, but occupy a ≈3 km long zone, significantly larger than the 90% limits of confidence which are typically less than 0.5 km from the epicenters. This zone is parallel to the NNE striking plane in the FPS which is tentatively interpreted as the plane of rupture: a reverse east dipping fault with a large component of right-lateral slip. Paleozoic structural features in the immediate vicinity of the epicenters appear to be prominently discordant with the inferred rupture. In contrast, a prominent Jurassic dike is parallel and adjacent to the inferred fault.

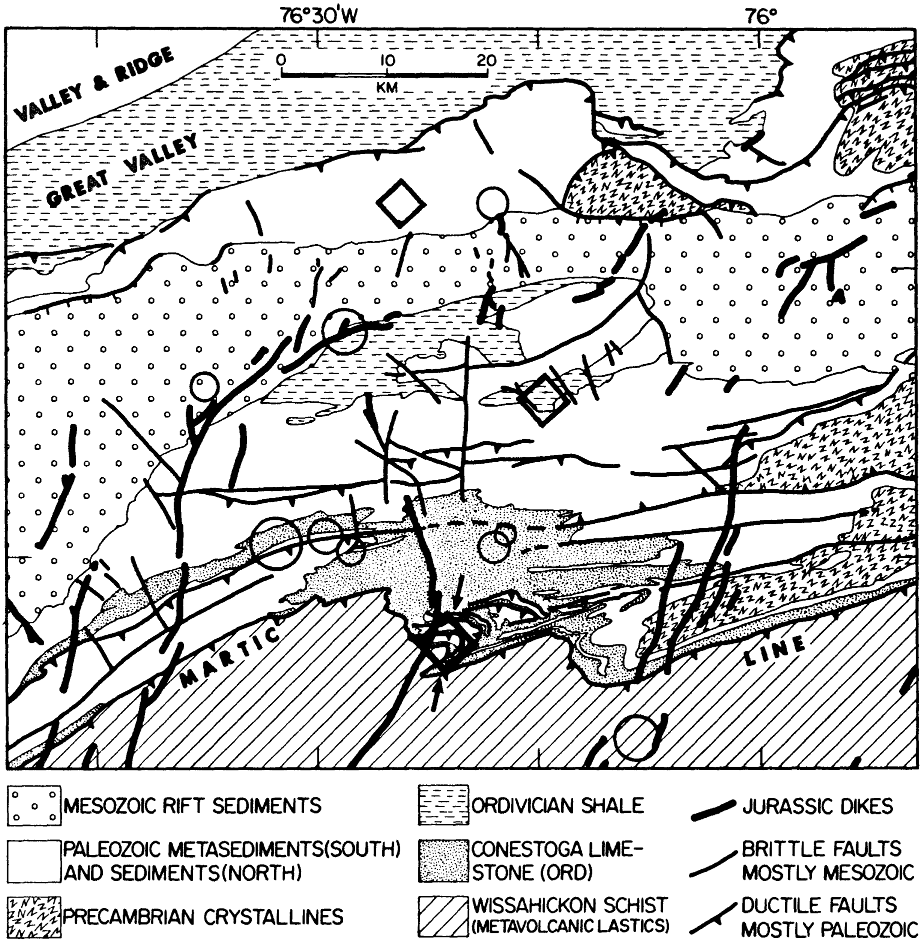

Figure 2. The Lancaster seismic zone, as identified by macroseismic epicenters of pre-instrumental earthquakes (circles), instrumental epicenters relocated by Dewey and Gordon (1984; squares) and by the Martic 1984 epicenter (square with arrows indicating strike of aftershock zone), viewed in a broad geologic contest. Paleozoic structural features in this portion of the inner crystalline Appalachians tend to strike nearly E-W. The Gettisburg Mesozoic rift basin closely follow the Paleozoic trend. However a set of Jurassic basic dikes, the youngest prominent tectonic feature recognized in this area, cuts the E-W trends at high angles. The Lancaster seismic zone is confined within two crustal blocks delimited by three adjacent dikes. The inferred NNW rupture of the Martic event is aligned with a N-S fault which seems to control one of these dikes.

Regional Microearthquake Network in the Central Mississippi Valley

14-08-0001-21887

William Stauder
Robert B. Herrmann
Department of Earth and Atmospheric Sciences
Saint Louis University
P.O. Box 8099 Laclede Station
St. Louis, MO 63156
(314) 658-3131

Goals

1. Monitor seismic activity in the New Madrid Seismic Zone, using data from a 60 station regional seismic array sponsored by the USGS and the USNRC.

2. Prepare seismic bulletins and archive seismic data for use with research projects.

Investigations

1. The project consists of monitoring data from a network of 32 USGS and 16 NRC seismograph stations located in the central Mississippi Valley. In addition telemetered data from eight Tennessee Earthquake Information Center stations in the southern part of the New Madrid Seismic Zone are recorded digitally. The seismic data are also recorded on 16mm film and on a PDP 11/34 digital computer. Operation, analysis and publication of quarterly bulletins are an ongoing task. Cooperative arrangements with other organizations, such as the Tennessee Earthquake Information Center and the University of Kentucky, have been made in order to make the quarterly published Central Mississippi Valley Seismic Bulletin as complete as possible.

The 181 earthquakes located by the USGS and other cooperating networks during the first quarter of 1984 are given in the attached figure. The size of the symbols is scaled to the magnitude of the events. Of particular interest is the tight grouping of events on the Ohio River, 25 km upstream of its confluence with the Mississippi River. An extensive swarm with several magnitude 3+ earthquakes occurred in February, 1984. Portable MEQ-800 were fielded for a two period to augment network coverage. This swarm accounts for the majority of the earthquakes located during the quarter.

2. The installation of the Berkeley 2.9BSD distribution of UNIX (TM ATT Technologies) has been successful. System performance is good. Minor changes have been made to the scheduler and other utilities.

Results

1. Quarterly Bulletin 39 of the Central Mississippi Valley Earthquake Bulletin had been issued. This bulletin covers the first quarter of 1984.

2. A paper entitled "Central Mississippi Valley earthquakes - 1983" has been submitted to Earthquake Notes for inclusion in the annual seismicity issue.

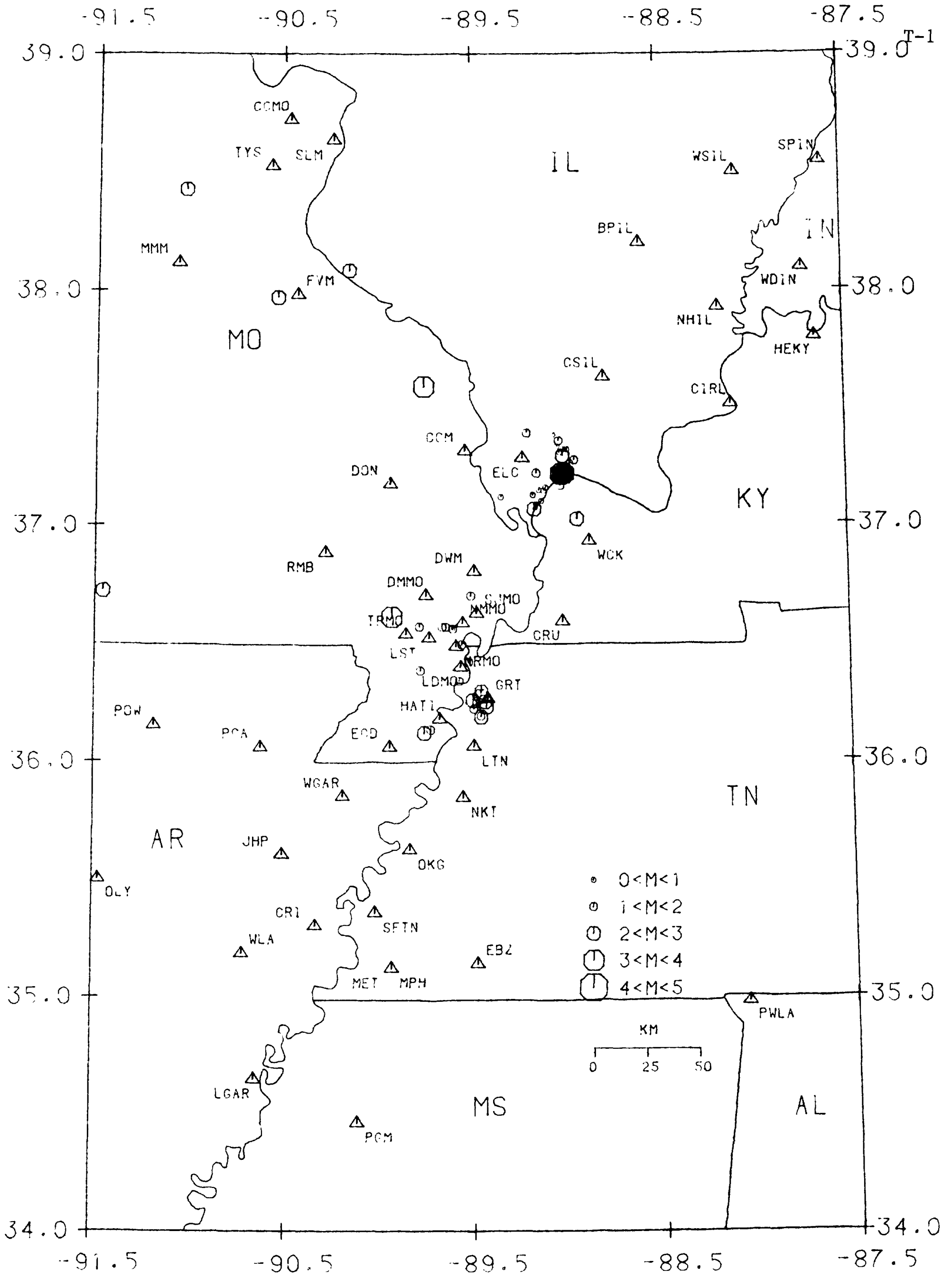

REPORTING PERIOD 01 JAN 1984 TO 31 MAR 1984

LEGEND . ⚠ STATION ⊙ EPICENTER

United States Earthquakes

9920-01222

Carl W. Stover
Branch of Global Seismology and Geomagnetism
U.S. Geological Survey
Federal Center, M.S. 967
Denver, Colorado 80225
(303) 236-1500

Investigations

1. One hundred three earthquakes in nineteen states and Puerto Rico were canvassed by a mail questionnaire for felt and damage data. Thirty-nine of these occurred in California and 17 in Alaska. The most significant event was the Morgan Hill, California earthquake of April 24, 1984 which was located at 37.320°N., 121.698°W., at a depth of 8 km, magnitude 5.7 mb, 6.1MS, and 6.2 ML. Three events; in California, Alaska, and Pennsylvania; caused damage. The most damaging was the Morgan Hill, California earthquake with a maximum intensity of VII.

2. The United States earthquakes for the period April 1, 1984 through September 30, 1984, have been located and the hypocenters, magnitudes, and maximum intensities have been published in the Preliminary Determination of Epicenters.

Results

A maximum Modified Mercalli intensity of VII was assigned to the April 24, 1984, Morgan Hill, California earthquake. Twenty-one people were injured and damage was estimated at $7.5 million. Most of the damage occurred in Santa Clara County in the Morgan Hill-San Jose area.

A preliminary report and isoseismal map for the April 24, 1984 Morgan Hill, California earthquake has been submitted to the California Division of Mines and Geology for publication in Special Publication 68.

Reports

Stover, C.W., Minsch, J.H., Baldwin, F.W., and Brewer, L.R., 1984, Earthquakes in the United States, October-December 1982: U.S. Geological Survey Circular 896-D, 33 p.

Stover, C.W., Reagor, B.G., and Algermissen, S.T., 1984, Seismicity Map of the state of Colorado: U.S. Geological Survey, Miscellaneous Field Studies Map MF-1694.

The Historical Seismicity of Central United States: 1811-1927

14-08-0001-21251

R. Street
Department of Geology
University of Kentucky
Lexington, Kentucky 40506-0059
(606) 257 4777

Objective: In recent years a number of cataloges of the earthquakes that occurred in central United States have been published; e.g., Docekal, 1971; Nuttli, 1979; and Barstow *et al*, 1981. As a consequence, the seismicity of the central United States has been fairly well documented with respect to such parameters as date, time, and general epicentral location. However, none of these studies have systematically documented the earthquakes by means of original accounts. The objective of this study is to review accounts of the larger CUS earthquakes that have occurred in the seven state area of Arkansas, Illinois, Indiana, Kentucky, Ohio, Missouri, and Tennessee between the years of 1811 when the "New Madrid" earthquake sequence began, and 1928 when the U. S. Coastal & Geodetic Survey began to collect "felt" reports.

Discussion: Sixty earthquakes, including the four major earthquakes of the 1811-1812 "New Madrid" sequence, were sufficiently documented during the course of the study to be described in detail. Several other earthquakes were partially documented (and are still being investigated), or were deemed to be too small to be of interest. Table 1 is a list of those earthquakes that have been reasonably well documented, to date, in the seven state area. Included in the table are the date and time (GMT) of the events, their apparent epicentral locations, m<bLg> magnitudes, and maximum Modified Mercalli (MM) intensities.

REFERENCES

Barstow, N. L., Brill, K. G., Nuttli, O. W., and P. W. Pomeroy (1981). An Approach to Seismic Zonation for Siting Nuclear Electric Power Generating Facilities in the Eastern United States, prepared for the Office of Nuclear Reactor Regulation, publication NUREG/CR-1577.

Docekal, J. (1971). Earthquakes of the Stable Interior: With Emphasis on the Midcontinent (vols. 1 and 2), Ph. D. dissertation, University of Nebraska, Lincoln, Nebraska.

Nuttli, O. W. (1979). "Seismicity of the central United States", Reviews in Eng. Geology, IV, 67-93.

Street, R. (1981). "A contribution to the documentation of the 1811-1812 Mississippi valley earthquake sequence", Earthquake Notes, 53, 39-52.

TABLE 1

EARTHQUAKES STUDIED

Epicentral Location, Manitude, and Maximum Intensity

DATE Mo/Day/Year	TIME (GMT) H - M	LAT/LONG East/North	MAGNITUDE m<bLg>	MAXIMUM MM INTENSITY *
DEC 16, 1811	08-15	(36 /90)	7.2	XI #
DEC 16, 1811	14-15	(36 /90)	7.0	X @
Jan 23, 1812	15	(36.3/89.6)	7.1	X-XI #
FEB 07, 1812	09-45	36.5/89.6	7.4	XI @
JUL 05, 1827	11-30	38.0/87.5	5.0	VI
AUG 07, 1827	04-30	38.0/88.0	4.8	V
JUN 09, 1838	14-45	38.5/88.0	5.0	VII
DEC 28, 1841	05-50	36.6/89.2	4.6	V-VI
JAN 05, 1843	02-45	35.5/89.6	5.8 #	VII
APR 05, 1850	02-05	(37.0/88.0)	4.9	V
FEB 28, 1854	09	37.6/84.0	4.0	IV
NOV 09, 1856	10	36.6/89.5	4.6	V
OCT 08, 1857	10	38.7/89.2	5.1	VII
AUG 07, 1860	15-30	(37.5/87.5)	4.5	VI
AUG 17, 1865	15	36.5/89.5	4.6	VI-VII
SEP 25, 1876	06-15	38.5/87.0	4.8	VII
NOV 19, 1878	05-52	35.5/90.7	(5.2)	VII
SEP 27, 1882	10-20	38.7/89.5	4.7	VI
JAN 11, 1883	07-12	37.0/88.5	4.7	VI
DEC 05, 1883	15-20	35.7/91.2	4.2	V-VI
SEP 19, 1884	20-14	40.7/84.1	5.1	VI-VII
FEB 06, 1887	22-15	39.0/88.5	4.6	VI
AUG 02, 1887	18-36	(37.2/88.5)	5.2	VI
JUL 27, 1891	02-28	37.9/87.5	4.0	VI-VII
SEP 27, 1891	04-55	38.3/88.5	5.5	VII
OCT 31, 1895	11-08	37.0/89.4	6.0 #	VIII-IX
JUN 14, 1898	15-26	36.5/88.7	4.5	V
APR 30, 1899	02-05	38.5/87.4	4.5	VII
FEB 15, 1901	00-15	36.0/90.0	4.4	IV
JAN 24, 1902	10-18	42.3/89.0	5.0	V-VI
FEB 09, 1903	00-21	37.8/89.3	4.8	VII
OCT 05, 1903	02-56	38.3/90.2	3.9	V
NOV 04, 1903	18-18	36.5/89.5	4.4	VI-VII
NOV 04, 1903	19-14	36.5/89.8	4.8	VII
NOV 27, 1903	07	37.0/89.5	4.0	V
AUG 22, 1905	05-08	37.2/89.3	5.2	VI-VII
DEC 27, 1908	21-15	37.5/88.0	4.1	IV
MAY 26, 1909	14-42	40.6/88.1	5.0	VII
JUL 19, 1909	04-34	40.3/90.7	4.4	V-VI
Sep 27, 1909	09-45	39.3/89.5	5.4	VII

MAR 31, 1911	16-57	34.0/91.8	4.2	VII
JAN 02, 1912	16-21	42.3/89.0	4.7	VI
DEC 07, 1915	18-40	36.0/90.0	4.6	VI
APR 09, 1917	20-52	37.0/90.0	5.0	VII
OCT 04, 1918	09-21	35.0/91.1	4.4	IV-V
OCT 16, 1918	02-15	36.0/90.0	4.6	V
MAY 25, 1919	09-45	38.3/87.5	4.4	V
MAY 01, 1920	15-15	38.0/89.6	4.1	V
MAR 14, 1921	12-15	40.0/88.0	4.5	VI
MAR 22, 1922	22-30	37.4/89.4	4.2	VII
MAR 23, 1923	04-30	37.4/89.4	4.5	VI-VII
NOV 27, 1922	03-31	37.4/88.2	4.1	VII
OCT 28, 1923	17-10	35.3/90.0	3.9	V
JAN 01, 1924	03-05	36.0/90.0	4.5	VI
APR 02, 1924	11-15	37.0/88.8	4.0	V
JUN 07, 1924	05-42	36.5/89.8	3.9	V
APR 27, 1925	04-05	38.0/88.2	5.0	VII
SEP 02, 1925	11-55	37.9/87.2	4.7	VI
SEP 20, 1925	09	37.9/87.2	3.9	IV
MAY 07, 1927	08-28	36.0/90.2	4.7	VI

---

* Maximum MM intensity refers to the maximum intensity documented during this study

\# Data presented for these earthquakes are those of Nuttli (1979)

@ Data presented for these earthquakes are those of Street (1981)

Note: Parentheses are used to indicate parameters that are not well defined

Seismic Monitoring of the Shumagin Seismic Gap, Alaska

USGS-14-08-0001-21919

John Taber and Klaus Jacob
Lamont-Doherty Geological Observatory of Columbia University
Palisades, New York 10964
(914) 359-2900

Investigations

Seismic data from the Shumagin seismic network were processed to obtain origin times, hypocenters, and magnitudes for local and regional events. The processing resulted in files of hypocenter solutions and phase data, and archive tapes of digital data. These files are used for the analysis of possible earthquake precursors, seismic hazard evaluation, and studies of regional tectonics and volcanicity.

Results

The seismicity of the Shumagin Islands region from January 1 to June 30, 1984 is shown in map view in Figure 1 and in cross section in Figure 2. The overall pattern over this time period is similar to the long-term seismicity, though the time period is too short to permit the delineation of the double-planed seismic zone. The highest concentration of events occurs at the base of the shallow thrust zone with the thrust zone itself poorly defined. West of the Shumagins the seismicity is more diffuse and extends closer to the trench.

The yearly servicing of the network was successfully completed in July 1984. The network is capable of digitally recording and locating events as small as M_l=0.9 with uniform coverage at the 2.0 level. Onscale recording is possible to at least Ml=5.0 on a telemetered 3-component force-balance accelerometer. Larger events are recorded on photographic film by 10 strong-motion accelerometers.

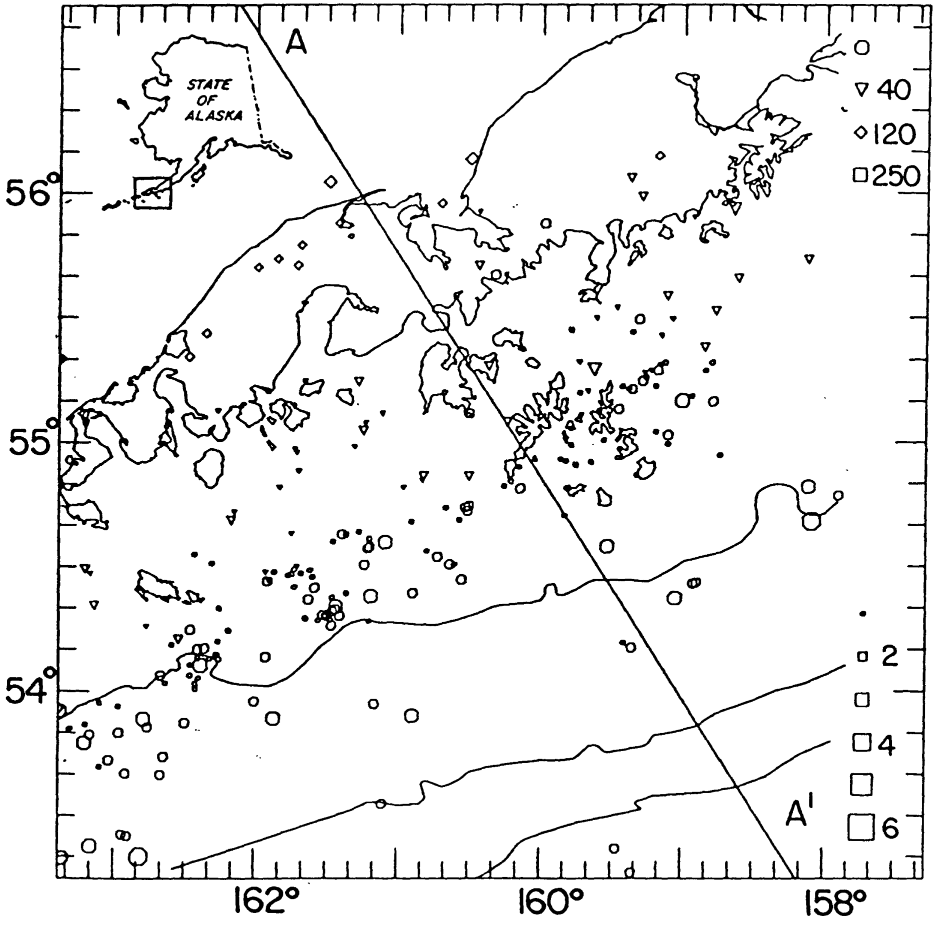

Figure 1. Seismicity recorded by the Shumagin Island seismic network from January 1 to June 30, 1984. Depth (km) is shown by symbol type (upper right corner) and magnitude by symbol size (lower right corner).

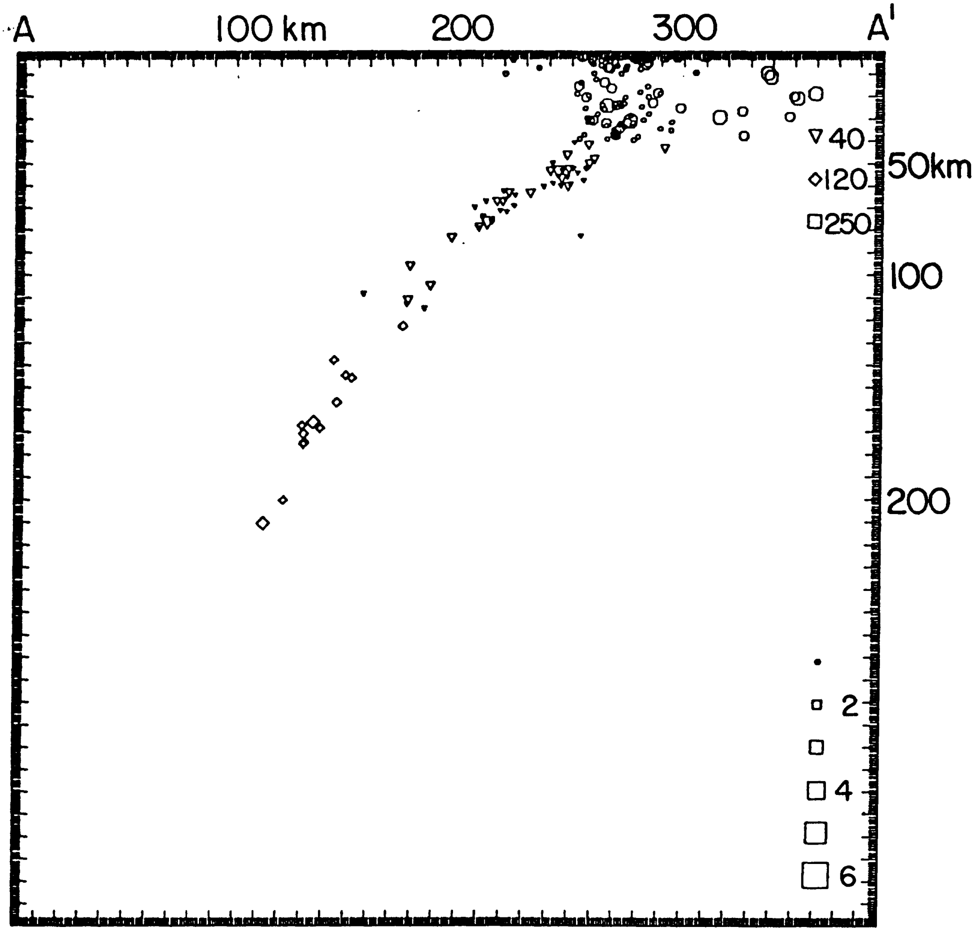

Figure 2. Cross section of seismicity projected along the line A-A' in Figure 1. Symbols are the same as in Figure 1.

Earthquake Hazard Research in the Greater Los Angeles Basin and Its Offshore Area

#14-08-0001-21858

Ta-liang Teng
Thomas L. Henyey
Egill Hauksson
Center for Earth Sciences
University of Southern California
Los Angeles, CA 90089-0741
(213) 743-6124

INVESTIGATIONS

(1) Upgrade recording of the seismic network data from analog to digital using a dedicated PDP 11/34 computer. Write software to carry out the data analysis using a VAX 11/750 computer that runs under the VMS (version 3.2) operating system.

(2) Monitor earthquake activity in the Los Angeles Basin and the adjacent offshore area.

(3) Seismotectonic analysis of recent earthquakes (1970-1984) along the Newport-Inglewood fault zone.

RESULTS

(1) Since early March 1984, the USC Los Angeles Basin seismic network has been digitally recorded by our PDP 11/34 computer. All the necessary software and significant remote support was made available by R. Bookbinder of Lamont-Doherty Geological Observatory of Columbia University in New York. Currently the computer records both the L.A. Basin and the Dos Cuadras oilfield (Santa Barbara) networks that consist of 19 USC stations and 16 USGS/CIT seismic stations. During April 20-24, 1984 a large swarm of at least 400 recorded microearthquakes occurred within the Dos Cuadras network. Approximately 90% of the earthquakes that were recorded by the continuously recording data acquisition system were also recorded digitally by the PDP 11/34 computer.

Beginning July 1, 1984 all local earthquakes recorded by the PDP 11/34 computer are routinely located. Since we still operate our analog data acquisition system in a continuous mode, any small earthquakes not detected by the PDP 11/34 are played back using analog strip-chart recorders.

The seismic data are analyzed using our VAX 11/750 computer. We have written a computer program that is similar to ping.c developed by seismologists at University of Washington to interactively pick P- and S-arrival times, amplitude, period and coda duration. The earthquake hypocenters are calculated using the latest version of HYPOINVERSE, Klein (1984).

(2) The earthquake activity that occurred in the Los Angeles Basin and the adjacent offshore area during 1983 and the first six months of 1984, is shown in Figures 1 and 2. The seismicity rate during this time period is similar to what was reported during the previous three years. The earthquake activity is dominated by single shocks that are scattered throughout the Los Angeles Basin. In 1983 the most noticeable activity consists of several events of

magnitude 3-3.5 that occurred in the northwestern part of the Los Angeles Basin. The largest earthquake that occurred during the first half of 1984 within the Los Angeles Basin (M=3.9) was located at 33°N 28.28' and 118°W 4.62' at a depth of approximately 14 km. The focal mechanism determined from first motions of P-wave arrivals indicates right-lateral strike-slip motion (Figure 3).

(3) We are analyzing earthquake data recorded by USC and USGS/CIT during the last ten years in the Los Angeles Basin. Forty earthquakes in the magnitude range from 2.5 to 4.0 have been relocated and special effort has been made to recheck available USC seismic records to add as many S-arrivals as possible for accurate depth determination. The first motions have been utilized to construct single event focal mechanisms. The results so far reveal that the deepest earthquakes that occur along the Newport-Inglewood fault zone have depths to 16 km. Second, most of the focal mechanisms show either almost pure right-lateral strike-slip or almost pure thrust with a small component of right-lateral strike-slip.

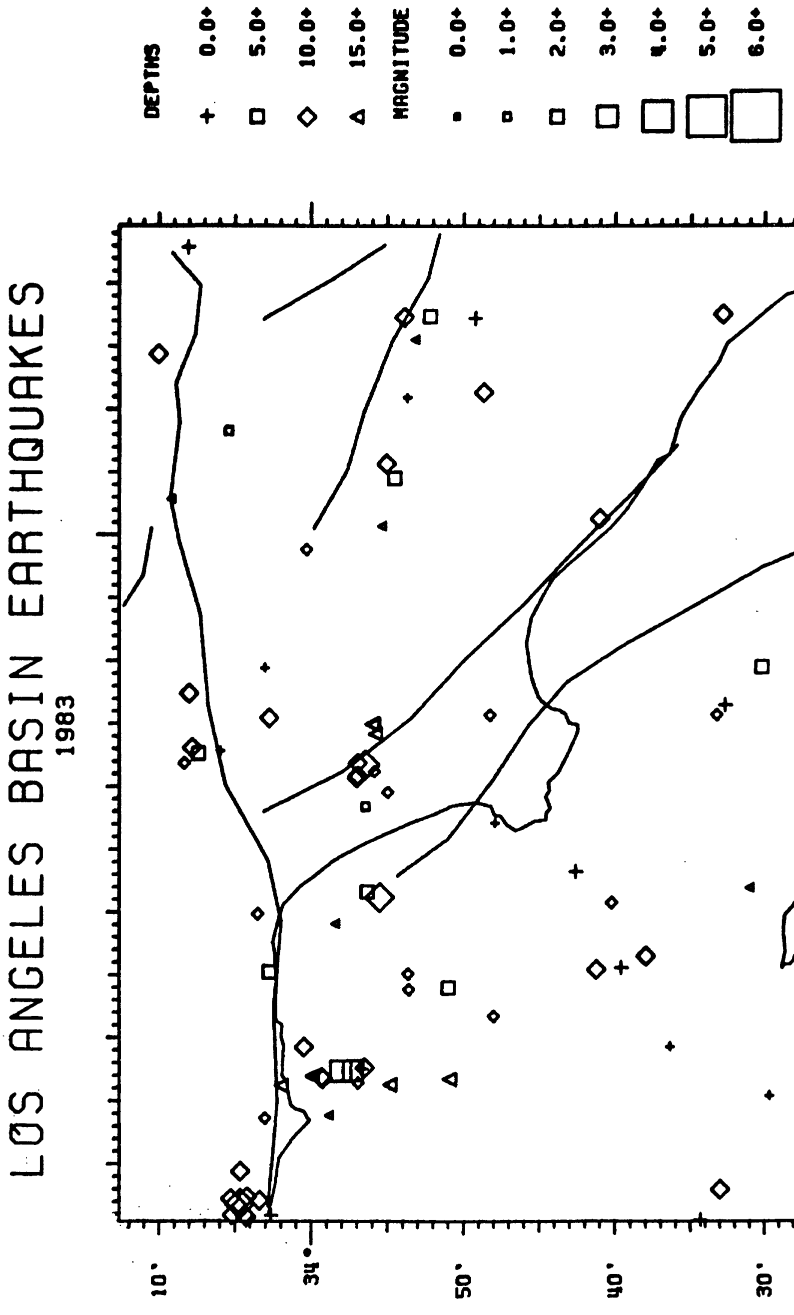
LOS ANGELES BASIN EARTHQUAKES
1983
DEPTHS
0.0+
5.0+
10.0+
15.0+
MAGNITUDE
0.0+
1.0+
2.0+
3.0+
4.0+
5.0+
6.0+
20 KM
10'
34°
50'
40'
30'
50'
40'
30'
20'
10'
118°
50'
40'

FIGURE 1

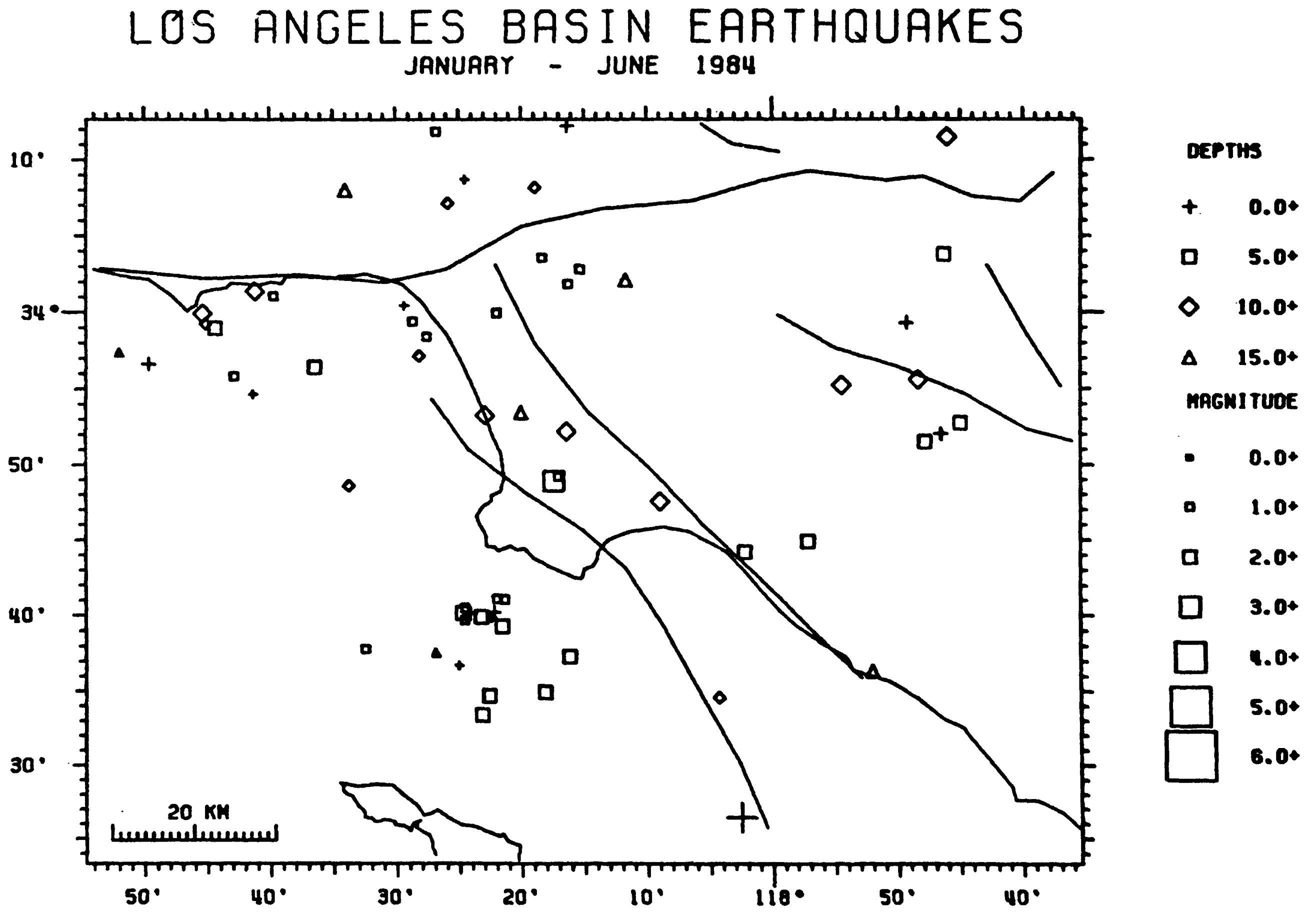
LØS ANGELES BASIN EARTHQUAKES
JANUARY - JUNE 1984
DEPTHS
+ 0.0+
□ 5.0+
◇ 10.0+
△ 15.0+
MAGNITUDE
0.0+
1.0+
2.0+
3.0+
4.0+
5.0+
6.0+
10'
34°
50'
40'
30'
50'
40'
30'
20'
10'
118°
50'
40'
20 KM

FIGURE 2

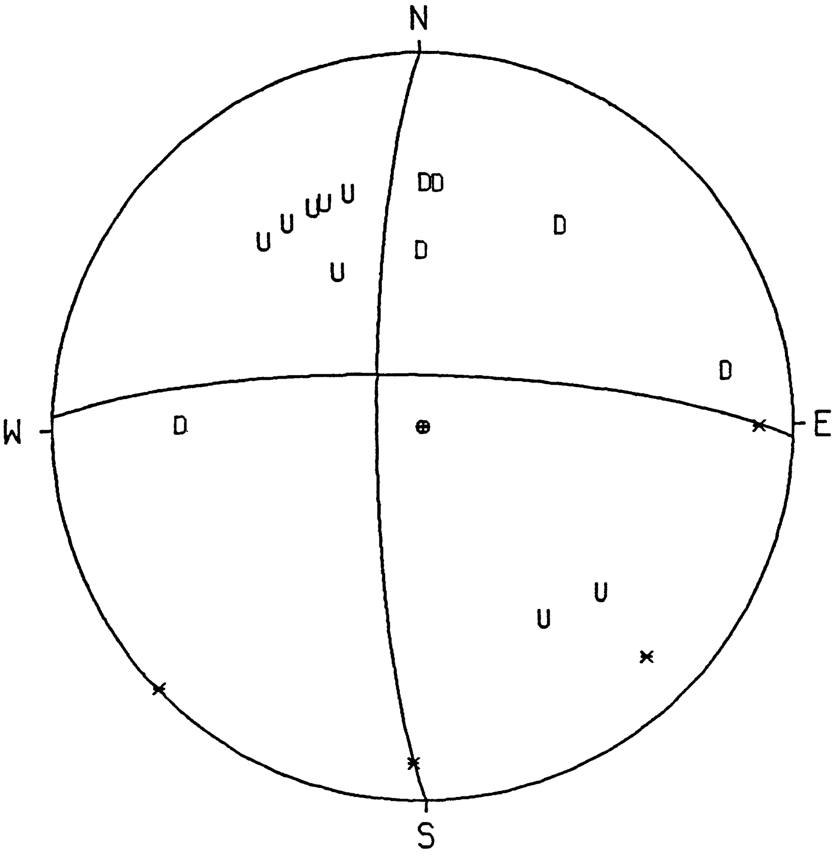

Figure 3. Focal mechanism of the San Pedro Earthquake of February 27, 1984. This is a lower hemisphere projection where U indicates compression and D indicates dilatation. Below the azimuths and dips of the two nodal planes are shown.

AZ1=180.0 DIP1= 80.0 AZ2=272.0 DIP2= 78.8

Palæoseismic studies using subsurface radar profiling.

USGS 14-08-0001-21926

Roger Bilham & Leonardo Seeber
Lamont Doherty Geological Observatory,
Palisades, New York, 10964
(914) 359-2900

Investigations

1. A large number of strike slip and normal faults were profiled using a commercial impulse radar system with an effective depth penetration of the order of 10m. The excavation of faults to obtain estimates of earthquake recurrence times is expensive and not always successful. Radar profiling is perceived to be a possible method for examining subsurface structure prior to excavation and for spatially extending trench-derived information. The surveys were conducted to examine the potential usefulness of radar profiling in different climatic conditions and in different soil types.

Results

1. Features associated with the Wasatch, Hebgen Lake, Borah Peak, Fairview Peak, Owens Valley, Concord, San Andreas and San Gabriel faults were investigated and additional studies were undertaken on the Macgregor and Ramapo Faults in N.Y. and at Mammoth Lakes and Coalinga in California. In cases where there exist stratigraphic layers possessing contrasting electromagnetic velocities in the upper 3m it was possible to locate palæoseismic features related to recent fault activity. However, a near-absence of dielectric layering was found to be typical of the coarse colluvium covering faulted range fronts in arid regions of Nevada, Utah and California. Notable successes of radar imaging were the detection of colluvial wedges associated with former movements of the Lost River Fault, Idaho and the identification of wide zones of fracturing on strands of the San Andreas fault system at Point Reyes, Hollister and the Salton Sea.

2. Fresh surface water was found to not significantly affect subsurface imagery. Successful profiles were obtained by floating the antenna across the surface of sagponds or fault crossing rivers. However, moistened salty soil was found to be opaque to radar. Reflections were obtained at 80Mhz

and 120Mhz from trees and tall bushes which limited activities occasionally to the use of an electrically screened 300MHz antenna. The 80MHz antenna was successfully used along roads in the Mammoth Lakes region to profile the 1-6m depth of the lava beneath gravel deposits at speeds of up to 40mph.

Reflections from buried and overhead cables are easily eliminated from the radar imagery particularly if they cross the profile at right angles but abrupt lateral changes in soil moisture (e.g. caused by irrigation or patches of impermeable cover) were found to distort subsurface imagery in an unpredictable manner. An attempt to map clay layer thickness near Coalinga was unsuccessful due to the dominating effects on travel time of soil moisture heterogeneity induced by intensive irrigation. Profiles in cities (Hollister and Concord) were not successful due to numerous reflections from water sprinkler systems, underground pipes, reinforcing bars and passing vehicles. Our results indicate that palæoseismic radar investigations can be used to examine the upper 1-3m in most soil types and climatic conditions but that certain easily identifiable environments should be avoided.

3. Approximately 80% of the 200 radar profiles obtained show palæoseismic features but the resolution (6-30cm) is inadequate to map the subsurface in detail. Impulse antennas with reduced beam divergence may soon be available that may improve the resolution of subsurface radar imagery especially if used in conjunction with methods to determine subsurface velocity structure. Our results indicate that radar profiling can provide useful subsurface structural information especially in those locations where polymodal sedimentation is likely to be important in subsequent trench investigations.

Reports

Bilham, R., W. Black and P. Williams Subsurface Radar Imagery of the San Andreas Fault, *EOS. Trans Amer Geophys. Un*, **64**, 18

Bilham, R. Impulse Radar Studies of the Borah Peak Earthquake, Idaho, *USGS Open File Report*, in the press 1984.

STUDY OF BROADBAND REGIONAL GROUND MOTIONS

14-08-0001-21897

Bruce A. Bolt
Seismographic Station
University of California
Berkeley, California 94720
(415) 642-7030

Project Plan

The project is to develop broadband recording at stations operated by the University of California, Berkeley, and carry out related analysis of seismic waves from strong regional earthquakes. Digital seismographs are being operated at the Berkeley and Jamestown stations which record the earthquake signals over a wide frequency band as digital samples on magnetic tape. The appropriate computer graphics, algorithms, and interactive methods of analysis of waveforms, spectra, location, seismic moment, and so on, are being constructed in order to relate the broadband recordings to earthquake risk problems. New methods of access and distribution to seismologists generally are being established. Work has begun to test how such enhanced recordings of seismic waves are crucial for high resolution of earthquake source properties and their temporal variation for more realistic prediction of strong ground motions.

Broadband Data Acquisition

Two three-component digital broadband stations (Berkeley and Jamestown) are telemetering continuously 16-bit digital data to Berkeley for archiving and analysis. The bandwidth of the digital data is 0-25 Hz for Berkeley and 0-10 Hz for Jamestown. The vertical-component broadband station at Whiskeytown Dam currently records analog only, with a bandwidth of 0-10 Hz. Hardware and software are being installed to facilitate archiving of all broadband data into a common format on a MODCOMP minicomputer and into a data base structure on an IBM-XT microcomputer. Such use of microprocessors has been discussed by Bolt (1983) and Husebye and Thoresen (1984). In addition TECMAR Lab Master hardware was installed in the IBM-XT with the capability of reading serial and parallel data (16 bit) and performing analog to digital conversion with 96 db (16 bit) resolution. This hardware will expedite the acquisition of high-resolution digital data from broadband seismographs (such as Whiskeytown) which do not yet record digitally.

Analysis

Analysis of the broadband regional ground motions has concentrated on four problems during the past six months.

1. Extensive spectral analysis of signal and noise samples has been made in order to determine the background noise characteristics and the minimum-sized earthquake which can be recorded at a given

distance with an acceptable signal-to-noise ratio. The principal result is that the magnitude threshold for a 20 db signal-to-noise ratio varies from M_L 2.5 at 10 km to M_L 5.5 at 400 km.

2. Seismic moments of moderate earthquakes have been estimated from the area of displacement pulses and from the asymptotic low-frequency spectral level. For instance, the P-wave displacement pulse recorded at Berkeley is $\Omega_o(P) = 0.31$ cm-sec for the M_L 6.6 earthquake which occurred off the coast of northern California on 10 September 1984. The corresponding seismic moment is 1.6×10^{26} dyne-cm. A further example of estimating seismic moment from broadband records is given by Uhrhammer and Darragh (1984) for the 24 April 1984 Halls Valley earthquake.

3. Regionally recorded crustal S phases are being analyzed to determine the wave propagation characteristics of the lower crust (Sibson, 1982). About 15 well-recorded S phases from regional earthquakes were available from magnetic tape storage. The data set samples epicentral distances from 7 km to 108 km and the ray paths sample the whole range of depths in the crust. The work bears on the important question of threshold focal depths in the light of Sibson's hypothesis.

4. Pattern recognition techniques to estimate earthquake parameters are being investigated and convolution operators have been shown to be effective in selection of prototype earthquakes from the comparison dictionary.

Computer Algorithms

Several computer algorithms have been developed and are being tested for the processing, archiving, and analysis of broadband digital records. These include:

1. Processing of Berkeley and Jamestown digital data in a common format on a MODCOMP minicomputer.

2. Transmission of digital data from the MODCOMPT minicomputer to an IBM-XT microcomputer.

3. Processing programs on an IBM-XT for spectral analysis, filtering, F-K analysis, deconvolution of instrument response, etc.

4. A relational data base for archiving the digital records on an IBM-XT.

References

Bolt, B.A., Seismology in the Digital Age, 1983 Assembly IASPEI, IUGG Chronicle (in the press), 1984.

Husebye, E. S., and E. Thoresen, Personal Seismometry Now, EOS, 65, 29, pp. 441-442, 1984.

Sibson, R. H., Fault zone models, heat flow, and the depth distribution of earthquakes in the continental crust of the United States, Bull. Seism. Soc. Am., 72, 151-163, 1982.

Uhrhammer, R. A., and R. B. Darragh, The 1984 Halls Valley ("Morgan Hill") earthquake sequence: April 24 through June 30, in the 1984 Morgan Hill, California earthquake, California Division of Mines and Geology, Special Publication 68, in press, 1984.

NORTHERN SAN ANDREAS FAULT SYSTEM

9910-03831

Robert D. Brown
Branch of Engineering Seismology and Geology
345 Middlefield Road, MS 977
Menlo Park, California 94025
(415) 323-8111, ext. 2461

Investigations

Historic seismicity between Monterey Bay and the Gorda Escarpment is scattered through a 60 km-wide belt that includes the Coast Ranges and extends a few kilometers offshore. To better understand the geometry of currently active faults and the distribution of severe earthquake hazards I am evaluating geophysical and geological evidence that help define modern and ancient members of the San Andreas fault system. This evidence includes:

1. Seismically active regions or belts, known from historic seismicity
2. Currently active faults, known from geomorphic, geologic, or seismic evidence
3. The structure and extent of mappable geologic units exposed at the surface.
4. The structure and extent of subsurface geologic units, as interpreted from geologic and geophysical data.

Results

Although the great San Francisco earthquake of 1906 was on the main San Andreas fault, most other northern California earthquakes of damaging magnitudes (Toppozada and others, 1981; Toppozada and Parke, 1982) and most smaller earthquakes located by modern seismic networks have been further east, chiefly along the trend defined by the southern Calaveras, Hayward, Rodgers Creek, and Maacama faults.

This trend and the San Andreas fault south of Hollister follow a small circle centered at the North American-Pacific pole of rotation (49.02°N, 76.05°W; Minster and Jordan, 1978) and passing through the segment of maximum aseismic slip, or fault creep, on the San Andreas fault in Bitterwater Valley (Burford and Harsh, 1980). Aseismic slip characterizes the faults along the small circle arc from San Pablo Bay to Parkfield, a distance of 290 km.

Cumulative strike slip on these eastern fault trends is much less than on the main San Andreas. As shown by mapped sedimentary and volcanic rocks of Neogene age and by buried bodies of magnetic serpentimized ultramafic rock, observed displacements on the eastern faults can be satisfied by, at most, tens of kilometers of strike slip compared to more than 300 km for the main San Andreas. Fault-formed geomorphic features and strike continuity are also weaker on the eastern faults, which may signify that rates of Quaternary slip, as well, are low.

The disparity between geologic slip rates and historically observed seismicity and aseismic slip may indicate that 1) historic activity is typical -- large infrequent earthquakes on the main San Andreas fault occur against a background of frequent smaller, but still damaging, earthquakes along the eastern fault trend, 2) historic activity is atypical and a short term (hundreds of years) departure from normal patterns of movement, which are dominated by frequent activity on the San Andreas, or 3) activity along the eastern trend signals a shift in the location of the master shear in northern California from the main San Andreas fault to a fault trend 30 km further inland.

Although the evidence is insufficient to choose between these and other alternatives, accurate assessment of earthquake hazards and the design of a reliable predictive model depend on choosing the correct explanation.

References cited

1. Burford, R.O. and Harsh, P.W., 1980, Slip on the San Andreas fault in central California from alinement array surveys: Bulletin of the Seismological Society of America, v. 70, no. 4, p. 1233-1261.

2. Minster, J.B., and Jordan, T.H., 1978, Present day plate motions: Journal of Geophysical Research, v. 83, p. 5331-5354.

3. Toppozada, T.R., Real, C.L., and Parke, D.L., 1981, Preparation of isoseismal maps and summaries of reported effects for pre-1900 California earthquakes: California Division of Mines and Geology Open-File Report 81-11 SAC, 182 p.

4. Toppozada, T.R., and Parke, D.L., 1982, Areas damaged by California earthquakes, 1900-1949: California Division of Mines and Geology Open-File Report 82-17 SAC, 65 p.

Late Pleistocene and Holocene (?) Faulting beneath San Francisco Bay, California

14-08-0001-21917

Charlotte Brunner
Paleontology Department
University of California
Berkeley, CA 94720
(415) 642-7873

Objective: To investigate the extent, timing and sense of movement of probable faults beneath San Francisco Bay. Previous stratigraphic studies (Sloan, 1981; Laws, 1983) identified offset of late Pleistocene bay sediments in borehole samples along a transect between San Francisco and Alameda. This project continues the stratigraphic study of bay sediments along two additional transects across the Bay.

Investigations: In the first phase of the study, 85 tube samples from 6 boreholes along a transect between San Mateo and Hayward were analyzed to determine the late Pleistocene (Sangamon) stratigraphy. Biofacies were defined primarily on the basis of foraminifers, sand-size diatoms and seeds. Investigation of diatom biofacies is continuing.

Results: Preservation of calcareous microfossils was not as good as expected in the tube samples. Only 31% of the Sangamon sediments contained identifiable foraminifers. This level of preservation is insufficient to permit stratigraphic resolution detailed enough to confirm (or not) the presence of faulting offset at the San Mateo-Hayward transect. It is anticipated that analysis of diatom biofacies will provide better stratigraphic resolution, from which fault offset can be determined.

Foraminiferal biofacies confirm that Sangamon stratigraphy at the San Mateo-Hayward transect is the same as that at the Southern Crossing about 15 km to the north (Sloan, 1981). Sediments indicative of marsh to subtidal depositional environments are present and record the filling of the Bay during the Sangamon transgression.

NEOTECTONICS OF NEW ZEALAND: INSIGHT TO SAN ANDREAS FAULT SYSTEM TECTONIC BEHAVIOR

14-08-0001-21882

William B. Bull and Peter L. K. Knuepfer
Geosciences Department
University of Arizona
Tucson, Arizona 85721
Bull: 602-621-2219; Knuepfer: 602-621-6002

INVESTIGATIONS

Most studies of earth deformation involve historical seismicity and earth movements, or deal with the long time spans used by those who study relative motions of plates based largely on reversals of the earth's magnetic field. A more complete assessment of vertical and horizontal fault movements, either for scientific models or for hazards assessments, should include evaluations of variations of earth movements in the age range of 10^3-10^5 yr. Landforms such as uplifted marine terraces and displaced stream terraces provide one of the few bases for quantitative estimates of late Quaternary rate histories across major fault systems, such as the San Andreas shear system in California and the Alpine shear system in New Zealand.

The major right-lateral transcurrent faults of the Alpine shear system form a transpressive continental plate boundary between the Tonga-Hikurangi and Fiordland-Puysegur troughs. Our studies concern the Alpine fault and its splays in Marlborough (northeastern South Island). The Alpine shear system has a geometry that is quite similar to the San Andreas shear system in southern California and even in the San Francisco Bay region. Accordingly, an understanding of the temporal and spatial patterns of fault slip on the New Zealand faults studied by us and the associated regional deformational patterns can yield insight into the behavior of this complex plate boundary, and, by analogy, to the San Andreas fault system as well.

Our studies of the neotectonics of New Zealand during the last six months have continued to emphasize two primary concerns: (1) the amounts of uplift of marine terraces and of vertical and horizontal displacements of stream terraces, and (2) the development and/or improvement of methods to estimate the ages of late Quaternary geomorphic surfaces that have been subject to earth deformation.

RESULTS

Uplifted Marine Terraces

Our additional studies continue to show that the marine terraces of New Zealand are part of a population of global marine terraces. The terraces are difficult to date directly, particularly in the South Island, so the basis for dating is correlation of flights of New Zealand terraces with dated flights of uplifted coral reef terraces on New Guinea in the Pacific Ocean, Barbados in the Atlantic Ocean, and elsewhere. For each uniform uplift rate there is a unique number and altitudinal spacing of terraces within a given flight. Correlation of local flights of marine terraces with dated flights of global marine terraces is based on the altitudes of inner edges of shore platforms determined by surveys or estimated from topographic maps. These altitudinal data are used to construct several inferred uplift rate graphs for different age assignments -- generally, one graph reflects a uniform uplift style.

Beveled bedrock and rounded gravel directly above the active surf zone are regarded as being marine in origin by most workers. Montane terraces are more controversial, but appear to be common to altitudes of more than 2000 m in the Southern Alps. The highest parts of the Southern Alps are within 100 km of the present coastlines, and have been sites of marine processes during the late Quaternary. Three principal lines of evidence support the conclusion that marine-terrace remnants are ubiquitous throughout most of the Southern Alps: (1) the presence of exhumed shore platforms and degraded sea cliffs, especially along the crests of spur ridges; (2) widely scattered, but ubiquitous, rounded quartz pebbles on notched spur ridges and on flat-topped ridges and summits. These pebbles have abrasion textures and impact marks that are identical to quartz pebbles on the modern high energy beaches along the northwest coast of the South Island. And, lastly, (3) flights of as many as 19 of the youngest New Zealand marine-terrace remnants have altitudinal spacings that allow them to be correlated with the dated coral reef terraces on New Guinea in the age range of 30,000-336,000 yr.

Studies of uplifted marine terraces along 300 km of the northwestern flank of the Southern Alps show a systematic pattern of uplift rates and styles. The presence of beach pebbles was documented at 187 sites during the December 1983-March 1984 field season. Topographic map analyses reveal that uplift rates have been rapid and uniform during the last 130,000 yr. Inferred uplift rates reach a maximum of 8.2 mm/yr adjacent to the highest part of the Southern Alps and decrease to about 5.6 mm/yr to the northeast and southwest. Uplift rates during the 200,000 yr prior to 130,000 yr b.p. were much less, ranging from 2.6 mm/yr in the north to a maximum of 3.7 mm/yr in the area of highest metamorphic rock grade for materials that have been exposed to erosion by uplift along the Alpine fault. The time of change between these two periods of uniform uplift appears to be the same at five sites and is estimated to have occurred between 134,000 yr and 142,000 yr b.p. The abrupt increase in inferred uplift rates since about 136,000 yr b.p. is attributed to continuing long term increases in convergence betwen the Pacific and Australian plates.

Faulted Stream Terraces

Our additional studies on faulted post-glacial stream terraces have focused on improving our age-estimation techniques by analyzing soil and rock-weathering data collected during our 1983-84 field season and using these techniques to determine rates of slip across faults of the Alpine shear system. The terraces are difficult to date directly, since the high-energy rivers tend to remove datable materials from the gravelly river beds. We have used rates of rock weathering rind development and soil morphologic and chemical change to establish high-quality age-estimation techniques, building on previous studies by New Zealand and U.S. workers. Weathering rinds yield age estimates of Holocene stream terraces with a precision of 5%-20%. Soil chemical data show systematic changes in iron, aluminum, and total element chemistry with time in Holocene soils, and these are calibrated at dated chronosequences. Soil chemical and morphologic data yield age estimates of Holocene soils with a typical precision of 20%-30%.

These age estimation techniques have allowed us to determine latest Quaternary fault-slip rates at 20 sites distributed along the Alpine fault and its splays. We recognize a latest Quaternary right-lateral slip rate of 30-45 mm/yr across the main Alpine fault. Slip rates of 5-15 mm/yr are found across each of three main splays of the Alpine fault in the northeastern South Island, while the fourth — the Hope fault — has a latest Quaternary slip rate of 20-35 mm/yr.

The fault-slip data indicate a systematic decrease in late Holocene rates from early-mid Holocene rates. The total early-mid Holocene fault slip across the Alpine shear system is 35-70 mm/yr, but the rate is only 15-30 mm/yr during the last 3000 yr. This decrease in Holocene fault-slip rates occurred on each of the faults, so it must indicate some regional shift in rates of fault slip of the plate boundary.

Applicability to San Andreas

The techniques we have established for estimating ages of tectonically-affected landforms have wide potential application to the San Andreas system. The use of global marine terrace chronologies has already been used successfully by other workers to obtain uplift rates along portions of the California coast. Our experience in New Zealand suggests that uplift rates should vary spatially in response to proximity to zones of tectonic transition, such as the Mendocino triple junction, and that they may vary temporally in response to changing rates of plate convergence. Relative-absolute dating techniques should be particularly useful in regions of grossly constant lithology, such as the coastal belt Franciscan. Although the soils and weathering-rind techniques must be recalibrated in specific study regions, the general approach should be applicable in California. Our experience in New Zealand suggests that variations in lateral fault-slip rates may be apparent over time intervals of a few thousand years. Sharp recognized such a change on the San Jacinto fault, but similar changes are not documented on the San Andreas fault or other major strike-slip faults in California. Nonetheless, the similarity in tectonic setting and style between the Alpine and San Andreas shear systems is suggestive that tectonic behavior should be similar for the two regions, and that time-dependent changes in lateral slip and uplift can be expected for the San Andreas system.

Comparative Earthquake and Tsunami Potential for Zones in the Circum-Pacific Region

9600-98700

George L. Choy
Stuart P. Nishenko
William Spence
Branch of Global Seismology and Geomagnetism
Denver Federal Center, MS 967
Denver, Colorado 80225
(303) 236-1506

Investigations

1. Prepare detailed maps and text of comparative earthquake potential for the west coasts of Mexico, Central America, and South America.

2. Conduct survey of video-image processing systems to determine optimal system for digitization of historic seismograms.

3. Conduct investigations of the rupture processes of large earthquakes that have produced tsunamis. The faulting parameters of these earthquakes to be compared with parameters determined for other tsunami-producing earthquakes. Study of tectonic mechanisms in subduction zones to be used to assess the likelihood of major earthquakes in these zones.

Results

1. A study of comparative earthquake potential is complete for the west coasts of Chile and southern Peru. A paper describing the results is in press with the Journal of Geophysical Research. It is found that the Valparaiso region of central Chile has a relatively high potential for large earthquake occurrence in the next 20 years. Southern Chile in the vicinity of the rupture zone of the 1960 earthquake has the lowest potential. The potential in northern Chile is apparently somewhat higher than for the south, but existing data provide poor constraints. Work on earthquake potential in Mexico is to be presented at meetings of the American and the Mexican Geophysical Unions. The Mexican subduction zone has been divided into 11 zones based on patterns of prior earthquake occurrence. Four of the segments have low probabilities (<30%) for earthquake recurrence. Five segments have conditional probabilities of greater than 30% for large earthquakes during the next 20 years.

2. The best candidate for this system is currently one which can produce a rasterized data set (a gridded set of data points).

3. We have detailed the rupture processes of three large earthquakes which have produced tsunamis. The Samoa Islands earthquake of 1 September 1981 which occurred at the extreme northern end of the Tonga trench ruptured two separate but offset faults. The Peru earthquake of 1974 was a shallow focus thrust event consisting of several small breaks. It is concluded that the maximum likely earthquake to occur in central Peru would be MS 8.4. The great Sumba earthquake of 1977 was the largest normal faulting earthquake to occur

since 1933. It is concluded that this earthquake and its aftershock series are the direct result of slab pull forces.

Reports

Choy, G. L., 1984, Broadband body-wave analysis of the complex rupture process of the Samoa earthquake of September 1, 1981; submitted to the J. Geophys. Res.

Nishenko, S. P., 1984, Seismic potential for large and great interplate earthquakes along the Chilean and southern Peruvian margins of South America: J. Geophys. Res. (in press).

Nishenko, S. P., and Singh, S. K., 1984, Conditional probabilities for the occurrence of large plate boundary earthquakes along the Mexican subduction zone: 1984-2004: to be presented at the 1984 Annual Meeting of the Mexican Geophysical Union and at the Annual Fall Meeting of the American Geophysical Union.

Spence, W., 1984, Slab pull and the 1977 Sumba earthquake: to be presented at the 1984 Annual Fall meeting of the American Geophysical Union.

Spence, W., 1984, The 1977 Sumba earthquake series: direct evidence for slab pull: submitted to the J. Geophys. Res.

Global Seismology

9920-03684

E. R. Engdahl
Branch of Global Seismology and Geomagnetism
U.S. Geological Survey
Denver Federal Center
Box 25046, Mail Stop 967
Denver, Colorado 80225
(303) 236-1506

Investigations

1. Depth Phases. Establish criteria for the proper identification of depth phases from sub-oceanic subduction-zone earthquakes.

2. Earthquake Location in Island Arcs. Develop practical methods for accurately locating earthquakes in island arcs.

3. Subduction Zone Structure. Develop techniques to invert for subduction zone structure using seismic travel times.

4. Global Synthesis. Synthesize recent observational results on the seismicity of the earth and analyze this seismicity in light of current models of global tectonic processes.

Results

1. Depth Phases. Broadband data recorded by the Grafenberg array were used to study the frequency dependance of depth phases from moderate-sized earthquakes in the central Aleutians. It was found that in the presence of a water layer the short-period band is usually dominated by pwP energy and the long-period band by pP and sP energy. A technical article is being prepared on these findings.

   Analysis of depth phases recorded both analog and digitally from a large set of moderate-sized central Aleutian earthquakes has been completed. Depths accurate to a few kilometers were determined for a large number of events by matching theoretical times of depth phases based on local structure to observed data. The new hypocenters provide a means to accurately locate the plate interface across the subduction zone. A journal article is in preparation.

2. Earthquake Location in Island Arcs. An extended data set of central Aleutian earthquakes, that includes events with well determined depths as previously described, has been relocated using the JHD approach. It is shown that by careful selection of observing stations, proper analysis of depth phases and the availability of local network calibration events, this approach can reduce hypocentral uncertainties to less than 15 kilometers over a broad region of the subduction zone. These results and their tectonic significance will be the subject of a paper to be prepared.

3. Subduction Zone Structure. A cooperative project with Dr. D. Gubbins at Cambridge University to jointly invert seismic travel times for hypocenters and for structure in the central Aleutian subduction zone has been undertaken.

4. Global Synthesis. A framework for this synthesis study has been developed.

Reports

Engdahl, E. R., Billington, S., and Dewey, J. W., 1984: Redefined spatial distribution of teleseismically recorded earthquakes in the central Aleutian Islands, abstract submitted to the Anchorage Seismological Society of America meeting.

Seismic Hazard Studies, Anchorage

9950-03643

A. F. Espinosa
Branch of Engineering Geology and Tectonics
U.S. Geological Survey
Box 25046, MS 966, Denver Federal Center
Denver, CO 80225
(303) 236-1597

Investigations

1. A damage evaluation for the City of Anchorage, sustained from the 1964 Alaskan earthquake, is being performed with damage data which have not been published previously. This information and local surficial geological data is planned to be used in order to evaluate transfer function amplification curves in Anchorage and to ascertain any existing correlation between damage and soil conditions in the area.

2. A "completeness" of the seismicity catalog is being investigated in order to use lower magnitude thresholds in (a) spatial and magnitude-temporal distribution of shallow ($h \leq 33$ km) and intermediate ($34 \leq h \leq 100$ km) seismicity ($M_s \geq 5.5$) occurring within a specified area in the period of time which uses (a) historical and (b) instrumentally recorded earthquakes. b-values are being determined likewise for the region under study. This effort is part of the seismicity study being carried out in this project for the Anchorage and vicinity region in Alaska.

3. A surficial geologic map of the southeastern part of Anchorage and vicinity is being drawn. Geologic field data is being collected and mapped.

4. Two geological cross-section maps for the City of Anchorage are being drawn.

5. A suite of seismicity maps and depth cross sections for the Anchorage and vicinity region in Alaska are being plotted.

Reports

Brockman, S. R., Espinosa, A. F., Michael, J. A., and Navarro, R., 1984, Near-field strong-motion data from nuclear explosive sources: U.S. Geological Survey Open-File Report 84- , 226 p.

Espinosa, A. F., 1984, Inconsistencies in the Modified Mercalli Intensity Scale: The El Asnam, Algeria, earthquake [abs.]: International Conference on Seismic Microzoning, Ech Cheliff, Algeria, October 10-12, 1984, Proceedings.

Mayer-Rosa, D., Lopez-Arroyo, A., and Espinosa, A. F., 1984, An analysis on available earthquake catalogues for hazard and microzonation studies in Algeria [abs.]: International Conference on Seismic Microzoning, Ech Cheliff, Algeria, October 10-12, 1984, Proceedings.

Schmoll, H. R., and Barnwell, W. W., 1984, East-west geologic cross section along the DeBarr Line, Anchorage, Alaska: U.S. Geological Survey Open-File Report 84-791.

Investigation of Seismic Wave Propagation for Determination of Crustal Structure

9950-01896

Samuel T. Harding
Branch of Engineering Geology and Tectonics
U.S. Geological Survey
Box 25046, MS 966, Denver Federal Center
Denver, CO 80225
(303) 236-1572

Investigations

1. Conducted high-resolution seismic reflection surveys
    a. N and T tunnels at the Nevada test site
    b. Lines across the Carpetbag and Yucca fault, Nevada test site
    c. Lines across the Beatty and Crater Flats fault scarps, Nevada
    d. Lines across a fault scarp at Taylorsville and Granger, Utah
    e. Continued to expand coverages near Beck Hot Springs, Utah.

2. Began processing New Madrid seismic reflection data

Results

1. a. The work in N and T tunnel shows a great number of reflectors. Considerable difficulty was encountered interpreting these data due to the difficulty of separating up and down going events. We have shown that this can be done, however. In the future, it may be necessary to pick an area with greater structure in order to differentiate between events occurring above the tunnel with those below the tunnel.
    b. The line across the Carpetbag fault shows quite a bit of structure. The processing of these data was difficult, due more to the existence of considerable scattered energy. We did not have trouble getting good coupling of the source energy into the ground. The data across the Yucca fault has not been processed at this time.
    c. The data across the Beatty and Crater Flats fault scarps is generally of poor quality. The reason for this is again the scattered energy. A fault can be seen on the Beatty fault scarp line on the migrated section. Migration was used as a signal enhancement tool in order to remove some of the scattered energy. More work on processing must be done. A definite change in structure at Crater Flats can be seen, but how this is associated with the fault scarp is not well understood.
    d. The data from Granger and Taylorsville Flats has not been processed at this time.
    e. Only preliminary processing and no interpretation has been conducted with the data from Beck Hot Springs, Utah.

2. We have run a brute stack on one New Madrid line. This line was processed to 7 s using an extended sweep technique. We see a traceable reflector at about 6 s. The rest of the data have been recorrelated to 11 s and we see coherent energy at about 10 s.

Report

Harmsen, S. C., and Harding, S. T., 1984, A comparison of three numerical techniques for modeling P-SV wave propagation across slanting interfaces: Colorado School of Mines Quarterly, v. 79, no. 2, p. 65-82.

Earthquake Hazard Research in the Central Mississippi Valley

14-08-0001-21886

Robert B. Herrmann
Department of Earth and Atmospheric Sciences
Saint Louis University
P.O. Box 8099 Laclede Station
St. Louis, MO 63156
(314) 658-3131

Goals

1. Perform research on the earthquake process in the New Madrid Seismic Zone to delineate the active tectonic processes. 2. Perform more general research relating to the problems of the eastern U. S. earthquake process and of the nature of eastern U. S. earthquakes compared to western U. S. earthquakes.

Investigations

1. The comparison of the m_{Lg} and M_L magnitude scales continues. Using California strong motion data, the Kanamori and Jennings (1978) M_L study is extended to included M_{Lg}. The vertical component strong motion data are passed through a WWSSN short period instrument while the horizontal components are passed through a Wood-Anderson. The magnitudes are determined from the synthesized seismograms according to normal convention. For large California earthquakes ($M_L > 5.2$),

$$m_{Lg} = 0.81M_L + 0.88$$

The relation between these magnitudes and seismic moment is not as well defined given the greater scatter in the data set. Expressing peak strong ground motion in terms of M_L or m_{Lg} may be a way of extrapolating the western U. S. strong motion data to the east.

2. Focal mechanisms have been determined for five earthquakes which occurred in January 1982. These earthquakes include the magnitude 5.7 and 5.1 New Brunswick earthquakes of January 9, the 5.4 magnitude New Brunswick earthquake of January 11, the 4.5 magnitude New Hampshire earthquake of January 19, and the 4.5 magnitude Arkansas earthquake of January 21. The moment-magnitude relation for the three New Brunswick earthquakes are

$$\log_{10}M_o = 1.87m_b + 13.66.$$

Combining these two regressions, assuming that the m_{Lg} and M_L interrelations will also apply in the east, we obtain

$$\log_{10}M_o = 1.51M_L + 15.30$$

which is similar to the California relation, except that according to

Bakun (1984), the California region works down to M_L=3, whereas the eastern U. S. relation only works down to M_L=4.5. Indirectly, this supports a different spectral scaling law for the eastern U. S.

Results

1. A Master's Thesie by B. Nguyen has been submitted. This thesis concerns the focal mechanisms of the five January, 1982 earthquakes.

2. Research results are listed in the papers given below.

3. Two volumes of a planned eight volume set entitled "Computer Programs in Seismology" have been completed. In these two volumes, a total of 27 computer programs are documented. The documentation consists of program description, program listing, sample input and output, and representative graphic output. The complete set will be finished in early 1985.

Reports

Chulick, J. A. and R. B. Herrmann (1984). The relationship between M_L and m_{Lg} using California strong-motion data, 56 th Annual Meeting, Eastern Section Seiamological Society of America, Saint Louis University, October 10 - 12.

Shin, T.-C. T. and R. B. Herrmann (1984). Source parameters and L_g attenuation of New Brunswick earthquakes, 56 th Annual Meeting, Eastern Section Seiamological Society of America, Saint Louis University, October 10 - 12.

Pleistocene Faulting in Coastal San Diego County

14-08-21898

Philip Kern

Dept. of Geological Sciences
San Diego State University
San Diego, California 92182
(619) 265-6443

Investigations

This study is part of a project to map the Pleistocene geology of coastal San Diego County. During the past half year field mapping of marine and nonmarine shorelines, associated sediments, and geologic structures has been carried out in the coastal zone of the Del Mar and Encinitas quadrangles. Field work also was completed in the La Jolla and Point Loma quadrangles, bringing to completion mapping of the faulted coastal area from south San Diego to north of Leucadia.

Results

Detailed mapping of deformed shorelines has revealed the presence of a much more extensive system of Pleistocene faults than was previously recognized in the area from San Diego to Leucadia. Very large numbers of closely-spaced, subparallel faults are oriented northeast-southwest across the through-going Rose Canyon fault. The apparent normal and strike-slip character of the secondary faults is consistent with their apparent origin in the initial phase of right-slip wrenching along the Rose Canyon zone. The geometric relationship between the through-going fault and its associates is that of known right-slip faults in nature, in model experiments, and as predicted by strain-ellipse analysis. Further, the apparently still-active Rose Canyon fault has cut and substantially displaced all the Pleistocene shorelines, including that of the 125,000-year-old Nestor terrace, while the secondary faults, representing the early phase of wrenching, cut only the older terraces (probably 500,000 years or more).

Reports and Publications

Kern, J. P., 1984a, Chronology, Paleoenvironments, and Tectonics of California Pleistocene shorelines, San Diego to Oceanside (poster session abstract). Pacific Section, A.A.P.G./S.E.P.M./S.E.G., Programs and Abstracts, p. 84-85.

Kern, J.P., 1984b, Anatomy and ontogeny of small-scale, right-slip wrenching: the Rose Canyon fault zone, San Diego, California (abstract). Pacific Section, A.A.P.G./S.E.P.M./S.E.G., Program and Abstracts, p. 85.

Postglacial uplift in northeastern United States
9510-03207

Carl Koteff
U.S. Geological Survey
National Center, MS928
Reston, VA 22092
703/860-6503 FTS 928-6503

INVESTIGATIONS

The postglacial uplift profile for the Connecticut River valley from Connecticut to northern Vermont and New Hampshire was refined and extended and now covers a total distance of over 245 km from south to north. Altitudes of the contact between topset and foreset beds in ice-marginal deltas constructed in former glacial lakes were obtained there as well as in the Merrimack River valley in Massachusetts and New Hampshire. The topset/foreset contacts are believed to represent the former water level with an accuracy of 1 m. Ice-marginal deltas were especially singled out because they provide a relative physical chronology of the northward growth of a glacial lake during ice retreat. The ice retreat is known to have been very systematic in this region for the time represented by the glacial lakes, from about 17,000 BP to about 14,000 BP. Thus, the profile derived from the delta altitudes is a time-transgressive depiction of about 3,000 years.

RESULTS

Plotted altitudes of topset/foreset contacts for 30 separate ice-marginal deltas that were constructed in the Connecticut Valley during the northward growth of glacial Lake Hitchcock show a profile of postglacial uplift that bears N20W. The profile is a very straight line; only four of the plotted altitudes depart from the projection by more than one meter, and the largest departure of these four is only two meters. The projected altitude of the water level of Lake Hitchcock at the threshold in the spillway at New Britain in central Connecticut is about 25 m, and the measured altitude of the topset/foreset contact in the northernmost ice-marginal delta at South Ryegate in northeastern Vermont is 244 m. The differential uplift is 219 m over a distance of 245.78 km along the N20W projection and shows a gradient of 0.89 m/km up to the northwest. This gradient is the steepest known for postglacial uplift in North America and is thought to represent the largest possible gradient.

Because the profile is so straight and because it represents a time transgression of 3,000 years, the concept of a considerable delay to uplift response during the early stages of deglaciation is confirmed. It is reasonable to extend this delay to include the beginning of deglaciation at about 19,000 years BP. Thus there appears to have been a 5,000-year period of ice unloading before upward crustal movement. Also, the N20W projection of the profile points directly towards Hudson Bay, which strongly suggests that that region was the locus of crustal depression and hence the locus of thickest ice. This conflicts with current ideas of Canadian workers on the nature and location of ice centers for the late Wisconsinan ice sheet.

REPORTS

Koteff, Carl, Stone, B. D., and Caldwell, D. W., 1984, Glacial lake history of the Merrimack Valley, southern New Hampshire, in New England Intercollegiate Geologic Conference, 76th Annual Meeting, Guidebook for field trips in the coastal lowlands, Boston, Massachusetts to Kennebunk, Maine, p. 381-393.

Determining Landslide Ages and Recurrence Intervals

9950-03789

Richard F. Madole
Branch of Engineering Geology and Tectonics
U.S. Geological Survey
Box 25046, MS 966, Denver Federal Center
Denver, CO 80225
(303) 236-1617

Investigations

Fieldwork in 1984 focused primarily on large, recent landslides on the west flank of the Wasatch Plateau. The Manti and Twin Lakes slides, Sanpete County, were discovered to contain abundant exposures in which to develop methods for dating landslides that would be applicable to other areas.

Results

Materials suitable for ^{14}C-age determinations and amino-acid dating of landslide deposits are relatively common in the areas studied. The materials most useful for determining landslide recurrence intervals are found in translocated pond deposits and presssure ridges.

Translocated pond deposits have been moved laterally downslope by flow or slide from the sites where they accumulated, and they are now high, dry, and exposed for study. On some slides, there has been a tendency for pond-forming depressions to remain in relatively the same position during successive landslide events; whereas the deposits that accumulated in these depressions after each landslide were translocated downslope. In such places, repetitive landslides may give rise to a series of spatially separate pond deposits. Translocated pond deposits, therefore, have the potential for recording the number of landslide events, as well as providing ^{14}C ages for dating the events.

Radiocarbon ages of soils buried by pressure ridges combined with data from the soils developed on the crests of the pressure ridges also provide a means for calculating landslide recurrence intervals. The buried soils provide ^{14}C ages that date the event that formed the pressure ridge and at the same time serve to calibrate relative-dating techniques based on properties of the surface soils.

Pressure ridges form within and along the margins of some landslides. Their form is similar to that of lateral moraines and end moraines of small valley glaciers. They are composed of material thrust or squeezed up from depth during a major episode of flow or sliding. Pressure ridges formed along the margins of a slide area tend to overlap and bury the adjacent land surface. Radiocarbon ages of organic material buried on these surfaces give maximum dates for the flow or slide events. Examination of the pressure ridge along the northeast margin of the Manti slide (Fleming and others, 1978) revealed that it is composed of segments of more than one age. Hence, lateral pressure ridges are also a source of information about the number of mass-movement events that have occurred in a given area.

Because unweathered material is brought to the surface of pressure ridges during their formation, the degree of soil development on the ridge crests can be used to assign ages to these deposits. Several soil properties appear to be age dependent, including depth of leaching, amount of organic matter (measured in g/cm^3 x soil thickness), horizon thickness, profile thickness, and complexity of horizon sequence. Soil study sites, however, must be selected with care. On older landslides (late Pleistocene), erosion has stripped much of the relict profiles on sloping sites, and on many slides, older soils exist on landslide blocks that remained intact during sliding. On landslide deposits of all ages, soil study sites must be limited to locations where unweathered material was brought to the surface by the mass-movement event being dated.

Soils considered to be of late Holocene age (0-5 ka) are 5-25 cm thick and have simple profiles composed of a sequence of A/C or A/AC/C horizons. Soils interpreted to be of early Holocene age (5-10 ka) are 5-25 cm thick and have profiles composed of a sequence of A/Bw/C horizons. Strongly oxidized B horizons, well-developed Bt horizons, and Cca horizons were observed in landslide deposits of Pleistocene age, but not in deposits considered to be Holocene. The soil parent materials in the areas studied were derived from the Flagstaff Limestone and North Horn Formation and are highly calcareous. Apparently, strongly oxidized B horizons do not form in these parent materials until leaching has removed the carbonate.

Most of the large landslide deposits in Manti Canyon appear to have formed during the latter part of late Pleistocene time (10-30 ka). Several landslides, however, including the Manti slide, have had recurring movement during Holocene time, although on a much smaller scale than in Pleistocene time. Information obtained by R. W. Fleming, R. L. Schuster, and R. B. Johnson (written commun., 1984) indicate that debris from the Manti and North slides began to accumulate on the floor of Manti Canyon about 20,000 B.P. Most of the debris apparently accumulated after the time of the Pinedale (late Wisconsin) glacial maximum, possibly during the intervals when the extent of large, perennial snowfields were being reduced on the Wasatch Plateau.

Weathering of clasts including pitting, etching, granular disintegration, decomposition, and rind formation are not useful relative-dating techniques in the area studied. Similarly, lichenometry does not show promise for dating geologically young deposits in this area. Morphological parameters, such as a progressive decrease in the slope angle of pressure-ridge sides with increased age, may be useful for dating landslide deposits. Morphological parameters, however, were not studied systematically during the 1984 field season.

References

Fleming, R. W., Schuster, R. L., Johnson, R. B., and Robinson, S. L., 1977, Recent movement of the Manti, Utah, landslide: Symposium on Engineering Geology and Soils Engineering, 15th Annual, Pocatello, Idaho, April 6-8, 1977, Proceedings, p. 161-178.

Data Processing, Golden

9950-02088

Robert B. Park
Branch of Engineering Geology and Tectonics
U.S. Geological Survey
Box 25046, MS 966, Denver Federal Center
Denver, CO 80225
(303) 236-1638

Investigations

The purpose of this project is to provide the day to day management and systems maintenance and development for the Golden Data Processing Center. The center supports Golden based Office of Earthquakes, Volcanoes, and Engineering investigators with a variety of computer services. The systems include a PDP 11/70, several PDP 11/03's and PDP 11/23's, a VAX/780 and two PDP 11/34's. Total memory is 6.4 mbytes and disk space will be approximately 2.2 G bytes. Peripherals include four plotters, eight mag-tape units, an analog tape unit, five line printers, 5 CRT terminals with graphics and a Summagraphic digitizing table. Dial-up is available on all the major systems and hardwire lines are available for user terminals on the upper floors of the building. Users may access any of the systems through a Gandalf terminal switch. Operating systems used are RSX11 (11/34's), Unix (11/70), RT11 (LSI's) and VMS (VAX).

The three major systems are shared by the Branch of Global Seismicity and Geomagnetism and the Branch of Engineering Geology and Tectonics.

Results

Computation performed is primarily related to the Global Seismology and Hazards programs; however, work is also done for the Induced Seismicity and Prediction programs as well as for DARPA, ACDA, MMS, U.S. Bureau of Reclamation, and AFTAC among others.

In Global Seismology and Geomagnetism, the data center is central to nearly every project. The monitoring and reporting of seismic events by the National Earthquake Information Service is 100 percent supported by the center. Their products are, of course, a primary data source for international seismic research and have implications for hazard assessment and prediction research as well as nuclear test ban treaties. Digital time series analysis of Global Digital Seismograph Network data is also 100 percent supported by the data center. This data is used to augment NEIS activities as well as for research into routine estimation of earthquake source parameters. The data center is also intimately related to the automatic detection of events recorded by telemetered U.S. stations and the cataloging of U.S. seismicity, both under development.

In Engineering Geology and Tectonics, the data center supports research in assessing seismic risk and the construction of national risk maps. It also provides capability for digitizing analog chart recordings and maps as well as analog tape. Also, most if not all of the research computing related to the hazards program are supported by the data center.

The data center also supports equipment for online digital monitoring of Nevada seismicity. Also it provides capability for processing seismic data recorded on field analog and digital cassette tape in various formats. Under development is a portable microprocessor based system to be used by the field investigations group to do preliminary analysis and editing of temporary local networks and the GOES Satellite Event Detect System. Recent acquisitions include the replacement of the PDP 11/40 used for analog input with a PDP 11/34, expansion of the Nevada Network 11/34 for collection of Western Slope data for the U.S. Bureau of Reclamation, a second Versatec plotter and a Tektronix 4014 graphic system.

Northeastern U.S. Seismicity and Tectonics

9510-02388
Nicholas M. Ratcliffe
U.S. Geological Survey, MS 925
Reston, Va. 22092
(703) 860-6406

Investigations

1. Vibroseis reflection profiling of Ramapo seismic zone in cooperation with Virginia Polytechnical Institute and State University

2. Geologic mapping along vibroseis routes

3. Two dimensional gravity modeling of data from vibroseis profiles of Newark Basin

Results

1. Collection of 40 miles of 12 and 24 fold, 5 sec. reflection data are planned for early November across the central parts of the Newark Basin, Hudson highlands of New Jersey and the Green Pond syncline in the vicinity of Wayne, New Jersey, to near Sparta, New Jersey.

2. Twenty nine miles of 48 fold vibroseis data across the Newark Basin in eastern Pennsylvania have been acquired from industry. At present these proprietary data may be used only in confidential internal reports for N.R.C.'s evaluation of seismicity.

3. Geologic mapping in Dutchess County, New York, along our vibroseis profile was completed this summer and fall. A complex system of previously unrecognized Paleozoic thrust faults and zones, Mesozoic normal faulting is present along the northern extension of the Ramapo fault system extending into the Lower Hudson River Valley.

4. Field study of the Mesozoic Flemington fault in New Jersey south of our southern vibroseis profile indicates that this north trending normal fault dips at shallow angles 25-30° east and underlies significant areas of the central part of the Newark Basin. If the principal compressive stress axis is located in the northeast quadrant as some fault plane solutions of Woodward Clyde and limited hydrofracture data suggest (Statton, Quittmeyer and Houlday, 1983), then the Flemington fault is one if not the largest Mesozoic fault in the Ramapo area that is suitably oriented for thrust reactivation. Further study of these features is planned.

5. Ken Kodama (Lehigh University) completed a preliminary two dimensional model of the gravity data collected in 1983 along our Ramapo No. 1 seismic line. These results fit well with the distribution of sediments and deep diabase interpreted to be present from the vibroseis data.

Basement Tectonic Framework Studies
Southern Sierra Nevada, California

9910-02191

Donald C. Ross
Branch of Engineering Seismology and Geology
U.S. Geological Survey
345 Middlefield Road, MS 977
Menlo Park, CA 94025
(415) 323-8111, ext. 2341

Investigations

1. Field studies of plutonic and metamorphic rocks west of the White Wolf-Breckenridge-Kern Canyon fault.

2. Revision of Professional Paper manuscript and illustrations on basement rock geology of the southernmost Sierra Nevada, California, following editing by Western Branch of Technical Reports.

3. Petrographic study of selected granitic rocks collected last field season for chemical analysis.

4. Update a compilation of locations of samples containing sillimanite and (or) andalusite in the southern Sierra Nevada.

5. Preparation for outside publication (Geology) of a manuscript entitled: "A mafic complex (batholithic root?) in the southernmost Sierra Nevada, California."

6. Petrographic study of thin sections of a suite of basement rocks of the Scodie Mountains Roadless area east of Isabella Lake (sections furnished to me by J. L. Harner and J. F. Seitz).

Results

1. Recent field studies (July, 1984) have delineated several mappable plutonic units in a previously little-studied area west of the White Wolf-Breckenridge-Kern Canyon that extends west to the east edge of the San Joaquin Valley. Preliminary results suggest the presence of a nested granitic suite, about 20 km across, that consists of three facies that become progressively more felsic toward the core of the suite. Mapping to the westernmost exposures of the Sierra Nevada batholith has also finally put a northern limit to the seemingly endless exposures of the tonalite of Bear Valley Springs.

2. Study of thin sections (the hand specimens were unfortunately discarded) from the Scodie Mountains Roadless area has enabled me to expand the area of exposure of the coarsely porphyritic granodiorite of Castle Rock and the darker granodiorite of Rabbit Island. These two units are grossly equivalent to parts of two rather loosely defined, but widely used, rock names in the southern Sierra Nevada (the Isabella Granodiorite and the Sacatar Quartz diorite of Miller and Webb, 1940). The thin sections also indicated evidence of rather large plutons of the fine-grained granite of Onyx, a widespread and distinctive granitic rock type in the area east of Isabella Lake. Study of these thin sections provided me with valuable help in planning traverses for the coming fall field season in this relatively inacessible area.

Reports

Ross, D. C. (in press), A mafic gneissic complex (batholithic root?) in the southernmost Sierra Nevada, California: Geology (Director's approval, August, 1984).

Earthquake Hazard of the Red River Fault and Related Faults Deduced from Geological Field Studies in Western Yunnan, P.R.C.

Contract No. 14-08-0001-21289

Kerry Sieh
California Institute of Technology
Division of Geological and Planetary Sciences
Pasadena, CA 91125
(818) 356-6115

Investigations

In the Spring of 1983, Ray Weldon and I went to Yunnan Province, China, to study the Red River and related faults. A summary of our accomplishments in the field appeared in a previous "Summaries...." volume.

Results

Since my previous summary (vol. XVIII, p. 79), we have received several radiocarbon analyses which indicate that at least 5 large slip events have occurred on the Red River fault in the past approximately 20,000 years. Based on a preliminary ^{14}C date, we also estimate a slip rate for the fault of about 3 mm/yr for the past 40,000 years.

Publications since previous report

Allen, C.R., Gillespie, A.R., Han Yuan, Sieh, K., Zhang Buchun and Zhu Chengnan, 1984, Study of the Quaternary activities of the Red River fault (I) -- General Survey of its contemporary activities and evidence of the active faulting: in Chinese with English abstract: Journal of Seismological Research, Yunnan People's Publishing House, Kunming, China, 7, no. 1, pp. 39-51.

Allen, C.R., Han Yuan, Sieh, K., Zhang Buchun, Gillespie, A.R. and Zhu Chengnan, 1984, Study of the Quaternary activities of the Red River fault (II) -- Its features of activity, slip rate and recurrence intervals of earthquakes in Chinese with English abstract: Journal of Seismological Research, Yunnan People's Publishing House, Kunming, China, 7, no. 2, pp. 171-186.

Allen, C.R., Gillespie, A.R., Han Yuan, Sieh, K., Zhang Buchun and Zhu Chengnan, 1984, "Red River and associated faults, Yunnan Province, China: Quaternary Geology, Slip Rate and Seismic Hazard": Geological Society of America Bulletin, vol. 95, pp. 686-700.

INTEGRATED STUDIES OF EARTHQUAKE POTENTIAL, PREDICTION, AND HAZARDS IN THE WASATCH FRONT URBAN CORRIDOR AND ADJACENT INTERMOUNTAIN SEISMIC BELT

14-08-0001-21856

R.B. SMITH, W. J. ARABASZ, J.C. PECHMANN, and W.D. RICHINS*
Department of Geology and Geophysics
University of Utah
Salt Lake City, Utah 84112
(801)581-6274

Investigations

1. New perspectives on Wasatch Front and Utah earthquake hazards.
2. Earthquake behavior in the Wasatch Front area: association with geologic structure, space-time occurrence, and stress state.
3. Study of an M_L 4.3 earthquake in the western Salt Lake Valley using digital seismic data.
4. Deformation rates across the Wasatch fault from seismicity, geodetic data and paleoslip.
5. Computer generated movies of space-time patterns of Utah earthquakes.
6. Borah Peak earthquake studies.
7. Studies of normal faults from seismic reflection data and source properties (see D. I. Doser and K. A. Smith's theses).

Results

1. The M 7.3, Borah Peak earthquake, one of the three largest events in the western U.S. in the last thirty years, has had a profound effect on our understanding of large-magnitude normal faulting earthquakes. The Borah Peak earthquake nucleated on an $\sim 50^o$ dipping planar fault at a depth of approximately 15 km near the base of the seismogenic layer and near the hypothetical shear stress maxima for a brittle/ductile model. Comparisons of the Borah Peak earthquake with the two other large Basin-Range earthquakes, the M 7.1, 1954 Dixie Valley, Nevada (Okaya and Thompson, 1984), and the M 7.5 1959 Hebgen Lake (Doser, 1984) earthquakes also show nucleation depths of ~ 15 km on 40^o to 60^o dipping planar faults. With respect to the potential for equivalent large earthquakes on the Wasatch Front, seismic reflection data show a variation of fault plane geometries with dips varying from 40^o to 65^o at depths of 4-6 km, while the surface

---

*G. Chen, D. I. Doser, P. Eddington, E. Kjartansson, L L. Leu, J. F. Peinado, K. Renggli, K. A. Smith, and B. Thorbjarnardottir also contributed to this project during the report period.

expressions in unconsolidated materials have steeper dips, $>75^{o}$. Large through-going planar faults, deeper than 6 km, have not yet been detected on the Wasatch fault. From the similarities in age and structural style of the Wasatch fault to the large, M7+ Basin-Range earthquakes, a hypothetical model for a large earthquake on the Wasatch Front suggests an 40^{o}-60^{o} west dipping fault nucleating at approximately 15 km depth--at locations beneath the populated urban corridor.

Individual segments of the Wasatch fault differ in background seismicity, degree of quiescence, and inferred fault geometry; properties similar to that of the Lost River fault zone. In the Borah Peak earthquake, the 34 km long segment that broke appeared to have had at least one Holocene event while adjacent segments have older slip events, greater than 30,000 years. Thus, we must also consider a plausible model in which an active Holocene segment may remain active for several slip cycles compared to adjacent quiescence segments. This suggests that the Ogden, Salt Lake and Provo segments (Schwartz and Coppersmith, 1984) are candidates for more detailed investigations.

A heretofore unidentified hazard that could be produced by a future large normal-faulting event on the Wasatch Front is that of flooding induced by asymmetric ground subsidence. From empirical measurements of ground deformation produced by the 1959 Hebgen Lake earthquake (a maximum credible event) we have calculated the effects of hypothetical faulting placed at arbitrary locations on the Wasatch fault. These calculation shows a maximum vertical displacement of ~ 5 m and an area of asymmetric eastward tilt of the ground surface that extends westward from fault ~ 20 km intersecting the Great Salt Lake. For two hypothetical locations; one in Bountiful and one in Salt Lake City (for the lake level at 4209 MSL, the 1984 peak run-off level) deformation induced flooding could inundate major urban areas, industrial centers and transportation links on the west sides of Bountiful and Salt Lake City. For a hypothetical event near Provo, Utah, with the Utah Lake level at 4494 feet (the 1984 peak run-off level) deformation-induced flooding would cover areas on the west and south of the city, including transportation links, extensive urban developments and farm areas. The effects of earthquake induced flooding must be considered in an appraisal of Wasatch Front earthquake hazards even for events in the range $6.5 > M > 7.5$.

2. On the basis of special earthquake studies in the southern Wasatch front area, neighboring parts of central Utah, and SE Idaho, background seismicity appears to be fundamentally controlled by variable mechanical behavior and internal structure of horizontal plates within the seismogenic upper crust(Arabasz, 1984a,b)--resulting from relict pre-Neogene thrust belt structure and/or Neogene extension. Diffuse epicentral patterns arise from the superposition of seismicity occurring within individual plates, and also perhaps from favorable conditions for block-interior rather than block-boundary microseismic slip. Seismicity gaps associated with the Wasatch fault zone on both local and regional scales have been re-examined by Arabasz (1984a). A significant decrease in rate of seismicity in the region of the Wasatch fault occurred during the 1960's, but statistical analysis indicates that the change may be explained by larger inter-event

times consistent with a Poisson process. A critical issue is whether north-central Utah has a long-term flux for small to moderate-size earthquakes that is different--and lower--than that for neighboring parts of the seismic belt. Regarding stress state, data summarized by Arabasz (1984a,b; see also last semi-annual rept.) indicate: (1) near-critical in situ stress differences (at 5 km depth) for frictional sliding near the southern Wasatch fault, (2) average ESE-WNW (102^o-282^o) orientation of minimum horizontal compressive stress along the main seismic belt south of lat. 40^oN, and (3) significant mixing of strike-slip and normal faulting from the southern Wasatch fault southward--suggestive that maximum horizontal compressive stress is close to the lithostat.

3. An earthquake of M_L 4.3 occurred on October 8, 1983, within a seismically active region of the western Salt Lake Valley. A well-constrained focal mechanism for this event indicates normal faulting on a north-northwest striking fault that dips either 68^o-80^o east or 10^o-22^o west. A time domain technique for measuring rupture duration (Frankel and Kanamori, 1983) was successfully applied to determine a source radius of 1.1-1.4 km. Combining this with a moment estimate of 1.3 x 10^{23} dyne-cm inferred from the moment-magnitude relation for Utah earthquakes (Doser and Smith, 1982) we calculate a stress drop of 21-43 bars.

All earthquakes with preliminary locations within 20 km of the M_L 4.3 mainshock during the time period January 1981 through November 1983 were relocated relative to the mainshock, using the master event technique. The most conspicuous feature of the seismicity in the area during the three years preceding the mainshock was a cluster of six events located 12 km northeast of the mainshock epicenter. Five of these 6 events have very similar waveforms. Cross correlation of bandpass-filtered seismograms for these events suggests that their hypocenters lie within about 200 m of each other. Analysis of waveform data for 9 aftershocks shows that some of events are tightly clustered as well. The breaking of a asperity or group of asperities during the earthquakes in the 'preshock' cluster may have released a locking point on a fault resulting in a transfer of stress to the location of the main shock. However, the location of the preshock cluster at a distance of several fault lengths from the mainshock epicenter weakens the case for a direct connection between this cluster and the M_L 4.3 earthquake. (See Pechmann and Thorbjarnardottir, 1984.)

4. Crustal deformation (horizontal components) inferred from contemporary seismicity and geodetic measurements was compared with Quaternary-Holocene slip rates on the Wasatch Front as a means of assessing possible areas of strain accumulation. Seismic moment rate tensors (magnitude and direction of maximum moment release) were calculated by a new method that diagonalizes the strain-rate tensor. Individual source areas were selected on the basis of homogeneous strain, similarities in fault plane solutions and similarities in Quaternary geology.

The northern Wasatch fault showed a 0.1 mm/yr deformation rate due to earthquakes while geodetic data from triangulation and trilateration inferred a rate of approximately 1.0 mm/yr. These rates compare to estimates of paleoslip of approximately 1 mm/yr. This result suggests that considerable strain release may be accommodated by aseismic slip. For the southern Wasatch Front, earthquake related slip accounted for ∿0.1 mm/yr compared with 0.4 mm/yr measured geodetically and 0.8 mm/yr from paleoslip. Hansel Valley had the greatest contemporary strain release of earthquakes of 1.5 mm/yr compared to relatively poor estimates of 0.3 mm/yr from paleoslip. No geodetic data are available in areas off the Wasatch fault. The Bear River Range and East Cache fault zone show considerably less deformation at 0.3 mm/yr from active seismicity and 0.2 mm/yr for paleoslip.

The average slip rate for the ISB in Utah was 0.5 mm/yr for active seismicity compared to 0.6 mm/yr paleoslip estimates--a suggestion of an overall strain balance for the 500 km length of the active seismic zones in Utah. From these results we infer that the current seismicity rate is generally representative of the Holocene deformation

5. To evaluate the spatial and temporal variations of seismicity in Utah, two computer generated movies prepared with the help of Einar Kjartansson. The movies cover: (1) pre-instrumental seismicity, 1850-1961, and (2) The recent and most accurate network coverage 1962-1983. Earthquake epicenters superimposed on a state map were plotted on a colored CRT where earthquake magnitudes were scaled by color and screen duration. Spatial trends, temporal progressions and relationships of seismic gaps to surrounding microseismicity will be examined with these movies. We thank the Stanford Exploration Laboratory for allowing the use of their computer facilities for generating the movies.

6. The Borah Peak, Idaho earthquake ($M_S = 7.3$) sequence was examined in detail using a 25 station regional network ($\Delta < 600$ km) and a dense temporary network ($\Delta < 50$ km) for the time period October 28, 1983 to August 22, 1984. No foreshock activity above magnitude 2.0 was detected. The main shock and first 3 weeks of aftershock activity define a 75 km x 15 km zone parallel to the surface rupture but displaced laterally to the southwest by 5 to 10 km. Seismicity does not appear to have migrated spatially during the first 3 weeks after the main shock. The location of the main shock is at the base of the seismogenic zone SW of the surface rupture suggesting unilateral rupture to the NW. Analysis of later aftershocks through August 22, 1984 shows an increase of activity 10 to 15 km north of the surface rupture including a magnitude 5.8 event on August 22, 1984. Fault plane solutions for the entire sequence indicate predominately normal faulting with varying components of strike slip.

The 1983 Borah Peak earthquake occurred in an area of Basin -Range style tectonics at the base of a block faulted mountain range and occurred in an area geologically considered to have the potential for a large magnitude earthquake. However, the event was not preceded by perceptible foreshock activity nor was it associated with regional seismicity trends. Crustal structure in the Borah Peak area appears to be transitional between the Basin-Range to the south and the northern Rocky Mountains. The regional pattern of historic seismicity shows a concentration of seismicity throughout central Idaho that is associated with the large area of hot springs and a possible northeast-trending boundary of an extinct caldera.

The northwest trending belt of seismicity associated with the Borah Peak earthquake is orthogonal to that of the central Idaho area suggesting a complex zone of stress interaction.

Regional fault plane solutions from historic earthquakes in central Idaho suggested northeast-southwest regional extension, the same as that inferred from the main shock fault plane solution. Borah Peak fault kinematics inferred from accurate hypocenters, and hypothesized crustal rheologies suggest that the earthquake occurred at a peak in the shear stress versus depth curve for a quartz rheology and a strain rate of 10^{-14} s^{-1}. Ninety percent of the aftershocks occurred above the maximum shear stress depth and it appears that the main shock nucleated near region of the hypothesized transition from brittle to quasiplastic flow.

Reports and Publications

Arabasz, W. J., 1984a, Earthquake behavior in the Wasatch Front area: Association with geologic structure, space-time recurrence, and stress state: Proceedings of USGS Workshop on "Evaluation of Regional Urban Earthquake Hazards and Risk in Utah," Salt Lake City, Utah, August 1984, 32 p.

Arabasz, W. J., 1984b, Geometry of seismically active faults and crustal deformation within the Basin and Range-Colorado Plateau transition in Utah: (preprint, Geological Society of America Special Paper; includes earthquake studies of southern Wasatch Front area supported by USGS contract research).

Bruhn, R. L. and Smith, R. B. 1983, Relation of Wasatch fault zone to ancient thrust belt structures: Implications for normal fault geometry and maximum expectable earthquake magnitude (abs.): EOS, Trans. Am. Geophys. Union, v. 64, p. 842.

Doser, D. I., 1984, Source parameters and faulting processes of the August 1959 Hebgen Lake, Montana earthquake sequence, Ph.D. dissertation, Univ. of Utah, Salt Lake City, 152 p.

Doser, D. I., 1984, The 1983 Borah Peak, Idaho and 1959 Hebgen Lake Montana, earthquakes: Models for normal fault earthquakes in the Intermountain seismic belt: Proceedings of USGS Workshop on "The Borah Peak Earthquake," Sun Valley, Idaho, October 1984.

Pechmann, J. C. and Thorbjarnardottir, B., 1984, Investigations of an M_L 4.3 earthquake in the western Salt Lake Valley using digital seismic data: Proceedings of USGS Workshop on "Evaluation of Regional and Urban Earthquake Hazards and Risk in Utah," Salt Lake City, Utah, August 1984, 27 p.

Richins, W. D. Smith, R. B., Langer, C. J., Zollweg, J. E., King, J. D., and Pechmann, J. C., 1984, The 1983 Borah Peak, Idaho earthquake: Relationship of aftershocks to the main shock, surface faulting, and regional tectonics: Proceedings of USGS Workshop On "The Borah Peak Earthquake," Sun Valley, Idaho, October 1984, 26 p.

Smith, K. A., 1984, Normal faulting in an extensional domain: Constraints from seismic reflection interpretation and modeling: M.S. thesis, Univ. of Utah, Salt Lake City, Utah.

Smith, K. A. and R. B. Smith, 1984, Normal faulting in an extensional domain: constraints from seismic reflection interpretation and modeling: Abstracts with Programs, 97th Ann. Meeting, Geol. Soc. America, p. 661.

Smith, R. B. and Bruhn, R. L., 1983, Extensional tectonics of the intraplate U.S. Cordillera: Inferences on structural style from reflection data, tectonics and rheologic models (abs): EOS, Trans. Am. Geophys. Union, v. 64, p. 844.

Smith, R. B. and Bruhn, R. L., 1984, Intraplate extensional tectonics of the western U.S. Cordillera: Inferences on structural style from seismic reflection data, regional tectonics, and thermal-mechanical models of brittle/ductile deformation: Jour. of Geophys. Res., v. 89, no. B7, p. 5733-5762.

Smith, R. B. and Richins, W. D., 1984, Seismicity and earthquake hazards of Utah and the Wasatch Front: Paradigm and paradox: Proceedings of USGS Workshop on "Evaluation of Regional and Urban Earthquake Hazards and Risk in Utah", Salt Lake City, Utah, August 1984, 35 p.

Smith, R. B., Eddington, P. K., and Leu, L. L., 1984, Strain rates in Utah from seismic moments, geodetic surveys and paleoslip (abs.): Proceedings of USGS Workshop on "Evaluation of Regional and Urban Earthquake Hazards and Risk in Utah", Salt Lake City, Utah, August 1984.

Smith, R. B., Richins, W. D., Doser, D. I., Pechmann, J. C., and Langer, C. J., 1984, The 1983, M_s 7.3 Borah Peak, Idaho, earthquake: A model for active crustal extension, Abstracts With Programs, 97th Ann. Meeting, Geol. Soc. America, p. 661.

Smith, R. B., Richins, W. D., Doser, D. I., Eddington, P. K., Leu, L. L., and Chen, G., 1984, The Borah Peak earthquake: Seismicity, faulting kinematics and tectonic mechanism: Proceedings of USGS Workshop on "The Borah Peak Earthquake," Sun Valley, Idaho, October 1984, 31 p.

Zollweg, J. E. and Richins, W. D., 1984, Later aftershocks of the 1983 Borah Peak, Idaho, earthquake and related activity in the Central Idaho seismic zone; Proceedings of USGS Workshop on "The Borah Peak Earthquake," Sun Valley, Idaho, October 1984, 11 p.

Seismicity and Tectonics

9920-01206

William Spence
Branch of Global Seismology and Geomagnetism
U.S. Geological Survey
Denver Federal Center, MS 967
Denver, Colorado 80225
(303) 236-1506

Investigations

Studies carried out under this project focus on detailed investigations of large earthquakes, aftershock series, tectonic problems,and earth structure. Studies in progress have the following objectives:

1. Provide tectonic setting for and analysis of the 1977 Sumba earthquake series (W. Spence).

2. Provide tectonic setting for and analysis of the 1974 Peru gap-filling earthquake (W. Spence, C. J. Langer, and J. N. Jordan).

3. Determine faulting parameters (strike, dip, slip) for aftershocks of the great (M_S 7.7) Colombia earthquake of December 1979 and infer rupture characteristics of the main shock (C. Mendoza).

4. Determine the maximum depth and degree of velocity anomaly beneath the Rio Grande Rift and Jemez Lineament by use of a 3-D, seismic ray-tracing methodology (W. Spence, R. S. Gross, and L. H. Jaksha).

Results

1. The great ($M_o = 4 \times 10^{28}$ dyne-cm), normal-faulting Sumba earthquake of 1977 occurred at the Java Trench, just west of the zone where the Australian continental lithosphere is in collision with the Java arc. Aftershocks of the Sumba earthquake have been relocated by the joint hypocenter method and occur in two zones: an east-west trending zone, mostly east of the main shock, and a triggered northwest- southeast-trending zone located about 180 km northwest of the main shock. Both sets of earthquakes are confined to the 40-km-thick brittle portion of the oceanic lithosphere. Focal mechanism data for the aftershocks in the main shock zone and in the triggered zone combined with study of the detailed tectonic setting support the conclusion that both the Sumba main shock and the triggered group of earthquakes occurred directly as a result of the slab pull. The main shock may be part of a continuing process of detachment of the subducted oceanic lithosphere from the Australian continental lithosphere, rather than being a simple plate-bending event.

2. The great 1974 Peru thrust earthquake (M_S 7.8, M_W 8.1) occurred in a documented seismic gap, between two earthquakes each with magnitude of about 8, occurring in 1940 and 1942. Additional major earthquakes occurred in this region in 1966 and in 1970; all but the 1970 shock represent thrust faulting. The stress release of the October 3, 1974 main shock and aftershocks occurred in a spatially and temporally irregular pattern. The

multiple-rupture main shock produced a tsunami with wave heights of 0.6 ft at Hawaii and which was observed, for example, at Truk Island and at Crescent City. The aftershock series essentially was ended with the occurrence of a M_S 7.1 aftershock on November 9, 1974.

3. Three large earthquakes, occurring in 1942, 1958, and 1979, have reruptured the zone of the single great Colombia-Ecuador earthquake (M_S 8.6, M_W 8.8) of January 31, 1906. The last of these (December 12, 1979; M_S 7.7) ruptured the northernmost part of the 1906 rupture. This thrust earthquake was followed by numerous aftershocks as large as magnitude 5.5. A joint hypocenter relocation of these aftershocks indicates that most of them occurred at or near the interface between the Nazca plate and the overriding South American Plate. Long-period Love- and Rayleigh-wave spectra in the 30-80 second band, as recorded by the Global Digital Seismograph Network, are being used to determine the fault parameters (strike, dip, and slip) at the corresponding source depths of many of these aftershocks. The procedure is to compare the observed spectra with a suite of theoretical source models until a best fit is obtained. The best fit is further constrained by taking ratios of the observed spectra to that of a standard, reference event. The latter procedure serves to remove perturbations of the observed spectra due to path effects. The final set of aftershock magnitudes, hypocenters, and faulting parameters will be used to infer the detailed rupture characteristics of the 1979 main shock and thus to provide insight into the nature of earthquake occurrence at this segment of plate convergence.

4. To a depth of about 160 km, the upper mantle P-wave velocity beneath the Rio Grande rift and Jemez lineament is 4-6 percent lower than beneath the High Plains Province. A 3-D, P-wave velocity inversion shows scant evidence for pronounced low P-wave velocity beneath the 240-km-long section of the Rio Grande rift covered by our array. However, the inversion shows a primary trend of 1-2 percent lower P-wave velocity underlying the northeast-trending Jemez lineament, down to a depth of about 160 km. The Jemez lineament is defined by extensive Pliocene-Pleistocene volcanics and late Quaternary faults. The upper mantle low-velocity segment beneath the Jemez lineament is at most 100 km wide and at least 150-200 km long, extending in our inversion from Mt. Taylor through the Jemez volcanic center and through the Rio Grande rift. A Backus-Gilbert resolution calculation indicates that these results are well-resolved.

Reports

Mendoza, C., and Dewey, J. W., 1984, Seismicity associated with the great Colombia-Ecuador earthquakes of 1942, 1958, and 1979: implications for barrier models of earthquake rupture: Bulletin of the Seismological Society of America, v. 74, no. 2, p. 577-593.

Spence, W., 1984, Slab pull and the 1977 Sumba earthquake series: EOS (American Geophysical Union, Transactions), v. 65 (in press).

Tectonic Analysis of Active Faults

9900-01270

Robert E. Wallace
Office of Earthquakes, Volcanoes and Engineering
345 Middlefield Road, MS 977
Menlo Park, California 94025
(415) 323-8111, ext. 2751

Investigations

1. Evaluation of fault scarps and tectonics of the central Nevada and eastern California seismic belts.

2. Active Tectonics--Impact on Society. A project under the auspices of the Geophysics Study Group, National Research Council, National Academy of Sciences.

3. International Geological Correlation Program - Active Faults of the World.

4. U.S. Geological Survey/State Seismological Bureau, People's Republic of China. Investigations of active faults in Ningxia and Ganzu Provinces, PRC.

Results

1. Completed a report for publication (Dave Hill, first author) on the potential for major earthquakes in the Long Valley-Mono Craters region of eastern California.

2. Completed first draft of volume on Active Tectonics - Impact on Society.

3. Attended organizational workshop for IGCP project on Active Faults of the World in Kobe, Japan, May 1984.

4. Active faults in People's Republic of China. - Bob Bucknam, Tom Hanks and I spent June 1984 studying the faults that offset the Great Wall near Shizuishan, Ningxia Province, PRC, in 1739. Among of our findings were that a free face was well preserved along much of the southern segment of the scarp. The free face was 2-3 m high in many places. I had previously published an estimate, based on work in Nevada, that free faces might last more than 300 years, and possibly as much as 2,000 years. The free face along the 1739 scarp, and a small remnant of free face along a manmade cut near Gaotai (see later paragraph) which is possibly 2,000 years old seem to support the earlier estimates. The total height of the scarp ranged up to 8 m. The Great Wall was offset in three places by branches of the fault. At the westernmost break, the wall was offset 1.4 m right laterally and 0.95 m vertically, east side down; at the main break, the offsets were about 2 m both right laterally and 2 m vertically, east side down. The easternmost break offset the wall 0.75 m vertically, west side down, and left lateral offset was questionable, but possibly as much as 0.2 m.

The Great Wall had been built in 1531 across the fault scarp along which the 1739 break occurred. The profile of the older scarp, also reflected in the shape of the Great Wall, indicated an age of 12-15,000 years. The profile, analyzed according to an error function solution of the diffusion model, proved to be nearly identical to the profiles of wave-cut cliffs at the high stands of glacial Lakes Lahontan and Bonneville, the ages of which are between 12,000 and 15,000 years B. P.

Near Gaotai, Ganzu province, an earthquake struck in 180 AD. We examined some high angle reverse faults in an alluvial fan and pediment south of Gaotai that conceivably could have been the causative faults. The pediments and fan surfaces are warped at the faults and little new gravel and sand have been deposited across displaced units. Prominent scarps, which had been reported to be possibly related to the earthquake, proved to be manmade and parts of a great irrigation project. Four to five more-or-less parallel channels extend for 40 km parallel to the north flank of the Yu Mu Shan (mountains) south of Gaotai. The channels slope at about 1 m per km westward toward the walled City of Camels. The construction of the channels suggests that they may also have served as a defensive barrier. The channels are said to have been dug in the Han dynasty, 206 BC to 220 AD, but that is yet to be confirmed.

We have been told by China scholars that our measurements and report about the Great Wall of China are the "first scientific report" about defensive trenches along the Great Wall. Apparently, we have gathered both unusual archaeological as well as geological data.

Reports

Wallace, R. E., 1984, Variations in slip rates, migration and grouping of slip events on faults in the Great Basin Province: Proceedings of conference on the Borah Peak, Idaho 1983 earthquake, Stein, R., and Bucknam, R. [eds.], U.S. Geological Survey open-file report (in press).

Hill, D. P., Wallace, R. E., and Cockerham, R. S., 1984, Potential for major earthquakes and volcanism in the Long Valley-Mono Craters regions of eastern California: Proceedings Volume, U.S.-Japan Conference on Earthquake Prediction (in press).

Hanks, T. C., Bucknam, R. C., Lajoie, K. R., and Wallace, R. E., 1984, Modification of wave-cut and faulting-controlled landforms: Journal of Geophysical Resarch, v. 89, n. B7, p. 5771-5790.

Hanks, T. C. and Wallace, R. E., 1984, Morphological analysis of the Lake Lahontan shoreline and Beachfront fault scarps, Pershing County, Nevada: Bulletin of the Seismological Society of America

Schultz, S. S. and Wallace, R. E., 1984, The San Andreas fault: Department of Interior/U.S. Geological Survey Pamphlet.

Harms, K.K., Clark, M.M., Rymer, M.J., Bonilla, M.G., Harp, E.L., Herd, D.G., Lajoie, K.R., Lienkaemper, J.J., Mathieson, S.A., Perkins, J.A., Wallace, R.E., and J.I. Ziony, 1984, The April 24, 1984 Morgan Hill, California Earthquake: The Search for Surface Faulting in The Morgan Hill, California Earthquake of April 24, 1984 (A Preliminary Report), v. 1, Open-File Report 84-498A.

Wallace, R. E., Davis, J. F., and McNally, Karen C., 1984, Terms for expressing earthquake potential, prediction and probability: Bulletin, Seismological Society of America, v. 74, n. 5, p. 1819-1825.

Wallace, Robert E., 1984, Notes on surface faulting in Dixie Valley, Nevada: Geological Society of America, Field Guide Volume (in press).

Wesson, R. L., and Wallace R. E., 1984, Preparing for the next great earthquake in California: Scientific American (in press).

Geophysical and Tectonic Investigations of the Intermountain Seismic Belt

9930-02669

Mary Lou Zoback
U.S. Geological Survey
Branch of Seismology
345 Middlefield Road, Mail Stop 977
Menlo Park, California 94025
(415) 323-8111, Ext 2367

Investigations

1. Investigation of crust and upper mantle structure beneath the western United States using an integrated analysis of gravity, seismic refraction, heat flow, and surface elevation data.

2. Analysis and compilation of stress data from circum-Pacific continental regions.

3. Analysis of the current state of stress along the Wasatch front region, Utah

Results

1. An integrated analysis of gravity, seismic refraction, surface elevation, and heat flow data has been used to constrain crust and upper mantle structure beneath the Western United States. A simple model in which the level of isostatic equilibrium lies at the base of a thermally defined lithosphere has been found to fit the data quite well. The model specifies surface elevation in terms of lithosphere buoyancy, which is a simple function of lithospheric thickness, the difference between mean lithosphere and asthenosphere density, and a constant related to the level to which asthenospheric material would rise if not overlain by lithosphere. This latter constant is obtained using a midocean ridge standard mass column. The crustal component of lithosphere buoyancy is computed from density models derived from seismic refraction studies. Mantle lithosphere density is computed from thermal expansion, using a mean lithospheric temperature. This temperature is derived from the lithosphere base temperature (assumed to be 1350°C) and a crustbase temperature estimate from heat flow and heat production data. Lithospheric thicknesses computed from buoyancy considerations for different regions in the Western United States are as follows: northern Basin and Range province, 55-65 km; southern Basin and Range province, 50-60 km; Colorado Plateau, 90-100 km; and the Southern Great Plains, 170 km. Four long (approximately 1000-1500 km) gravity profiles have been constructed to check the results of this buoyancy-elevation model. All four profiles intersect near the center of the Colorado Plateau; two originate in the northern Basin and Range province and the other two cross the southern Basin and Range. The computed lithosphere thicknesses and densities provide an excellent fit to the gravity data and are similar to thermal lithosphere thicknesses that would be predicted from a simple downward extrapolation of temperature gradients.

2. Stress data were collected for the entire circum-Pacific region as part of the Circum-Pacific Geodynamic Map Series. Most data were obtained from the literature and through collaboration with foreign scientists. In addition to the stress data, the Geodynamic Map includes earthquake epicenters (color-coded by depth), focal mechanisms, free-air gravity contours, active volcanoes and historic faulting. The map series consists of 4 quadrant maps (1:10,000,000), an Antartica sheet (1:10,000,000), and an entire Pacific Basin sheet (1:17,000,000). To date only the northeast quadrant map has been published, the other 5 maps are in various stages of proofing and are scheduled for publication some time before the end of 1984.

3. Available stress data along the Wasatch front including earthquake focal mechanisms, Holocene slickenside studies, and hydraulic fracturing tests have been integrated with analysis of stress-induced well bore elongation ("breakouts") in six deep wells in the vicinity of the southern Wasatch fault. The available data indicate high stress differences between the maximum principal stress, S_1, (assumed vertical) and the minimum horizontal stress, S_3. The data also suggest that both horizontal stresses (S_2 and S_3) are approximately equal in magnitude and that there is no strongly preferred orientation for the minimum horizontal stress other than that dictated by the generally N-S striking normal faults which are currently active.

Reports

Rapp, R. H., Zoback, M. L., Mauk, F. J., Tarr, A. C., Moore, G. W., Simkin, T., Siebert, L., Soller, D. R., and Brown, R. D., 1984, Geodynamic map of the Circum-Pacific region, northeast quadrant, American Association of Petroleum Geologists, scale 1:10,000,000.

Zoback, M. L., 1984, Constraints on the in-situ stress field along the Wasatch front, in Proceedings of a Workshop on Evaluation of Regional and Urban Earthquake Hazards and Risk in Utah: U.S. Geological Survey Open File report, in press.

Zoback, M. L., and Lachenbruch, A. H., 1984, Upper mantle structure beneath the western United States: Geological Society of America, Abstracts with Programs, v. 16, p. 705.

Holocene deformation near Coalinga, California

9540-02190*

Brian F. Atwater, Project Chief
Branch of Western Regional Geology
U. S. Geological Survey
345 Middlefield Road, MS 975
Menlo Park, CA 94025
(415) 323-8111 x2031 FTS 467-2031

GOAL AND APPROACH

The project's goal is to place constraints on Holocene earthquake history near Coalinga. The approach is to measure Holocene deformation on the Coalinga Nose anticline. This anticline grew as much as 0.5 m during the Coalinga earthquake of May 1983. The anticline is crossed by a major Coast Range stream, Los Gatos Creek. Deposits of Los Gatos Creek may thereby express earthquake frequency by expressing anticlinal uplift, providing aseismic uplift is negligible and large Holocene earthquakes were accompanied by uplift comparable to that of 1983.

Ideal structural datums in Los Gatos Creek alluvium would be alluvial plains having similar initial profiles and substantially different ages. Such plains should converge over a rapidly growing anticline, diverge over a rapidly growing syncline. For example, if the anticline grows 25 cm per century, then alluvial plains differing in age by 2000 years should converge 5 m over the anticline. The project thus consists of efforts to identify and trace such alluvial plains, chiefly through study of the physical stratigraphy and radiocarbon ages of Holocene deposits exposed in banks of Los Gatos Creek.

COLLABORATING SCIENTISTS

John C. Tinsley and David A. Trumm (Branch of Western Regional Geology, USGS, Menlo Park)
Ross E. Stein (Branch of Tectonophysics, USGS, Menlo Park)
Allen B. Tucker (Dept. of Physics, San Jose State Univ.)
Douglas J. Donahoe and A. J. T. Jull (Dept. of Physics, Univ. of Arizona)

INVESTIGATIONS

1. Measurement and description of 28 stratigraphic sections in Holocene alluvium along Los Gatos Creek. Six of the sections are located on the Coalinga Nose anticline; the remainder are in adjacent synclines. Vertical control for the sections has been established by vertical-angle surveying with closure error 18 cm over a line 20 km long.

2. Radiocarbon dating of detrital charcoal and burned-in-place charcoal from the measured sections. About 100 charcoal-rich samples have been

---

*For administrative convenience, the project has no number of its own, and its funds have been banked with those of the Foothills Fault System project (9540-02190; D. E. Stuart-Alexander, project chief).

collected and cleaned. Thirteen bulk samples (weight greater than 1 g) have been submitted to the USGS lab in Menlo Park for conventional beta-decay ^{14}C dating. In addition, 28 small (5-65 mg) samples have been submitted for accelerator ^{14}C dating at the NSF Regional Facility for Radioisotope Dating, University of Arizona. None of the conventional dates are available at this time, but 13 of the accelerator dates have been determined.

RESULTS

1. A buried alluvial plain about 500 years old does not measurably converge toward the modern alluvial plain over the axis of the anticline. But the difference in age between these plains may be as little as 100 years because the modern alluvial plain appears to be relict. Therefore the approximate parallelism of the plains merely argues against extremely rapid latest-Holocene uplift (say, uplift of 2 m per century, which would entail a repeat time of 25 years for earthquakes accompanied by 0.5 m of anticlinal uplift).

2. Radiocarbon control is as yet too sparse to reveal the amount of convergence, if any, of alluvial plains older than 500 years. But available ^{14}C results do show that the measured sections contain Los Gatos Creek alluvium as old as 5000 years. Therefore it may be possible to detect the relatively gradual uplift (say, uplift of 0.1 m per century) that could express repeat times of 500 years for earthquakes comparable to the 1983 event.

REPORTS

Atwater, B. F., Tinsley, J. C., Stein, R. E., Trumm, D. A., and Wert, S. L., 1984, Late Holocene alluvial plains as structural datums across the Coalinga Nose - Guijarral Hills anticline, Fresno County, California in Rymer, M. J., and Ellsworth, W. L., eds., Proceedings of Conference XXVI -- Mechanics of the May 2, 1983, Coalinga earthquake: U. S. Geological Survey Open-File Report 84-____.

Tucker, A. B., Tinsley, J. C., Atwater, B. F., Trumm, D. A., Robinson, S. W., Donahue, D. L., and Jull, A. J. T., 1985, Acclerator dating of detrital and burned-in-place charcoal from the alluvium of Los Gatos Creek, Fresno County, California, U.S.A., submitted to the 12th International Radiocarbon Converence, to be convened at the Norwegian Institute of Technology, Trondheim, Norway, June 24-28, 1984 (Director's approval received 10/23/84).

SURFACE FAULTING STUDIES

9910-02677

M. G. Bonilla
Branch of Engineering Seismology and Geology
U.S. Geological Survey
345 Middlefield Road, MS 977
Menlo Park, California 94025
(415) 323-8111, Ext. 2245

Investigations

1. Statistical data related to surface faulting.
2. Appearance of active faults in exploratory trenches.
3. Field investigations of surface faulting.

Results

1. Two manuscripts relating earthquake magnitude to rupture length and fault displacement at the ground surface were revised after review by Seismological Society of America referees and submitted for publication.

2. Data on the effect that material penetrated and fault displacement have on the visibility of faults in exploratory trenches was entered in the computer. Preliminary analysis indicates that about 10% of the fault strands shown in the trench logs have obscure segments (i.e., segments in which the fault is not visible or is very obscure). Obscure strand segments are more common on strike-slip faults than on dip-slip faults and more common in coarse-grained than in fine-grained sediments. Recognition of the possibility that obscure segments can exist is important when inferring time of last displacement on a fault and recurrence times of displacement.

3. Draft reports were prepared concerning surface faulting accompanying the Idaho earthquake of October 28, 1983 and the Guinea earthquake of December 22, 1983 (see preceding volume of "Summaries of Technical Reports"). Part of the epicentral area of the magnitude 6.1 Morgan Hill, California earthquake of April 24, 1984, was searched for surface faulting but only minor fractures of uncertain origin were found.

Reports:

Bonilla, M. G., Villalobos, H. A., and Wallace, R. E., 1984, Exploratory trench across the Pleasant Valley fault, Nevada: U.S. Geological Survey Professional Paper 1274-B, 14 p.

Bonilla, M. G., Mark, R. K., and Lienkaemper, J. J., 1984, Statistical relations among earthquake magnitude, surface rupture length, and surface fault displacement: U.S. Geological Survey Open-File Report 84-256.

Bonilla, M. G., Mark, R. K., and Lienkaemper, J. J., 1984, Statistical relations among earthquake magnitude, surface rupture length, and surface fault displacement: Seismological Society of America Bull., v. 74, no. 6 (in press).

Lienkaemper, J. J., 1984, Comparison of two surface-wave magnitude scales: M in Gutenberg and Richter (1954) and M_s of Preliminary Determination of Epicenters: Seismological Society of America Bull., v. 74, no. 6 (in press).

Harms, K. K., Clark, M. M., Rymer, M. J., Bonilla, M. G., Harp, E. L., Herd, D. G., Lajoie, K. R., Lienkaemper, J. J., Mathiesen, S. A., Perkins, J. A., Wallace, R. E., and Ziony, J. I., 1984, The April 24, 1984 Morgan Hill, California earthquake: The search for surface faulting: U.S. Geological Survey Open-File Report 84-498A, The Morgan Hill, California, earthquake of April 24, 1984 (A Preliminary Report), p. 92-108.

SOIL DEVELOPMENT AND DISPLACEMENT ALONG THE HAYWARD FAULT

14-08-0001-21929

Glenn Borchardt
Division of Mines and Geology
California Department of Conservation
380 Civic Drive
Pleasant Hill, CA 94523-1997

(415) 671-4926

Investigations

Its high rate of activity (>5 mm/yr) and urban location make the Hayward fault potentially more destructive than any other fault in the San Francisco Bay Area. Many of the area's most important lifelines cross the fault as they enter the metropolitan area from the east (Davis and others, 1985). But aside from sketchy historical accounts mentioning that between 8 and 36 inches of ground surface rupture occurred over a distance of up to 60 km during the 1868 event, very little information is available for estimating future catastrophic displacement. If evidence of the amount of displacement per event exists at all, it would be found primarily in the most recent sediments and soil horizons straddling the fault. The objective of this research program is **to determine the recurrence interval and the amount of displacement to be expected for major earthquakes on the Hayward fault.**

Recent efforts in using soil mineralogical techniques to determine the amount of displacement and the relative ages of surficial materials have met with great success in studies of the Foothill fault system (Borchardt, Taylor, and Rice, 1980; Borchardt, Rice, and Taylor, 1980), the bedding plane faults of the Point Conception LNG terminal site (Borchardt, Rice, and Treiman, 1982), and the Raymond fault (Borchardt and Hill, 1985). Just getting underway, this project will entail:

1. Compiling a list of soil series offset by the fault.

2. Preparing a map of all archaeological sites within the Alquist-Priolo Special Studies Zone encompassing the fault.

3. Evaluating consultants' reports prepared for the Alquist-Priolo Special Studies Zone for precise fault locations and for information on soil sites that might yield information on displacement history and recurrence interval.

4. Excavating four seismic investigation trenches, two planar excavations, and several soil pits.

5. Describing, sampling, and characterizing in detail four soil profiles displaced by the Hayward fault by using physical, geochemical, and soil mineralogical methods.

Results:

1. At least 25 different soil types are offset along the Hayward fault. About half of these are developed on Holocene materials young enough to be of special interest to this project. Some of these soils have Bt, Bg horizons, contain gypsum, carbonate, or saline-alkali accumulations that are expected to aid in discovering microgeomorphological features useful for determining fault displacement per event during the late Holocene.

2. Offset vertisols were described and sampled at Appian Way in Union City, Alquire Rd. in Hayward, and at High St. in Fremont.

3. The first site selected for detailed investigation is at Point Pinole at the northwestern end of the fault. The fault was precisely located from 1939 aerial photos and from projections of creep evidence in a housing development to the southeast. Reyes silty clay, a late Holocene soil developed on the tidal flat and characterized by a gleyed B horizon, is clearly offset by the fault. The southwest side of the fault at Point Pinole appears to consist entirely of landslides and coastal slumps interspersed with soils and materials possibly useful for determining displacement history.

References Cited

Borchardt, Glenn, and Hill, R. L., 1985, Smectitic pedogenesis and late Holocene tectonism along the Raymond fault, San Marino, California, in D. L. Weide, ed., Quaternary soils and geomorphology in the American Southwest: Geological Society of America Special Paper (forthcoming).

Borchardt, Glenn, Rice, Salem, and Taylor, Gary, 1980, Paleosols overlying the Foothills fault system near Auburn, California: California Division of Mines and Geology Special Report 149, 38 p.

Borchardt, Glenn, Rice, Salem, and Treiman, Jerome, 1982, Mudflow deposits and horizonation in Holocene soils near Point Conception, California: Geological Society of America Abstracts with Programs (Cordilleran Section), p. 150.

Borchardt, Glenn, Taylor, Gary, and Rice, Salem, 1980, Fault features in soils of the Mehrten Formation, Auburn Damsite, California: California Division of Mines and Geology Special Report 141, 45 p.

Davis, J. F., and others, 1985, Earthquake planning scenario for a magnitude 7.4 earthquake on the Hayward fault in the San Francisco Bay Area: California Division of Mines and Geology Special Publication (forthcoming).

Soil-Structure and Structural Response Studies

9910-02760

A. G. Brady & G. N. Bycroft

Branch of Engineering Seismology and Geology
U.S. Geological Survey
345 Middlefield Road, MS 977
Menlo Park, CA 94025
(415) 323-8111 X2881

Investigations

1. Instumentation of San Francisco Bay Area structures.

As a result of the agreement between the ambient tests and the dynamic computer study of the Great Western building in Berkeley, 12 accelerometer sites have been chosen for the permanent instrumentation of this building. An electrical contractor familiar with our requirements for cabling has investigated the facility, and work will commence as soon as he has finished a similar cabling job on the Pacific Park Plaza in Emeryville.

A complete report on the recommended list of structures for seismic instrumentation in the San Francisco Bay region by the USGS San Francisco Bay Region instrumentation advisory committee has been prepared (M. Celebi, chairman). The contribution from this project is the selection procedure by which the structures were placed in a priority list.

2. Time-dependent structural response.

At the seminar and workshop on Earthquake Ground Motion and Building Damage Potential held by the Applied Technology Council in San Francisco, March 27, 1984, interest was expressed in the contribution by Perez and Brady describing the demands made on a structure's ductility as the structure moves through many cycles of response during earthquakes. The paper has been added to and reworked and has been accepted in the first, introductory, issue of Earthquake Spectra, the journal of the EERI.

Work continues on the effects on structures with different damping than the standard 5% of critical, and on structures exhibiting non-linear characteristics, namely elasto-plastic force-displacement behavior. Current results show that the assumptions made regarding the displacements attained by these structures, whether they remain elastic or enter the elasto-plastic regime, are valid.

3. Soil-structure interaction and field testing.

SRI International, Menlo Park, California, has completed a series of aligned explosive shots near a model structure to demonstrate the feasibility of producing a simulated earthquake motion at the foundation of a structure. We took the opportunity to carry out three important procedures during this series of seven shots.

(a). Refining our skills at placement of accelerometers and digitally recording under a timed explosive environment rather than ambient (wind-excited) or earthquake environment.

(b). Experimental verification of soil-structure interaction affects by constructing a simple structure (4 ft diameter, 3 ft high, pedestal) and measuring motion on the structure, and at two of its symmetric image locations.

(c). Comparison of the technical requirements in day-long setting up of equipment (for example, film recorders and two different manufacturers' digital recorders); the reliability of their recording; and the handling of problems associated with synchronizing of master/slave instruments when no external time source (WWVB or time code generator) is available.

4. Soil-structure interaction and differential ground motions.

Research on the effect of soil-structure interaction and differential ground motions on the motion of structures was continued. The effect of soil structure interaction on the recording of accelerograms has been studied further with a paper in preparation. Initial design of experiments to verify corrections of accelerograms for soil structure interactions was made.

Papers on soil-structure interaction and its effect on seismograms are in preparation.

Reports

Perez, V., and Brady, A.G., 1984, Reversing cyclic demands on structures during earthquakes and application to ductility requirements. Accepted for publication, Earthquake Spectra.

"Report on recommended list of structures for seismic instrumentation in the San Francisco Bay region", USGS San Francisco Bay region instrumentation advisory committee, M. Celebi (Chairman), USGS Open-File Report 84-488.

Holocene and Quaternary Geologic Studies

9540-03787

Robert O. Castle
Branch of Western Regional Geology
345 Middlefield Road MS 975
Menlo Park, CA 94025
(415) 323-8111, ext. 2293

Investigations

1. Resumed studies of historic surface deformation along the Newport-Inglewood zone between the Dominguez Hills and Newport Beach. These studies are aimed primarily toward the discrimination of tectonic deformation, where the major vertical displacements consist chiefly of movement associated with changes in the underground fluid regime.

2. Continued investigations of historic deformation within and adjacent to the Salton Trough and the contrast in tectonic activity between southeastern California and southwestern Arizona.

3. Continued preparation of two reports on the magnitude and predictability of the so-called unequal-refraction error in geodetic leveling.

Results

1. Comparisons among the results of repeated geodetic levelings propagated eastward through southern California into southwestern Arizona tend to confirm the geologically inferred tectonic stability of this part of Arizona. This stability, moreover, is consistent with the virtual absence of seismic activity east of the Colorado River. Analyses of the results of the more recent levelings has been complicated by the occurrence of compaction-induced subsidence, attributable to ground-water withdrawals, at critical connecting bench marks during junction intervals ranging up to a year or more. Disregarding the effects of compaction-induced displacements during the cited junction intervals could lead to an interpretation requiring broad, regionally developed historical block movement over much of southwestern Arizona. Preliminary analyses of the results of third-order, wooden-rodded leveling (the least accurate geodetic leveling carried out in the United States during the 20th century), coupled with the acceptance of the geologically inferred premise of tectonic stability over most of southwestern Arizona, suggests that these surveys were characterized by a much higher accuracy than heretofore believed.

Reports

Castle, R. O., Elliott, M. R., Church, J. P., and Wood, S. H., The evolution of the southern California uplift, 1955 through 1976; U.S. Geological Survey Professional Paper 1342 (in press).

LATE QUATERNARY SLIP RATES ON ACTIVE FAULTS OF CALIFORNIA

9910-03554

Malcolm M. Clark
Branch of Engineering Seismology and Geology
345 Middlefield Road, MS 977
Menlo Park, CA 94025
(415) 323-8111, Ext. 2591

Investigations

1. Search epicentral area of April 24, 1984, Morgan Hill, California, earthquake for surface rupture (K. K. Harms, M. M. Clark, M. J. Rymer, and J. J. Lienkaemper).

2. Dig three trenches across the Nunez fault, northwest of Coalinga, to determine near-surface structure of the fault and its late Quaternary history of movement. Remeasure nine leveling lines across the fault (M. J. Rymer and J. J. Lienkaemper).

3. Convene a symposium, with W. L. Ellsworth, on mechanics of the May 2, 1983, Coalinga earthquake (M. J. Rymer).

4. Continue investigation of soils and ages of offset of fluvial terraces of Tres Pinos Creek along Calaveras fault south of Hollister, California (J. W. Harden, K. K. Harms, M. M. Clark, and S. N. Hoose).

5. Continue analysis of Lone Pine fault in Owens Valley, California (Lester Lubetkin, U.S.F.S., and M. M. Clark).

Results

1. Post-earthquake investigation of abundant ground cracks associated with the April 24, 1984, Morgan Hill earthquakes revealed no unequivocal evidence of surface faulting. Cracks in two places in San Felipe Valley were aligned with late Quaternary fault traces, but showed no tectonic displacement. Cracks near the southeast end of Anderson Reservoir showed right slip of more than 0.1 m, but were either in or near active landslides or in short zones that had no continuity of displacement or trend along strike in the fault zone. We think the evidence does not demonstrate surface faulting, but we cannot deny the possibility that some cracks were tectonic.

2. The Nunez fault as exposed in the walls of one trench in Holocene fluvial deposits and two trenches dug in Cretaceous rocks, shows great complexity and a variable dip of 65 to 86° E. in the upper 3-4 m. The trench in Holocene flood and overbank deposits revealed a nearly completely homogeneous pebbly, silty sand overlying a pebble to boulder gravel. Near the top of the section are 1- to 2-cm-thick sand and silt laminae. A discreet planar surface does not cut these materials, but a 10 cm vertical warp is noticeable in the sand

and silt laminae. Fourteen charcoal samples were taken from deposits in the walls of this trench for ^{14}C dating and will give a minimum age for recurrence of faulting in this segment of the Nunez fault. In Cretaceous rock near the northern end of the south Nunez break the trench walls revealed a main trace, with a 5- to 7-cm-thick fault gouge, and four parallel slip planes, one being west of the main trace. Measurement of the rake of mullions on a slickensided surface along the main trace indicate that the proportion of right-lateral slip relative to reverse slip in the 1983 event was about 24 percent, similar to other localities along the 1983 rupture where right-lateral and reverse slip components were measured.

Remeasurement of nine leveling lines across the Nunez fault revealed continued afterslip on the five lines in the southern segment and the northernmost line in the northern segment. Remeasurements in May and August, 1984 show linear decay of slip with the logarithum of time along these six lines. Leveling line N2 at the north end of the southern Nunez break has consistently had the largest vertical (reverse) movement in all measurement periods. Cumulative afterslip on this line from July 17, 1983, to August 18, 1984, is 63 mm, approximately 60 percent as large as the coseismic slip at this locality. Measurement of right-lateral afterslip on line N7, also in the southern break, by Beth Brown in November, 1983, and April and June, 1984, similarly shows decay of movement along the fault in time. The proportion of right-lateral to vertical (reverse) movement measured on leveling line N7 is the same as measured for coseismic slip in the northern segment of the fault.

3. A symposium was convened at Asilomar, California, to discuss the mechanics of the May 2, 1983, Coalinga earthquake. Thirty-five investigators participated in the interdisciplinary meeting. A symposium volume (OEVE redbook) is in preparation.

4. Measurements on multiple stream terraces of Tres Pinos Creek yield horizontal slip rates along the Calaveras fault. Two approaches, using offset late-Quaternary features, provide four independent slip rates for different periods along this segment of the fault.

One method of determining slip rates is to constrain ages on horizontally displaced terrace risers. At one location the offset has a large uncertainty because apparent displacements could have been formed by mass wasting, fluvial action, fault movement, or a combination of these processes. We determine the minimum and maximum ages of offsets by using quantification of soil development (calibrated to that of other soils of known age) to date those terraces older and younger than the offset. The three resulting horizontal slip rates using this method are 0.6-4.2, 2.8-10.4 and 3.2-12.9 mm/yr.

A second approach we have used is to determine the timing of a major change in the course of the Tres Pinos Creek and to relate this change to a hill offset along the fault. This hill has been offset approximately 450 m beyond the location where it blocked the present drainage. By determining the age of the youngest deposits associated with the abandoned course, and that of the oldest deposits associated with the present course, the age of the offset can be constrained to 80-600,000 yrs. The resulting slip rate is 0.8-5.6 mm/yr. Our excavations on this hill, however, revealed a relatively young soil, suggesting either stripping of the soil or substantial vertical uplift across the fault. If the uplift has occurred, the hill may not have blocked the present drainage.

5. Offset surficial features and scarp morphology along the Lone Pine fault in Owens Valley combine to yield distinctly different slip rates from sites only 220 m apart. This inconsistency may be real or only apparent, but it must be resolved before a reliable slip rate for the fault can be determined.

Average maximum dip-slip displacement of an abandoned outwash fan is 5.5 m, measured from many profiles of a 1.5-km-long fault scarp across this fan. This scarp is younger than the offset fan surface, whose age is bracketed by a 21,000-yr-old shoreline of Lake Owens and by the time of abandonment of the fan surface at least 10,000 B.P. The average dip-slip rate for the past 10,000-20,000 yr at this fan is 0.3-0.6 mm/yr.

A young debris flow that crosses the fault scarp on the same outwash fan has been offset 6-7 m right laterally and 1-1.5 m vertically, apparently all from slip during the great 1872 earthquake. An assumed average recurrence interval of 3,000-10,000 yr for 1872-type earthquakes at this site (derived from scarp morphology) and net oblique slip of 6-7 m yield a total oblique-slip rate at this site of 0.6.2 mm/yr for the past 3,000-10,000 yr. The horizontal-slip component here, however, contrasts sharply with that at a site only 220 m south along the scarp, where no horizontal slip is recognizable in an abandoned stream channel that predates the offset debris flow, and the total slip rate equals the dip-slip rate of 0.3-0.6 mm/yr. This discrepancy suggests that either: (1) horizontal slip is present but not detectable at the abandoned channel, (2) postslip erosion of the debris-flow deposit has caused an apparent offset greater than the actual offset, or (3) horizontal slip can vary greatly over relatively short lateral distances.

Reports

Bakun, W. A., Clark, M. M., Cockerham, R. S., Ellsworth, W. L., Lindh, A. G., Prescott, W. H., Shakal, A. F., and Spudich, P. A., 1984, The 1984 Morgan Hill, California, earthquake: Science, v. 225, p. 288-291.

Harms, K. K., Clark, M. M., Rymer, M. J., Bonilla, M. G., Harp, E. L., Herd, D. G., Lajoie, K. L., Lienkaemper, J. J., Mathieson, S. A., Perkins, J. A., Wallace, R. E., and Ziony, J. I., 1984, The April 24, 1984, Morgan Hill, California, earthquake: The search for surface faulting, U.S. Geological Survey Open-File Report 84-498.

Rymer, M. J., Harms, K. K., Lienkaemper, J. J., and Clark, M. M., in press, Rupture of the Nunez fault during the Coalinga earthquake sequence, in Rymer, M. J., and Ellsworth, W. L., eds., Mechanics of the May 2, 1983, Coalinga, California, earthquake: U.S. Geological Survey Open-file report.

Holocene Styles of Surface Faulting Along the Creeping Segment of the San Andreas Fault, San Juan Bautista

21335

W. R. Cotton, N. T. Hall, and E. A. Hay
Foothill-De Anza Community College District
Los Altos Hills, California 94022
(415) 948-8590

Investigation

This project is designed to recognize and evaluate localities along the creeping segment of the San Andreas fault capable of yielding information about 1) characteristics of the style of rupturing in a creeping segment (as opposed to locked segments), 2) slip rates for creep that extend back into pre-historic time, and 3) recurrence interval determinations if discrete rupture events are recognizable.

Results

1. All preliminary conclusions pertaining to this investigation were reported in Volumes XVII and XVIII of the Summaries of Technical Reports, December 1983 and June 1984, respectively.

2. We have been waiting since February, 1984 for ^{14}C age determinations of twenty (20) small charcoal samples collected from offset paleostream channels and the older fan sediments into which the channels were incised. Professor Allan Tucker (San Jose State University) agreed to use facilities at the University of Arizona to evaluate these small samples, using the accelerator technique. We are awaiting these determinations before estimating slip rates for the last few hundred years along this segment of the San Andreas fault.

HOLOCENE BEHAVIOR OF THE SAN GABRIEL FAULT SAUGUS/CASTAIC AREA LOS ANGELES COUNTY, CALIFORNIA

14-08-0001-21950

William R. Cotton
William Cotton and Associates
314 Tait Avenue
Los Gatos, California 95030
(408) 354-5542

Investigation

The goal of this investigation was to locate exploratory trench sites along the San Gabriel fault in the Saugus/Castaic area of southern California that contain well-defined and datable Holocene records.

Results

1) The initial phase of our work entailed a systematic analysis of the field conditions along a 25-mile segment of the fault between Placerita Canyon and Frazier Mountain. Geologic data from our previous investigations in the area, local oil well information, and the site selection criteria that we have developed from other EHRP projects allowed us to identify eight sites along the southern part of the study area that had high potential for productive research. As of this date, our work has been confined to a 3-mile segment of the fault located between the Santa Clara River and Castaic Creek.

2) Preliminary test trenching and detailed bedrock mapping along the fault trace established our primary investigation sites to be in the Rye Canyon area located north of the community of Valencia (between Santa Clara River and Castaic Creek).

3) A series of exploratory trenches were excavated across a broad alluvial valley floor near the head of Rye Canyon. At this location, the fault trace was well constrained in several bedrock ridges located to the north and south of the site. The trenches exposed well stratified fluvial sediments and buried soil horizons that contained limited, but significant, charcoal materials. In addition to the trenches used in active fault investigations, we utilized a very large excavation from an earlier investigation. This excavation was placed on a narrow canyon floor and measured approximately 500 feet long, 60 feet wide, and 40 feet deep. The alluvial section is about 45 to 50 feet thick and probably represents the entire Holocene record.

4) Fault displacements within the alluvium were well defined in all of the exploratory trenches. Preliminary radiocarbon dates indicate that the fault cuts Holocene beds that yield radiocarbon dates of 8,140 ± 60 yrs BP, 7,700 ± 60 yrs BP, and 3,500 ± 250 yrs BP, and does not displace beds that contain charcoal that provide a date of 1,550 ± 190 yrs BP. Radiocarbon dates were obtained by conventional methods from the University of Washington and by the accelerator method (for very small charcoal samples) from the University of Arizona Nuclear Accelerator Laboratory, under the operation of Alan Tucker (San Jose State University).

5) The zone of faulting as displayed in the bedrock areas is approximately 80 to 100 feet wide. The *active* trace of the San Gabriel fault, however, is confined to a narrow zone ranging in width from a few inches to about 1 or 2 feet in the bedrock, and from 1 to 2 inches to 4 feet in the overlying alluvium. This active trace appears to be at the western margin of the fault zone. Active fault ruptures can be traced clearly to within about 7 feet, and possibly to within 4 feet, of the ground surface.

6) The trend of the fault throughout the Saugus-Castaic field area is N40°W; however, a range of N25°W to N67°W was measured on fault splays within the exploratory trenches. The general attitude of the active fault plane in the bedrock is either near vertical, or steeply dipping to the east ($80^{+\circ}$). Within the overlying alluvium, the fault divides into several splays which generally flatten upward to dips of about 30° to the west.

7) The displacements observed within exploratory trenches are primarily right-lateral strike slip. The *apparent* vertical displacement of the active splays is uniformly east-side down. As of this date, we have been unable to establish (a) whether multiple faulting events have taken place within the Holocene section, (b) the interval of time between repeated earthquake events, (c) the amount of slip per event, and (d) the actual slip direction of the most recent episode of faulting.

8) A detailed ground penetrating radar survey of all of our trench sites was conducted by Rodger Bilham (Lomont-Doherty Geological Observatory). The survey was conducted at sites where we had clearly constrained the location of the fault within both the bedrock and the alluvium. Within the range of 0 to 12 feet, the GPR survey was unable to detect (a) layered alluvial sediments, (b) thin alluvium over bedrock, or (c) fault alluvium. The GPR survey proved to be of no value in locating subsurface discontinuities within our research area.

Seismic Hazard Investigations in the Pacific Northwest

14-08-0001-21861
14-08-0001-21862

R.S. Crosson & S.D. Malone
Geophysics Program
University of Washington
Seattle, WA 98195
(202) 543-8020

Investigations

1. Operation of the western Washington regional seismograph network, and routine preliminary analysis of seismic events in western Washington

2. Analysis and interpretation of Pn observations for both eastern and western Washington

3. Development and implementation of automated processing of seismic events using digital network data

4. Crustal structure determination in the vicinity of Mt. St. Helens and in the greater Puget Sound region from earthquakes and explosions recorded digitally on the local and regional networks

5. Locations, focal mechanisms and occurrence characteristics of crustal and subcrustal earthquakes beneath western Washington and their relationship to subduction processes

6. Automated spectral analysis of digital seismic data for determination of source parameters for local earthquakes in the Pacific Northwest

Results

1. Network operation for stations in western Washington, eastern Washington, and northern Oregon continued normally. No unusual regional earthquake activity was recorded outside of the Mt. St. Helens region. A new station (OSD) which provides critical data for depth determination in the subduction complex beneath the Olympic Peninsula was established in the central Olympic Mts. Reconfiguration of the telemetry routes and the installation and reinstallation of stations in the northeast part of the Puget Sound basin is underway and scheduled for completion for autumn 1984. An analysis of magnitude thresholds for catalog completeness was done for the network, and will be utilized henceforth in report and catalog presentations. Efforts are underway to establish a uniform data base of earthquake phase data for the greater western Washington region, from 1970 through the transition to digital data acquisition in 1980 to the present. Eventually, pre-network instrumental and historic data will be merged into

a uniform data base with appropriate quality indicators.

2. Results from Pn analysis reinforce the existence of significant differences in structure between eastern and western Washington. East of the Cascade Range, Pn velocity averages 8.18 +/- 0.02 km/sec, whereas the average for western Washington is 7.77 +/- 0.02 km/sec. Anisotropy appears to be significant east, but relatively unimportant west, of the Cascades. Calculated Moho dip east of the Cascades, assuming no lateral change in crustal velocity, is about 0.7 degree whereas the calculated regional dip for the west is about 2.1 degrees in a southeasterly direction. There is little direct evidence in the regional Pn data for Moho dip associated with a dipping slab beneath western Washington.

3. A new algorithm for phase picking has been developed and incorporated into an automated processing program for digital network data. In the current configuration, feedback is provided between phase picking and location processing to reduce the number of blunders due to noise spikes and poor signal-to-noise ratio. An important aspect of automated processing is making quantitative and consistent estimates of phase picking errors for both P and S phases and coda length estimates. We are undertaking a complete recalibration of our auto-processed coda duration measurements for the purpose of improving the consistency and accuracy of local magnitude determinations. The current version of our program is being run in a test mode and is also being used for special studies. Use of automatic processing in our routine network data analysis is feasible based on results to date. We view these efforts as being important in the long range to improve the quantity, quality and consistency of network data analysis. In recently completed work on structure inversion, for example, we exclusively utilized auto-picked phase data.

4. A joint P/S layered structure inversion program was developed to use earthquake and explosion arrival times, providing additional constraint on structure determination where high quality S arrivals are measured. The method uses coupled P and S models, and makes use of an an independently determined VP/VS ratio. Using the joint P/S inversion program, crustal structure at Mt. St. Helens was inverted from both earthquake and explosion arrival times. The incorporation of S phases offers significantly greater stability to the modeling process than the use of P phases alone. Our final model indicates that the P velocity in the vicinity of St. Helens rises rapidly to about 6.1 km/sec at 1 km depth (very high shallow velocity) and then increases slowly in approximately a linear fashion to about 6.5 km/sec at 20 km depth. In comparison with the Puget Sound region, higher velocities are reached at shallower depths but mid-crustal values are somewhat lower. Using auto-picked digital data for 58 seismic events (48 earthquakes, 10 explosions), we inverted for a coupled P and S velocity model for the greater Puget Sound region. The final model, although similar to our previous model in the depth range from about 12 km to 30 km, has a thinner surface layer of velocity 5.4 km/sec and a slight velocity reversal in the interval 30-40 km. km. The constraint on the velocity in the 30-40 km depth range, an earthquake free zone, with our new model appears to be better than that previously obtained. This structure inversion

effort is preliminary to undertaking a careful analysis of deep earthquake seismicity.

5. Focal mechanisms for small earthquakes are commonly utilized to infer tectonic stress directions and trajectories. In the Puget Sound region, the volumetric distribution of earthquakes offers an excellent opportunity to study stresses associated with subduction. Such studies provide one of the most reliable methods to assess the degree of coupling between the overlying North American and the subducted Juan de Fuca plates. McKenzie (1969) has shown quantitatively how preexisting faults or fractures can distort the interpretation of stress directions when these are based on the common assumption of fracture of previously unbroken rock. Since there are probably no regions of the earth's crust or upper mantle that behave as unfractured rock, caution is required. With reasonable assumptions as to the effect of the earth's free surface and the relative magnitudes of the principal stresses, we can use McKenzie's results to show that substantial error may be introduced if strike-slip earthquakes are used to determine the P axis for the Pacific Northwest. By contrast, thrust or normal earthquakes should provide better estimates of the azimuth of P or T axes. We are studying a data base of well recorded regional earthquakes in order to test this hypothesis, and possibly reconcile varying values of P axis azimuth estimated from northwest earthquakes. These studies of regional tectonics are critically dependent on the data base efforts discussed in (1) above.

6. Routines for determining seismic moment, corner frequency, and stress drop from digital seismic data are being tested. A synthetic source spectrum is fit to the amplitude density spectrum for P, S, and coda waves corrected for instrument response and Q. All events located by the routine processing will ultimately have source parameters determined by this process. Periodic testing of the process is underway. Calibration of amplitude-frequency responses of network stations is crucial to this effort, and is ongoing.

Reports

Crosson, R.S. and D.A. Bame, 1984, A Spherical Source Model for Volcanic Earthquakes (abs), EOS, (in press).

Ludwin, R.S. and R.S. Crosson, 1984, The Azimuth of Regional Tectonic Compression in the Pacific Northwest from Shallow Thrust Earthquakes (abs), EOS, (in press).

Noson, Linda Lawrance, R.S. Ludwin, and R.S. Crosson, 1984, Compilation of Earthquake Hypocenters in western Washington, 1979, Washington Division of Geology and Earth Resources Information Circular, (in press).

Univ. of Wash. Geophysics Program, 1984, Earthquake Hazard Evaluation in the Pacific Northwest, 1981-1982 Final Technical Report U.S.G.S.

Contract 14-08-0001-19274.

Univ. of Wash. Geophysics Program, 1984, Earthquake Hazard Evaluation in the Pacific Northwest, 1982-1983 Final Technical Report U.S.G.S. Contract 14-08-0001-21192.

Univ. of Wash. Geophysics Program, 1984, Quarterly Network Report 84-A on Seismicity of Washington and Northern Oregon Jan 1 through March 31, 1984,27p.

Univ. of Wash. Geophysics Program, 1984, Quarterly Network Report 84-B on Seismicity of Washington and Northern Oregon April 1 through June 30, 1984,26p.

Zervas, C., 1984, A Time-Term analysis of Pn Velocities in Washington, M.S. Thesis, Univ. of Washington.

PALOS VERDES FAULT ZONE
EARTHQUAKE POTENTIAL AND SURFACE FAULTING

14-08-0001-21304

S. T. Freeman and P. D. Guptill(1)
Woodward-Clyde Consultants
203 North Golden Circle Drive
Santa Ana, California 92705
(714) 835-6886

Investigations: Field studies are continuing on the Palos Verdes fault and related secondary faulting on the Palos Verdes Peninsula, in southern California. The object of the field studies is to locate fault traces and evluate offsets of late Quaternary geologic units. The methods being used include describing the youngest marine terraces, drilling and sampling, and trenching across fault traces.

Data Acquisition and Analysis

1. The initial phase of our investigation has involved analysis of aereal photographs, preliminary geologic mapping, and subsurface drilling. The results of this phase of the research was used to select candidate sites to trench the fault. Efforts are continuing to obtain access permits from city and private landowners to complete the trenching program.

2. A comprehensive mapping, sampling, and age dating program of old shorelines found near the Palos Verde fault has begun. At this time, the stratigraphy and relationships of old shorelines is not well defined along the trend of the fault. The basic importance of resolving some of the stratigraphic and age-relationships has become more apparent as our program has progressed. The stratigraphic relations have become essential to understanding the tectonic deformation (rate and style) and nature of faulting along the trend of the Palos Verdes fault.

---

(1) P. D. Guptill is a former employee of Woodward-Clyde Consultants.

Detailed Analysis of 1906 Faulting in Marin County, California

21242

N. T. Hall, W. R. Cotton, and E. A. Hay
Foothill-De Anza Community College District
Los Altos Hills, California 94022
(415) 948-8590

Investigation

The investigation is being focused on a 12 kilometer segment of the 1906 trace of the San Andreas fault. The research area lies between the Marin County localities of Dogtown and the Vedanta Retreat, and is an area where Holocene activity along the fault has occurred in a narrow zone. The investigation is designed to produce a set of detailed geologic and geomorphic maps of the seismotectonic features. This information will be augmented by the rich historic record of the 1906 faulting that was compiled by G. K. Gilbert shortly after the 1906 earthquake.

Results

1. All field work and photo interpretation activities are now complete. Large scale topographic maps (1" = 100', C.I. = 2') were used to map the following: 1) the rupture traces of 1906 as shown on G. K. Gilbert's photographs; 2) additional traces as determined from photo interpretation and field mapping of geomorphic features; 3) camera stations for Gilbert's 1906 - 1907 photographs; 4) fault-related geomorphic features such as sag ponds, tectonic ridges, scarps, etc.; and 5) Holocene deposits associated with active faulting.

2. We have completed detailed mapping at (3) localities:

   a. Boucher Ranch of 1906 (approximately one mile southeast of the Vedanta Retreat; approximately 9,000 feet southeast of Olema): Mapping covers about 3,600 feet along the fault zone. Five of Gilbert's camera stations are located (his numbers 3044, 3039, 3043, 3042, and 3045). Approximately 900 linear feet of 1906 ruptures are shown here, along with 9 sags and numerous other rift related geomorphic features.

   b. Five Brooks site (approximately 3 1/2 miles southeast of Olema): Mapping covers about 3,800 feet along the fault zone. There aren't any Gilbert photographs here, but a locality to the southeast is the location of his photos numbers 3036, 3035, 3034 (this region is now heavily vegetated and not at all like its 1906 appearance). Four sags, one sharply defined expression of offset drainage, and numerous other rift features are located.

c. Bondieti Ranch of 1906 (approximately 5 1/2 miles southeast of Olema; west of the Randall trailhead): Mapping covers about 5,300 feet along the fault zone. Six of Gilbert's camera stations are located (his numbers 3047, 3037, 2952, 2850, 3041 and 2851). Approximately 2,200 linear feet of 1906 ruptures are shown here, along with 8 sags and numerous other rift related gemorphic features.

Soil Development as a Time-Stratigraphic Tool

9540-03852

Jennifer W. Harden
Branch of Western Regional Geology
U.S. Geological Survey
345 Middlefield Road, MS 975
Menlo Park, California 94025
(415) 323-8111 ext. 2039

Investigations

1. Use soil development as age control for studies on the recency and timing of tectonic events. Geomorphic surfaces that have been offset by faults are correlated across the fault and approximately dated by the degree of soil development. In some studies, the surfaces include Pleistocene as well as Holocene deposits, thereby providing information on the evolution of fault activity.

2. Develop methods for sampling and data analysis to (a) establish rates of soil development in areas where soils have been studied and dated radiometrically; (b) test comparability of development rates between different geographical and geologic settings; and (c) establish statistical methods for estimating the ages of deposits based on soil development and calibration curves in (a), in areas found to be comparable in (b).

3. Collect and analyze soils along faults such as the San Andreas and Calaveras (in conjunction with J. C. Matti and M. M. Clark, U.S. Geological Survey; FY-85, 86).

Results

1. Sampling was completed for the study near Tres Pinos along the Calaveras fault. Three stream terraces on the north side of Tres Pinos Creek are probably about 20,000 to 50,000, 30,000 to 70,000, and 100,000 to 150,000 years old. Using soils to correlate these surfaces across the fault, three separate slip rates range from about 1 to 13 mm/yr. Most of the uncertainty in these rates is due to uncertainty in ages of the soils and geomorphic surfaces. In order to reduce these uncertainties, we conducted a sampling program on four dated deposits in the area, that should provide more accurate and more precise estimates of the ages of surfaces (result no. 2). (J. W. Harden; K. K. Harms; M. M. Clark).

2. Soils were sampled on four dated deposits in the San Francisco Bay Region in order to improve our methods of age estimation. Charcoal had been dated previously near the Mt. View dump; Palo Alto Avenue near downtown Palo Alto; Stanford Shopping center; and Butano Creek. All four soils are Holocene and are being analyzed at U.C. Davis under contract no. 4-9540-0074. (J. W. Harden; K. K. Harms; M. M. Clark).

3. Soils sampled near Tres Pinos in 1983 were prepared and analyzed for particle size, bulk density, dithionite iron and percent magnetite. Approximately 150 samples were analyzed for a total of about 600 samples runs

(M. J. Singer, P. Janitzky, J. Aniku contract no. 4-9540-0074).

Publications

Harden, J. W., 1984, Techniques and uncertainties in using soil development for stratigraphic, geomorphic, and age analyses (abs): Earthquake Notes, Vol. 55, no. 1, p. 7.

Harms, K. K., Harden, J. W., Hoose, S. N., and Clark, M. M., 1984, Estimating slip rates along Calaveras Fault, California, using soil chronology and geometry of stream terraces: Earthquake Notes, Vol. 55, no. 1, p. 9.

Tectonics of Central and Northern California

9910-01290

William P. Irwin
Branch of Engineering Seismology and Geology
U. S. Geological Survey
345 Middlefield Road, MS 977
Menlo Park, CA 94025
(415) 323-8111, ext. 2065

Investigations

1. Field studies of suture relations and origin of accreted terranes of northern California, and preparation of geologic maps of the Dubakella Mountain and Hyampom 15-minute quadrangles.

2. Determination of metamorphic state of limestone from localities in various terranes of the Klamath Mountains, by X-ray analysis.

3. Paleomagnetic study of various tectonic elements of the Eastern Klamath terrane: collaboration with E. A. Mankinen and C. S. Gromme.

Results

During the report period, paleomagnetic sampling of the Mule Mountain stock and Shasta Bally batholith was done to (1) test our ideas regarding tectonic rotation of the Eastern Klamath terrane, and (2) more closely date the suturing of the Klamath Mountains to the North American continent. Our present ideas regarding preaccretionary rotation of the Eastern Klamath terrane are based almost entirely on our studies of the stratified rocks. These studies indicate that the Klamath Mountains experienced a series of rotational movements before being accreted to the North American continent. The Permian and Triassic strata of the Eastern Klamath terrane rotated clockwise approximately 100 degrees, the Jurassic strata 50 degrees, and the overlying Lower Cretaceous strata perhaps as much as 12 degrees. The small amount of rotation of the Lower Cretaceous presumably occurred after suturing of the terrane to North America. However, several Jurassic plutons in terranes lying west of the Eastern Klamath terrane have been measured by other investigators, and these show rotations that compare favorably on average to the Jurassic strata of the Eastern Klamath terrane.

We drilled the Mule Mountain stock (400 m.y.; Devonian) with the expectation of measuring a rotation perhaps even greater than the 100 degrees of clockwise rotation of the Permian strata. The Shasta Bally batholith (136 m.y.; Early Cretaceous) was selected for drilling, as it is one of several plutons in the Trinity Alps region that form the youngest plutonic belt of the Klamath Mountains province. If the Eastern Klamath terrane had virtually ceased rotation by the Early Cretaceous, we would expect Shasta Bally batholith to show little or no rotation, in contrast to the substantial rotation of older plutons of the Klamath Mountains. Plutons that have been studied in the Sierra Nevada show no rotation relative to stable North America. A similar lack of rotation of Shasta Bally batholith would suggest that the emplacement of the batholith was coincident with the accretion of the Klamath Mountains to North America. Laboratory work on the drill cores from our latest sampling has not yet been completed.

Reports

Irwin, W. P., 1984, Plutonic belts in allochthonous terranes of the Klamath Mountains, California and Oregon: Geological Society of America, Program with Abstracts, v. 16, no. 5, p. 290.

Irwin, W. P., 1984, Accreted terranes and plutonic belts of the Klamath Mountains, California and Oregon, in Howell, G.D., ed., Tectonostratigraphic Terranes of the Circumpacific Region: Earth Science Series, v. 1, Circumpacific Council for Energy and Mineral Resources (AAPG Bookstore), in press.

Barnes, I., Irwin, W. P., and White, D. E., 1984, Map showing world distribution of carbon-dioxide discharges and major zones of seismicity: U.S. Geological Survey, Miscellaneous Investigations Map I-1528, scale 1:40,000,000, with text, 10 p.

Mankinen, E. A., Irwin, W. P., and Gromme, C. S., 1984, Tectonic rotations suggested by paleomagnetic studies of the Eastern Klamath terrane: Society of Economic Paleontologists and Mineralogists, Pacific Section, San Diego meeting, abstract, p. 94-95.

Urban Hazard Seismic Field Investigations

9950-01919

Kenneth W. King
Branch of Engineering Geology and Tectonics
U.S. Geological Survey
Box 25046, MS 966, Denver Federal Center
Denver, CO 80225
(303) 236-1591

Investigations

The objective is to improve fundamental knowledge about how the ground response along the Wasatch is affected by local and regional geology.

An investigation of the feasibility of using reflection methods to identify the soil parameters controlling ground response is continuing in cooperation with the Kansas Geological Survey.

A Wasatch strong-motion program was developed with the cooperation of the Utah Geological and Mineral Survey.

A National Park investigation at Chaco Canyon was expanded to include seismic investigations at Hovenweep National Park.

Results

1. During this time period one article was published in the Eighth World Conference on Earthquake Engineering, and two were also submitted to the "Proceedings of the Conference on Earthquake Hazards along the Wasatch Urban Corridor," dealing with the ground-shaking hazard in Utah. A report on the results of the shallow-reflection program was also presented at the Urban Hazards Evaluation Workshop in Salt Lake City and will be in the proceedings.

2. The Mini Sosie (high-resolution reflection system) system has enabled us to finish several high-resolution profiles in the Wasatch area. A shallow-reflection experiment was made in Kansas along a test profile with very good results; however, the followup experiments in the Wasatch area have been delayed because of poor weather conditions. These experiments are developing the use of shear-wave reflection techniques to study structure in the upper 50-100 m.

3. A network of six strong-motion instruments was deployed at pertinent geologic areas in the Salt Lake urban areas. An additional network of 14 sites was selected by the USGS/UGMS committee. These sites will be instrumented with seismoscopes.

4. Additional data has been obtained from induced seismic motions on pertinent National Park archaeological sites; a report on the findings is now in preparation.

Reports

Hays, W. W., and King, K. W., 1984, The ground shaking hazard along the Wasatch Fault zone, Utah: Eighth World Conference on Earthquake Engineering, San Francisco, July 1984.

______1984 (in press), The ground shaking hazard along the Wasatch Fault zone, Utah, in Proceedings of conference, A workshop on evaluation of regional and urban earthquake hazards and risk in Utah, Salt Lake City, August 14-16, 1984: U.S. Geological Survey Open-File Report.

Rogers, A. M., Carver, D. L., Hays, W. W., King, K. W., and Miller, R. D., 1984 (in press), Preliminary estimates of geographic variation in relative ground shaking in the Wasatch Front urban corridor, in Proceedings of conference, A workshop on evaluation of regional and urban earthquake hazards and risk in Utah, Salt Lake City, August 14-16, 1984: U.S. Geological Survey Open-File Report.

Steeples, D. W., Miller, R. D., and King, K. W., 1984, An effort to determine Poisson's ratio in situ for near-surface layers, in Proceedings of conference, A workshop on evaluation of regional and urban earthquake hazards and risk in Utah, Salt Lake City, August 14-16, 1984: U.S. Geological Survey Open-File Report.

Coastal Tectonics, Western U. S.

9940-01623

Kenneth R. Lajoie
Branch of Engineering Seismology and Geology
U.S. Geological Survey
345 Middlefield Road, MS 977
Menlo Park, CA 94025
(415) 323-8111, ext. 2642

Investigations

1. Uplift and deformation of Pleistocene and Holocene marine strandlines.

2. Stratigraphic/geomorphic analysis of neotectonics along the Palos Verdes fault, Los Angeles, California.

3. Amino-acid geochronology of fossil molluscan faunas from uplifted and deformed Pleistocene terraces and deposits.

4. Stratigraphic/geomorphic analysis of Neogene tectonics of the Mendocino triple junction, Humboldt County, California.

5. Coastal erosion, San Mateo County, California.

6. Post-earthquake investigations of April 24, 1984 Morgan Hill, California earthquake.

Results

1. A set of equations relating the present and initial elevations of marine strandlines has been derived from basic principles. These equations and their graphical representations permit correlation and relative age dating of emergent strandlines in areas undergoing different rates of uplift even if no strandline is independently dated. If the age and initial elevation of at least one strandline in a sequence is known, the ages and initial elevations of all other strandlines can be determined. These equations also provide tests for constant rates of uplift.

2. D. Ponti mapped the deformed late Pleistocene marine sediments exposed in roadcuts and quarries along the NE flank of the Palos Verdes Hills. Along Gibson Boulevard, Palos Verdes Sand (~120 ka B.P.) unconformably overlies the San Pedro Sand (200-300 ka B.P. (?)) on the NE limb of the Gaffey anticline (SW side of the Palos Verdes fault).

Sediment and fossil samples from boreholes on the NE side of the fault are being analyzed to correlate across the fault and determine amounts and rates of vertical fault displacement.

3. D. Ponti and S. Mathieson set up and debugged amino-acid equipment used to analyze fossil materials for correlating and dating purposes. P. McKereghan prepared 200 fossil samples and L. Conlan ran 1200 amino-acid analyses on Ponti's collections in samples from the Palos Verdes area. Preliminary results indicate that the Palos Verdes Sand may represent more than one paleo-sea level highstand. (85-140 ca B.P.(?)). Also, the slightly dipping (2°-4°) sediments exposed along Gibson Boulevard probably correlate with steeply dipping (30°-40°) strata exposed on the east wall of the Chandler gravel pit about 4 km to the NW.

Preliminary amino-acid data indicate that each molluscan family has a distinct amino-acid "fingerprint," which can be used to identify small or worn shell fragments. Such identification is important because the rates of amino-acid racemization differ among different families. Therefore, only data from the same family can be compared for correlation and dating purposes. Many outcrop and borehole fossil assemblages consist only of broken and worn shell fragments.

4. P. McCrory completed sampling and describing the Eel River beds near the Mendocino triple junction and submitted planktic foraminifera samples for oxygen-isotope analysis to date the section and correlate it with the DSDP section offshore. McCrory is also working with Stanford geologists to create a computer graphics program to integrate Cenozoid plate tectonics and geology of western North America (timing and rates of faulting and basin formation and ages of volcanism).

5. Lajoie and Mathieson completed a study of coastal erosion in San Mateo County. Exceptionally high tides and storm waves caused considerable damage along the Pacific coast during the winter of 1982 and 1983. Extreme cliff erosion (up to 30 m) occurred mostly on the northern sides of headlands and small promontories. Single severe storms or short periods (decades(?)) of higher than normal storm activity related to minor climatic changes may be recorded as beach berms and erosional notches in the Holocene geologic record. The record of these "storm events" may be interpreted as coseismic uplift events in areas of rapid crustal deformation. On the Island of Iwo Jima, a volcanic edifice steadily rising at 20 cm/yr (for at least 200 yrs), Kaizuka mapped numerous emergent storm-cut terraces that might be misinterpreted as coseismic notches.

6. Mathieson and Lajoie helped in post-earthquake investigations of primary and secondary geologic effects of the April 24, 1984 Morgan Hill earthquake. No primary ground rupture was found along any of the well-delineated segments of the Calaveras fault. The pattern of structural damage indicates seismic energy was focused along the southwest part of the epicentral region.

Reports

Lajoie, K. R., and Mathieson, S. A. (in press), Coastal erosion and hazards, San Mateo County, California: *in* Griggs (ed.), Coastal erosion in California (map and text).

Ponti, D. J., and Tinsley, J. C., 1984, Inherent uncertainties in Quaternary dating methods and slip-rate evaluations (abs): Earthquake notes, Seismological Society of America, v. 55, no 1.

Mathieson, S. A., 1984, Comparison of glacial sequences between the Yuba-Feather divide, northern Sierra Nevada and Mono Basin, Central Sierra Nevada, California: Evidence for an Illinoian Tahoe glaciation (abs): U.S. Geological Survey, Abstracts with programs, v. 16, no. 5.

Harms, K. K., Clark, M. M., Rymer, M. J., Bonilla, M. G., Harp, E. L., Herd, D. G., Lajoie, K. R., Lienkaemper, J. J., Mathieson, S. A., Perkins, J. A., Wallace, R. E., and Ziony, J. I., 1984, The April 24, 1984, Morgan Hill, California earthquake: The search for surface faulting, *in* Hoose (compiler), U.S. Geological Survey Open-File Report 84-498A.

Mathieson, S. A., 1984, Damage to engineered structures associated with the April 24, 1984 Morgan Hill earthquake, Santa Clara County, California: *in* Hoose, S. (compiler), U.S. Geological Survey, Open-File Report 84-498A.

Clark, M. M., Harms, K. K., Lienkaemper, J. J., Harwood, D. S., Lajoie, K. R., Matti, J. C., Perkins, J. A., Rymer, M. J., Sarna-Wojcicki, A. M., Sharp, R. V., Sims, J. D., Tinsley, J. C., Ziony, J. I., 1984, preliminary slip-rate table and map of late-Quaternary faults of California: U.S. Geological Survey Open-File Report 84-106.

Ponti, D. J., 1984, Amino-acid composition of Pleistocene bivalves: Preliminary results from the San Pedro area, California (abs): Western Society of Malacologists, Santa Cruz.

Neogene Paleomagnetic Stratigraphy, Transverse Ranges, California: Timing and Deformation Rates of Potentially Active Faults

14-08-0001-21901

Shaul Levi
Geophysics, College of Oceanography
Oregon State University
Corvallis, Oregon 97331
(503) 754-2912

Neogene formations are widely exposed in parts of the Transverse Ranges, in areas undergoing rapid urbanization north and west of Los Angeles. These formations from oldest to youngest include the Modelo, Towsley, Pico and Saugus. Our paleomagnetic (PM) investigations of the continental Saugus Formation, in the East Ventura basin just west of Newhall along the Santa Clara River and the transmission line sections, indicate that the Saugus was deposited mostly during the Matuyama reversed polarity epoch and is younger than 2.48 MY (million years). The youngest Saugus exposed in both sections was deposited during the normal polarity Brunhes epoch and is younger than 0.7 MY. Moreover, our PM results indicate an average sedimentation rate of 0.9 km/MY for the transmission line and Santa Clara River sections. The marine Pico Formation is less well suited for PM investigations and many of its finer-grain deposits are severely overprinted. However, reversed sites from the upper Pico suggest that they too were deposited during the Matuyama. The sections of Pico in Lyons Canyon and Towsley and Modelo in the Towsley Canyon were severely overprinted by the present field and have thus far not yielded useful PM results.

This year we have extended our study to the southern foothills of the San Gabriel and Santa Susana Mountains in Los Angeles County. We conducted initial sampling along Little Tujunga Canyon (Saugus and Towsley/Pico Formations), Kagel Ridge (Saugus and Towsley/Pico Formations), and Lower Van Norman Lake (Sunshine Ranch and upper members of the Saugus Formation). Our results to date are as follows: 1) nine of the ten sites sampled along the Lower Van Norman reservoir are reversed, presumably of Matuyama age. The lowest site of the approximately 890 m stratigraphic section is normal. 2) Thirty-two sites were sampled along Kagel Ridge. The section is predominantly reversed, but four normal polarity events were identified in Saugus strata of the approximately 690 m stratigraphic section. As in the Newhall area, the Saugus PM results were clearly superior to those of the Towsley and Pico, for reasons that are not yet known. Additional sampling is necessary along both Kagel Ridge and Lower Van Normal Lake sections to ascertain which Matuyama normal polarity events were observed.

Earthquake Hazards Studies, Upper Santa Ana Valley and Adjacent Areas, Southern California

9540-01616

Jonathan C. Matti
Branch of Western Regional Geology
U. S. Geological Survey
345 Middlefield Road, MS 975
Menlo Park, California 94025
(415) 323-8111 ext. 2358, 2353

Investigations

1. Studies of the Quaternary history of the upper Santa Ana River Valley. Emphasis currently is on: (a) generation of a liquefaction susceptibility map; and (b) the three-dimensional distribution of the valley fill and its lithologic, lithofacies, and pedogenic character.

2. Neotectonic studies of the Crafton Hills-Yucaipa Valley, Banning, and San Andreas fault zones. The study has focused on: (a) mapping fault strands that deform crystalline basement rocks, Tertiary sedimentary rocks, and Quaternary surficial units; (b) identification of Quaternary units to establish Quaternary depositional patterns and the relative ages of displacements along various fault strands; and (c) interpreting relationships between the Banning fault system and the south branch of the San Andreas fault.

Results

1. S. E. Carson and J. C. Matti have reached the report-writing stage of a liquefaction evaluation for the San Bernardino Valley. No new results to report.

2. Mapping by J. C. Matti adjacent to the San Andreas fault in the Mill Creek region of the southwestern San Bernardino Mountains and the Liebre Mountain region of the northwestern Transverse Ranges has led to the recognition of distinctive crystalline rocks that provide a new constraint for palinspastic reconstruction on the San Andreas fault in southern California. The San Andreas fault system here consists of several fault zones (San Andreas, Banning, San Gabriel) that together have produced cumulative right-lateral offsets comparable to the 300-km post-Miocene offsets originally proposed for the San Andreas fault in central California. In southern California, the San Andreas fault alone accounts for a large fraction of the total 300-km offset, but a comparison of palinspastic reconstructions proposed in the literature shows that significant disagreement exists regarding both the amount of offset on the fault (180 to 270 km) and the timing and amount of offset on associated right-lateral and left-lateral faults. The most widely cited reconstructions require about 240 km of right-lateral offset on the San Andreas fault; this figure is based on restoration of sedimentary and crystalline rocks of the Soledad Basin region and the northwestern San Gabriel Mountains to the Orocopia Mountain region northeast of the Salton Trough.

Crystalline rocks in the San Bernardino Mountains provide a possible piercing point that constrains total offset on the San Andreas fault zone to about 160 km in southern California, and yields a long-term different reconstruction for the San Andreas and San Gabriel faults. The San Bernardino Mountains are underlain by Mesozoic batholithic rocks and older prebatholithic rocks that are truncated on the west and southwest by several strands of the San Andreas fault zone. Although the mountains now form a massive, high-standing crystalline terrain undergoing dissection, before Pliocene uplift the region included lowlands that received sedimentary deposits. Western parts of this region largely were covered with upper Miocene and Pliocene sediment derived from the Mojave Desert; however, eastern parts of the terraine included emergent crystalline highlands that formed local sources for upper Miocene and Pliocene sediment. This paleogeographic setting is relevant to recognizing crystalline rocks offset from the region since middle Miocene time: if the San Bernardino Mountains were a region of highlands and sedimented lowlands during Miocene and Pliocene time, then crystalline highlands that were truncated and offset by the San Andreas fault still should be recognizeable as emergent highlands to the northwest on the opposite side of the fault (assuming they have not been obscured or buried by subsequent tectonism or sedimentation).

In the Mill Creek region of the San Bernardino Mountains, a distinctive belt of rocks that is truncated by the San Andreas fault provides a possible key to recognizing rocks offset from the San Bernardino Mountains. These rocks include a body of megaporphyritic hornblende monzogranite to quartz monzonite characterized by subhedral to euhedral phenocrysts of potassium feldspar as much as 8 cm long (monzogranite of Manzanita Springs of Matti and others, 1983). If the megaporphyry formed a crystalline highland in the San Bernardino terrane prior to Miocene truncation by the San Andreas fault system, then only three regions exist where offset counterparts of this rock might crop out: The San Gabriel Mountains, the Liebre Mountain region, and the Frazier Mountain region. Because the Frazier Mountain and San Gabriel Mountain regions contain prebatholithic rocks not found in the San Bernardino Mountains, the Liebre Mountain block remains as the only region where the offset megaporphyry might crop out. There, in the northwestern part of Liebre Mountain, porphyritic granitoid rock occurs that is indistinguishable in hand specimen from the megaporphyry of the Mill Creek region.

I propose that the two bodies represent segments of a formerly continuous pluton that was cut by the San Andreas fault zone. The severed parts have been offset 160 to 170 km, although I favor the smaller figure. Cross-fault correlation of the two megaporphyry bodies is supported by geochemical and isotopic studies by V. A. Frizzell, J. M. Mattinson, and J. C. Matti, who demonstrated that the Liebre Mountain and Mill Creek rocks have similar chemical compositions, intrusive ages (Triassic, about 215 m.y.), and thermal histories.

Restoration of the megaporphyritic bodies leads to a palinspastic reconstruction for the San Andreas and San Gabriel faults that reassembles crystalline and sedimentary terranes differently from conventional reconstructions. The new reconstruction allows only about 220 km of offset on the San Andreas and San Gabriel fault zones (160 km + 60 km), which is about 80 to 100 km short of the 300-km post-Miocene offsets that have been documented for the San Andreas fault in central California. This shortfall requires the existence of another Miocene strand of the San Andreas fault system in southern California.

Only 160 km of offset on the San Andreas fault since its inception south of the Garlock fault yields a long-term slip rate of 3.2 to 4 cm/year during the last 4 or 5 m.y. This rate compares well with Holocene slip rates of about 3.5 cm/year on the San Andreas fault north of the Garlock fault, but contrasts with long-term rates of 4.8 to 6 cm/year for conventional reconstructions that require 240 km of Pliocene and Quaternary offset on the San Andreas fault during the last 4 or 5 m.y. If the megaporphyry is a valid piercing point for total offset on all strands of the San Andreas fault, and if the San Andreas has been slipping uniformly since the opening of the Gulf of California 4 or 5 million years ago, then the long-term slip rate for the San Andreas is compatible with short term rates.

Reports

Matti, J. C., Cox, B. F., and Iverson, S. R., 1983, Mineral resource potential map of the Raywood Flat Roadless Area, San Bernardino and Riverside Counties, California: U.S. Geological Survey Miscellaneous Field Studies Map MF-1563-A, scale 1:62:500.

Matti, Jonthan C., Distinctive megaporphyritic monzogranite offset 160 km by the San Andreas fault, southern California: a new constraint for palinspastic reconstructions. (Received Director's approval Nov. 13, 1984, submitted to GEOLOGY).

Quaternary Fault History and Earthquake Potential of the Hansel Valley area, north-central Utah

14-08-001-21899

James McCalpin
Department of Geology
Utah State University
Logan, Utah 84322
(801) 750-1220

Objective: The 1934 M_L 6.6 Hansel Valley earthquake was the largest earthquake in Utah history and one of only three events (besides the 1959 M 7.1 Hebgen Lake and 1983 M 7.3 Borah Peak) to rupture the ground surface in the Intermountain Seismic Belt. The Hansel-Pocatello Valleys area has been a source of continuing, intense post-1934 seismic activity, including a 1975 M 6.0 shock and thousands of smaller events. The purpose of this study is to examine Hansel Valley for evidence of pre-historic earthquakes, either as fault scarps, offset Quaternary lacustrine or alluvial deposits, or as seismic-induced liquification phenomena. If possible, the magnitude and recurrence of such events would be calculated using standard techniques.

Surficial Geologic Mapping: Quaternary alluvial and lacustrine deposits have been subdivided into approximately 20 map units, based on genesis and age, on a 1:50,000 scale map. The Bonneville, Provo, and Gilbert shorelines are well-developed and define the major age subdivisions. As many as 42 recessional shorelines occur below the Provo level, but are discontinous and have not been correlated across the valley.

Bonneville-cycle (Jordan Valley cycle of Scott et al, 1983) and Little Valley(?)-cycle deposits are exposed in several 5 m to 12 m-deep arroyos along the valley margins and in the valley center. Well laminated silts and clays of Little Valley(?) age are unconformably overlain by transgressive beach gravels of Jordan Valley age in gully walls at an elevation of about 4450 feet msl; no inter-cycle soils have been observed. Transgressive gravels are overlain by up to 10 m of alternating laminated versus intensely convoluted silts, the latter though to result from periodic seismic shaking of saturated lake-bottom sediments.

Arroyos in the central and northern valley area expose pre-Little Valley(?) alluvial and lacustrine sediments within less than 2 m of the surface. These semi-indurated strata dip up to 25° and are offset by faults with up to 4.5 m normal displacement; no faults offset the ground surface. The exact age of these deposits is presently unknown; some may be as old as late Tertiary, equivalent to the Salt Lake Formation (Oligocene-Pliocene).

Neotectonics: The Bonneville and Provo shorelines rise approximately five feet per mile from the north to south ends of Hansel Valley. Because the shoreline deflections are similar, it is implied that major isostatic rebound occurred after the abandonment of the

Provo shoreline. Preliminary observations indicate that the shorelines on the west and east sides of the valley are at similar elevations, suggesting that no major post-Bonneville eastward tectonic tilting has occurred like that reported for nearby Pocatello Valley (McCalpin and Garr, 1984).

Two small fault scarps occur along the inferred trace of the North Promontory fault on the east valley margin. The northern scarps faces west, is 0.6 km long, 10.0 m high and offsets a Bonneville delta. A shorter splay fault east of Bulls Pass offsets pre-Bonneville alluvial fans as much as 9.5 m, also down to the west. Slope-angle vs scarp height data suggest the northern scarp is younger than the Bonneville shoreline, while the southern one is older.

The trace of the 1934 surface break across the mudflats of southwestern Hansel Valley is still expressed as a degraded east-facing scarp up to 49 cm high. North of the mudflats the trace continues for about 10 km as an east-facing scarp 1.6 m to 9.0 m high which offsets numerous shorelines below 4600 feet. The variation in scarp height, the arcuate shape of some scarp segments, and control of recessional shoreline positions by the scarp strongly suggests that it was formed underwater, probably by a single 2 m displacement event. Post-1952 gully erosion across the fault zone exposes a complex of 11 normal faults within a 240-m long zone, both down to the east and west, with displacements of up to 2.5 m in a single event. Most faults offset Little-Valley (?) and the transgressive Bonneville deposits, but are truncated by a Holocene unconformity (Fig. 1). However, some faults are truncated by the Bonneville transgression indicating that at least three fault events have occurred on this strand in late Pleistocene time.

Two faults are well exposed in roadcuts of Interstate 84 at the north end of Hansel Valley. The Rattlesnake Pass cut (Fig. 2) exposes a 2.6 m down-to-the-east normal offset of early to mid-Pleistocene channel fills and superposed soils which overlie Tertiary basalts. Evidence of only a single very recent event is present, despite the fact that soil development supports an age of several hundred thousand years for the channel-fill sequence. The inferred main trace of the down-to-the-west North Promontory fault (not exposed) is about 100 m west of the exposed fault, suggesting the exposed fault is an antithetic feature. The Hansel Valley Exit cut 2 km further west exposes shattered Paleozoic carbonates (Oquirrh Formation?) in fault contact with locally-derived Quaternary alluvium, loessy colluvium, and volcanic ash (Fig. 3). The ash is dragged up into the fault zone and offset an unknown amount down to the east; it may be of mid-Pleistocene age. Ash identification and C 14 and amino acid dating of snails is currently underway to fix the absolute age of deformed deposits.

References Cited:

McCalpin, James, and Garr, J. D., 1984, Late Pleistocene lake shorelines in Pocatello Valley, Utah-Idaho and their use in neotectonic reconstruction; GSA, Abstracts with Programs, vol. 16, no. 4, p. 247.

Scott, W. E., McCoy, W. D. and Shroba, R. R., 1983, The last two cycles of Lake Bonneville; GSA, Abstracts with Programs, vol. 15, no. 5, p. 300.

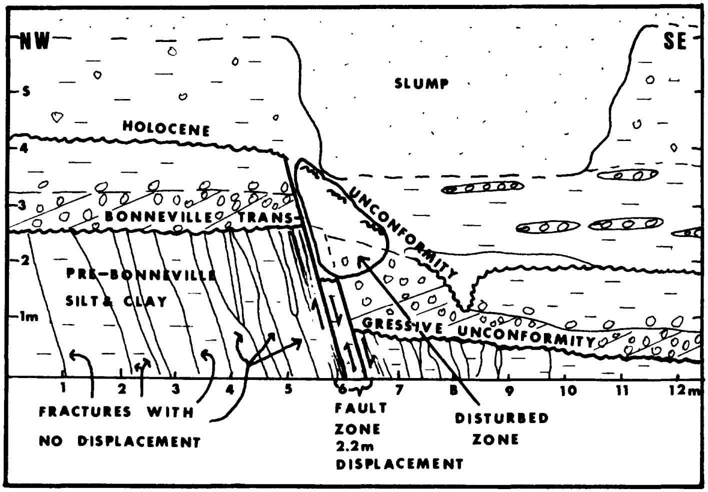

Fig. 1. Westernmost fault in the complex fault zone on the west side of Hansel Valley. The fault here represents a single post-Bonneville transgression event. Holocene sediments overlie the fault in an undeformed cut-and-fill terrace.

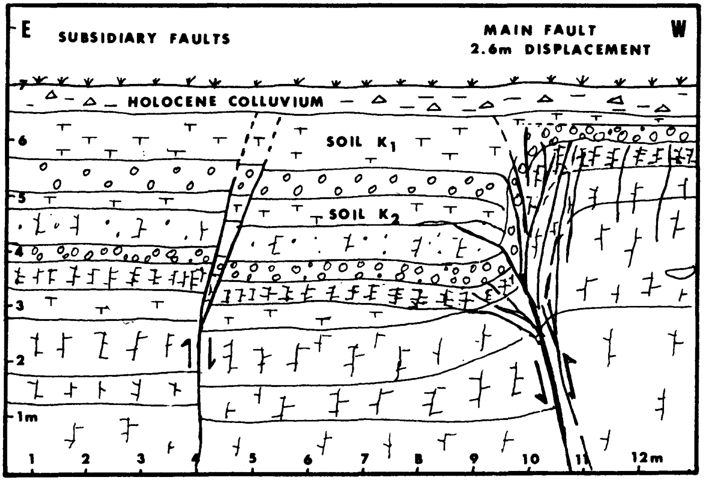

Fig. 2. Detail of the fault in the Rattlesnake Pass roadcut. A single 2.6 m displacement offsets all deposits except the surface Holocene colluvium. The upper part of the soil carbonate in Soil K1 also extends across the fault, suggesting it is younger than faulting. Intensity of line patterns in soil B horizons indicates degree of development

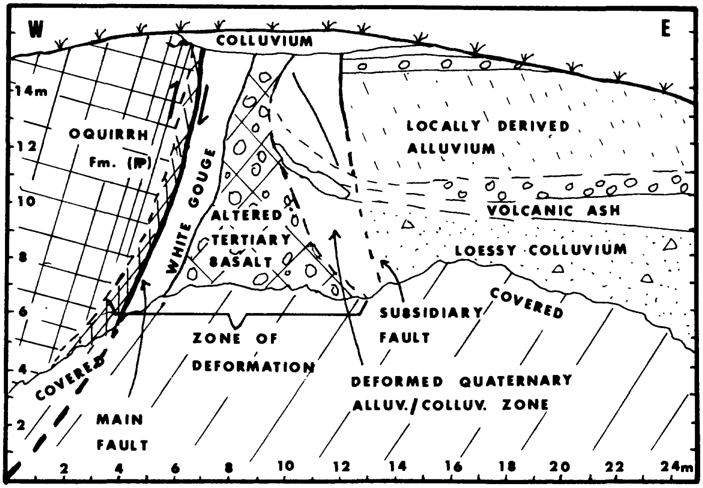

Fig. 3. Fault in the Hansel Valley Exit roadcut which juxtaposes progressively more shattered and altered Paleozoic carbonates against Tertiary basalts and Quaternary alluvium/colluvium. The east side of the cut represents a depositional swale, so the complete Quaternary section was not necessarily ever deposited to the west of the fault; thus, displacements can only be estimated.

Mississippi Valley Seismotectonics

9950-01504

F. A. McKeown
Branch of Engineering Geology and Tectonics
U.S. Geological Survey
Box 25046, MS 966, Denver Federal Center
Denver, CO 80225
(303) 236-1575

Investigations

1. Interpretation of 320 km of seismic-reflection profile data.

2. Preliminary reprocessing of seismic-reflection data to investigate deep structure.

3. Quantitative geomorphic study of stream profiles in the southeastern part of the Ozark Mountains.

4. Processing and interpretation of seismic-reflection data recorded on the Mississippi River.

5. Analysis of level line data.

Results

1. A report by A. J. Crone, F. A. McKeown, S. T. Harding, R. M. Hamilton, D. P. Russ, and M. D. Zoback describing a structural disrupted zone along the axis of the Reelfoot Rift was written and technically reviewed and is currently being revised for submission to Geology. The disrupted zone is coincident with the northeast-trending zone of epicenters between Caruthersville, Mo., and Marked Tree, Ark., and underlies the area with the greatest number of sandblows in the New Madrid region. On seismic-reflection profiles the disrupted zone is characterized by loss of coherent reflectors below an antiform of Cambro-Ordovician rocks. The relfectors in the antiform diverge from a reflector identified as magnetic basement suggesting that the antiform is the result of intruded material. The origin of the antiform and disrupted zone is unknown but is important because they are associated with a major seismogenic zone.

2. Reprocessing of field tape records of seismic-reflection profiles to 11 s two-way traveltime has begun and shows discontinuous but strong deep reflectors, particularly at depths of about 15 and 30 km. Preliminary interpretation of these zones suggests that they may correlate with the tops of crustal layers with velocities of 6.60 and 7.30 km/s shown on refraction data by Mooney and others (1983).

3. Analysis and interpretation of stream-profile data is continuing and a report on the data has been started. The data consist mostly of digitized elevations of every contour crossed by a stream and the distance of the

crossing from the stream source for 70 streams in the southeastern part of the Ozark Mountains. Geologic data from E. E. Glick and Boyd Haley (written commun., 1983) and discharge data from Lamb and others (1983) and Waite and others (1983) are also included in the data base. From these data the following plots and parameters have been made or calculated:

(1) Stream profiles on Cartesion and semilog coordinates
(2) Stream-gradient indices
(3) Stream gradients
(4) Gray-tone scale map of stream-gradient indices
(5) Two-dimensional hypsometric analysis for total stream length
(6) Subenvelope map
(7) First derivatives of gradients
(8) Plots and statistical analyses of various combinations of stream length, gradients, gradient indices and discharge.

Interpretations to date have led to a number of paradoxical relationships among gradient, stream length, discharge and drainage basin area. In general, discharge information indicates lower stream gradients in the Ozarks than in a geologically similar region in central Pennsylvania as reported by Brush (1961). Calculated mean and median gradients are also lower. The rate of change of gradient to stream length, however, for streams on the Salem Plateau (a carbonate terrain) of the Ozarks is much less than for streams in central Pennsylvania, regardless of lithology, and for streams in sandstone and shale in the Ozarks. Reaches more than 10 and 100 km from drainage divides in the Salem Plateau have steeper gradients than streams in shale and sandstone, respectively. This may account for profiles of the plateau streams being less concave than streams south of the plateau in sandstone and shale. Explanations of the anomalous gradient stream length, discharge, and drainage basin area relationships are quite speculative. Current thought is that they are related to the large changes in base level during the Pleistocene and Holocene with resulting periods of much aggradation and degradation.

4. Progress on the interpretation of the seismic-reflection data recorded on the Mississippi River has been slow because of unanticipated redirection of the work of the investigators.

5. Compilation and analysis of level line data for the upper Mississippi embayment and vicinity was completed by Richard Dart. Compilation and analysis of breakout zones in drill holes for Mark and Mary Lou Zoback has precluded timely preparation of an open-file report planned for the level line data.

Reports

McKeown, F. A., 1984, New Madrid seismic zone, Part I, Historical review of studies; Part II, Contemporary studies by the U.S. Geological Survey, _in_ Proceedings of the New Madrid seismic zone symposium, Cape Girardeau, Missouri, April 27-28, 1984: U.S. Geological Survey Open-File Report 84-770.

References cited

Brush, L. M., Jr., 1961, Drainage basins, channels, and flow characteristics of selected streams in central Pennsylvania: U.S. Geological Survey Professional Paper 282-F, p. 145-181.

Lamb, T. E., Porter, J. E., Lambert, B. F., and Edds, J., 1983, Water resources data, Arkansas, water year 1982: U.S. Geological Survey Water-Data Report AR-82-1, 504 p.; available from U.S. Department of Commerce National Technical Information Service, Springfield, VA 22161 as Report USGS/WRD/HD-84/010.

Mooney, W. D., Andrews, M. C., Ginzburg, A., Peters, D. A., and Hamilton, R. M., 1983, Crustal structure of the northern Mississippi embayment and a comparison with other continental rift zones: Tectonophysics, v. 94, p. 327-348.

Waite, L. A., Hatten, D. O., and Cross, P. W., 1983, Water resources data, Missouri, water year 1982: U.S. Geological Survey Water-Data Report MO-82-1, 341 p.; available from U.S. Department of Commerce National Technical Information Service, Springfield, VA 22161 as Report USGS/WRD/HD-83/079.

Historical Seismicity in the Southern Appalachian Seismic Zone

14-08-0001-21902

Donald J. Reinbold, Arch C. Johnston
Tennessee Earthquake Information Center
Memphis State University
Memphis, Tennessee 38152
(901) 454-2007

Objective: The Southern Appalachian Seismic Zone (identified by Bollinger, 1973) is a region in the eastern United States for which existing historical earthquake catalogs are clearly inadequate for delineating seismic source zones and/or evaluating seismic hazard. These inadequacies result from incompleteness, mislocation of epicenters, and incorrect assessment of intensity/magnitude. This study is designed to produce a thorough and consistent catalog of historical seismicity.

Data Acquisition and Analysis: Work on this project has been divided into 2 phases.

1. Phase 1 objectives were to complete compilation and editing of data from over 170 published sources previously begun by P. I. Reinbold at the Tennessee Valley Authority. These data will be integrated into a master file which includes source parameters for each earthquake in addition to all available reference data complete to the most basic source cited, e.g., personal interviews, newspaper accounts, diaries, etc. These data are included so that users of the catalog may easily add to it or reinterpret it if desired. Analysis of the data from these published sources must take into consideration: (a) the objectives of each contributing author in compiling his information; (b) how he acquired it and from where; and (c) any temporal and/or areal constraints on data collection. Phase 1 has now been completed.

2. Phase 2 of this project is intended through a systematic search of archived newspapers to: (a) insure the completeness of the catalog; (b) provide more information to aid in refining locations, either through interpretation of Imax or through associations of foreshock/aftershock sequences; and (c) help estimates of size from either additional reports on maximum effects or through delineation of the area of perceptibility. Obviously, demographics will play a large part in the assessment of these data. Phase 2 is well under way; the location and availibility of archived newspapers have been determined and data collection efforts have begun.

EARTHQUAKE RESEARCH IN THE WESTERN GREAT BASIN

Contract 14-08-0001-21863

A.S. Ryall, U.R. Vetter, and E.J. Corbett
Seismological Laboratory
University of Nevada
Reno, NV 89557-0018
(702) 784-4975

Investigations

This program supports continued studies with research focused on: (1) seismicity and focal mechanisms associated with magma injection in Long Valley area; (2) geometry of magma bodies in Long Valley caldera; (3) systematic variations in focal mechanisms along the Sierra Nevada - Great Basin boundary zone; (4) premonitory seismicity patterns preceding the 1980 Mammoth Lakes earthquakes; (5) re-analysis of the May 1980 Mammoth Lakes earthquake sequence; and (6) digitization of field tapes for a more detailed analysis of the 1978 Wheeler Crest earthquakes. Progress in selected areas of this program is described below.

Results

A. *Systematic variations in focal mechanisms.*

Continuing studies by Vetter (1984, 1985) appear to confirm that in the Mammoth Lakes area, there is a clear relation between focal mechanism type and focal depth. First motions from over 100 earthquakes indicate that shallow earthquakes are primarily strike-slip events while deeper events exhibit oblique and normal mechanisms. This is taken to mean that the direction of maximum compression is horizontal for the shallow crust and becomes more vertical with increasing depth. The transition takes place in the depth range of 6-9 km, which is also the depth range of maximum earthquake occurrence. Also, 95% of the seismicity is restricted to the upper 12 km of the crust. A possible explanation may be made if one assumes that the temperature gradient is somewhat greater in the Mammoth Lakes area than it is in the Great Basin to the east, and that 12 km represents the depth at which silicate rocks behave plastically, corresponding to a temperature of 450°−500° C. If the gradient is linear, this would imply that strike-slip events occur in a regime where the temperature is below 300° C., while the normal and oblique events occur at depths where the temperature is higher. Considering other models of earthquake mechanics, this may indicate that strike-slip earthquakes occur in the brittle regime, while the normal events occur in the brittle-plastic transition zone.

B. *Studies of the 1980 Mammoth Lakes earthquake sequence*

Soon to be published work by Priestley *et al.* (1985) studies the spectral amplitudes and derives moments for 24 of the 1980 Mammoth Lakes earthquakes. The spectra do not show the pronounced spectral peaks that would be predicted by theoretical models of tensile cracks opening with fluid injection, and have been observed in other volcanic areas. They observe that these spectra are similar to the spectra from "tectonic" earthquakes and conclude that the complexities observed in the regional and teleseismic seismograms are the result of complexities in double-couple sources and are not due to compensated linear vector dipole sources.

A Master's thesis by C.S. Lide has given new insight into the 1980 earthquake sequence. Lide (1984) used only data from a select group of stations, chose a well-controlled earthquake for a master event, and located 344 aftershocks relative to it. The most striking features of his locations are two parallel zones of aftershocks that strike N20°E and dip vertically. These features are in agreement with the vertical strike-slip focal mechansims derived from short-period first-motion data for the three largest shocks ($M_L > 6$). These locations also indicate that the tectonic process was quite complex as many of the earthquakes occurred on other structural trends that are discussed in detail by Lide and Ryall (1985).

Since 1978, much of the seismicity and most of the large earthquakes have occurred in the Sierran mountain block south of the Long Valley caldera. The prevailing poor station coverage in this area was alleviated this summer by the repair of one station and the installation of five new ones. With the the addition of these six stations we are building up a high quality digital data base on the earthquakes that are continuing to occur in the same locations as those of the 1980 sequence, and since. We anticipate that we will soon have enough data to use well-controlled present-day earthquakes to systematically relocate the earlier events.

C. *Geometry of magma bodies in the Long Valley area.*

There is a growing body of evidence that magma bodies in the Long Valley area may not be limited to the Long Valley caldera. Seismic signals with anomalous characteristics have now been observed by Ryall and Ryall (1984) for earthquakes in the mountain block south of the caldera recorded at stations to the east and northeast. These data indicate the presence of a possible magma body 10-12 km south of the caldera in the vicinity of the southern termination of the Hilton Creek fault, and just west ot the Wheeler Crest. New stations installed in the mountain block and in the White Mountains to the east are expected to provide data to better delineate this feature. Seismograms from stations in the mountain block are already showing unexpected phases arriving prior to S that bear the appearance of replicated P-phases. These phases may be body-wave reflections which suggests a strong reflecting body in this same region.

D. *Study of the 1978 Wheeler Crest earthquakes.*

Research conducted at UNR has identified a number of factors which point to the importance of the Wheeler Crest earthquake of October 4, 1978: 1) it was evidently the event which initiated the Mammoth Lakes earthquake sequence; 2) the above-mentioned evidence for a magma body just west of the Wheeler Crest; and 3) suggestions by other workers that, like the 1980 Mammoth Lakes earthquakes, this event too has a complicated source that cannot be explained by a single double-couple. In 1978 the University of Nevada monitored the aftershocks of this earthquake with 6 continuously recording analog stations and two 3-component digital event recorders (Peppin, 1984). We have recently finished construction and testing of a hardware device designed to digitize the analog field tapes directly onto our 11/70 computer. W.A. Peppin has just begun the effort of transferring a sample of the data to disc for waveform analysis and for precise master-event location of the aftershocks, with the aid of a team of graduate students. An initial sampling of the tapes indicates that approximately 4,500 aftershocks were recorded on the field tapes.

E. *Reports*

Lide, C.S. (1984). Aftershocks of the May 1980 Mammoth Lakes earthquakes, *M.S. thesis*, Univ. Nevada.

Lide, C.S. and A.S. Ryall (1985). Relationship between aftershock locations and mechanisms of the May, 1980 Mammoth Lakes earthquakes, *J. Ceophys. Res.*, submitted.

Ryall, A.S. (1984). Mammoth Lakes earthquake sequence: Seismological investigations. *in* Western Geological Excursions, volume 2, *Geol. Soc. Amer. annual meeting guidebook*, 72-79.

Ryall, A.S., and F.D. Ryall (1984). Shallow magma bodies related to lithospheric extension in the western Great Basin, western Nevada and eastern California, *Earthquakes Notes*, **55, no. 1**, 11.

Peppin, W.A. (1984). The University of Nevada, Reno, portable digital event recording seismograph system, *Seismological Laboratory rpt.*, Univ. Nevada, 115p.

Priestley, K.F., and J.N. Brune (1984). Source mechanism, surface wave excitation, and m_b-M_S analysis of a volcanic earthquake sequence, Mammoth Lakes, California, *Terra Cognita*, **4**, 373.

Priestley, K.F., J.N. Brune, and J.G. Anderson (1984). Surface wave excitation and source mechanism of Mammoth Lakes, California earthquakes, *Earthquakes Notes*, **55, no. 1**, 14.

Priestley, K.F., J.N. Brune, and J.G. Anderson (1985). Surface wave excitation and source mechanisms of the Mammoth Lakes earthquake sequence, *J. Geophys. Res.*, submitted.

Sanders, C.O. (1984). Location and configuration of magma bodies beneath Long Valley, California, determined from anomalous earthquake signals, *J. Ceophys. Res,* **89**, 8287-8302.

Vetter, U.R. (1984). Focal mechanisms and crustal stress patterns in western Nevada and eastern California, *Annales Geophysicae*, in press.

Vetter, U.R. (1984). Relations between focal mechanism and temperature in the western Great Basin, *Terra Cognita*, **4**, 374.

Vetter, U.R. (1985). Focal mechanisms and frequency-depth distribution of earthquakes in the Mammoth Lakes area, *J. Geophys. Res.*, submitted.

Late Holocene Behavior San Andreas Fault

Contract No. 14-08-0001-21275

Kerry Sieh
Division of Geological and Planetary Sciences 170-25
California Institute of Technology
Pasadena, CA 91125
(818) 356-6115

Investigations

Field work at the Indio site for 1984 was completed in the late Spring, and will be resumed in January 1985. Radiocarbon samples are being analyzed currently. Weldon continues toward completion of his Ph.D. dissertation on the neotectonics of the San Andreas and related faults in the Cajon Pass region.

Results

See previous summary report (vol. XVIII, p. 126-128).

Publications since previous report

Sieh, K., 1984, Lateral offsets and revised dates of large earthquakes at Pallett Creek, California, J. Geophys. Res., 89, 7641-7670.

Sieh, K., and R. H. Jahns, 1984, Holocene activity of the San Andreas fault at Wallace Creek, California, Geol. Soc. America Bull., 95, 883-896.

Sieh, K., and R. Weldon, in press, GSA Bull., Oct. 1984, Holocene rate of slip and recurrence interval for large earthquakes on the San Andreas fault in Cajon Pass, southern California.

Quaternary Framework for Earthquake Studies
Los Angeles, California

9540-01611

John C. Tinsley
Branch of Western Regional Geology
U. S. Geological Survey
345 Middlefield Road, MS 975
Menlo Park, California 94025
(415) 323-8111, x 2037

Investigations

1. Continued revising drafts of 5 chapters for inclusion in the U.S. Geological Survey's forthcoming Professional Paper 1360 "Evaluating earthquake hazards in the Los Angeles region -- an earth science perspective," J. I. Ziony, Editor.

2. Completed initial loading of geotechnical data pertaining to the San Fernando Valley into the USGS VAX computer (S. Wert, J. Tinsley, D. Ponti).

3. Completed field studies and sampling of a late Holocene alluvial sequence that ranges in age from 5000 YBP to present and that crosses the anticlinal axis of the Coalinga anticline. Well-exposed along Los Gatos Creek, these deposits contain abundant detrital charcoal and angular charcoal formed in-situ as artifacts of past fires. In addition to an appraisal of the detrital charcoal problem in the central California Coast Ranges, the Los Gatos Creek basin affords an opportunity to study the effect of tectonics on patterns and rates of alluvial sedimentation, and to use the upper Holocene stratigraphy to determine the relative rate of deformation (uplift) along the Coalinga Nose anticline during late Holocene time. These results help constrain the likely repeat times of damaging earthquakes in the Coalinga area (Brian Atwater, John Tinsley, Allen Tucker, Ross Stein, Dave Trumm, Sandra Wert).

Results

1. U.S. Geological Survey Professional Paper 1360, a multi-authored volume, presents an integrated set of studies that identify the principal geologically controlled earthquake hazards (surface faulting, strong ground shaking, ground failure, and tsunamis), summarizes methods for evaluating their areal extent and severity, and suggests opportunities for their reduction. To demonstrate some of the techniques, many of which are newly developed, the geologic and seismologic effects of a magnitude 6.5 earthquake along the northern part of the Newport-Inglewood fault zone are predicted. The methods described can be used for evaluating and mapping earthquake hazards in other urban regions threatened by earthquakes.

2. The completed data base enables us to make rapid comparisons among several geotechnical parameters as a function of depth and areal distribution in the San Fernando Valley. We anticipate testing models of liquefaction and ground shaking using the data base and our regional Quaternary stratigraphy.

3. Initial returns fron the NSF Accelerator Facility for Radiocarbon Dating, Tucson, Arizona, indicate that substantial errors in late Holocene geochronology may be incurred if detrital charcoal has been used to assign ages to strata. Investigators have acknowledged that detrital charcoal can be reworked in the alluvial environment, and that ages obtained from detrital charcoal can only be maximum ages for the host deposit. Recent studies at Coalinga along Los Gatos Creek indicate that the detrital charcoal ages there may be as much as 2000 years too old, compared to ages of 4800 and 5300 ^{14}C years obtained from angular charcoal collected from growth position in lenses of fire-baked silt. The increased use of particle accelerators to date milligram-size carbon samples may result in this sampling problem becoming acute, especially when detrital charcoal is used to calibrate estimates of earthquake recurrence in the range of hundreds of years. Detrital charcoal may be of little value where host deposits are very young and where the carbon cycle in the sedimentary basin exceeds the recurrence intervals of faulting.

Reports

Tinsley, J. C. and Fumal, T. E., 1985, Mapping Quaternary sediments for areal variations in shaking response--Chapter 5 in U.S. Geological Survey Professional Paper 1360.

Fumal, T. E. and Tinsley, J. C., 1985, Mapping shear-wave velocities of near-surface geologic materials: Chapter 6 in U.S. Geological Survey Professional Paper 1360.

Rogers, A. M., Tinsley, J. C., and Borcherdt, R. D., 1985, Predicting relative shaking response: Chapter 9 in U.S. Geological Survey Professional Paper 1360.

Tinsley, J. C., Youd, T. L., Perkins, D. M., and Chen, A. T. F., 1985, Evaluating liquefaction potential: Chapter 11 in U.S. Geological Survey Professional Paper 1360.

Ziony, J. I., Evernden, J. F., Fumal, T. E., Harp, E. L., Hartzell, S. H., Joyner, W. B., Keefer, D. K., Spudich, P. A., Tinsley, J. C., Yerkes, R. F., and Youd, T. L., 1985, Predicted geologic and seismologic effects of a postulated magnitude 6.5 earthquake along the northern part of the Newport-Inglewood zone: Chapter 15 in U.S. Geological Survey Professional Paper 1360.

Atwater, B. F., Tinsley, J. C., Stein, R. S., Trumm, D. A., and Wert, S. L., 1984, Late Holocene alluvial plains as structural datums across the Coalinga Nose - Guijarral Hills anticline, Fresno County, California in Rymer, M. J. and Ellsworth, W. L., (eds.), Proceedings of Conference XXVI - Mechanics of the May 2, 1983, Coalinga earthquake: U.S. Geological Survey Open-File Report 84 - ____.

Tucker, Allen B., Tinsley, J. C., Atwater, B. F., Trumm, D. A., Robinson, S. W., Donahue, D. L., and Jull, A. J. T., 1985, Accelerator dating of detrital and burned in-place charcoal from the alluvium of Los Gatos Creek, Fresno County, California, U.S.A., submitted to the 12th International Radiocarbon Conference, to be convened at the Norwegian Institute of Technology Trondheim, Norway, June 24-28, 1985. (Director's Approval Received 9/23/84).

Geothermal Seismotectonic Studies

9930-02097

Craig S. Weaver
Branch of Seismology
U. S. Geological Survey
Geophysics Program AK-50
University of Washington
Seattle, Washington 98195
(206) 442-0627

Investigations

1. Continued analysis of the seismicity and volcanism patterns of the Pacific Northwest in an effort to develop an improved tectonic model that will be useful in updating earthquake hazards in the region. (Weaver, Michaelson, Yelin).

2. Continued acquisition of seismicity data along the Washington coast, directly above the interface between the North American plate and the subducting Juan de Fuca plate. (Weaver, Michaelson, UW contract).

3. Test the hypothesis: An area of crustal spreading exists in southwestern Washington between the St. Helens seismic zone to the northeast and a still poorly defined seismic zone that probably parallels the Portland Hills to the southwest. Both zones strike north-northeast, and are offset by about 40 km. The proposed opening is in a west-to-northwest direction. (Weaver, UW contract).

4. Continued seismic monitoring of the Mount St. Helens area, including Spirit Lake (where the stability of the debris dam formed on May 18, 1980 is an issue) and Elk Lake. (Weaver, Grant, UW contract).

5. Study of an earthquake sequence between 1958-1962 that occurred near Swift Reservoir (the largest event has an M_L=5.1). The events near Swift Reservoir were probably on the southern segment of the SHZ. (Grant, Weaver).

Results

1. Focal mechanisms have been calculated for all earthquakes greater than magnitude 2.0 that have occurred at depths greater than 4 km directly beneath Mount St. Helens for the period May 19, 1980 to the present. Mechanisms were well determined for 29 of the 41 events that met the abvove criteria; 8 of the events that do not give a double-couple mechanism are directly north (within 2 km) of the surface position of the lava dome located within the crater at Mount St. Helens. East of the lava dome, the focal mechanisms are dominated by nearly pure strike-slip faulting on either north-south or east-west striking fault planes. These earthquake locations and the orientation of the north-south striking fault planes suggest that these events are occurring on the southern extension of the Elk Lake fault zone. West of the lave dome, two general classes of focal mechanisms are observed: 1) Strike-slip faulting with a

thrust component on either northeast or northwest striking faults, and 2) thrust faulting on northeast striking faults. The strike of the northwest fault planes is nearly identical with that calculated for earthquakes near Marble Mountain to the southeast. We conclude that the Marble Mountain fault zone continues beneath Mount St. Helens to the west of the lava dome. Together, the Elk Lake fault zone and the Marble Mountain seismic zone (both segments of the larger St. Helens seismic zone), form a right-stepping center of crustal opening beneath Mount St. Helens. This suggests the possibility that accumulated slip on the SHZ may be responsible for driving the localized volcanism at Mount St. Helens.

2. Relocation of the magnitude 5.1 earthquake of September 17, 1961, indicates that this event was along the southern part of the St. Helens seismic zone, within a few kilometers of Swift Reservoir (Figure 1). Thus, two of the four earthquakes known to be greater than magnitude 5 that have occurred in the crust of Washington since 1960, have occurred along the SHZ. A relatively well constrained focal mechanism has been calculated using 5 stations operating in the Pacific northwest in 1961 and a number of stations at Pn distances throughout the western U.S. The mechanism is largely strike-slip, with north-northwest and east-northeast fault planes (Figure 2). This mechanism is very similar to focal mechanisms calculated in the same area for events recorded by the modern short period University of Washington seismographic network (Figure 2).

Reports

Grant, W. C., Weaver, C. S., and Zollweg, J. E., 1984, The February 14, 1981, Elk Lake Washington, earthquake sequence, Bulletin of the Seismological Society of America, v. 74, p. 1289-1309.

Weaver, C. S., and Grant, W. C., 1984, Seismic fault zones beneath Mount St. Helens, Washington, (abs), Eos, Transactions American Geophysical Union, v. 65, p. 242.

Grant, W. C., and Weaver, C. S., 1984, Spatial-temporal characteristics of two earthquake sequences in southwestern Washington, (abs), Eos, Transactions American Geophysical Union, v. 65, p. 242.

Michaelson, C. A., 1984, Large scale heterogeneities in the crust and upper mantle of the Pacific Northwest, (abs), Abstracts with Programs, Geological Society of America, v. 16, p. 321.

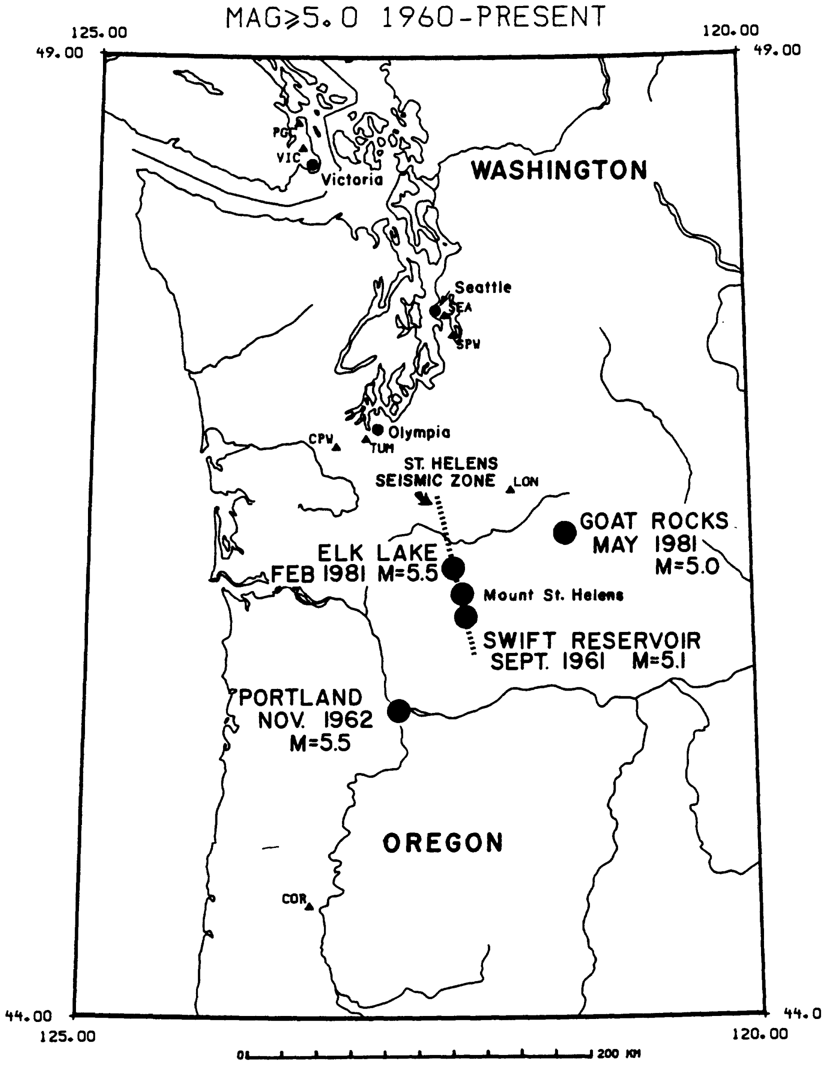

Figure 1. Known crustal earthquakes greater than magnitude 5, from 1960 to the present, in Washington and northern Oregon.

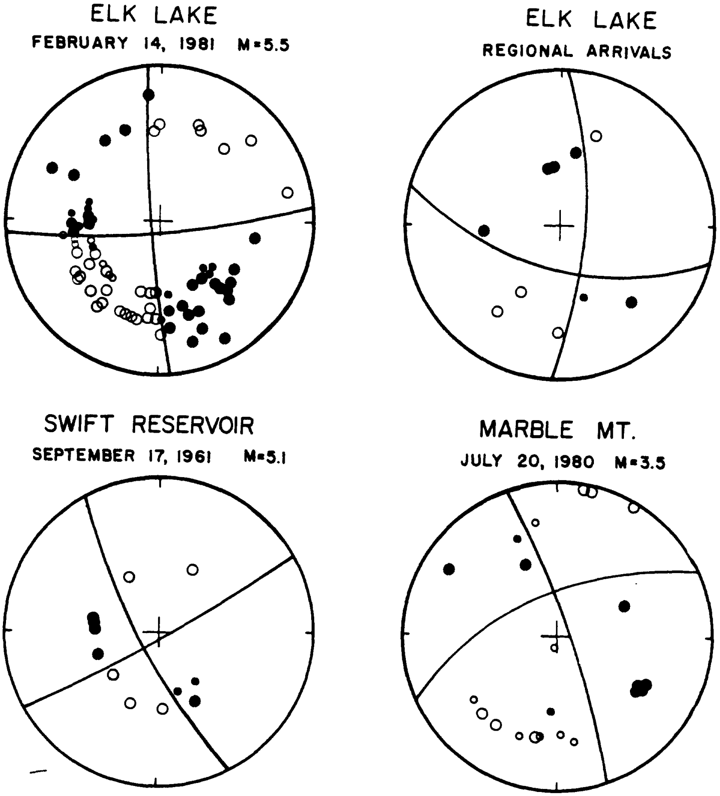

Figure 2. Focal mechanisms for the Elk Lake, Swift Reservoir, and Marble Mountain earthquakes. The upper left solution for Elk Lake is the short period mechanism, calculated with data from the University of Washington network. Upper right solution is based on Pn arrivals at stations used for the Swift Reservoir mechanism (lower left) plus data from the 5 stations operating in the northwest for both events. Lower right mechanism is for an event recorded on the modern network that is located near the Swift Reservoir earthquake. Darkened circles are compressions, open circles dilatations.

Evaluation of Activity of the San Gabriel Fault Zone, Los Angeles and Ventura Counties, California

14-08-0001-21928

F. Harold Weber, Jr. and Allan G. Barrows
State of California
Department of Conservation
Division of Mines and Geology
107 South Broadway, Room 1065
Los Angeles, California 90012

Objective: Studies of the San Gabriel fault zone made by Weber beginning in 1975 indicate that the zone has been active in late Pleistocene time. More recent studies by W. R. Cotton and others show that the fault zone has been active during Holocene time in the Saugus area. The fault previously had been considered by most geologists to be no longer active. The objective of this project is to study in detail the fault zone at widespread localities along its 130-km length in order to determine how widespread youthful activity has been and to evaluate the nature of this activity. Both detailed field mapping and trenching will be utilized to evaluate localities.

Investigations: Investigation of trench sites has been initiated along the northwest portion of the fault zone, from the vicinity of Wayside Honor Rancho, near Castaic, to the apparent northwest end of the fault zone west of Hungry Valley. The investigation so far has included detailed site examination and mapping to determine precise location of fault segments in the Smith Fork area of Piru Creek and the segment of Piru Creek that contains Hardluck campground. The Smith Fork area contains landslide, terrace, and younger alluvial deposits that may be displaced by faulting. The Hardluck area contains a variety of sedimentary deposits within the area traversed by the fault zone. Landslide deposits in the Beartrap and Violin canyons areas may be displaced by faulting but are inaccessible to trenching equipment. These localities will be investigated in more detail by field mapping. The portions of the fault zone within Wayside Honor Rancho and to the east of Saugus are next to be evaluated for trenching potential.

Central California Deep Crustal Study
(Neotectonic Synthesis of U.S.)

9540-02191

Carl M. Wentworth
Branch of Western Regional Geology
U.S. Geological Survey
345 Middlefield Road, MS 975
Menlo Park, California 94025
(415) 323-8111 ext. 2474

Investigations

The objective of the project is to examine crustal structure between the California Coast Ranges and the Sierran Foothills using deep seismic reflection profiling in concert with surface geology, aeromagnetic and gravity analysis, and seismic refraction profiling. Reflection profiles and associated refraction data have been obtained at three principal E-W crossings in the San Joaquin Valley (fig. 1): (a) line SJ-6, which extends from the coast at Morro Bay through Cholame and Delano and onto foothills crystalline rock (lat. 35.75° N); (b) lines SJ-3 and SJ-19 across Coalinga anticline (lat. 36.18° and 36.26° N); and (c) lines CC-1 and CC-2, which together form a profile that extends from the core of the Diablo Range north of Pacheco Pass at Mustang Peak eastward through Gustine to Merced and, with a 13-km offset to the south, eastward almost to crystalline rock (approximately lat. 37.25° N). Reflection data have also been obtained in the northern Sacramento Valley.

1. Work has continued on developing velocity structure along reflection lines CC-1 and CC-2 (15 s, 800-channel, SIGN-BIT data), both for further processing of the reflection data and for interpretation. Constant velocity panels for data in the Diablo Range are ambiguous and even CDP gathers corrected for normal movement with our best estimates of velocity structure have proved ambiguous, possibly due to a crooked line over cross dip. Single-shot profiles in the San Joaquin Valley have been used as reversed refraction profiles to examine basement velocity.

2. Interpretative work has continued on the Coalinga data, particularly through comparison with COCORP results (Fielding et al, 1984, Geology, v. 12, p. 268-273) and with Allan Walter's refraction results.

3. Gravity and magnetic modeling has been carried out by A. Griscom and R. Jachens along SJ-19.

4. Many more well records have been gathered to better define structure in the Coalinga area.

5. A careful compilation at 1:500,000 has been made of basement lithologies and depth in basement-penetrating wells in the Great Valley of California, involving new petrography by Clark Blake and Angela Jayko, to explore control on distribution of Sierran, possible ophiolitic, and other rock types beneath the Great Valley.

6. A contract has been signed to extend reflection line CC-2 eastward for 32 km across Foothill metamorphics into batholithic rocks. Field acquisition is planned for late November, 1984.

Results

1. A basic interpretation of structure at the west margin of the Great Valley is emerging (fig. 2) that is supported at all four latitudes along the length of the Great Valley where we have data. Structure along the eastern margin of the Coast Ranges, where the Franciscan assemblage and Great Valley sequence are juxtaposed, seems to be marked by tectonic wedges. These are allochthonous masses thrust between underlying basement and overlying rocks peeled up by the wedge. Structure inferred from reflection and refraction profiles in the San Joaquin Valley requires that the buried east boundary of Franciscan rocks is the tip of a tectonic wedge. Great Valley basement extends westward from beneath flat-lying Great Valley sequence at the west edge of the valley (depths of 6 to 10 km) to beneath the Franciscan wedge at depths of 12 to 15 km. In this interpretation, the Coast Range thrust, long viewed to be a subduction zone suture between Franciscan assemblage and the Great Valley sequence with its ophiolitic basement, becomes the roof thrust of the Franciscan wedge.

2. Recorrelation of lines SJ-3 and SJ-19 to obtain an additional 6 seconds of record (total of 12 s) is now complete. In contrast to our success with SJ-6, this did not reveal any evident deep reflections, although the quality of events between 5 and 6 seconds is improved. Interpretation of the reflection records alone is difficult below the top of the Cretaceous Panoche Formation, but in combination with Allan Walter's refraction model the results are striking (fig. 3). Basement dips westward from the western valley to 13 to 14 km beneath the Diablo Range, and may be marked by the deepest reflections in SJ-19. A prominent wedge of intermediate velocity material overlying the deep basement is inferred to be Franciscan rocks. The top of the wedge seems to coincide with a prominent reflection in the record, which is broken by faults. Numerous layered reflections lie within the wedge, as well as above it. The 1983 Coalinga mainshock occurred within the wedge and the gently southwest-dipping focal plane is consistent with rupture on a thrust that steepens up dip to the northeast.

3. A structure contour map on the top of the Eocene Kreyenhagen Formation in the Coalinga area has been prepared and is being expanded. This defines the shape of structure in the area at least down into the Panoche Formation. Of particular importance are distinction of Coalinga anticline as a separate fold that abuts the southern limb of Joaquin Ridge anticline, and recognition that the syncline west of the Coalinga anticline is much shallower than the east flank of the fold.

4. Both the reflection data and Allan Walter's refraction work at SJ-19 indicate low velocity zones (LVZ's) that seem due to anomalously high pressure of pore fluids. Cooperative work with Bob Yerkes demonstrates clear correlation in the Coalinga area between these LVZ's and high fluid pressure and abrupt decrease in sonic velocity in logged wells. Diagenetic and metamorphic reactions that produce excess fluids, demonstrably

underway in the region and superimposed on compaction loading in the thick marine section, make development of high fluid pressures simply a matter of adequate fluid containment. Extensive reduction of effective normal stress across low-angle surfaces may enhance thrusting as a deformational mechanism.

5. We will propose, at a special session at AGU in San Francisco in December, 1984, that our work is identifying some worthwhile targets for scientific drilling. Important locations along line CC-1 include: (a) within the Diablo Range, to examine the east-dipping reflection at 5 km and test for overlying serpentinite (indicated by magnetic analysis) and underlying Franciscan (fig. 4) and; (b) near or east of the range front to examine the Franciscan wedge.

Reports

Wentworth, C. M., Blake, M. C., Jr., Jones, D. L., Walter, A. W., and Zoback, M. D., 1984, Tectonic wedging associated with emplacement of the Franciscan assemblage, California Coast Ranges, *in* Blake, M. C., Jr., ed., Franciscan Geology of Northern California: Society of Economic Paleontologists and Mineralogists, Pacific Section, Book# 43, p. 163-173.

Wentworth, C. M., Zoback, M. D., and Bartow, J. A., 1984, Tectonic setting of the 1983 Coalinga earthquake from seismic reflection profiles: a progress report, *in* Rymer, M. J., and Ellsworth, W. L., eds., Mechanics of the May 2, 1983 Coalinga, California, earthquake: U.S. Geological Survey Open-File Report 84---, in press.

Wentworth, C. M., Zoback, M. D., and Walter, A. W., 1984, Tectonic models of Franciscan and Nevadan obduction by seismic drilling in central California (abs.): American Geophysical Union, abstract for Fall 1984 meeting, in press.

Figure 1. Location of seismic reflection lines in central California obtained for the deep crustal studies project. SJ-3, 6, and 19 are 6-S VIBROSEIS records recorrelated to 12 s (SJ-6, only central 100 km recorrelated); CC-1 and 2 are 15-s SIGN-BIT VIBROSEIS records, S lines are 5-s explosion records.

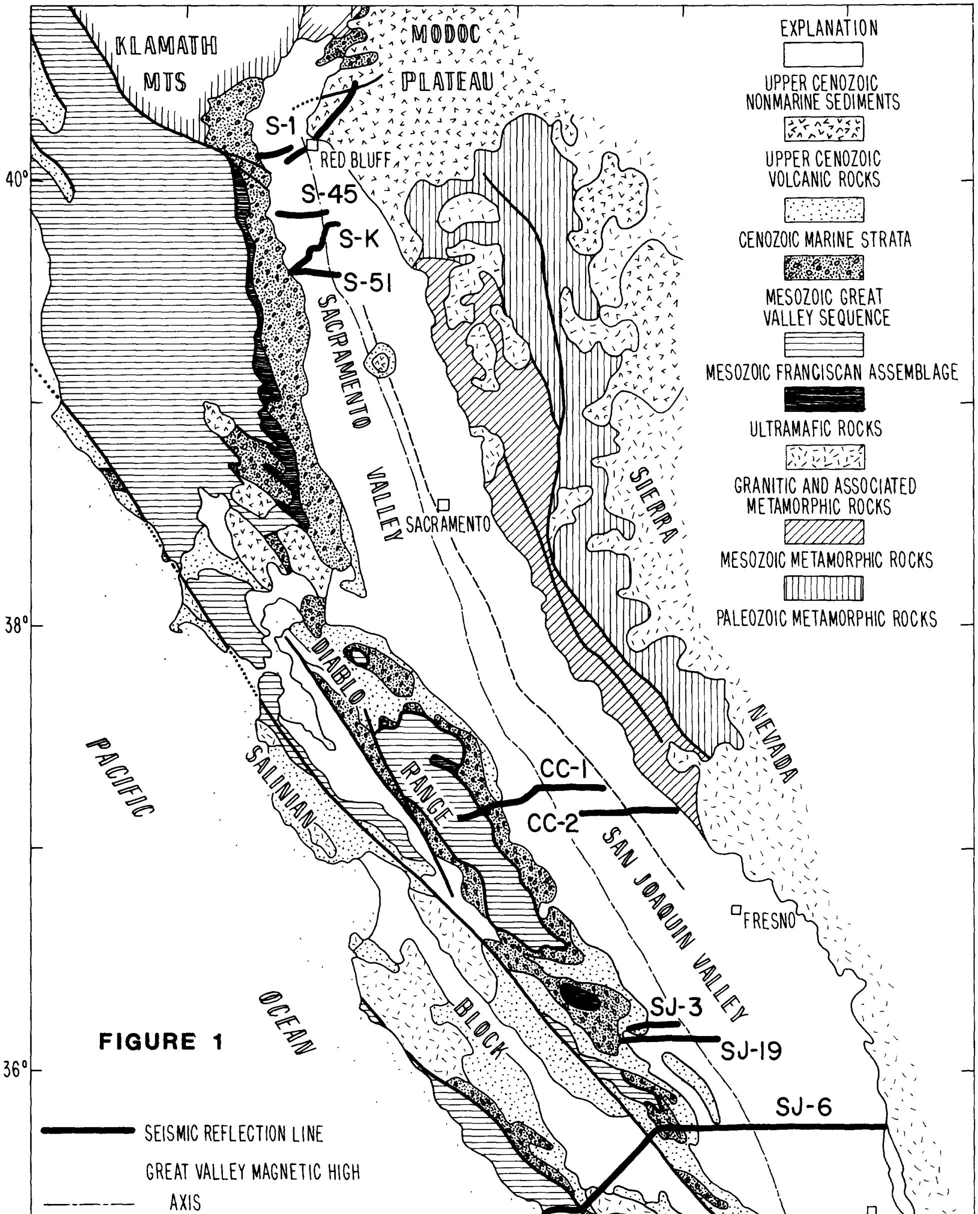
KLAMATH MTS
MODOC PLATEAU
EXPLANATION
UPPER CENOZOIC NONMARINE SEDIMENTS
UPPER CENOZOIC VOLCANIC ROCKS
CENOZOIC MARINE STRATA
MESOZOIC GREAT VALLEY SEQUENCE
MESOZOIC FRANCISCAN ASSEMBLAGE
ULTRAMAFIC ROCKS
GRANITIC AND ASSOCIATED METAMORPHIC ROCKS
MESOZOIC METAMORPHIC ROCKS
PALEOZOIC METAMORPHIC ROCKS
S-1
RED BLUFF
S-45
S-K
S-51
SACRAMENTO VALLEY
SACRAMENTO
SIERRA NEVADA
DIABLO RANGE
SALINIAN BLOCK
PACIFIC OCEAN
CC-1
CC-2
SAN JOAQUIN VALLEY
FRESNO
SJ-3
SJ-19
SJ-6
BAKERSFIELD
SEISMIC REFLECTION LINE
GREAT VALLEY MAGNETIC HIGH
AXIS
CENTER OF STEEP EAST GRADIENT
0
100km
40°
38°
36°
122°
120°

FIGURE 1

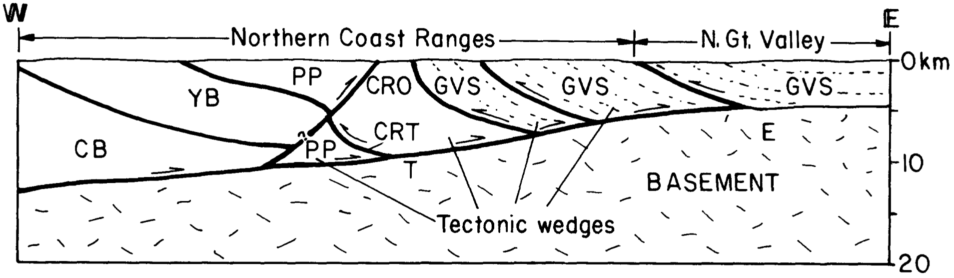

Figure 2. Schematic cross section between the northern Coast Ranges and northern Great Valley at latitude 39.88° N. Inferred roof faults of wedges in Great Valley sequence presumably merge northward with large, southeast-trending tear faults that offset exposed Great Valley sequence. GVS - Great Valley sequence; CRO - Coast Range ophiolite; CRT - Coast Range thrust; PP - Pickett Peak Terrance, Eastern Franciscan belt; YB - Yolla Bolly terrane, Eastern Franciscan belt; CB - Central Franciscan belt.

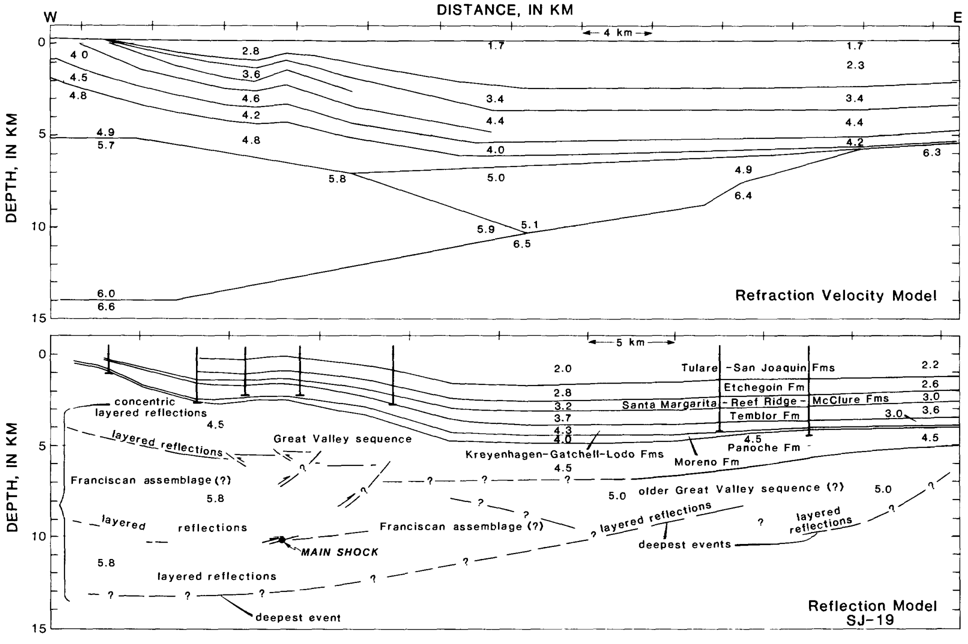

Figure 3. Refraction velocity model and associated reflection interpretation along line SJ-19 across Coalinga anticline. Velocities below about 5 km in the reflection model are based largely on the refraction model. "Deepest event" marks deepest clear reflection in 12-s record. Vertical bars show drill holes used in identifying stratigraphic units.

Lake Levels and Geodetic Leveling to Monitor Vertical Tectonics: Wasatch Front

9950-02396

S. H. Wood
Branch of Engineering Geology and Tectonics
U.S. Geological Survey
Boise State University
Boise, Idaho 83725
(208) 386-3629

Investigations

Geologic evidence indicates that vertical deformation and major earthquakes are a continuing process along segments of the Wasatch Fault zone. First-order geodetic level lines that cross the fault zone in Weber Canyon south of Ogden, Utah, show an apparent elevation change of 110 mm and a land-surface tilt of 11.4 microradians developed between 1958 and 1983. Results shown here are derived from recalculation of the 1958 elevations using rod recalibrations and a theoretical correction for sight-line refraction. The 1983 elevations were leveled using methods especially designed to overcome slope-dependent systematic errors. Acceptance of these relatively high rates of vertical deformation along the Wasatch Fault zone rests largely upon the validity of the 1958 elevations. Taken at face value the relevelings indicate a 25-year average rate of uplift of at least 4 mm/yr and a tilt rate of 0.46 microradians/yr. The 1983 to 1979 comparison suggests a tilt rate of no more than 0.82 microradians/yr. The fact that much of the land-surface tilt appears to occur in the hanging wall of the fault is consistent with the configuration of coseismic land-surface deformation that accompanies major earthquakes on normal faults.

Report

Wood, S. H., and Till, John, 1984, Repeated geodetic leveling across the Wasatch Fault near Ogden, Utah: Geological Society of America Abstracts with Programs, v. 16, no. 6, p. 700.

Potentially Active Reverse Faults of Eastern Ventura Basin, Los Angeles County, California

USGS Contract No. 14-08-0001-21279

Robert S. Yeats, James W. McDougall, and Leonard T. Stitt
Department of Geology
Oregon State University
Corvallis, Oregon 97331-5506
(503) 754-2484

Investigations

Geologic maps of the Val Verde and the south half of the Whitaker Peak 7½ minute quadrangles will be open-filed by USGS. The open-file report will include an oil-well base map and several cross sections showing critical relations as revealed by oil-well data. The two quadrangles are critical to an understanding of the relation of reverse faults in the eastern Ventura basin to the San Gabriel fault to the east and the San Cayetano and Oak Ridge faults to the west.

Results

1. Several northeast-dipping reverse faults in the Whitaker Peak quadrangle are Miocene in age. The Whitaker thrust is overlain unconformably by the Devil Canyon anorthosite-bearing conglomerate of Mohnian age (4-12 m.y.), confirming field relations reported by Crowell (1954). In SW/4 Sec. 6, T5N, R17W, the Whitaker fault could be interpreted alternatively as cutting the basal Devil Canyon conglomerate, but if it does so, it is overridden by the Devil Canyon fault 150 m east of the base of the Devil Canyon conglomerate. The Devil Canyon fault does not cut uppermost Modelo fine-grained strata, and the overlying Hasley Conglomerate Member of the Towsley Formation is not faulted, thereby constraining the age of the Devil Canyon fault as Mohnian.

The Canton fault cuts the basal Devil Canyon conglomerate and is overlain unconformably by younger beds of this conglomerate, as mapped by Crowell (1954, 1975). We agree with the relations illustrated in Fig. 2 of Crowell (1975) except that we consider the Canton fault to be an abandoned strand of the San Gabriel fault. The fault, which separates Palomas gneiss on the east from Whitaker granodiorite on the west, can be traced in the subsurface for more than 7 km southeast of its surface termination (Stitt and Yeats, in press). As at the surface, the Canton fault in the subsurface is overlain unconformably by Mohnian strata.

2. Structural growth continued during deposition of the Towsley and Pico formations. In Violin Canyon, immediately west of the San Gabriel fault, the Towsley and Pico formations are relatively thin. To the west, these formations greatly increase in thickness. From north to south in the Val Verde quadrangle, successively younger Pico members appear beneath the base of the Saugus: a lower conglomerate-sandstone member, an upper siltstone-fine-grained sandstone member,

and an upper conglomerate-sandstone member which grades laterally into Saugus in its upper part. Locally, the Hasley Conglomerate is absent over structural highs.

3. Post-Saugus structures were formed in the late Quaternary. The youngest Saugus could be as young as 0.1 to 0.2 m.y. based on extrapolation upsection of sedimentation rates derived from paleomagnetic stratigraphy (Levi and Yeats, 1984), and even the youngest Saugus strata are strongly deformed.

Major south-dipping reverse faults are, from south to north, the Del Valle, Holser, Hasley, Oak Canyon, and Santa Felicia faults. The Del Valle fault is not in contact with the Saugus, but the Holser and Hasley faults do cut the Saugus. The Santa Felicia fault does not cut the Saugus, but it cuts the main strand of the San Gabriel fault near the mouth of Violin Canyon, and the San Gabriel fault cuts the Saugus. The Santa Felicia fault brings Towsley and Pico formations over Violin Breccia and Castaic Formation, and the fault dips 50° southwest.

In the subsurface, these reverse faults in the Whitaker Peak and Val Verde quadrangles continue to dip at moderate angles to bedding and do not steepen to vertical. In the western part of these quadrangles, these faults dip at such a low angle to bedding that they may become bedding faults at depth.

4. Tectonic landforms are less apparent in the east Ventura basin than they are in the western Ventura basin. The south-dipping Oak Ridge fault and the north-dipping San Cayetano fault die out in the Santa Clara River Valley north of Tapo Canyon. These faults are mapped in the subsurface, and they reach the surface at places where older alluvium is separated from younger alluvium by linear topographic steps, possibly eroded fault scarps which are modified by the present Santa Clara River. These topographic steps have not been trenched. East of these fault traces, no linear topographic steps have been found in the Santa Clara River Valley. The Santa Clara River flows down the axis of the syncline north of the Oak Ridge fault, but east of the Oak Ridge and San Cayetano faults, the Santa Clara River cuts diagonally across the Santa Clara syncline, Newhall-Potrero anticline, Del Valle anticline, and the southeast termination of the Del Valle fault.

5. River terraces are preserved along the axis of the Santa Clara syncline southeast of the Santa Clara River north of Potrero Canyon. The broad, alluviated valley of Potrero Canyon may be controlled by downwarping on this late Quaternary syncline.

San Martinez Grande Canyon is located on the downthrown north block of the Del Valle fault, crossing the fault only at the mouth of the canyon near the termination of the fault. A broad terrace is preserved in Section 16, T4N, R17W, east of the point where the Del Valle fault bends to the south. The axis of the canyon is north of the present fault trace. Possibly the canyon developed very close to the fault at a higher erosion level when the fault trace was farther north. Subsequent downcutting of the canyon resulted in a southward migration of the fault trace away from the canyon, and large landslides were directed northward into the canyon.

In the western part of Val Verde quandrangle, the Holser fault follows the south side of Holser Canyon, a relation similar to that between the Del Valle fault and San Martinez Grande Canyon. Farther east, the fault follows the axis of San Martinez Chiquito Canyon where it trends east, and still farther east, it follows a side tributary to Castaic Creek. The Santa Felicia fault follows Santa Felicia Canyon for part of its length, but it crosses mountainous terrain farther east. The Hasley and Oak Canyon faults show no relation to topography.

In conclusion, the reverse faults of the east Ventura basin do not exhibit the youthful tectonic geomorphology that reverse faults do farther west in the Ventura basin. No evidence of Holocene movement was found. Oil fields in the region have not experienced any documented damage from active tectonism, including the 1971 San Fernando earthquake. Careful study of river terraces may show evidence of late Quaternary folding, and trenching may reveal evidence of late Quaternary movement on the Oak Ridge and San Cayetano faults, which appear to be the youngest faults in the two quadrangles.

Crowell, J. C., 1954, Strike-slip displacement of the San Gabriel fault, southern California: California Division of Mines Bull. 170, Chapter IV, p. 49-52.

Crowell, J. C., 1975, The San Gabriel fault and Ridge basin, southern California: California Division of Mines and Geology Special Report 118, p. 208-219.

Levi, S., and Yeats, R. S., 1984, Magnetostratigraphy and paleomagnetism of the Saugus Formation, Los Angeles County, California: U.S. Geological Survey Open-File Report 84-628, p. 109-117.

Stitt, L. T. and Yeats, R. S., in press, A structural sketch of the Castaic area, northeastern Ventura basin and northern Soledad basin, California, in Geology and Mineral Wealth of the California Transverse Ranges: Santa Ana, Calif., South Coast Geological Society.

Earthquake Hazards Studies, Metropolitan Los Angeles-Western Transverse Ranges Region

9540-02907

R. F. Yerkes
Branch of Western Regional Geology
345 Middlefield Road MS 975
Menlo Park, California 94025
(415) 323-8111 x2350

Investigations and results

1. Historic earthquake data (W. H. K. Lee). Continued organizing and merging phase data from several sources into a common format.

2. Earthquake hazard studies (Yerkes). Completed collection and evaluation of fluid-pressure data for more than 300 deep wells in south San Joaquin Valley. The study generally verifies, expands, and completes findings previously reported (Summary XVIII, Open File Report 84-628). The study infers the presence of near-lithostatic fluid pressures in Franciscan and Great Valley rocks at seismogenic depths below Coalinga anticline on the basis of 1) mapped seismic low-velocity zones (correlated with high fluid pressures); 2) the active generation of metamorphic fluids in Franciscan and Great Valley rocks, which pond and increase fluid pressure below relatively impermeable clayey layers; 3) a model that explains variations of fluid pressure in the overpressured zone as a function of permeability (lithology), and hence effective normal stress; 4) thus explaining the more than 400-fold range in crustal strength of rocks in the seismogenic zone reported by McGarr and others (OFR). Completed first draft of Professional Paper report, an open-file rport, and an abstract for AGU Fall Meeting on this topic.

3. Quaternary stratigraphy, chronology, and tectonics, Ventura area (A. M. Sarna-Wojcicki)

(a) Continued analyses and correlation of Quaternary ash layers in the Ventura basin to develop and improve age control of upper Cenozoic deposits in this area and quantify rates of late Cenozoic crustal deformation. Results of neutron-activation analysis of volcanic glass separated from samples of ash layers from the Ventura area identify the Bailey ash bed (1.2 m.y. b.p.) at six new locations, including the north limb of the Ventura Avenue anticline west of the Ventura River, near the base of the Santa Barbara Formation (also identified previously from the south limb), and the west flank of South Mountain southeast of Ventura, in the Pico Formation. The new analyses also confirm a previous tentative identification of the Bishop ash bed (0.74 m.y. b.p.) at a locality near Sexton Canyon, on the south limb of the Ventura Avenue anticline in the upper part of the Santa Barbara Formation, where the ash bed lies approximately 600 m below the Lava Creek ash bed (0.62 m.y. b.p.), in the lower part of San Pedro Formation. Combined with amino-acid racemization age estimates on fossil mollusk shells in the San Pedro Formation (K. R. Lajoie, BESG), the horizontal-compression rate across the Ventura Avenue anticline is about 3-10 mm/yr in the past 0.2-0.6 m.y.

(b) Continued study of oxygen-isotope analysis of foraminifera in on-land Quaternary marine sections, Ventura basin, in order to improve existing age control for upper Cenozoic sections by correlation with deep-sea secular oxygen-isotope variations, and in order to derive a climatic history that can be correlated to non-marine sections in the western United States (see vol. XVIII, p 148).

Reports

Lajoie, K. R., Sarna-Wojcicki, A. M., Kennedy, C. L., Mathieson, S. A., McCrory, P. A., Morrison, S. D., and Stephens, T. A., 1984, Late Quaternary coastal tectonics of the Pacific coast of the United States: Abstracts for the International Symposium on Recent Crustal Movements of the Pacific Region, Wellington, New Zealand, Feb., 1984, p. 28.

Sarna-Wojcicki, A. M., Meyer, C. E., and Slate, Janet, 1984, Application of tephrochronology and tephrostratigraphy to Quaternary chronology, stratigraphy, and tectonics in the western United States: Abstracts for the International Symposium on Recent Crustal Movements of the Pacific Region, Wellington, New Zealand, Feb. 1984, p 48.

Sarna-Wojciki, A. M., Meyer, C. E., Bowman, H. R., Hall, N. T., Russell, P. C., Woodward, M. L., and Slate, J. L., in press, Correlation of the Rockland ash bed, a 400,000 year-old stratigraphic marker in northern California and western Nevada, and implications for mid-Pleistocene paleogeography of central California: Quaternary Research.

Sarna-Wojcicki, A. M., Meyer, C. E., Roth, P. H., and Brown, F. H., Ages of early hominids in East Africa by correlation of tuff beds to sediments in the Gulf of Aden. Submitted to Nature. Approved.

Segall, P., and Yerkes, R. F., Stress and fluid pressure changes associated with oil field operations: a critical assessment of effects in the focal region of the 1983 Coalinga earthquake: U.S. Geological Survey Open File Report and Professional Paper.

Yerkes, R. F., Levine, Paia, and Wentworth, C. M., in press, abnormally high fluid pressures in the region of the Coalinga earthquakes--a preliminary report: U.S. Geological Survey Open File Report.

Yerkes, R. F., McGarr, A. F., Wentworth, C. M., and Walter, A. W., 1984, Abnormally high fluid pressures near the Coast Range-Great Valley boundary, CA, may aid northeast-directed thrusting responsible for the 1983 Coalinga earthquakes (abs.): EOS, vol , no, , p. .

Regional Syntheses of Earthquake Hazards in Southern California

9910-03012

Joseph I. Ziony
Branch of Engineering Seismology and Geology
U.S. Geological Survey
345 Middlefield Road, MS 977
Menlo Park, California 94025
(415) 323-8111, ext. 2944

Investigations

1. We have started field studies to search for and evaluate offset late Quaternary features that would provide better estimates of the style and rate of slip along the Whittier and the northern Elsinore fault zones. Geologic controversy exists concerning the slip history of these fault zones, and published estimates of slip rate range from 0.6 to 7.0 mm/yr. Our efforts initially focus on the sector between Corona and Agua Tibia Mountain, within which slip is concentrated along a few well-mapped fault strands and where Quaternary deposits are widespread.

   An intermediate goal is to develop a soils chronosequence for the Elsinore Trough region that could provide improved time constraints for evaluating measured horizontal and vertical separations across the faults. Therefore, the project is supporting analysis of relative soil-profile development and detailed Quaternary geologic mapping by two graduate students: Douglas Millman (San Diego State University) is working in the Temescal Valley area on Holocene sag pond deposits and soils formed across a faulted sequence of late Quaternary alluvial fans and terraces. Patrick Vaughan (University of Colorado) is investigating a soils sequence and Quaternary stratigraphy along a graben flanking Agua Tibia Mountain near Pala.

2. The professional paper manuscript evaluating the earthquake hazards of the Los Angeles region has received Director's approval and will be published in the summer of 1985. A conference addressing the evaluative methods described, and their applications to hazard reduction, is being organized for November, 1985 in Los Angeles.

Reports

Ziony, J.I., and Yerkes, R.F., 1984, Fault slip-rate estimation for the Los Angeles region--challenges and opportunities [abs.]: *Seismological Society of America, Fastern Section, Earthquakes Notes*, v. 55, no. 1, p. 8.

Clark, M.M., Harms, K.K., Lienkaemper, J.J., and Ziony, J.I., 1984, Slip-rate table and map of late Quaternary faults of California [abs.]: *Seismological Society of America, Eastern Section, Earthquake Notes*, v. 55, no. 1., p. 7.

Harms, K.K., Clark, M.M., Rymer, M.J., Bonilla, M.G., Harp, E.L., Herd, D.G., Lajoie, K.R., Lienkaemper, J.J., Mathieson, S.A., Perkins, J.A., Wallace, R.E., and Ziony, J.I., 1984, The search for surface faulting in Hoose, S.N., compiler, The April 24, 1984 Morgan Hill, California earthquake: *U.S. Geological Survey Open-File Report 84-498*, p. 92-108.

An Analysis of the Haicheng Aftershock Sequence, and an Animated Color Graphical System for Displaying Earthquake Prediction Data

14-08-0001-G-885

Keiiti Aki*
Department of Earth, Atmospheric and Planetary Sciences

Steven P. Ellis
E40-113
Statistics Center
Massachusetts Institute of Technology

Objectives: In the first study the catalog of aftershocks of the 1975 Haicheng earthquake through 1978 was analyzed with a view of developing new statistical methods for analyzing nonstationary seismic data and to gain insight into how the aftershocks depend on one another. The second study is an attempt to create a graphics system for displaying seismicity and precursory data in four dimensions. It is hoped that an analyst using this tool will get new insights into the prediction problem.

Analysis of the Aftershocks: This study concentrated on the temporal aspects of the data.

The first step was to fit Omori's law to the catalog. In order to accomodate a change in the lower Richter magnitude threshold from 3 to 2 early in the catalog, the data was modeled as a point process on the time-magnitude plane whose intensity is the product of the expressions for the Omori and magnitude-frequency laws.

Next, the parameters in the intensity function were estimated from the time-magnitude data by maximum likelihood under the assumption that the data was generated by a Poisson process. Using the results, it was shown that the data is too clustered to be Poisson. In particular a large, magnitude 6, aftershock 1200 days into the sequence produces its own aftershock sequence. To overcome this problem an iterative "robust" method was used in which each observation is weighted.

Unsing the robust estimates, a "second order" analysis of the dependence between pairs of events was carried out. The usual methods for doing this are designed for stationary data. Since the rate of occurrence of aftershocks decays with time, the Haicheng aftershock catalog is not stationary. Three different methods are tried to get around this problem. In the first, the data is assumed to be stationary on on a different time scale. The second and third assumes that "auto-intensity function" of the sequence equals the product or sum of a "stationary" component and the intensity function of the times of occurrence.

These methods are checked by applying them to the first and second halves of the data set and then comparing the results. If the model underlying the method is correct, the results for the two halves should be the same. All three methods fail this test. However, once it is "robustified" to withstand the influence of the aftershock subsequence produced by the largest aftershock, the third or "additive", model seems to fit the first and second halves of the data in comparable ways. This model has the interpretation that

---

*Now at: University of Southern California
Los Angeles, CA 90089-0741
(213) 743-3510

an aftershock affects the catalog, e.g. by producing its own aftershocks, in a way which does not depend on where it falls in the sequence.

The statistical methods developed for this study should prove useful in other areas of seismology, e.g. in earthquake risk assessment.

The Graphics Package: This set of programs will portray earthquakes and possible precursors in the following way. "Viewing-time", the time during which the data is viewed, is used to represent the times of occurrence of the events (on a highly compressed scale). Each event appears as a colored square on a map of the region under consideration. The square remains on the screen for a time proportional to the duration of the event being portrayed.

The center of the square representing an event is located at the position on the map corresponding to the actual location of the event. The size of the square is used to represent the size of the event. Finally, the color of the square indicates the type of the event (e.g. earthquake, water level anomaly, animal behavior anomaly, etc.)

Thus, besides event type, four dimensions are portrayed: Time, two dimensions of location, and magnitude.

The programs are organized as follows. Since viewing time is used as an axis, it is important that the timing of various calculations associated with the graphical portrayal be predictable. This is hard to achieve, especially on a time-sharing system. For this reason the portrayal is created in two passes. The first involves practically all the calculations. It produces a "compiled" version of the data which consists of graphical commands for the terminal plus the amounts of time that the computer should wait between execution of these commands. The second program takes the "compiled" file, reads each sequence of commands, writes it to the terminal and then waits the appropriate amount of time before reading the next sequence. The first pass need be performed only once on each data set. After that the data can be viewed as often as one likes using the second program.

At present, an experimental program combining both phases is running. Once a "final" version is ready, we will use it first to view some Japanese data.

The programs are being written in C on a VAX 11/730 with Berkeley 4.2 UNIX. The terminal used is a Tektronix 4105. (The programs should run with any Tektronix 4100 series terminal.)

Analysis of Central California Network Data
and Earthquake Prediction

Contract Number 14-08-0001-21292

Keiiti Aki*
Department of Earth, Atmospheric and Planetary Sciences
Massachusetts Institute of Technology

Investigations

The goals of this study are twofold: 1) to examine the site effect in order to understand its spacial and frequency dependent behavior; and 2) to acquire the ability to extend single station coda wave techniques to a large array of stations by applying a site correction. This will enable us to carry out coda source and path effect studies using the U.S.G.S. Calnet.

Results

We use digital data from over 85 earthquakes, each recorded by a subset of some 150 stations in the Coast Ranges of central California between San Francisco and San Luis Obispo. A moving window FFT is applied to over 1200 codas to study their spectral characteristics. The site amplification for a given frequency band is determined by least squares from:

$$d_{ijk} - \overline{d_{ijk}}^{(jk)} = r_i - \overline{r_i}^{(jk)}$$

where the d_{ijk} are the data (after taking the logarithm), the r_i are the site terms, and indecies i, j, k represent site, source and time respectively. The average represented by the bar is taken for source and time held constant. This equation can be derived from the assumption that coda power decay with time is independent of source and receiver location (Aki, 1969). The data variance indicates the degree to which the data fits our model, and is 12 % of the total variation at worst. This is satisfactory, however there is evidence that certain sediment sites contribute heavily to the error.

Results indicate that site amplification depends strongly on surface geology and frequency. At low frequencies (1.5 - 3.0 Hz) changes in amplification up to a factor of 20 are observed; amplification generally varying inversely with age at sediment sites and is lowest at granite and Franciscan (basement) sites. At high frequencies (6 - 24 Hz) the pattern changes. Many granite sites, the majority in the Gabilan range, exhibit

---

*now at: University of Southern California
Los Angeles, California 90089-0741
(213) 743-3510

increasing amplification with frequency relative to the average station. This behavior differs strikingly from that observed at sediment and Franciscan sites which roll off at an intermediate rate, and many sediment sites adjacent to the San Andreas fault zone which decay away even more rapidly with frequency (Figure 1). These results can be explained qualitatively by appealing to variable near site impedance and attenuation properties; however, complicating phenomena such as mode excitation in valley sediments at low frequencies, and resonance of smaller structures at high frequencies must exist. At a few sediment sites the low frequency excitation is so strong that the coda envelopes begin to take on different shapes. This contradicts the assumption based on previous observations that the coda shape is independent of source-receiver location.

References

Aki, K., Analysis of the seismic coda of local earthquakes as scattered waves, J. Geophys. Res., 74, 615-631, 1969.

Publications

Phillips, W. S. and K. Aki, The site effect of coda waves in central California for frequencies from 1 to 24 Hz, to be submitted to B.S.S.A.

Phillips, W. S., Observations of coda waves in central California, Ph.D. thesis, M.I.T. Cambridge, in preparation.

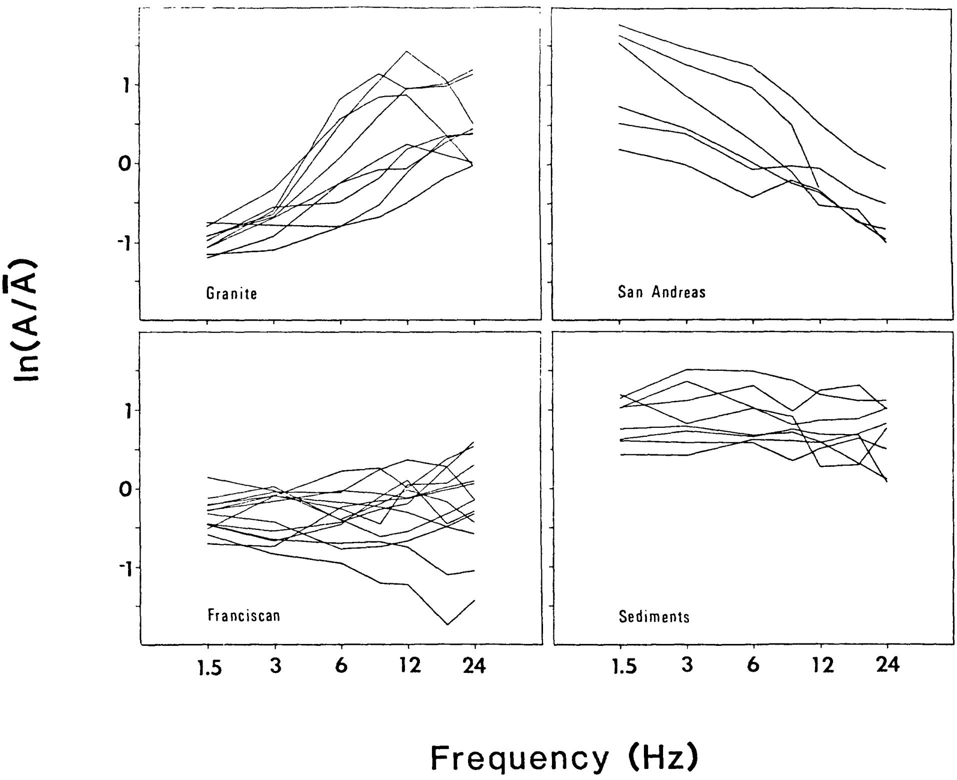

FIGURE 1: Site amplification with respect to the "average" station as a function of frequency. Results are grouped by surface geology. "Granite" sites include those in the Gabilan and Santa Lucia ranges, "Franciscan" sites are from the Diablo range and a strip alongside the Sargent fault, "San Andreas" sites are from the Hollister and Bear Valley areas, located in the fault zone, and "sediments" sites are Pliocene to Quaternary sediments not located in the fault zone, including many sites near Watsonville. Standard errors are rarely greater than 0.1. Differences in near site attenuation are responsible for the variation in high frequency behavior between these groups of stations, except at a few granite sites where small scale resonances result in peaks at 6 - 12 Hz.

Regional and Local Hazards Mapping in the Eastern Great Basin

9950-01738

R. E. Anderson
Branch of Engineering Geology and Tectonics
U. S. Geological Survey
Box 25046, MS 966, Denver Federal Center
Denver, CO 80225
(303) 236-1584

Investigations

1. Completed the study of paleostress in central Utah using fault-slip data collected from exposed faults in the transition zone between the Central Colorado Plateau and the Basin and Range province. (Anderson and Barnhard)

2. Studied paleostress in the Hoover Dam area, Nevada, using fault-slip data from exposed faults. (Anderson and Angelier)

3. Completed field mapping and began compiling map of surface faulting associated with the 1983 M_s 7.3 Borah Peak, Idaho, earthquake. Collected data to examine the relationship between the morphology of newly formed scarps and the composition of the faulted sediments. (Crone)

4. Collaborated with David P. Schwartz (Woodward-Clyde Consultants) to reexcavate a pre-1983 trench across the Borah Peak fault scarps and examine the effects of the M_s 7.3 earthquake on the trench stratigraphy. (Crone)

5. Completed interpretation of seven high-resolution reflection profiles along the Wasatch Fault zone, Utah. Collected data at three additional sites in the vicinity of Salt Lake City, and two sites in western Nevada. (Crone and Harding)

6. Completed reconnaissance mapping of Quaternary deposits along the surface trace of Nephi and Levan segments of the Wasatch fault zone (Machette), and initiated mapping along the surface trace of the Odgen and Collinston segments of the Wasatch fault zone (Personius).

7. Crone and Machette attended a U.S. Geological Survey sponsored conference on the 1983 Borah Peak earthquake (Oct. 3-6, Sun Valley, Idaho). Both presented technical papers and Crone led a one-day field trip.

8. Anderson, Crone, Wheeler, and Machette attended a workshop on "Evaluation of regional and urban earthquake hazards risk in Utah" (Aug. 14-16, Salt Lake City, Utah). Anderson and Crone presented technical papers, and Crone, Wheeler, and Machette submitted papers for publication in the workshop proceedings.

9. Machette repeated photographs of some scarps formed during the Borah Peak, Idaho, earthquake from terrestrial benchmark stations established in 1983.

10. Wheeler continued fieldwork (4 sessions totaling 7 weeks) aimed at identifying pre-Tertiary structures that may have localized a proposed segment boundary in the Wasatch fault zone, near Payson, Utah.

11. Wheeler continued completion of manuscripts left over from project 02653 (Structural framework of Eastern United States seismic zones).

Results

1. Fault-slip data were collected from several major faults in the transition zone between the Colorado Plateau and Basin and Range provinces near Richfield, Utah, including: (1) The Teasdale and Thousand Lakes faults in Emery County, (2) the Paradise fault in Wayne County, and (3) several major faults including the Sevier fault and faults that cross Salina Canyon in Sevier County. The area is of special interest because focal mechanisms from microseismicity are dominated by strike slip; whereas, previously available geologic data would predict dip-slip fault events. The youngest displacements on the Paradise fault, the Thousand Lake Fault, the faults that cross Salina Canyon, and graben-bounding faults in the Pavant Range appear to be mainly dip slip consistent with the regional geology. Some faults west of the townsite of Sevier are predominantly strike slip consistent with the seismicity. Many other faults, including the Sevier and Dry Wash faults, appear to be capable of strike-slip, or dip-slip displacements. This study is the first known documentation of major strike-slip faulting in the area.

2. At Hoover Dam 40 km southeast of Las Vegas, Nevada, where previous geologic studies indicate clockwise rotation of paleostress and a nearness to a major strike-slip fault zone boundary, sense of slip was determined on about 500 separate faults. The fault-slip data show internal consistency with respect to lithology, size of faults, and location within the small area. With respect to fault slip, however, the data represent an inhomogeneous mixture of primarily strike-slip and dip-slip motions. If, however, the data are first separated into strike-slip and dip-slip faulting modes and subsequently searched for subpopulations that correspond to contrasting paleostress orientations, the computations yield tightly constrained tensors that illustrate two distinct stress fields with subhorizontal σ_3 axes that trend N. 50° E. and N. 75° W. The σ_1 and σ_2 axes permutate in two vertical planes that strike N. 40° W. and N. 15° E. because σ_1 and σ_2 are close in value relative to σ_3. These relationships suggest that strike-slip and dip-slip faulting belong to the same tectonic regime.

   Qualitative observations of polyphase slip, fault-fault offsets, and fault-bedding geometric relationships, when evaluated in the context of changes in σ_3 orientation and permutations of σ_1 and σ_2, provide a basis for a two-stage late Cenozoic structural evolution at Hoover Dam, (1) strike-slip faulting (partly pre-tilt) and dip-slip faulting and associated stratal tilting and (2) mostly post-tilt complexly interrelated strike-slip, oblique-slip, and dip-slip faulting. The qualitative evaluations indicate that strike-slip and dip-slip faulting alternated in time during the second stage of deformation and may have done so during the first. These mixed-mode movements probably represent stress oscillations in time and space rather than discrete stress reorganizations. In contrast, the two different orientations of σ_3 either represent a major clockwise rotation of the stress field or a major counterclockwise rotation of the rocks during the faulting history. Each alternative is consistent with regional geologic relationships, and the choice of which is correct cannot be made within the small area that was studied.

3. The 36-km-long zone of fault scarps and surface ruptures associated with the Borah Peak earthquake occur primarily along the Lost River fault and follow the pre-1983 surface ruptures in extraordinary detail.

   The Borah Peak scarps show that diverse morphologies occur in the newly formed scarps and that the morphologies are influenced by many factors including sorting, grain size, and water saturation of the faulted material. In general, scarps formed in poorly sorted, subangular gravel colluvium with a silty to clayey matrix have prominent vertical to overhanging free faces. Locally, where scarps extend into rounded, well-sorted coarse sand and pebble-cobble gravel, they have lost most of the free face and raveled to maximum slope angles of 30°-37°. Another morphologic variation occurs where the scarps cut fine-grained water-saturated sediments near springs. Adjacent to the springs, the scarps in the poorly sorted colluvium have sharp, well-defined free faces but in the water-saturated sediments near the springs, the ground surface is locally warped into a broad monocline, often with tension cracks at the crest. The water-saturated sediments have deformed plastically whereas the colluvium deformed as a more brittle material. The morphologic data of these scarps will permit comparison of how these various morphologies degrade in the future.

   Several sets of slickensides occur on a bedrock face exposed in the newly formed fault scarp on the flank of Dickey Peak. The rakes of the slickensides show that past movements on the fault have been dominantly normal slip with both left- and right-lateral components. All of the observed slickensides predate the Borah Peak earthquake.

4. In 1976, M. H. Hait, Jr. (U.S. Geological Survey, Denver) excavated and mapped a trench across the prehistoric fault scarp along the Lost River fault at Doublespring Pass road. The Borah Peak earthquake ruptured the scarp at the trench site and exposed the trench in the newly formed scarp. Studies of the reexcavation of Hait's trench are continuing but to date there are two important observations about the behavior of the Lost River fault at this site. Many small 1983 scarps overlie pre-1983 shear zones indicating that very small displacement faults (tens of centimeters) were reactivated during the Borah Peak earthquake and that the pattern of ground breakage in 1983 was very similar to the breakage associated with the prehistoric earthquake. Furthermore, the displacements associated with the prehistoric earthquake were very similar in size to those produced by the Borah Peak earthquake.

5. High-resolution reflection profiling is an effective method to examine near-surface structure and faulting associated with Holocene fault scarps along the Wasatch fault zone. The main fault scarps overlie either vertically displaced reflections, zones of incoherent reflected energy or

fault zones in the shallow subsurface are not associated with scarps; thus, areas of potential surface faulting defined solely on the basis of recognizable fault scarps may underestimate the surface faulting hazards. Poorly constrained data suggest that the Quaternary slip rate for the East Bench fault in Salt City is considerably less than the Holocene rates estimated from trenching studies of other parts of the Wasatch fault zone. At Hobble Creek, south of Provo, a broad area of back rotation extends west of the scarp for more than a kilometer in the shallow sursurface.

Reflection data collected across two suspected intrabasin faults in the Jordan River Valley and at the Salt Lake salient new Beck's Hot Springs north of Salt Lake City have not yet been processed. Similarly, reflection data from the Beatty fault and Crater Flats in western Nevada awaits processing.

6. The most interesting result of Machette and Personius's studies is the estimation of cumulative slip rates during various time intervals along two segments of the Wasatch fault zone (WFZ). These data show that Quaternary slip rates may have culminated in latest Pleistocene time (table 1) during the rapid growth and contraction of Lake Bonneville. Slip rates calculated from fault offset in both pre-Bonneville and post-Provo-age deposits are much less than rates calculated from fault offset in Provo- and Bonneville-age deposits.

Faulted fan deposits of pre-Bonneville age are preserved at the mouth of Gardner Creek, just north of Nephi, and near Jim May Canyon, just north of Brigham City. Mid(?)-Holocene alluvium, most of which may have been deposited during the warm, dry Altithermal (about 4,000-6,000 yrs ago), is the youngest deposit for which we have reliable slip data. Conversely, the oldest deposit for which we can calculate a slip rate is fan alluvium that contains a soil with strongly developed K horizons of 200,000-250,000 yrs age.

The mid-Holocene alluvium is vertically offset about 3.9 m at Gardner Creek, and if one uses an average age of 5,000 yrs for the alluvium, the average slip rate is about 0.8 m/ka. Fault scarps formed in 250,000(?)-yr-old alluvium at Gardner Creek are 26-28 m high and are probably associated with 30 m (-5 m, + 10 m) of fault offset. On the basis of this offset value and an age of 250,000 yrs, the cumulative late Quaternary slip rate on the WFZ at Gardner Creek is 0.12 m/ka (the range in values is 0.10-0.18 m/ka; table 1). The latter slip rate is only 15 percent of the mid-Holocene slip rate (0.78 m/ka).

Pre-Bonneville alluvium near Jim May Canyon is vertically offset 30 m by the WFZ. Comparison with soils studied elsewhere in the region suggests a reasonable age estimate of 200 ka (± 50 ka) for this deposit. These data yield a cumulative pre-Bonneville slip rate of 0.15 m/ka (compare with 0.12 m/ka for the Gardner Creek area). To the north and east of Brigham City, Provo and associated recessional shoreline gravels (12-14 ka) are offset 12-15 m. Average values of these data (13.5 m and 13 ka) yield a slip rate of about 1.0 m/ka: this value more than six times the pre-Bonneville slip rate.

Most of the post-Provo alluvial-fan deposits near Brigham City are of latest Pleistocene to early Holocene age (12-8 ka); fault offset in these deposits is 4-6 m. The youngest faulting in the area offsets a mid(?) Holocene (6-4 ka) alluvial-fan deposit 1.5 m. Average values of these data yield slip rates of 0.50 and 0.30 m/ka since early and middle(?) Holocene time, respectively. No evidence of post-mid(?) Holocene faulting has been recognized in the Brigham City area.

Table 1. Cumulative slip rates (m/ka) recorded in offset Quaternary deposits (age in ka) along the Wasatch fault zone

Time interval	Jim May Canyon (Personius)	Hobble Creek	North Creek	Gardner Creek (Machette)
Mid(?) Holocene (5 ka)	0.30 (6 ka)	[1]1.3 (4.5 ka)	[2]1.3	0.78
Early(?) Holocene (10 ka)	0.50			
Post-Provo (13.5 ka)	1.0 (13.5 ka)	[1]0.85-1.0	n.d.	n.d.
Post-Bonneville	n.d. (17 ka)	[3]<1.8	n.d.	n.d.
Pre-Bonneville (200 ka)	0.15	n.d. (250 ka)	[4]0.20 (250 ka)	0.12
Late Cenozoic	0.4 for the central Wasatch fault zone[5]			

[1] Data from Swan and others (1980).
[2] Data from Schwartz and others (1983).
[3] Most likely rate of Swan and others (1980); range is <1.7 to <3.3 m/ka.
[4] Calculated from ratio of pre-Bonneville to mid-Holocene slip rates at Gardner Creek times mid-Holocene slip rate at North Creek.
[5] Data from Naeser and others (1983).

7. The central problem in developing source zones for the east is how to generalize to large regions the detailed understanding of seismogenic structure that exists for a few small locales. Few schemes for generalization take advantage of new interpretations of Appalachian tectonics. Wheeler and Bollinger (1984) suggest that the concept of suspect terranes is a natural vehicle for such generalization, and show that proposed terrane boundaries are consistent with spatial characteristics of southeastern seismicity and with structural models of seismicity in central and southwestern Virginia and southeastern South Carolina.

Reports

Anderson, R. E., 1984, Strike-slip faults associated with extension in and adjacent to the Great Basin: Geological Society of America Abstracts with programs, v. 16, no. 6, p.

Anderson, R. E., and Barnhard, T. P., 1984, Late Cenozoic fault and fold patterns in Sevier County, Utah, and their relationship to seismicity in the area: Geological Society of America Abstracts with Programs, v. 16, no. 6, p. 430.

Anderson, R. E., Irwin, W. P., and Thenhaus, P. C., 1983 [1984], Southern Rocky Mountains seismic source zones--Summary of workshop convened January 23-24, 1980, *in* Thenhaus, P. C., ed., Summary of workshops concerning regional seismic source zones of parts of the conterminous United States, convened by the U.S. Geological Survey 1979-1980, Golden, Colorado: U.S. Geological Survey Circular 898, p. 14-18.

Angelier, Jacques, Colletta, Bernard, and Anderson, R. E., in press, Neogene paleostress changes in the Basin and Range--A case study at Hoover Dam, Nevada-Arizona: Geological Society of America Bulletin.

Arabasz, W. J., and Wheeler, R. L., 1984 (in press), Summary and recommendations of discussion group 1--Synthesis of geological, geophysical, and engineering data for evaluation of earthquake hazards, *in* Proceedings of conference, A workshop on evaluation of regional and urban earthquake hazards and risk in Utah, Salt Lake City, August 14-16, 1984: U.S. Geological Survey Open-File Report, 10 p.

Barnhard, T. P., and Anderson, R. E., 1984, Extensional and compressional paleostress states in the western Colorado Plateau, central Utah: Geological Society of America Abstracts with Programs, v. 16, no. 6, p. 437.

Crone, A. J., and Harding, S. T., 1984 (in press), Near-surface faulting associated with Holocene fault scarps, Wasatch fault zone, Utah--a preliminary report, *in* Proceedings of conference, A workshop on evaluation of regional and urban earthquake hazards and risk in Utah, Salt Lake City, August 14-16, 1984: U.S. Geological Open-File Report, 35 p.

Crone, A. J., and Machette, M. N., 1984 (in press), Surface ruptures associated with the 1983 Borah Peak earthquake, Idaho: Geology.

Machette, M. N., 1984 (in press), Late Cenozoic geology of the Beaver basin, southwestern Utah: Brigham Young Studies in Geology.

Machette, M. N., 1984 (in press), Preliminary investigations of Quaternary geology along the southern part of the Wasatch fault zone, central Utah, *in* Proceedings of conference, A workshop of evaluation of regional and urban earthquake hazards and risk in Utah, Salt Lake City, August 14-16, 1984: U.S. Geological Survey Open-File Report, 15 p.

Machette, M. N., and May, R. J., Thermoluminescence dating of soil carbonate--feasibility, techniques, and results from two areas of New Mexico: submitted to Quaternary Research (7/25/84), 30 ms. p., 9 figs., 3 tables.

Machette, M. N., and Personius, S. F., 1984, Map of Quaternary and Pliocene faults in the eastern part of the Aztec 1° x 2° quadrangle and western part of the Raton 1° x 2° quadrangle, northern New Mexico: U.S. Geological Survey Miscellaneous Field Studies Map MF-1465-B, scale 1:250,000. (Accompanied by 18-page text.)

Personius, S. F., and Machette, M. N., 1984, Quaternary and Pliocene faulting in the Taos Plateau region, northern New Mexico, in Rio Grande Rift--northern New Mexico: New Mexico Geological Society Guidebook, 35th Field Conference, p. 83-90.

Wheeler, R. L., 1983, Stratigraphic evidence for Devonian tectonism on lineaments at Allegheny Front, West Virginia--Supporting material: U.S. Geological Survey Open-File Report 83-243, 23 p.

______1984 (in press), A plan for evaluating hypothesized segmentation of the Wasatch fault, in Proceedings of conference, A workshop on evaluation of regional and urban earthquake hazards and risk in Utah, Salt Lake City, August 14-16: U.S. Geological Survey Open-File Report, 33 p.

Wheeler, R. L., and Bollinger, G. A., 1984, Seismicity and suspect terranes in the southeastern United States: Geology, v. 12, p. 323-326.

References cited

Naeser, C. W., Bryant, Bruce, Crittenden, M. D., Jr., and Sorensen, M. L., 1983, Fission-track ages of apatite in the Wasatch Mountains, Utah--an uplift study, in Miller, D. M., Todd, V. R., and Howard, K. A., eds., Tectonic and stratigraphic studies in the eastern Basin and Range: Geological Society of America Memoir 157, p. 29-36.

Schwartz, D. P., Hanson, K. L., and Swan, F. H., III, 1983, Paleoseismic investigations along the Wasatch Fault zone--an update, in Gurgel K. D., ed., Geologic excursions in neotectonics and engineering geology in Utah; Guidebook, Part IV: Utah Geological and Mineral Survey Special Studies 62, p. 45-49.

Swan, F. H., III, Schwartz, D. P., and Cluff, L. S., 1980, Recurrence of moderate to large magnitude earthquakes produced by surface faulting on the Wasatch fault zone, Utah: Seismological Society of America Bulletin, v. 70, no. 5, p. 1431-1462.

Crustal Deformation Measurement in the Shumagin Seismic Gap, Alaska

USGS-14-08-0001-G944

John Beavan and Roger Bilham
Lamont-Doherty Geological Observatory of Columbia University
Palisades, New York 10964
(914) 359-2900

Investigations:

1. Nine short (≈1 km) level lines (Fig. 2) are measured approximately annually within the Shumagin Islands seismic gap, Alaska. Surface tilt data are interpreted in terms of tectonic deformation at the Pacific-North American plate boundary.

2. Five absolute-pressure sea level gauges are operated in the Shumagins (Fig. 1) in an attempt to measure vertical deformation associated with the Aleutian subduction zone. A continuously recording two component tiltmeter is operated at one site.

3. Data from the sea level and tilt sensors are transmitted to Lamont in near real time and are examined for possible tectonic signals. Studies of noise level as a function of frequency are underway to determine the relative usefulness of different types of measurement, and to evaluate the minimum size of tectonic signal which will be visible above the noise.

Results:

The leveling results are shown in Fig. 3. Long-term sea level signals are shown in Fig. 4. The best site has an up-time of 74%, the worst 26%. Failures are due about equally to damage to the sensorto-shore cable, and to transmitter failures. Fig. 5 shows initial results from the new tiltmeter installation. Fig. 6 shows log power spectra of the tiltmeter data, and of a tilt signal generated by differencing two sea level signals and dividing by the distance between them (sea slope). The lowest frequency in these spectra is 1c/month and the sea slope is noisier than the tiltmeter at all frequencies above this. As more tiltmeter data become available this analysis will be extended to lower frequencies; we expect that the sea slope data will become quieter than the tiltmeter data (and hence more useful for detecting tectonic signals) at periods longer than several months.

Reports

Beavan, J., R. Bilham, and K. Hurst, 1984. Coherent tilt signals observed in the Shumagin seismic gap; detection of time-dependent subduction at depth? J. Geophys. Res., 89, 4478-4492.

Bilham, R., J. Beavan, K. Hurst and K. Evans, 1984. Crustal deformation metrology at Lamont-Doherty Geological Observatory, J. Geod. Soc. Japan, in press.

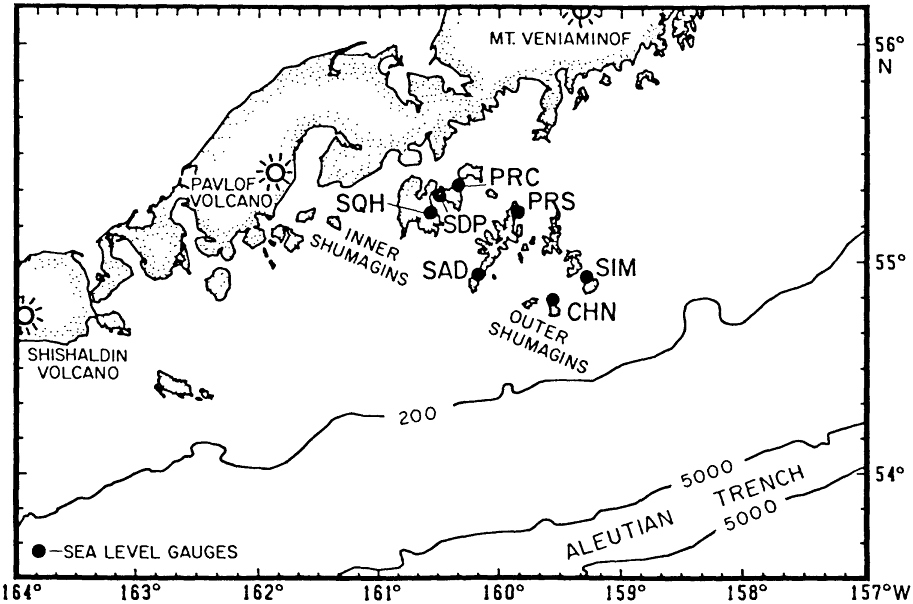

Figure 1. Locations of sea level gauges in the Shumagin Islands.

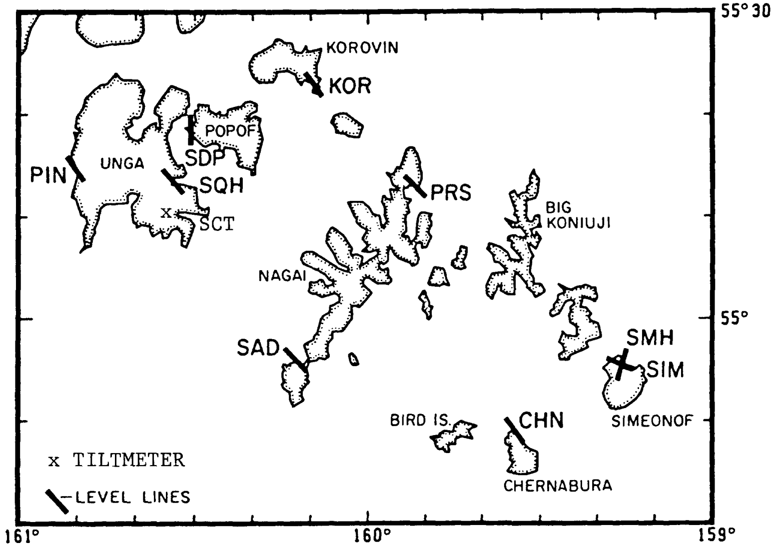

Fig. 2 The Shumagin Islands, showing the locations and directions of first-order level lines, whose lengths vary between 600 m and 1200 m.

A two-component mercury level tiltmeter was installed at SCT during 1984.

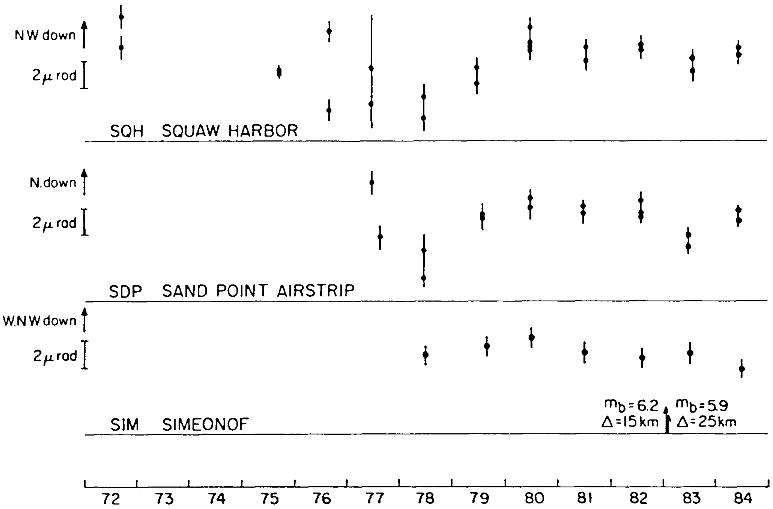

Figure 3. Tilt in the Shumagin Islands, as determined from level line measurements. Tilt rates are typically a few tenths of a microradian per year down towards the trench. A significant 5 microradian reversal occured between 1978 and 1980. This has been interpreted as due to a slip episode on the Benioff zone between approx. 20 km and 70 km depth (Beavan et al 1984). The one line oriented perpendicular to the relative plate motion vector (SMH) shows no significant tilt.

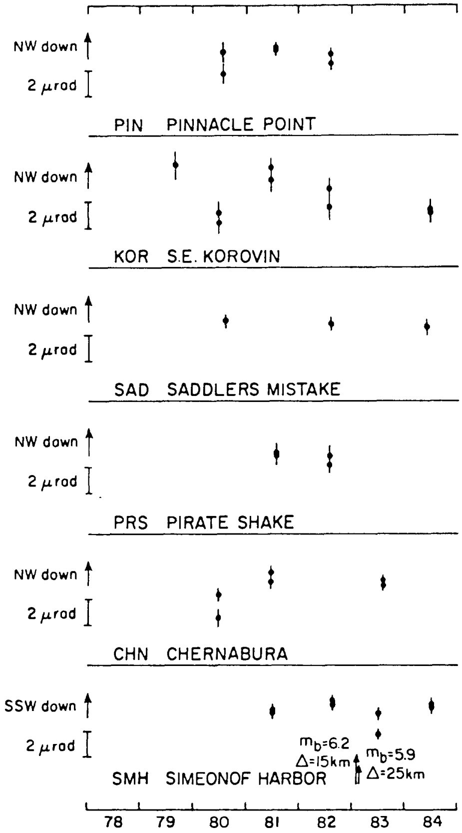

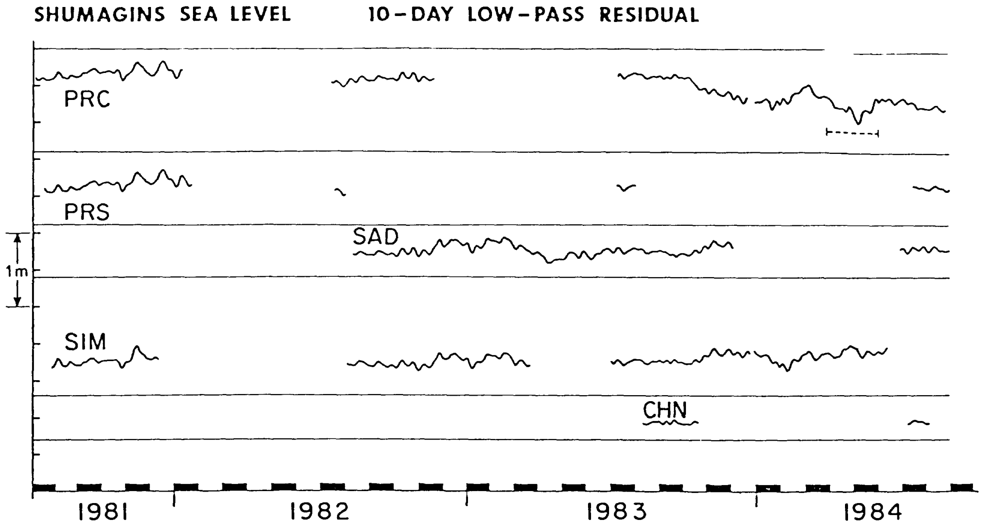

Figure 4. Three years data from sea level gauges. Tides have been removed, and the data low-pass filtered with a 10 day cut-off. Long period signals of oceanographic origin are correlated between gauges and can be removed by differencing. Note that the data from PRC have a offset since late 1983; this is due to an electronic malfunction, and it may be correctable by further processing.

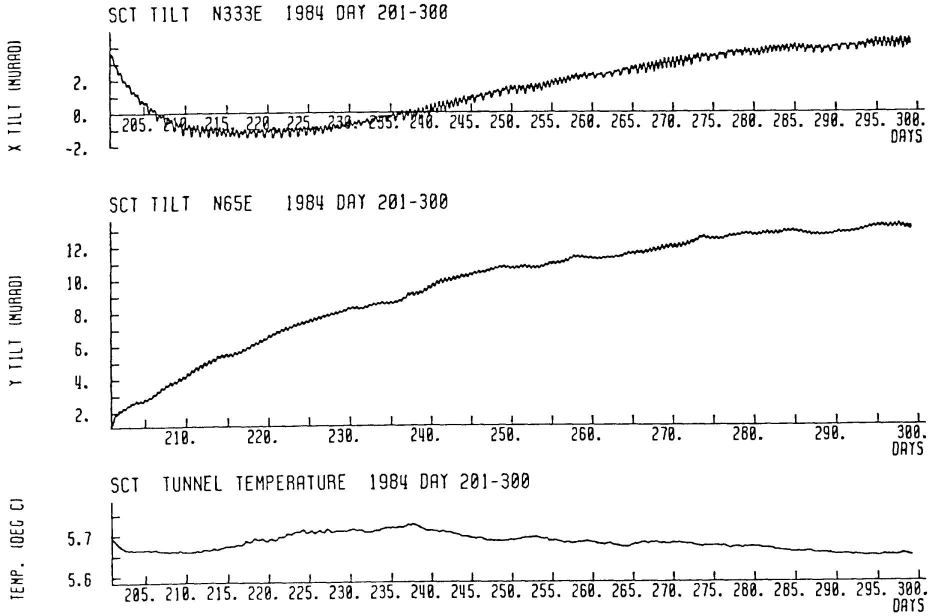

Figure 5. The first 100 days data from a two-component mercury level tiltmeter on Unga Island. The decreasing exponential drift is probably due to mount settling.

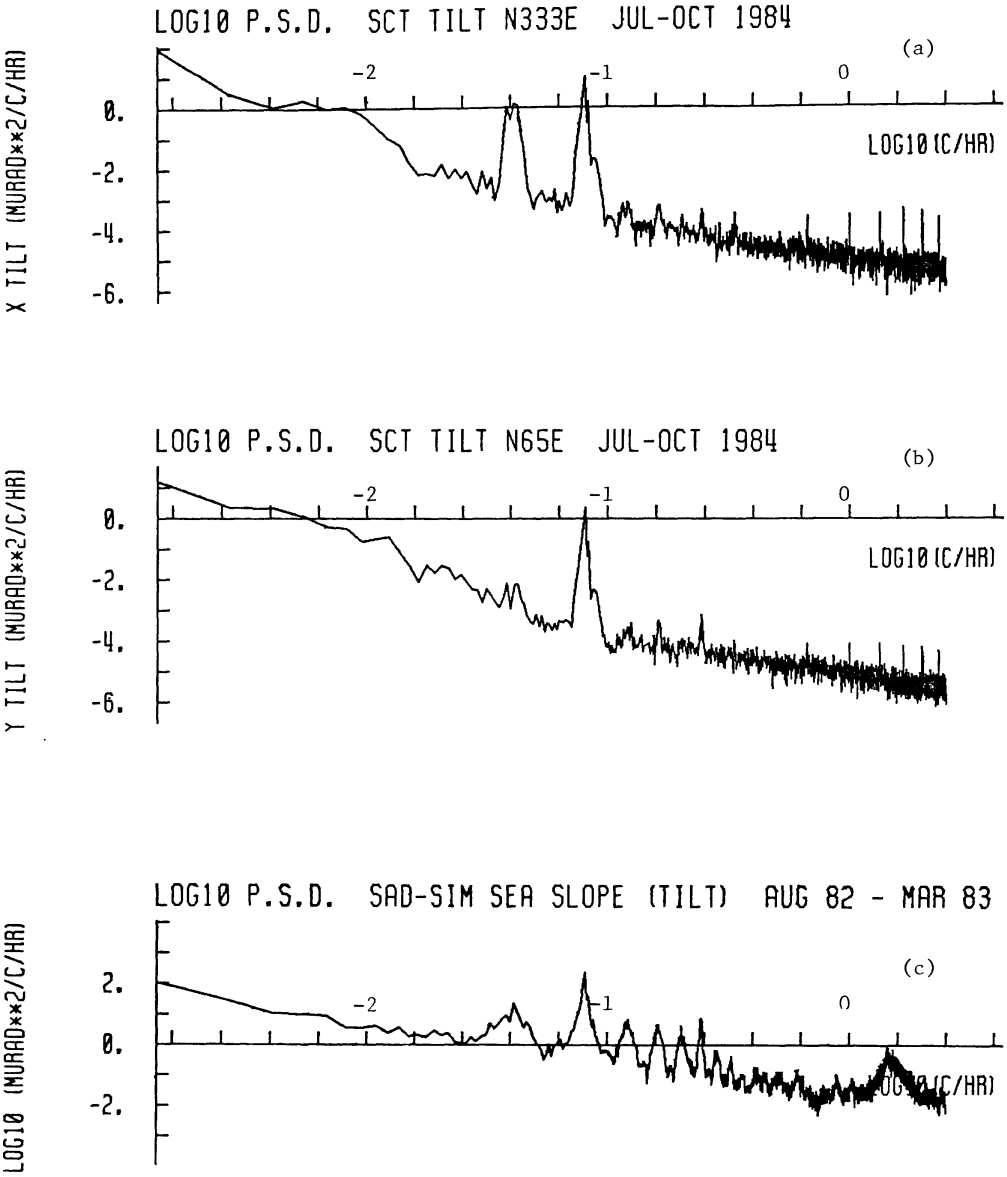

Figure 6. (a), (b) Log_{10} power spectral density (psd) of two components of tiltmeter. (c) Log_{10} psd of tilt calculated by differencing two sea level measurements and dividing by the distance between them. At all frequencies above 1 c/month the tilt measurements are quieter than the sea slope measurements. By extrapolating the spectra, we expect that the sea slope measurements will be quieter at periods longer than a few months.

Seismological Data Processing

9930-03354

Barbara Bekins

Branch of Seismology
U.S. Geological Survey
345 Middlefield Rd. MS 977
Menlo Park, California, 94025
(415) 323-8111 ext. 2965

Investigations

Computer data processing is absolutely necessary in modern seismological research; digital seismic data can be analyzed in no other way, and problems of earthquakes and seismic wave propagation usually require numerical solution. On the other hand, the interface between computers and people usually makes data processing unnecessarily difficult. The purpose of this project is to develop and operate a simple, powerful, well human-engineered computer data processing system and to write general application programs to meet the needs of scientists in the earthquake prediction program and monitor earthquakes in northern California. This goal includes maintaining the ability to transfer data and programs over a network and the ability to share data and programs with external contractors.

Results

The PDP11-70 UNIX system has continued to operate smoothly, and performs a large amount of computing for program projects. Some current statistics:

194	registered users
446703	1024-byte disk storage blocks used
84	login sessions per weekday

The Calnet operations plus the Mammoth project and the Crustal Heterogeneity project have moved to the new Vax 750. The current usage on that machine is:

524064	1024-byte disk storage blocks used
43	login sessions per weekday

To address a concern that the Vax 750 is slower than the 11/70 two additional megabytes of memory, and a massbus interface for the tape drive were purchased.

This project is beginning to investigate the database needs of the Seismology Branch. Some commercial databases available for UNIX have been investigated. Also being investigated are super microcomputers which run the UNIX system. Such a system is desired to replace the VAX 750 which may be used to support work under the VMS system in the future.

This project also handles one third of the support for the office Vax 780 operation. This support consisted of weekly and monthly disk backups to tape, authorizing new users, redistributing Seismology branch disk quotas, assisting users, and occasional miscellaneous activities related to computer operations.

Earth Structure and its Effects upon Seismic Wave Propagation

9920-01736

George L. Choy
Branch of Global Seismology and Geomagnetism
U.S. Geological Survey
Denver Federal Center, MS 967
Denver, Colorado 80225
(303) 236-1506

Investigations

1. Source parameters from broadband data. We are developing methods to extract more accurate source parameters from waveforms by determining corrections for propagation effects such as frequency dependent attenuation.

2. Shear wave interaction with the earth's mantle. We are seeking constraints on the frequency dependence of shear wave attenuation and on velocity structure in the earth's mantle by synthesizing broadband body waves with frequency content from tens of seconds to several Hz.

Results

1. We have developed a method of computing radiated energy for shallow, complex ruptures that directly incorporates the effects of frequency dependent attenuation. Application of the method to two recent earthquakes (the Coalinga earthquake of 2 May 1983 and the Borah Peak earthquake of 28 October 1983) indicates that indirect methods, which do not adequately exploit spectral information above the corner frequency, may overestimate radiated energy.

2. We have obtained broadband body waves from deep earthquakes recorded at the GRF array and by stations of the GDSN. We have found that even moderate-sized earthquakes display significant rupture complexity, so a critical aspect of the analysis is that realistic source models must be considered. Preliminary results indicate that S-wave attenuation is nearly proportional to P-wave attenuation up to 2 Hz. The behavior of S-waves across the GRF array at distances about the S-wave cusp is contrary to that expected for models which propose a discontinuous velocity jump just above the core-mantle boundary. Possible explanations for the observed waveform behavior include source complexity and/or anomalous shear-wave polarization across laterally inhomogeneous structure.

Reports

Choy, G. L., 1984, FWT (Full Wave Theory) Documentation, in Documentation of Earthquake Algorithms, World Data Center A for Solid Earth Physics.

Boatwright, J. and G. L. Choy, 1984, Teleseismic estimates of the energy radiated by shallow earthquakes, in preparation.

Remote Monitoring of Source Parameters for Seismic Precursors

9920-02383

George L. Choy
Branch of Global Seismology and Geomagnetism
U.S. Geological Survey
Denver Federal Center, MS 967
Denver, Colorado 80225
(303) 236-1506

Investigations

1. Broadband analysis of moderate-sized earthquakes. We are applying methods of seismogram synthesis to study the rupture characteristics of the Coalinga earthquake of May 2, 1983.

2. Teleseismic estimates of radiated energy from shallow earthquakes. We are developing a method for computing radiated energy directly from teleseismic body waves, rather than through indirect methods (such as empirical relationships with moment).

Results

1. The broadband content of digitally recorded body waves from the GDSN permits detailed resolution of the rupture process. The modelling technique combines realistic source models with propagation operators computed by the full-wave or reflectivity methods. We have determined that the Coalinga mainshock was a complex rupture consisting of two events, occurring 3.2 seconds apart. The depth of nucleation, focal mechanism, radiated energy, moment and bounds for associated stress drops for each event were determined.

2. We have applied our method to compute the radiated energy of two events: the Coalinga earthquake of 2 May 1983 and the Borah Peak earthquake of 28 October 1983. Advantages of the method are: (1) it analyses frequencies about and above the corner frequency by using digitally recorded broadband data; (2) it accounts directly for frequency dependent attentuation; and (3) its accuracy is unaffected by rupture complexity. Indirect estimates of energy (e.g., those depending on simplistic relations with seismic moment) may overestimate energy if the rupture process involves a sizeable component of aseismic slip.

Reports

Choy, G. L., 1984, Inferring rupture characteristics of shallow moderate-sized (m_b~6.0) earthquakes from broadband body waves: Earthquake Notes, 55, 13.

Choy, G. L., 1984, Source parameters of the Coalinga, California earthquake of May 2, 1983 inferred from broadband body waves: U.S. Geological Survey Professional Paper, submitted.

Boatwright, J., and G. L. Choy, 1984, Teleseismic estimates of the energy radiated by shallow earthquakes, in preparation.

Search for Electromagnetic Precursors to Earthquakes

66730

William D. Daily
Lawrence Livermore National Laboratory
P. O. Box 808, L-156
Livermore, CA 94550
(415) 422-8623

Objective: Observations of electromagnetic (EM) precursors have been reported for large earthquakes in Japan, Iran, Chile and the Soviet Union (e.g., by Gokhberg et al., 1980 a). Mechanisms and semiquantitative models advanced to explain the observations have been discussed by Gokhberg, et al., (1980 b) and Warwick, et al. (1982). Laboratory demonstration of radio frequency emission from cracking rocks has also been reported (Nitsan, 1977; Vorobev, 1977). Although the Soviet Union, Japan and China have programs to evaluate EM emissions near a fault as a precursor to fault rupture, the United States has conducted little research in this area. The objective of the research reported herein is to determine if measurable EM precursors exist for earthquakes originating along the San Andreas Fault system.

Data Acquisition: Five radio frequency receivers have been built to monitor the broadband EM noise spectrum along the fault. Each has been placed at a location determined by: (1) the estimated probability of an earthquake of Richter magnitude greater than about 5, (2) accessibility to site to facilitate deployment and periodic equipment checks, (3) isolation from cultural sources of wide band EM noise, (4) reasonable security. To allow some discrimination of source location, monitoring stations are spaced far enough apart that signals from an event will not be seen equally well by all sensors. If the source region for these signals is deep (a few kilometers), signals at the surface should be confined near the epicenter--attenuation will be high due to propagation long distances through high loss crust from the source. If the source region is near the surface, signals will be measurable at larger distances. From these considerations and published measurements of precursors, we estimate that the locations monitored should be a few hundred kilometers apart, but also chosen for their high potential as an epicenter for a large earthquake. Monitoring stations are operating at (1) Coyote Lake (near Morgan Hill), (2) Bear Valley (near Pinnacles National Park), (3) Parkfield, (4) Adobe Mountain (near Palmdale) and (5) Pinon Flat Observatory (near Palm Springs).

Each monitor is a broadband receiver covering 3 frequency bands: 200 Hz to 1 kHz, 1 kHz to 10 kHz, 10 kHz to 100 kHz. Each channel has 60 dB dynamic range (logarithmic amplifiers) and data is recorded on a strip chart recorder. The first monitor was deployed in October 1983; the most recent deployed in May 1984. All five stations are currently operational.

The signal received by each monitor is very site specific. At some sites, the signal in all frequency bands is continuously highly variable on a time scale of a few hours. At other sites, the measured signal levels are nearly constant for periods of weeks at a time. The reason for this difference is unknown but some sites may have high levels of cultural noise which would be variable in amplitude. An example of data collected is shown in the figure. This data is from an electromagnetically quiet station. Note the signal amplitude decrease on April 18, 1984. This was about six days before a magnitude 6 earthquake with epicenter a few kilometers from the monitoring station. This signal decrease is not typically seen in the data. This earthquake is the only one of comparable magnitude along the San Andreas system during the time the stations have been deployed. Only the Coyote Lake station was operational at the time of this event.

References

Gokhberg, M. B., I. L. Gufeld, and I. P. Dobrovolsky, "On the Sources of Electromagnetic Earthquake Precursors," Preprint N 10, Acad. of Sci. of the U.S.S.R., Moscow, 1980 a.

Gokhberg, M. B., I. L. Gufeld, I. P. Dobrovolsky, G. I. Shevtsov, "Studies of Mechanoelectric Effects Under Laboratory Conditions," Preprint N 9, Acad. of Sci. of the U.S.S.R., Moscow, 1980 b.

Vorob'ev, A. A., "Electromagnetic Radiation in the Process of Crack Formation in Dielectrics," Difektoskopiya, No. 3, 128, 1977.

Nitsan, U., "Electromagnetic Emission Accompanying Fracture of Quartz-Bearing Rocks," Geophys. Res. Letters, 4, 333, 1977.

Warwick, J. W., C. Stoker, and T. R. Meyer, "Radio Emission Associated with Rock Fracture: Possible Application to the Great Chilean Earthquake of May 22, 1960," J. Geophys., Res., 87, 2851, 1982.

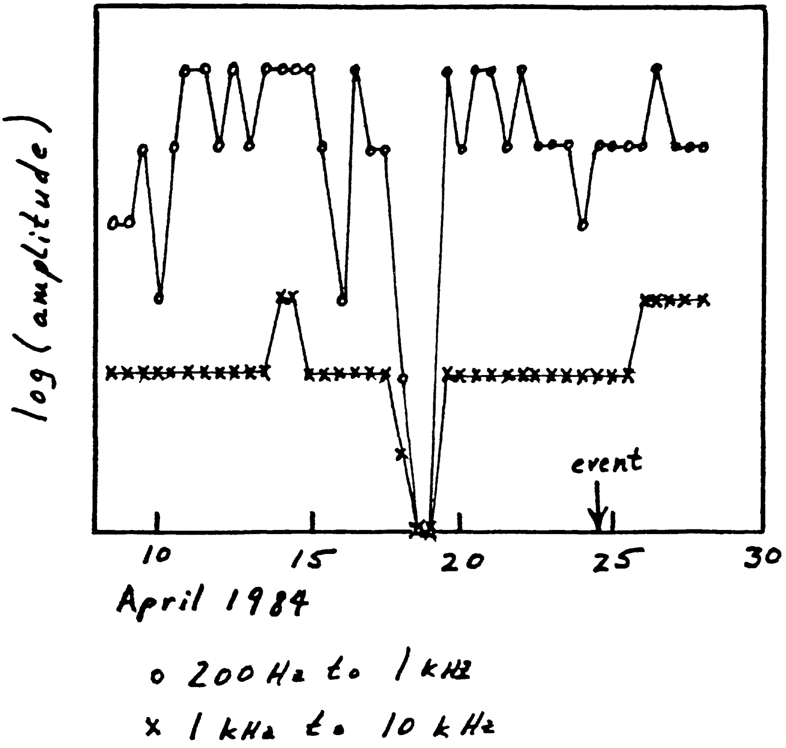

Amplitude of received signal measured at Coyote Lake, California in two low frequency electromagnetic bands during April 1984. Each point is a 12 hour average of data. The event marked was a magnitude 6 earthquake with an epicenter near Morgan Hill, California. Six days before the event, the signal level fell to a value below the instrumental logarithmic scale minimum.

Central California Network Operations

9930-01891

Wes Hall
Branch of Seismology
U.S. Geological Survey
345 Middlefield Road, MS-977
Menlo Park, California 94025
(415) 323-8111, Ext 2509

Investigations

1. Maintenance and recording of 406 seismograph stations, located in Northern Calif., Central Calif., Oregon, and Yellowstone National Park. The area covered is approximately 91,000 square miles.

Results

1. Replaced Terra Technology instrumentation at four locations in the Parkfield area with 3-component modified J402 VCO's (Middle Mountain, Vineyard Canyon, Hog Canyon, Turkey Flat). All VCO's were retrofitted with a new temperature compensation circuit, checked for improved noise specs, and environmentally checked from 60° to -15°.

2. Completed installation of a microwave transmitter facility at Hog Canyon. Installation included construction of a 10'x10' building, 30 ft. tower, 6 ft. parabolic antenna, 430 watt solar array and microwave transmit equipment.

3. Williams Hill - Co-located a microwave site within a commercial television facility. Installed a 10 ft. and 4 ft. parabolic antennas.

4. Mt. Tamalpais - Co-located a microwave site within the U.S. Corps of Engineer radio facility. Installed 30 ft. tower and a 8 ft. parabolic antenna.

5. Serviced the Southern Oregon seismic array. Installed new sites at Ichabad Quarry (VIQ), Klammath Pt. (VKP), Solomon Butte (VSO). Installed 20 ft. tower at Haymaker (VHA) and moved the Herd Peak relay site to Deer Mountain.

Northwest U.S. Subduction Zone
Risk Assessment
4-9930-03790

Thomas H. Heaton and Stephen H. Hartzell
Branch of Seismology
U.S. Geological Survey
525 S. Wilson Avenue
Pasadena, CA 91106
(818) 356-6956

The purpose of this project is to assess the potential seismic hazard due to great shallow thrust earthquakes along the Juan de Fuca subduction zone which is located along the coasts of Washington and Oregon. There is good evidence that the Juan de Fuca and North American plates are converging at a rate of between 3 and 4 cm/yr along the Juan de Fuca subduction zone. However, present day seismicity is extremely low and there is no historic (150 years) evidence of significant earthquakes along the shallow portion of the subduction zone. One explanation for this situation is that aseismic creep is occurring over the entire fault which is approximately 900 km long and 100 km wide. Although aseismic creep is thought to be common for many subduction zones where old oceanic lithosphere is subducted, it is usually accompanied by a moderate level of occurrence of shallow thrust earthquakes of magnitude greater than 6. Such earthquakes are remarkably absent in the historic record of Washington and Oregon. Furthermore, very young crust is being subducted in the Juan de Fuca subduction zone and it appears that the Juan de Fuca subduction zone is clearly different from the most common class of aseismic subduction zone. Instead, it has noteable similarities to other subduction zones where very young oceanic lithosphere is being subducted and which have experienced very large shallow subduction earthquakes.

Investigations

1. The first phase of work is a comparative study of subduction in the northwestern United States with other world wide subduction zones. Due to the lack of large historic earthquakes in the Pacific Northwest, the seismic risk is evaluated by drawing analogies with other subduction zones having similar characteristics. Physical parameters which are considered include; a) plate age, b) convergence rate, c) shallow seismicity, d) trench bathymetry and gravity, e) overall geometry of the subducted slab.

2. A short reconnaissance field survey of coastal terraces in northernmost California, Oregon, and Washington has been completed. The general pattern of coastal uplift since the last interglacial period (120,000 YBP) was investigated. We also searched for evidence of episodic Holocence uplifts that may be associated with great shallow subduction earthquakes. This was a cooperative project with the Japanese geomorphologists, Yoko Ota and Atsumasa Okada, who have extensive experience in the study of coastal deformation at other subducting boundaries.

3. Using the information obtained from investigations 1 and 2, the source dimensions of potential northwestern United States shallow subduction earthquakes are estimated.

4. Broad-band teleseismic P-wave recordings of large shallow subduction earthquakes from a variety of subduction zones are studied in order to investigate their overall source characteristics. Systematic evaluations are made to determine; a) total moment release, b) rupture duration, c) rupture complexity, and d) spectral characteristics of radiated energy.

5. The final phase of the project is the estimation of potential strong ground motion and Tsunami hazard based on the results of the above investigations.

Results

1. Heaton and Kanamori (1984) note that the Juan de Fuca subduction zone is clearly different from the most common class of aseismic subduction zone that is characterized by the subduction of very old oceanic crust. On the basis of the age of subducted lithosphere, geometry of the subducted plate, and the convergence velocity, they noted that the Juan de Fuca subduction zone is similar to other zones that have experienced great shallow subduction earthquakes. As a follow-up to this earlier work, we have systematically compared trench bathymetry, free-air gravity anomalies, and temporal seismicity for all major circum-Pacific subduction zones. We find that there is a very good correlation of trench depth and size of free-air gravity anomaly with the age of the subducted lithosphere. The extreme young age of subducted lithosphere (5-15 my) in the Pacific Northwest is consistent with the fact that no bathymetric trench is observed.

   We also compared shallow circum-Pacific subduction seismicity for the period from 1933 to 1980. At a magnitude cutoff of 6.0, low seismicity levels are seen for both strongly coupled and weakly coupled subduction zones whereas moderately coupled subduction zones have relatively high seismicity levels. However, the Juan de Fuca subduction zone is conspicuous for having the lowest seismicity level of any zone studied.

   Our comparison of the physical features of subduction zones has reinforced the earlier observation of Heaton and Kanamori (1984) that the Juan de Fuca subduction zone shares many features with other strongly coupled subduction zones. However, the Juan de Fuca subduction zone may be considered as an end member in that it involves some of the youngest subducted lithosphere anywhere. This, in itself, suggests that the Juan de Fuca subduction zone belongs in a class (perhaps aseismic) by itself. However, there are several other localities where comparably young crust appears to be subducting. These are southern Chile between 40° and 45° south latitude, Colombia near 2° north latitude, and the Rivera plate off western Mexico. These regions all appear to be strongly coupled and Colombia and southern Chile have experienced earthquakes with energy magnitudes of 8.8 (1906) and 9.5 (1960), respectively. Bathymetric profiles across the subduction zones of Colombia and southern Chile are strikingly similar to those in the Pacific Northwest. There is also evidence that these regions have experienced significant periods of seismic quiescence. Unfortuntely the NOAA catalog is not sufficiently complete to allow a comparison of seismicity at small magnitude earthquakes. However, at a magnitude cutoff of 6, the rate of seismicity in the 50 years preceding the 1960 earthquake in the region between 40° and 45° south latitude seems comparable to that reported for the Juan de Fuca subduction zone.

2. Investigations into the nature of marine terraces along the Juan de Fuca subduction zone indicates significant variation in the long-term uplift rate along the coasts of northern California, Oregon, and Washington. Regions of both apparent uplift and subsidence were identified. In general, the highest uplift rates appear to occur in southern Oregon and northern California. Points of land closest to the trench appear to be uplifting the most rapidly, with uplift rates of greater than 3 mm/year and 1 mm/year inferred for Cape Mendocino and Cape Blanco, respectively. Uplift at a rate lower than .5mm/year are generally found between these two points. Sea level appears to be relatively stable in northern Oregon and southern Washington with some areas of potential subsidence. The action of glacial erosion and deposition makes estimation of previous sea levels difficult in northern Washington. However, we believe that uplift in this region may not exceed 0.5 mm/year.

   Except in the triple junction region of Cape Mendocino, no obvious Holocene terraces were observed. However, the extreme erosion action along this coastline would make the preservation of such features difficult except in areas of very high uplift rates.

3. Using the age-rate relationship vs. maximum magnitude relationship obtained by Ruff and Kanamori (1980), the maximum projected earthquake is 8.4 (M_w). There is some question about the applicability of this relationship for very young oceanic crust, however. The worst case model of good coupling everywhere would be a single event along the entire boundary. This boundary has the same approximate dimensions as the 1960 Chilean (M_w 9.5) earthquake, and thus such an event cannot presently be ruled out. If the zone were to break in two or three separate segments, then earthquakes of M_w 8 3/4 can be postulated. However, lacking direct evidence of any prehistoric great earthquakes, we cannot rule out the possiblity that this zone is incapable of supporting any major subduction earthquakes.

4. Broad-band teleseismic P-wave records from the 63 largest, shallow, subduction earthquakes that have occurred in the circum-Pacific since 1938 were systematically analyzed. These earthquakes were recorded by the Pasadena vertical 1-90 seismometer. Teleseismic time functions have been computed using a constrained, least-square inversion procedure. The time functions give a picture of the overall rupture characteristics for these events. This information is important for the estimation of potential strong ground motions.

   Fourier power spectra have been computed for the P-wavetrains of these large events. These spectra yield information about the nature of the spectral scaling relationships for large earthquakes. The average spectral fall off between 30 sec and 2 sec for all the events is $(\text{frequency})^{-1.5}$.

References

Heaton, T.H., and H. Kanamori (1984). Seismic potential associated with subduction in the northwestern United States, *Bull. Seism. Soc. Am.*, 74, 933-941.

Ruff, L, and H. Kanamori, (1980). Seismicity and the subduction process, *Phys. Earth Pl. Inter.*, *25*, 240-252.

Data Processing

4-9920-02217

John Hoffman
Branch of Global Seismology and Geomagnetism
U.S. Geological Survey
Albuquerque Seismological Laboratory
Building 10002, Kirtland AFB-East
Albuquerque, New Mexico 87115-5000
(505) 844-4637

Investigations

1. Data Management Center for the China Digital Seismograph Network: The data processing equipment required to process the station tapes from the China Network has been purchased, assembled, and tested at the Albuquerque Seismological Laboratory (ASL). Two Chinese software specialists spent three months at ASL this summer and received training on the UNIX Operating System, Fortran 77, C Language, and operation of the computer system.

2. Data Processing for the Global Digital Seismograph Network: All of the digital data received from the Global Network and other contributing stations are reviewed and checked for quality.

3. Network-Day Tape Program: Data from the Global Network stations are assembled into Network-Day Tapes which are distributed to regional data centers and other government agencies.

4. Event Detection Program: This program has been revised and converted into C Language for incorporation into the software for the China Digital Seismograph Network.

Results

1. Data Management Center for the China Digital Seismograph Network: All of the computer hardware, parts, and supplies for the Data Management Center have been received at ASL. The computer system has been installed and completely checked out by the supplier. Four Chinese scientists spent July, August, and September 1984 at the ASL where they were trained in hardware maintenance and computer programming. The two engineers trained in hardware maintenance spent seven weeks at the Digital Equipment Corporation training school in Boston, Massachusetts. Some of the software which will be supplied to the Chinese is still being written and tested at ASL. The data processing system is scheduled for shipment to China in January 1985, and will be installed and checked by ASL personnel in March, April 1985.

2. Data Processing for the Global Digital Seismograph Network: During the past six months, 572 digital tapes (191 SRO/ASRO, 228 DWWSSN, and 153 RSTN) from the Global Network and other contributing stations were edited, checked for quality, corrected when feasible, and archived at ASL. The Global Network is now comprised of 11 SRO stations, 4 ASRO stations, and 15 DWWSSN stations which comprise the Global Digital Seismograph Network (GDSN) and are supported by ASL. In addition, there are six contributing stations which include Glen Almond, Canada and the five RSTN stations installed and supported by Sandia National Laboratories.

3. Network-Day Tape Program: The Network-Day Tape Program is a continuing program which assembles all of the data recorded by the Global Digital Seismograph Network plus the contributing stations for a specific calendar day onto one magnetic tape. This tape includes all the necessary station parameters, calibration data, frequency response, and time correction information for each station in the network. A fifth edition of the Network-Day Tape Newsletter containing information on all of the Global stations was distributed in July 1984. These newsletters are published twice a year and copies are forwarded to all digital data users. A new 405 megabyte disc recording system, manufactured by Systems Industries Corporation, was installed in July 1984. This new disc system replaced two obsolete RP06 units.

4. Event Detection Program: The short-period and intermediate-period event detector algorithm has been written in C Language for implementation on the systems that will be installed in China. Murdock has presented a paper on this algorithm to the 'Interactive Workshop on Advances in Remote Sensing Retrieval Methods' which was held in Williamsburg, Virginia from October 30 to November 2, 1984.

Reports

Newsletter:

Hoffman, J.P., R. Buland, and M. Zirbes, Network-Day Tape Newsletter, July 1984, V. 3, No. 1, 16 pp., available from Albuquerque Seismological Laboratory, Albuquerque, New Mexico.

SEARCH FOR PRECURSORS TO EARTHQUAKES IN THE VANUATU ISLAND ARC BY MONITORING TILT AND SEISMICITY

14-08-0001-G-822

Bryan L. Isacks
Department of Geological Sciences
Cornell University
Ithaca, NY 14853
(607)256-2307

Investigations

This report covers the period April 1,1984 to September 30, 1984 for the operation and analysis of data from the Vanuatu seismograph and tilt networks. The networks include twenty stations distributed along 500 km of the arc, seven bubble-level tiltmeter stations, two periodically releveled arrays of benchmarks (1 km aperature), and a 100 m two-component water tube tiltmeter. Our investigations include continued examination of the tilt data for possible earthquake related signals, continued development of the water-tube tiltmeter and detailed studies of the evolving pattern of seismicity recorded by the seismograph network. The most important earthquake sequence so far captured includes three magnitude(Ms) 6 events and one magnitude 7 event. These events occurred between 1978 and 1981 in a spatially coherent sequence located between Efate and Malekula islands. Detailed analyses of this sequence continues to be a focus of our research.

Results

1. The six month period covered by the previous report was one of the quietest during the past 5 1/2 years. This trend continues during the six month period covered by this report, and further highlights the 1978-1981 sequence as an important episode in the evolving seismicity of the region of Efate Island. The largest shallow events within or near the network include only five magnitude(mb) 5-5.5 events. Locations from the network at the time of this report are only available through June, 1984. Preliminary results for the rest of the six month period indicate little remarkable activity.

Only one of these had a surface magnitude reported by the PDE (Ms = 5.0, mb = 5.0, local magnitude = 5.1). This earthquake occurred in one of the small areas near Efate island that are repeatedly activated in clusters of events. This particular area is located right between the epicenters of the two magnitude 6 earthquakes that occurred 10 days apart in August, 1979. The area is located on the boundary between the aftershock sequences of the two 1979 events; it was the site of a marked cluster of events which occurred 3 months before the August, 1979 sequence; and it was again activated in the aftershock sequence of the July, 1981 shock (Ms = 7). Twenty km arcward of this area is another "hot spot" of concentrated seismicity also repeatedly activated by clusters but also accounting for much of the ongoing background of seismicity in the Efate Island region. Both these areas were activated during April in a series of clusters.

Ten days after the April 1 event another magnitude 5 (mb = 5.4, local magnitude = 5.0) occurred 20 km farther down-dip and landward of the two nests described above and was located at a depth of 72 km. No aftershocks or clusters were located near this event, in striking contrast to the aftershocks and clusters associated with the April 1 event. The seismicity of this part of the subduction zone is characterized by a more or less continuous rate of occurrence of small events instead of the sporadic the tightly clustered sequences found farther up-dip (trenchward). This deeper activity may be related to creep along the parts of interplate boundary located down-dip of the discrete seismogenic patches producing the organized spatial pattern of shallow seismicity near Efate.

The April events produced the usual coseismic transient signals on the tiltmeters located on Efate Island (about 30-50 km distant from the clusters) with no indications of precursory tilts on a time scale of minutes to hours accessible to visual inspection of the records.

2. The long-baseline water tube tiltmeter has continued to produce data during the period of this report. During June-September, 1984, G. Hade improved the end pot sensors, calibrated all four ends of the two component system and built new housing for the recording instrumentation and power.

One result of this work is to understand better the nature of the remarkable oscillatory signal recorded by tiltmeter component oriented perpendicular to the nearby coastline. It is probable that this signal is a seiche in the 100 m tube driven by the loading effects of another seiche set up in ocean water in the nearby embayment of the coast. Although the tube seiche is only slightly underdamped, it is effectively driven by the bay seiche because of the fortuitous near coincidence of the two natural periods (about 5 minutes). The loading effect of the main ocean tides is stronger on the end nearest the coast, in agreement with our previous work on the effect of a low-rigidity near surface layer on tidal loading. The loading effects of the bay seiche, however, are more nearly equal at the two ends of the tube because of the excitation of the tube seiche.

Releveling of the Devils Point benchmark array on Efate Island in May, 1984 showed little tilt change from the previous leveling in November, 1983. The May, 1984 leveling is the 22nd leveling of the Devils Point array since 1975. We are undertaking further analysis of this unique data set. Changes in the techniques and, especially, expansion of the network configuration introduce identifiable noise in the results that we did not take fully into account in our previous analysis. However, the overall pattern of tilt change remains significant and similar to that previously determined. Approximately 5 microradians of north-south tilting appears to have occurred mostly prior to the 1978-1981 sequence of magnitude 6-7 events, although the exact form of the tilt signal is difficult to resolve. The latest results reinforce a suggestion of increased tilting during the past 1-2 years in the same sense and direction as the 1976-1978 episode, but further levelings are required to verify this trend.

Reports

Coudert,E., R.K. Cardwell, B.L. Isacks, and J.-L. Chatelain, 1984, P-Wave velocity of the uppermost mantle and crustal thickness in the central Vanuatu Islands (New Hebrides island arc), Bull. Seismol. Soc. Amer.,74,913-924.

Socorro Magma Bodies

9920-03379

Lawrence H. Jaksha
U.S. Geological Survey
Geoscience Dept.
New Mexico Tech.
Socorro, New Mexico 87801
(505) 835-5501

Investigations

1. Albuquerque basin seismicity.
2. Crustal structure
3. Source parameters
4. Instrumentation

Results

1. Analysis of over 1000 hypocenters obtained near Albuquerque, New Mexico during 1976-1981 revealed that most of the seismicity fell into three regions: (1) the Socorro-Belen area of the Rio Grande rift, (2) the Mt. Taylor area of the Jemez lineament, and (3) the Estancia basin.

The earthquakes can be roughly divided into two categories: those related to block faulting and those related to intrusive volcanism. Events from both groups have occurred within and near the city of Albuquerque. Because of their proximity to a major metropolitan area, earthquakes of moderate magnitude (~4.0) can do substantial property damage.

2. The logistics for an experiment to determine the Pn velocity beneath the Jemez lineament in western New Mexico and eastern Arizona have been determined. An areal array consisting of seven temporary seismograph stations was deployed for four days across the lineament near St. Johns, Arizona. Explosions originating at Farmington, Santa Rita, and Tyrone, New Mexico and Morenci, Miami, and Kayenta, Arizona were recorded.

3. John Ake is studying the source parameters of some small earthquakes near Socorro. His prelimianry results for earthquakes in the magnitude range ~1.3 - 2.0 suggest fairly large source radii (>150 m) and rather small (<3 bar) stress drops.

4. A new radio telemetered station was added to the network in September. The station is on the Servillota Wildlife Refuge and brings the number of stations in the net to ten.

A substantial amount of time has been spent clearing up radio interference problems this report period.

Reports

Jaksha, L. H., and Evans, D. H., 1984, Reconnaissance seismic refraction--reflection surveys in northwestern New Mexico: Bulletin of the Seismological Society of America, v. 74, no. 4, p. 1263-1274.

Wong, I. G., Cash, D. J., and Jaksha, L. H., 1984, The Crownpoint, New Mexico earthquakes of 1976 and 1977: Bulletin of the Seismological Society of America, (in press).

Jarpe, S. P., Sanford, A. R., and Jaksha, L. H., 1984, Evidence for magmatic intrusion during an earthquake swarm in the central Rio Grande rift: EOS Abstracts for fall meeting (in press).

Instrument Development and Quality Control

9930-01726

E. Gray Jensen
Branch of Seismology
U. S. Geological Survey
345 Middlefield Road - Mail Stop 977
Menlo Park, California 94025
(415) 323-8111, ext. 2050

Investigations

This project supports other projects in the Office of Earthquake, Volcanoes and Engineering by designing and developing new instrumentation and by evaluating and improving existing equipment in order to maintain high quality in the data acquired by the Office. During this period some personnel from this project were assigned to the GEOS project (9940-03009) on a part-time basis.

Results

Development of a hardware teleseismic trigger device is nearing completion. This unit, which is a mostly-hardware implementation of John Evan's teleseismic trigger software, consists of a analog section which performs filtering and STA/LTA ratio detection and an NSC-800 microprocessor board which handles timing, control and operator interfacing. The analog section prototyping is complete and circuit board production is proceeding. Software development should be completed soon. Work has also been done on developing improvements to the J402 preamp/VCO package to increase stability and reduce noise. One development involves redesign of the temperature compensation and power supply sections as well as implementing more detailed testing and screening procedures. The other development replaces the existing VCO with one that is inherently more stable but also uses more power.

Nine "mini-master clock" units were built and sent to China. These will allow time transfer from radio standards to event recorders located in underground vaults. A computer-aided schematic design and drawing system has been set-up and is currently facilitating project design work. Several items of test equipment have been acquired to aid maintenance of microwave telemetry equipment. This project assisted in installing and connecting a new GOES satellite telemetry ground station.

Test have been performed on the Calnet on-line digitizer which show that shielding cables carrying seismic signals within the computer room greatly reduces noise on the digitized signals. Consequently the process of shielding all such cables has been initiated. A parallel I/O link has been installed between the two on-line digitizer PDP11/44's. This will allow a fail-safe cabability. The arrival of a new VAX 11/750 has brought about a reorganization involving tranfer of facilities and terminal lines from the PDP 11/70 which is still in progress. In addition 14 terminals and 7 computer parts have been added to the Gandalf port switching device.

The Seismic Cassette Recorder (SCR) system has been maintained and supported through several field programs including Sutter Buttes, Alaska, Hanford and Newberry Crater. Also, special VHF radio repeater systems were built for communication during the Alaska project. During this period approximately 125 telemetry radio transmitter and receivers were repaired or aligned and 60 seismometers were calibrated.

Southern California Cooperative Seismic Network
9930-01174

Carl Johnson
Branch of Seismology
U.S. Geological Survey
Seismological Laboratory 252-21
Pasadena, California 91125

Investigations

1. Southern California Network Operations
   Operations and maintenance of the southern Caifornia seismic network continued through the reporting period without significant failure. At present 248 predominantly short-period, vertical instruments are telemetered to Caltech for analysis.

2. Routine Network Analysis
   Routine processing using stations of the southern California cooperative seismic network was continued for the period April through September, 1984. Routine analysis in cooperation with Caltech personnel includes the interractive timing of phases, event location, magnitude calculation, and final catalog production using the CUSP analysis system. At present 2000 events detected each month are being analyzed in this manner with a regional magnitude threshold approaching 1.2. In addition, the analysis of earlier data that has been maintained in a preliminary form has begun with current efforts focussed on finalizing network data from mid-1981 through June, 1983. Phase data for this period is being prepared for distribution in a form identical to that being used for the distribution of current data.

3. Conditional Foreshock Probability
   We have been conducting a statistical analysis of the 52 year southern California catalogue to determine the probability that an earthquake will be a foreshock to a larger event and from this the short term earthquake hazard as a function of time after the occurrence of an earthquake in southern California. In addition to the independent probability, the conditional probability that an earthquake will be a foreshock given certain characteristics of the earthquake, such as its location, the number of aftershocks immediately following it, is being determined.

4. Seismicity Increase in the Southern Sierra Nevada
   We are conducting a special study of the seismicity of the southern Sierra Nevada. Although the Sierra Nevada has traditionally been relatively quiet seismically, this year it has been one of the most active areas of southern California. The spacial and temporal distribution of this activity is being analyzed to examine the cause of the increase in seismicity and the probability of future larger earthquakes in the region. The mechanisms of the earthquakes are also being studied from first motion data and waveform modeling to elucidate the tectonic causes of these events.

5. Seismicity Statistics Based on 2nd Order Moment

   Analysis of the second order seismic moment of the southern California catalogue is being carried out in collaboration with Paul Reasenburg in Menlo Park, CA. With this technique, spatial and temporal patterns of seismicity associated with moderate earthquakes are examined. In addition, Reasenburg's clustering algorithm is being applied to the southern California catalogue. The resulting clusters will be analyzed to quantify seismic patterns and search for possible seismic precursors in southern California.

Results

1. Conditional Foreshock Probability

   The probability that an earthquake in southern Caifornia ($M \geq 3.0$) will be followed by an earthquake of larger magnitude within 5 days and 10 km (i.e., will be a foreshock) is shown to be 6% ± .5% (1 S.D.), and to be independent of the magnitude of the possible foreshock between $M=3$ and $M=5$. The probability that an earthquake will be followed by a $M \geq 5.0$ mainshock, however, increases with magnitude of the foreshock from less than 1% at $M \geq 3$ to 6.5% ± 2.5% (1 S.D.) at $M \geq 5$. The mainshock is most likely to occur in the first hour after the foreshock and the probability that a mainshock will occur decreases with elapsed time from the occurrence of the possible foreshock by approximately the inverse of time. Hence, the occurrence of an earthquake of $M \geq 3.0$ in southern California increases the earthquake hazard within a small space-time window several orders of magnitude above the normal background level.

2. Seismicity Increase in the Southern Sierra Nevada

   Studies of the recent seismicity in the southern Sierra Nevada have shown that these earthquakes are concentrated along a line parallel to but 10 km east of the Kern Canyon fault. This north south lineation extends over 100 km north from the eastern end of the 1952 Kern Co. earthquake ($M = 7.7$) rupture zone. The depth distribution of seismicity is close to vertical so these earthquakes are not occurring on the Kern Canyon fault. Focal mechanisms of these events show almost pure normal faulting along a north-south striking plane. This movement is the same as that on the Sierra Nevada frontal fault (which is parallel to and 20 km east of this structure) suggesting that the large earthquake proposed by Wallace for the southern Sierra could occur along this structure rather than the frontal fault.

Reports

1. Jones, L.M., C. Johnson, R.S. Dollar, Swarms in the southern Sierra Nevada, *Earthq. Notes*, v. 55, p. 22, 1984.

2. Jones, L.M., Foreshocks and time-dependent earthquake hazard assessment in southern California, submitted to *Sceince*, 1984.

Seismic Study on Rupture Mode of Seismic Gaps

Contract No. 14-08-0001-G-814

Hiroo Kanamori
Seismological Laboratory, California Institute of Technology
Pasadena, California 91125 (818-356-6914)

Investigations

Monitoring the spatio-temporal pattern of stress release along subduction zones (Kanamori, H. and Dziewonski, A., EOS, 65, No. 16, April 17, 1984).

Results

Several methods have recently been developed to rapidly determine earthquake mechanism solutions from digital seismograms of the IDA and GDSN networks (Dziewonski et al., 1981; Kanamori and Given, 1981). The number of stations in both networks became sufficient in 1977 to obtain reliable moment tensor solutions for large shallow earthquakes with $M_s \geq 6.5$ or, for deep events, with $m_b \geq 5.5$. Further increase in the number of stations decreased this threshold to $M_s \geq 5.5$ for shallow events. The Harvard group (Dziewonski, Franzen, Friedman, Giardini and Woodhouse), compiled a catalog of over 1,200 centroid-moment tensor solutions for the years 1977-1983. The catalog is nearly complete for shallow events with $M_s \geq 6.5$ and deeper events ($h > 80$ km) with $m_b \geq 5.5$; it is also complete for $M_s \geq 5.5$ beginning with the year 1981. We use these solutions, supplemented by results for larger earthquakes obtained at Caltech, to examine current earthquake stress release patterns along various subduction zones. The quality of the solutions is examined by comparing the moment tensor elements determined by different methods.

Notable patterns we found include: (1) a sequence of outer-rise normal-fault events and of thrust events near the Simushir-Onekotan gap in the Kurile-Kamchatka region following a large thrust-event in 1978 (see Figure 1), (2) a large normal-fault event in the Tehuantepec, Mexico, region, following a sequence of large earthquakes along the Mexican subduction zone and (3) large tear-fault event in the Loyalty Is. region following the 1980-1981 sequence of thrust events. These patterns suggest migration and diffusion of stress in subduction zones on time scales of a few years which are comparable to the Maxwellian time of the lithosphere-asthenosphere system.

The figure illustrates seismicity patterns of the Kurile Islands subduction zone for year 1977-1983. It shows the double-couple representation of moment tensor solution obtained for the Kurile Islands region for the period from January 1, 1977 through September 30, 1983. The figure shows all events with M_w of 6.5 or greater and it is also complete for $M_w \geq 6.0$ from January 1, 1981. The radius of the "beach-ball" is a linear function of M_w. The figure also shows the area of faulting associated with major earthquakes in the past: the events of 1952, 1958, 1963 and 1969. There is a distinct gap in seismicity between the islands of Simushir and Onekotan, covering some 300 km of the trench axis; no major earthquake has occurred in this region since, at least, 1915. The existence of this gap has been recognized for some time.

The major burst of seismic activity occurred as a sequence of large thrust events from March 22 to 24, 1978, with the largest events exceeding M_w of 7.5. The pattern of seismicity following this series seems to be consistent with the hypothesis of stress diffusion along a subduction zone.

The normal fault, outer rise, event on 4/30/81 is consistent with the concept of relaxation of stresses in the subducted lithosphere following a major thrust earthquake. The seismicity migrates towards north-east with a magnitude 6.9 earthquake on 12/31/80 and 7.1 on 6/30/82; the latter event is located on the trench axis and has a rather atypical mechanism dominated by strike-slip. The most recent event illustrated (5/1/83) is a thrust on the south-western edge of the gap itself.

The northeastern end of the gap borders the fault area of the 1952 Kamchatka earthquake. This area has been quiescent since 1977, except for three outer rise events in 1981. Two in the northeast were tensional, but one near the southwestern end was compressive, perhaps diagnostic of the overall high stress in the entire region. Then, in 1983, two thrust events occurred on the southwestern end of the gap: M_w of 6.3 on 2/26/83 and M_w of 6.5 on 4/4/83.

Whether this pattern of migrating seismicity is indicative of an impending major event in the Simushir Onekotan gap is an open question. Increase of seismicity at the edges of a gap was noted before some major events (1952 Kamchatka M_w = 9.0, 1964 Alaska M_w = 9.2).

Reports and Publications

Astiz, Luciana and Hiroo Kanamori, An earthquake doublet in Ometepec, Guerrero, Mexico, Physics of the Earth and Planetary Interiors, 34, 24-45, 1984.

Heaton, Thomas H. and Hiroo Kanamori, Seismic potential associated with subduction in the northwestern United States, Seismol. Soc. Amer., Bull., 74, No. 3, 933-941, 1984.

Kanamori, H. and A. M. Dziewonski, Spatio-temporal variation of seismic stress release along subduction zones, AGU Spring Meeting, Cincinnati, Ohio, May 14-18, 1984.

Kanamori, Hiroo and Adam M. Dziewonski, Monitoring the spatio-temporal pattern of stress release along subduction zones, Mathematical Geophysics Conference, Loen, Norway, June 24-30, 1984.

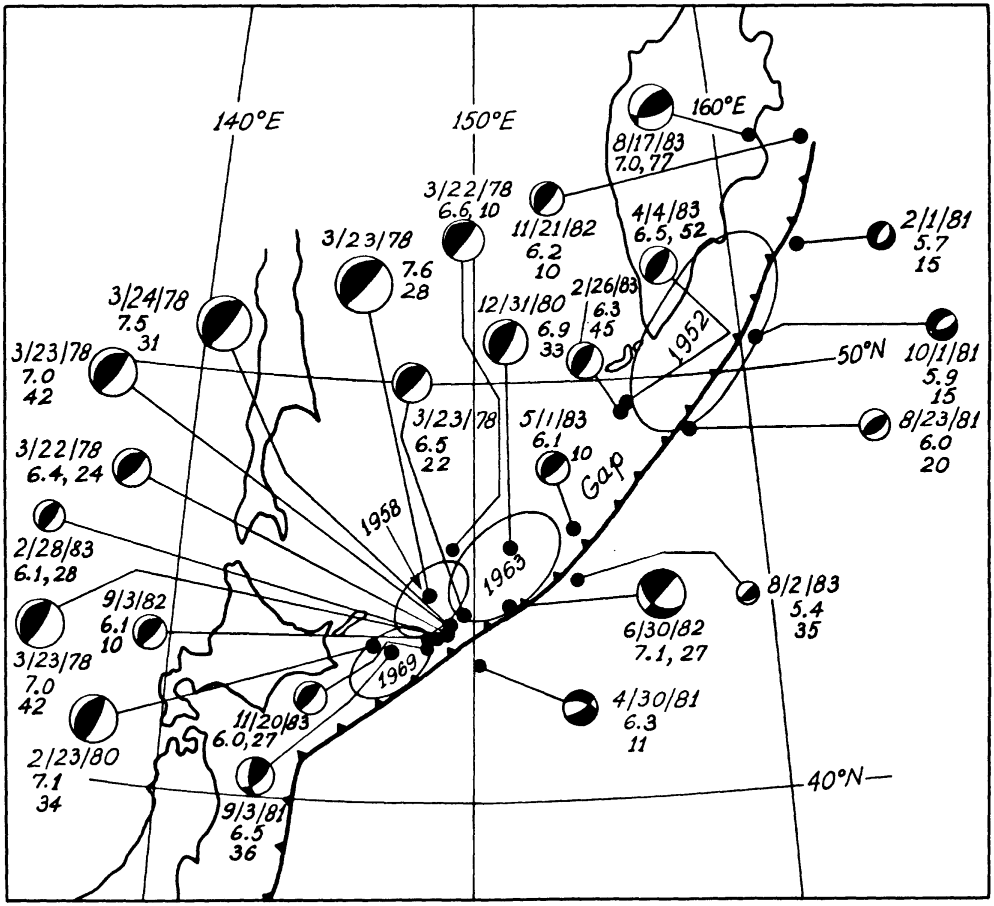

Figure 1. Seismicity along the Kurile Trench for years 1977-1983.

SEISMICITY, TOPOGRAPHY AND PRE-EARTHQUAKE LOADING PROCESSES ALONG THE SAN ANDREAS SYSTEM

Contract No. 14-08-0001-21282

John Kelleher
REDWOOD RESEARCH,INC.
San Mateo, CA 94401
(415) 342-8276

Investigations

Research supported under this contract includes a) an investigation into the relationship between topographic features and the locations of larger strike-slip earthquakes along the San Andreas system; b) a study of the depth distribution of events along the San Andreas system. Some evidence suggests a time-dependent component to deeper earthquakes (h 10 km) whereby the distribution of deeper events may be an important indication of regional stress accumulation; c) continued study of the patterns of seismic activity which precede larger strike-slip earthquakes.

Results

The major observations to date of seismicity before significant ($M \cong 5 - 6$) earthquakes along the San Andreas include the following:

1. During the final year or two before rupture, noticeable seismicity, particularly smaller shocks ($M \cong 2$), develops near the pending rupture blocks along the inferred direction of maximum compressive stress. Thus before the larger strike-slip shocks of the northern San Andreas (1979 Coyote Lake, 1984 Morgan Hill) or the Imperial Valley (1979), the late seismicity developed to the north and/or south of the pending rupture. However, before the 1983 Coalinga earthquake the late seismicity was strongest along an east-west line while before the 1968 Borrego Mtn. earthquake the late seismicity was strongest along a NE-SW line.

2. In several cases the late seismicity referred to above appeared to be the final stage of a migration of activity toward the pending rupture over a period of five years or more.

3. These zones of important late seismicity appear to be characterized by uplifted and extremely rough topography. Thus, in association with a rupture zone along the NW striking San Andreas zones of particularly rough topography might occur to the east of the northern end of the rupture and west of the southern end. The seismicity which develops in these two key areas may provide important information about the timing of the pending shock. Under this interpretation the strong pattern of seismic activity (approximately 1974 - 1984) in a region of rough topography in the vicinity of Coalinga may be related to a pending large shock on the San Andreas near and south of Parkfield. Contrast for example

this seismic activity and topography with the much quieter area of smoother topography directly west of the San Andreas.

4. These seismicity patterns suggest that stress accumulation before significant shocks may sometimes exhibit a simple and straight forward geometry. For this reason a project has been started to model the pattern of strain-deformation in time before significant strike-slip earthquakes. A modified finite element model is being used which incorporates earthquake fault movements and clusters of seismicity. Our goal is to reproduce the location and timing of seismicity patterns before significant shocks.

FAULT MECHANICS AND CHEMISTRY

9960-01485

C.-Y. King
Branch of Tectonophysics
U.S. Geological Survey
345 Middlefield Road, MS/977
Menlo Park, California 94025
(415) 323-8111, ext. 2706

Investigations

1. Water temperature and radon content were continuously monitored at two water wells in San Juan Bautista and a newly prepared well in Parkfield, California.
2. Water level was continuously recorded at six other wells.
3. Water samples were periodically taken from most of these wells for chemical analyses.
4. Radon content of ground gas was continuously monitored at two sites (Limekiln A and Cienega Winery) along the San Andreas fault in the Bear Valley area, California, and at a site in Nevada Test Site.
5. Slip events generated along a laboratory fault were studied.

Results

This report presents some preliminary data recorded at two springs and two shallow wells situated along the Hayward fault, where the ground water seems to have shown some anomalous changes in quality beginning two years before the magnitude 6 Morgan Hill earthquake on April 24, 1984. Temperature, salinity and conductivity of ground water have been measured with a portable instrument (Yellow Springs Instrument Co., Model 33) about once a month since late 1975 at two springs in Alum Rock park east of San Jose and approximately 15 kilometers from the epicenter of the Morgan hill earthquake (fig. 1). Water flow rate has also been recorded at the orifice of one of the springs (Sulfur Spring #11). Both springs are located within the middle member of the Monterey formation which consists of thin bedded opaline chert and cherty shale (Crittenden, 1951).

The measured conductivity and salinity values show a gradual decline of 40% from about the end of 1981 to April 9, 1984 (fig. 2). This result is corroborated by an independent study of William C. Evan (USGS Water Resources Division) who has been regularly collecting water samples from one of the springs, Sulfur Spring #4, for chemical analysis. Evans' data show a similar decline in HCO_3^- content in the water. Our post-earthquake measurements taken on May 9 and June 8, 1984 show a small recovery of conductivity (and salinity) at both springs (fig. 2).

Dave Basler visited the springs on April 25, the day after the earthquake, and observed an appreciable increase of flow at Sulfur Spring #4 and recorded a large increase in flow rate at Sulfur Spring #11 (more than twice as high as measured on April 9 and highest since our study began in 1975). The flow increase cannot be attributed to rainfall, which has been extremely small for the 1983-84 winter season, but may be induced by the stress-field changes associated with the earthquake because the springs are situated in a compressional quadrant of the earthquake (Wakita, 1975). Also the color of the water in the springs changed from whitish to greyish-brown because of the large amount of sediments in the water. The flow rate at Sulfur Spring #11 was measured again on May 9 and June 8, and was found to have dropped back considerably but was still higher than normal (fig. 2a). The water color had returned to normal (whitish) by May 9.

Measurements have also been made at two shallow wells in east Oakland near the Hayward fault (Oakland and Chabot, fig. 1). A gradual decline in conductivity and temperature during the past two years (1982-83) is noticeable in the data, although it is dominated by seasonal variations (fig. 3).

It is not clear at the present whether the observed groundwater changes are due to tectonic or climatic effects (the 1981-82 and 1982-83 winter seasons had an above normal amount of rainfall). Radon content of ground water has been continuously monitored for several years at an artesian well south of San Juan Bautista near the San Andreas fault (fig. 1). The radon data show no significant changes.

References

Crittenden, M. D., Jr., 1951, Geology of the San Jose-Mount Hamilton area: California Division of Mines Bulletin 157.

Wakita, H., 1975, Water wells as possible indicators of tectonic strain, Science, v. 189, p. 553.

Reports

King, C.-Y. and D. Basler, 1984, Ground-water changes before the Morgan Hill earthquake, U.S. Geological Survey, Open-File Report 84-498A, p. 122-127.

King, C.-Y., 1985, Impulsive radon emanation on a creeping segment of the San Andreas fault, California, *Pure and Applied Geophysics*, in press.

King, C.-Y., 1984, Application of gas geochemistry to earthquake prediction (abstract), The 1984 International Chemical Congress of Pacific Basin Societies, Honolulu, Hawaii.

King, C.-Y., 1984, In the forecasting movement (a review on Earthquake Prediction Research), *Nature*, v. 311, p. 328.

King, C.-Y., 1984, Earthquake prediction: hydrologic and geochemical approaches, *Nature*, in press.

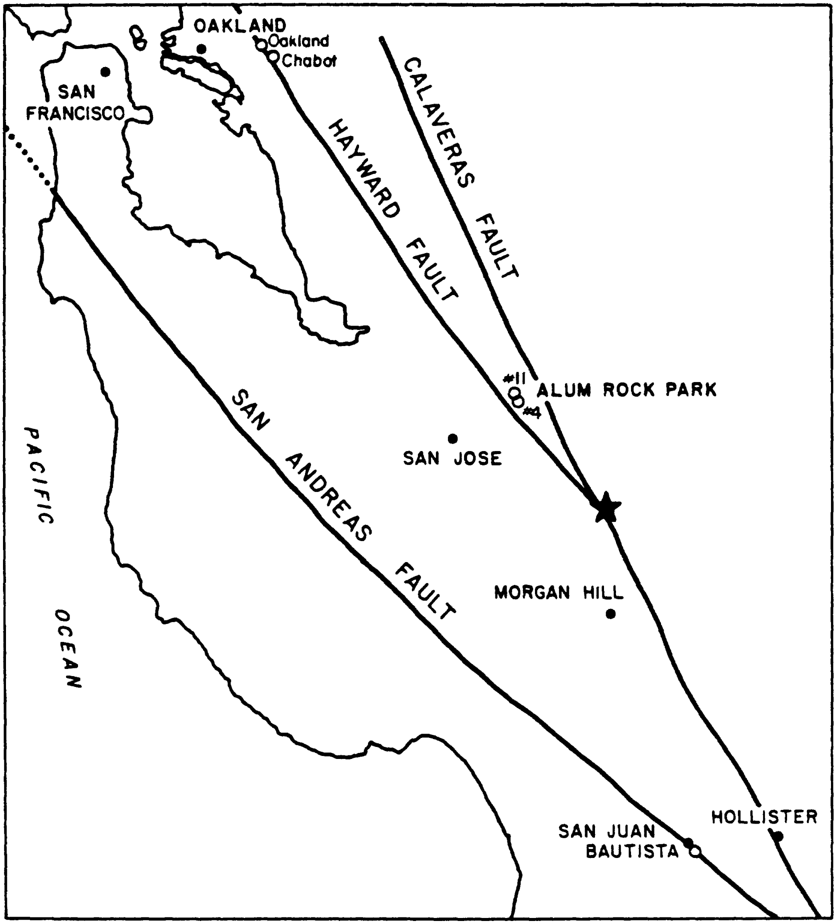

Figure 1. Location of ground water measurement sites (circles) and epicenter of the Morgan Hill earthquake (star).

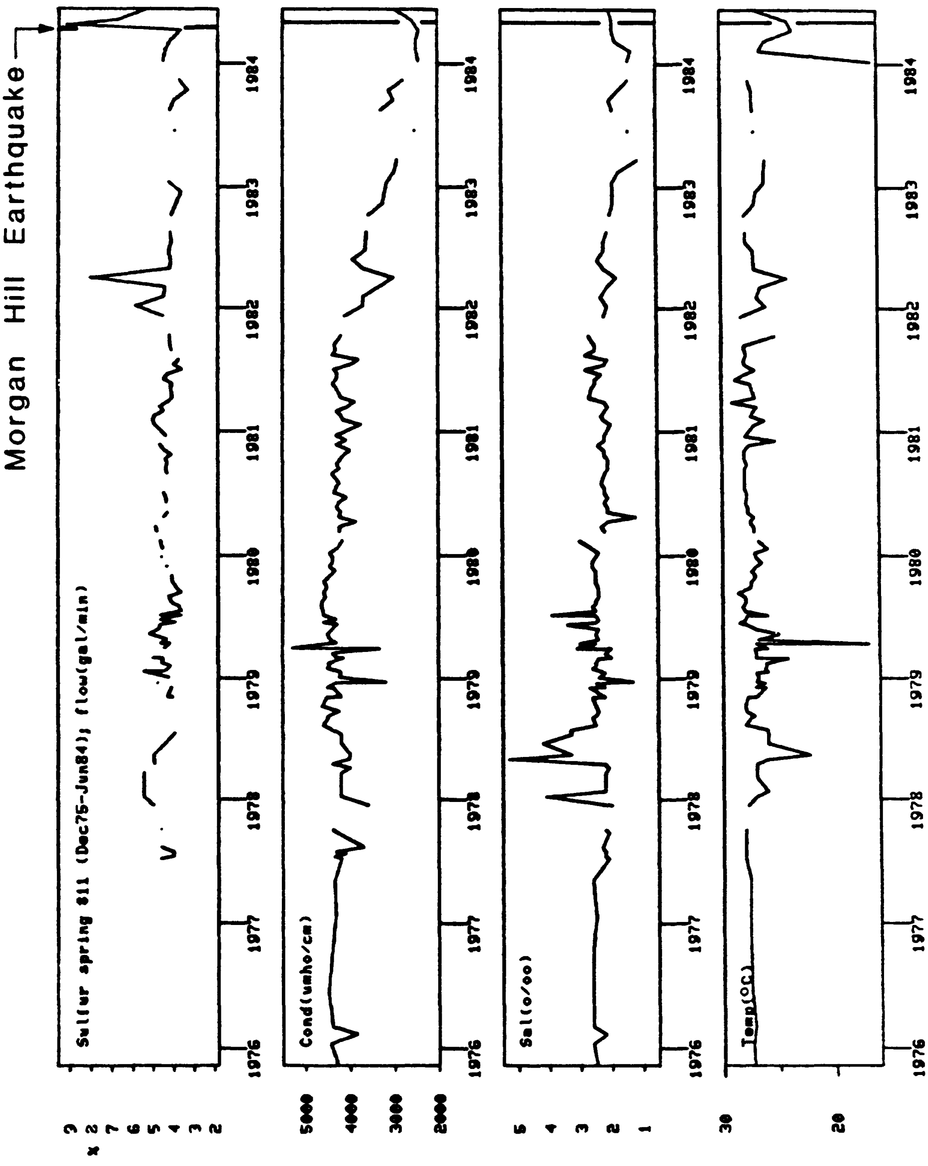

Fig.2 (a)

Figure 2. Flow rate, conductivity, salinity and temperature data from two springs in Alum Rock park. (a) North; (b) South.

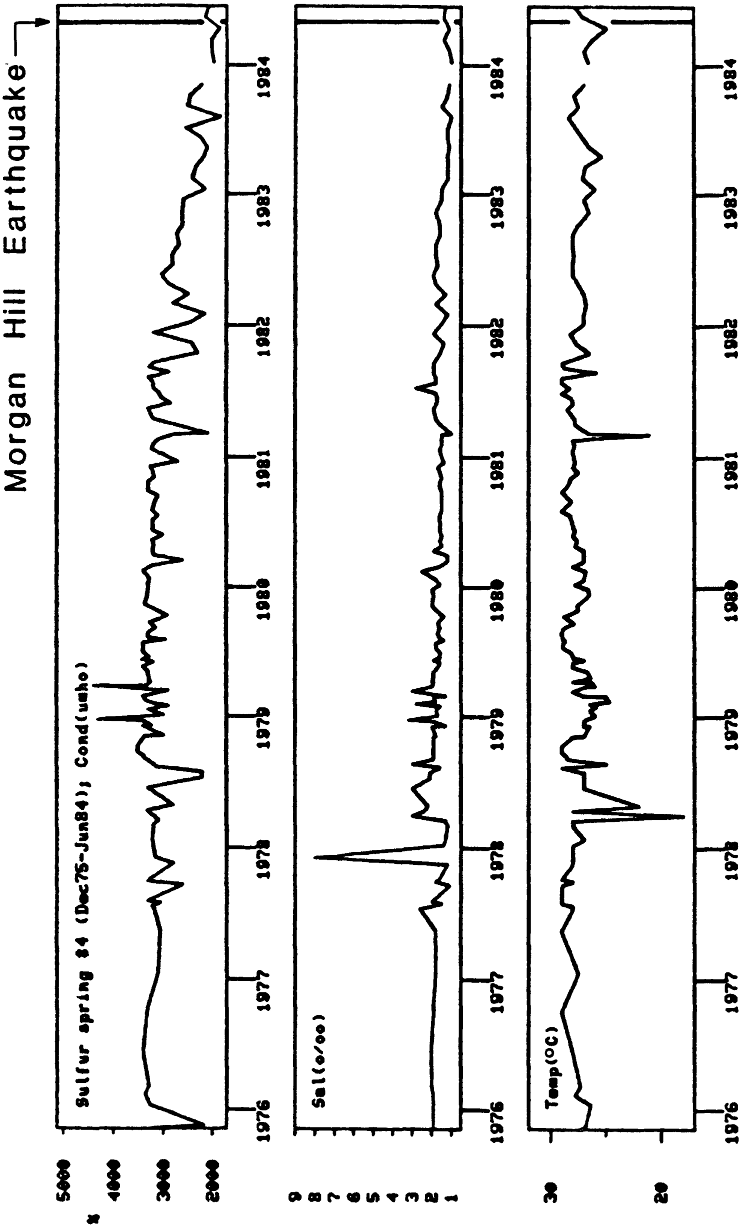
Morgan Hill Earthquake
Sulfur spring 84 (Dec75-Jun84); Cond(umho)
5000
4000
3000
2000
x
Sal(o/oo)
9
8
7
6
5
4
3
2
1
Temp(°C)
30
20
1976
1977
1978
1979
1980
1981
1982
1983
1984

Fig.2 (b)

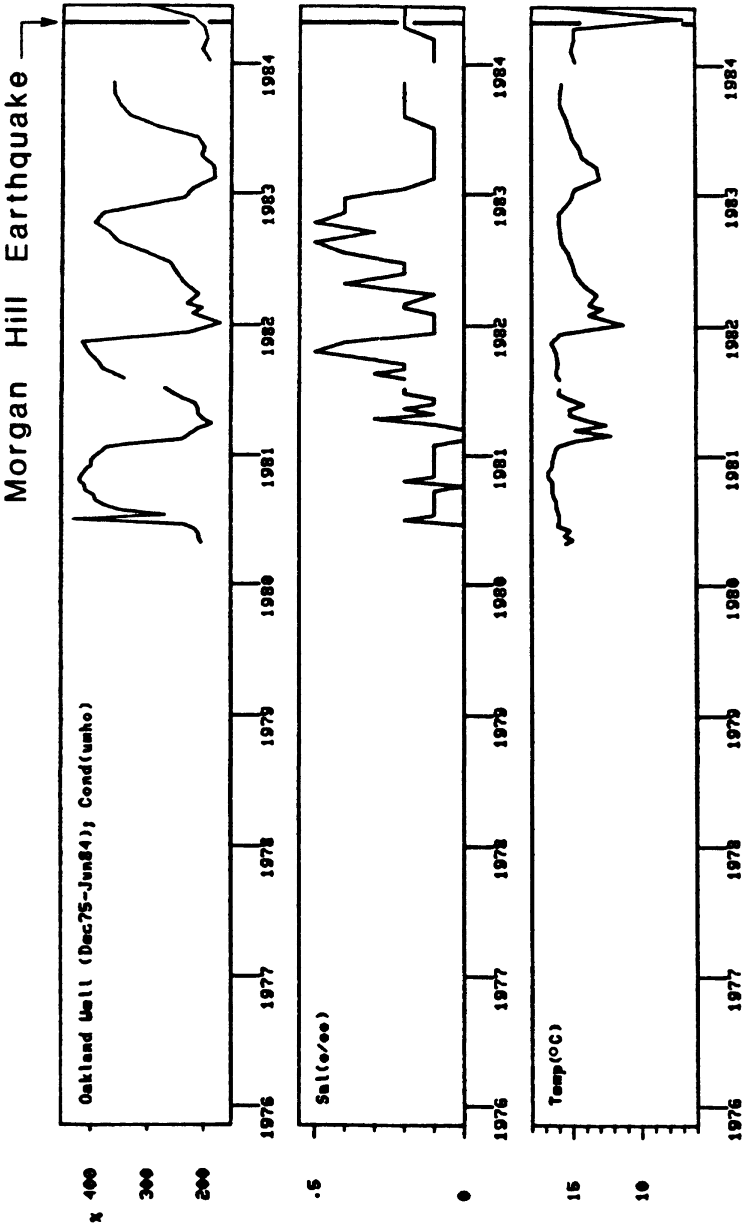

Fig.3 (a)

Figure 3. Conductivity, salinity and temperature data from two wells in east Oakland. (a) Oakland; (b) Chabot.

]

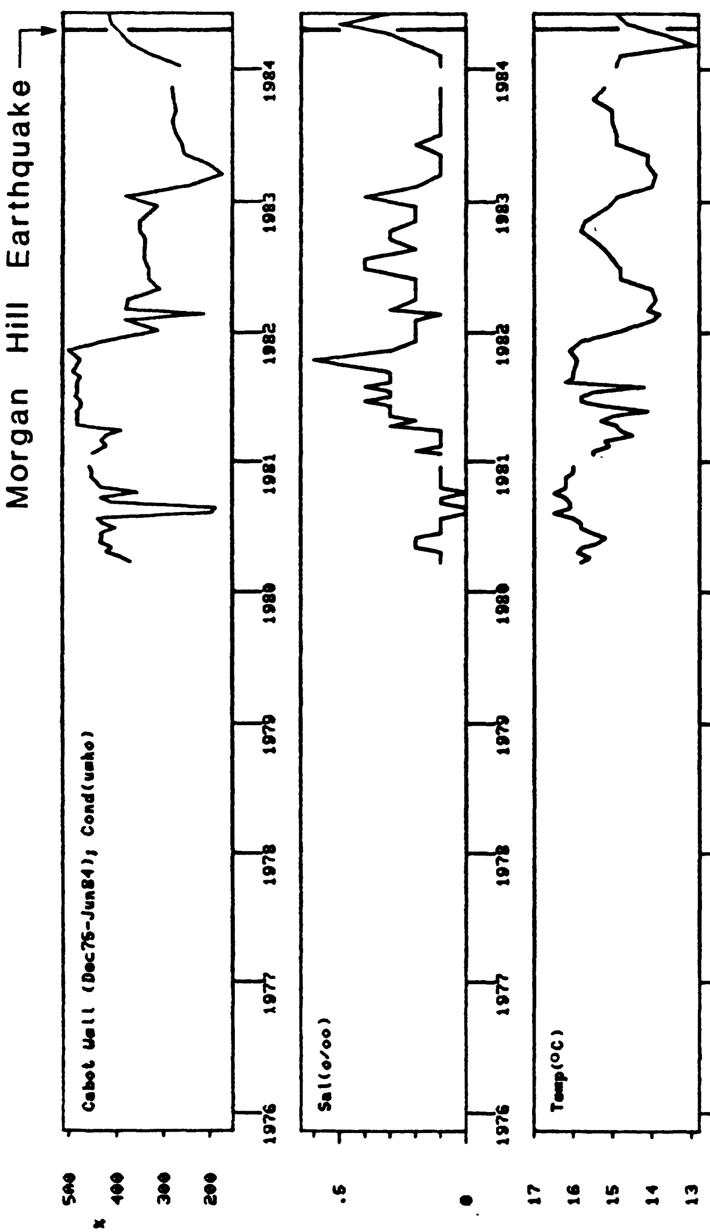
Morgan Hill Earthquake
Cabot Well (Dec75-Jun84); Cond(umho)
500
x
400
300
200
Sal(o/oo)
.5
0
Temp(°C)
17
16
15
14
13
1976
1977
1978
1979
1980
1981
1982
1983
1984

Fig.3 (b)

Central Aleutian Islands Seismic Network
and
Prediction Methodology for Subduction Zone Earthquakes, Central Aleutian Islands

Contract No. 14-08-0001-21896 and Grant No. 14-01-0001-G-881

Carl Kisslinger and Selena Billington
Cooperative Institute for Research in Environmental Sciences
Campus Box 449, University of Colorado
Boulder, Colorado 80309
(303) 492-8028

Network Operations

The primary objectives of the network contract are the operation of the Adak Seismic Network and the production of a catalogue of earthquakes in the Adak seismic zone from the data acquired by this network. The Adak seismic zone is defined as that portion of the Aleutian arc within which the network is capable of providing hypocenter locations with adequate precision and accuracy. This zone extends from approximately 50.25°-52.25°N latitude and 175°-178.5°W longitude. The network consists of 14 stations deployed on Adak and nearby islands. Thirteen of these are two-component, short-period, high-gain stations, connected by radio telemetry to the Adak Observatory; the other is a conventional six-component earthquake station, ADK.

Network Maintenance. Maintenance of this network requires the solutions of difficult problems of the natural environment, remoteness from our headquarters and difficulty of access to the individual stations even after reaching Adak Island. After ten years of experience S.T. Morrissey, the project engineer, has developed stations capable of operating unattended for two years, if no extreme natural catastrophes strike. A successful maintenance trip was carried out in July-August, 1984, during which all of the stations except one were reached and serviced with the aid of a rented small craft. The station that could not be reached by surface transport is inoperative and will remain so until we can once again get to it by helicopter. This trip did restore some of the coverage of the western part of the seismic zone that had been lost during 1982 through the first part of 1984.

Seismicity in the Adak zone. Earthquake locations are complete through July, 1984. The location task has fallen behind the normal lag of three to four weeks because of disruptions in data flow during the summer maintenance trip and the diversion of personnel to other essential tasks. Temporary experienced staff has been added and we expect the backlog to be eliminated by the end of November.

The seismicity patterns in terms of the locations of concentrations of earthquakes are not unusual during the past six months, but the continuation of the low rate of occurrence of events in all magnitude bands is still an important feature. We consider this seismic quiescence, which has been in progress since September, 1982, to be a possible precursor to a major earthquake, as discussed in the Research section of this summary.

Research on Prediction Methodology

The research program has had two long-term goals since its inception in 1974: improved understanding of the relation of the seismic activity to local and regional tectonics, through seismotectonic investigations; and the discovery, documentation and explanation of phenomena indicative of the approach of the occurrence of a large earthquake in order to make possible the prediction of earthquakes in this subduction zone. Data provided by the Adak network are the primary basis of these studies, but teleseismic data and theoretical approaches have also been incorporated. This work is currently supported under Grant G-881, but research under other, non-USGS support is an integral part of the program and some of the results obtained from these other efforts are included for completeness.

Forecast of the Location of the 6May1984 Earthquake. An earthquake, m_b 5.8 (NEIS), occurred in sub-region SW2 of the Adak seismic zone on May 6, 1984. This earthquake, the largest to occur in this part of the Adak zone since we started work here in 1974, was located at the place which we had selected and announced as the likely site of a strong earthquake in the indefinite but near future. This forecast may be found, among other places, in our entry in Volume XVII of these Technical Summaries, December, 1983, and in a letter to the Chief, Office of Earthquakes, Volcanoes, and Engineering, U.S.G.S., January 4, 1984. The forecast was based on our conclusion that sub-region SW2 enclosed an asperity on the main thrust plane that had become activated in July 1980, as evidenced by a cluster of moderate earthquakes between that time and the end of 1983, Fig. 1 (Bowman and Kisslinger, 1985). The occurrence of the May 6 event is taken as confirmation of this interpretation, but leaves open the other part of our forecast, that a major earthquake will occur in the Adak zone soon.

In a related study based on Adak network data but carried out with other support, the state of stress (apparent stresses and stress drops from microearthquakes) in SW2 and adjacent parts of the main seismic zone was examined on the basis of the spectra of S-waves (Scherbaum and Kisslinger, 1984.) They found that the higher stress microearthquakes occurred in the same place as the cluster of moderate events mentioned above, Fig. 2a, and the stresses associated with these stronger microearthquakes have been increasing steadily since the latter part of 1982, Fig. 2b. We do not yet have comparable results for earthquakes after May 6. The gradual increase in these seismically determined stresses began at about the same time as the overall quiescence in the Adak seismic zone.

Quiescence in the Adak Seismic Zone. We have reported previously that a pronounced decrease in the rate of occurrence of earthquake located by our network started in mid-September, 1982. The decrease in the rate for the year before and the year after this time was about 60 percent in all magnitude bands, as given by our Adak catalogue. In view of Habermann's discovery of a clear quiescence that lasted for three years prior to the strong event of February 7 and May 2, 1971, we were led to the conclusion that this quiescence had to be considered as a possible precursor to the next major earthquake in this zone. The fact that no event of magnitude 7 or greater has occurred in the neighborhood of Adak for more than 13 years lends credence to this expectation. If the 1971 scenario is followed, an event of magnitude 7 or larger should occur within the next 12 months.

After the May 6 event, we hypothesized that another feature of 1971 might be observed again. In that case a smaller earthquake, magnitude 6.7, occurred east of Adak Canyon three months before (Feb. 7) the large event in Adak Canyon (May 2). We, therefore, announced the highly speculative outlook that a major event would occur in August, 1984. This did not happen, and we conclude that the May 6 event is not related directly to the occurrence of a larger event. However, the May 6 event did not change the observed rate of occurrence of local earthquakes, so whatever is responsible for the quiescence had not ceased operating.

An independent check on the reality of the quiescence indicated by the local network catalogue has been made by an examination of the rate of occurrence of events reported in the Preliminary Determinations of Epicenters by NEIS. The results for earthquakes with m_b 4.5 and greater are the most reliable, because the catalogue of these events is more likely to be complete than a listing including smaller events. The average rate of occurrence during the 247 months was 0.891 events per month, or just under 11 per year. The teleseismic data show a strong decrease in activity during October 1982 through March 1983, with an increase after that. Further analysis confirmed that much of the teleseismic activity during the supposed quiescence occurred within SW2, the activated sub-region. The rate of occurrence of earthquakes in the region of study, with SW2 eliminated, with m_b greater than or equal to 4.5 during the two year period prior to September, 1982 was about 0.9 per month, during 1983 was 0.67 per month, and during 1984 has been 0.17 per month, one of the lowest rates seen in the 20 years covered, and about the same as 1969. It is, however, not the lowest rate ever seen, as 1975 was marked by extremely low rate of 0.1 per month. The 1975 drop in teleseisms lasted only one year and was not followed by a large event.

The teleseismic data do not contradict the data from the local network, but they do not provide strong confirmation. They do indicate that sharp drops in rates of activity can last as long as one year without being precursors to strong events. Only continued observations will tell if they can last two years or longer and still not be followed by a major event.

Research on local and regional tectonics

Work has been completed and manuscripts are being prepared on two seismotectonic studies: (1) the study of shallow-focus earthquakes seaward of the main thrust zone; and (2) the search for possible precursors to the m_b 5.8 June 4, 1982, Adak Canyon earthquake. No precursors to this earthquake were found in an examination of the time-space patterns of seismicity or in the focal mechanisms of preceding earthquakes. Spectral analyses of small events occurring in the vicinity prior to the 1982 event are in progress.

The shallow-focus earthquakes trenchward of the main thrust zone are infrequent, occur in both spatial and temporal clusters, have thrust mechanisms in which the probable fault plane dips with a very shallow angle to the northwest, and occur at depths near 17 km under a prominent bathymethric forward rise called "Hawley Ridge". The "Hawley Ridge earthquakes" are particularly interesting in light of the seismicity pattern associated with the 1971 earthquakes discussed above: the February event occurred under Hawley Ridge, the larger May event occurred north of the western edge of the February aftershock zone. The 1982 Adak Canyon event was followed five days later by events under Hawley Ridge at the same longitude. These sequences suggest a correlation between events on the plate interface under Hawley Ridge and those occurring farther north within the main thrust zone. The further interpretation of this observation in terms of the details of failure along the plate interface must wait for more examples, either at Adak or in other subduction zones.

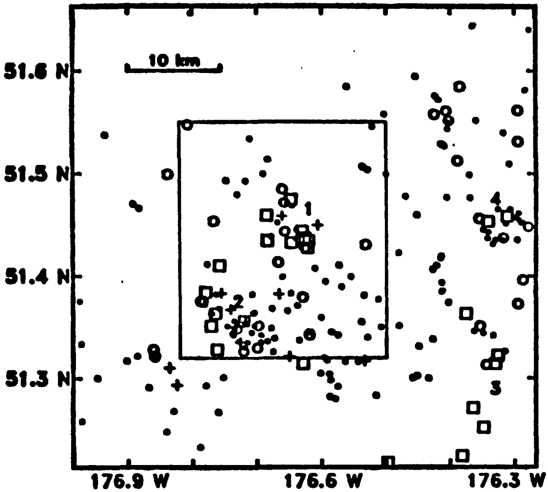

1.

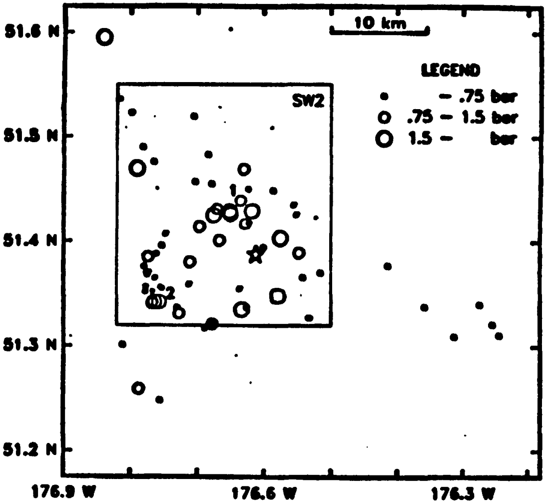

2a.

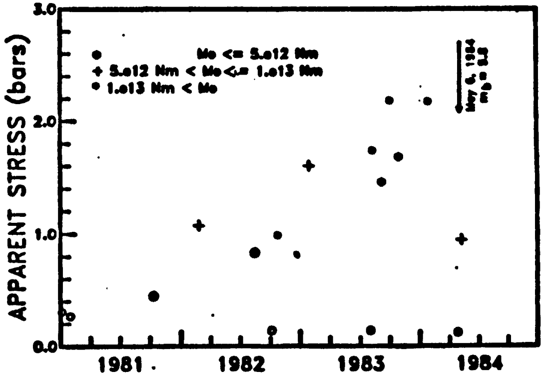

2b.

Figure 1. Shallow (<70 km) seismicity in and around SW2, August 1974-June 1983. The squares are local network locations of events on the PDE, circles are microearthquakes. Clusters 1 and 2 are associated with the asperity.

Figure 2a. Apparent stresses of SW2 earthquakes. The higher stresses concentrate at the clusters in Fig. 1. The star is the 6May1984 earthquake.

Figure 2b. Apparent stress as a function of time for earthquakes within 7.5 km of the 6May1984 earthquake.

References

Bowman, J.R. and C. Kisslinger, 1985, Seismicity associated with a cluster of m_b>4.5 earthquakes near Adak, Alaska: evidence for an asperity, *Bull. Seis. Soc. Amer.*, *75*(1): in press.

Scherbaum, F. and C. Kisslinger, 1984, Variations of apparent stresses and stress drops prior to the earthquake of 6May1984 (m_b 5.8) in the Adak Seismic Zone, *Bull. Seis. Soc. Amer.*, *74*(6): in press.

Publications and Abstracts, April-September, 1984

Toth, T. and C. Kisslinger, 1984, Revised focal depths and velocity model for local earthquakes in the Adak Seismic Zone, *Bull. Seis. Soc. Amer.*, *74*(4): 1349-1360.

Billington, S., C. Kisslinger and E.R. Engdahl, 1984, Features of locally-recorded seismicity in the central Aleutian islands (abstract), *Abstracts with Program*, G.S.A. Cordilleran Section Meeting, volume 16, number 5, p. 270.

Engdahl, E.R., J. Dewey and S. Billington, 1984, Redefined spatial distribution of teleseismically recorded earthquakes in the central Aleutian islands (abstract), *Abstracts with Program*, G.S.A. Cordilleran Section Meeting, volume 16, number 5, p. 282.

Scherbaum, F. and C. Kisslinger, 1984, Stress monitoring, source parameters and scaling laws in the Adak region, Aleutian Islands (abstract), *Earthquake Notes*, S.S.A. Eastern Section, volume 55, number 1, p. 16.

ALASKA SEISMIC STUDIES

9930-01162

John C. Lahr, Christopher D. Stephens, and Robert A. Page
Branch of Seismology
U. S. Geological Survey
345 Middlefield Road, MS 977
Menlo Park, California 94025
(415) 323-8111, Ext. 2510

Investigations

1) Continued collection and analysis of data from the high-gain short-period seismic network extending across southern Alaska from Juneau to Cook Inlet and inland across the Chugach Mountains. Two new stations were installed near the Copper River Delta to investigate a persistent source of shallow seismicity that is located along the inferred boundary of the Yakataga seismic gap. On September 11, 1984 two stations also were installed on the southern edge of the Talkeetna mountains near the m_b 5.7 earthquake that occurred on August 14, 1984. These stations will help to resolve more precisely the spatial configuration of the aftershock zone.

2) With funding from the Division of Geological and Geophysical Surveys of the State of Alaska, continued operation of four seismic stations in the northern Prince William Sound region which experienced two magnitude 6 earthquakes during 1983.

3) Continued monitoring of the region around the proposed Bradley Lake hydroelectric project on the Kenai Peninsula, a cooperative effort with the Alaska Power Authority. The level of monitoring was reduced at the request of the Alaska Power Authority on completion of the design phase for the hydroelectric project. Four cooperatively run stations and two nearby U.S.G.S. stations were terminated; a vertical-component high-gain seismograph and a strong motion instrument remain near Bradley Lake. Monitoring the level of seismicity near the project will continue but the precise location of microearthquakes will no longer be possible.

4) Cooperated with the Engineering Seismology and Geology Branch in operating strong motion accelerographs in the vicinity of the seismic network, including 13 between Icy Bay and Cordova in the area of the Yakataga seismic gap. Fourteen accelerographs are connected to the high-gain station telemetry network so that absolute trigger times can be obtained.

Results

1) During the past six months preliminary hypocenters were determined for 1691 earthquakes that occurred between February and July 1984 (Figure 1), which is 572 fewer events than were located for the preceding six-month period. Two major factors contributing to this decrease are a continuing decline in the rate of aftershock activity from the 1983 Columbia Bay shocks, and a change in criteria used to select earthquakes for processing, which was implemented to exclude earthquakes north of 62.5°N and events smaller than about magnitude 1 which occur within the aftershock zone of the 1979 St.

Elias earthquake northeast of Icy Bay. Sixteen events of magnitude 4 m_b and larger occurred, of which all but four were located in the Aleutian Benioff zone west and north of Cook Inlet. Two of the larger shocks were located above 15 km depth within the St. Elias aftershock zone, one was about 27 km deep beneath Blying Sound southeast of the Kenai Peninsula, and one was within the crust just east of Mt. Katmai on the Alaska Peninsula. The largest shock had a magnitude of 5.3 m_b and was located at 85 km depth in the Aleutian Benioff zone southwest of Cook Inlet. In and around the Yakataga gap the pattern of microearthquake activity was similar to that which has been observed over the past several years.

2) On August 14, 1984 a magnitude 5.7 m_b (5.2 M_s) crustal earthquake occurred near Sutton, Alaska approximately 80 km NE of Anchorage. Aftershock hypocenters define an east-west striking zone 9 km long which ranges in depth from about 11 to 21 km. The main shock is located near the deeper limit of the aftershock distribution. This sequence is of particular interest because of its location just a few km north of the surface trace of the Castle Mountain fault, which exhibits Holocene offset in the Susitna lowlands about 55 km to the west. Locally the fault strikes N 65° E and dips steeply northward (Detterman and others, 1976), subparallel to a steeply north-dipping nodal plane of the focal mechanism for the main shock which was derived from regional first-motion data. If this nodal plane is taken as the fault plane, then the earthquake resulted from right-lateral slip. Both the focal mechanism and distribution of hypocenters are consistent with slip on the Castle Mountain fault. Field inspection and aerial reconnaissance by T. Miller and S. Nelson of the Alaskan Geology Branch along the mapped trace two weeks after the earthquake failed to reveal any surface breakage, so the rupture probably did not extend to the earth's surface. This earthquake provides the strongest evidence yet available that the Talkeetna segment of the Castle Mountain fault is currently active.

3) During the summer of 1984 a proto-type earthquake logging device (ELOG) was successfully field-tested in Alaska. ELOG is a microprocessor-based earthquake detection and data collection instrument which is capable of operating from three 2.5 volt, 1000 amp-hr batteries for a period in excess of one year. The hardware is based on the RCA Microboard series, and timing is provided by a Swiss-manufactured clock synchronized to the Omega navigational radio signal. Data is currently stored on cassette tape. ELOG runs FORTH, a high-level computer language well-suited for applications with limited memory.

The proto-type ELOG was deployed at the site of the regional seismograph station SAW 30 km east-northeast of Sutton, Alaska. About 1500 triggers were recorded during a five-week period that included part of the early aftershock sequence following the August 14 shock. The data are being analyzed and compared with the signals recorded by SAW to check the ability of the ELOG to detect earthquake arrivals and its accuracy in picking the onsets of the phases.

Since the field test, low-power CMOS programmable memory was incorporated into the unit and a memory expansion board was added to increase the available program memory by a factor of five. Future plans call for a solid-state mass-storage unit to replace the cassette, and for expanded software to pick the S as well as the P phase.

References Cited

Detterman, R. L., Plafker, George, Russell, G. T., and Hudson, Travis, 1976, Geology and surface features along part of the Talkectna segment of The Castle Mountain - Caribou fault system, Alaska, U.S. Geological Survey Miscellaneous Field Studies Map, MF-738.

Reports

Fogleman, K. A. and Rogers, J. A., 1984, Regional earthquake monitoring in Southern Alaska, 1971-83 [abs.], Earthquake Notes, Eastern Section, Seismological Society of America, v. 55, p. 15.

Lahr, J. C., Stephens, C. D., and Page, R. A., 1984, Resolution of seismic source zones in the Anchorage area, Alaska [abs.], Earthquake Notes, Eastern Section, Seismological Society of America, v. 55, p. 16.

Page, R. A., 1984, Seismological aspects of the great 1964 Alaska Earthquake [abs.], Earthquake Notes, Eastern Section, Seismological Society of America, v. 55, p. 17.

Pelton, J. R., and Page, R. A., 1984, Focal depth estimates for selected Alaskan teleseisms [abs.], Earthquake Notes, Eastern Section, Seismological Society of America, v. 55, p. 15.

Stephens, C. D., Fogleman, K. A., Lahr, J. C., and Page, R. A., 1984, The Wrangell Benioff zone, southern Alaska, Geology, v. 12, p. 373-376.

Stephens, C. D., Page, R. A., and Lahr, J. C., 1984, Variations in the style of convergence across southern Alaska inferred from regional seismic data [abs.], Earthquake Notes, Eastern Section, Seismological Society of America, v. 55, p. 16.

Figure 1. Earthquakes located by the USGS southern Alaska seismograph network during February through July 1984. Epicenters of 1691 events are plotted. Magnitudes are determined from coda-duration or maximum amplitude, and for events of magnitude 3 and larger can be as much as one unit smaller than the teleseismic m_b magnitude. The lowest magnitude level to which data is processed varies within the mapped area due to uneven station distribution and to criteria used to select earthquakes for processing. Heavy dashed contour indicates inferred extent of Yakataga seismic gap. Abbreviations are: A - Anchorage, BL - Bradley Lake, BS - Blying Sound, C - Cordova, CB - Columbia Bay, CI - Cook Inlet, CR - Copper River Delta, IB - Icy Bay, PWS - Prince William Sound, S - Sutton.

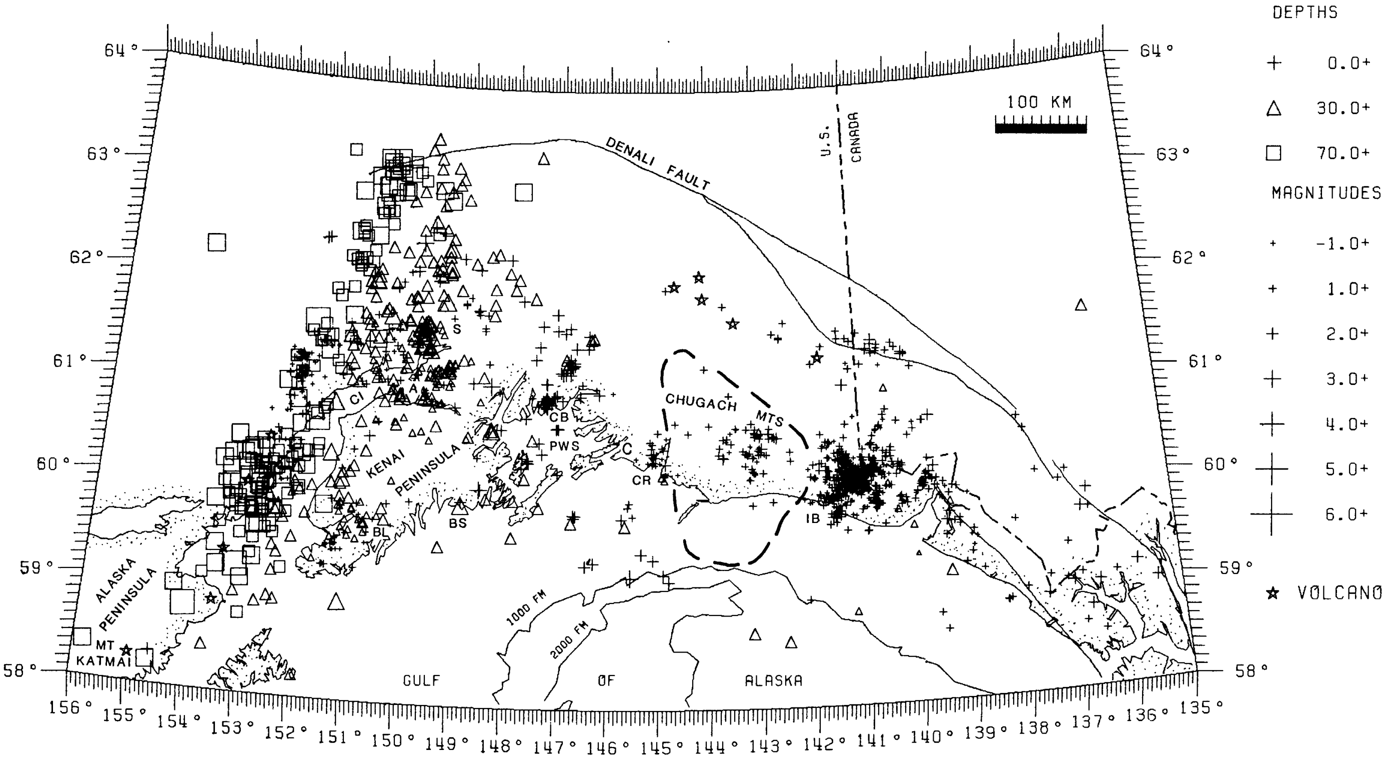

Figure 1. Earthquakes located by the USGS southern Alaska seismograph network during February through July 1984. Epicenters of 1691 events are plotted. Magnitudes are determined from coda-duration or maximum amplitude, and for events of magnitude 3 and larger can be as much as one unit smaller than the teleseismic m_b magnitude. The lowest magnitude level to which data is processed varies within the mapped area due to uneven station distribution and to criteria used to select earthquakes for processing. Heavy dashed contour indicates inferred extent of Yakataga seismic gap. Abbreviations are: A - Anchorage, BL - Bradley Lake, BS - Blying Sound, C - Cordova, CB - Columbia Bay, CI - Cook Inlet, CR - Copper River Delta, IB - Icy Bay, PWS - Prince William Sound, S - Sutton.

Seismological Field Investigations

9950-01539

C. J. Langer
Branch of Engineering Geology and Tectonics
U.S. Geological Survey
Box 25046, MS 966, Denver Federal Center
Denver, CO 80225
(303) 236-1593

Investigations

1. Borah Peak, Idaho, earthquake aftershock study--regional investigation of aftershocks resulting from M_s 7.3 earthquake of October 18, 1983.

2. Guinea, West Africa, earthquake aftershock study--local investigation of aftershocks resulting from $M_s = 6.2$ earthquake of December 22, 1983.

3. Laramie Mountains, Wyo., earthquake aftershock study--local investigation of aftershocks resulting from $M_L = 5.5$ earthquake of October 18, 1984.

Results

1. The distribution of 374 aftershocks resulting from the 1983 Borah Peak, Idaho, earthquake shows an aftershock zone approximately 75 km long by 15 km wide that extends roughly parallel to the surface rupture and is displaced laterally to the southwest about 5-10 km. Depths range from near surface to 13 km with the majority of activity occurring in the interval between 5 and 11 km. Dense clustering of aftershocks is evident near the westward splay of the surface rupture in the Willow Creek Pass area. Hypocentral cross sections taken perpendicular to the surface rupture, using the best located aftershocks ("A" quality only) south of the splay, indicate that the fault zone may be dipping at or near 60°.

   A magnitude 5.8 (M_L) aftershock occurred on August 22, 1984, near Red Hill, about 10 km east-southeast of Challis. A network of 18 smoked paper recording seismographs and 5 digital systems was installed 3 days later by the U.S. Geological Survey (USGS) and University of Utah personnel. Almost 2 weeks of records were obtained during this sequence of intense aftershock activity. Analysis of these data are in process.

2. A magnitude 6.2 (M_s) earthquake occurred in northwestern Guinea, West Africa, on December 22, 1983, that was felt in six neighboring countries. The epicentral area is coastal margin, intraplate locale with a very low level of historical seismicity. The main shock was accompanied by some 9 km of east-southeast to west-northwest-trending surface faulting that was discovered and mapped by M. G. Bonilla. The fault displacement was right-lateral strike slip of at least 13 cm with an additional small component of vertical movement, southwest side down in several places. Main shock focal mechanism solutions derived from teleseismic data by other workers show a strong component of normal faulting motion that was not observed in the ground ruptures. The surface faulting occurred on a preexisting fault whose field characteristics suggest a low-slip rate with

very infrequent earthquakes. There were extensive rockfalls and minor liquefaction effects at distances less than 10 km from the faulting and main-shock epicenter.

A 15-day period of aftershock monitoring, commencing 22 days after the main shock, was conducted. Eleven portable, analog short-period vertical seismographs were deployed in a network with an aperture of 25 km and an average station spacing of 7 km. Over 200 aftershocks, with duration magnitudes of two or greater, were recorded. Analysis of a sample of 94 of these events revealed a tabular aftershock volume (27 km long by 14 km wide by 2 km thick) trending east-southeast to west-northwest and dipping steeply ($\sim 60^0$) to the south-southwest. Four composite focal mechanisms for groups of events, distributed throughout the aftershock volume, all exhibit right-lateral, strike-slip motion on a steeply dipping (near-vertical) plane striking east-northeast to west-southwest. Thus, the general agreement between the field geologic and seismologic results is good, but does not support the large component of normal faulting reported for the main shock.

3. The magnitude 5.5 (M_L) Laramie Mountains, Wyoming, earthquake of October 18, 1984, is the largest documented earthquake to occur in the south-eastern Wyoming area during historical time. This earthquake is considered to be of significant importance because of its proximity to a large metropolitan and industrial region in neighboring Colorado as well as the industry and several cities and towns in Wyoming. Although the shock was felt over a six-State region, it caused only minor structural damage to houses and businesses close to the epicenter.

   A 23-station portable seismic network was installed around the epicentral area to monitor aftershocks for a period of 10 days (October 19-29). The fieldwork was conducted with the assistance of personnel and equipment from the U.S. Bureau of Reclamation, Geologic Services Branch which considerably enhanced the network coverage. Several hundred aftershocks were recorded and preliminary locations of six events indicate that their epicentral locale is about 8 km east-northeast of Marshall, under Mule Creek Mountain (approximately lat $42^o19'$ N., long $105^o44'$ W). Depths of these aftershocks range from 20 to 27 km. A focal mechanism constructed by Dave Gordon and Russ Needham, USGS Branch of Global Seismology and Geomagnetism, shows a high-angle strike-slip fault, right-lateral motion, produced by east-west compressive stresses.

Northern and Central California Seismic Network Processing

9930-01160

Fredrick W. Lester
Branch of Seismology
U.S. Geological Survey
345 Middlefeld Road M/S 977
Menlo Park, California 94025
(415) 323-8111, ext. 2149

Investigations

1. Signals from 433 stations of the multipurpose Northern and Central California Seismic Network (Calnet) are telemetered continuously to the central laboratory facility in Menlo Park where they are recorded, reduced, and analyzed to determine the origin times, magnitudes, and hypocenters of the earthquakes that occur in or near the network. Data on these events are presented in the forms of lists, computer tape and mass data files, and maps to summarize the seismic history of the region and to provide the basin data for further research in seismicity, earthquake hazards, and earthquake mechanics and prediction. A magnetic tape library of "dubbed" unprocessed records of the network for significant local earthquakes and teleseisms is maintained to facilitate futher detailed studies of crust and upper mantle structure and physical properties, and of the mechanics of earthquake sources.

2. Project personnel also conducted investigations of significant earthquakes or earthquake sequences that occurred in northern and central California.

3. Quarterly reports were prepared on seismic activity around Lake Shasta, Warm Springs Dam, the Auburn Dam site and Melones Dam for the appropriate funding agencies.

Results

1. Figure 1 shows the seismic activity of Northern and Central California for the period April 1, through September 30, 1984. The 10443 earthquakes plotted are all reliable locations using 4 or more phase readings in the solution. The phase readings were obtained either by hand timing or by the Real Time Picker (RTP) or they are a combination of both sources. The Coast Ranges have been screened for quarries and those data have been eliminated. Identification of quarries in the Sierra Nevada Foothills is a constant problem so that all quarry data have not yet been eliminated from the catalog. We feel that the catalog of location data maintained by Calnet is relatively complete for earthquakes M 1.5 and larger.

2. Processing of data for the first half of calendar year 1978 and 1983 is nearly complete and those data will be open-filed as soon as they are ready.

3. The investigation of the Coalinga earthquake sequence that began

on May 2, 1983 is continuing. The results of the investigation will be published in the spring of 1985 as part of a U.S.G.S. Professional Paper. Aftershocks continued in the region at a rate of 3 to 5 per day.

4. Close monitoring of the Long Valley caldera area of the eastern California is still underway. Included on Figure 1 are locations of 4064 earthquakes that were located in and around the caldera for this time period. Events in the region are located and analyzed on a daily basis so as to keep abreast of possible new situations that may arise since this area is still considered to be a potentially hazardous volcanic region.

5. The Morgan Hill, California, earthquake (magnitude 6.1) of 24 April 1984 ruptured a 30-kilometer-long segment of the Calaveras fault zone to the east of San Jose. Although it was recognized in 1980 that an earthquake of magnitude 6 occurred on this segment in 1911 and that a repeat of this event might reasonably be expected, no short-term precursors were noted and so the time of the 1984 earthquake was not predicted. Unilateral rupture propagation toward the south-southeast and an energetic late source of seismic radiation located near the southeast end of the rupture zone contributed to the highly focused pattern of strong motion, including an exceptionally large horizontal acceleration of 1.29g at a site on a dam abutment near the southeast end of the rupture zone. Figure 2 shows 1901 well recorded earthquakes with reliable locations that occurred in the Morgan Hill area. The largest aftershock was magnitude 4.5. Some published results of the investigation of this sequence are now available and other investigations are currently underway.

Reports

Bakun, W. H., Clark, M. M., Cockerham, R. S., Ellsworth, W. L., Lindh, A. G., Prescott, W. H., Shabal, A. F., and Spudich, P., 1984, The 1984 Morgan Hill, California earthquake, Science, 225, 288-291.

Cockerham, R.S., 1984 Evidence for a 180-km-long subducted slab beneath northern California, BSSA, 74, 569-574.

Eaton, J. P., 1984, Location, focal mechanism, and magnitude of the Morgan Hill earthquake derived from Calnet records, in the Morgan Hill, California earthquake of April 24, 1984 (a preliminary report) USGS Open-File Report 84-492A, p. 10-17.

Eaton, J. P., 1984, Noise analysis of the seismic system employed in the northern and southern California seismic nets, USGS Open-File Report 84-657, 43p.

Oppenheimer, D. H., and Eaton, J. P., 1984, Moho orientation beneath central California from regional earthquake traveltimes, Journal of Geophysical Research (in press).

Savage, J. E., and Cockerham, R. S., 1984, Earthquake swarm in Long Valley caldera, California, January 1983: Evidence for dike inflation, Journal of Geophysical Research, 89, 8315-8324.

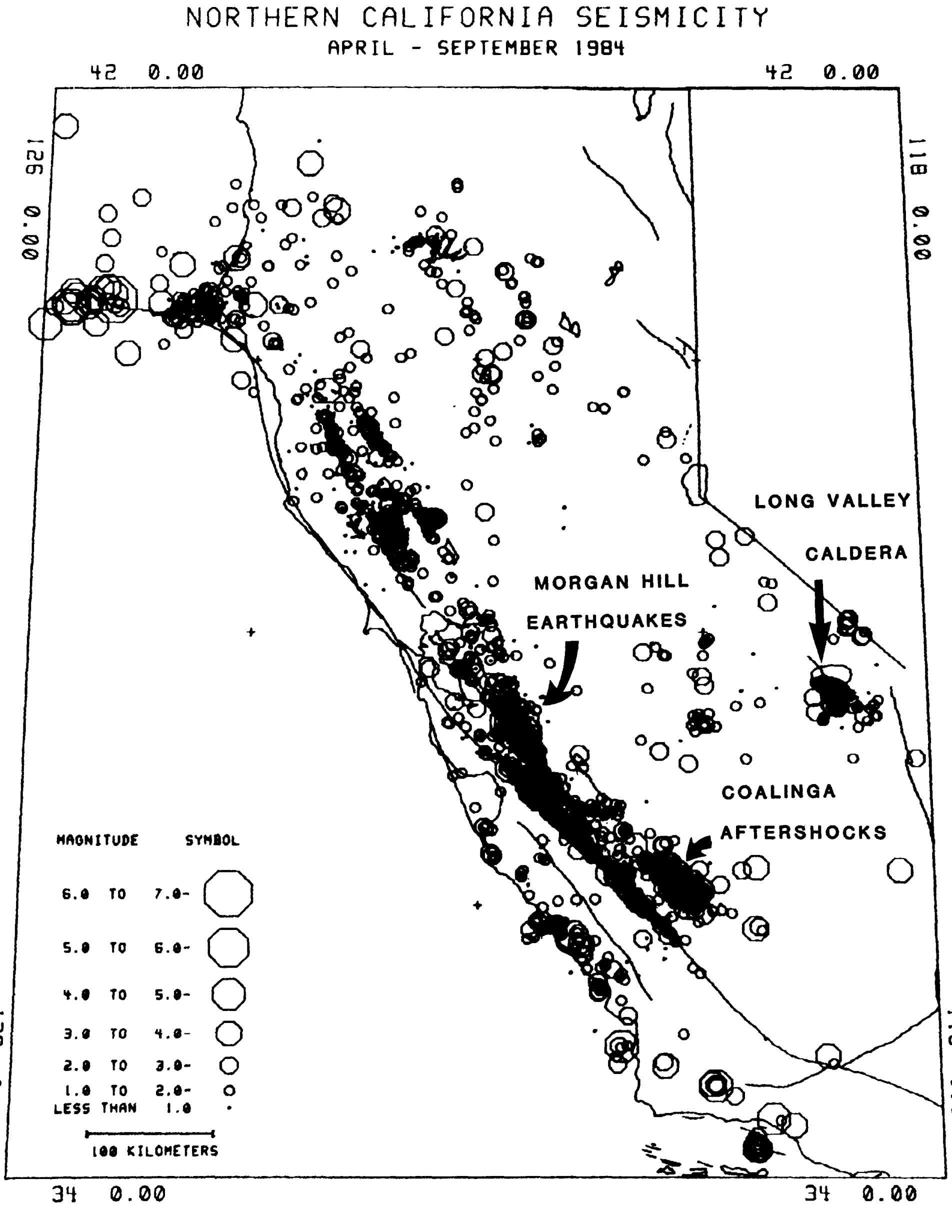
NORTHERN CALIFORNIA SEISMICITY
APRIL - SEPTEMBER 1984
42 0.00
42 0.00
126 0.00
118 0.00
126 0.00
118 0.00
34 0.00
34 0.00
LONG VALLEY
CALDERA
MORGAN HILL
EARTHQUAKES
COALINGA
AFTERSHOCKS
MAGNITUDE
SYMBOL
6.0 TO 7.0-
5.0 TO 6.0-
4.0 TO 5.0-
3.0 TO 4.0-
2.0 TO 3.0-
1.0 TO 2.0-
LESS THAN 1.0
100 KILOMETERS

FIGURE 1

MORGAN HILL EARTHQUAKES
APRIL 24 - SEPTEMBER 30, 1984

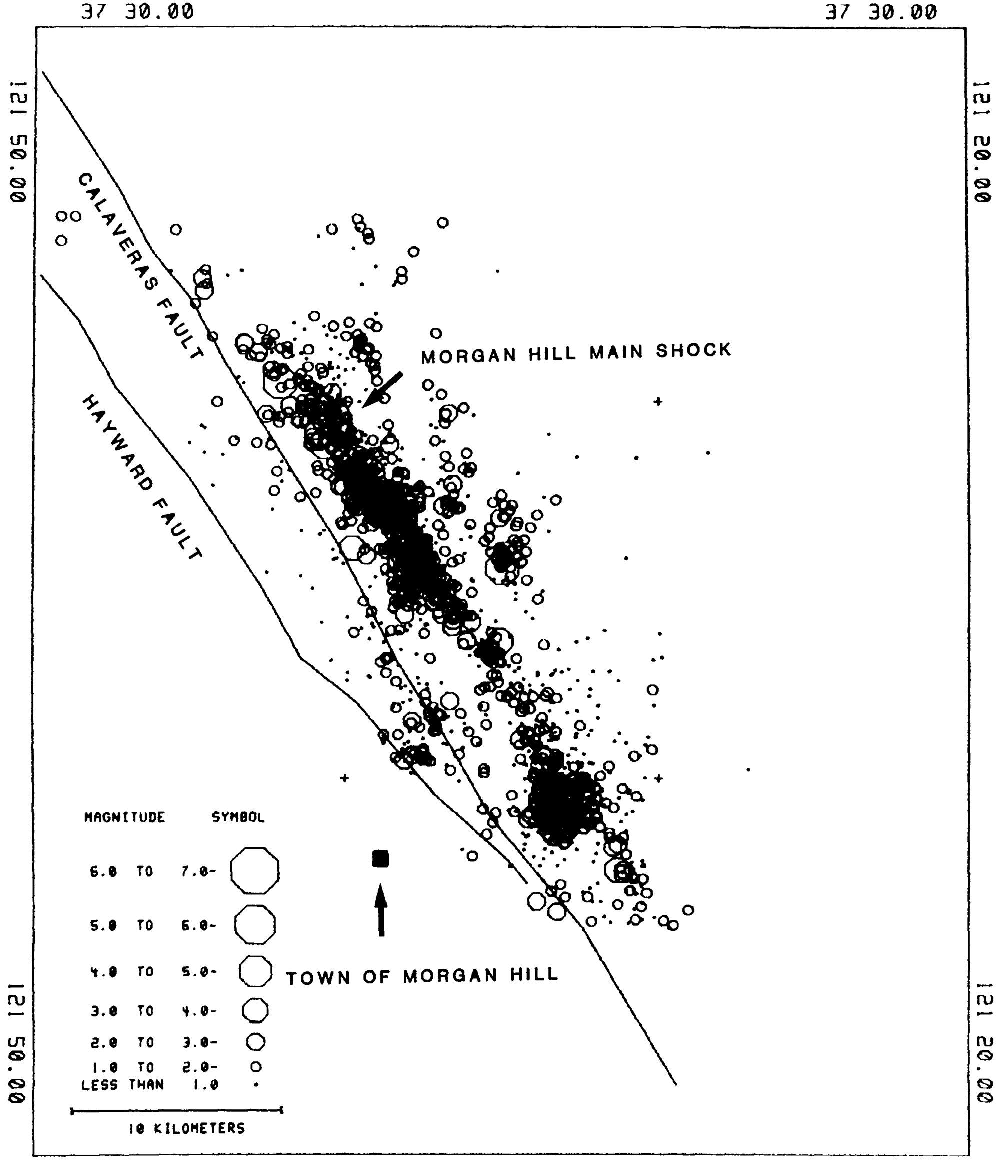

FIGURE 2

CONSTRUCTION OF AN ELECTROMAGNETIC DISTANCE-MEASURING SYSTEM

66701

Judah Levine

Time and Frequency Division
National Bureau of Standards
Boulder, Colorado 80303
(303) 497-3903

Investigations

We have continued our testing and evaluation of a three- wavelength system for measuring baselines up to 50 km long with fractional uncertainties of about 0.02 ppm. The instrument is designed to measure the refractivity of the atmosphere by measuring the path differences between three signals: two optical and one microwave. The optical wavelengths used are 632 nm (He-Ne red) and 441.6 nm (He-Cd blue); the microwave frequency is 8.1 GHz.

Results

WE have made substantial progress in eliminating the angle dependent errors which we discussed in our previous progress report. The error has been traced to an interaction between the modulators and the interference filters used to separate the red and blue beams. We do not yet understand the physical basis for the error, but it is possible to reduce it to an insignificant level by removing the interference filters. We are undertaking two parallel efforts to understand the source of the error to be sure that it will be finally eliminated, and to proceed with the field testing without the interference filters for the time being.

Earthquake Prediction and the Tectonics of the Northeastern Caribbean: Analysis of Seismic Data from a Regional Network

USGS-14-08-0001-21233

W. R. McCann and L. R. Sykes
Lamont-Doherty Geological Observatory of Columbia University
Palisades, New York 10964
(914) 359-2900

Investigations

1. Model local P-wave velocities and jointly locate microearthquakes recorded by LDGO operated seismic network in the northeastern Caribbean.

2. Estimate seismic hazard of Puerto Rico and the Virgin Islands.

3. Terminate recording at central recording site in St. Thomas and redirect signals from 5 stations in the Virgin Islands and eastern Puerto Rico to Cayey, Puerto Rico.

4. Remove all remaining equipment from the field stations and central recording site to LDGO.

Results

1. We have successfully determined P-wave velocities in the upper 50 km of the Virgin Islands region (18°N-19°40'N, 64°-66° W). Arrival times from over 250 microearthquakes were used in the velocity inversion program written by R. Crosson to determine seismic velocities and station delays. Location and time information from 3 2-ton shots were used to initially constrain the velocity model. As a result of this study we have more clearly defined the downgoing seismic zone that delineates the upper surface of the underthrust North American plate. We have also identified two shallow, intraplate faults near the islands of St. Thomas and Virgin Gorda.

2. We have qualitatively estimated the seismic hazard for Puerto Rico and the Virgin Islands. A possible great eathquake (8-8 1/2 M_s) appears to have occurred along the main seismic zone near Puerto Rico. Other destructive shocks in 1918 (7.5 M_s, NW Puerto Rico) and 1867 (7.5 M_s, Virgin Islands) occurred on intraplate faults. Maximum dimensions of future large earthquakes as inferred from lengths of faults in the intraplate region suggest that events as large as 7.5 M_s can occur to the west and south of Puerto Rico and near the Virgin Islands as well. Although strain rates on these faults may be an order of magnitude less than on faults in the Puerto Rico trench, the large number of potential sources suggest that damaging earthquakes in this part of the Caribbean can come from either the Puerto Rico trench or the intraplate faults with nearly equal probability.

Average repeat times for damaging earthquakes may be about 100 years. It has been 70 years since the last damaging earthquake.

3. We have terminated operations at our central recording site in St. Thomas. That site is now used to repeat signals from the Virgin Islands region to Cayey, Puerto Rico the site of central recording of the Puerto Rico seismic network. Of the 17 stations in the LDGO network monitoring seismic activity in the northeastern Caribbean 12 are now closed; five in eastern Puerto Rico and the Virgin Islands have been integrated into the Puerto Rico seismic network.

4. Equipment at the central recording site in St. Thomas not needed for the integration of seismic signals into the Puerto Rico network have been removed to LDGO. Also, equipment at the various field stations have also been removed to LDGO.

MAGNETIC FIELD OBSERVATIONS

9960-03814

R. J. Mueller
Branch of Tectonophysics
U.S. Geological Survey
345 Middlefield Road, MS/977
Menlo Park, CA 94025
(415) 323-8111 ext. 2533

INVESTIGATIONS

1) Investigation of total field magnetic intensity measurements and their relation to seismicity and strain observations along active faults in central and southern California.

2) Recording and processing of synchronous 10 minute magnetic field data and maintenance of the 25 station telemetered magnetometer network and its receive telemetry system for central and southern California.

3) Processing and analysis of on-site recorded data from the 64 station portable magnetometer network in California.

RESULTS

1. The epicenter of the Morgan Hill earthquake (M_L=6.0±0.3) of April 24, 1984 is located on the Calaveras fault and within an array of magnetometer stations. The magnetometer stations, located along the Calaveras fault, were not operational at the time of, or for the 16 month period prior to the earthquake, but were reinstalled within hours of the main shock. Comparison of magnetic field differences after the earthquake with those 16 months prior indicate no significant variations >0.75 nT. Analysis of hourly magnetic field differences for the 12 day period following the earthquake indicate no significant variations >1.0 nT associated with the aftershock activity. A seismomagnetic model of the earthquake, using uniform magnetization, indicates the magnetometer stations along the Calaveras fault are poorly located to detect stress-generated magnetic field changes. The same model, using a distribution of magnetic material only on the west side of the fault, indicates station C1Y was located near the point of maximum expected field change. The lack of any magnetic field change >1.0 nT at station C1Y, requires a stress change <1.2 MPa for the 12 day period following the Morgan Hill earthquake.

2. Designed and bench tested a digital circuit to monitor the output from dilatometer stations and automatically rezero the instrument. The circuit is presently being field tested.

3. Designed and bench tested a digital circuit to convert 16 parallel data outputs to a serial output which is compatible with the serial input of the Sutron model 8004D satellite data collection platform.

4. Conversion of 2 magnetometer stations to solar powered batteries. Only 4 of the 25 stations are presently not solar powered and only 1 of these 4 have suitable locations for conversion.

5. Completed construction and testing of magnetometer and geodetic equipment for shipment to China.

REPORTS

Johnston, M. J. S., Mueller, R. J., and Davis, P. M., Precision of magnetic measurements in a tectonically active region: J. Geomag. Geoelectr., 36, p. 83-94, 1984.

Mueller, R. J. and Johnston, M. J. S., Magnetic field measurements near the Morgan Hill earthquake of April 24, 1984: U.S. Geol. Survey Open-File Report 84-498A, p. 76-85, 1984.

Mueller, R. J., Johnston, M. J. S., Keller, V., and Silverman, S., Magnetic field observations in the Long Valley caldera of central-eastern California, 1976-1984: Trans. A.G.U. (in press).

Probabilistic Approach to Earthquake Forecasting

USGS Contract No. 14-08-0001-21916

Mansour Niazi
TERA Advanced Services Corporation
2150 Shattuck Avenue
Berkeley, California 94704
(415)845-5200

Investigations

The earthquake recurrence characteristics of a region, as a byproduct of the tectonic loading and regional fracture pattern, play a key role in providing long-range forecasting capability. We would like to determine how the observation of one or more potential precursors may modify the long term probability estimates for occurrence of an earthquake of $M > M_x$. The procedure is expected to be of application in probabilistic forecasting within intermediate-and possibly short-term range. Southern California has been selected as the test region to which the procedure may be applied.

Results

Since the authorization of this study in May, we have been focusing on the development of the methodology as well as the application of screening procedures to the subsets of precursory information reported for southern California earthquakes. Both the methodology and preliminary results will be presented during the upcoming AGU Fall meeting in San Francisco.

Global Seismograph Network Evaluation and Development

9920-02384

Jon Peterson
Branch of Global Seismology and Geomagnetism
U.S. Geological Survey
Building 10002, Kirtland AFB-East
Albuquerque, New Mexico 87115-5000
(505) 844-4637

Investigations

Work continued in accordance with the Protocol Agreement between the State Seismological Bureau (SSB) of the People's Republic of China and the U.S. Geological Survey (USGS), in which the USGS is assisting in the design and establishement of the China Digital Seismograph Network (CDSN).

Results

A delegation of seven SSB personnel, headed by Professor Chen Junliang, received three months of familiarization training in CDSN hardware and software. Two of the delegation members attended a DEC school and the other five received training at the Albuquerque Seismological Laboratory where the equipment is being assembled and tested.

The assembly and test of the demonstration data system and the data management system continues. Slow delivery of DEC hardware caused delays; however, all equipment is now in hand and software is being tested.

The testing of the sensor systems that will be used in China has been completed. The results of noise tests on the DJ-1 seismometers and low-noise short-period amplifiers have confirmed that these instruments are suitable for use out to the Nyquist frequency (20 Hz). Extensive noise tests were performed on the STS-1 seismometers that will be used to generate broadband, long-period, and very-long-period signals. The principal purpose of the testing was to determine the best installation technique. The results show that when the instruments are properly installed in good vaults the noise levels of both the vertical and horizontal components are consistently lower than the noise levels recorded from an SRO borehole seismometer during windfree periods in the period range from 50 to 10,000 seconds. A report describing the CDSN sensor system and the test results is being prepared.

CRUSTAL STRAIN

9960-01187

W.H. Prescott, J.C. Savage, M. Lisowski
Branch of Tectonophysics
U.S. Geological Survey
345 Middlefield Road, MS/977
Menlo Park, California 94025
(415) 323-8111, ext. 2701

Investigations

The principal subject of investigation was the analysis of deformation in a number of tectonically active areas in the western United States.

1. The Morgan Hill, California Earthquake of 24 April 1984

As reported previously the Morgan Hill earthquake involved about 420 mm of slip on the coseismic rupture plane. Since the earthquake an additional 330 mm of slip have occurred. This postseismic slip continues to be deeply buried. There is no evidence for near surface slip like that which occurred following the Coyote Lake earthquake. The small aperture array in Hall's Valley has been surveyed a number of times since the main shock. The most recent survey was after the M_L=4.5 aftershock on 26 September 1984. There is no evidence of any slip at the surface in Hall's Valley.

2. Creep Rates From Small Aperture Geodetic Networks Near San Francisco, California

Current fault slip rates have been calculated for faults of the San Andreas system near San Francisco from about 8 to 10 years of HP 3800 series measurements. All of the networks are located either along the 1906 rupture zone or on other faults adjacent to it. The data imply that neither the San Andreas fault itself nor the San Gregorio fault are creeping (with a detection threshold of 2-3 mm/yr). Both the Hayward and Calaveras faults along the eastern side of San Francisco Bay are creeping. The Hayward fault creep rate is well determined at 6 ± 1 mm/yr from observations at several sites. The Calaveras fault is more problematic. At its southern end near the Morgan Hill epicenter the creep rate is 9 ± 1 mm/yr. There is ambiguous evidence at Concord suggesting over a centimeter per year of creep. One of two fault crossing lines shows the change and the other does not.

3. Observed Strain Rates Near New York City

Analysis of historic triangulation data near New York City indicates that the strain rates for two areas are surprisingly large. One arc, located in a relatively seismic region on the Ramapo fault (see Figure), has a strain rate of 0.18 ± 0.05 µstrain/yr, the other high strain area is in western Long Island, where the observed strain rate is 0.57 ± 0.14 µstrain/yr. At Ramapo the plane of maximum shear is oriented N-S and on Long Island it is oriented N25°W. At other sites in the vicinity, no significant strain accumulation was detected.

4. Monitoring Deformation in the Long Valley 1983-1984

Deformation continued in the Long Valley caldera at about the same rate as in 1982-1983. A resurvey of the 40-line, regional trilateration network suggests an outward expansion centered on the resurgent dome. Horizontal displacements as large as 30 mm were measured within the caldera for the interval August 1983 to August 1984. The leveling surveys will not be completed before the end of October, but preliminary results indicate a 45 mm uplift of Casa Diablo Hot Springs relative to Toms Place. The uplift does not fall off to the north, however, and it would appear that June Lake Junction is up 60 mm with respect to Toms Place. We suspect that this latter result may be a product of leveling error as some problems have been encountered in closing sections.

During the period August 1983 to September 1984 deformation of the caldera was monitored monthly by leveling surveys of six, 1-km aperture, L-shaped leveling arrays and distance measurements of three 10-km-long lines radiating from near Casa Diablo Hot Springs. The accumulated tilt measured over the 10 month interval amounted to only a few microradions at each array and is only marginally significant. Nevertheless, the tilt vectors are all directed approximately radially outward from the center of the resurgent dome. The length measurements showed a linear trend with time; the line to Lookout Mountain lengthened at a rate of 33 ± 4 mm/a and the line to the top of Mammoth Mountain lengthened at a rate of 19 ± 3 mm/a. The monitoring measurements leave little doubt that deformation is accumulating approximately linearly with time.

5. Reanalysis of Deformation Data Near Palmdale 1971-1984

Although the long-term (1971-1984) strain accumulation across the San Andreas fault near Palmdale, California, is simply right-lateral shear at the rate of 0.20 ± 0.01

μstrain/a (tensor shear), annual measurements indicate that an anomalous contraction perpendicular to the fault accumulated in the interval 1973-1978 and was abruptly released in mid-1979. This anomaly is referred to as the 1979 Palmdale strain event. More frequent measurements of strain since 1979 suggest a more irregular accumulation of strain than prior to 1979. This irregularity may be due to measurement errors larger than previously estimated. As a consequence of this post-1979 irregularity, the 1979 strain event no longer appears as anomalous as it had in the shorter (1971-1980 record). To provide independent support for existence of the 1979 Palmdale strain event we have reviewed gravity measurements at Palmdale by Jachens and water level measurements in wells near Palmdale by Merifield and Lamar that have previously been shown to provide a marginal correlation with the 1979 strain recovery. These data taken together with the original strain observations suggest a real strain anomaly did occur near Palmdale in 1979, but the evidence is not overwhelming.

Reports

Bakun, W. H., M. M. Clark, R. S. Cockerham, W. L. Ellsworth, A. G. Lindh, W. H. Prescott, A. F. Shakal, P. Spuduch, The 1984 Morgan Hill, California, earthquake, Science, 225, p. 288-291, 1984.

Savage, J. C., and M. Lisowski, Deformation in the White Mountain seismic gap, California-Nevada, 1972-1982, J. Geophys. Res., 89, p. 7671-7687, 1984.

Savage, J. C., and R. S. Cockerham, Earthquake swarm in Long Valley caldera, California, January 1983: Evidence for dike inflation, J. Geophys. Res., 89, p. 8315-8324, 1984.

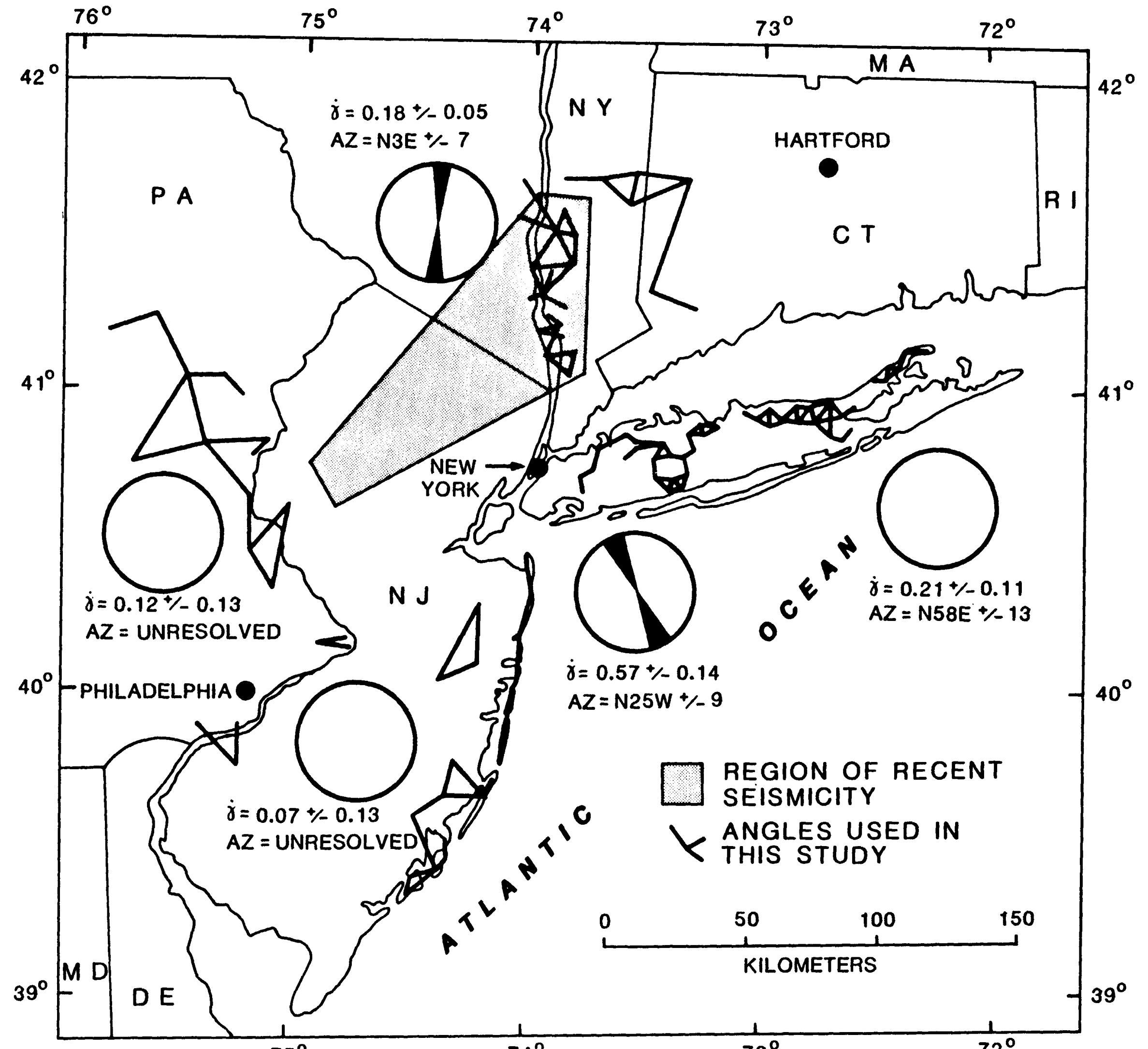
76°
75°
74°
73°
72°
42°
41°
40°
39°
MA
NY
PA
CT
RI
NJ
MD
DE
HARTFORD
NEW YORK
PHILADELPHIA
OCEAN
ATLANTIC
$\dot{\delta}$ = 0.18 +/- 0.05
AZ = N3E +/- 7
$\dot{\delta}$ = 0.12 +/- 0.13
AZ = UNRESOLVED
$\dot{\delta}$ = 0.07 +/- 0.13
AZ = UNRESOLVED
$\dot{\delta}$ = 0.57 +/- 0.14
AZ = N25W +/- 9
$\dot{\delta}$ = 0.21 +/- 0.11
AZ = N58E +/- 13
REGION OF RECENT SEISMICITY
ANGLES USED IN THIS STUDY
0
50
100
150
KILOMETERS

Helium Monitoring for Earthquake Prediction

9570-01376

G. M. Reimer
U.S. Geological Survey, MS 963
Denver Federal Center
Denver, CO 80225
(303) 236-7886

Investigations

The variations of helium in soil-gas from sample collecting stations along the San Andreas Fault near San Benito, California continue to be observed and related to nearby seismic activity. A specific investigation to understand the source of the seasonal helium variations was undertaken during the summer of 1984. Samples were collected daily, meteorological conditions were measured, and the samples were analyzed for nitrogen, oxygen, methane, and carbon dioxide in addition to helium.

Results

Figure 1 shows the plot of helium concentrations as a function of time, plotted through October 22, 1984. The April Morgan Hill earthquake and aftershocks fit the criteria of precursory helium decreases as outlined in the Summaries of Technical Reports, v. 18 of this series.

The daily sampling and comparison of helium variations to meteorologic parameters and other gases was conducted during June and July, 1984, during a typical period of the helium concentration reversal. The data are still being analyzed but preliminary observations reveal a strong link between the helium concentration and the near-surface soil moisture content. If a simple variable could be found to correlate with seasonable helium changes, it would permit the reduction of the seasonal influence and allow greater confidence in separating true helium variations from the seasonal pattern. This is particularly important to help resolve helium decreases in the spring when the seasonal pattern is also in a decreasing mode.

Reports

Reimer, G. M., 1984, Prediction of central California earthquakes from soil-gas helium fluctuations: Journal of Pure and Applied Geophysics, in press.

Figure 1.--Helium soil-gas concentrations near San Benito, CA from May 1979 to October 1984. Date divisions are in months. Breaks in the helium record are periods when samples were not collected.

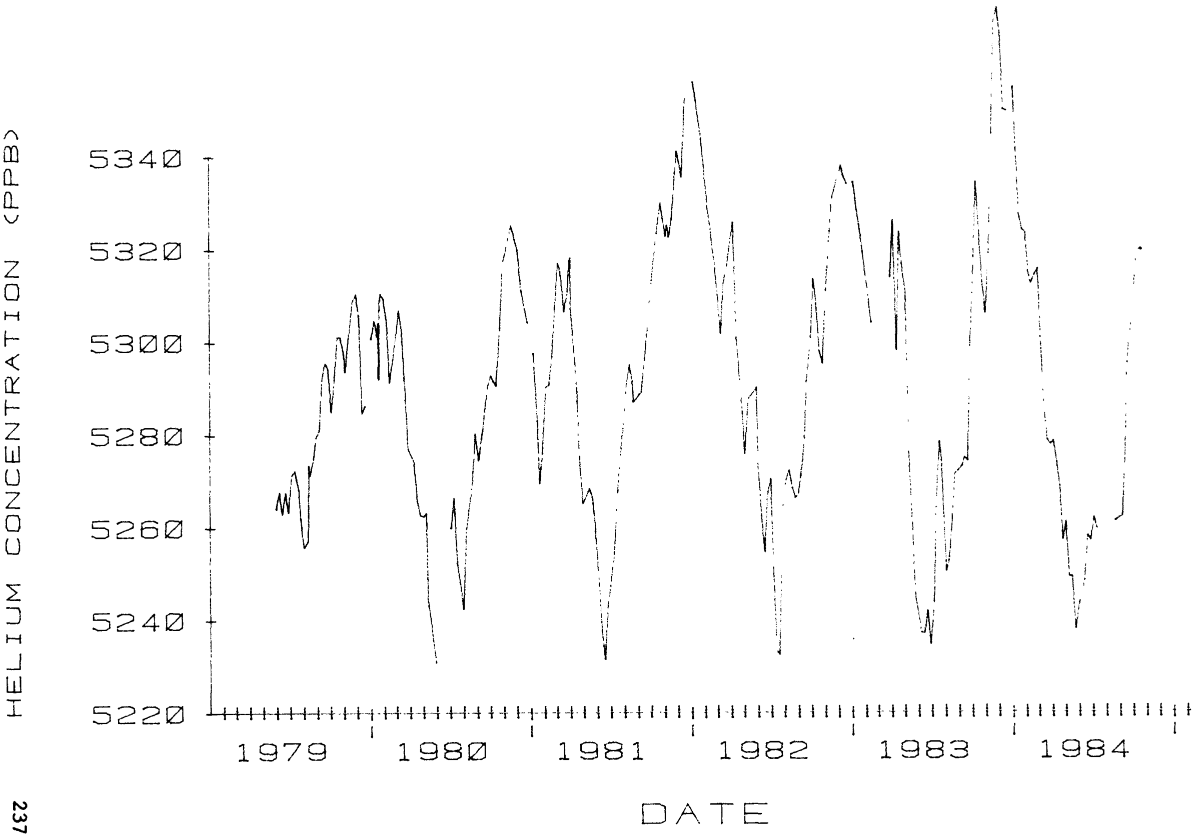

Global Digital Network Operations

9920-02398

Robert D. Reynolds
Branch of Global Seismology and Geomagnetism
U.S. Geological Survey
Albuquerque Seismological Laboratory
Building 10002, Kirtland AFB-East
Albuquerque, New Mexico 87115-5000
(505) 844-4637

vestigations

e Global Network Operations continued to provide technical and operational pport to the SRO/ASRO/DWWSSN observatories which include operating supplies, placement parts, repair service, redesign of equipment, training and on-site aintenance, recalibration and installation. Maintenance is performed at cations as required when the problem cannot be resolved by the station ersonnel. One field engineer was added to the Bendix O.&M. contract during his period. This brings the personnel level to a team leader, four field ngineers, and a digital technician.

he SRO enhancement program continued at the SRO stations. These enhancements onsist of adding the two short-period horizontal components to the digital ata, removal of the six second notch from the long-period filters, and installation of clip detectors on each seismometer module.

The following station maintenance activity was accomplished:

ANMO - Albuquerque - SRO
Two maintenance visits

ANTO - Ankara, Turkey - SRO
One maintenance visit

BCAO - Bangui, Central African Republic - SRO
Two maintenance visits

BOCO - Bogotta, Colombia - SRO
Two maintenance visits

CHTO - Chiang Mai, Thailand - SRO
Two maintenance visits

CTAO - Charters Towers, Australia - ASRO
One maintenance visit

KONO - Kongsberg, Norway - ASRO
One maintenance visit

SNZO - Wellington, New Zealand - SRO
One maintenance visit

ZOBO - La Paz, Bolivia - ASRO
Two maintenance visits

DWWSSN

BER - Bergen, Norway
One maintenance visit

SCP - State College, Pennsylvania
One maintenance visit

TOL - Toledo, Spain
One maintenance visit

WWSSN

ARE - Arequipa, Peru
One maintenance visit

GIE - Galapagos Islands, Ecuador
One maintenance visit

LPB - La Paz, Bolivia
One maintenance visit

NNA - Nana, Peru
One maintenance visit

ASL Repair Facility

As much routine repair as possible was done this period to support the field maintenance activity. Delivery was taken on an IBM-XT computer system during this period. The purpose of this system is to computerize the electronic components inventory and to develop computerized station maintenance files. Software development was started during this period.

Special Activity

The Global Telemetered Seismic Network noise survey was started in South America but was cancelled directly by the decision of an outside agency.

Formal training in the operation and maintenance of the SRO system was provided to a technician from Wellington, New Zealand.

Results

The digital network continues with a combined total of 29 SRO/ASRO/DWWSSN stations. The maximum effort is now to perform as much on-site maintenance and training as possible to provide the most quality digital data for the worldwide digital data base.

Hydrogen Monitoring

9980-02773

Motoaki Sato, K. A. McGee*, A. J. Sutton*
Branch of Igneous and Geothermal Processes, U.S. Geological Survey
MS 959, National Center, Reston, VA 22092
(703) 860-6600
(* now at 5400 MacArthur Blvd., Vancouver, WA 98661)

Investigations

Hydrogen (H_2) concentration in soil along major seismogenic faults in California is continuously monitored at a dozen sites by using a small H_2/O_2 fuel cell sensor. Because H_2 is highly mobile and buoyant, and has a low solubility in water, it is likely to escape to the atmosphere as soon as an incipient fracture develops at or above the depth where H_2 is generated or accumulated. Anomalous H_2 emission would signal increased permeability or incipient fracturing of rocks at depth, depending on the pattern of the emissions. This report covers results obtained in FY83, during which the principal investigator (Sato) was on a Gilbert Fellowship and was unable to summarize the results. More recent data are pending processing.

Results

(1) The present H_2 monitoring sites in California are shown in Fig. 1. Except for H2CY (Coyote Reservoir) the data are telemetered via phone links to Menlo Park, CA, or via the NOAA/NESS west geostationary satellite. The Coyote Reservoir site has an on-site recording system. All but one station along the San Andreas and Calaveras faults were non-functional during the winter and spring months of 1984 due to the P.I.'s health and staff relocation problems. They were restored to the operational status in June 1984.

(2) Three stations produced very noteworthy data in 1982 and 1983. The Cienega Winery site has recorded two major peaks, one in early November in 1982 and the other in early April 1983 (Fig. 2). Detailed examination of seismic records from July 1982 through December 1983 showed that the peaks appeared at times of very low seismic energy release within a radius of 50 km (Fig. 3). An increase in baseline and three minor peaks that appeared between May 3 and May 15, 1983, appear to be coseismic with the widespread aftershocks of the May 2 Coalinga earthquake. The spike-like pattern and aseismic nature of the large H_2 peaks require a tectonic mechanism which is abrupt but quiet; a combination of characteristics seemingly in contradiction.

Theoretical models were constructed on the basis of tensional opening of already-fractured fault zone due to outward stress exerted by the underlying ductile layer. The scenario assumes that the ductile layer is an ophiolitic crust -- an assumption supported by numerous serpentinite intrusions found along the faults. Penetration of groundwater through the fractured fault zone to the ophiolitic crust causes serpenitization of peridotites, a process which generates both H_2 and heat, forms magnetite, and causes a substantial volume expansion. The volume expansion at this depth would result in a tensional stress in the overlying brittle layer. Eventually the fault zone opens up aseismically. As soon as such a gap is created the H_2 accumulated during serpentinization would escape rapidly and be gone. Some serpentinites may even intrude plastically into the fault zone and lubricate the fault blocks. When such openings propagate laterally over some distance, an earthquake of a substantial magnitude may be triggered in the presence of lateral stress. Serpentinization can account for low electrical resistivity, attenuation of seismic velocity, high magnetic susceptibility, high heat flow, and aseismic bulging, observations that are often reported in the vicinity of a seismogenic fault.

Model calculations of relative H_2 concentrations expected to be observed at the Cienega Winery site for earthquakes within a radius of 50 km show that each of the two major H_2 peaks preceded an earthquake that scored a very high computed H_2 concentration values (manuscript in review).

(3) The H_2 data from July 1981 through 1983 are plotted for the Slack Canyon site (H2SC) in Fig. 4 and that for the Parkfield site (H2PK) in Fig. 5. We have not analyzed the details of correlation with seismicity for these sites, but the magnitudes of the anomalies recorded in the second half of 1982 and the first half of 1983 are very large. The highest H_2 concentration exceeded 0.1%. Because the changes are so drastic, we did not fully comprehend the nature of the anomalies until we made multi-year plots. Also only these two stations were operating on recirculating air-pump system to supply oxygen to the sensor, we did not fully trust the data until we replaced the pumps with oxygen cylinders and observed changes of comparable magnitudes at Parkfield in early July 1984. Seismicity in the vicinity of these sites during the high H_2 emission periods was low until the Coalinga earthquake shook the area. The patterns of the aftershocks suggest that incipient fractures probably extended to these sites over the distance of 35 km. There is a high possibility that the anomalous H_2 emissions that started more than one year prior to the Coalinga earthquake were related to the chain of tectonic events that eventually triggered the M6.5 earthquake. In this sense, the enormous H_2 anomalies at both Slack Canyon and Parkfield in late 1982 and early 1983 may be construed as precursory to the Coalinga earthquake. Model studies are impending at present.

(4) Multitudes of H_2 events were observed at the Casa Diablo site at Long Valley caldera from late 1982 through early 1984. The station was vandalized in March 1984, and we missed the data till May. The H_2 peaks often preceded an earthquake swarm under the resurgent dome area by a few to several days. Detailed analyses of the data are underway. The Laurel Spring site, which is located outside of the caldera, behaved differently. This site, which is on the Laurel Canyon fault, appears to be sensitive to events along the extension of the fault and two other adjacent parallel faults. We can not make multi-year plots of the data for these sites yet.

Reports

Sato M., McGee K. A., Sutton A. J., and Schultz S. S. (1982) Hydrogen monitoring along seismogenic faults. Abstract, EOS 63, 1043.

Sato M., McGee, K. A., Sutton A. J., and Casadevall, T. J. (1983) Continuous hydrogen monitoring for predicting earthquakes. Abstract, EOS 64, 758.

One manuscript is being reviewed.

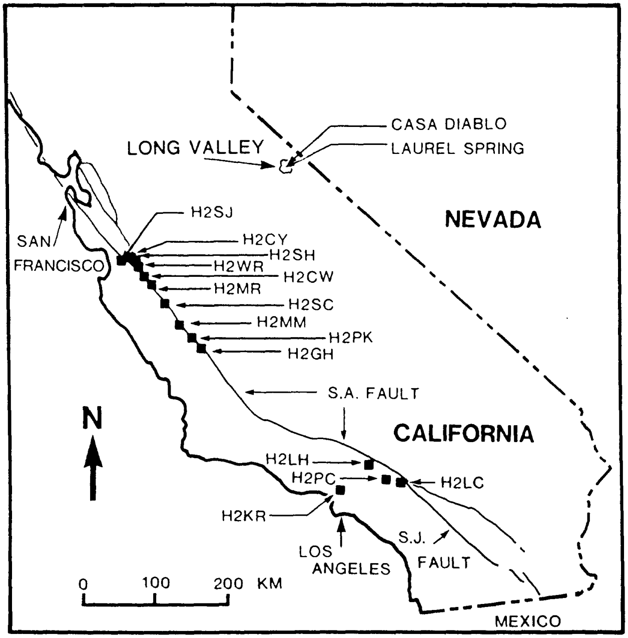

Fig. 1. A map showing current locations of hydrogen monitoring stations in central and southern California. Those in southern California are operated by the Kellog Radiation Laboratory of CIT as a part of their monitoring effort. The station codes are as follows: H2CY(Coyote Reservoir), H2SJ(San Juan Bautista), H2SH(Shore Road), H2WR(Wright Road), H2CW(Cienega Winery), H2MR(Melendy Ranch), H2SC(Slack Canyon), H2MM(Middle Mountain), H2PK(Parkfield), H2GH (Gold Hill), H2LH(Lake Hughs), H2PC(Pacoima Dam), H2KR(Kresge Observatory), H2LC(Lytle Creek).

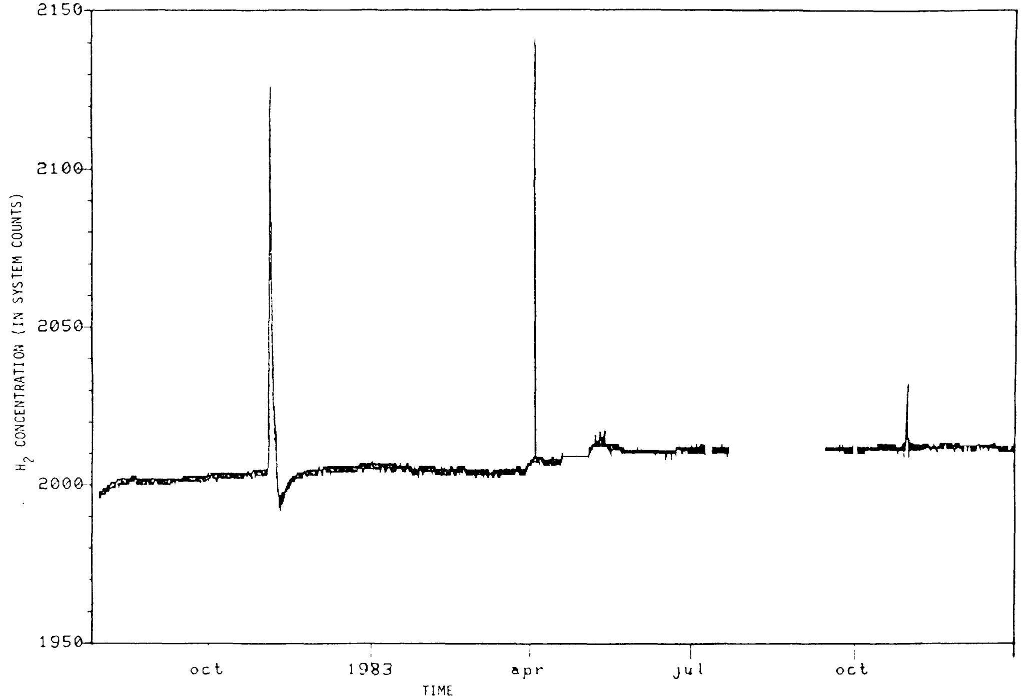

Fig. 2. H_2 emissions observed at the Cienega Winery site (H2CW) from July 30, 1982, through December 1983.

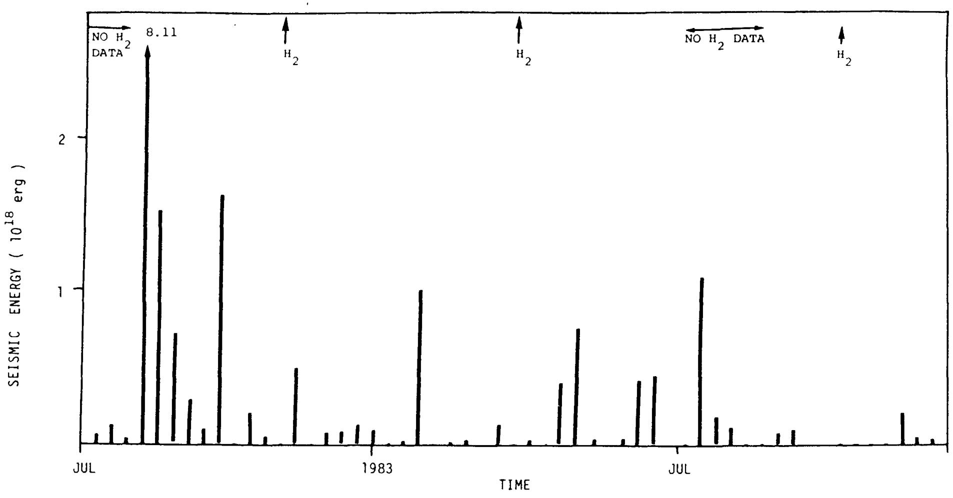

Fig. 3. Comparisons of H_2 events with seismic energy released within 50 km of Cienega Winery for each 10-day intervals between July 5, 1982, and December 31, 1983.

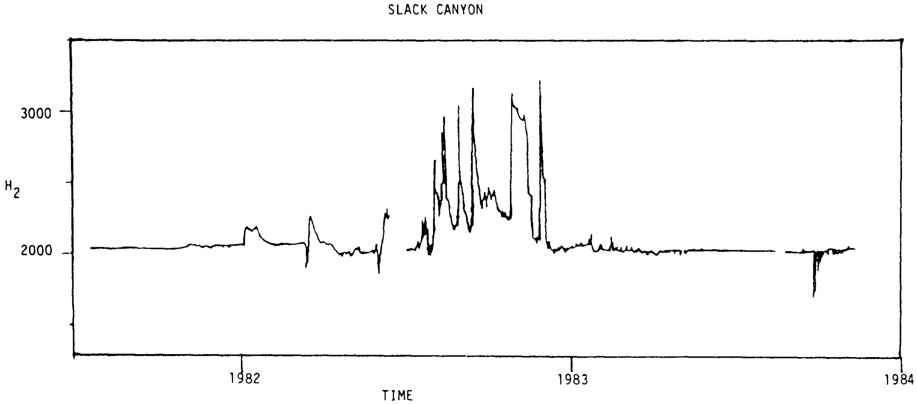

Fig. 4. Hydrogen emissions observed at the Slack Canyon site (H2SC) from July 1982 through November 1983.

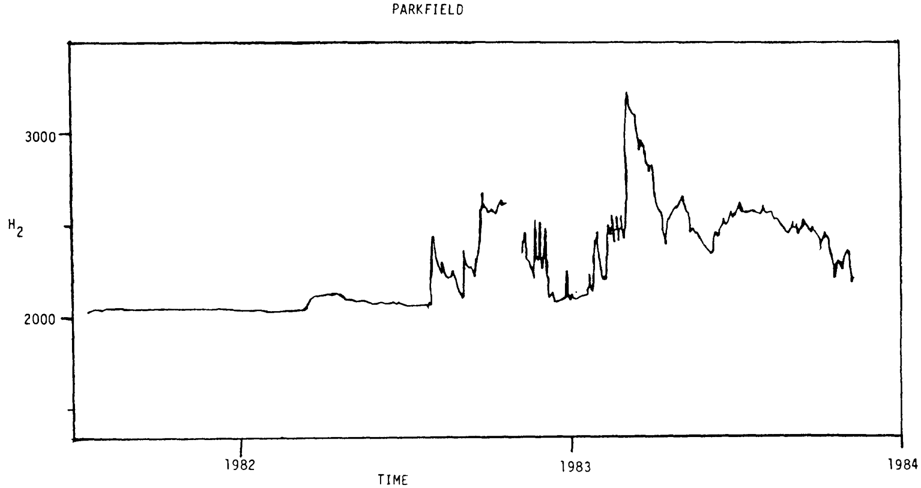

Fig. 5. Hydrogen emissions observed at the Parkfield site (H2PK) from July 1982 through November 1983.

Systems Analysis of Geologic Rate Processes

9980-02798

Herbert R. Shaw and Anne E. Gartner
Branch of Igneous and Geothermal Processes, U.S. Geological Survey
MS-910, 345 Middlefield Road, Menlo Park, CA 94025
(415) 323-8111, X4169, X4170

Investigations

The maximum moment model of Wesnousky and others (1983) implies that faults are activated over a characteristic length which is correlative with earthquakes of characteristic magnitudes and recurrence times. By comparison, Shaw and Gartner (1981a) showed that, in general, many possible combinations exist for partitioning of slip among subsets of individual faults of characteristic lengths in a branching system of faults with a hierarchy of lengths. This general relation is described by a nomogram that outlines possible combinations of segment lengths, numbers and recurrence times relative to coordinates of frequency and magnitude. End-member models in this diagram represent, on the one hand, b-value type trends and, on the other hand, maximum moment type trends. Hence, the Wesnousky and others (1983) maximum moment model represents one type of set in the Shaw and Gartner (1981) nomogram. In any general case of unconstrained fault motion (by observation or by model), a zigzag path of b-valuelike and maximum-momentlike intervals is likely. This is in agreement with the overall behavior described by Wesnousky and others (1982, 1983), by the compilation of Shaw and others (1981b) and with other published data.

Reports

Shaw, H. R., and A. E. Gartner, 1981a, Statistical data on faulting rates in the United States and deduced seismicity: Geological Society of America Abstracts with Programs, 13, p. 552.

Shaw, H. R., A. E. Gartner, and F. Lusso, 1981b, Statistical data for movements on young faults of the conterminous United States; paleoseismic implications and regional earthquake forecasting: U.S. Geological Survey Open File Report 81-946, 353 p.

Wesnousky, S. G., C. H. Scholz, and K. Shimazaki, 1982, Deformation of an island arc: Rates of moment release and crustal shortening in intraplate Japan determined from seismicity and Quaternary fault data: Journal of Geophysical Research, 87, p. 6829-6852.

Wesnousky, S. G., C. H. Scholz, K. Shimazaki, and T. Matsuda, 1983, Earthquake frequency distribution and the mechanics of faulting, Journal of Geophysical Research, 88, p. 9331-9340.

Consolidated Digital Recording and Analysis
9930-03412

Sam Stewart
Branch of Seismology
U.S. Geological Survey
345 Middlefield Road, M/S 977
Menlo Park, California 94025
(415) 323-8111 Ext. 2577

Investigations

The goal is to operate, on a routine and reliable basis, a computer-automated system that will detect and process earthquakes occurring within the USGS Central California Earthquake Network (also known as CALNET). Presently, the output from more than 450 short-period seismic stations is telemetered to a central recording point in Menlo Park, California. Two DEC PDP11/44 computers are used on this project. The 11/44A is dedicated to the task of online, realtime detection of earthquakes and storing the waveforms for later analysis. The 11/44B is used for offline processing and archiving of earthquakes. Both computers have a 512 channel analog-to-digital converter, so the 11/44B can serve as backup to the online system whenever necessary. The two computers can communicate with each other via a simple digital-bit I/O "semaphore" system, and can transfer large amounts of data via a dual-ported disk subsystem or a dual-ported magnetic tape subsystem.

Both computers use the RSX11M-PLUS (v2.1) operating system. Software has been developed largely by Carl Johnson in Pasadena, but with considerable modification by Peter Johnson, Bob Dollar and myself, to meet Menlo Park's specific needs. Our applications are all written in Fortran-77, but with heavy use of system functions unique to the RSX operating system.

Results

1. During the period April-September 1984 approximately 9200 earthquakes were processed through the CUSP system. This represents an annual rate of about 18400 earthquakes per year.

2. A detailed comparison of events detected by the realtime CUSP system and the "hand processed" develocorder film scanning system was made for the data from May 1984. The CUSP system missed 4.6 percent (i.e., 95) of the 2072 events, magnitude 1.3 or greater, that were listed in the "hand processed" event summary files. The missed events included (1) those in the Cape Mendocino area, where the telemetry lines are so noisy that the CUSP system usually is not monitoring stations in that region, (2) the Geysers area, where small events are so numerous that the CUSP detection thresholds are set high enough so that all events purposely are not recorded, (3) some quarry shots north of San Francisco Bay that are quite emergent and the station distribution is rather sparse, (4) some events from Coalinga that are very emergent and are seen on only a few, noisy stations.

3. Additional capability was added to the CUSP offline processing system. Specifically, digital tapes generated by digitizing analog earthquake recordings on the Eclipse digitizing system can be read directly into the CUSP system, and merged with the rest of the data. This was developed for the Shasta-Lassen networks in northern California. Routine processing of these Eclipse tapes started at the end of this report period.

4. An automatic bootstrap and complete startup sequence following restoration of power after a power outage has been implemented on both PDP 11/44 computers. Both computers will attempt to restart with the online detection system. The idea here is that, if the power outage damaged one computer, perhaps the other is still functioning.

5. The transfer of earthquake waveform data and other parameters from the online data disk to the offline data disk now occurs completely automatically. Using a simple digital-bit I/O "semaphore" system, the online computer notifies the offline computer that there is enough data to start the transfer. A data transfer takes about 15-30 minutes. The automatic transfer scheme permits the system to run unattended overnight or on weekends for example, and greatly reduces the possibility of filling up the online data disk completely. Depending upon seismic and noise activity, disk data transfers occur about 2-4 times per day. Of course, the earthquake detection and data storage process is not interrupted while the disk data transfer is going on.

6. A second high speed, triple density System Industries tape drive was added to the online 11/44A computer. These tape drives also serve as a backup, to "catch" online data in the event that earthquake or noise detections are occurring too rapidly for the online system to complete the processing of each detected event. Each tape drive is also dual ported, one to the offline 11/44B, the other to the Branch VAX-750.

Reports

None.

Great Earthquakes and Great Asperities, Southern California: A Program of Data Analysis

14-08-0001-G-948

L. R. Sykes and L. Seeber
Lamont-Doherty Geological Observatory of Columbia University
Palisades, New York 10964
(914) 359-2900

Investigations

Analysis of recent seismic activity along the San Andreas fault between San Bernadino and Desert Hot Springs and between Yucca Valley and the Salton Sea is being carried out. We are utilizing enhanced station coverage to look at the 3-dimensional configuration of seismicity. We are also mapping related groups of earthquakes as distinguished by their focal mechanisms. Space-time relationships over the last several years are being examined for distinguishable patterns and any changes in the overall level of activity.

In light of our results suggesting the widespread occurrence of block rotations in southern California, we are considering kinematic models to explore possible roles of block rotations in the long term evolution of the transform boundary in California as well as in the short term behavior of the right lateral transform system during interseismic periods between great earthquakes. The interaction between the rotation and the stress built up on the master fault is also being explored.

Results

1. Earthquake hypocenters and first-motion data from the CIT-USGS network reveals an unusual pattern of deformation along fault zones in southern California. Major strands of the San Andreas fault south of Cajon Pass are currently aseismic. Earthquakes shallower than 10-12 km exhibit left-lateral oblique strike-slip motion along short faults oriented northeasterly. This pattern, in conjunction with normal and reverse focal mechanisms, suggests rigid blocks undergoing contemporary clockwise rotation as a result of regional right-lateral shear. The presence of the rotating blocks presupposes a detachment surface at depth. In fact, the mechanisms of microearthquakes below ≈10 km are distinctly different. At greater depths, N-S shortening near San Gorgonio Pass is accommodated by a combination of strike-slip and shallow-angle thrust faults. Few earthquakes, however, can be directly related to slip on the detachment itself. Velocity structures determined from earthquake arrival times suggest a low-velocity zone at or above ≈10 km below the San Bernardino Mts., but not below the San Jacinto Mts. This low velocity is nearly at the same depth as the transition between the two layers of different kinematic behavior and suggests that the upper crust in the San Bernardino block is allochthonous. This model provides several new concepts for understanding the kinematic behavior and fault tectonics for southern California.

Shallow-angle structures like detachments need to be examined and, in the analysis of regional strain data, rotations must be considered. More importantly, the pattern of deformation presently observed during the interseismic period differs from the type expected from a large earthquake. Current seismicity cannot be then used to extrapolate the effects of a large event on the San Andreas. However, a systematic change in this pattern of predominantly left-lateral slip may signal an approaching failure and the occurrence of large right-lateral displacements.

2. Several major transcurrent faults in California exhibit significant offsets or side-steps at the surface. Accurate hypocentral locations of small earthquakes confirm that in many cases these offsets are continuous down to the deepest seismogenic depths, suggesting there is no real coalescing of the individual fault strands. These side-steps affect rupture propagation in large earthquakes and the time-space distribution of aftershocks. Right-stepping faults in a right-lateral system are commonly associated with pull-apart basins; however, an exception is Coyote Ridge between the right-step of the Coyote Creek and San Jacinto faults. We propose a block rotation model where the crustal wedge between the two parallel over-lapping en-echelon branches of the major bounding faults is deformed and rotated by a system of subparallel faults oriented nearly orthogonal to the major master faults. Clockwise rotation of the individual block slices can then accommodate right-lateral shear across the major NW-striking faults even when these master faults are locked. This model accounts for several geologic features associated with Coyote Ridge including the timing and ages of various faults, the uplift, the amounts of slip and the amounts of rotation involved. Other cases where this model may be applicable include Parkfield and the deformation associated with the Coyote Lake earthquake on the Calaveras fault.

3. Microearthquake activity along the southern San Andreas fault (SSAF) between the San Bernardino Mts. and the Salton Sea has been systematically located northeast of the easternmost mapped surface fault trace. That much of this seismicity orginates on the SSAF has been often taken for granted. The offset in earthquake epicenters has then been used to infer either an easterly dip to the SSAF itself, or a possible location bias resulting from strong lateral velocity inhomogeneities. Recent data, however, from newly installed stations close to the earthquake activity show that 1) the seismicity defines a zone 10-15 km in width; 2) the zone is sharply bounded to the SW by the SSAF; and 3) the epicenters align along a well defined system of short en echelon faults oriented northeasterly. Focal mechanisms of the larger events confirm that the motion along these northeasterly planes is left-lateral. These results suggest that the SSAF is currently aseismic and that the present activity is in fact occurring on a set of secondary structures oriented nearly orthogonal to the major fault strands. Geomorphology of the SSAF surface traces indicates that significant right-lateral movement occurs repeatedly only within a narrowly defined fault zone. This suggests a bimodal distribution of deformation where "interseismic" activity takes place on secondary structures, but major right-lateral slip occurs along the mapped surface faults. This implies that earlier interpretations of earthquake

activity along the SSAF may need to be revised, and that the role of the magnitude 6.5 Desert Hot Springs earthquake of 1948 may need to be re-examined.

Reports

Nicholson, C., L. Seeber, P. Williams, and L. R. Sykes, A new paradigm for understanding southern San Andreas fault tectonics, EOS, v. 65, 1984.

Seeber, L., C. Nicholson, P. Williams, and L. R. Sykes, Block rotations and discontinuous faults: Solving the problem of slip continuity with examples from southern California, EOS, v. 65, 1984.

Sykes, L. R., and S. Nishenko, Probabilities of occurrence of large plate rupturing earthquakes for the San Andreas, San Jacinto and Imperial Faults, California, Journal of Geophysical Research, v. 89, pp. 5905-5927, 1984.

Williams, P., C. Nicholson, L. Seeber, and L. R. Sykes, Seismicity of the southern San Andras fault, California, EOS, v. 65, 1984.

Analysis of Seismic Data from the Shumagin Seismic Gap, Alaska

USGS-14-08-0001-G-946

John Taber and Klaus Jacob
Lamont-Doherty Geological Observatory of Columbia University
Palisades, New York 10964
(914) 359-2900

Investigations

Digitally recorded seismic data from the Shumagin seismic gap in the eastern Aleutian arc, Alaska, are analyzed for detecting space-time variations in seismicity, focal mechanisms, and of dynamic faulting parameters that could be precursory to a major earthquake expected in this seismic gap. The seismic results obtained from the network data are being integrated with crustal deformation data that are independently collected, with volcanicity data of nearby Aleutian volcanoes, and with teleseismic information, to identify basic tectonic processes which may be potentially precursory to a great earthquake.

Results

1. Analysis of an earthquake sequence. Two moderate events (M_s=6.3 and 5.6) occurred within a five-hour period just outside the Shumagin network on February 14, 1983. Thirteen additional events associated with the sequence and ranging from M_l=2.5-4.0 where recorded digitally and located. The focal mechanisms of the two events show similar nodal planes with P axes in the approximate direction of plate convergence and near-vertical T axes (Figure 1) but their aftershock zones do not appear to overlap. The depth of both main events was well constrained at 26 km by teleseismic body wave modelling. The aftershock zones were not sufficiently constrained to determine the slip plane but the thrust plane along the subducting plate boundary is the preferred plane.

There do not appear to be any foreshocks before the first main event but there were 3 small events that occurred before the second main event and north of the cluster of aftershocks around the first event (Figure 2). These three events have a higher frequency content than aftershocks in the same region (Figure 3). Thus a change in frequency may be a useful precursory phenomena in the Shumagin region.

From two strong-motion records it appears that the first earthquake was a complex event rupturing towards the northeast for about 10 seconds with an initial dynamic stress drop of 80 bars and a moment of 2.4×10^{25} dyne-cm. The second earthquake has a dynamic stress drop of 70 bars and a moment of 1.0×10^{25} dyne-cm. These stress drops are in contrast to the high values (650-890 bars) calculated by House and Boatwright (1980) for two events near the base of the main thrust zone. A possible interpretation is that stress increases with depth in the main thrust zone and that large or great earthquakes would be expected to initiate in the high-stress region.

2. The Shumagin network monitors seismicity and tremor at Pavlof Volcano, the dominant active volcano in the Shumagin seismic gap. Eruptions of Pavlof are periodic and correlate with annual variations in sea-level unless disturbed, as in 1978 to 1980, by a major aseismic slip event which caused a net volume increase (dilatation) in the crust and upper-mantle root zone of the volcano; during this time no eruption occurred. The volume of lava that erupted before and afterwards is estimated to be time-predictable and is apparently modulated by external strain events (tectonic, oceanographic, or precursory). Therefore, Pavlof may be considered a useful volume strainmeter for earthquake prediction purposes. The main task lies to establish false-alarm rates and causative relations to stress/strain changes in the seismogenic zone (main thrust).

References

House, L., and J. Boatwright, Investigation of two high-stress drop earthquakes in the Shumagin seismic gap, Alaska, J. Geophys. Res., 85, 7151-7165, 1980.

Reports and Presentations

Hauksson, E., J. Armbruster, and S. Dobbs, Seismicity patterns (1963-1983) as stress indicators in the Shumagin seismic gap, Alaska (abstract), Earthquake Notes 55, 16, 1984.

Jacob, K. H., Estimates of long-term probabilities for future great earthquakes in the Aleutians, Geophys. Res. Lett., 11, 295-298, 1984.

McNutt, S. R., Eruption characteristics, cycles, and the state of stress at Pavlov volcano, eastern Aleutians, as inferred from seismicity (abstract), Earthquake Notes, 55, 12, 1984.

Taber, J. J., J. Mori, and J. Beavan, February 14, 1983 earthquake sequence in the Shumagin seismic gap, Alaska (abstract), EOS, 16, 241, 1984.

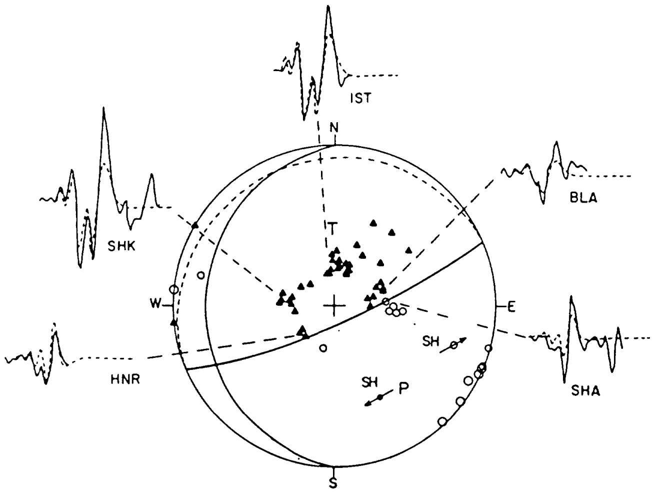

02/14/84 03:20 DEPTH 26 $M_s = 6.3$

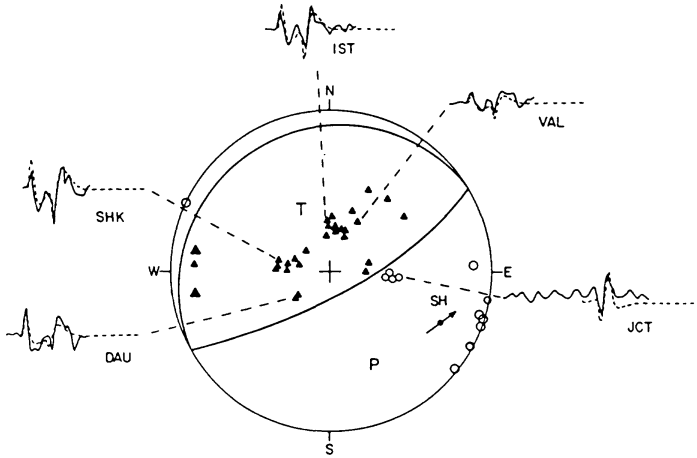

02/14/84 08:09 DEPTH 26 $M_s = 5.6$

EQUAL AREA LOWER HEMISPHERE

▲=COMPRESSION O=DILATATION

Figure 1. Lower-hemisphere focal mechanisms for the two main events during the February 14, 1983 earthquake sequence. Solid fault planes from both teleseismic and local first motions and SH polarizations from strong-motion accelerometers. Dotted fault plane (shown where different from solid fault plane) from the long-period teleseismic body wave modelling shown around the outside of focal mechanism. The 60-seconds long synthetic trace is superimposed on the data from each station.

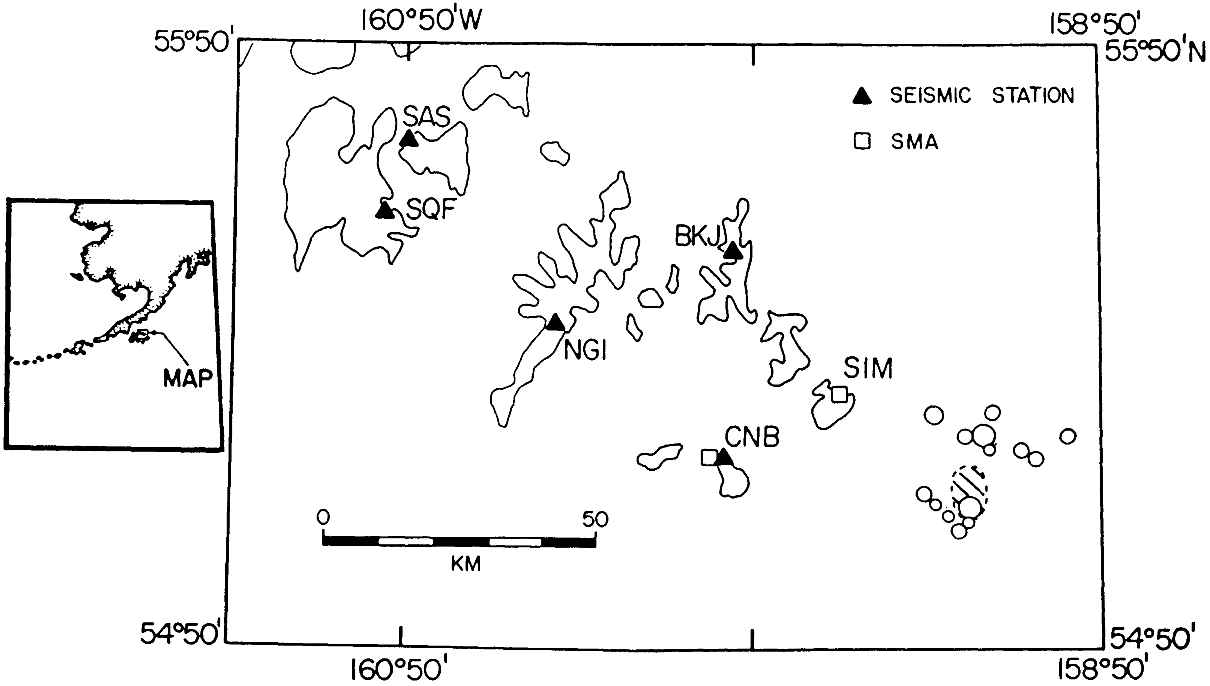

Figure 2. Location map for earthquake sequences. Shaded area around first main event is the inferred rupture area. The rupture area of the second main event (north of the first main event) is no larger than the epicenter circle. The aftershocks are not well located though it does appear that the north and south groups form separate zones. SMA = strong-motion accelerometer site.

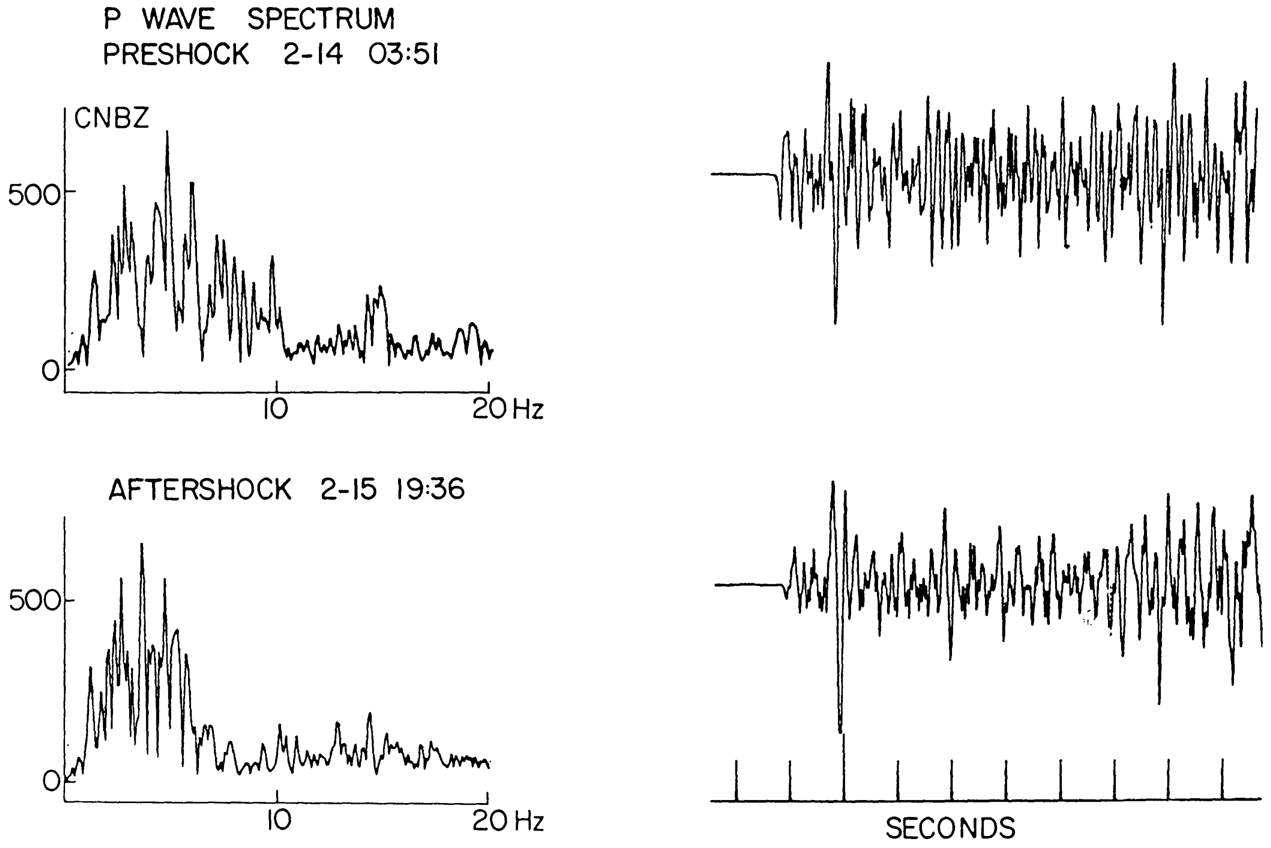

Figure 3. Short-period waveforms and spectra of a foreshock and aftershock of the second main event. Note that while the frequency content is different, the same phases are seen on both records, suggesting that the events had nearly the same locations.

National Earthquake Catalog

9920-02648

J. N. Taggart
Branch of Global Seismology and Geomagnetism
U.S. Geological Survey
Denver Federal Center, MS 967
Denver, Colorado 80225
(303) 236-1506

Investigations

1. Completed an annotated bibliography of technical references to large California earthquakes, 1900-present.

2. Developed a character string database format, which includes all parameters from local network and standard teleseismic hypocenter computations.

3. Completed several codes for input to and output from the new character-string database.

4. Assembled a trial catalog of large Alaskan earthquakes, 1786-1982.

Results

1. Karen Meagher completed an annotated bibliography of technical references to large ($M \geq 5$) California earthquakes, 1900-present, with cross references to authors. The bibliography will be useful for identifying uncertainties in reported parameters for some historically important earthquakes.

2. Taggart expanded the character string database format from 188 to 300 characters to include all parameters routinely published in local network and teleseismic hypocenter determinations. An important advantage of character representation of parameters is that all data can be stored with the originally published precisions. Data can be selected and written out with operating system software much faster from the expanded character record than from a previous developed 120-byte numerical record, which requires extensive decoding in order to recover the published precisions.

3. Taggart completed several codes for interfacing with the expanded character string database. Input codes convert the original database format and three local network data formats into the expanded format of the new database. All unused parameters in the new database are padded with blanks. An extensive output code provides data in any of several formats for events identified by sets of independent selection criteria.

4. From the Alaska database Carol Thomasson and Taggart assembled a trial catalog of 2290 earthquakes with magnitudes $\geq$ 5.5 and/or M.M. intensities ≥ 5. The listing also contains many large earthquakes that occurred between 1904 and 1963 for which values of magnitude and intensity are unavailable.

Development of General Earthquake Observation System

9910-03009

John Van Schaack

Branch of Engineering Seismology and Geology
U.S. Geological Survey
345 Middlefield Rd. MS 977
Menlo Park, California 94025
(415) 323-8111, ext. 2584

Investigations

The objectives of this program are to complete the assembly, testing, and documentation of the General Earthquake Observation System (GEOS). Approximately thirty of the systems have been assembled and partially tested. Twenty systems are being deployed on a regular basis for evaluation of all operating parameters. Tests are being conducted to locate the sources of system noise and to reduce the noise while recording. Tests were also run to determine and isolate the cause of sporadic tape drive misbehavior.

Results

The tests run to date indicate that it is possible to reduce the total system noise in the band .1Hz to 50Hz to about .5 microvolt peak to peak referred to the input at 60db gain. This test was run with separate power for the analog section of the system. The problems with the tape drive have been identified and are being corrected in hardware and software.

Reports

None.

Field Experiment Operations

9930-01170

John Van Schaack
Branch of Seismology
U. S. Geological Survey
345 Middlefield Road MS/77
Menlo Park, California 94025
(415) 323-8111, ext. 2584

Investigations

This project performs a broad range of management, maintenance, field operation, and record keeping tasks in support of seismology and tectonophysics networks and field experiments. Seismic field systems that it maintains in a state of readiness and deploys and operates in the field (in cooperation with user projects) include:

a. 5-day recorder portable seismic systems.
b. Smoked paper-recorder portable seismic systems.
c. "Cassette" seismic refraction trucks.
d. Portable digital event recorders.

This project is responsible for obtaining the required permits from private landowners and public agencies for installation and operation of network sensors and for the conduct of a variety of field experiments including seismic refraction profiling aftershock recording, teleseism P-delay studies, volcano monitoring, etc.

This project also has the responsibility for managing all radio telemetry frequency authorizations for the Office of Earthquakes, Volcanoes and Engineering and its contractors.

Results

Seismic Refraction

120 seismic cassette recorders were used in 5 separate experiments to gather deep crustal velocity and structural data. Preliminary analysis and record sections were produced in the field. In each deployment all 120 instruments are used. The following projects were carried out:

1. Sutter Buttes. May. The Sacramento Valley, one deployment. Four shotpoints were detonated.
2. TACT. June, July. The Alaskan Refraction Study. Four deployments, one by helicopter, with five lake shots, were made. Thirty shots were fired.
3. Hanford, Wash. Two deployments were made in southeastern Washington in mid-August. Eight shotpoints were fired.
4. Newberry Crater. The last week in August all 120 instruments were deployed around the crater area by truck, back-pack and horse train. Nine shotpoints of 6000 pounds each, and 3 of 500 pounds each were fired.
5. Maine. Two of eight deployments were completed during the last week of Sept. The project will continue through Oct.

Telemetry Networks

The network in Yellowstone was reconditioned during the summer and is now in operation.

Micro-wave telemetry systems have been installed between Mt. Tamalpais and Parkfield and are being tested. Signals are received in Menlo Park.

Portable Networks

Fifteen 5-day recorders have been operating in the Mammoth Lakes area all summer primarily collecting P-delay data; however, the local seismicity is being digitized and used with the data collected by the telemetry net.

Exploiting the Precision Inherent in NAVSTAR/GPS Geodetic Measurements

14-08-000121378

Randolph H. Ware

Cooperative Institute for Research in Environmental Sciences
University of Colorado, Box 449
Boulder, CO 80309
(303) 492-8028

Investigations. It has been predicted that corrections based on water vapor radiometer (WVR) observations will be required to attain relative positioning accuracy routinely on the order of a centimeter over 100-km baselines using the NAVSTAR Global Positioning System (GPS) [1,2]. Such corrections account for the refractive phase delay of satellite radio signals by tropospheric water vapor. Dual-frequency GPS receivers to correct for ionospheric refraction effects will also be required to attain centimeter accuracy [1,2].

We have carried out GPS baseline measurements during which simultaneous WVR observations along the line-of-sight to NAVSTAR satellites were obtained. A single-wavelength GPS receiver (Macrometer) and a WVR (developed by NOAA) were operated at each end of a 22-km baseline near Boulder, Colorado, on three consecutive evenings in July 1983. The WVR's were pointed toward each satellite sequentially at 15-minute intervals during GPS data acquisition. The baseline vector was calculated using single, double and triple difference processing of the GPS receiver data. Corrections for tropospheric water vapor were based on a model or on WVR data. Improvements in the repeatability of the baseline vector components are found when WVR corrections are applied, and the vertical, east-west, and north-south components are systematically shortened.

Instrumentation. Two single-frequency GPS receivers (Macrometers) operated by the National Geodetic Survey (NGS) [3,4] and two dual-frequency water vapor radiometers developed and built by the National Oceanic and Atmospheric Administration (NOAA) [5] were operated simultaneously at both ends of a 22-km baseline located near Boulder, Colorado. Survey marks were placed at both sites in June 1983 by the NGS.

Five NAVSTAR satellites were observed during three hours starting at about 17:30 local time for three consecutive evenings in July 1983. Ephemeris data were provided for each three minute epoch by NGS, allowing the Macrometer to compute the Doppler frequency and track each satellite. Also, the radiometers were pointed using the NGS ephemerides. Each of the WVR's, which are normally used for meteorological studies, occupies a small portion of a forty-foot trailer van. They were located close to each GPS receiver, and were pointed toward each satellite every fifteen minutes. This allowed two minutes to change the pointing and one minute of observation for each of the five satellites.

Data Processing and Results. Baseline coordinates were calculated using software developed by the NGS. For tropospheric correction, we used either a model or WVR data. In the modeling approach, phase corrections to the receiver data were calculated from the Saastamoinen/Hopfield atmospheric model [8,9]. This calculation uses the surface temperature, pressure, and relative humidity at the receiver locations, and depends on the elevation angles of the satellites. The model cannot correct for any azimuthal variation in water vapor, or any unusual vertical distribution, such as temperature or humidity inversions. Using WVR data, the tropospheric phase corrections were calculated by multiplying the measured integrated water vapor along the line-of-sight to each satellite by a factor of 6.5 [7], and dividing by the wavelength of the GPS carrier signal.

The excess path errors resulting from water vapor between the sites and the satellites are shown for the three evenings of measurements in Figures 1-3. Spline fits which were used to estimate excess paths during the 15-minute intervals between WVR observations of each satellite are shown. The general sloping curvature seen in Figures 1-3 is caused by the change of observed water vapor with elevation angle and azimuth as the satellites track across the sky at 30 degrees per hour. The short term variations or "bumps" are the signatures of local thunderstorms that were present during the three evenings of observations. Included in Figures 1-3 are the differences in excess path between the Boulder and Erie sites. On day 198, the excess path observed from Boulder is initially larger than the excess path observed from Erie, and then it crosses over and becomes smaller than Erie. In spite of this variability observed by WVR's, surface measurements of humidity at the two sites by the NGS showed differences of less than a few per cent during the same period.

Tables 1-3 list the results of baseline calculations using the single, double and triple difference processing techniques (SD, DD and TD). The baseline components differ by up to 8 cm depending on the processing technique. This difference may result, in part, from the use of a different datum for DD processing (NAD1927) and SD or TD processing (WGS72). Both the DD and the TD use Gram-Schmidt orthonormalization to avoid correlation to a reference satellite [6].

The mean and rms of the baseline length and components over the three observing days are listed in Tables 1-3 and are also shown in Figures 4-7. Here, the rms is a measure of the repeatability over the three days of observations. Three sets of processed data were analyzed for each day including: (1) the total set of all receiver data corrected using the Saastamoinen/Hopfield model, (2) the subset of receiver data for which WVR data were available, corrected using the Saastamoinen/Hopfield model, (3) the same subset corrected using WVR measurements.

Tables 1-3 also list the total number of data points available versus the points used. The total of points available was determined by the number of epochs when measurements were taken times the number of satellites that were received at each of these epochs and also by the processing technique that was used. Fewer data points are available for DD processing than for SD because the difference between two SD's (for 2 satellites at one epoch) gives only one DD data point. Similarly fewer data points enter the TD algorithm than the DD program. All three programs are allowed to discard 'bad' data that occur outside of a credible window. Thus the number of points used can differ from one program to the other, even if the number of available points is the same. These numbers are listed to reveal the size and quality of the data sets. For a sampling rate of one measurement every 3 minutes a 'good' 3-hour GPS survey session aquires about 300 data points. As seen in Tables 1-3 between 113 and 247 data points were acquired for each session. The subsets with WVR data include a smaller number of points. The rms of the fit, also listed in Tables 1-3, is a measure of how well the model for the least square solution of the baseline agrees with the phase data.

A comparison of the net effect of WVR correction, regardless of the processing technique used, is seen in the differences between the corrected and uncorrected baseline lengths and components listed in Table 4. The baseline length is shortened by 10 cm, the vertical component by 3 cm, east-west by 10 cm, and north-south by 0.3 cm. This shortening depends only slightly on the processing technique, as shown by the rms values of less than 1 cm.

Conclusions. These results demonstrate that errors in GPS baseline determinations resulting from refraction in the wet troposphere can be present at the several parts per million level. The observations were carried out during disturbed weather conditions and may represent worst-case variability of atmospheric water vapor. Surface measurements appear to be unable to correct adequately for the observed variability in water vapor with respect to azimuth and elevation. However, WVR measurements of line-of-sight water vapor were able to improve baseline repeatability. We caution that only three baseline measurements with less than optimal data sets were used in this analysis.

Although GPS baselines can be averaged over a number of observing sessions to reduce tropospheric and ionospheric refraction errors, it appears that consistent centimeter accuracy from several-hour observing sessions in a variety of weather conditions will require the use of two receiver frequencies and line-of-sight WVR's. The WVR-corrected baseline measurements have a repeatability of 1 ppm, which is consistent with published results of GPS baselines measured during fairly calm weather conditions without WVR corrections [3].

References.

[1] Spilker, J. J., Jr., GPS signal structure and performance characteristics, Nav. 25,, 121-146, 1978.

[2] Bossler, J. D., C. C. Goad, and P. L. Bender, Using the Global Positioning System (GPS) for geodetic surveying, Bull. Geod., 553-563, 1980.

[3] Goad, C. C., and B. W. Remondi, Initial relative positioning results using the Global Positioning System, Bull. Geod., 58, 193-210, 1984.

[4] Counselman III, C. C., and D. H. Steinbrecher, The Macrometer: a compact radio interferometry terminal for geodesy with GPS, in Proc. Third International Geodetic Symposium on Satellite Doppler Positioning, Vol. 2, Physical Sciences Lab, New Mexico State Univ., 1165-1172, 1982.

[5] Hogg, D. C., F. O. Guiraud, J. B. Snider, M. T. Decker and E. R. Westwater, A steerable dual-channel microwave radiometer for measurement of water vapor in the troposphere, J. App. Meteorol. 22,, 789-806, 1983.

[6] Remondi, B. W., Using the Global Positioning System (GPS) phase observable for relative geodesy: modeling, processing, and results, Ph.D. Thesis, University of Texas at Austin, 1984.

[7] Hogg, D. C., F. O. Guiraud and M. T. Decker, Measurement of excess radio transmission length on Earth-space paths, Astron. Astrophys. 95, 304-307, 1981.

[8] Goad C.C., Wallops Island Tropospheric refraction study and analysis, Prepared for H.R.Stanley Geos-C Project Scientist NASA/Wallops Station Contract No. NAS 6-2173, 1974.

[9] Saastamoinen, J., Contributions to the theory of atmospheric refraction, Bull. Geod., 105, 279-298, 106, 383-397, 107, 13-34, 1972.

Table 1. Single Difference Processing

data set and corrections	Julian day	#of points: total/used	rms of fit (cm)	baseline (cm)			
				length= 22,035m+	vertical= 11m+	EW= 21,979m+	NS= 2058m+
all receiver data, no WVR corrections	198	113/113	0.6	79.6	32.9	62.5	36.9
	199	224/224	1.1	83.4	40.6	66.8	35.8
	200	247/210	1.1	79.4	38.9	62.5	33.6
			mean:	80.8	37.5	63.9	35.4
			rms:	2.3	3.3	2.4	1.7
subset having receiver and WVR data, no corrections	198	103/103	0.6	80.6	31.5	63.3	36.9
	199	133/133	0.9	97.1	41.0	80.4	34.7
	200	237/201	1.1	81.2	39.6	64.2	33.6
			mean:	86.3	37.4	69.3	35.0
			rms:	9.4	4.2	9.6	1.7
subset having receiver and WVR data, with corrections	198	103/103	0.5	72.1	36.6	54.8	34.7
	199	133/133	1.0	80.8	32.0	64.2	34.7
	200	237/199	1.0	76.3	33.4	59.9	33.6
			mean:	76.4	34.0	59.6	34.3
			rms:	4.4	1.9	4.7	0.6

Table 2. Double Difference Processing

data set and corrections	Julian day	#of points: total/used	rms of fit (cm)	baseline (cm)			
				length= 22,035m+	vertical= 11m+	EW= 21,979m+	NS= 2058m+
all receiver data, no WVR corrections	198	84/84	1.1	87.6	38.1	69.4	45.6
	199	172/172	1.6	86.4	45.9	68.5	42.3
	200	161/161	1.7	82.6	44.3	65.1	41.2
			mean:	85.6	42.8	67.7	43.0
			rms:	2.6	3.4	2.3	2.3
subset having receiver and WVR data, with corrections	198	76/76	1.0	87.9	36.4	69.4	45.6
	199	100/100	1.3	96.1	46.3	78.8	41.2
	200	154/154	1.7	84.1	44.7	66.0	41.2
			mean:	89.4	42.5	71.4	42.7
			rms:	6.2	4.3	6.6	2.6
subset having receiver and WVR data, with corrections	198	76/76	0.9	78.8	40.9	60.8	44.5
	199	100/98	1.3	80.0	37.9	61.7	42.3
	200	154/151	1.6	81.7	38.6	64.2	41.2
			mean:	80.2	39.0	62.3	42.6
			rms:	1.5	1.4	1.8	1.7

Table 3. Triple Difference Processing

data set and corrections	Julian day	#of points: total/used	rms of fit (cm)	baseline (cm) length= 22,035m+	vertical= 11m+	EW= 21,979m+	NS= 2058m+
all receiver data, no WVR corrections	198	79/79	0.9	81.4	31.7	64.2	36.9
	199	167/167	1.5	83.5	40.6	66.8	35.8
	200	183/157	1.4	80.6	36.1	63.3	34.7
			mean:	81.8	36.1	64.8	35.8
			rms:	1.5	3.6	1.8	1.1
subset having receiver and WVR data, no corrections	198	73/73	0.9	80.7	31.3	63.3	36.9
	199	96/95	1.2	89.6	40.3	72.7	33.6
	200	176/151	1.4	82.6	36.7	65.9	34.7
			mean:	84.3	36.1	67.3	35.0
			rms:	4.7	3.7	4.9	1.7
subset having receiver and WVR data, with corrections	198	73/73	0.9	72.1	36.3	54.8	34.7
	199	96/95	1.2	70.4	31.1	53.9	34.6
	200	176/150	1.4	72.8	32.7	55.7	35.5
			mean:	71.8	33.4	54.8	35.0
			rms:	1.3	2.2	0.9	0.5

Table 4. Reduction in baseline length and components (mean of 3 days) resulting from WVR corrections for single, double, and triple difference processing.

		l-l(wvr)	z-z(wvr)	x-x(wvr)	y-y(wvr)
single difference:		9.9cm	3.4cm	9.7cm	0.7cm
double difference:		9.2	3.5	9.1	0.1
triple difference:		12.5	2.7	12.5	0.0
	mean:	10.5	3.2	10.4	0.3
	rms:	0.8	0.2	0.9	0.2

P-1

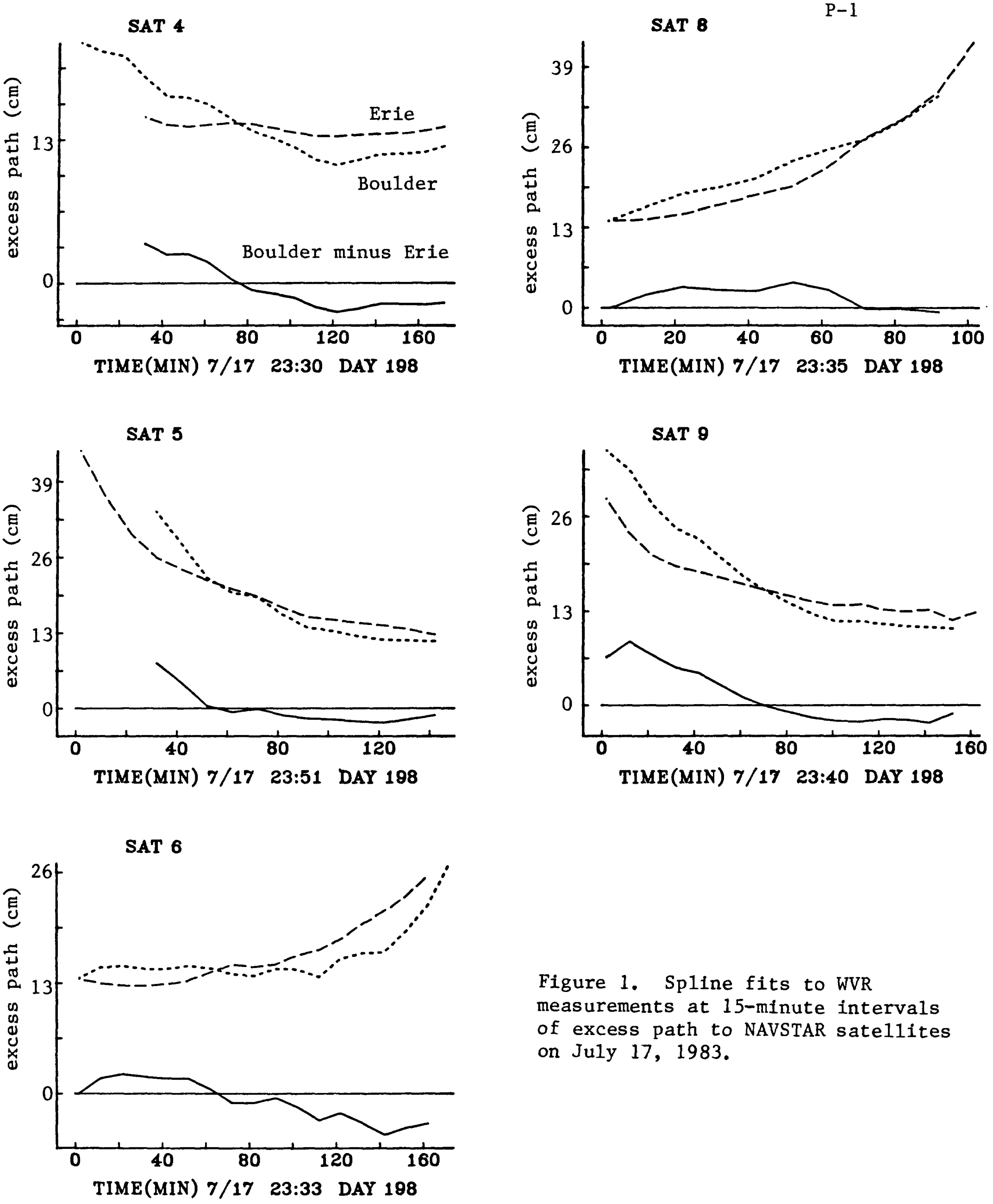

Figure 1. Spline fits to WVR measurements at 15-minute intervals of excess path to NAVSTAR satellites on July 17, 1983.

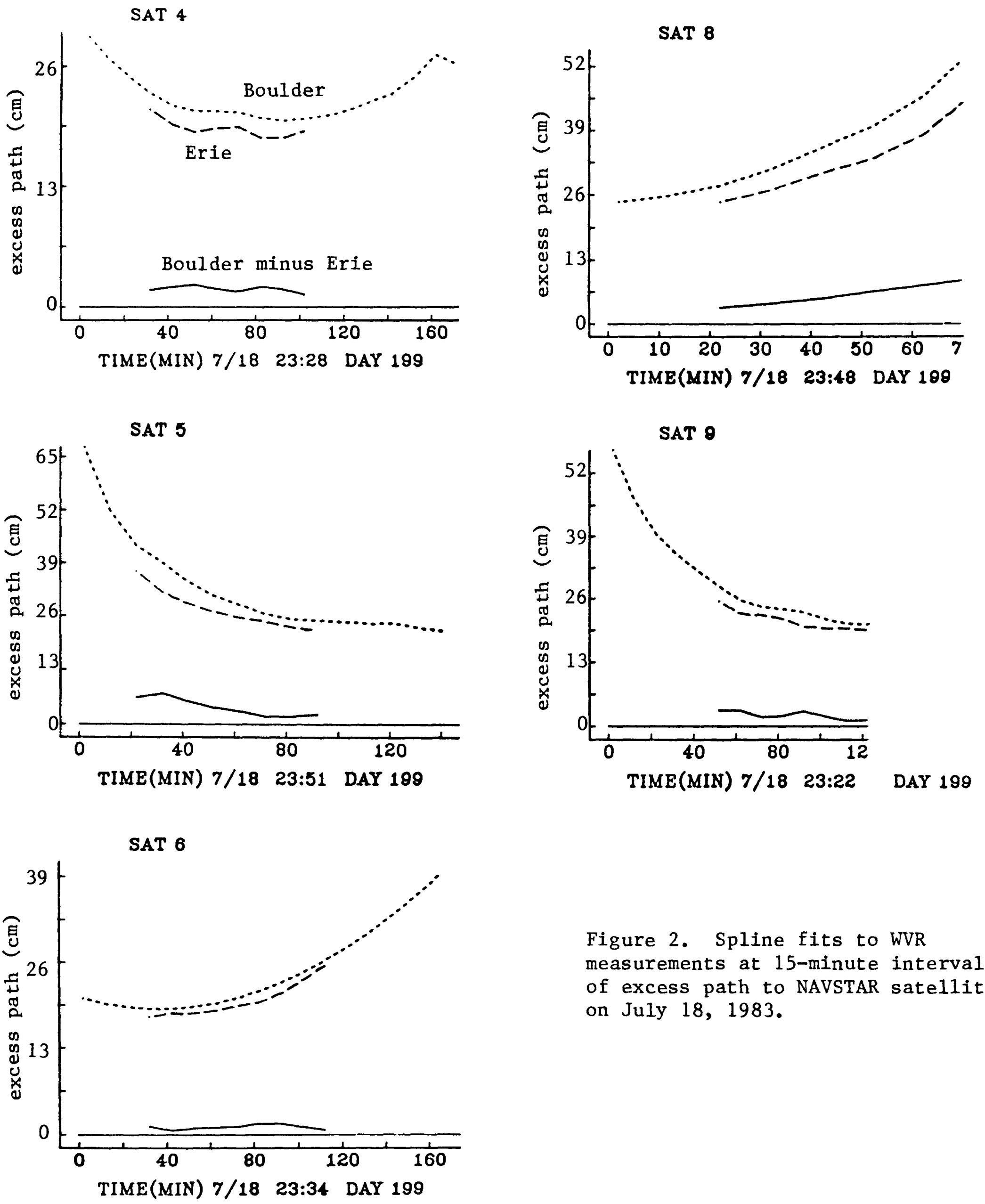

Figure 2. Spline fits to WVR measurements at 15-minute intervals of excess path to NAVSTAR satellites on July 18, 1983.

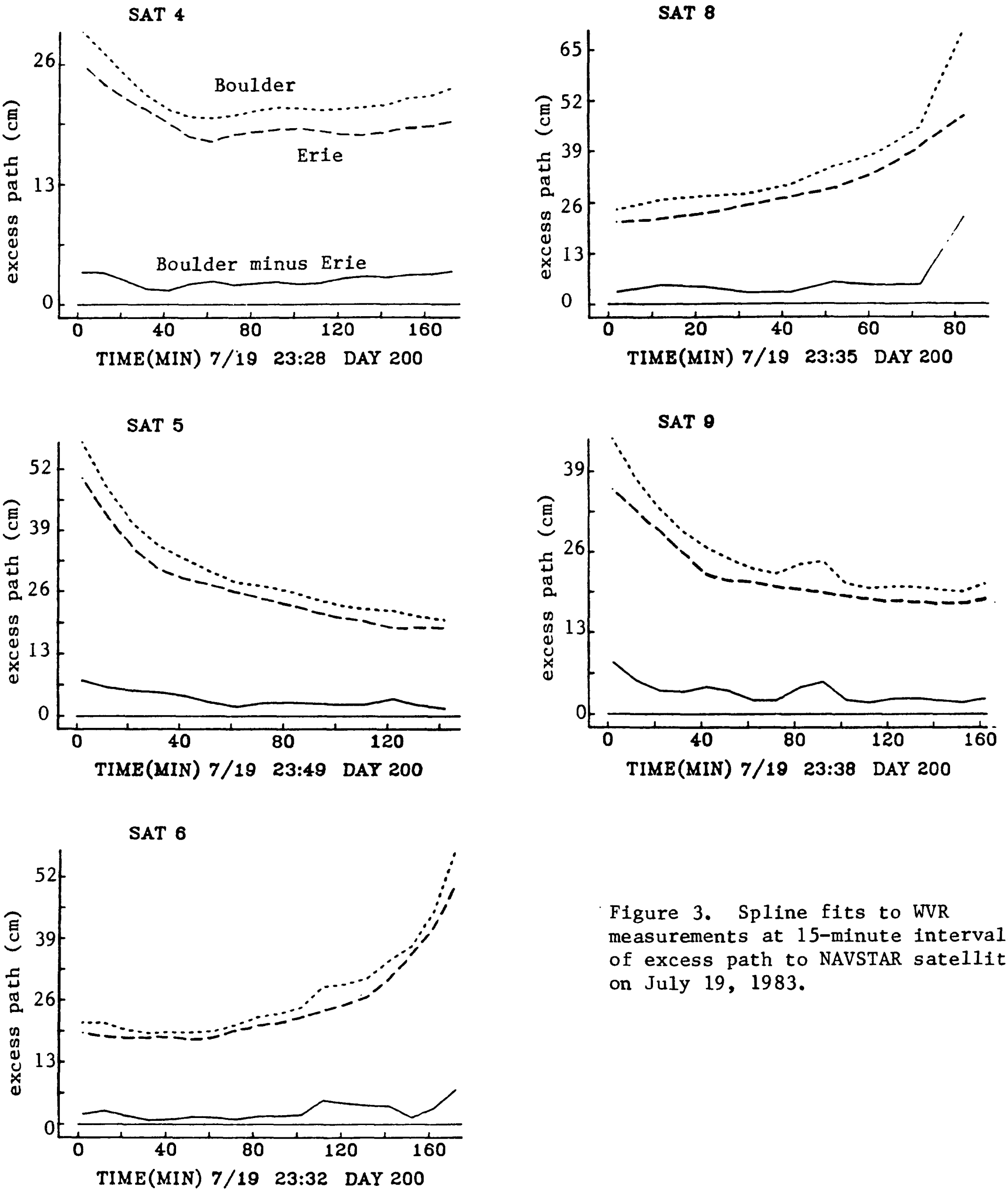

Figure 3. Spline fits to WVR measurements at 15-minute intervals of excess path to NAVSTAR satellites on July 19, 1983.

Figure 4.

GPS baseline vector repeatability with and without water vapor correction, single difference computation with single wavelength Macrometer, ▨ **with WVR** ░ **without WVR**

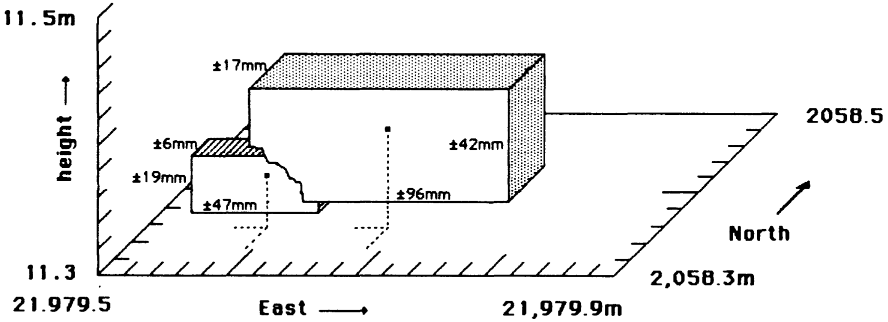

Figure 5.

GPS baseline vector repeatability with and without water vapor correction, double difference computation with single wavelength Macrometer, ▨ **with WVR** ░ **without WVR**

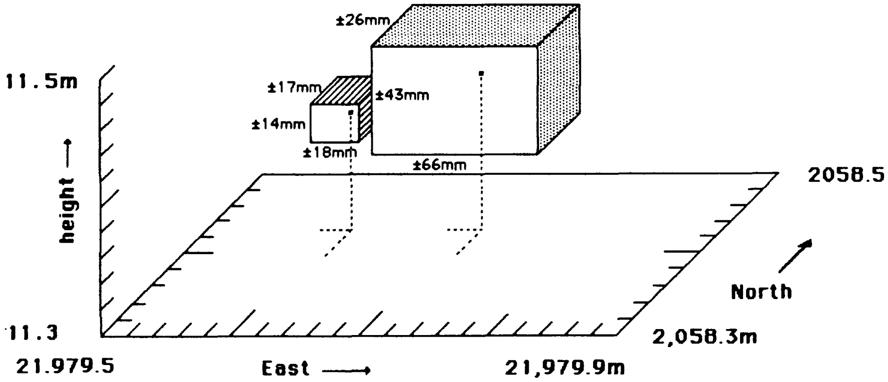

Figure 6.

GPS baseline vector repeatability with and without water vapor correction, triple difference computation with single wavelength Macrometer, ▨ **with WVR** ▩ **without WVR**

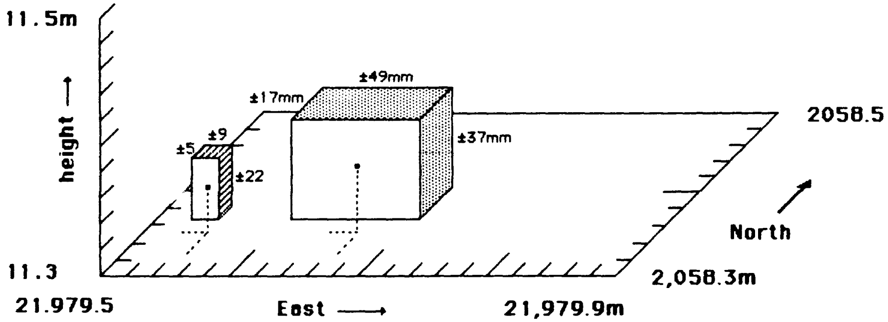

Figure 7.

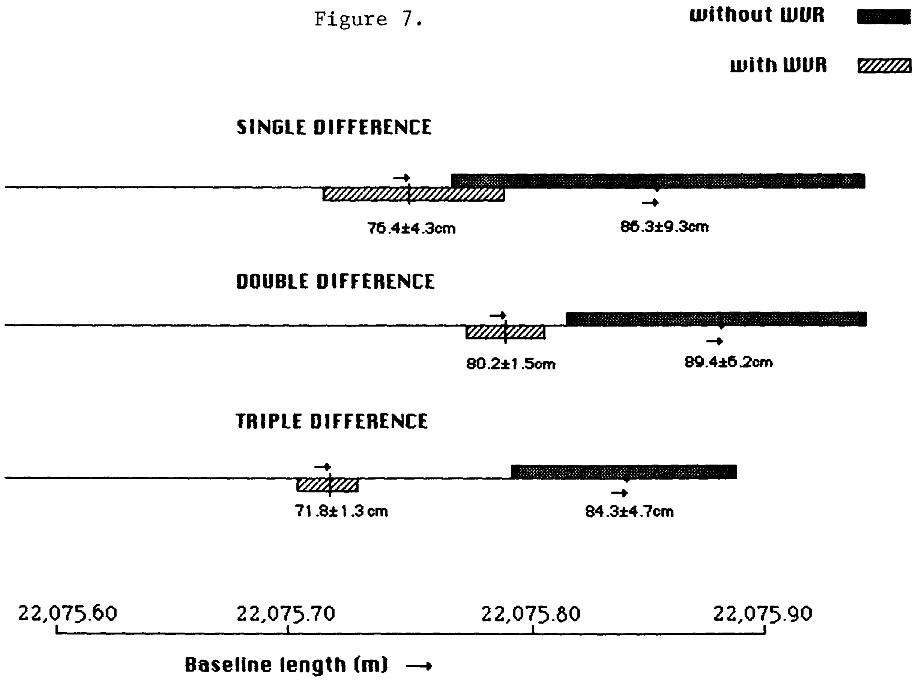

Seismicity and Structure of the San Pablo Bay-Suisin Bay Seismic Gap from Calnet and Explosion Data

9930-02938

David H. Warren
Branch of Seismology
U.S. Geological Survey
345 Middlefield Road, Mail Stop 977
Menlo Park, California 94025
(415) 323-8111, Ext. 2531

Investigations

In previously unreported work plots were made of the clusters. The percentage of events was plotted vs. radius with the center of swarm at zero.

The Willits aftershock study was completed but work remains to meet the referee's criticisms.

Results

The plots of percentage of events vs. radius show great variety presumably due to varying shape of the swarms. The clusters that can be categorized as spherical show similar plots. The vast majority of events fall within 2 km of the center. Those with fewer events peak within 1 km of the center.

Reports

Warren, D. H., Scofield, C., and Bufe, C. G., Aftershocks of the November 22, 1977 earthquake at Willits, California: Activity in the Maacama fault zone: accepted by the Bulletin of the Seismological Society on September 12, 1984.

Central American Seismic Studies

9930-01163

Randall A. White, David H. Harlow
Branch of Seismology
U.S. Geological Survey
345 Middlefield Road, MS/977
Menlo Park, California 94025
(415) 323-8111, ext. 2570

Investigations

We are examining the tectonic origin and the seismic characteristics of shallow ($Z < 15$ km), destructive earthquakes along the volcanic chain in Central America. We are focusing on these earthquakes because the historical record indicates that these earthquakes produce a greater impact than do large subduction zone earthquakes which are typically small (magnitude 7.5 to 8.0) compared to other circum-Pacific thrust zones and whose effects are mitigated by their infrequency and greater hypocentral distance. The shallow earthquakes, on the other hand, are more frequent and occur in or near major population centers which are concentrated along the volcanic chain.

Results

1. Magnitudes have been determined for the largest damaging earthquakes (since 1910) at 10 different locations along the volcanic chain. All of the magnitudes lie within the range $6 \leq M \leq 6\ 1/4$. Lower magnitude earthquakes do not cause significant damage and larger events do not appear to occur (see figure).

2. Historical records indicate that repeat times for these "characteristic" damaging earthquakes may be 30 to 100 years.

3. Reports indicate that most if not all of these damaging earthquakes were preceeded by days to weeks of felt earthquakes.

4. Several swarms have been recorded by micro-earthquake networks at different segments of the volcanic chain in Central America. The swarms occur with no clear main shock or with the main shock embedded well within the sequence. The b-values of all swarms studied to date (3 in Guatemala and 5 in Nicaragua), range between 1.3 and 1.5. This narrow range is midway between the range typical for tectonic earthquakes ($0.8 \leq b \leq 1.0$) and the range for volcanic earthquakes associated with eruptions ($1.8 \leq b \leq 3.5$).

5. From focal mechanisms, alignment of epicenters, and geologic features we conclude that at least in Nicaragua the volcanic chain is a diffuse zone of slow right-lateral slip.

The persistent reports of foreshocks and the nature of recently recorded microearthquake swarms at the volcanoes lead to the intriguing suggestion that, at a minimum, these earthquakes could be forecast within a socially useful timeframe. Recent moderate sized earthquakes in Central California, however, do not have foreshock activity that clearly broadcasts the future mainshock. Therefore, we plan to carefully evaluate these reports and to examine closely the possibility that the style of tectonic deformation along the volcanic chain creates a rupture process that is characterized by foreshock activity.

Reports

Yuan, Annette T. E., McNutt, Stephen R., and David H. Harlow, 1984. Seismicity and eruptive acitivity at Fuego Volcano, Guatemala: February 1975-January 1977: Journal of Volcanology and Geochemical Research, 21: 277-296.

White, Randall H., 1983. The Guatemala earthquake of 1816 on Chixon-Polochic fault: Seismological Society of America Bulletin (in press).

White, Randall H., Harlow, David H., and Edgar R. Quevec, 1984. Microseismicity of the western Motagua fault prior to the 4 February 1976 Guatemala earthquake: EOS (in press).

McNutt, S. R., and Harlow, D. H., 1984, Seismicity at Fuego, Pacaya, Izalco, and San Cristobal Volcanoes, Central America, 1973-1974, Bull. Volcanol. (submitted).

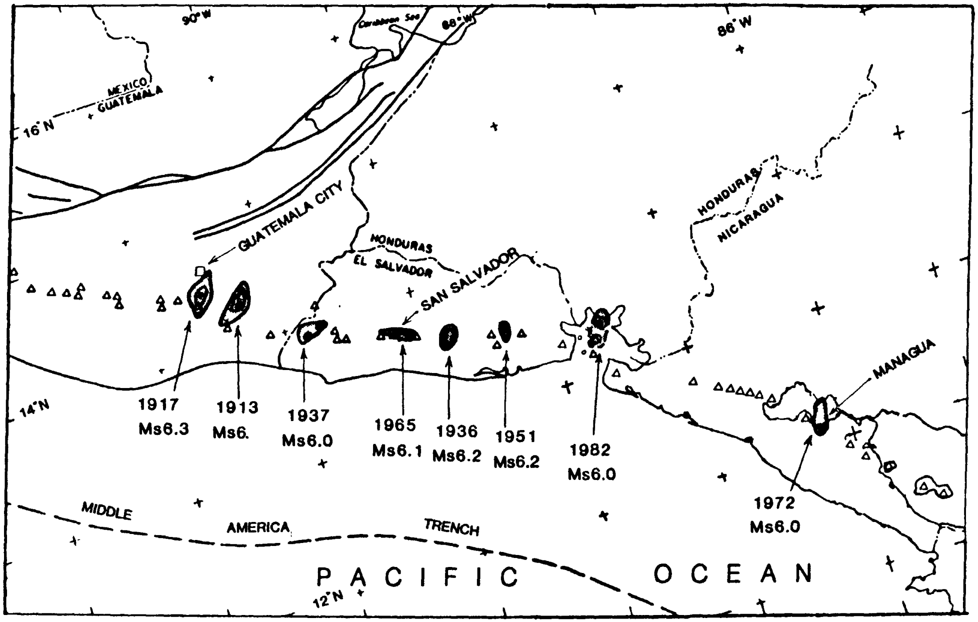

VOLCANIC CHAIN EARTHQUAKES - INTENSITY VII OR GREATER

Recognition of Individual Earthquakes on Thrust Faults (New Zealand)

14-08-0001-21379

Robert S. Yeats, Sarah A. Barrow
Department of Geology
Oregon State University
Corvallis, Oregon 97331-5506
(503) 754-2484

Kelvin R. Berryman, Sarah Beanland
Earth Deformation Section
New Zealand Geological Survey, D.S.I.R.
P.O. Box 30368
Lower Hutt, New Zealand
(644) 699-059

Investigations: Field and subsurface studies of the Dunstan, Pisa, and Nevis-Cardrona fault systems in the range and basin reverse-fault province of Central Otago were completed by the Earth Deformation Section, New Zealand Geological Survey in 1984. Immediate reports have been published and are listed below under "Reports." One set of these reports was delivered to the U.S. Geological Survey, Menlo Park by Sarah Beanland. Two copies of the Clyde Dam Site final report on the Dunstan fault (Officers of the NZGS, 1983) are at Oregon State University, and one of these will be turned over to the USGS library at Menlo Park at the completion of the second year of this contract. Copies of the Pisa fault final report (Officers of the NZGS, 1984) and the Nevis-Cardrona fault study (Officers of the NZGS, in prep.) will be obtained next year for the USGS library with contract funds.

USGS-supported scientists (R. S. Yeats, S. A. Barrow) contributed to field work on the Dunstan, Cardrona, and Nevis faults.

Results: Central Otago is underlain by Haast Schist, which consists of metamorphosed sedimentary rocks and minor interbedded volcanic rocks of late Paleozoic and early Mesozoic age. These rocks were metamorphosed predominantly in the greenschist facies during the Rangitata orogeny, which ended 140-130 million years ago. In Late Cretaceous time, the schist basement was uplifted and eroded to a deeply-weathered peneplain. The region apparently received no sediments during the Paleogene, when coastal areas to the east and west were receiving largely marine sediments. In the Neogene, Central Otago received relatively fine-grained nonmarine sediments, in part lacustrine, resting on quartz gravels which themselves rest on deeply-weathered schist. The fine grain size of these nonmarine sediments indicates that central Otago continued to be an area of low relief as recently as Miocene and Pliocene. These fine-grained strata are overlain by weathered gravels (Maori Bottom, Schoolhouse), reflecting uplift of nearby ranges. Tectonic activity in Central Otago may be a response to the change in stress regime along the Alpine transform fault from pure strike slip to oblique convergence. Clast composition of these weathered gravels commonly does not correspond with that of alluvial fans directly overlying them, suggesting that the geomorphic configuration in early Pleistocene time did not correspond to the present distribution of ranges and basins. The weathered gravels are overlain with angular unconformity by late Quaternary outwash gravels, alluvial fans, moraines, fluvial deposits and colluvium responding to the present topography and drainage. These late Quaternary sediments are faulted.

In Central Otago, the northeast-trending ranges and basins are asymmetric, with major reverse faults dipping northwest beneath the southeast edge of the range front, and the synclinal axis in the adjacent basin close to this range front. The peneplain surface tends to be well preserved on the gently-sloping northwest flank of the range. On the steep southeast flank, the peneplain is not preserved, and foliation becomes steep to overturned close to the range-front fault. Some of the basins (Manuherikia, Cromwell) are as large in area as the flanking ranges, whereas others (Cardrona, Upper Nevis, Lower Nevis) are very narrow relative to flanking ranges. In addition to range-front reverse faults marking the boundary between schist and sediment, there are other faults within the basin itself, and these faults have provided most of the documentation for late Quaternary fault history. Some of these faults dip away from the ranges (labeled antithetic), and others dip toward the ranges (labeled synthetic), parallel to the range front. The zones of faulting are from 0.1 to 3 km wide, in some cases forming horsts within the basin.

The Dunstan fault zone is somewhat lobate in plan, convex toward the Manuherikia basin. The Waikerikeri segment (6.5 km long) and Devonshire segment (14 km long) have more surface expression within the basin and thus may be more active than the intervening Brassknocker segment (6.5 km long). Vertical displacements for a single faulting event are estimated at about 2 m, implying a dip-slip displacement of 2.8 to 4 m, depending on the dip of the fault at depth. The estimated recurrence interval of faulting is about 8,000 years; others suggest a figure of 5,000-7,000 years. The length of a possible surface rupture for a single fault movement is estimated to range from 20 to 60 km, with 20 km more likely.

The Pisa fault is divided into three segments, a NNW-trending segment south of the Kawarau River, the main segment flanking the Pisa Range, and an apparently less active segment north of the Lindis River and east of the Clutha River. The north-trending Grandview fault, extending to Lake Hawea, is part of the Pisa fault system. Both antithetic and synthetic faults are present in the Cromwell basin adjacent to the main segment of the Pisa fault, and a late Quaternary subsurface fold extends along the north half of the Pisa segment and is continuous along the Grandview fault. The range-front fault is exposed in the Kawarau River gorge and is seen to be a zone of sheared and crushed rock 500 m wide. The schist-sediment contact dips 60° northwest. Schist foliation dips more steeply as the fault zone is approached. The Pisa fault was active 70,000 to 36,000 years ago and prior to 140,000 years ago, but inactive 140,000 to 70,000 years ago and since 36,000 years ago. Ages are based on correlation of faulted sequences with the Quaternary glacial stratigraphy of the upper Clutha Valley.

The Nevis-Cardrona fault system comprises two NNE-trending segments which are stepped left in relation to one another and bifurcated in the region of stepover north and south of the Kawarau River. The system is characterized by infaulted slices of Tertiary sediments, by relatively short fault traces with evidence of late Quaternary activity, and by three narrow basins (Upper Nevis, Lower Nevis, Cardrona) containing Tertiary sediments and Quaternary gravels. The Upper Nevis basin contains a mid-valley horst, and the west-dipping fault on the east side of this horst (Nevis fault) appears to be the youngest fault. A west-dipping range-front fault bounds the basin on the west and is older than the faults of the horst. The vertical component of displacement for each event on the Nevis fault over the last 22,000 years is 0.25 to 0.4 m. Average recurrence interval of faulting is about 5,000 to 7,000 years, and the last event took place several thousand years ago.

Late Quaternary faulting in the Lower Nevis basin occurred on very short fault traces near the major throughgoing fault, which is not at the range front. The Coal Creek fault trace represents at least two faulting events in the last 22,000 years with a total vertical offset of 2 m at the surface. The Ben Nevis fault does not appear to have moved in the last 22,000 years.

Cardrona Valley contains a basin bounded by a relatively active fault on the west (NW Cardrona fault) and a poorly-exposed fault on the east (SE Cardrona fault). The fault system bifurcates at the southern end of the basin into the Crown and Coalpit segments on the west and the Roaring Meg and Doolans segments on the east. These segments rejoin at the north end of the Lower Nevis basin. A trench on an antithetic fault 500 m east of the NW Cardrona fault at Branch Creek Road yielded evidence of 3 faulting events in the last 22,000 years with a total vertical offset of 4 m. On the Crown segment of the NW Cardrona fault, one locality (Blackmans Creek) contains evidence of vertical offset of a stream terrace of 7 m and lateral offset of 10 m in the last 22,000 years. A younger fan surface 500 m south of this locality is offset by 1 m, which may represent a single event. Farther south, at the Kawarau River, a west-dipping fault displaces a surface with an age estimated as 22,000 years in 3 to 6 discrete events. The Roaring Meg segment warps a surface estimated as 22,000 years old.

In adjacent regions, the Ostler fault in the Mackenzie basin (illustrated on page 14 of the August, 1984 Geotimes) has a recurrence interval of 3,500 years. In coastal Otago south of Dunedin, the Akatore fault has a recurrence interval which may be less than 1,000 years, with events 1,500 and 900 years BP.

Estimates of recurrence interval depend on estimates of ages of surfaces or deposits that are offset, and these ages are not well constrained. There are relatively few ^{14}C dates, probably because the semiarid climate of Central Otago results in poor preservation of organic matter. Accumulation of loess causes problems in dating surfaces by soils chronosequences, and there are no ash deposits for tephrachronology. Profiles of fault scarps have been compared with profiles used in quantitative studies of scarp degredation. In the Upper Nevis basin, the calculated age of the scarp produced by the last fault event [4,500 years] correlates well with ages based on geological constraints. The scarp profile immediately after reverse faulting is more complex than normal faults of the western U.S. For example, the Ostler and Lake Heron reverse-fault scarps tend to be broad, low angle, and convex near the top and steep only at the base, possibly due to a tank-tread-like movement of the leading edge of the hanging wall near the surface. Finally, the ages of the glacial/interglacial sequence beyond the range of radiocarbon dating of the Upper Clutha Valley are very poorly constrained.

A major finding of the Central Otago fault studies is that the prediction of future fault behavior in Central Otago must be based upon late Quaternary fault history rather than instrumental and historical seismicity. Central Otago is characterized by very low seismicity, yet there is abundant evidence for Holocene faulting. The Nelson-Buller area of northwestern South Island is much more active seimsically, and this is the site of the 1929 Murchison earthquake (M 7.8) and the 1968 Inangahua earthquake (M 7.1), both reverse-fault events. Despite the high seismicity of the Nelson-Buller area, the fault recurrence interval of the Inangahua fault is 6,000 to 9,000 years, and the White Creek fault, which moved during the 1929 Murchison earthquake, last moved at leat 18,000 years ago.

It is also of interest that the Pisa fault is characterized by periods of frequent faulting alternating with periods of inactivity. During the last 36,000 years, the Pisa fault has been inactive whereas the Dunstan and the Nevis-Cardrona faults have been active during this time.

Reports:

Barrow, Sarah A., in prep., Geology and neotectonics of the Upper Nevis Basin, Central Otago, South Island, New Zealand: MS thesis, Oregon State University.

Beanland, Sarah, 1984, Late Quaternary faulting in the Cardrona valley, Central Otago: NZGS/EDS Immediate Report 84/017, 15 p.

Beanland, Sarah and Barrow, Sarah A., 1984, Trenching investigations of active faulting in the Upper Nevis basin, central Otago: NZGS/EDS Immediate Report 84/004, 21 p.

Beanland, Sarah and Barrow, Sarah A., 1984, Geology of the Upper Nevis basin in relation to active tectonics: NZGS/EDS Immediate Report 84/005, 14 p.

Beanland, Sarah, and Barrow, Sarah A., 1984, Quaternary geology and late Quaternary tectonic deformation of the Upper Nevis basin, central Otago: NZGS/EDS Immediate Report 84/006, 21 p.

Beanland, S., Berryman, K., Hull, A., and Wood, P., in press, Late Quaternary deformation at the Dunstan fault, Central Otago, New Zealand: Proceedings of the Symposium on Recent Crustal Movements: Bulletin of the Royal Society of New Zealand.

Beanland, S., Berryman, K., Hull, A., Wood, P., Barrow, S., and Yeats, R., 1984, Active reverse faulting in central Otago, South Island, New Zealand: Geol. Soc. America Abs. with Programs, v. 16, p. 440.

Beanland, S., Fellows, D. L., and Barrow, S. A., 1984, Late Quaternary faulting in the Lower Nevis basin central Otago: NZGS/EDS Immediate Report 84/018, 19 p.

Beanland, Sarah, and Fellows, Debbie L., 1984, Late Quaternary tectonic deformation in the Kawarau River area Central Otago: NZGS/EDS Immediate Report 84/019, 17 p.

Officers of the New Zealand Geological Survey, 1983, Seismotectonic hazard evaluation of the Clyde Dam site: NZGS EG 375, 2 vols.

Officers of the New Zealand Geological Survey, 1984, Seismotectonic hazard evaluation for Upper Clutha power development: NZGS Report EG 377.

Yeats, Robert S., 1984, Evidence for coseismic folding in the South Island, New Zealand: Geol. Soc. America Abs. with Programs, v. 16, p. 702.

Yeats, Robert S., in press, Faults related to folding, including examples from New Zealand: Proceedings of the Symposium on Recent Crustal Movements: Bulletin of the Royal Society of New Zealand.

Yeats, Robert S. and Berryman, K. R., in prep., Northern South Island, New Zealand and Transverse Ranges, California - a tectonic comparison.

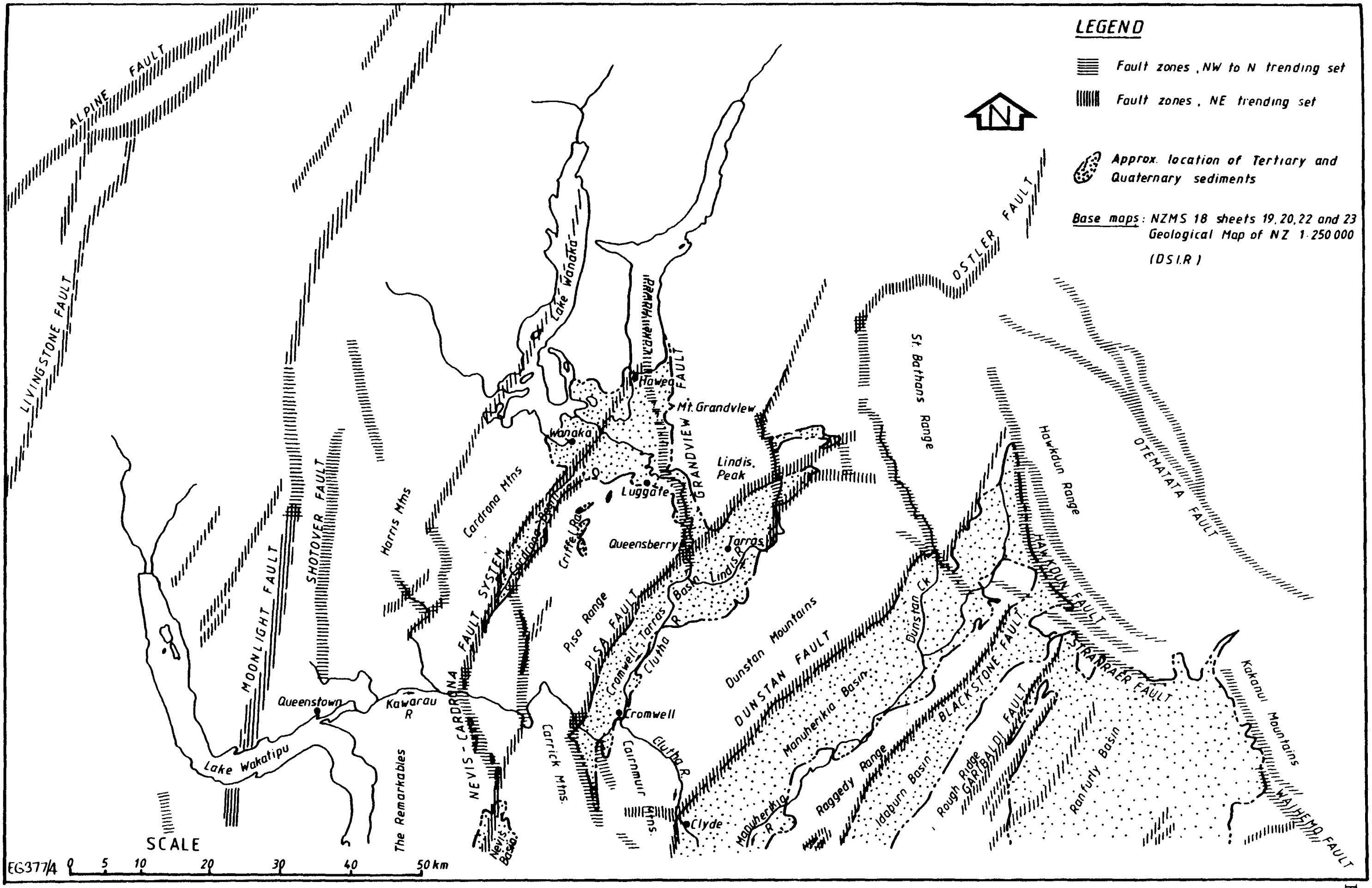

FIGURE 1 KNOWN ACTIVE AND POTENTIALLY ACTIVE FAULTS OF CENTRAL OTAGO

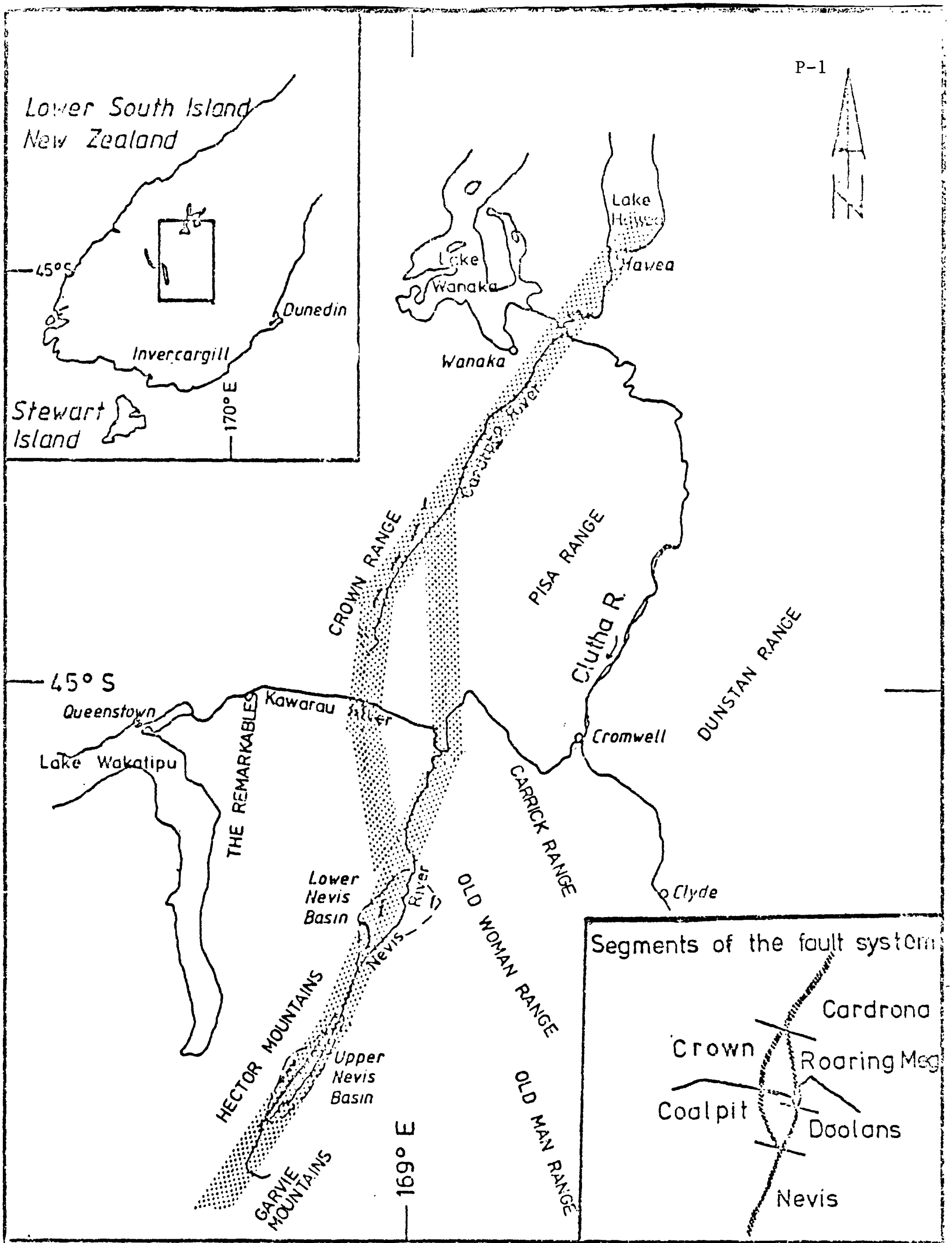

GRAPHIC SCALE

10 0 10 20 km

EXPLANATION

— Late Quaternary fault trace

▨ Nevis Cardrona Fault System (limits)

LOCATION DIAGRAM
NEVIS-CARDRONA FAULT SYSTEM
CENTRAL OTAGO

FIG 2

No. 963/53/027 sheet 1 of 1 EDSI 84/019

Creep and Strain Studies in Southern California

Contract No. 14-08-0001-21212

Clarence R. Allen and Kerry E. Sieh
Seismological Laboratory, California Institute of Technology
Pasadena, California 91125 (818-356-6904)

Investigations

This semi-annual report summary covers the six-month period from 1 April 1984 to 30 September 1984. The contract's purpose is to monitor creepmeters, displacement meters, and alignment arrays across active faults in the southern California region. Primary emphasis focuses on faults in the Coachella and Imperial Valleys.

During the reporting period, resurveys of theodolite alignment arrays were carried out at **Anza**, **Bertram**, **Cajon**, **Highway 80**, and **Pallett Creek**. Nail-file arrays were resurveyed at **Anderholt**, **Ross Road**, and **Worthington Road**. Creepmeters were serviced and records collected at **North Shore**, **Mecca Beach**, **Superstition Hills**, **Harris Road**, **Ross Road**, **Heber Road**, and **Tuttle Ranch**. In addition, the telemetry unit (TIM) at **Mecca Beach** was replaced due to failure caused by corrosion. The data from this installation continues to be monitored at the Seismological Laboratory on a weekly basis.

Results

The measurements of fault slip taken over the last 9 months show few changes in the overall picture of activity. Surveys as recent as July of the alignment arrays at **Cajon**, **Pallett Creek**, and **Una Lake** show that significant slip has not occurred on the section of the San Andreas fault between Palmdale and San Bernardino for at least the last 15 years. On the San Jacinto fault system, the array at **Anza** has not shown significant motion from 1977 to the February survey, while the array at **Baileys Well** on the Coyote Creek fault continues to show dextral slip at a rapid rate. The March survey there requires, however, that the average rate over the 13 years since the establishment of the array be revised downward to 5.2 mm/year. In the Imperial Valley, the Superstition Hills fault has not shown detectable slip at an alignment array and a creepmeter up to July, although the creepmeter records suggest dextral slip possibly averaging 0.5 mm/year between 1968 and 1979. On the Brawley fault zone, an array at **Keystone Road** and a creepmeter at **Harris Road** have both demonstrated a lack of significant slip since the 1979 earthquake up to July. The Imperial fault, however, has remained the most active in southern California. As of July, dextral afterslip of the Imperial Valley earthquake has continued to be recorded on creepmeters at **Ross** and **Heber Roads**, and on the array at **Highway 80**, on the southern half of the 1979 rupture, at rates from 13 to 15 mm/year. These rates are twice what the average rate of continuing slip at these locations was prior to the 1979 event. However, as the resurveys of **Highway 80** show, the post-seismic slip rate may not have been decreasing with time during the last few years, as would be expected. At the extreme southern end of the 1979 surface rupture, at **Tuttle Ranch**, where the post-seismic slip died out within 2.5 years of the event, the creepmeter there has not shown significant slip to the July servicing.

The only real change this year has been a dramatic increase in the amount of slip activity on the section of the San Andreas fault near the Salton Sea, at **Mecca Beach**. For the first time, creep events and more-or-less continuous slip have been recorded instrumentally on this section of the San Andreas. Beginning at some time between 28 March and 2 April, two dextral creep events were recorded with a total slip of 0.81 ± 0.06 cm over a period of 140 ± 10 hours, ending between 2 and 4 April (Fig. 2). The first event was itself of a dual character and lasted more than 20 hours, with a magnitude of 0.67 ± 0.06 cm. The second event had a duration of about 15 hours, and a magnitude of 0.15 ± 0.01 cm. In addition, 2 tilt events were recorded at the same site, each probably coincident in time with the respective creep events, and having a similar magnitude relationship. Unfortunately, although the data from this site are usually telemetered to Pasadena, the telemetry unit was inoperative at the time of the event. Therefore the absolute time of the events can only be determined to within the limits given above. However, soon after the new unit was installed it began to record additional, though smaller, creep events (Fig. 3). The larger event began at 0450 hours on 7 July GMT, and continued for 97 ± 18 hours for a total of 0.08 ± 0.01 cm of dextral slip. During the first 19 hours the average slip velocity was 6.9×10^{-7} cm/s, which slowed gradually afterwards. Interestingly enough, the creep event was actually preceded by a tilt event by more than a day. Tilting began on the N-S axis between 1800 on 5 July GMT and 0600 on 6 July GMT and continued for 44 ± 6 hours. The E-W axis began tilting about 7 hours later and continued for 17 ± 6 hours. Thus the creep event began when the tilt event was about half complete and continued long after the tilt had ceased to change. The rate of change of the tilt was fairly constant through the event at about 2.5×10^{-5} μradian/s, for a total change of 4.4 ± 0.2 μradian along a line oriented at N21°E. The line of maximum tilt forms about a 65° angle with the local trend of the San Andreas fault. The last fairly clear event recorded was a tiny 0.03 cm creep episode that peaked on 21 August.

The creepmeter micrometer readings at **Mecca Beach** (Fig. 1) show that the instrument had recorded less than 0.1 cm of dextral slip from its installation in April 1981 up to February 1984. It has subsequently recorded a total of 1.18 ± 0.08 cm of slip up to October 1. However, discrete events recognizable in the records account for only 0.92 ± 0.06 cm, so it is likely that 0.26 ± 0.1 cm has occurred as more-or-less continuous slip. Thus, so far, discrete slip events have accounted for more than 75% of the slip at **Mecca Beach**, while the creepmeters on the Imperial fault have typically recorded only 50% or less of their slip as events.

Despite the fact that dextral slip has been continuing on the section of the San Andreas through the Coachella Valley, north of the Salton Sea, at rates from 1 to 3 mm/year for at least 14 years, significant slip had not been previously observed on the fault where it is adjacent to the Salton Sea, with the exception of slip coincident with the 1968 and 1979 earthquakes that was observed in some areas. The latest readings, in July, of the creepmeter at **North Shore**, just a few km to the north of **Mecca Beach**, do show a possible 0.1 cm of dextral motion, but such fluctuations have been observed often during the 14-year life of the instrument, which does not indicate any slip overall. The alignment array at **Bertram**, about 10 km south of **Mecca Beach**, was resurveyed in July and shows that any slip through this unreliable site would have been less than a few mm. Thus the creep event appears to have been limited to the area of the fault immediately adjacent to **Mecca Beach**.

Seismic moments calculated from local magnitudes of events located in the Salton Sea area by the southern California seismic array do show a moderate increase in the release of seismic moment in early June in the North Shore and Bombay Beach areas. While this increase was certainly the largest that has occurred during the life of the **Mecca Beach** instrument, it is hardly unprecedented. Much larger releases of seismic moment have occurred previously in all three areas, and during those periods slip was not measured at either the **North Shore** or the **Bertram** site.

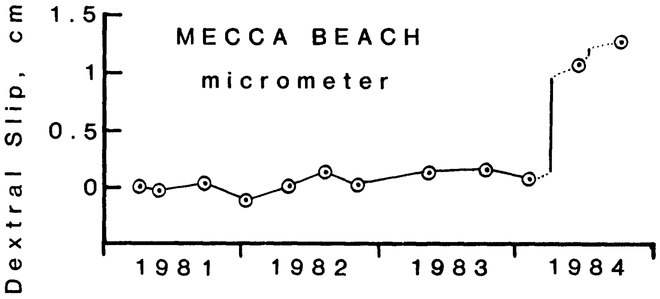

Figure 1. Record of cumulative slip from readings since April 1981 of the micrometer at the **Mecca Beach** creepmeter on the San Andreas fault in the Coachella Valley. The readings are represented by circled dots; the vertical lines separated from the readings by dotted lines after February 1984 represent the two largest creep events, as measured on the chart records.

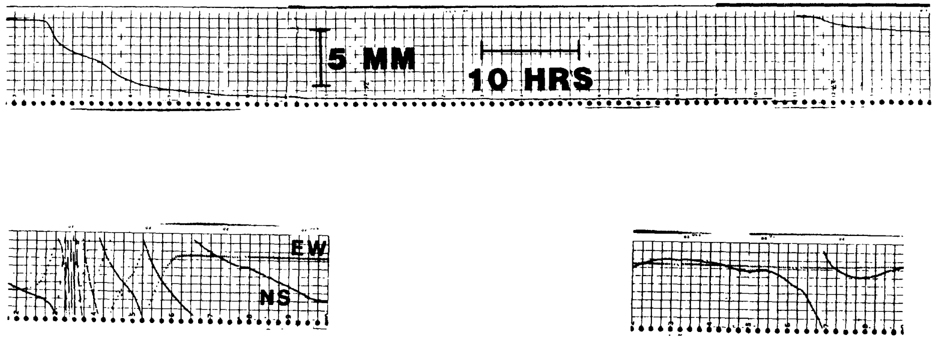

Figure 2. Chart records of the creep (top) and N-S and E-W tilt (bottom) events at **Mecca Beach** at the beginning of April 1984. The recorder impresses a small dot every 2 seconds. Time runs from left to right. The large offsets from one side of the chart to the other are automatic scale resets.

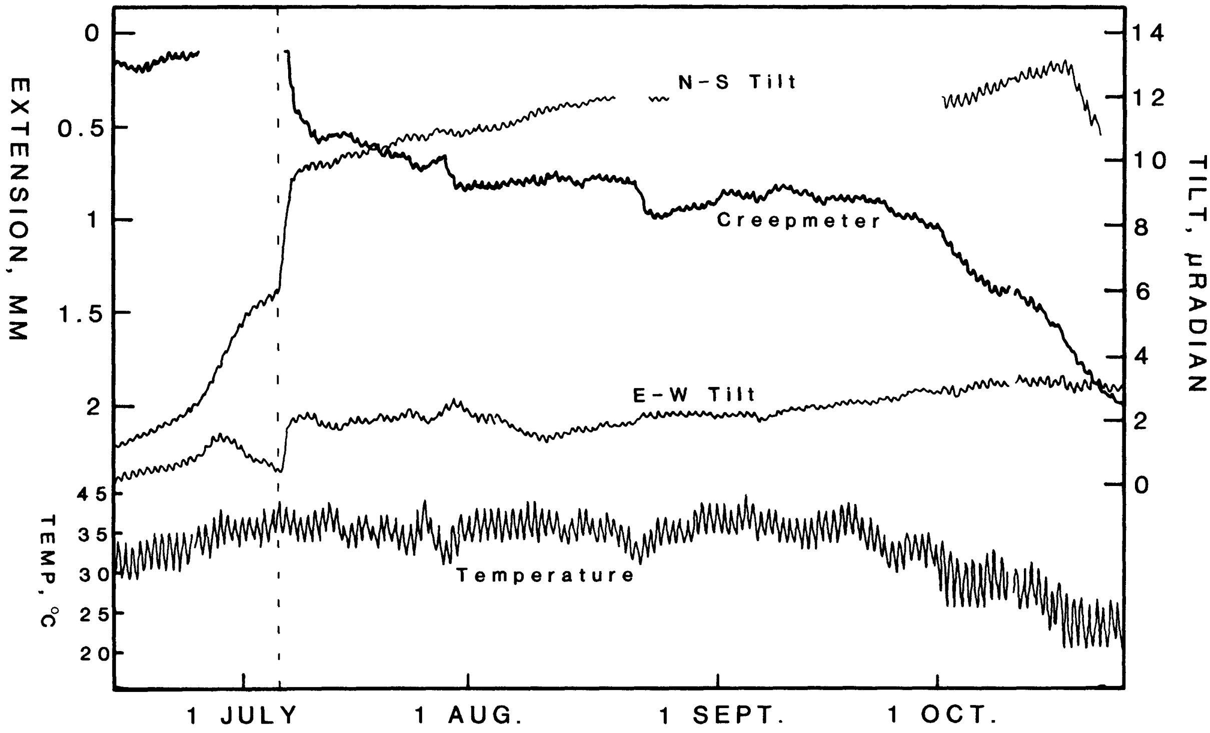

Figure 3. Composite of telemetered records from the **Mecca Beach** instruments on the San Andreas fault near the Salton Sea for the period from 13 June to 26 October 1984. The creepmeter record represents the raw extension between the piers and is corrected for temperature and instrument geometry to yield the slip. Note the apparent extension in late September and October following the fall in temperature. The dashed vertical line shows the position of 6 July 1984, when the creep and tilt events began.

On-Line Seismic Processing

9970-02940

Rex Allen
Branch of Seismology
U.S. Geological Survey
345 Middlefield Road, MS 77
Menlo Park, California 94025
(415) 323-8111 ext 2240

Investigations and Results

Implementation of the Mark II real-time processor (RTP) using 68010 processors is proceeding, although somewhat more slowly than we had hoped. Time-intensive sections of the picker algorithm have been identified, and assembly language routines have been written to be called from the fortran picker program. The principal time sinks are the digital filters, and these are quite amenable to this treatment. Fortran routines used in the associator are being transferred to the 68000 development system for compilation.

Hardware for the first system has been ordered and is now being delivered. Local field support engineers from the manufacturer are working with us in bringing up the hardware for test as it arrives, and in dealing with problems encountered. We expect to have a prototype system in operation in December.

The Mark I RTP continues to function satisfactorily. A few small modifications were made in the associator software on the suggestion of Mitch Pitt, and a significant improvement was observed, especially in the unit at the University of Washington for the stations monitoring Mt St. Helens.

Digital Signal Processing of Seismic Data

9930-02101

W. H. Bakun
U.S. Geological Survey
345 Middlefield Road, MS/977
Menlo Park, California 94025
(415) 323-8111, ext. 2777

Investigations

1. Main shocks of the earthquake sequences that occurred on the Parkfield section of the San Andreas fault in central California in 1922, 1934, and 1966 are characterized by southeast rupture expansion over the same 20- to 30-km-long section of the fault. Whereas the seismic moments for the 1922 and 1934 events are identical to within a precision of 10 percent, the seismic moment for 1966 is 20 percent greater than for the earlier events to within a precision of 20 percent. The Parkfield area seismicity, in general, seems well described by a recurring moderate size characteristic earthquake, repeating the same epicenter, magnitude, seismic moment, rupture area, and southeast direction of rupture expansion. An unexplained 10 year advance of the 1934 event is the only discrepancy in the hypothesis that the Parkfield earthquakes in 1857, 1881, 1901, 1922, 1934, and 1966 represent a strictly periodic process. Assuming the strictly periodic model and the absence since 1966 of the perturbations hypothesized for the 1922 to 1934 period, the next characteristic Parkfield earthquake should occur between 1983 and 1993.

2. Onscale seismograms recorded at stations in the U.S. Geological Survey's (USGS) central California seismic network (CALNET) have been used to estimate the seismic moment M_0 and local magnitude M_L for earthquakes of $1 \leq M_L < 4$ located on the San Juan Bautista and Parkfield sections of the San Andreas fault, the Coyote Lake section of the Calaveras fault, the Sargent fault, and near Livermore. These data, together with M_0 and M_L estimates for $4 \leq M_L \leq 6$ earthquakes in these areas, cannot be fit with a single linear log M_0-versus-M_L relation. Rather, the data are consistent with $\log M_0 = 1.5 M_L + 16$ for $3 \lesssim M_L \lesssim 6$, with $\log M_0 = 1.2 M_L + 17$ for $1\ 1/2 \lesssim M_L \lesssim 3\ 1/2$ and with a slope of 2/3 to 1 for $1/2 \lesssim M_L \lesssim 1\ 1/2$. Whereas USGS coda duration magnitude M_D is consistent with M_L for $1\ 1/2 \lesssim M_L \lesssim 3\ 1/4$, M_D is larger than M_L at $M_L \lesssim 1\ 1/2$ and smaller than M_L at $M_L \gtrsim 3\ 1/4$. Log M_0 can be estimated to a precision of 0.2 for $1 \leq M_D \leq 3\ 1/2$ earthquakes in central California by applying $\log M_0 = 1.2 M_D + 17$ to the M_D that have been routinely published by the USGS.

3. The Morgan Hill, California, earthquake (magnitude 6.1) of 24 April 1984 ruptured a 30-kilometer-long segment of the Calaveras fault zone to the east of San Jose. Although it was recognized in 1980 that an earthquake of magnitude 6 occurred on this segment in 1911 and that a repeat of this event might reasonably be expected, no short-term precursors were noted

and so the time of the 1984 earthquakes was not predicted. Unilateral rupture propagation toward the south-southeast and an energetic late source of seismic radiation located near the southeast end of the rupture zone contributed to the highly focused pattern of strong motion, including an exceptionally large horizontal acceleration of 1.29g at a site on a dam abutment near the southeast end of the rupture zone.

Reports

Bakun, W. H., and T. V. McEvilly, Recurrence models and Parkfield, California, earthquakes, J. Geophys. Res., 89, 3051-3058.

Bakun, W. H., 1984, Seismic Moments, Local Magnitudes, and Coda Duration Magnitudes for Earthquakes in Central California, Seismological Society of America Bulletin, 74, no. 2, p. 439-458.

Bakun, W. H., and A. G. Lindh, 1984, The Parkfield, Califiornia prediction experiment, Earthq. Pred. Res. (in press).

Bakun, W. H., M. M. Clark, R. Cockerham, W. L. Ellsworth, A. G. Lindh, W. H. Prescott, A. F. Shakal and P. Spudich, 1984, The Morgan Hill, California, earthquake, Science, v. 225, no. 4659, pp. 288-291.

Bakun, W. H., and A. G. Lindh, 1984, Characteristic earthquakes on the San Andreas fault (abs.), Abstract Book of IASPEI Regional Assembly (in press).

Li Y. Z., W. H. Bakun, Y. Jin, and F. G. Fischer, 1984, Magnitude and seismic moment scales in Yunnan Province, Peoples Republic of China (abs.), Abstract Book of IASPEI Regional Assembly (in press).

Tectonic Tilt Measurement: Salton Sea

USGS 14-08-0001-21918

John Beavan and Roger Bilham
Lamont-Doherty Geological Observatory of Columbia University
Palisades, New York 10964
(914) 359-2900

Investigations: Thirty-one years of data exist from water level gauges on the Salton Sea. Twenty-six years of these data were analysed in 1978 (Wilson & Wood, 1980) to reveal that crustal deformation was down to the SE until 1970 when it reversed. The tilt rate appears to be approximately 0.1 microradians per year, at times increasing to 0.4 microradians/year (Figure 2, Wilson & Wood, 1980). The rate of tilting and the timing of the 1970 inflection in the tilt rate are in good agreement with levelling profiles run in 1956, 1968, 1972, 1974, and 1978 along the Salton Sea coast. For this reason the Salton Sea may be considered to act as a long baseline tiltmeter producing nearly continuous measurements of crustal deformation. The importance of the Salton Sea in tilt measurement is that it straddles a region in which stresses have been increased by major earthquakes in the last century and where a major event will occur in the future.

We are using weather records to identify and remove noisy data in an attempt to improve the noise level of the data set. We are also analyzing the data up to date, which includes the times of the 1979 Imperial Valley and 1981 Westmorland earthquakes.

Results:

(1) Although the USGS Water Resources Division reports its water level measurements from Sandy Beach to 0.1 foot at the end of each month, the data have in fact been recorded continuously for the past 10 years and the paper charts can be read to 3 mm or better accuracy (Figure 3). From these records it is possible to estimate the short term noise level (<2 cm during quiet spells) and to observe the size and duration of the response of the Sea to storms (Figure 3).

(2) Between 1952 and 1970 two independent sea level data sets were collected within 1 km of each other at Fig Tree John Springs (FTJS). One was collected by Imperial Immigration District (reported by Wilson & Wood (1980)), the other by Coachella Valley Water District (before they changed their recording site to Salton Sea State Park (SSSP) in 1970). We may use these data to check on the stability of the recording staffs, a point which was not addressed by Wilson and Wood. The two data sets are shown in Figure 4, where the two traces have been offset by 0.1 foot for clarity of presentation. It is not possible to detect any instability at the cm level from this plot, but with further processing this will be possible.

(3) Weather observations (in particular atmospheric pressure, wind speed and direction) have been obtained from Thermal just to the north of the Sea for 1951 through 1982, and from El Centro (1951-1960) and Imperial (1960-1982) to the south. We will use these in conjunction

with the USGS continuous water level measurements to determine the response of the Sea to particular pressure and wind inputs.

(4) The continuous recorder at SB was unfortunately down for much of 1978 and 1979, prior to the Imperial Valley earthquake. However, we have obtained copies of the records prior to and during the 26 April 1981 Westmorland earthquake, whose epicenter was ≈10 km from the gauge. A section of the record at the time of the quake is shown in Fig. 5; we are examining the preceding records for any possible precursory signal.

References

Wilson, M.E. and S.H. Wood, 1980. Tectonic tilt rates derived from lake-level measurements, Salton Sea, California, Science, 207, 183-186.

Fig. 1 Map of the Salton Sea area, southern California, showing routes of repeated first-order leveling and locations of terminal benchmarks [13(CSHD), G516, H70, R1230, V614, W89, and G577]. Years in brackets indicate the dates of leveling. The water-level staffs are located at Fig Tree John Springs (*FTJS*), Salton Sea State Park (*SSSP*), and Sandy Beach (*SB*). Locations of the aftershock areas of the 1968 Borrego Mountain earthquake are adapted from Hamilton (*9*). Locations of the 1975 Brawley swarm area are from Johnson and Hadley (*10*), and locations of the 1976 Northern Imperial Valley swarm are from Schnapp and Fuis (*11*): $M_L = 6.2$ and $M_L = 6.4$ are Richter magnitudes for moderate-size earthquakes during the years indicated.

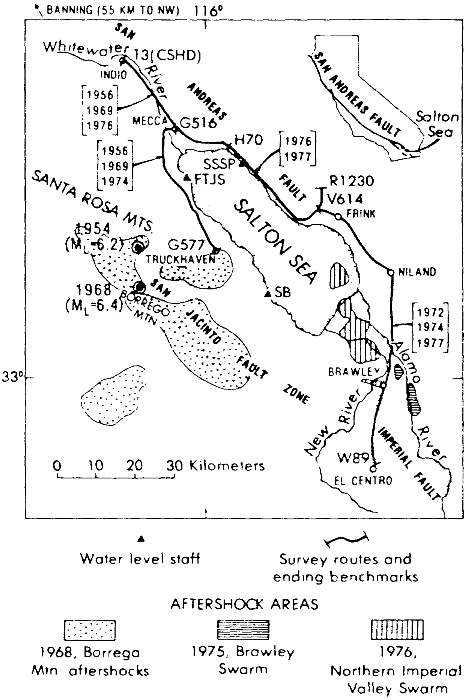

0036-8075/80/0111-0183$00.50/0 Copyr

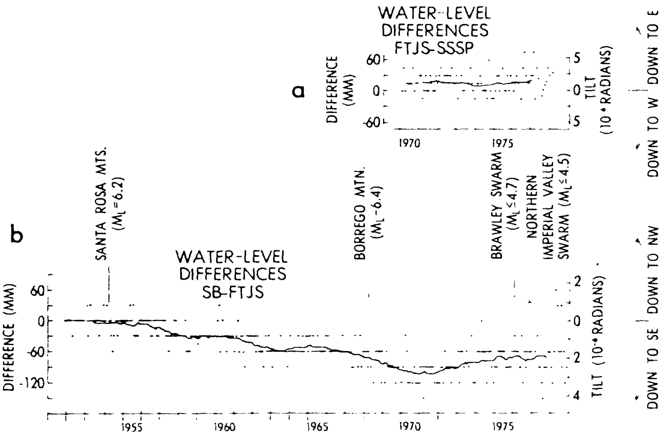

Fig. 2. History of water-level differences between pairs of stations on the Salton Sea. The continuous line is a 27-point running average: (a) water-level differences for the *FTJS-SSSP* pair; (b) water-level differences between *SB* and *FTJS*. Original data are shown as points.

From Wilson and Wood (1980)

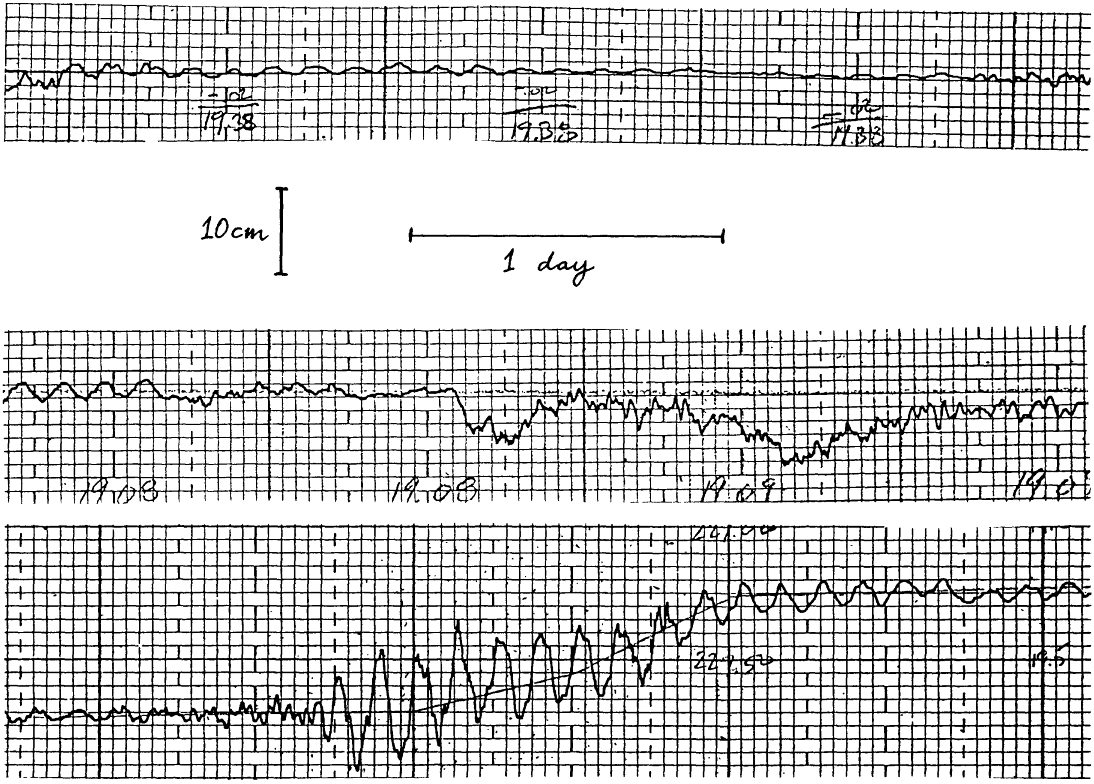

Figure 3. Typical quiet and noisy data as recorded by the USGS gauge at Sandy Beach.

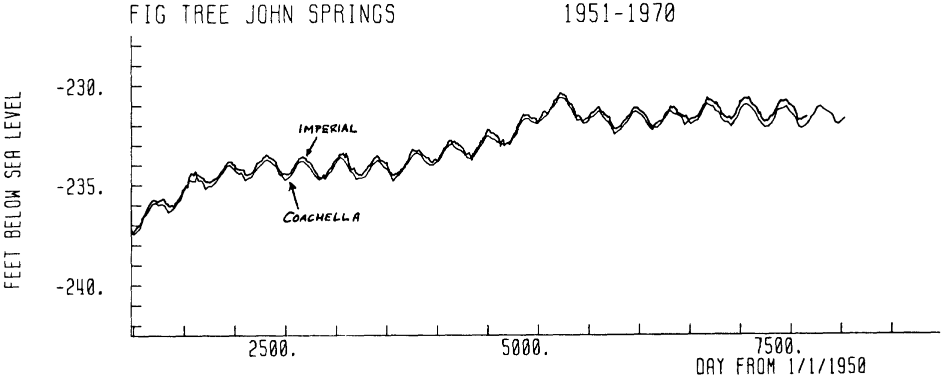

Figure 4. Simultaneous Salton Sea level data sets from adjacent (<1 km) sites. These data will be used to check on possible datum drift.

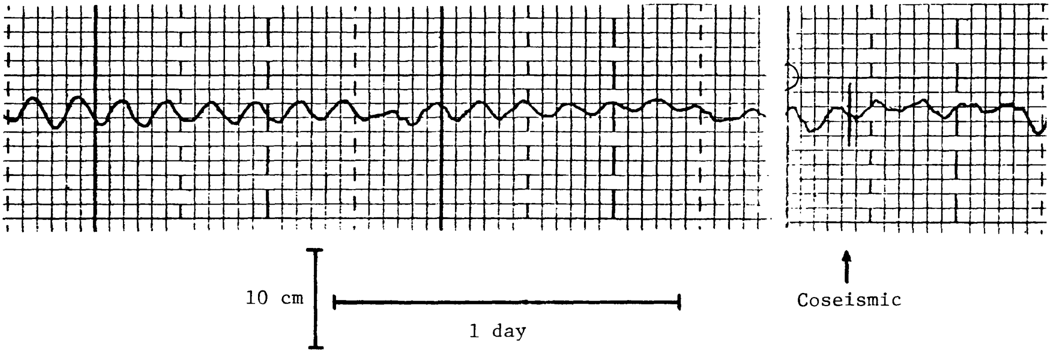

Figure 5. Sandy Beach data at the time of the 26 April 1981 Westmorland earthquake (epicentral distance approx. 10 km). Coseismic ground motion of 6cm peak-peak amplitude is visible.

Crustal Deformation Observatory: Part F

USGS 14-08-0001-21864

Roger Bilham and John Beavan
Lamont Doherty Geological Observatory
Palisades, New York 10964
(914) 359-2900

Investigations

1. The LDGO tiltmeter at Pinion Flat Observatory continues to be maintained in an investigation of coherence between data from various forms of long-baseline tiltmeter.

2. One of the principal difficulties in obtaining uninterupted long-period tilt data from the existing LDGO tiltmeter at PFO is due to occasional malfunctions of the laser-interferometer water height transducers. While we have provided a mechanical system for recovering the tiltmeter datum in the event of an electronic system failure the method is inconvenient since it must be performed manually. We have tested an alternative form of water level sensor that promises to provide long-term stability with low maintenance. The sensor combines the advantages of a direct micrometer readout with a non-interferometric optical tracking system based on an LED light source.

Results

1. Long period tilt data from the UCSD and LDGO tiltmeters appear to differ by less than 0.2 microradian/a. This estimate may be biased by the filling of gaps in data from the LDGO tiltmeter with secular signals observed on the UCSD instrument (Wyatt et al 1984). A divergence of 0.2 microradian/a is equivalent to a vertical displacement of one end monument of 106 microns/a relative to the other. Vertical motions of the end-mounts of the LDGO tiltmeter relative to the base of 26m boreholes beneath them have an annual displacement signal that is approximately sinusoidal with a amplitude of approximately 250 microns but with a 50 day phase difference. The phase of the monument-corrected tilt signal differs from the vertical extensometer signals but its amplitude is similar suggesting that a thermoelastic signal in the ground with a

wavelength of the order of a few hundred meters may be responsible for some of the discrepancies between the UCSD and LDGO tilt data. Deeper vertical extensometers beneath each end mount could suppress the signal but would be a costly solution. An alternative scheme is possibly to measure the gradient of vertical strain as a function of depth from the surface in an attempt to estimate displacements of the base of the borehole relative to an arbitrary deeper datum.

Tiltmeter data from the PFO installations are significantly more accurate than data obtained from leveling between the same end mounts using conventional leveling methods. This is not an unexpected result since it can be shown that thermally induced errors in the tiltmeters are equivalent to vertical displacement errors of less than 5 microns in 535m, whereas Class I leveling errors exceed 200 microns in the same distance. The micrometer-pointer readout of the LDGO tiltmeter can be read to better than ±2microns at each end and is essentially drift free. Note that this comparison of leveling with tilt data is independent of motion of the end monuments. Elastic depression of the LDGO end platforms by approximately 10microns occurs as the leveling rods are lowered on to them for measurements. Since the depression is identical at each end (±1micron) this does not contribute significantly to the leveling error.

2. The new sensor under development consists of a Light Emitting Diode (LED) focussed onto silicon bicell after reflection from the lower surface of water contained in a transparent, cylindrical vessel. Vertical movement of the water surface results in the displacement of the image of the LED vertically by precisely twice the displacement of the water surface. The bicell generates a signal whose polarity is determined by the sense of water surface motion and this signal after amplification causes a motorized micrometer to translate the bicell to a null position. The position of the micrometer is monitored remotely using an LVDT. The theoretical displacement resolution of the bicell/LED combination is better than 1nm although the precision of the present prototype is limited by servo-motor inaccuracies to approximately ±1micron. We are presently testing improved servo-control methods to achieve sub-micron accuracy over a range of several mm.

Reports

Bilham, R., J. Beavan and K. Evans Long baseline water-tube tiltmeter geometry, the detection of flexure and tilt and the supression of locally generated signals. *9th Intl. Symp. Earth Tides New York*, 85-94. E Schweitzerbartsche Verlagsbuchhandlung, D-7000, Stuttgart. 1982

Bilham, R., J. Beavan, K. Hurst and K. Evans, Crustal Deformation Metrology at Lamont-Doherty Geological Observatory. *J. Geod. Soc. Jap.* In the press 1984.

Bilham, R. Crustal Deformation Metrology in the U. S. , U.S./Japan Earthquake Prediction Conference. Washington, February 1984.

Wyatt, F., R. Bilham, J. Beavan, A. G. Sylvester, T. Owen, A. Harvey, C. Macdonald, D. D. Jackson, and D. C. Agnew. Comparing tiltmeters for Crustal Deformation Measurement, *Geophys. Res. Lett.* in the Press 1984

GEODETIC STRAIN MONITORING
PARKFIELD, CALIFORNIA

9960-02943

Robert Burford
Branch of Tectonophysics
U.S. Geological Survey
345 Middlefield Road, MS/977
Menlo Park, California 94025
(415) 323-8111, ext. 2574

and

Larry Slater
CIRES
University of Colorado
Boulder, Colorado 80309
(303) 492-8028

Investigations

Development of the 2-color laser network at Parkfield was continued during the period April 1 through September 30, 1984. Construction of the central observatory building adjacent to VABM Car (Car Hill, 1683-ft. elev.), about 1.4 km SSE of Parkfield, was completed in June. Reflectors were emplaced at 6 sites by late July, 1984. Only one of these reflector sites provide a fault crossing line. The remaining 5 reflectors provide monitoring lines that are situated within the block southwest of the main trace of the San Andreas fault. Five additional reflector sites have been completed within the block northeast of the fault, and more are planned, but no distance readings other than to the 6 initial sites were obtained prior to September 30.

Results

Distance readings on the line CAR-MID-E, which crosses the San Andreas fault at a shallow angle in a direction NNW of Car Hill, show a 1.8-mm contraction in response to a 3.4-mm creep event recorded near Car Hill on August 23, followed by a contractional trend of about 22 mm/yr (~ 2.1-mm contraction within 35 days during August and September). This trend is due to right-lateral slip on the fault at the same rate or the equivalent in shallow strain. The other 5 lines measured during June-September show some significant fluctuations in length, but the trends on these lines are nearly flat. If the larger distance fluctuations reflect actual strain changes, then the approximate strain field could be represented as uniaxial contraction of $\sim 7 \times 10^{-7}$ in a NNE-SSW orientation during July 20-August 4, followed by uniaxial extension of about the same magnitude during the remainder of August. Standard deviations of individual line-length readings retained in a data file for plotting ($1\sigma < 0.8$ mm) averaged about ± 0.5 mm for the 6 lines (strain uncertainty of about ± 0.14 μstrain).

Reports

No reports were completed during this period.

STRONG GROUND MOTION ANALYSIS

9910-02676

J. Boatwright, J.B. Fletcher, T.C. Hanks and A. McGarr
Branch of Engineering Seismology and Geology
U.S. Geological Survey
345 Middlefield Road, MS 977
Menlo Park, California 94025
(415) 323-8111 ext. 2485, 2384, 2184, 2708

Investigations

1. Measurement and analysis of ground motion and source parameters of the Coalinga, California earthquake sequence of 1983.

2. The 10-station digital array along the San Jacinto fault near the town of Anza was installed in 1981 to collect high-quality seismograms for the calculation of precise earthquake source parameters.

3. Analysis of the mainshock and aftershock sequence of the October 28, 1983, Borah Peak, Idaho, earthquake.

Results

1. Ground motion and source parameters were measured for 30 events of the Coalinga sequence from a large set of digital and analog ground motion data recorded in the epicentral region. For each event ground motion parameters $\rho R\underline{a}$ and $R\underline{v}$, where ρ is density, R is hypocentral distance, $\underline{a}$ is peak acceleration and $\underline{v}$ is peak velocity, were determined as well as the more usual source parameters, seismic moment M_0 and source radius r_0; the static stress drop (Brune model) is related to the other two source parameters according to $\Delta\sigma = 7/16\ M_0/r_0^3$. One of the more useful outcomes of this study is the development of a method to estimate the source radius in terms of the ground motion parameters in conjunction with the seismic moment. This relationship was determined to be

$$r_0 = \frac{\rho R\underline{a}\ M_0}{58\mu\ \rho(R\underline{v})^2} \tag{1}$$

where μ is the modulus of rigidity. This relationship is especially useful in instances for which spectral estimates of r_0 are difficult, as was the case for the Coalinga mainshock. From the ground motion data in conjunction with the seismic moment determined in other studies r_0 for the Coalinga mainshock appears to be about 5.4 km with a corresponding stress drop of about 110 bars. In the case of events for which both M_0 and r_0 can readily be determined, equation (1) serves to couple the ground motion parameters for peak acceleration and velocity.

The most interesting outcome of the Coalinga study to date is the finding that both the ground motion parameters and the source parameters show unexpected scaling with M_0. $\rho R\underline{a}$, $R\underline{v}$ and $\Delta\tau$ all appear to be much stronger functions of M_O than anticipated from conventional scaling principles. Moreover, the analysis of $\overline{Rv}$ as a function of M_O for other earthquake sequences indicates that the Coalinga events are not unusual in this regard.

2. Source parameters for approximately 170 events have been determined in a year and a half since the array commenced operation in the fall of 1982. The largest moment is 1.4×10^{21} dyne-cm (moment-magnitude of 3.4) and the stress drops range up to several hundred bars. While the size of the events is relatively small, the stress drops are high. Stress drops are computed two ways (Brune and a_{rms}) and both estimates have approximately the same range. The high values of stress drop are in qualitative agreement with the observation of a heat flow anomaly on this section of the San Jacinto fault, which is not generally observed along other fault zones in California. It is also in agreement with the small source zone of the $M_L = 5.5$ 1980 event compared to that of other earthquakes which occurred in central California with a similar M_L.

   Earthquakes are not located uniformly along the San Jacinto fault but are bunched in clusters. The locations of some of these clusters are predicted by Segall and Pollard's model of <u>en echelon</u> faulting. Some cross-cutting trends are also present that are similar to those found for the San Andreas to the northeast by Sykes and his coworkers. The seismicity is moderate between the Elsinore and the San Jacinto, but practically non-existent between the San Jacinto and the San Andreas.

3. The teleseismic waveforms radiated by the Coalinga and Borah Peak mainshocks were analyzed to determine the source parameters of seismic moment, radiated energy, and the static and dynamic stress drop. A new direct method of estimating the radiated seismic energy was derived for this study. For dip-slip faults, the resulting estimates do not require a model of the seismic source other than an average focal mechanism, and they depend only weakly on this mechanism. Comparison of the energy radiated by the two events indicates that the Coalinga earthquake had a significantly stronger stress release than the Borah Peak earthquake.

   Immediately following the Borah Peak earthquake, an array of digital instruments were deployed in the epicentral area. During the subsequent two weeks after the mainshock, 70 locatable events were recorded; the largest of these events was a moment magnitude 5.1 event; five other events greater than moment magnitude 4.0 were also recorded. The source parameters of hypocentral depth, seismic moment, radiated energy and dynamic stress drop were determined for 57 of these earthquakes. The results from this compilation indicate that the average stress drop of the aftershocks is relatively low, particularly for events near the epicenter of the mainshock. The events with the strongest stress drops are clustered at the northern end of the rupture, at an apparent stress concentration. The aftershocks are restricted to depths between 5 and 16 km; most of the larger aftershocks occur at depths greater than 10 km, while the majority of smaller aftershocks occur at shallow depths.

   These two complementary studies significantly improve the seismological understanding of the large normal faulting events which are the major sources of seismic hazard in the Basin and Range Province.

Reports

McGarr, A., Scaling of ground motion parameters, state of stress, and focal depth, *J. Geophys. Res.* *89*, 6969-6979, 1984.

McGarr, A., C. Mueller, J.B. Fletcher, and M. Andrews, Ground motion parameters of the 1983 Coalinga, California earthquakes: Implications for crustal strength, to appear in U.S.G.S. Open-File Report on Coalinga Earthquake Conference at Asilomar in June, 1984.

Boatwright, J. and G.L. Choy, Teleseismic estimates of the energy radiated by shallow earthquakes, to appear in U.S.G.S. Open-File Report on the Borah Peak Earthquake Workshop at Sun Valley, Idaho, in October, 1984.

Boatwright, J., Characteristics of the aftershock sequence of the Borah Peak earthquake, determined from digital recordings of the events, to appear in U.S.G.S. Open-File Report on the Borah Peak Earthquake Workshop at Sun Valley, Idaho, in October, 1984.

Contract #14-08-0001-21868

SUMMARY OF RESULTS FOR FIRST HALF OF 1984
SOUTHERN CALIFORNIA STRESSMETER PROJECT

Bruce R. Clark
Leighton and Associates, Inc.
1151 Duryea Avenue
Irvine, California 92714
(714) 250-1421

Investigations

1. Continue to monitor the Net of 14 stations (Figure 1) along the San Andreas, San Jacinto, and Sierra Madre faults for small stress changes, as measured by vibrating-wire Stressmeters.

2. Develop methods to increase the sensitivity and depth of emplacement of strain-measurement instruments.

Results

1. Long-term trends continue to be essentially linear on the Stressmeter arrays at sites of good-quality bedrock. For example, the Valyermo site (Figure 2) continues to show an increase in stress levels (approximately 50 KPa/a) in the N-S direction and a slight decrease in stress levels (approximately 30 KPa/a) in the E-W direction. The general increase in the stress difference between N-S and E-W measurements is confirmed by the second array at the site, although the absolute trends do not coincide exactly. The N45°W sensors do not show coherent trends. At San Antonio Dam (Figure 3), the E-W sensor changed trend in mid-1982 and has since established a new, almost constant stress level after several years of increase.

2. Tracking of trends between individual arrays at the same site is generally not very good, and is interpreted to show the importance of borehole effects on the wedged Stressmeters. In poor boreholes, the entire array tends to be noisy rather than just a single sensor.

3. There have been no significant short-term events since the March 1983 event which was recorded at several sites and correlated with the passage of a severe low pressure (and storm) system through southern California (see Valyermo data, Figure 2).

4. At Pinyon Flat, we now have 8 months of fairly stable readings from the deep hole Strain Cell array (Figure 4), which was grouted into place at 60 m depth. The results indicate that we are approaching long-term stability of better than 10^{-7} strain. In Figure 8, the scale is expanded to 4 KPa/division (corresponding to 10^{-7} strain) for a more detailed examination. The continued slight compression of all sensors is thought to be related to continued curing of the grout. These data can be compared to the tilt data from the long-baseline tiltmeters (approximately E-W), which are only a few meters from the Deep Hole.

   The increase in useful sensitivity of at least 25X using the new Strain Cells greatly increases their potential value to the Prediction Program.

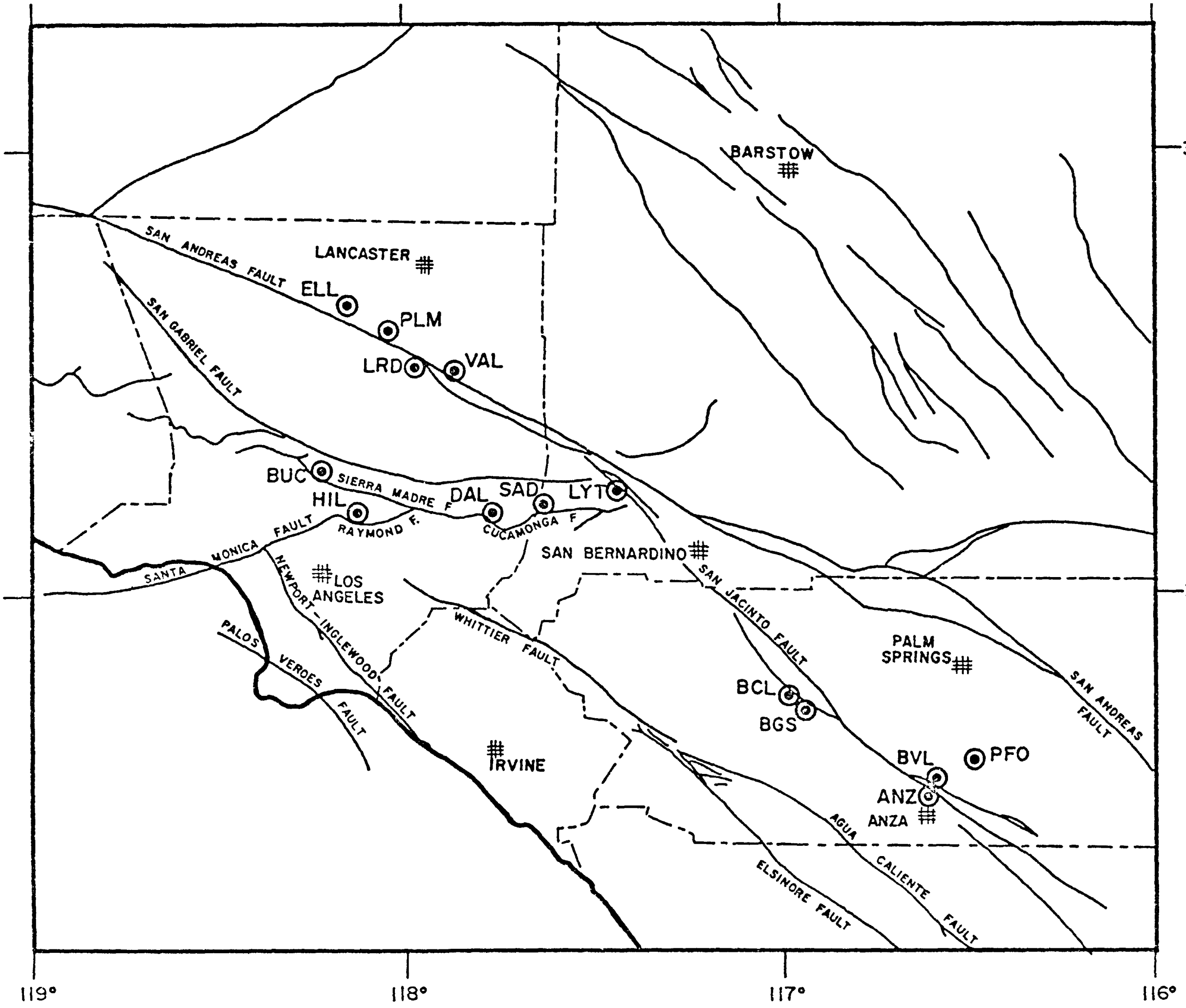

INDEX MAP SHOWING LOCATION OF ACTIVE STRESSMETER SITES

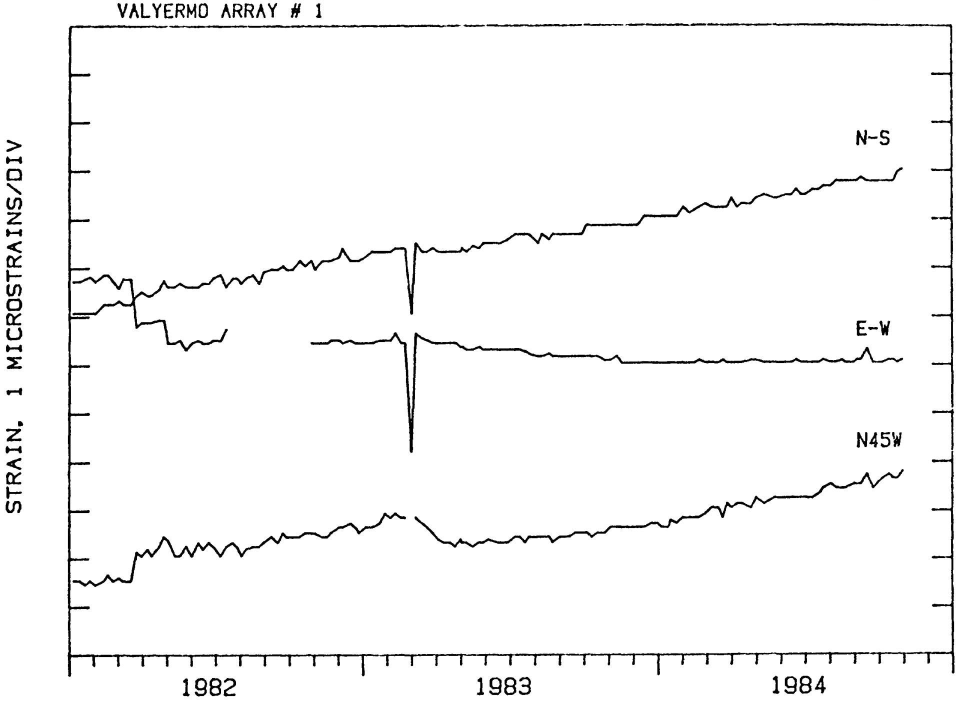
VALYERMO ARRAY # 1
STRAIN, 1 MICROSTRAINS/DIV
N-S
E-W
N45W
1982
1983
1984

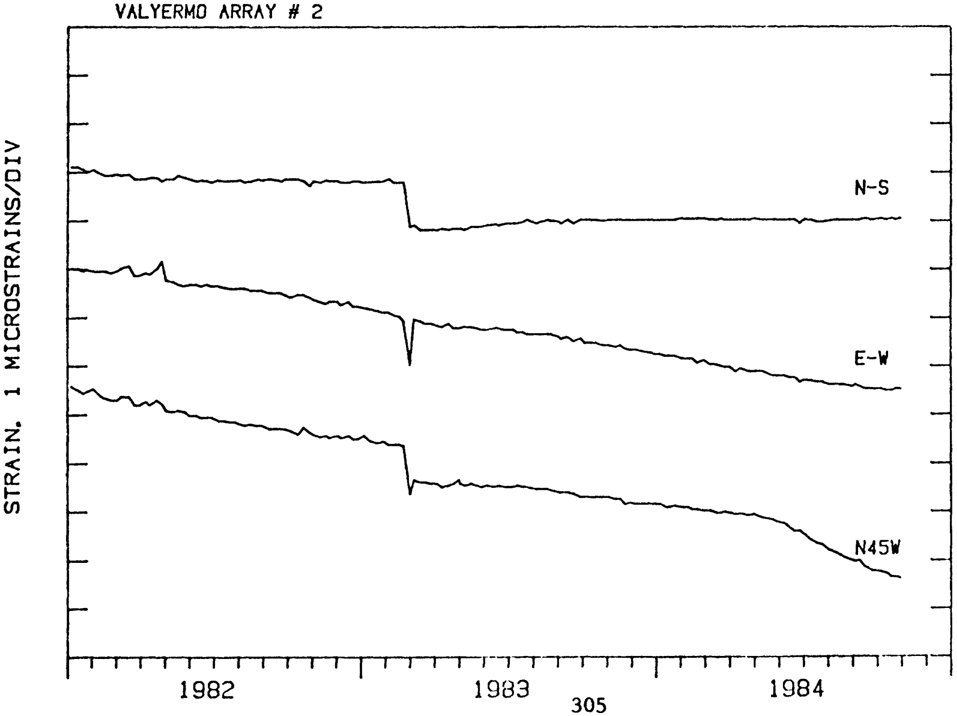
VALYERMO ARRAY # 2
STRAIN, 1 MICROSTRAINS/DIV
N-S
E-W
N45W
1982
1983
1984

P-2

SAN ANTONIO DAM ARRAY # 1

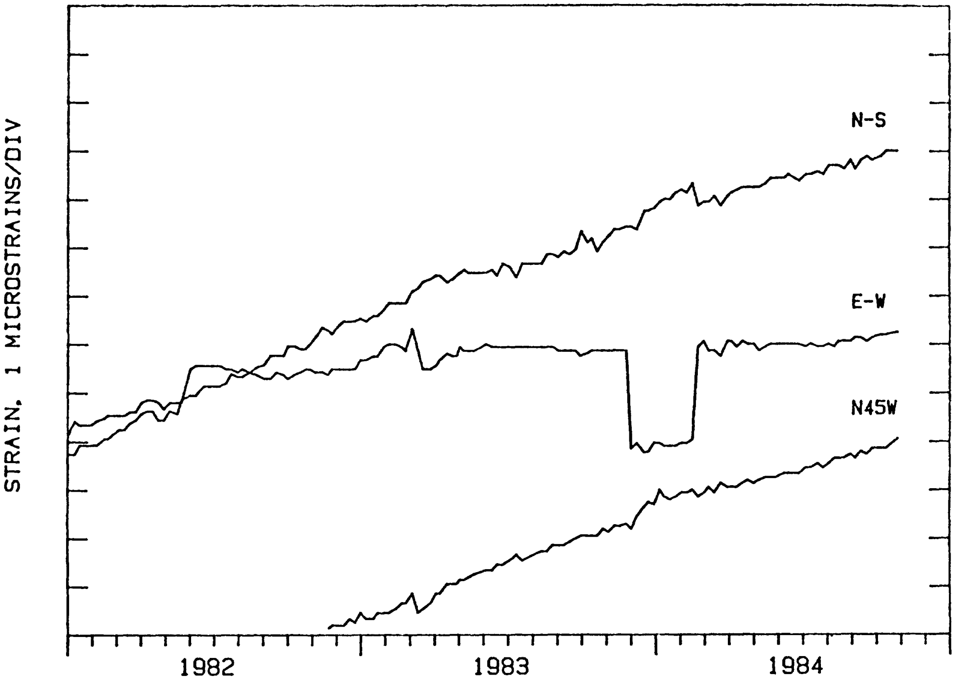

SAN ANTONIO DAM ARRAY # 2

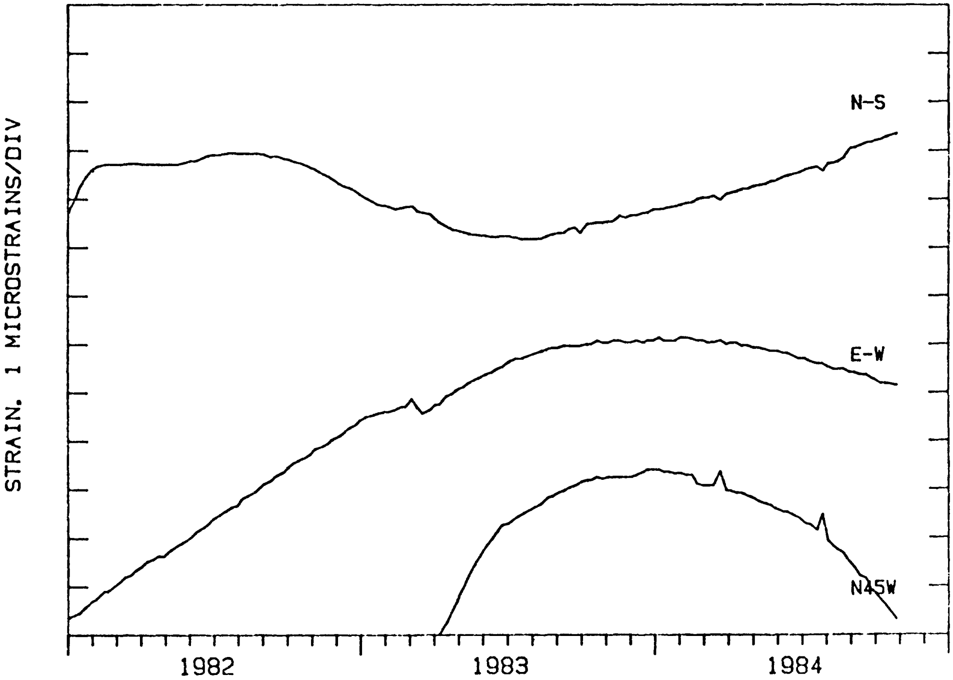

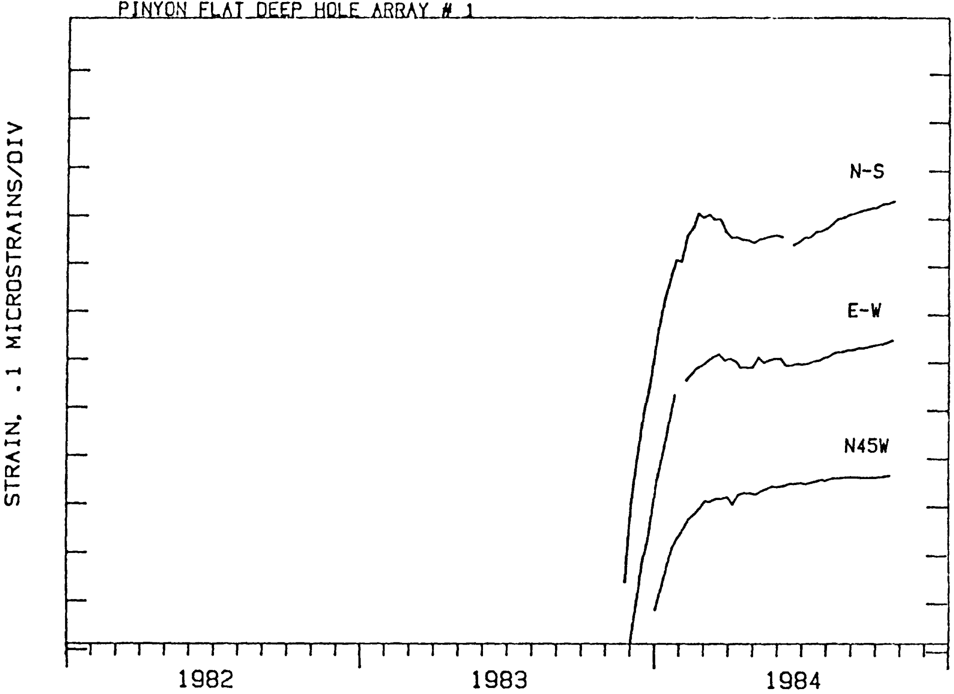
PINYON FLAT DEEP HOLE ARRAY # 1

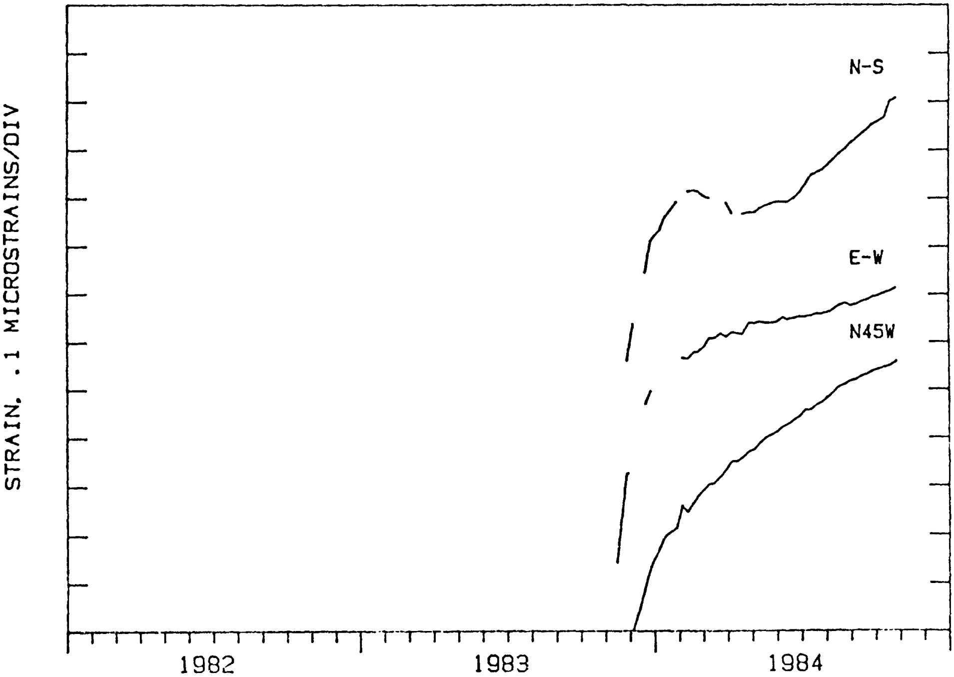
PINYON FLAT DEEP HOLE ARRAY # 2

Investigation of Radon and Helium as Possible Fluid-phase Precursors to Earthquakes

14-08-0001-21186

Y. Chung
Scripps Institution of Oceanography
University of California, San Diego
La Jolla, California 92093
(619) 452-6621

Investigations:

1. Monitoring radon, helium, and other geochemical parameters in a network of thermal springs and wells along the San Andreas, San Jacinto, and Elsinore faults, for possible percursory effects associated with earthquakes.

2. A general study of the relationships between these components, their origin, and variations which may be due to changes in flow rate of water, seasonal effects and meteorological factors.

3. Continuous radon monitoring at network sites with field-installed Continuous Radon Monitors (CRMs) for possible short-term anomalies that may be precursory to earthquakes.

4. Comparison study of long-term variations between the CRM and the discrete Rn data.

Results:

1. Discrete sampling and laboratory analyses of radon and helium at our Southern California network sites were carried out at monthly intervals for the last six months (April to September, 1984). No major earthquakes occurred in the network region during this period. Radon and helium at most of the sites were fairly constant at baseline levels.

2. Our discrete Rn and He data at the Arrowhead site show a monotonic decrease from a local peak in April toward the baseline in July. They have been at the baseline level since then. This concludes a period of one and a half years during which the Rn and He fluctuations are large and significantly above the baseline levels. Variations of this type were observed in 1979 when the Big Bear earthquakes occurred. Four earthquakes with magnitudes between 3.0 and 4.0 occurred nearby after the April peak. Rn and He are linearly correlated for the entire period.

3. The CRM variation at Arrowhead in 1984 is incomplete because the instrument often failed under the extremely humid and hot conditions in an underground cell during the summer months. Sporadic data collected during the last few months also indicate a systematic decrease from the April peak but only by about 15%. Direct comparison between the CRM and discrete Rn data in terms of concentration (dpm/ml) indicates that the Rn in the gas phase (CRM data) is enriched by a factor of 20 to 25 relative to the Rn dissolved in the water. Comparison of the CRM data between 1983 and 1984 indicates some similarity but the 1984 values are somewhat lower than 1983 values. The long-term CRM variations are smaller than the discrete Rn variations.

4. At Murietta Hot Springs where both the CRM monitoring and the discrete sampling for Rn and He are being carried out, weak correlation between the CRM and discrete Rn data may be observed: both increase from the beginning of the year to a maximum in April and May. However, the discrete Rn increases about 30% while the CRM Rn increases only about 20%. Rn and He variations as seen in discrete plots are quite parallel to each other for the entire monitoring years although He fluctuates more than Rn probably due to the fact that He sampling is more easily affected by trapped bubbles. On July 9, a swarm of events ($M \leq 3.2$) occurred about 30 km to the east of the Murrieta site. These events were preceded by significant Rn and He variations which show Rn and He maxima in April and May, minima in June, but maxima again in July and August. The water level dropped significantly after August, resulting in a total loss of bubble gas from the collector which feeds Rn into the CRM. Thus, no useful data have been collected since then.

5. In the Salton Sea area, Rn at the Hot Mineral Well shows much higher values during March and April probably due to a significant increase of trapped gas bubbles associated with a reduction of water flow (leakage of the well beneath the ground surface). Helium variation at the Hot Mineral Well is not correlated with Rn variation. At the Niland Slab Well southeast of the Hot Mineral Well, Rn has been constant at its baseline while He has decreased gradually to about 30% below its baseline values since mid-1983.

6. Along the San Jacinto fault zone, both the Indian Canyon and Robison's Well sites show some significant variations in both Rn and He during late 1983 and the beginning of 1984. These variations might have been associated with an earthquake ($M= 4.3$) which occurred about 6 km away from the Robison's Well on February 29, giving a lead time of about two months. No significant Rn and He variations have been observed at other network sites during the report period.

Theodolite Measurements of Creep Rates on San Francisco Bay Region Faults

Contract No. 14-08-0001-21260

Jon S. Galehouse
San Francisco State University
San Francisco, CA 94132
(415) 469-1204

We began measuring creep rates on San Francisco Bay region faults in September 1979. Amount of slip is determined by noting changes in angles between sets of measurements taken across a fault at different times. This triangulation method uses a theodolite set up over a fixed point used as an instrument station on one side of a fault, a traverse target set up over another fixed point used as an orientation station on the same side of the fault as the theodolite, and a second traverse target set up over a fixed point on the opposite side of the fault. The theodolite is used to measure the angle formed by the three fixed points to the nearest tenth of a second. Each day that a measurement set is done, the angle is measured 12 times and the average determined. The amount of slip between measurements can be calculated trigonometrically using the change in average angle.

We presently have theodolite measurement sites at 20 localities on faults in the Bay region. Most of the distances between our fixed points on opposite sides of the various faults range from 75-215 meters; consequently, we can monitor a much wider slip zone than can be done using standard creepmeters. The precision of our measurement method is such that we can detect with confidence any movement more than a millimeter or two between successive measurement days. We remeasure most of our sites about once every two months.

The following is a brief summary of our results thus far:

Seal Cove-San Gregorio fault - We began our measurements on the Seal Cove fault in Princeton, San Mateo County, in November 1979. For the next five years, the Seal Cove fault showed net movement at a rate of less than a millimeter per year in a right-lateral sense. However, details regarding the tectonic slip are difficult to ascertain because of seasonal effects involving apparent left-lateral slip that occur toward the end of each calendar year.

Various logistic problems have occurred at our site across the San Gregorio fault near Pescadero in San Mateo County. At the present time we are unable to determine whether or not the fault is creeping.

San Andreas fault - In the 4.6 years since March 1980 when we began our measurements across the San Andreas fault in South San Francisco, virtually no net slip has occurred. This indicates that the San Andreas

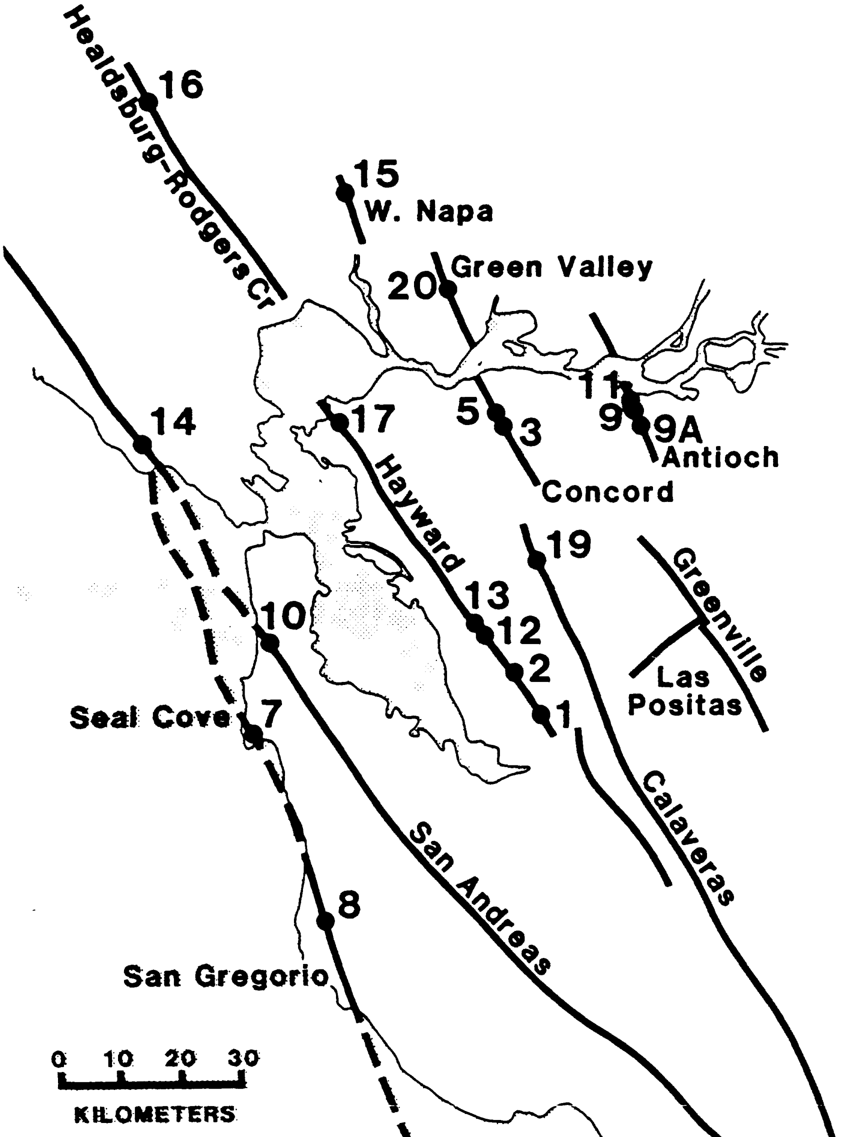

SAN FRANCISCO STATE UNIVERSITY
FAULT MEASUREMENT SITES

fault is locked in the San Francisco area. Our site in the Point Arena area has averaged slightly more than one millimeter per year of right-lateral slip in the three years from January 1981 to January 1984.

Calaveras fault - We have three measurement sites across the Calaveras fault and the nature and amount of movement are different at all three. We began monitoring our site within the City of Hollister in September 1979. Slip along this segment of the Calaveras fault is quite episodic, with times of relatively rapid right-lateral movement alternating with times of little net movement. For the past five years, the fault moved at a rate of about 8 millimeters per year in a right-lateral sense.

At our site across the Calaveras fault on Wright Road just 2.3 kilometers northwest of our site within the City of Hollister, the slip is much more steady than episodic. In the five years from October 1979, the Calaveras fault at this site has been moving at a rate of about 14.5 millimeters per year in a right-lateral sense, the fastest rate of movement of any of our sites in the San Francisco Bay region.

U.S.G.S. creepmeter results in the Hollister area are quite similar to our theodolite results. Creepmeters also show a faster rate of movement at sites on the Calaveras fault just north of Hollister than at sites within the City of Hollister itself.

The rate of movement is much lower at our site in San Ramon, near the northwesterly terminus of the Calaveras fault. Only about one millimeter per year of right-lateral slip has occurred during the past four years.

The epicenter of the 24 April 1984 Morgan Hill earthquake occurred on the Calaveras fault between our Hollister area sites which are southeast of the epicenter and our San Ramon site which is northwest of it. No surface displacement associated with the earthquake appears to have occurred at any of our three sites and no unusual movement occurred prior to it.

Rodgers Creek fault - In nearly four years from August 1980 to July 1984, the Rodgers Creek fault in Santa Rosa has slipped at a rate of about 1.7 millimeters per year in a right-lateral sense. However, our results show large variations in the amounts and directions of movement from one measurement day to another. These are probably due to seasonal and/or gravity-controlled mass movement effects, not tectonic slip.

West Napa fault - In the four years from July 1980 to July 1984, the West Napa fault in the City of Napa has shown very little net slip. Similarly to our results for the Rodgers Creek fault, however, large variations up to nearly a centimeter have occurred in both a right-lateral and a left-lateral sense between measurement days. The magnitude of these nontectonic effects is obscuring any tectonic slip that may be occurring. We hope that continued monitoring of these North Bay faults over a longer period of time will help clarify the situation.

Green Valley fault - We recently (mid-June 1984) established a new site on the Green Valley fault north of Suisun Bay. Preliminary results after only one remeasurement in mid-October 1984 indicate a few millimeters of right-lateral slip.

Hayward fault - We began our measurements on the Hayward fault in late September 1979 at sites in Fremont and Union City. During the past five years, the average rate of right-lateral slip has been about 4.6 millimeters per year in Fremont and about 4.3 millimeters per year in Union City.

We began measuring two sites within the City of Hayward in June 1980. In the 4.3 years since then, the average rate of right-lateral movement has been about 4.7 and about 4.2 millimeters per year.

We began measurements in San Pablo near the northwestern end of the Hayward fault in August 1980. For the past 4.2 years, the average rate of movement has been about 4.8 millimeters per year in a right-lateral sense. However, superposed on this overall slip rate are changes between some measurement days of up to nearly a centimeter in either a right-lateral or a left-lateral sense. Right-lateral slip tends to be measured during the first half of a calendar year and left-lateral during the second half.

Our theodolite triangulation results for the Hayward fault are quite comparable to those determined by U.S.G.S. creepmeters. The Hayward fault appears to be creeping at a rate of about four and one-half millimeters per year, making it the second fastest creeping fault in the San Francisco Bay region. Only the Calaveras fault in the Hollister area is moving faster.

Concord fault - We began our measurements at two sites on the Concord fault in the City of Concord in September 1979. Both sites showed about a centimeter of right-lateral slip during October and November 1979, perhaps the greatest amount of movement in a short period of time on this fault in the past two decades. Following this rapid phase of movement by about two months were the late January 1980 Livermore area moderate earthquakes on the nearby Grenville fault.

After the relatively rapid slip on the Concord fault in late 1979, both sites showed relatively slow slip for the next four and one-half years at a rate of about one millimeter per year right-lateral.

However, in late Spring-early Summer 1984, both sites again moved relatively rapidly, slipping about seven millimeters in a right-lateral sense in a few months. The rate has again slowed since late August (through mid-October 1984). Whether or not this unusual behavior on the Concord fault portends another San Francisco East Bay earthquake remains to be seen.

Antioch fault - We began our measurements at the more southeasterly of two original sites on the Antioch fault in the City of Antioch in January 1980. During the next 27 months, we measured a net right-lateral displacement of nearly two centimeters. However, large changes in both a right-lateral and a left-lateral sense occurred between measurement days. Three times left-lateral displacement occurred toward the end of one calendar year and/or beginning of the next. We abandoned this site in April 1982 because of logistic problems and relocated it just southeast of the City of Antioch in November 1982. In the 1.8 years until September 1984, the fault at this new site has had a net movement of about 2.6 millimeters in a right-lateral sense.

The more northwesterly of our original sites on the Antioch fault is located where the fault zone appears to be less specifically delineated. In the 4.4 years from May 1980 to September 1984, we have measured an average of about two millimeters per year of left-lateral slip. Much subsidence and mass movement creep appear to be occurring both inside and outside the Antioch fault zone and it is probable that these nontectonic movements have influenced our theodolite results. However, a recent (1984) trench across the Antioch fault within the City of Antioch showed soil horizons also offset in an apparent left-lateral sense.

DEEP BOREHOLE PLANE STRAIN MONITORING

14-08-0001- 21228

Michael T. Gladwin
Department of Physics
University of Queensland
St. Lucia
Australia 4067.

INVESTIGATIONS

An instrument capable of unattended deep borehole measurement of vector plane strain to 0.3 nanostrain has been developed and deployed at two sites in California. Response is from DC to 10 Hz on any single channel, dynamic range is approximately 10-4 in strain and total linearity better than 0.004%. The instrument is particularly relevant in California where shear strains dominate deformations, and provides a new dimension in continuous borehole deformation monitoring.

Normally, the instrument consists of seven independent modules of length 170 mm. Three measure strain in a plane perpendicular to the axis of the instrument. A further two measure tilt from the axis of the instrument, one component measures instrument azimuth by magnetic compass and the final component is a non-deforming reference cell. The instrument, of diameter 125mm, is cemented into 175 mm diameter boreholes at a target depth of 200 m. using expansive grout similar to that of the Sacks-Everton instrument to provide preload of the instrument. Strain is monitored using measurements of three instrument diameters spaced 120 degrees apart. The otherwize identical non-deforming reference cell is used to monitor the performance of the instrument cable and the surface electronics to guarantee the level of precision and long term stability. No tilt modules were deployed in these initial installations. The borehole is filled with the grout for some meters both sides of the instrument to produce a near homogeneous inclusion, and the hole is cemented to the surface to minimize groundwater and thermal contamination.

Operation is controlled by a microprocessor (RCA 1802), which sequences the transducers through measurement electronics common to all sensors. Gain and DC offsets for each channel are measured as a separate operation, and these parameters are used in production of a high stability data stream which is transmitted every three hours via a satellite link to the data retrieval centre at Menlo Park, California. Selected data is also printed on site for backup.

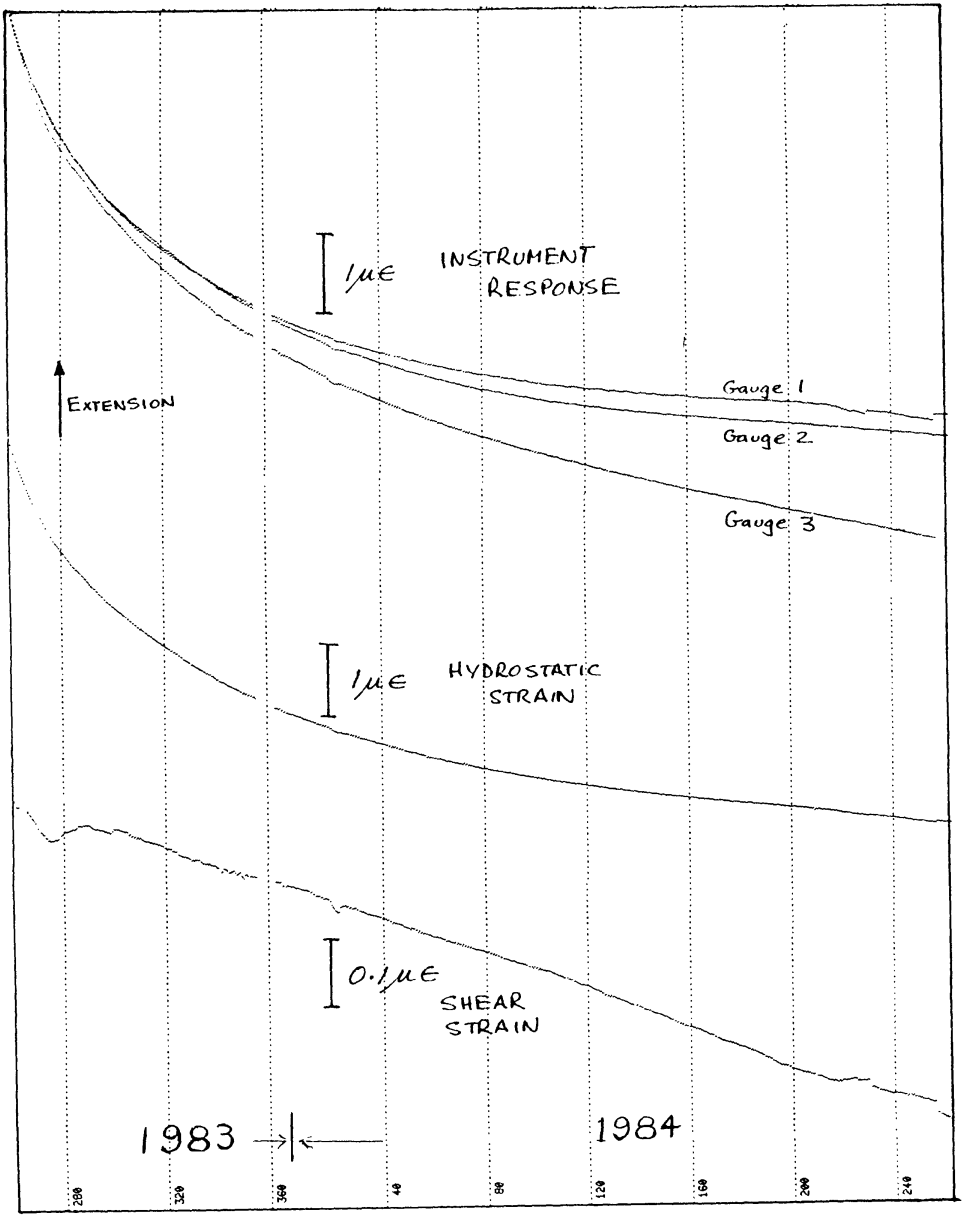

FIGURE 1. Strain measurements at Pinon Flat since installation. The upper three curves show the gauge responses, followed by the calculated hydrostatic and shear responses. Note that the scale for the shear (lower) plot indicates that the accumulated shear in the year since installation is less than 0.5 microstrain.

RESULTS

One instrument was installed at the Pinon Flat Geophysical Observatory at a depth of 151m in competent granite and was operational by September 16,1983. This location was chosen for direct comparison of the strain measurements with both the long baseline interferometer spanning the site (Wyatt(1982), Berger and Lovberg(1970)), and with a pair of DTM Carnegie Institution of Washington Sacks-Everton strain meters within 100m. The axis of gauge 2 was at 5 degrees east of North, with gauge 1 at 65 degrees east of North, and gauge 3 at 125 degrees east of North.

Figure 1 shows the results of strain measurements since installation. A volumetric compression over this period of order 5.6 microstrain is attributed to curing of the grout, with a time constant of order 6 months. During this period a constant rate of shear of less than 0.5 microstrain per year is evident. These strains are calculated from the observed instrument response, corrected by instrument response factors as calculated in Gladwin and Hart(1984), using estimates of grout and rock properties. This rate is comparable with rates obtained with Geodolite network measurements (Prescott et al,1979,or King and Savage, 1983). It should be noted that this low strain rate was established within two months of installation. This high common mode rejection of hydrostatic noise sources associated with installation procedures is a major advantage of the present instrument design.

Since initial installation, the data has shown excellent resolution of solid earth tides which in this location have amplitude of about 0.05 microstrain. Figure 2 shows the response of each gauge with a simple exponential compression caused by the curing of the grout removed. These are compared with theoretical plots of tide at corresponding azimuths, obtained using a time-series program package of D.Agnew. The lower amplitude on the gauge at 65 degrees east of north is similar to a reduced amplitude in the E-W long-baseline interferometer data from Pinon Flat (Wyatt,Private communication). The tidal phase observed on G2 (at 5 degrees east of north) also agrees well with the N-S results from that data set.

The second installation was at San Juan Baptista at a depth of 130 m in the close proximity of the multi-frequency laser ranging site and several USGS strain monitoring sites. The installation was completed on 1st October,1983, within five days of the completion of the drilling. For this site gauge 3 was oriented 25 degrees east of North, with gauge 2 and gauge 1 at 85 and 145 degrees east of North respectively.

Figure 3 shows the response of this site, which contrasts very strongly with the post installation behaviour at Pinon Flat. The traces indicate a very normal grout curing compression, on which is superimposed a very large shear, indicating the recovery of the pre-existing shear which was stress relieved during drilling. This post relief recovery is commonly observed following overcoring stress measurements (M.F.Lee, private communication). The amplitudes of the strain signals at this site are well above those expected from the grout parameters. The site was in a poorly sorted sandstone with high clay content. The procedure of rapid

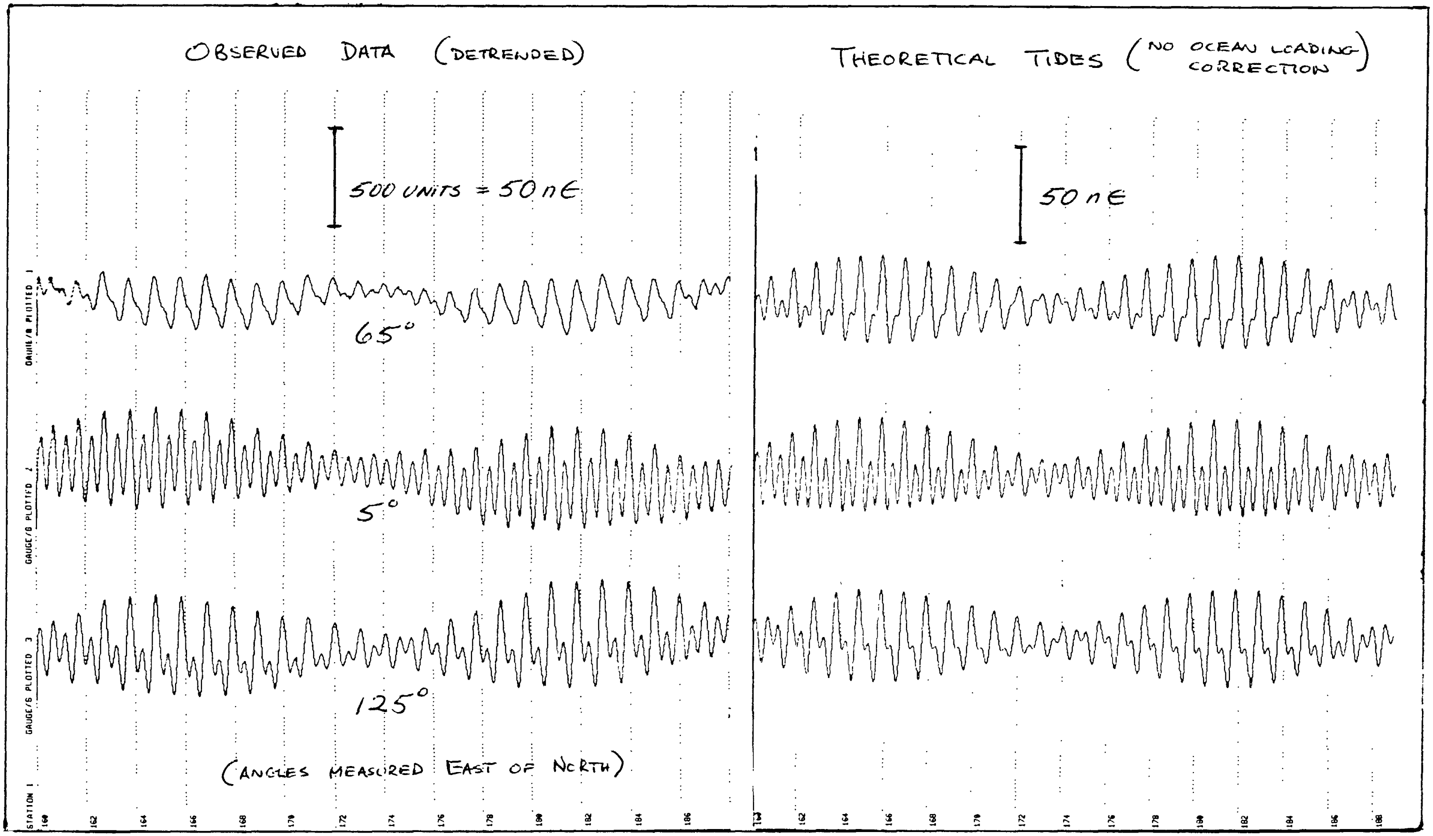

FIGURE 2. An earth tide record observed for the three gauges at Pinon Flat with the effect of grout curing removed. These are to be compared with the tides calculated theoretically for the same orientations, as shown on the right. Calibration is by comparison with selected data from UCSD laser strainmeter.

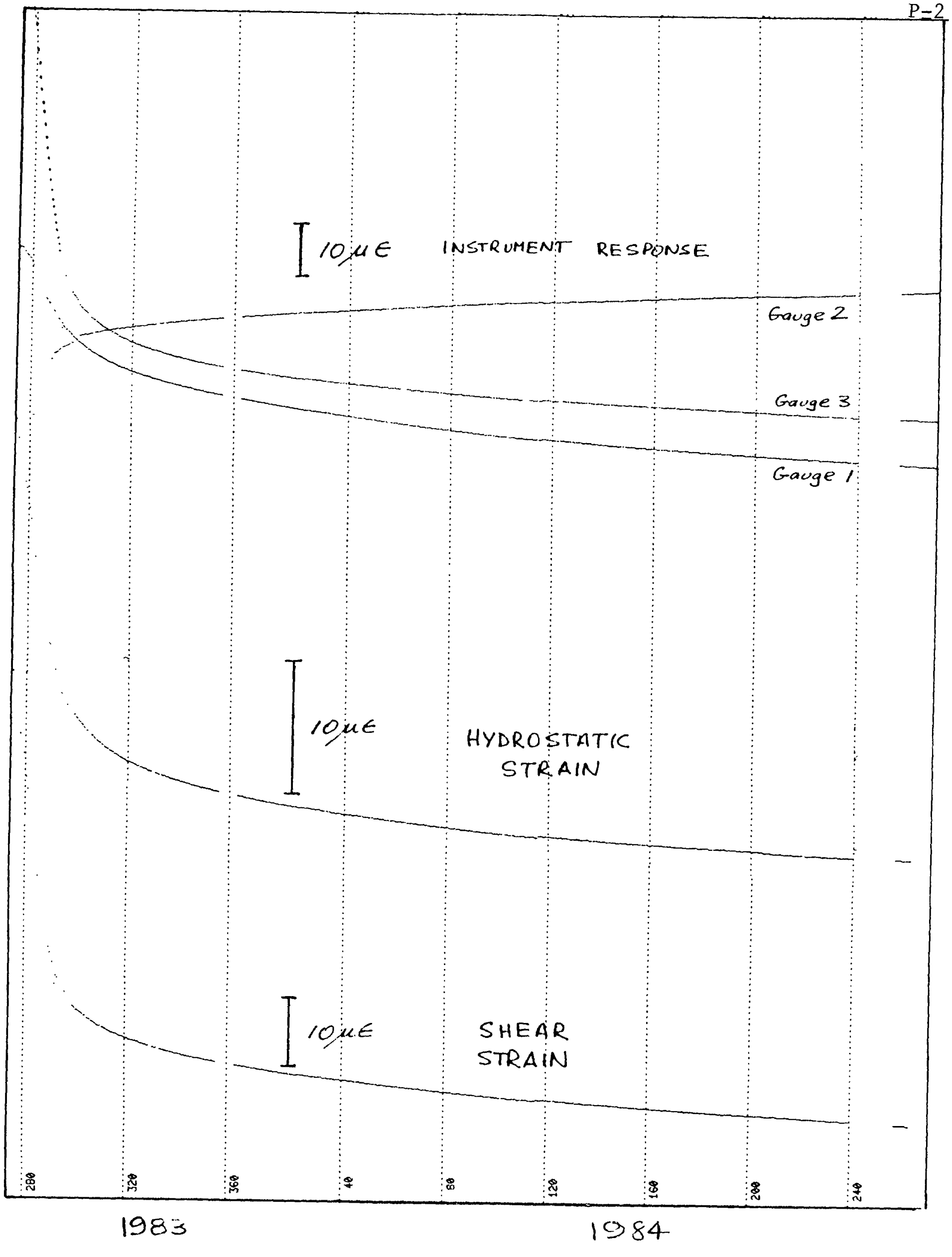

FIGURE 3. Strain measurements at San Juan Baptista since installation. The upper three curves show the gauge responses, followed by the calculated hydrostatic and shear responses. Calibration is uncorrected for site response.

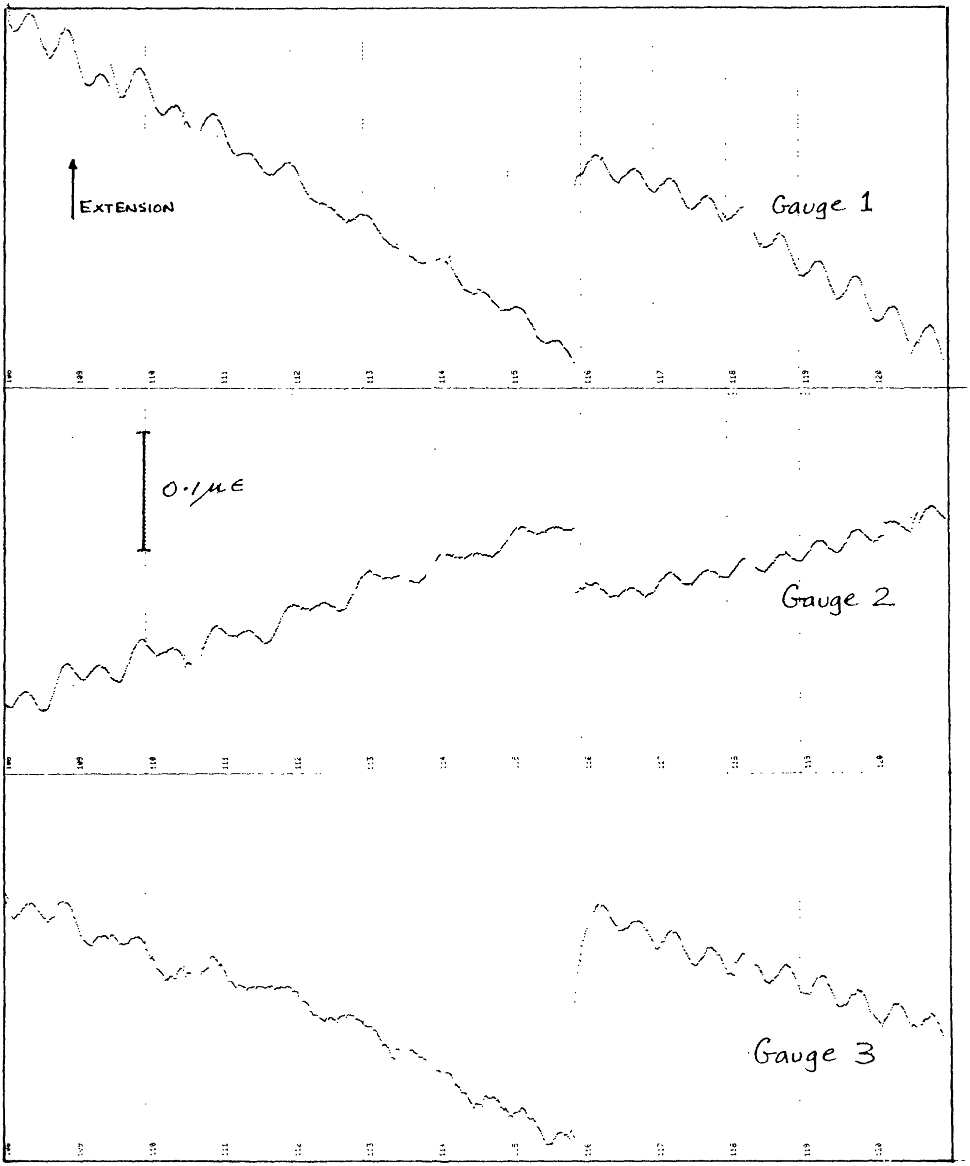

FIGURE 4. The response of the gauges of the instrument at San Juan Baptista to the Morgan Hill earthquake on 24 April,1984.

implementation of shear strain instrumentation following drilling allows an estimate of the initial state of stress of the region, without in any way preventing use of the installation for long term high resolution continuous monitoring. All three components are showing normal tidal signals with correct phase angles indicating proper coupling on each component. Tidal amplitudes indicate that the surrounding rock has quite low elastic modulii , so that the instrument is considerably harder than the host environment. Core samples were not available prior to fabrication to match the instrument/grout combination to the host environment.

Response of this instrument to the Morgan Hill earthquake (24 April,1984) is shown in Figure 4. Inversion of this response gives a shear of 0.03 microstrain, with the axis of maximum compression in an east-west direction. The sense of this shear is opposite to that of the accumulating shear for this site (as calculated from the long term data).

GLADWIN, M.T. (1984) High Precision Multi-Component Borehole Deformation Monitoring. (Accepted for publication in Rev. Sci. Inst.).

GLADWIN, M.T. and HART, R. (1984) Design Parameters for Borehole Strain Instrumentation. (in press)

Deepwell Monitoring along the Southern San Andreas Fault

14-08-0001-21879

Thomas L. Henyey and Steve P. Lund
Department of Geological Sciences
University of Southern California
Los Angeles, CA 90089-0741
(213) 743-6123

Investigations

We have monitored the variation in water level and temperature within an array of deep wells near the southern San Andreas fault (figure 1) for more than five years. Our data show no variations during 1984 that might be considered anomalous or related to potential seismic activity along the San Andreas fault.

Results

Short-Term Anomalies: We have noted in the past occasional water level anomalies, greater in amplitude than the solid-earth tidal and atmospheric pressure responses, that are coseismic with large earthquakes from California. The anomalies are characterized by quick (few hours) rise or drop in water level followed by long delays (few weeks) back to the pre-anomaly water level. The most recent example occurred at Phelan coseismically with the Coalinga earthquake. We have not identified anomalies of this waveform type in 1984.

Long-Term Anomalies: We have noted for several years that different portions of the array have distinct seasonal to multi-year water level variation. Water levels in the northwestern portion of the array have continuously risen or lowered between 1980 and 1983 (Figure 2), while water levels in the southwestern portion have oscillated on a yearly basis (in response to seasonal rainfall) or remained somewhat static. These patterns have continued in all wells through August, 1984 (Figure 5). A new site, Roberts well, within the San Andreas fault zone is similar to other northwestern sites in that it appears to have a long term trend in the water level. However, here the water level is dropping rather than rising. Until more is understood about the individual wells, i.e. what aquifers are tapped and what is their regional extent, it is impossible to attribute these variations to any fault related behavior.

Low-Amplitude Anomaly Detection: We are attempting to remove the water level variation that is induced by solid-earth tidal and atmospheric pressure variations, so that subtler potential water level anomalies can be detected. At present, we have not been able to satisfactorily remove all apparent periodic components from test data sets. We are beginning to evaluate whether our instrumentation is a possible source of noise in the water level variation that has been unnoticed without time series analysis.

Related Seismicity: Increased microseismic activity has occurred over the last year on the south side of the San Andreas fault near the center of the Palmdale array (Figure 3). The magnitudes of the earthquakes are all less than 3.0, and no apparent water level anomaly (greater than solid-earth tidal or atmospheric pressure induced variations) has been associated with the activity. The small magnitude of the earthquakes makes the lack of related water level variation unimportant, but it does raise an important issue. None of our water wells is located on the south side of the San Andreas Fault. It is certain that the ground water patterns on the south side of the fault will be quite different from those we observe on the north side of the fault. It is therefore important that we add suitable sites on the south side of the fault be the future.

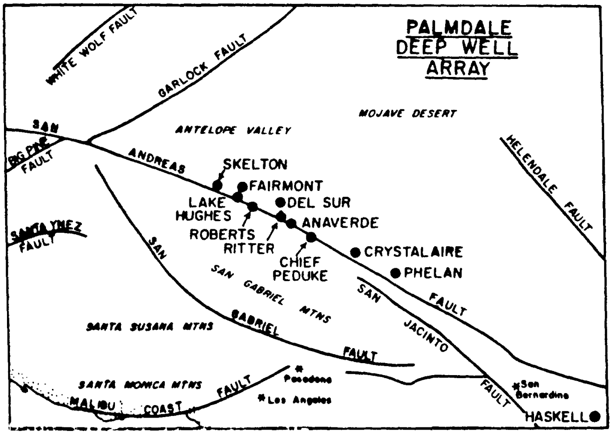

Figure 1: Location map for the Palmdale Deep Well Array.

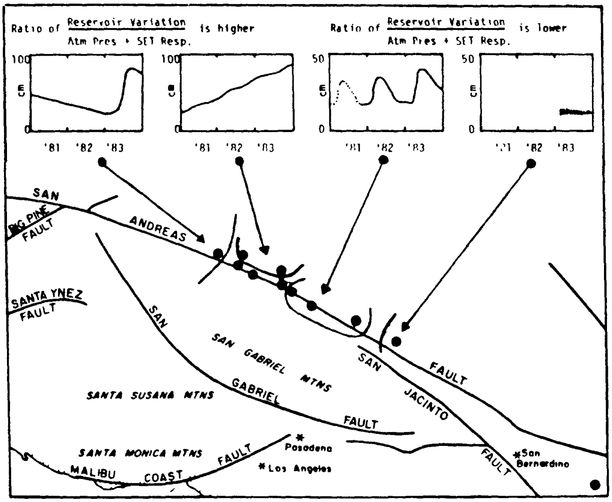

Figure 2: Long term water level trends in the Palmdale region for 1981 to 1983. These trends persist through August, 1984.

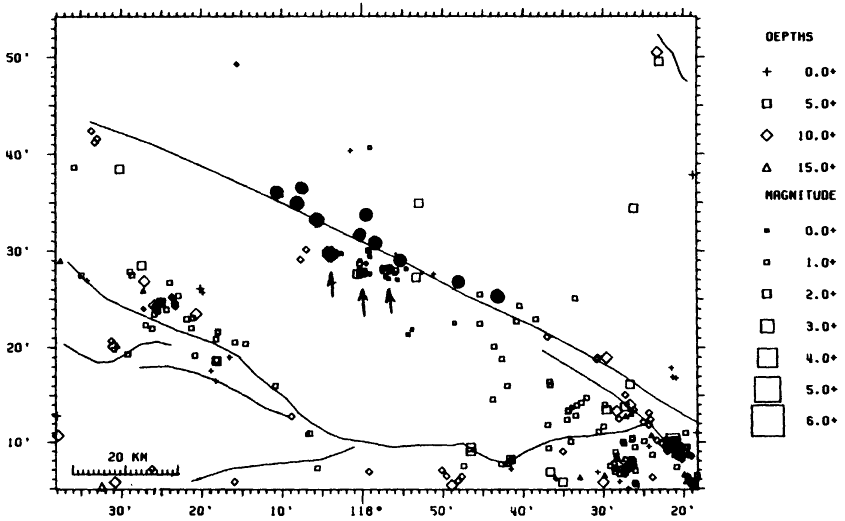

Figure 3: Seismicity near the Palmdale Array for September, 1983 to August, 1984. Three centers of microseismic activity (shown by arrows) occur within the array. Their magnitudes are below 3.0, and none of the wells record apparent variation that can be related to this activity.

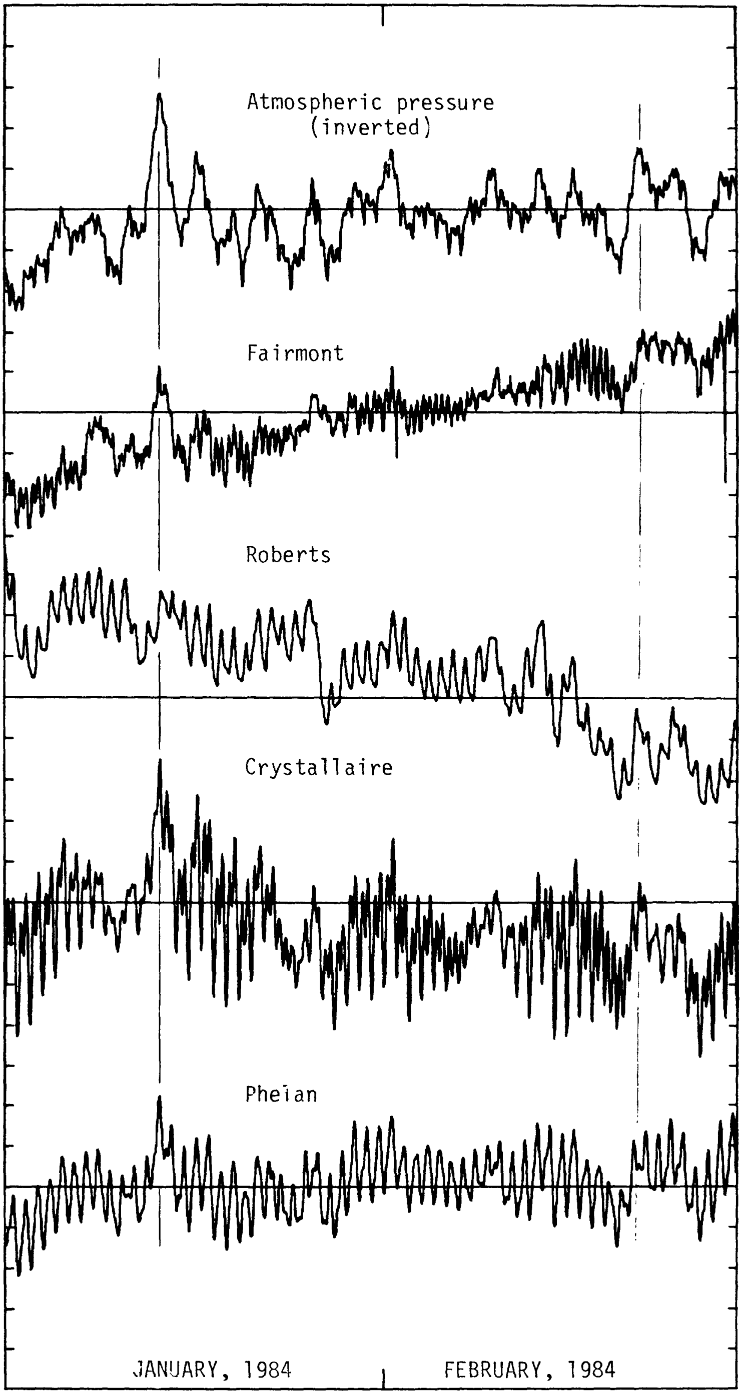

Figure 4: Hourly averaged water level variation for four typical wells compared to the Atmospheric pressure variation recorded at Roberts well.

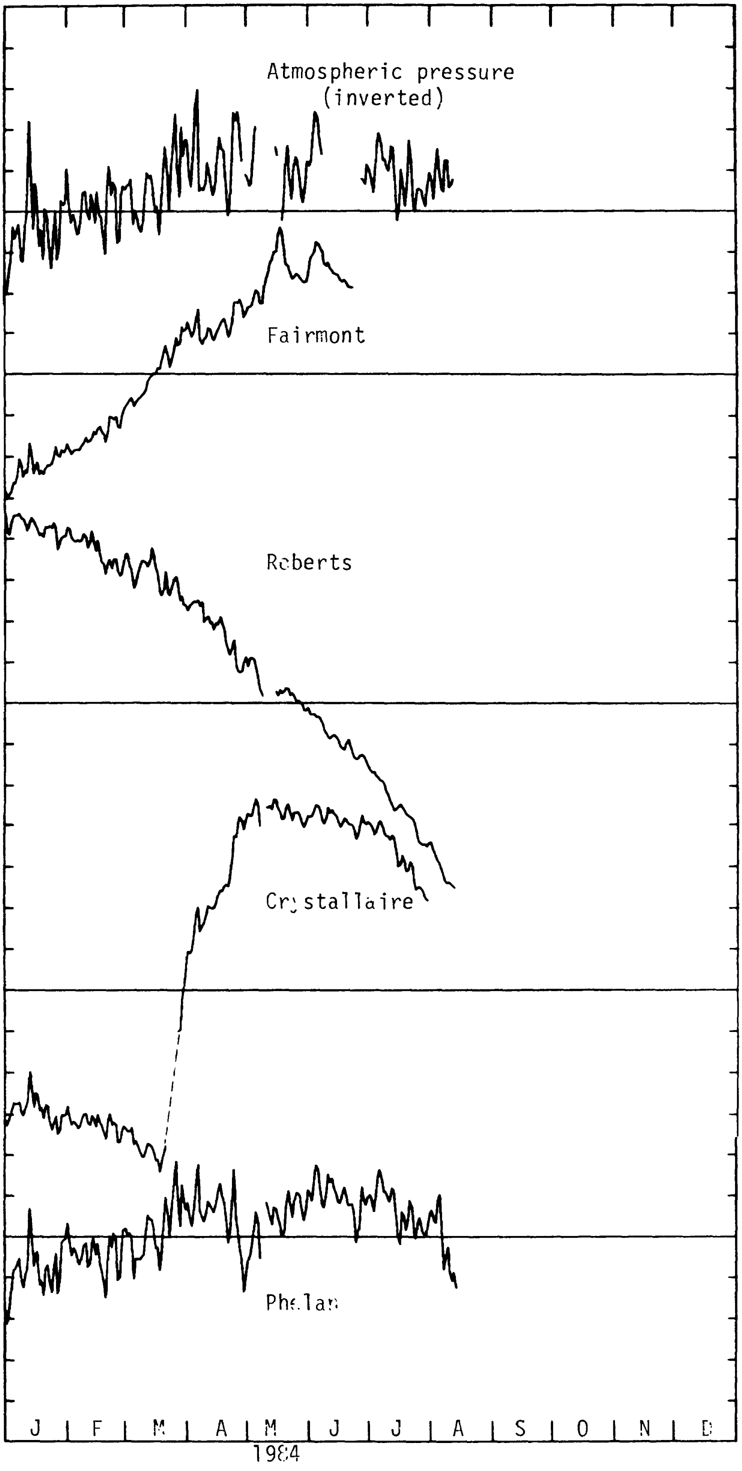

Figure 5: Daily averaged water level variation for four typical wells

Low Frequency Data Network

J. Herriot, K. Breckenridge, S. Silverman
Branch of Tectonophysics
U. S. Geological Survey
Menlo Park, California 94025
415/323-8111, ext 2932
October 15, 1984

9960-01189

Investigations

[1] Real-time monitoring, analysis, and interpretation of tilt, strain, creep, magnetic, and other data within the San Andreas fault system and other areas for the purpose of understanding and anticipating crustal deformation and failure.

[2] Compilation and maintenance of long-term data sets free of telemetry-induced errors for each of the low frequency instruments in the network.

[3] Development and implementation of graphical display systems for the purpose of monitoring seismic and surface deformation activity in real-time.

[4] Installation of satellite-based telemetry system for reliable real-time reporting and archiving of crustal deformation data.

Results

[1] Data from low frequency instruments in Southern and Central California have been collected and archived using the Low Frequency Data System. In the six months three million measurements from 125 channels have been received and subsequently transmitted on the Low Frequency 11/44 UNIX computer for archival and analysis.

[2] A major effort of the project has been to provide Real-time monitoring of designated suites of instruments in particular geographical areas. Terminals are dedicated to real-time color graphics displays of seismic data plotted in map or cross-sectional view or low frequency data plotted as a time series. During periods of high seismicity these displays are particularly helpful in watching seismic trends. This system was appreciated in the recent Morgan Hill earthquake.

[3] In November, 1983, Stan Silverman went to Reston to install the real-time graphics monitoring system there. Thus seismic activity at Mammoth and other active areas can now be displayed directly in Reston.

[4] Work continues on a creep alarm system. When finished creep events will be detected automatically as they occur and personnel can be contacted by radio pager or beeper.

[5] New software was written to improve access to the low Frequency data set for the uninitiated. Our goal is to facilitate access to the data without requiring any special training on our tools.

[6] The project continues to operate a configuration of one PDP 11/44 computer running the UNIX operating system and two PDP 11/03 running real-time data collection software. This 11/44 has been operational as our analysis machine with less than 1% down time. The two 11/03 machines operate redundantly for robustness. Accordingly, our real-time collection has had 0% down time.

[7] An additional DEC PDP 11/23 or comparable computer is being added to the present configuration for the purpose of collecting satellite telemetry data. The new computer is for satellite telemetry what the 11/03 systems are for telephone-based telemetry. Once fully operational the new system will be made redundant.

[8] A 5-meter satellite receiver dish was installed in Menlo Park for retrieval of real-time surface deformation data from Alaska to California, even the South Pacific islands. The GOES-6 geostationary satellite together with transmit and receive stations makes possible a greatly improved telemetry system. This new system is provided enhanced data quality as well as more flexibility in locating instruments over the old telephone-based telemetry system.

[9] Software has been developed to control and collect data from the newly installed ground receiving station in Menlo Park. The project has developed special purpose table-driven software which is very flexible with regard to adding and changing instrument and platform configurations while still being efficient on a small PDP 11/23 or equivalent computer.

[10] The data from the Network have been made available to investigators in real time. Data only minutes old can be plotted. Events such as creep events can be monitored while they are still in progress.

[11] The working prediction group of the Branch has made extensive use of the timely plots which are produced routinely by the project.

[12] The project continues to develop color graphics and color hardcopy capabilities for use in real-time seismic displays. Using the advanced graphics software with color graphics devices we have demonstrated our real-time seismic and low frequency data monitoring ability to visiting government officials, scientific investigators, and public interest groups.

[13] In October Jim Herriot lead a four person team to install real-time seismic and related software on a PDP 11/44 computer in China for the Beijing Seismic Network.

Reports

Johnston, M. J. S., Silverman S. A., and Breckenridge, K., 1984, Secular Variations and its Variations: EOS (Trans. Am. Geophys. Un.), v. 65, p. 203.

Repeat Gravity Studies

9380-03074

Robert C. Jachens and Carter W. Roberts
Branch of Geophysics
U.S. Geological Survey, MS 989
Menlo Park, CA 94025
(415) 323-8111, x4248

Investigations

1) Remeasured southern California precision base station network in May, including remeasurement of station at the Holcomb Ridge 2-color geodimeter site. Surveys coincided with measurements of areal strain by James Savage at sites along the San Andreas fault.

2) We again attempted to determine sources of short-term "drift" in LaCoste and Romberg gravimeters, one of two major error sources in repeat gravity observations.

3) Conducted a detailed areal gravity survey of about 240 stations in Long Valley caldera, California, primarily within the area of the south moat.

Results

1) The latest temporal gravity surveys in southern California show a continuing pattern of low-amplitude, short-period gravity fluctuations. No clearly anomalous gravity changes were seen in the most recent survey results.

2) Short-term daily "drift" experienced by all LaCoste and Romberg gravimeters is one of the two largest error sources in repeat gravity measurements made with spring-suspension gravimeters. Based on discussions with Lucien LaCoste, a likely cause of this "drift" is internal temperature fluctuations that arise when the gravimeters are operated in ambient temperatures that are close to their thermostat settings, situations that arises frequently in southern California. LaCoste and Romberg, Inc. currently is installing a modified temperature control system that may alleviate this problem.

3) A detailed gravity survey of a 20 km long portion of the south moat of Long Valley caldera has revealed 4 gravity highs of about 3-5 mGal amplitude spaced at about 5 km intervals along the base of the steep, linear gravity gradient which marks the south edge of the caldera. The two westernmost highs coincide with areas of recent earthquake swarms. A minimum source volume of 1.4 km^3 is required to account for each of these two anomalies even assuming a density contrast of 0.8 g/cm^3. Because these volumes are much greater than those associated with the recent deformation we believe that the gravity anomalies are caused by old, localized magma intrusions in the south moat.

Reports

1) Jachens, R. C., 1984, Vertical crustal motion based on gravity measurements: abstract for American Geophysical Union, Chapman Conference on Vertical Crustal Motion, Harpers Ferry, West Virginia, October 22-26, 1984, (in press).

2) Jachens, R. C., and Roberts, C. W., Temporal and areal gravity investigations at Long Valley caldera, California: (submitted to JGR)

3) Roberts, C. W., and Jachens, R. C., 1984, Gravity evidence for prior igneous intrusion beneath the south moat of Long Valley caldera, California: Transactions American Geophysical Union (Eos), (in press).

TILT, STRAIN, AND MAGNETIC MEASUREMENTS

9960-02114

M.J.S. Johnston, R. Mueller, C. Mortensen
D. Myren, A. Jones and V. Keller
Branch of Tectonophysics
U.S. Geological Survey
345 Middlefield Road, MS/977
Menlo Park, California 94025
(415) 323-8111, ext. 2132

Investigations

1. To investigate the mechanics of failure of crustal materials using deephole and surface strainmeters, tiltmeters and arrays of absolute magnetometers.

2. To investigate real-time records of these and other parameters for indications of incipient failure of the earth's crust.

Results

1. Earth Strain in the Period Range 0.1 - 10,000 Seconds at Six Borehole Sites Within the San Andreas Fault System, California

To utilize the high sensitivity, the wide dynamic range and the broad bandwidth of deep borehole three-component and dilational strainmeters in the short period range (0.1 seconds to 10,000 seconds), 16-bit digital recorders (GEOS) have been used at six sites in California to record earth strain noise, nuclear explosions, and seismic events. Limited dynamic range and bandwidth of standard recorders have not permitted such recordings previously. The power spectral density estimates for earth noise are similar in general characteristics for each of the sites. With the exception of about 10 db of 6 second microseismic noise, they decrease from about -170 dB at increasing frequency at about 10 dB per decade. Peak power in strain seismograms of local earthquakes and nuclear explosions occurs between 0.1 and 1 Hz. Detection of possible pre-rupture strains at the 10^{-10} strain level appears feasible in this period range.

2. Strain Episodes on the San Andreas Fault Following the April 24 Morgan Hill, California Earthquake

Static deformation followed by a strain episode on the San

Andreas fault were recorded on a cluster of borehole and surface strain monitoring instruments near San Juan Bautista following the April 24, Morgan Hill earthquake (M 6.1). The instruments include one 3-component strainmeter and two dilatometers installed at a depth of about 200 m, and one 3-component surface instrument. The theoretical strain field obtained by modeling the earthquake as a southward propagating rupture with a moment of 2 x 10^{25} x 10^{25} dyne-cms, rupture length of 30 km, and a slip of 42 cm between the depths of 5 and 10 km, are in general agreement with the observations from the instruments. A strain episode was detected by most instruments fifteen days to twenty days after the earthquake and is most easily modeled by slip on the San Andreas fault to the south of the array where, ten days later, a moderate shallow earthquake occurred.

3. Local Magnetic Fields, Uplift, Gravity, and Dilational Strain Changes in Southern California

Changes in regional magnetic field during gravity, strain and level surveys near the San Andreas fault at Cajon, Palmdale and Tejon are strongly correlated with changes in gravity, areal strain, and uplift in these regions during a seven-year period. This correlation is determined primarily by data taken during 1978-79 and 1981-82. During this period the Palmdale uplift event occurred. Because the relationships between these parameters is in approximate agreement with those inferred from simple deformation models, the preferred explanation appeals to short-term strain episodes independently detected in each data set. Transfer functions from magnetic to strain, gravity, and uplift perturbations are obtained by least-square linear fits to the data. A less likely explanation appeals to coincidental behavior of a common source of meteorologically generated crustal noise in the strain, gravity, and uplift data and an independent but undetermined disturbance in the magnetic data.

4. Magnetic Field Observations in the Long Valley Caldera of East-Central California, 1976-1984

Differential magnetic field intensity measurements collected near the Long Valley Caldera of central-eastern California between 1976-1984 indicate anomalous long period variations of 0.8-1.0 nT/a. Incomplete cancellation of the earth's secular magnetic field could account for 50% of these observed variations. The remaining amount could be caused by thermal demagnetization and/or tectonomagnetic effects resulting from dike injection or shear loading of the magma chamber. Magnetic models indicate thermal demagnetization of crustal rock at depths between 2 km to 5 km below the Long Valley Caldera could produce long-term magnetic field variations from +2.0 nT to -0.8 nT. If the observed variations are due to stress induced tectonomagnetic effects, then a stress rate of 0.15-0.30 MPa/a is required and a total stress change of 1.2-2.4 MPa for the period 1976-1984.

5. Secular Variation, Crustal Contributions and Tectonic Activity in California, 1976-1984

Five to ten years of data from an array of 34 total-field magnetometers are used to define the temporal and spatial characteristics of secular variation throughout central and southern California. For this period, well determined rates of secular variation are obtained at each site. These rates are temporally linear but spatially variable, ranging from -45 nT/a near San Francisco to -54 nT/a near the Mexican border. Least-square analysis of all rate data indicates secular variation decreases in a general southeasterly direction according to $F=k_1*\nu+k_2*\psi+K$ where F is in nT/a, ν and ψ are the geographic latitude and longitude, and k_1, k_2 and K are 1.67±0.13 nT/a.degree, -0.16±0.10 nT/a.degree, and -127.1±0.2 nT/a, respectively. Deviations of as much as one nanotesla per year occur on scales of a few tens of kilometers. These apparent small scale secular variation anomalies result, in part, from differences in local induction and remanent magnetization and may be reduced by determination of a site transfer function. A planar surface fit to the corrected data has the form $F=k_1*\nu+k_2*\psi+K$ where k_1, k_2, and K are now 1.54±0.08 nT/a.degree, -0.18±0.06 nT/a.degree, and -124.5±0.1 nT/a, respectively. Residual field variations obtained after correction of all data for secular variation are most apparent on the San Andreas fault in southern California between Palm Springs and the Salton Sea and less so along the recent Coyote (M_L=5.9 of August 6, 1979) and Morgan Hill (M_L=5.8 of April 24, 1984) aftershock zones. These residuals could be explained by stress localization in these regions and, particularly in the case of the southern San Andreas anomaly, may indicate the location of a future damaging earthquake. Incomplete correction for complex site effects may be an alternative explanation. In the first large-scale test of global secular variation models we find that the models for this region do not predict either the amplitudes or the mean isogram directions of these data to better than several tens of nanoteslas per year and several tens of degrees, respectively. This may result from a failure to correct for site response effects at some observatories before using the data in global spherical harmonic expansions. Local magnetization response can therefore bias estimate of secular variation and yield apparent impulsive behavior when external fields are perturbed.

Reports

Gladwin, M. T., Johnston, M. J. S., 1984, Strain Episodes on the San Andreas Fault Following the April 24 Morgan Hill, California, Earthquake, Trans. A.G.U. (in press).

Johnston, M. J. S., 1983, The Need for Interactional Earthquake Instability Models, (abs) I.U.G.G. Hamburg, Germany, 15-27 August, p. 151.

Johnston, M. J. S., 1984, Deep Creep, Earthquake Notes, v. 55, p. 19.

Johnston, M. J. S., 1984, Local Magnetic Fields, Uplift, Gravity and Dilational Strain Changes in Southern California, Trans. A.G.U. (in press).

Johnston, M. J. S., and Borcherdt, R. D., 1984, Earth Strain in the Period Range 0.1 - 10,000 Seconds at Six Borehole Sites Within the San Andreas Fault System, Trans. A.G.U. (in press).

Johnston, M. J. S., Silverman, S. A., and Breckenridge, K., 1984, Secular variations and its variations: EOS (Trans. Am. Geophys. Un.), v. 65, p. 203.

Johnston, M. J. S., Silverman, S. A., Mueller, R. J., and Breckenridge, K. S., 1984, Secular Variation, Crustal Sources and Tectonic Activity in California, 1976-1984, J. Geophys. Res. (in press).

Mueller, R. J. and Johnston, M. J. S., 1984, Magnetic Field Measurements near the Morgan Hill Earthquake of April 24, 1984, U.S. Geol. Surv. Open-File Report 84-498A.

Mueller, R. J., Johnston, M. J. S., Keller, V. G., and Silverman, S., 1984, Magnetic Field Observations in the Long Valley Caldera of East-Central California, 1976-1984, Trans. A.G.U. (in press).

Earthquakes and the Statistics of Crustal Heterogeneity

9930-03008

Bruce R. Julian

Branch of Seismology
U.S. Geological Survey
345 Middlefield Road - MS77
Menlo Park, California 94025
(415) 323-8111 ext. 2931

Investigations

Both the initiation and the stopping of earthquake ruptures are controlled by spatial heterogeneity of the mechanical properties and stress within the earth. Ruptures begin at points where the stress exceeds the strength of the rocks, and propagate until an extended region ("asperity") where the strength exceeds the pre-stress is able to stop rupture growth. The rupture termination process has the greater potential for earthquake prediction, because it controls earthquake size and because it involves a larger, and thus more easily studied, volume within the earth. Knowledge of the distribution of mechanical properties and the stress orientation and magnitude may enable one to anticipate conditions favoring extended rupture propagation. For instance, changes in the slope of the earthquake frequency-magnitude curve ("b-slope"), which have been suggested to be earthquake precursors and which often occur at the time of large earthquakes, are probably caused by an interaction between the stress field and the distribution of heterogeneities within the earth.

The purpose of this project is to develop techniques for determining the small-scale distributions of stress and mechanical properties in the earth. The distributions of elastic moduli and density are the easiest things to determine, using scattered seismic waves. Earthquake mechanisms can be used to infer stress orientation, but with a larger degree of non-uniqueness. Some important questions to be answered are:

** How strong are the heterogeneities as functions of length scale?

** How do the length scales vary with direction?

** What statistical correlations exist between heterogeneities of different parameters?

** How do the heterogeneities vary with depth and from region to region?

Scattered seismic waves provide the best data bearing on these questions. They can be used to determine the three-dimensional spatial power spectra and cross-spectra of heterogeneities in elastic moduli and density in regions from which scattering can be observed. The observations must, however, be made with seismometer arrays to enable propagation direction to be determined. Three-component observations would also be helpful for identifying and separating different wave types and modes of propagation.

The stress within the crust is more difficult to study. Direct observations require deep boreholes and are much too expensive to be practical for mapping small-scale variations. Earthquake mechanisms, on the other hand, are easily studied and reflect the stress orientation and, less directly, its magnitude, but are often not uniquely determined by available data.

This investigation uses earthquake mechanisms and the scattering of seismic waves as tools for studying crustal heterogeneity.

Results

Modelling seismic-wave codas

Most models of seismic-wave codas are either heuristic, assuming that coda shapes have arbitrarily-chosen functional forms, or are based on simplified physical assumptions, such as that scattering is isotropic or that mode conversion and multiple scattering can be ignored. Elastic-wave scattering is actually rather complicated, however, as theoretical work carried out earlier under this project has shown. Scattering is strongly anisotropic in all but one case (low-frequency P-to-P scattering from heterogeneities in compressibility) and for shear waves involves the phenomenon of polarization. On the other hand, since codas consist of a superposition of waves of different types scattered in different places and at different angles, they are expected to be somewhat insensitive to these complications. We have constructed a simple numerical model that predicts coda shapes for various physical assumptions about earth structure, earthquake mechanism, and station location. The approach used is very simple and not particularly efficient, consisting merely of adding the contribution to the seismogram of many rays scattered at different places. Investigations are now under way to use this model to find out whether coda shapes may enable one to make inferences about fine-scale earth structure.

Dike-intrusion earthquake mechanisms

Investigations are continuing into the processes responsible for the non-double-couple mechanisms of many of the earthquakes that have occurred since 1978 in and near Long Valley caldera. The large collection of estimated hypocenters now available for earthquakes since 1982 in Long Valley shows systematic spatial patterns that include several planar features which may be faults and fractures. In particular, one prominent plane has the correct position and orientation to be a tensile fracture associated with the largest and best-recorded earthquake, that of 1633:44 UTC on May 25, 1980. In order to be certain of the reality of this and other features, and to insure that they are not caused by systematic biases in the hypocenter-estimation process, we plan to analyze them using techniques that are comparatively immune to bias, such as the master-event method. Attention will also be devoted to earthquakes before 1982, whose connection with the large events of 1980 is more certain. Unfortunately, a dense seismograph network did not exist in Long Valley until 1982. Nevertheless, we hope to be able to assemble an adequate data base by merging data collected by various agencies.

Mechanism of unstable crack propagation - One question raised by the hypothesis that some Long Valley caldera earthquakes are caused by tensile failure is whether a fluid-driven crack can propagate fast enough to radiate far-field seismic waves. Many investigators have assumed that the tip of such a crack can extend only a short distance beyond the driving fluid, so that its propagation speed is limited by the speed with which the fluid can move. During the last six months, investigations into this question have been conducted in cooperation with Prof. Charles Sammis of the University of Southern California. We have found that although an isolated fluid-driven crack in an infinite homogeneous medium is indeed limited by the speed with which the fluid can move, for many other geometries unstable crack propagation is possible. These cases include, for example, a pair of cracks approaching each other and a crack approaching a free surface. The case that is probably most relevant to the Long Valley caldera earthquakes is that of a crack radiating from a pressurized reservoir. In all these cases, crack propagation at elastic-wave speeds is possible even if the driving fluid remains stationary. A journal article describing these investigations is being prepared.

Dilatometer installation - In order to gather data bearing on the earthquake mechanisms, a Sacks-Evertson dilatometer was installed last fall near the Devil's Postpile, immediately southwest of the caldera. This instrument will provide high-sensitivity measurements of areal strain changes, and will also be used as a high-quality seismometer. The installation is now complete, and low-frequency data are being telemetered to Menlo Park. The collection of high-frequency data will begin later this fall.

Reports

Bruce. R. Julian and Stuart. A. Sipkin, Earthquake processes in the Long Valley caldera area, California, J. Geophys. Res. (submitted), 1984

Bernard Chouet and Bruce R. Julian, Dynamics of an expanding fluid-driven crack, J. Geophys. Res. (submitted), 1984.

Bruce R. Julian, Scattering of elastic waves in anisotropically random media (abstract), Terra Cognita, vol. 4, no. 2, p 271, 1984.

Bruce R. Julian and Bernard Chouet, Dynamic response of a fluid-filled crack: a possible earthquake mechanism? (abstract), Terra Cognita, vol. 4, no. 2, p 278, 1984.

Earthquake and Seismicity Research Using SCARLET and CEDAR

Contract No. 14-08-0001-21210

Hiroo Kanamori, Clarence R. Allen, Robert W. Clayton
Seismological Laboratory, California Institute of Technology
Pasadena, California 91125 (818-356-6914)

Investigations

1) Earthquake focal mechanisms in southern California.

2) Crustal structure in southern California from array data.

Results

1) We determined earthquake focal mechanisms from P-wave first motions for the Eastern Transverse Ranges and the San Emigdio Mountains in southern California. The former region shows a predominance of strike-slip faulting whereas Quaternary faults in the region show thrust motion. Fault deformation in the San Emigdio Mountains inferred from focal mechanisms is in accord with displacements across Quaternary faults in the area. This study and a search of the literature have yielded 19 mechanisms with shallow-dipping nodal planes. Previous workers have interpreted such mechanisms as evidence for a regional decollement (see Figure 1). If such a regional decollement exists, these data give some indication of its regional extent. Slip directions inferred from the focal mechanisms with shallow-dipping nodal planes show some regional consistency, but this pattern cannot be entirely explained with current tectonic models. A comparison of the stress-drop of an event having a shallow-dipping nodal plane with an event with steeper planes gave inconclusive results. The details are described in a preprint entitled "Earthquake Focal Mechanisms in the Eastern Transverse Ranges and San Emigdio Mountains, Southern California and Evidence for a Regional Decollement" by Webb and Kanamori (1984).

2) Crustal structure in southern California is investigated using travel times from over 200 stations and thousands of local earthquakes. The data are divided into two sets of first arrivals representing a two layer crust. The Pg arrivals have paths that refract at depths near 10 km and the Pn arrivals refract along the Moho discontinuity. This data set is used to find lateral and azimuthal refractor velocity variations and to determine refractor topography.

The Pn raypaths are modeled using linear inverse theory. This enables statistical verification that static delays, lateral slowness variations and anisotropy are all significant parameters. However, because of the inherent size limitations of inverse theory, the full array data set could not be processed and the possible resolution was limited. A tomographic backprojection algorithm avoids these size problems. This algorithm allows us to process the data sequentially and to iteratively refine the solution. The variance and resolution for tomography are determined empirically using synthetic structures.

The Pg results spectacularly image the San Andreas Fault, the Garlock Fault and the San Jacinto Fault. The Mojave has slower velocities near 6.0 km/s while the Peninsular Ranges have higher velocities of over 6.5 km/s. The San Jacinto block has velocities only slightly above the Mojave velocities. It may have overthrust Mojave rocks. Surprisingly, the Transverse Ranges are not apparent at Pg depths. The batholiths in these mountains are possibly only surficial.

Pn velocities are fast in the Mojave, slow in southern California Peninsular Ranges and slow north of the Garlock Fault. Pn anisotropy of 2% with a NWW fast direction exists in southern California. A region of thin crust (22 km) centers around the Colorado River where the crust has undergone basin and range type extension. Station delays see the Ventura and Los Angeles Basins but not the Salton Trough, where high velocity rocks underlie the sediments. The Transverse Ranges have a root in their eastern half but not in their western half. The southern Coast Ranges also have a thickened crust but the Peninsular Ranges have no major root. The details are described in the thesis by Thomas Hearn, California Institute of Techology.

Reports and Publications

Hearn, Thomas M., Crustal Structure in Southern California from Array Data, California Institute of Technology doctoral thesis, November 1984.

Sanders, Chris O. and Hiroo Kanamori, A seismotectonic analysis of the Anza seismic gap, San Jacinto Fault zone, southern California, Jour. Geophys. Res., 89, 5873-5890, 1984.

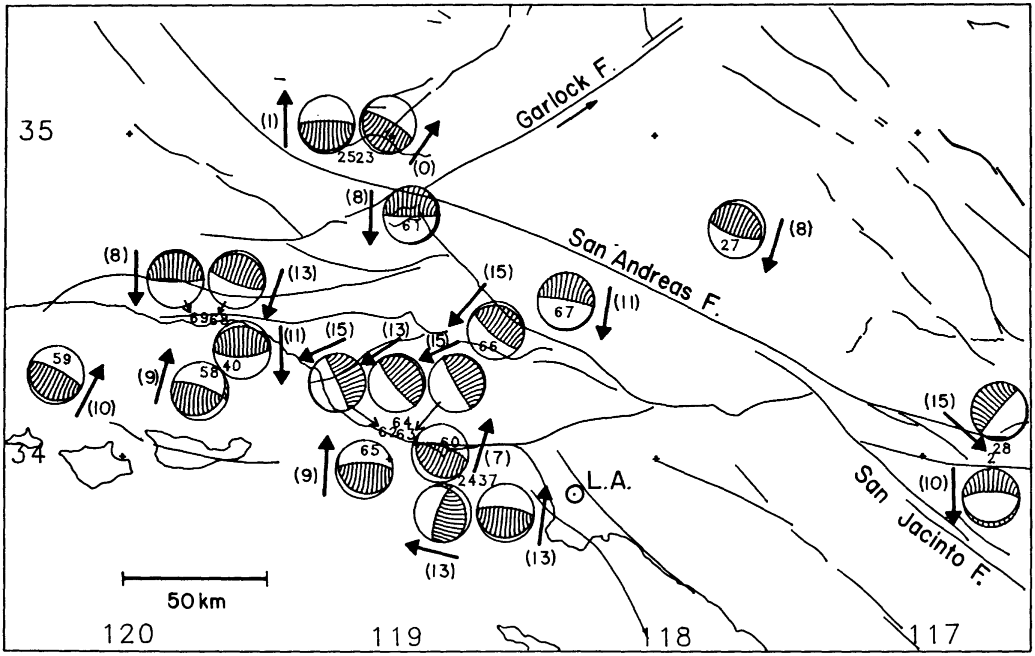

Figure 1. Map of focal mechanisms for all of the decollement-type events (one nodal plane dipping at less than 25 degrees) in the Transverse Ranges area. The arrows mark the direction of the horizontal projection of the slip vectors for the shallow-dipping nodal planes. Figures in parentheses are the respective focal depths. Events are from this work and other sources.

HYDROLOGICAL/GEOCHEMICAL MONITORING ALONG SAN ANDREAS AND SAN JACINTO FAULTS, SOUTHERN CALIFORNIA, DURING SECOND HALF OF FISCAL YEAR 1984

Contract 14-08-0001-21859

D. L. Lamar and P. M. Merifield
Lamar-Merifield Geologists, Inc.
1318 Second St., #25
Santa Monica, CA 90401

Investigations

Water levels in more than thirty wells along the San Andreas and San Jacinto fault zones were monitored during the current reporting period. Water levels in seven wells and barometric pressure at three wells were monitored by the Caltech Remote Observatory Support System (CROSS). Two of the Caltech units have been replaced by Envirolabs data loggers, Model DL-120-MCP, which are linked by telephone to our IBM Personal Computer. Another ten wells were monitored continuously with Stevens Type F recorders, two being maintained by W. R. Moyle, Jr., of the Geological Survey. The remaining wells were probed monthly, weekly, semiweekly or daily with the aid of volunteers.

Long-term water-level changes are displayed on computer-generated hydrographs for each well. Daily rainfall is plotted on the graphs for direct comparison with water levels. Long-term hydrographs of wells along the San Andreas fault typically show seasonal response to rainfall (Fig. 1). Most of the wells along the San Jacinto fault zone are in confined aquifers which are not affected by seasonal rainfall (Fig. 2). Short-term fluctuations in water level seen on the Stevens recorder charts, CROSS records, and Envirolabs plots are caused by barometric pressure changes related to weather fronts, earth tides and solar thermal tides.

Results

Sharp upward spikes in water level occurred in a well in Ocotillo Wells during periods of rainfall (Fig. 3). These spikes are believed to be caused by a sudden influx of rainwater into the well casing, and further demonstrate the importance of daily rainfall observations for the interpretation of water-level fluctuations in wells. A similar relationship between rainfall and sharp upward spikes in water level was previously reported for a well in Palmdale.

Water levels are measured every 15 minutes on the two wells equipped with Envirolabs data loggers. The measurements are stored on magnetic tape and data are sent to the IBM Personal Computer in our office via telephone once a week. To date the data loggers have operated without malfunction. Hydrographs are generated by a Bausch and Lomb digital plotter connected to the IBM Personal Computer.

Short-term water-level records of wells along the San Jacinto fault have shown anomalies interpreted to be strain events in the past (Merifield and Lamar, 1983,1984); no such anomalous water-level changes have been observed during the past six months.

Reports

Merifield, P.M. and D.L. Lamar, 1983, Ground water anomalies along the San Andreas and San Jacinto fault zones, southern California, EOS Trans. Am. Geophys. Union, v, 64, no. 45, p. 761.

Merifield, P.M. and D.L. Lamar, 1984, Possible strain events reflected in water levels in wells along San Jacinto fault zone, southern California, Pure and Applied Geophysics, in press.

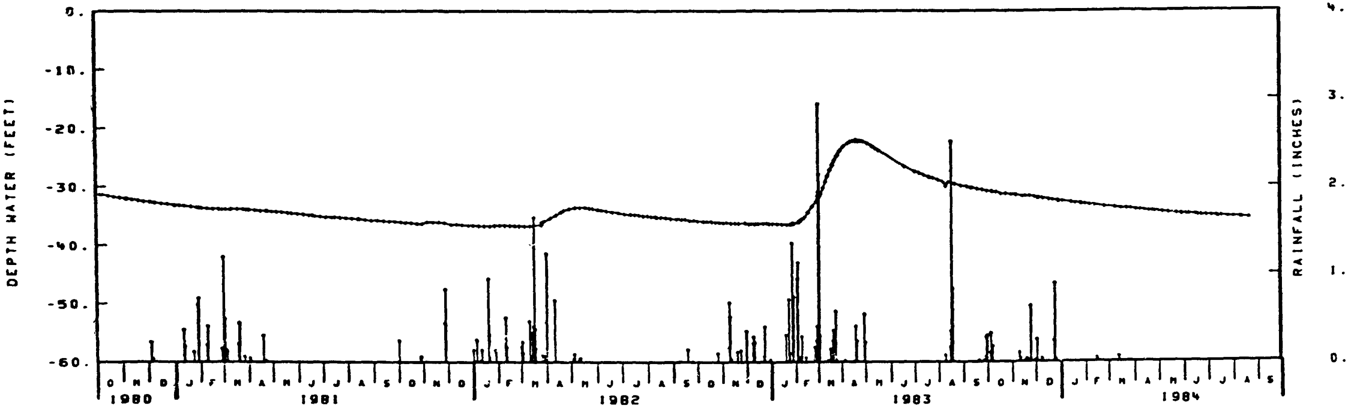

FIGURE 1 -- WEEKLY OBSERVATIONS OF WATER LEVEL (+) AND RAINFALL (.) IN WELL NUMBER 05N/12W-14C01 DURING 1980-1984 PALMDALE AREA SEASONAL RAINFALL AT ADJACENT STATIONS IN INCHES ACROSS TOP

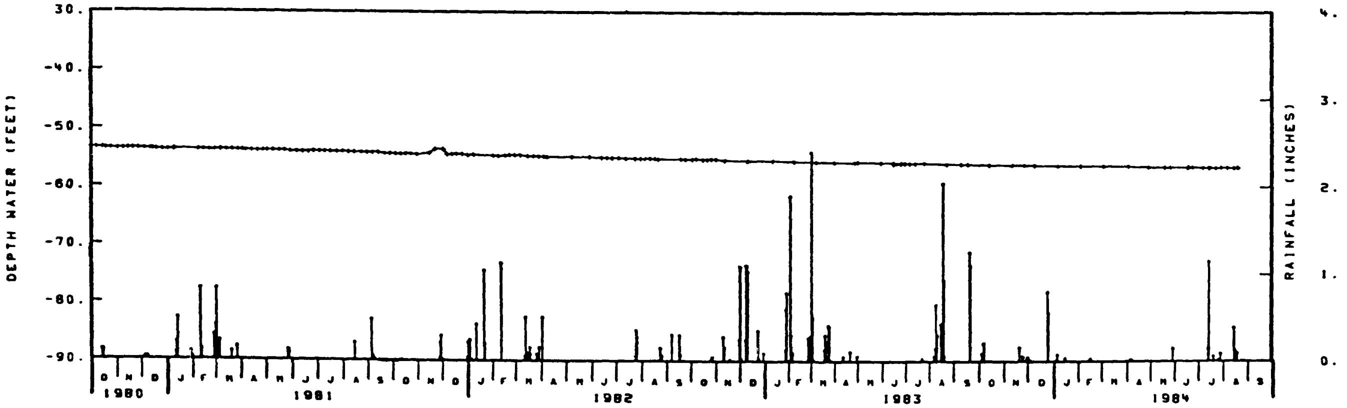

FIGURE 2 -- WEEKLY OBSERVATIONS OF WATER LEVEL (+) AND RAINFALL (.) IN WELL NUMBER 11S/06E-03N04 DURING 1980-1984, BORREGO SPRINGS AREA SEASONAL RAINFALL AT ADJACENT STATIONS IN INCHES ACROSS TOP

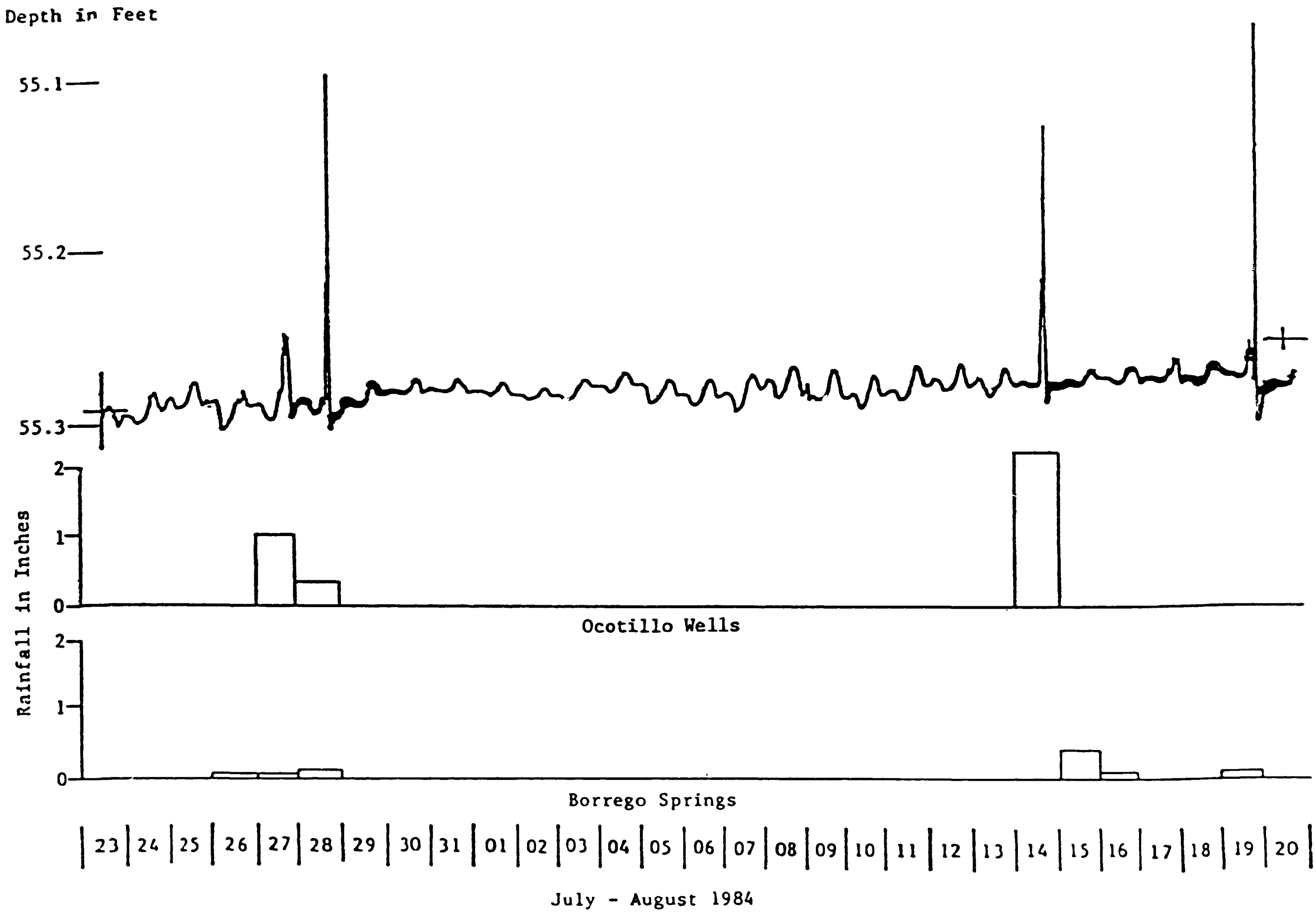

Figure 3 - Stevens water-level record 23 July - 20 August 1984, well 12S/8E-10E1, Ocotillo Wells and rainfall at adjacent precipitation stations.

GEODETIC STRAIN MONITORING

9960-02156

John Langbein
Branch of Tectonophysics
U.S. Geological Survey
345 Middlefield Road, MS/977
Menlo Park, California 94025
(415-323-8111, ext. 2038

Investigations

Two-color geodimeters are used to survey, repeatedly, geodetic networks within selected regions of California that are tectonically active. This distance measuring instrument has a precision of 0.1 to 0.2 ppm of the total line length.

Results

1) Pearblossom Network

Two-color geodimeter measurements of line-length changes for an 11 baseline network near Pearblossom, California have shown a dramatic increase in the shear-strain parallel to the local strike (N65°W) of the San Andreas fault during mid-1984. The changes in strain are shown in Figure 1. During the period between March and September, 1984, the shear strain (tensor quantity) has increased to an average rate of 0.8±0.2 ppm/a. The more recent observations in July, August and September indicate that the high rate of shear strain occurred primarily between March and late June, 1984. In contrast, the extensional components of strain parallel and normal to the strike of the fault show no substantial changes during the corresponding period of increasing shear strain.

The line length measurements between April and September were made at monthly intervals using a portable, two-color geodimeter. Previously, the measurements relied on the 2-color geodimeter that is owned by CIRES. The larger standard deviation of the inferred strain changes for the last 6 months are due to less frequent measurements and an apparent decrease in the precision of the portable geodimeter relative to the CIRES instrument.

Figure 1 also shows the strain rates averaged over yearly intervals and the strain changes observed for the nearby Palmdale network. The secular strain rate for the entire 4 year data set is written next to the title. The strains show substantial fluctuations about the long-term rates.

The inferred strain changes determined from yearly measurements of line-length changes of the nearby Palmdale network are shown with heavy lines in Figure 1. These measurements are made with a single color geodimeter using aircraft mounted probes to determine the refractive index of the atmosphere. The 5 measurements indicate that the shear strain appears to be correlated between these two networks that are separated by 35 km along the strike of the San Andreas fault. However, there is not enough data with a large signal to test the correlation hypothesis of the orthagonal components.

2) Long Valley Caldera

Since June of 1983, the line-lengths of several baselines have been monitored using a two-color geodimeter. This network is centered within the southwestern moat of the Long Valley Caldera. The data from the first year indicate that strain rates were as high as 6 ppm/yr on several baselines. The more recent data, however, reveals that these baselines are currently deforming at a lower rate. The apparent deceleration is shown in the Table for 7 baselines for which the deceleration is statistically significant term. Several other baselines show trends that are consistent with the deceleration. These rates are also tabulated. The remaining baselines are best represented by a single, secular rate of extension. The locations of the baselines within Long Valley are shown in Figure 2.

High rates of extension are primarily confined to the baselines that span the region of Casa Diablo Hot Springs and the zone defined by the earthquake swarm of January, 1983.

Table 1. Rates of Extension; Long Valley Geodetic Caldera

Baseline	Line Length (km)	Strain Rate ppm/yr			
		Secular Rate	Instantaneous Rates		
			July 1983	Feb. 1984	July 1984
Casa-Krakatau II	7.8	1.80±0.16	ND	2.4±0.2	0.3±0.4
Casa-Shark II	3.1	3.25±0.16	ND	3.6±0.2	2.0±0.4
Casa-Hot I	6.8	1.02±0.11	1.6±0.3	ND	0.1±0.4
Casa-Lomike	2.5	3.77±0.11	5.7±0.3	2.8±0.2	1.4±0.4
Casa-Rodger	2.6	4.00±0.17	5.8±0.4	ND	1.2±0.7
Casa-Sewer	3.9	4.17±0.10	5.3±0.3	3.7±0.2	3.0±0.4
Miner-Tilla I	4.9	4.46±0.18	8.4±1.2	ND	0.4±1.3
Miner-Hot I	9.7	2.30±0.24	3.8±1.8	ND	1.3±1.1
Miner-Shark I	5.3	4.84±0.20	6.8±1.2	ND	2.7±1.3
Casa-Knolls	7.1	2.22±0.17	ND	2.3±0.3	2.1±0.5
Casa-Sherwin II	4.8	4.34±0.15	ND	4.6±0.2	3.7±0.4
Miner-Lomike	4.0	-0.18±0.24			
Miner-Sewer	4.1	-0.10±0.32			
Casa-Hot II	6.8	0.84±0.17			
Casa-Tilla II	4.2	0.54±0.16			
Casa-Convict	8.1	-0.47±0.25			
Casa-Krakatau I	7.8	0.87±0.69			
Casa-Miner I	3.9	2.38±0.17			
Casa-Shark I	3.1	1.40±0.11			
Casa-Sherwin I	4.8	2.61±0.55			
Casa-Slide	3.2	2.09±0.25			
Casa-Taxi	5.5	0.10±0.50			
Casa-Tilla I	4.2	-0.16±0.16			

ND - No Data

3. Calibration of Two-Color Geodimeters

Calibration of instrument length using both the U.S.G.S.'s portable 2-color geodimeter and CIRES geodimeter have continued. Previous calibrations occurred in Pearblossom, but since the CIRES instrument is now located in Parkfield, California, the calibration experiments have continued there. The calibration measurements occurred in June and in August, 1984 where 7 baselines were measured simultaneously using both instruments. The data indicate that the instruments may have changed length by 0.16±.10 ppm relative to each other although the inferred change is not statistically significant. Because the CIRES instrument was moved from Pearblossom to Parkfield between March and June, 1984, the data from the previous calibration measurements in Pearblossom cannot be used with the more recent data.

Reports

None

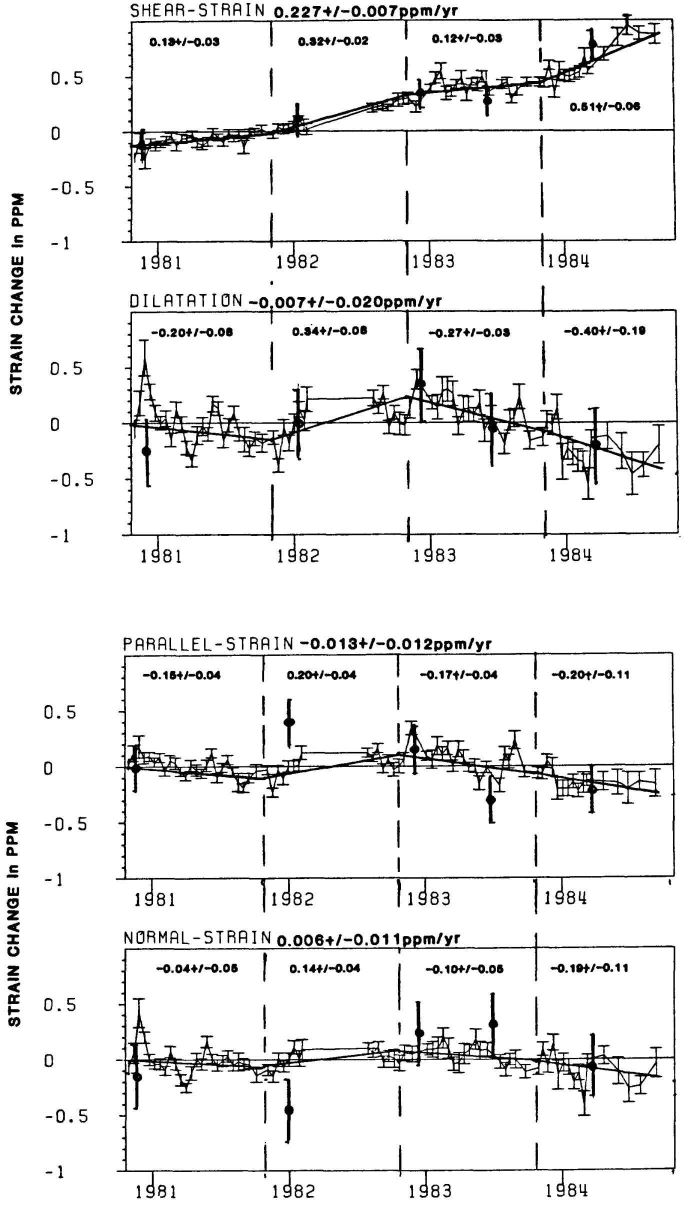

Figure 1. Strain changes for the Pearblossom and Palmdale Geodetic Networks. Data from the Pearblossom network is shown with light lines. Linear trends show secular rates for one year intervals. Palmdale data is shown with heavy lines and are not connected.

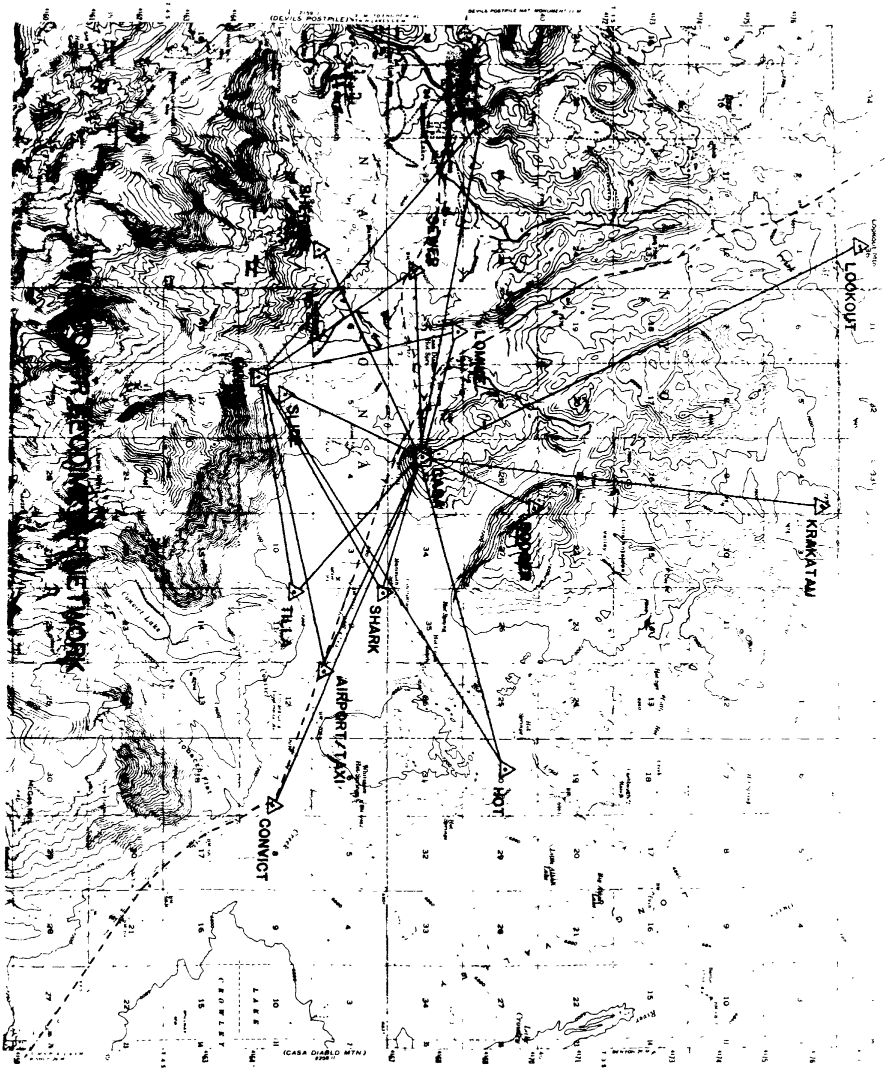

Figure 2. A map of the southern part of the Long Valley Caldera which shows the location of the baselines that comprise the two-color geodimeter network.

Carbon Fiber Strainmeter Studies in Southern California

14-08-0001-21240

Peter C. Leary and Yehuda Ben-Zion
Department of Geological Sciences
University of Southern California
Los Angeles, CA 90089-0741
(213) 743-8034

Objective: To monitor fault zone creep and fault block strain in the vicinity of major southern California faults.

Data Acquisition and Analysis: The USGS creepmeter XWR installation on the San Andreas fault between Palmdale and Pearblossom (coordinates N34° 29.6', W117° 58.2') was monitored at a creep step detection level of 5 microns between March and October, 1984. The 10 month XWR creep and temperature records (Figures 1 and 2) show the creep signal is dominated by temperature variations that are both seasonal and instrumental in origin. A greater degree of vault insulation should reduce the short term temperature variation in the creep signal. No steps greater than 5 microns are observed in the area of anomalous local seismic activity and the strain activity reported for the Pearblossom EDM instrument. The potential for creep steps in association with strain and/or seismic episodes was established at this creep site by the observation of a number of pre-seismic and co-seismic steps at the 5 to 20 micron displacement level during the 1979 regional strain episode (Leary and Malin, 1984).

Seasonal variations in temperatures and rainfall dominate the tunnel-situated carbon fiber strainmeter records at sites BQ (N34° 34.7', W118° 22.8'), DT (N34° 10.2', W117° 48.4') and JK (N34° 30.9', W118° 17.6'). The 1984 BQ and DT records are shown in Figures 3-6. Figure 7 shows the strong correlation between detrended strain at BQ (1.5 μstrain/yr removed) and the seasonal air temperature at a lag of 45 days. Equally apparent is the effect of rainfall; each episode of rain causes an expansion not predicted by the temperature function.

Publications: Leary, P. C. and P. C. Malin, Ground Deformation Events Preceding the Homestead Valley Earthquakes, B.S.S.A., vol. 74, p. 1799-1817, 1984.

Figure 1. XWR Creepmeter Record. Vertical scale: .13 microns/mV; extension is up.

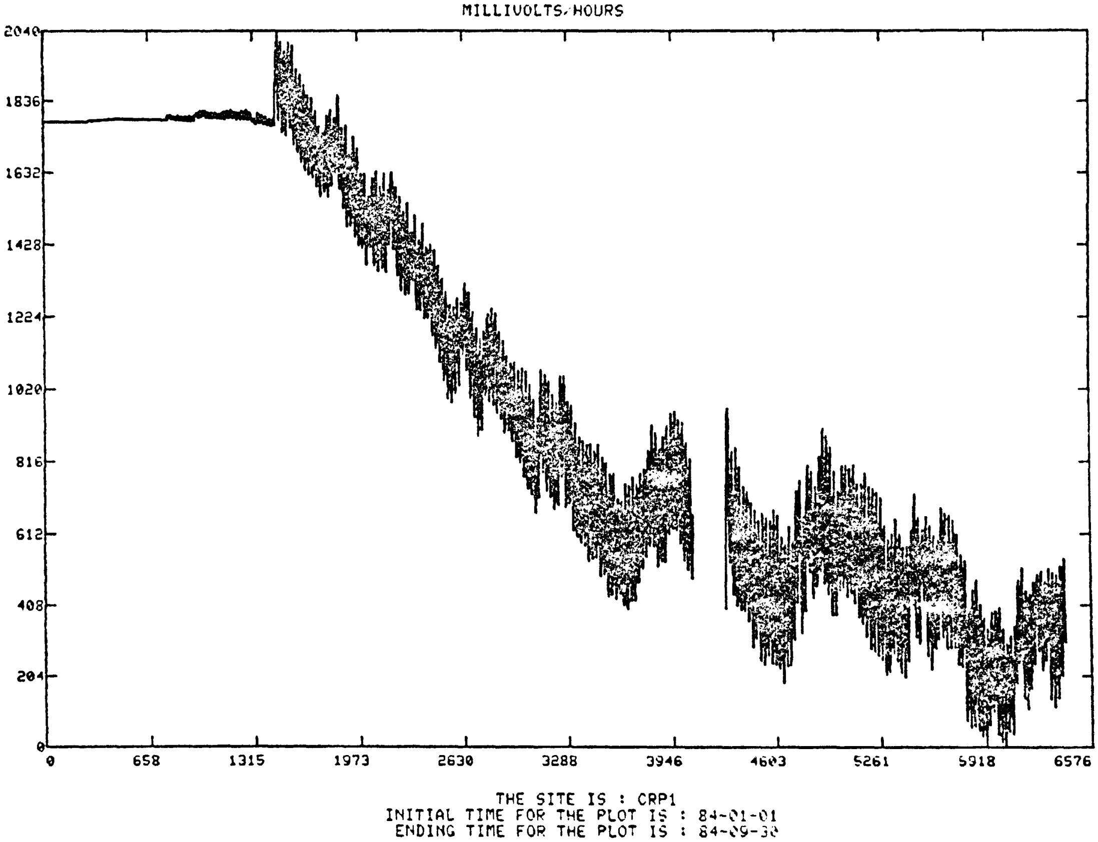

Figure 2. XWR Site Temperature Record. Vertical scale: 1.6 mdeg/mV; temperature increase is down.

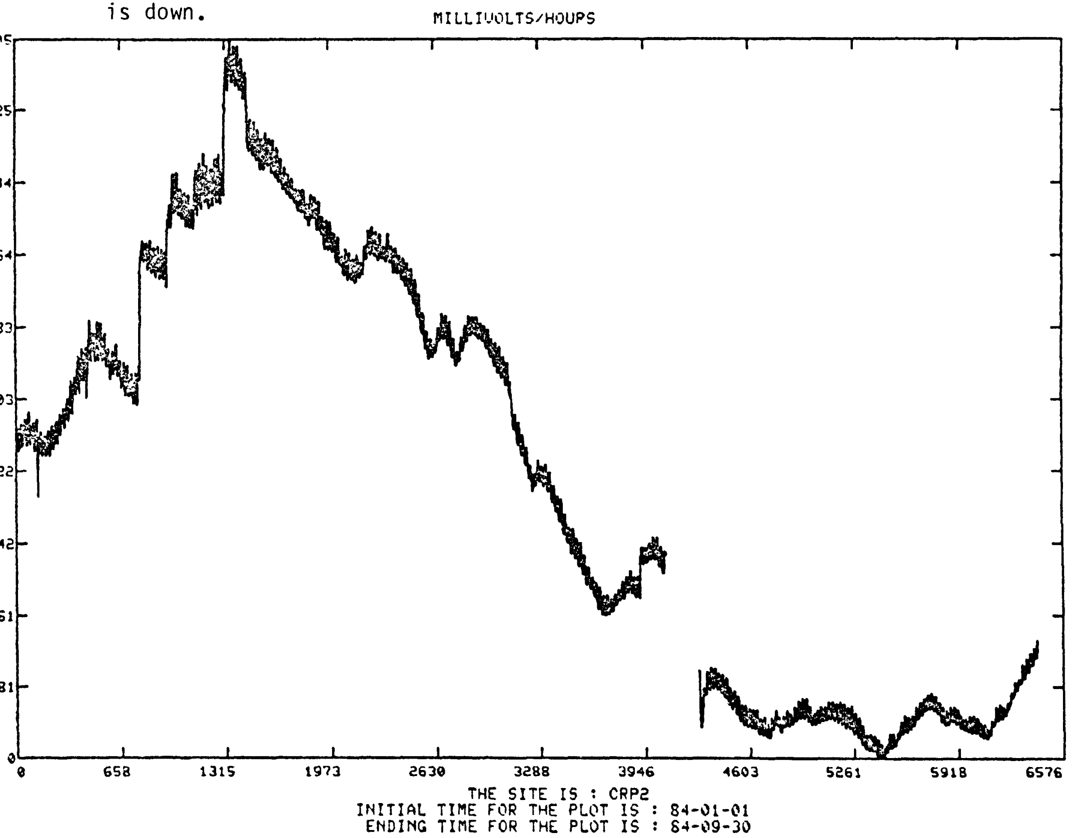

Figure 3. BQT1 Strainmeter Record. Vertical scale: .54 nstr/mV; extension is down.

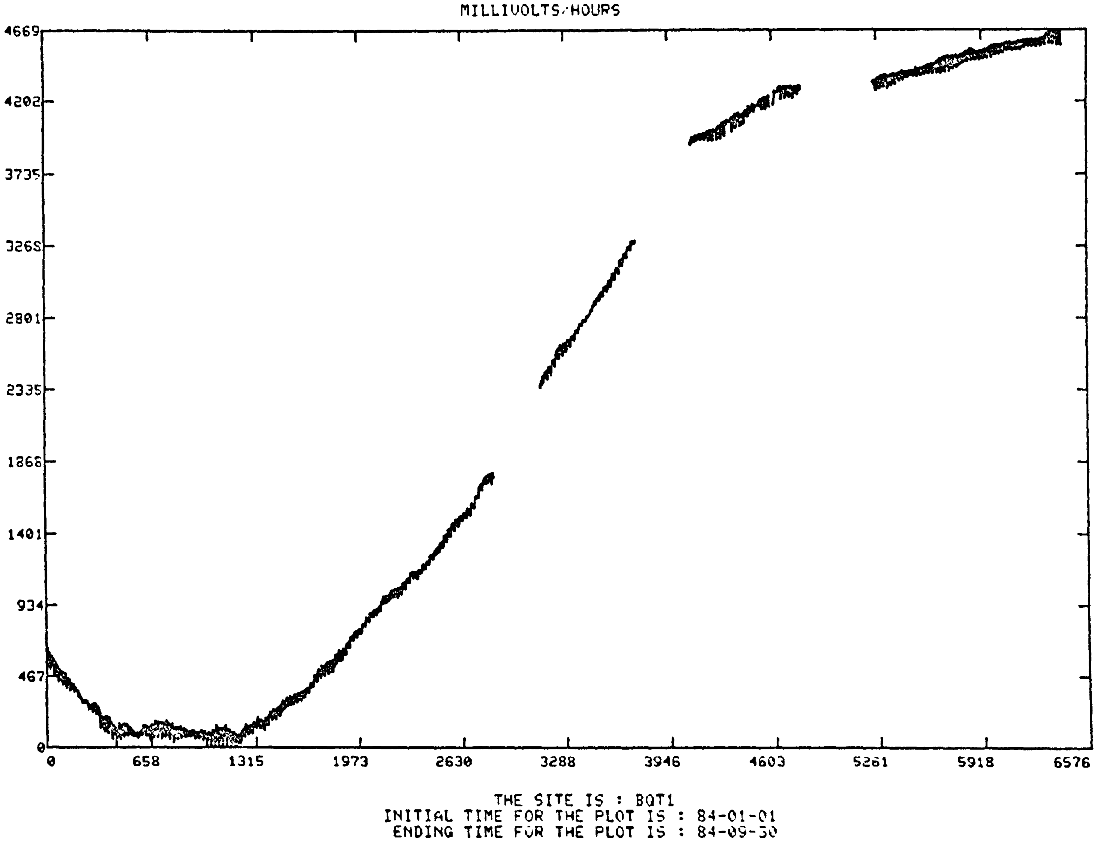

Figure 4. BQT2 Strainmeter Record. Vertical scale: .41 nstr/mV; extension is down.

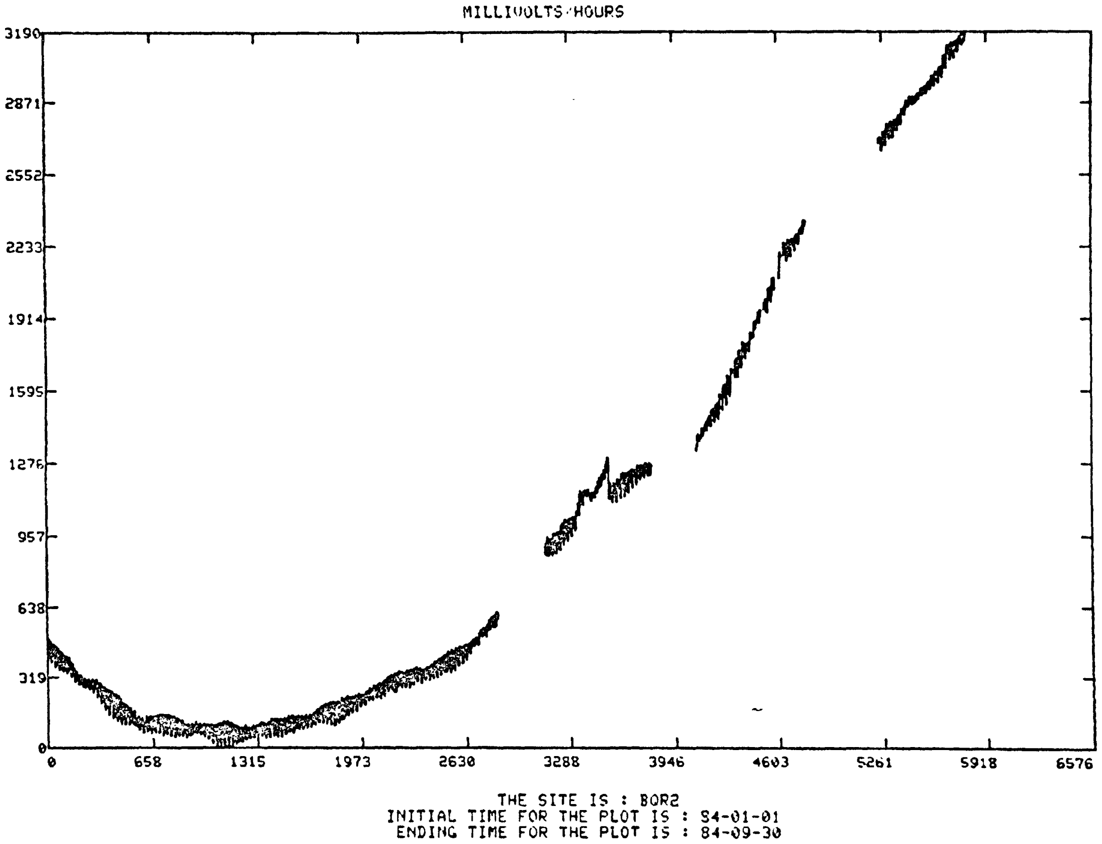

Figure 5. DT1 Strainmeter Record: Vertical scale: .18 nstr/mV; extension is down.

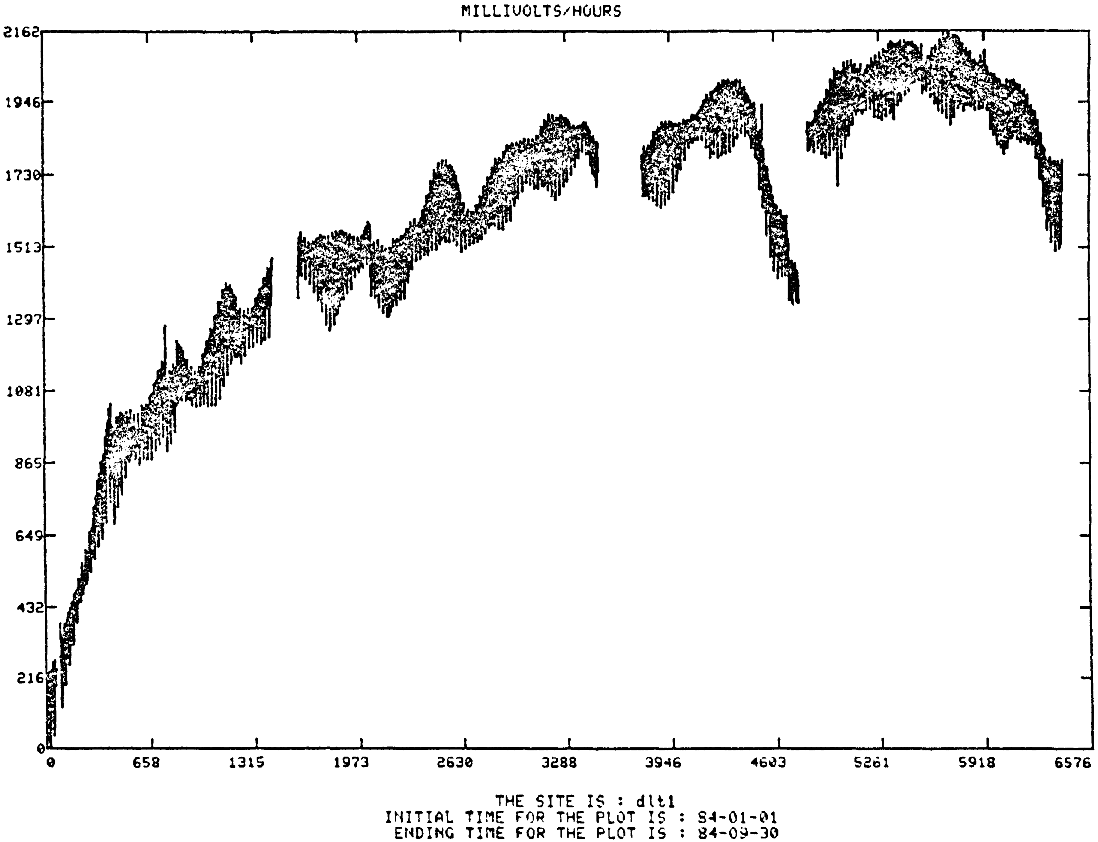

Figure 6. DT2 Strainmeter Record. Vertical scale: .38 nstr/mV; extension is down.

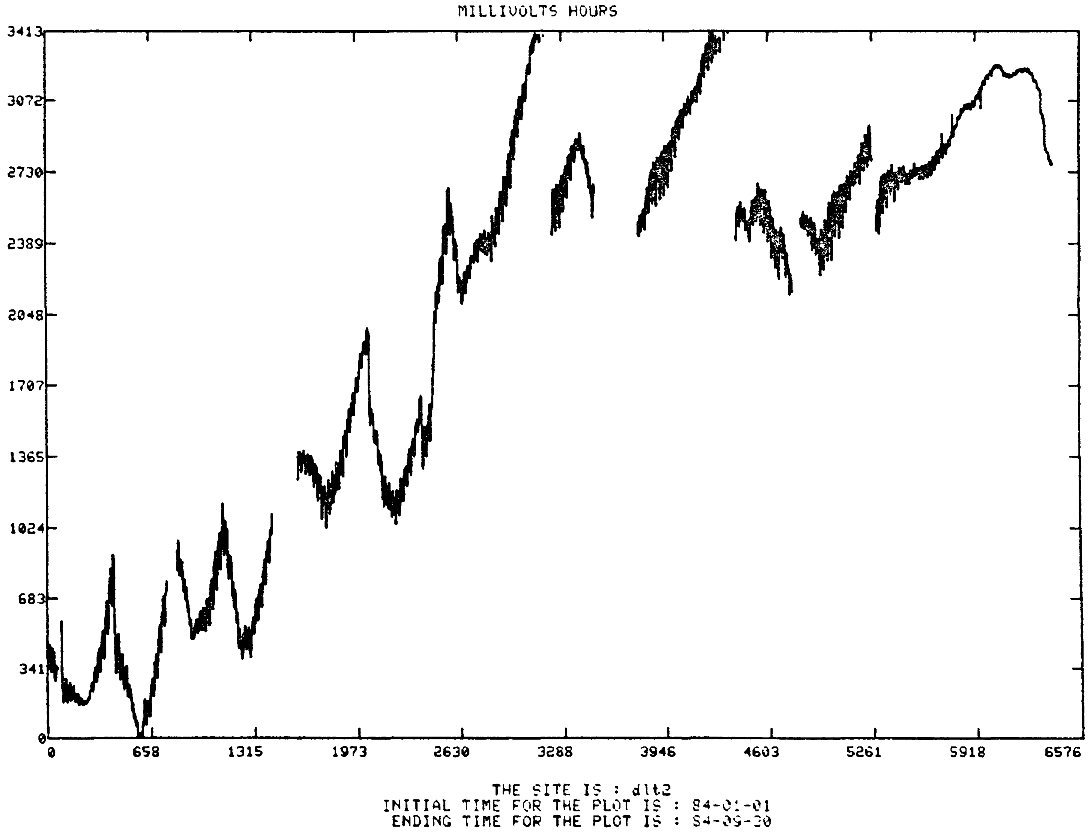

Figure 7. BQ1 strain (thick continuous curve), temperature predicted strain (thin continuous curve) and rainfall (spikes). Full scale strain is 2730 mV @ strain sensitivity of .54 nstr/mV. Full scale rainfall is 2.5 inches.

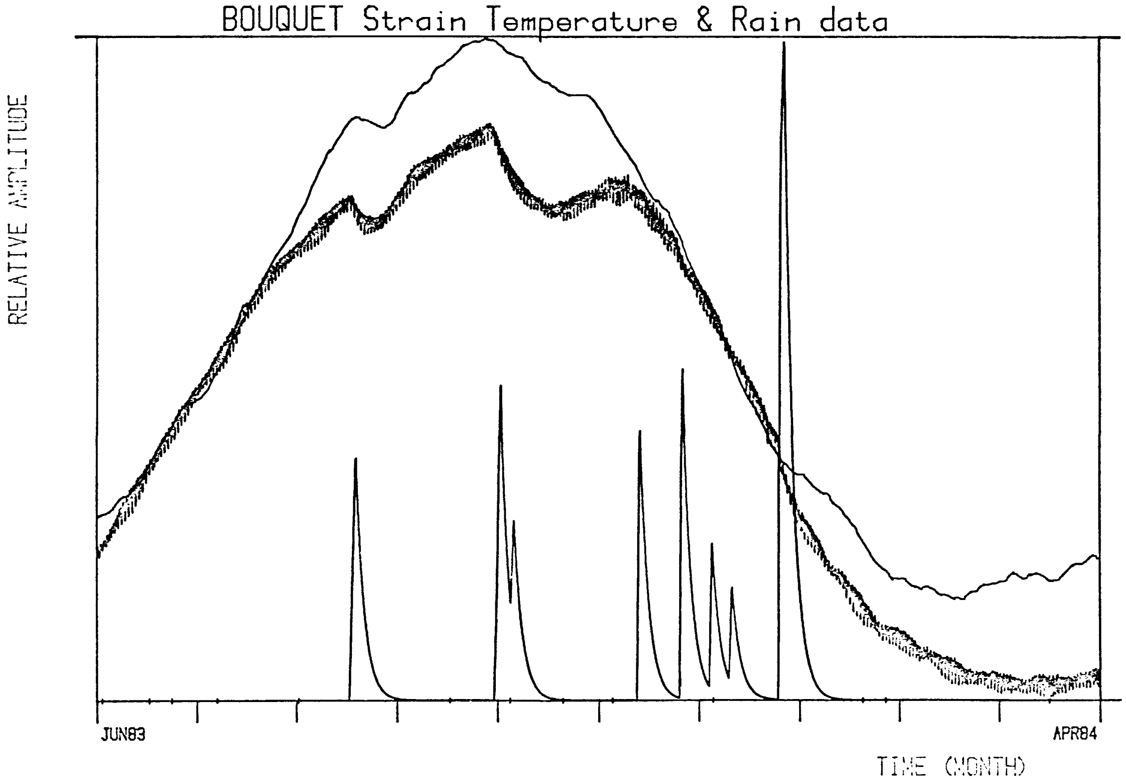

Microearthquake Data Analysis

9930-01173

W. H. K. Lee
Office of Earthquakes, Volcanoes, and Engineering
Branch of Seismology
345 Middlefield Road, MS 977
Menlo Park, California 94025
(415) 323-8111, Ext 2630

Investigations

The primary focus of this project is the development of state-of-the-art computation methods for analysis of data from microearthquake networks. For the past six months I have been involved in (1) setting up a computational procedure to study coda decay of local earthquakes, and (2) improving 2-D and 3-D seismic ray tracing techniques in heterogeneous media and applying them to study earthquake inverse problems.

Results

I. Coda Decay as an Earthquake Precursor

Earthquake prediction research must consider (1) the loading of tectonic stress, (2) the friction law governing fault slip, and (3) the structural heterogeneity of the earthquake source region. The tectonic stress has been monitored by geodetic observations and in-situ stress measurements. The friction law has been studied by rock deformation experiments. However, the structural heterogeneity of the earth's crust is yet to be extensively investigated.

The importance of "heterogeneity" in earthquake prediction has been emphasized by Mogi since 1962, but the quantification of the heterogeneity of the actual earthquake source region has not been rigorously attempted. Because the quality factor (Q) of shear waves at high frequencies may carry information about source heterogeneity, K. Aki suggested that we quantify heterogeneity by this parameter. In fact, Q can be systematically monitored by studying the coda decay of local earthquakes.

It is interesting to note that coda decay may be an effective earthquake precursor. For example, Jin Anshu observed that the coda duration is shorter for earthquakes before the great Tangshan earthquake than for those which occurred afterwards. Similar results were also obtained by Haruo Sato for a magnitude 6 earthquake in eastern Yamanshi. Because it is difficult to maintain instrument uniformity over a long period of time, and the subjectivity of measuring coda length by hand, it is better to determine Q directly from coda decay using digital waveform data.

We are now taking advantage of the Calnet digital waveform data provided by Sam Stewart's group. In collaboration with K. Aki and B. Chouet, a computer-based procedure has been developed to carry out the following analysis:

(1) For a given time period, select earthquakes that satisfy chosen magnitude and geographic limits, and label them by (t_i, x_i, y_i, z_i), $i = 1,2,3...$ (it can be shown that earthquakes with magnitude between 2 and 3 are best suited for the determination of source heterogeneity).

(2) Select stations that have recorded "healthy" signals, and label them by (x_j, y_j, z_j), $j = 1,2,3...$ Let us denote the signal traces of the ith earthquake at the jth station by $F_{ij}(l\Delta t)$, where l = 1,2,3... and Δt is the digitization increment.

(3) For each digitized signal $F_{ij}(l\Delta t)$, we perform FFT on moving windows to obtain the spectral power at various frequency bands and various times, i.e. $A^2_{ij}(\omega_k,t)$ where ω_k are octave frequencies (1.5, 3, 6, 12, and 24 Hz), and t is the center window time since the origin time t_i.

(4) If we fit a straight line through a plot of $\ln(t^2 A^2_{ij}(\omega_k,t))$ vs t, then the slope gives ω_k/Q_{ijk} and the intercept gives the combined source and site effects, S_{ijk}.

(5) If the earthquakes and stations are well distributed throughout a given geographical region, we can quantify the source heterogeneity by first dividing the region into 3-dimensional blocks, with block center coordinates (x_m, y_m, z_m), $m = 1,2,3...$, and then using 3-D ray tracing to help invert for Q_{ijk} at each block.

(6) The source and site effects, S_{ijk}, can be decomposed into:

$$S_{ijk} = \alpha_{ik} + \beta_{jk} + \varepsilon_{ijk}$$

where α_{ik} is the source effect of the ith earthquake at frequency ω_k, β_{jk} is the site effect of the jth station at frequency ω_k, and ε_{ijk} is the remaining random term. It is reasonable to assume $\Sigma\, \beta_{jk}$ = constant, and $\Sigma\, \varepsilon_{ijk}=0$, and we obtain by inversion, α_{ik} for earthquakes $i=1,2,3...$ Aki called α_{ik} the shape factor of the source.

(7) By repeating steps (1) through (6) for various time periods, we obtain temporal variations of Q^{-1} and α. Hopefully they may serve as effective precursors for earthquake prediction purposes.

Since the above analysis procedures involves massive data processing and keeping track of all the relevant numbers, we intend to apply it to a selected region for a feasibility demonstration. The area we have chosen is a strip of the San Andreas fault system from Santa Rosa to Parkfield.

II. Earthquake Inverse Problems

Most seismological problems (e.g. earthquake location, simultaneous inversion of hypocenter and velocity, inversion of Q^{-1}, etc.) are mathematical inverse problems. In engineering terms, we observe some output signals (i.e., seismic waveforms), we wish to infer the input signal (i.e., earthquake source parameters), as well as the nature of the "black box" (i.e., the earth). This is a very difficult problem, but considerable advances have been made by many disciplines of science, especially by mathematicians. In particular, we wish to apply recent mathematical advances in solving non-linear inverse problems to the simultaneous inversion of hypocenter and velocity, and simultaneous inversion of the quality factor Q^{-1} and source shape factor α (described in the previous section). Gene Golub, John Holt, and their colleagues and I have been developing computer codes to take advantage of the sparse nature of the Jacobian matrix in the earthquake inverse problems. Preliminary results indicate that we could speed up the computing time considerably, thereby making solution of large-scale earthquake inversion problems economical.

I was invited to the International Conference on "Inverse Problems of Acoustic and Elastic Waves" held at the Cornell University, Ithaca, N.Y. in June 1984. A paper on "Applications of Seismic Ray Tracing Techniques to the Study of Earthquake Focal Regions" was presented in collaboration with F. Luk and W. D. Mooney.

Reports

Lee, W. H. K., F. Luk, and W. D. Mooney, Applications of seismic ray tracing techniques to the study of earthquake focal regions, (Abstract), Proceedings of the International Conference on Inverse Problems of Acoustic and Elastic Waves, Cornell University, June, 1984.

Parkfield Seismicity Project

9930-02098

Allan Lindh
Branch of Seismology
U. S. Geological Survey
345 Middlefield Road, Mail - Stop 977
Menlo Park, California 94025
(415) 323-8111 ext. 2042

Work Underway

During the last six months I have:

1. Continued work on two manuscripts; one on Parkfield with Bill Bakun and one on long-term probabilities with Bill Ellsworth.
2. Started two new manuscripts: one on a model of the deformation at the end of the creeping zone that relates the Coalinga earthquake to the dislocation pile up near Parkfield, and a second paper that presents a simple model relating the micro-seismicity, the marco-seismicity, the geology, and the recurrence intervals of great earthquakes along the San Andreas system. The introduction to that paper is included in the results section of this report.

In addition I have continued processing and archiving the RTP data, maintained & upgraded the 11/23/watchdog system for the RTP, purchased a DEC 350 PC to upgrade our online use of the RTP data, and held weekly station quality meetings.

Results

In this short note I wish to sketch for the San Andreas system a reasonably comprehensive model for the detailed relations between:

1. The microseismicity,
2. The macroseismicity (ie. the largest plate boundary events along each segment and
3. The geology along each segment.

While this model derives to some degree from my own work at Parkfield, and on long-term recurrence along the entire San Andreas system, it also draws very heavily on Rick Sibson and Lynn Sykes recent work on the San Andreas. In addition it borrows freely from conversations I have had over the last few years with my friends, both those at the USGS and at the universities. As such it is put forth not as an original contribution, but rather as an edited summary of a large number of peoples thinking on this subject.

My motivation to attempt this model stems from my feeling that in California we should be able to understand what microearthquakes "mean", so to speak. This is important because of:

1. The lack of direct correlation between microseismicity and the source regions of large events,
2. The need to better utilize microseismic information in attempts to understand the tectonics and geologic structure of the San Andreas system, and

3. The need to "understand" the microseismicity of California, where the tectonics and seismic risk are relatively well understood, so as to be able to better the assess the risk in areas such as the eastern U.S., where scattered microseismicity is essentially all the information there is about the tectonics.

The major components of the model are:

1. That microseismicity on the San Andreas occurs at short wavelength gradients in the displacement on the fault,
2. That the width of the locked zone along the San Andreas depends on the rock-types juxtaposed across the fault at seismogenic depths,
3. The width of the locked zone determines the average strength of the locked portion of the fault, and
4. The average strength controls the average recurrence interval and the maximum displacement on the segment.

The distribution of microseismicity on the plane of the San Andreas fault has always been somewhat enigmatic, given that most of the microearthquakes occur along the creeping portions of the fault, while the segments that are known to have failed in large earthquakes are essentially aseismic. Another difficulty in understanding the distribution of microseismicity was pointed out by Joe Andrews, who showed that the short wavelength stress concentrations that result in small earthquakes cannot over the long run be the result of the long-wavelength loading that drives the plates, but must be produced locally by larger events (and thus be aftershocks of those larger events) or aseismic slip. Yet along much of the San Andreas it can easily be shown that the number of microearthquakes is not decaying with time, such as would be expected of aftershocks.

The solution proposed here is that the microearthquakes are driven by short-wavelength stress gradients created by the displacement gradients at the boundaries of regions of aseismic slip, or more generally at any boundary at which there is a short-wavelength change in displacement rate. Microearthquakes will only result, however, if the displacement gradients occur within a stick-slip portion of the P-T field for the geologic materials juxtaposed at the fault surface.

Thus microearthquakes will occur at:

1. The bottom edge of the locked zone, along locked portions of the San Andreas, but only where the bottom edge of the locked zone is within the stick-slip portion of the P-T field. Examples are the earthquakes at 8-10 km depth beneath the locked patch at Parkfield, the events at 10 km depth along the locked San Francisco Pennisula segment, and the events north of Simmler at 12-13 km depth on the Carrizo segment.
2. At the ends of the creeping zone (near Parkfield and San Juan Bautista) seismicity occurs at the vertical boundary between the creeping and locked segments, extending to the approximate depth of the locked zone.
3. Around locked (or partially locked) patches within the creeping zone, such as those at Bear Valley. In this model those locked patches will be the result of stronger lithologic units being embedded within the weak Franciscan melange matrix.

Microearthquakes will NOT occur where:

1. The base of the locked zone lies below the stick-slip field, examples being the Olema segment northwest of the Golden Gate, most of the Carrizo segment, and the Indio segment south of the Indio Hills.
2. Within the creeping zone where there are no stuck patches, such as south of Bitterwater Valley (where the highest creep rates are also observed).

In this model aftershocks are the transient response to the displacement gradient around the edge of the rupture, and decay away from it as the surrounding fault material relaxes. At Parkfield the microseismicity around the presumed locked patch occurs at the same places as did the aftershocks in 1966, but presumable due to strain gradients of opposite sign.

The fundemental model assumption made here is that the transition with depth from frictional to quasi-plastic behavior that controls the maximum depth of microearthquakes (Sibson, 1982), can occur at a different depth than the locking depth, above which failure only occurs in moderate to large earthquakes. Sibson (1982) argued that both these phenomenon might be the consequence of the friction to quasi-plastic transition; all we are adding to that is the suggestion that while closely related, the depth of the locking zone shows somewhat greater depth variation that the maximum depth of the microseismicity. When the transition to quasi-plastic behavior occurs above the locking depth, an aseismic fault segment results. When they are at about the same depth, scattered clusters of microseismicity at the base of the locked zone are observed, and when the locking depth is very shallow, a creeping segment with abundant microseismicity is the result.

Publications

Bakun, W. H., and A. G. Lindh, 1984, The Parkfield, California prediction experiment, Earthq. Pred. Res. (in press).

Bakun, W. H., M. M. Clark, R. Cockerham, W. L. Ellsworth, A. G. Lindh, W. H. Prescott, A. F. Shakal and P. Spudich, 1984, The Morgan Hill, California, earthquake, Science, v. 225, no. 4659, pp. 288-291.

Bakun, W. H., and A. G. Lindh, 1984, Characteristic earthquakes on the San Andreas fault (abs.), Abstract Book of IASPEI Regional Assembly (in press).

High Sensitivity Monitoring of Resistivity and Self-Potential Variations in the Hollister and Palmdale Areas for Earthquake Prediction Studies

U.S.G.S. Contract no. 14-08-0001-21235

P.I.: Theodore R. Madden

Department of Earth, Atmospheric and Planetary Sciences
Massachusetts Institute of Technology
Cambridge MA 02139
617/253-6384

No significant resistivity variations were observed during the first half of 1984 in either Hollister or Palmdale. We are still trying to identify and cure a noise problem on the Hollister array, however. A telephone and later an electrode outage on the San Juan Bautista electrode connection during the spring did temporarily eliminate the problem, so that we had good data for half the array during the period of the Morgan Hill earthquake. This data, which is derived from comparisons fo telluric signals across dipoles A,B,F and G, is shown in Figure 2.

The largest deviations were correlated with increased noise estimates and have been left out of the plotting. This data represents our first reliable data during a major event. (The Coyote Lake event took place just as the digital recording system was coming on stream). The size and distance of the event from our array probably precludes expecting any obvious results, and at our present level of signal to noise discrimination, none was seen.

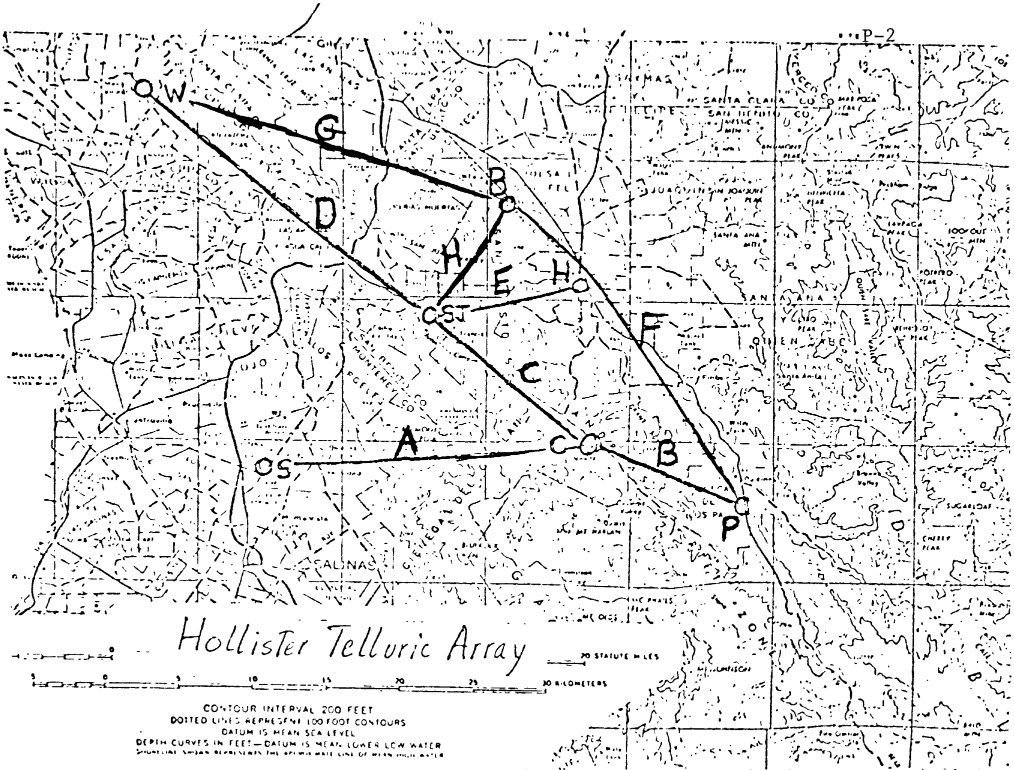

Hollister Telluric Array

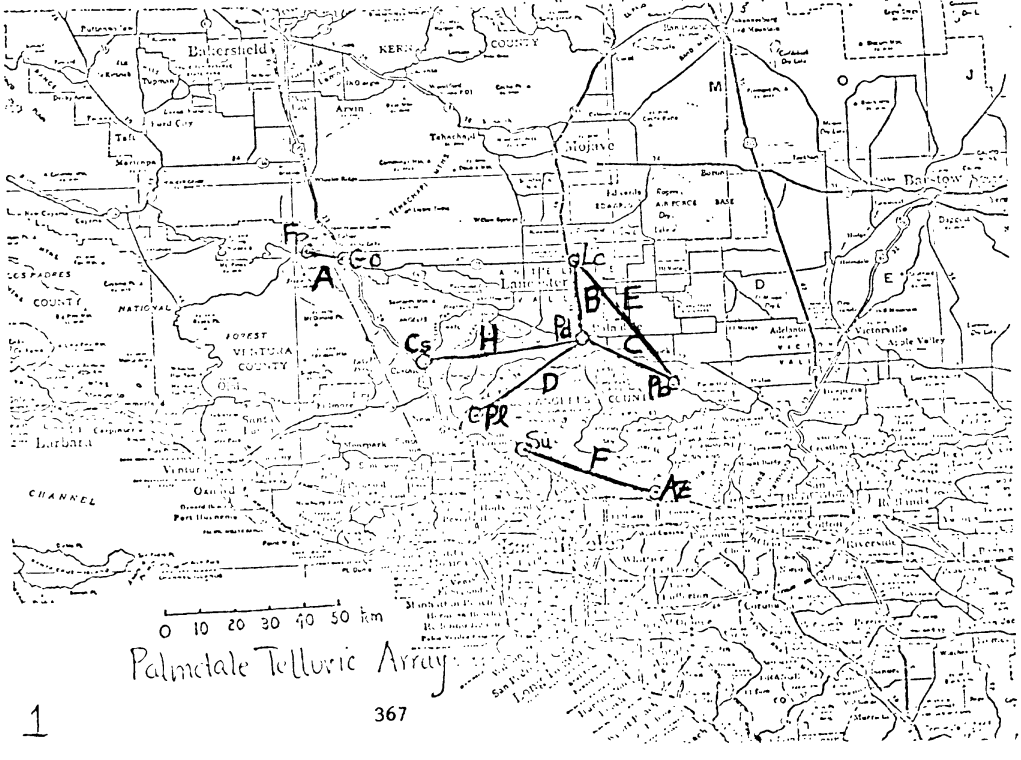

Palmdale Telluric Array

Fig 1

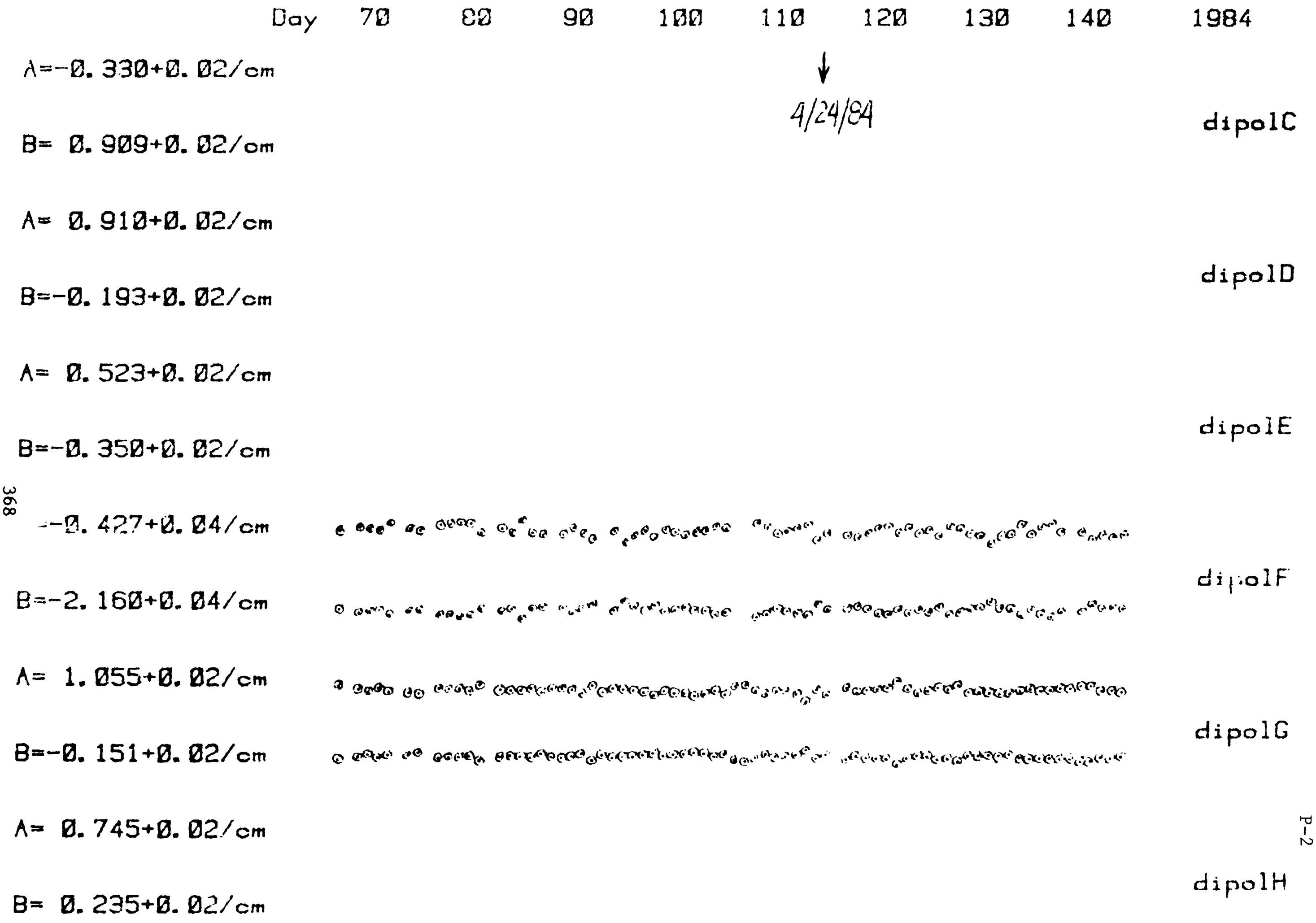

Figure 2

Hollister Array Resistivity Variations

In-Situ Seismic Wave Velocity Monitoring

14-08-0001-21222

T.V. McEvilly
R. Clymer
Seismographic Station
Department of Geology and Geophysics
University of California
Berkeley, California 94720
(415) 642-3977

Investigations

On-going monitoring of first-arrival travel times at sites adjacent to the San Andreas fault in central California (Figure 1) has continued in FY 83-84 with the collection of 2 to 4 data points on each path. Two measurements were made of deep reflections in the vicinity of Bear Valley. Measurements are made with a Vibroseis® system.

Results

Travel times, corrected for near-surface variations as measured in boreholes at most sites, are shown in Figures 2 and 3. There still appears to be a similarity of data sets from paths that share a common vibrator site. We suspect this is indicative of incomplete removal of near-surface variations occurring at the source end of each path.

It may be noted that the 1983 data in the present figures differ in some instances from those shown in the previous summary. The data shown here represent an average of an internally consistent set of first-arrival travel-time picks for each path. The '83 data shown in Volume XVIII of the Summaries were not in all cases from the same picks used for '80-'82.

Equipment

We have had few electronic equipment problems during this report period. However, the vibrator's diesel engine was overhauled in the spring of 1984, the expense of which caused us to forfeit one field session. The summer '84 field session was remarkably trouble-free, a welcome change.

The U.C. Seismographic Station has recently received a donation of a shear-wave vibrator, in excellent condition, from the Amoco Production Company Research Center. Included in the donation were an extra set of modern vibrator electronics, which will be used to upgrade our P-wave shaker, and a set of spare electronics modules which will greatly aid in field trouble-shooting.

Future Operations

For FY 84-85, we expect to make quarterly measurements at the Hollister arrays. In addition, we look forward to initiating another travel-time monitoring program on the San Andreas fault at Parkfield, using both the P and S vibrators with improved data collection methods, including multi-channel recording.

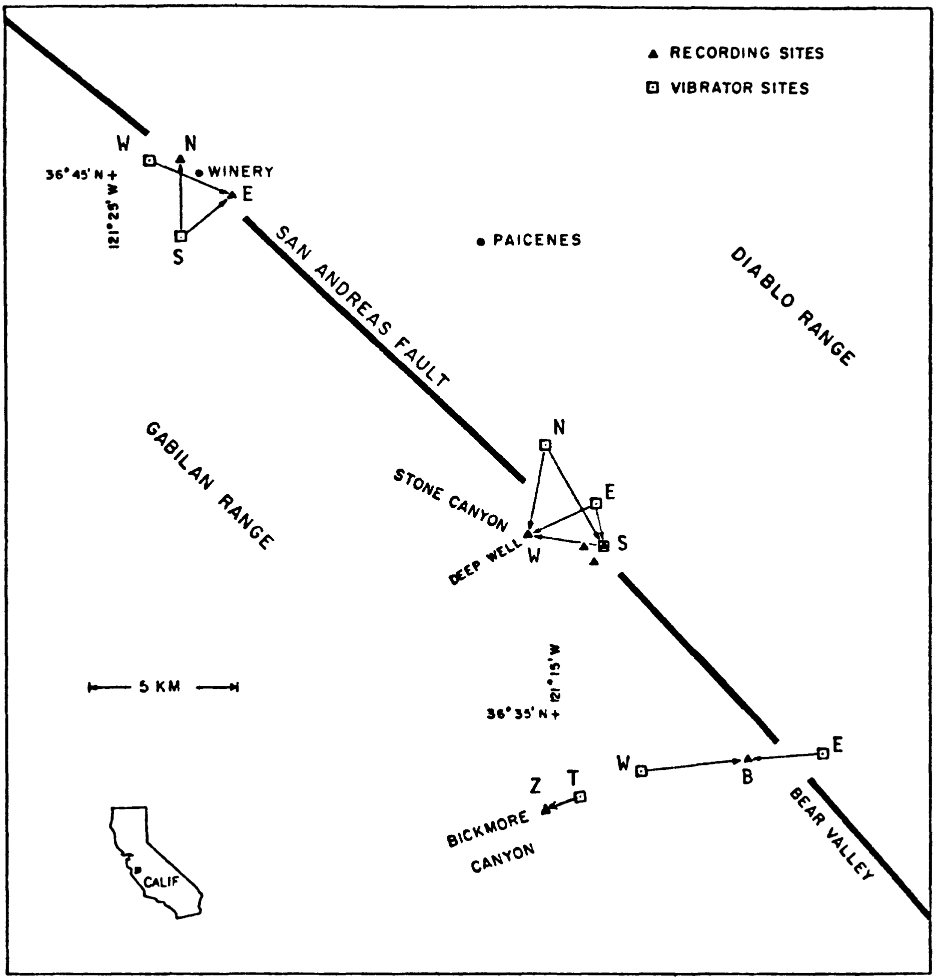

FIGURE 1. Source and receiver sites, Winery, Stone Canyon and Bickmore Canyon areas.

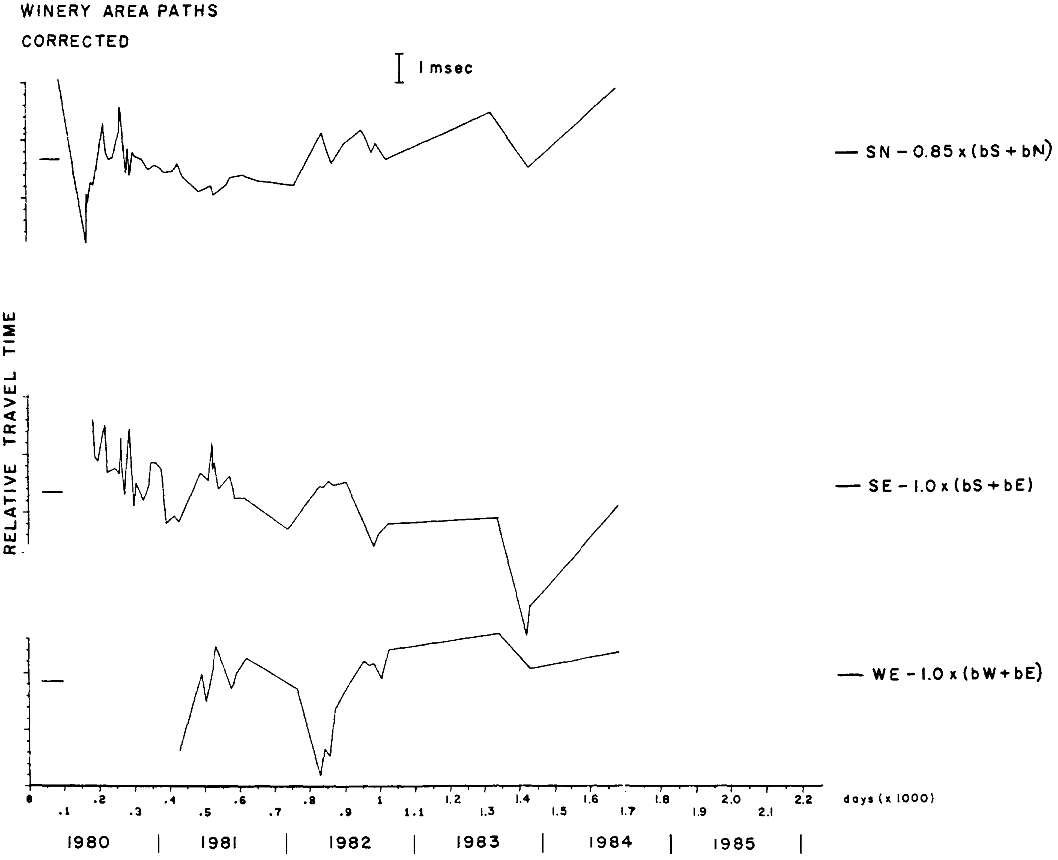

Figure 2. Winery area, seasonally-corrected data. Upper-case letters refer to site designations shown in Figure 1. Two upper-case letters indicate the source and receiver ends of a path, respectively. A lower-case 'b' followed by an upper-case letter implies that a borehole data set at that site was used for near-surface corrections to the path data.

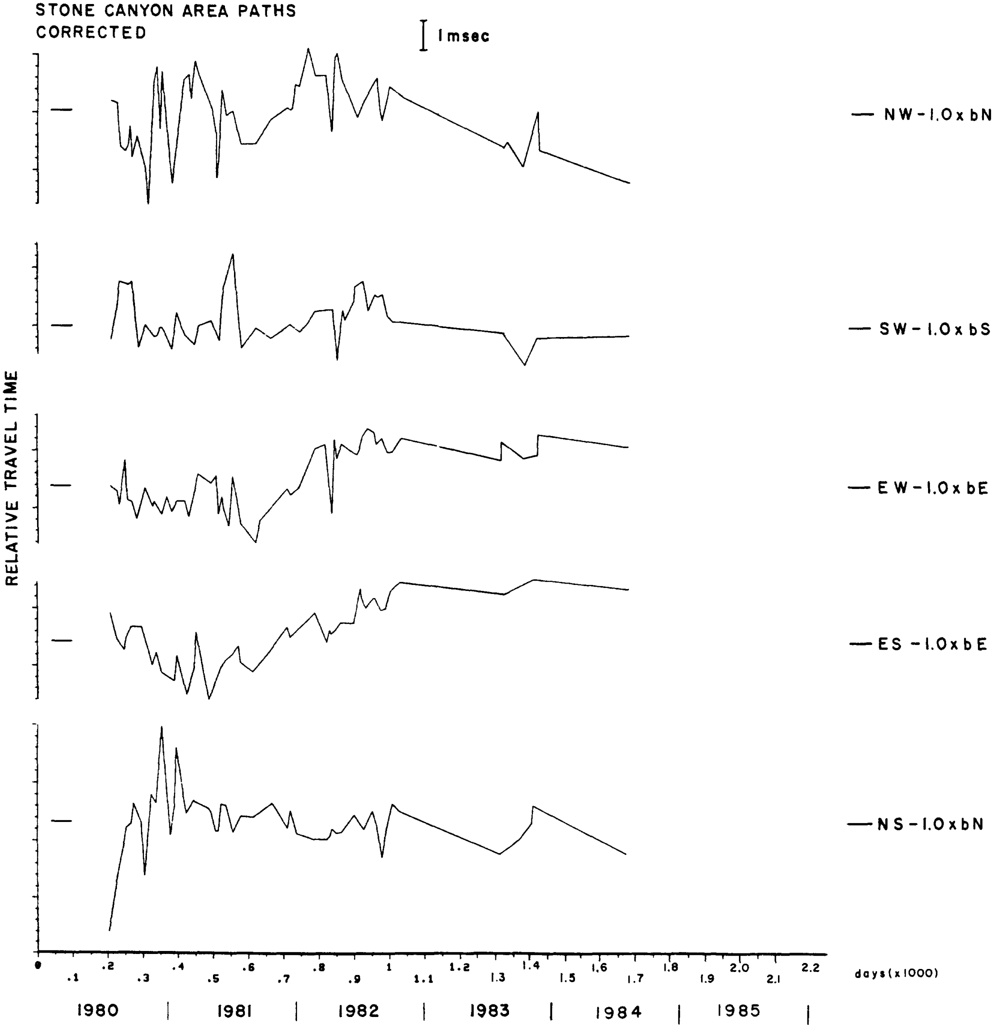

Figure 3. Stone Canyon area, seasonally-corrected data. Site W has a surface geophone array and no borehole for near-surface control. Thus paths NW, EW, and SW only have vibrator-end near-surface corrections applied. The receiver at site S is a borehole package, thus no receiver-end near-surface correction is necessary for paths NS and ES.

Tiltmeter and Earthquake Prediction Program in S. California and at Adak, AK

14-08-0001-21244

Sean-Thomas Morrissey
Saint Louis University
Department of Earth and Atmospheric Sciences
P.O. Box 8099 - Laclede Station
St. Louis, MO 63156
(314) 658-3129

I: Task 1: The Tiltmeter System

Objective: To continue to improve the performance of bubble sensor tiltmeter systems and to investigate other sensor systems for use in moderate depth boreholes, seeking relatively low-cost, readily deployed instrumentation.

Accomplishments: Five new tiltmeter electronics systems for the western Mojave have been tested for six months at the Tyson vault and are ready for installation. The bubble sensors operating on mirror blanks in a dynamically "noisy" environment (the whole vault wobbles) have shown similar response to the large thermoelastic noises and rainfall loading of the overburden.

A past weakness of the tiltmeter system has been the auto-zeroing servo system and its controller. A Swiss gear motor driven potentiometer unit has been evaluated and will be used in the future since it promises to be much more reliable than the earlier system. Its controller card is also greatly simplified, requiring only about half the components. Also in the new instrumentation effort, a new quadruple microtherometer system has been designed and built; it utilizes an intrinsically self-calibrated IC sensor, and provides 100 mv/^{o}C from four separate sensors from a single 7 cm x 10 cm circuit card.

Little further work has been done on the variable inductance pendulum sensor. Some mechanical drawings have been done for construction of a working scale prototype that will fit inside the present housing used for the bubble sensor. Smaller inductors than those used for the prototype linearity tests are required, but it is not anticipated that the linearity will be degraded in any way. The excitation oscillator has been modified for crystal control for much better frequency stability with a Statek programmable oscillator I.C.

II: Task 2: The Installation Method

Objective: To improve the installation methods for borehole instruments with a goal of installing them as deep as 100 meters.

Accomplishments: The tiltmeters prepared for installation at two sites in the Mojave have not been installed, partially due to the great amount of time required (most of the summer) for the Adak seismic network maintenance effort. There is also some discussion of installing some of the instruments in the Parkfield area because of the greater scientific interest there. (A separate project has been funded to install two instruments at each of two sites; this consideration would allow installing three additional instruments at an additional site at Parkfield rather than at Black Butte in the Mojave.

The deep hole installation system is complete. A variable speed reversible winch and portable headframe system has been designed for precise control of lowering the installation assembly with the tiltmeter attached; the entire assembly will weigh over 50 kgm, of which only the tapered borehole housing stays in the hole. The pre-leveling system of the installation tool can level the tiltmeter to ±1 ppm and hold it there for installing the bonding sand. A simple bi-axial electro-optical coarse level indicator has been added to facilitate initial adjustments of the installation system so that fine leveling adjustments are attempted only when the unit is within the operating range of the leveling system. The coarse level indicators have about 100 times the range of the lowest output of the bubble tiltmeter (±1500 ppm). Tests of the installation system and pre-leveling control are in progress at the CCMO test site, weather permitting. (We've had record rains in September and October.)

The Adak summer field trip was largely devoted to re-furbishing the seismic network, going by boat and hiking to replace the batteries. About 20% of the 2 months was spent on the tiltmeter program, mostly in battery replacement. All the records of the on-site Rustrak recorders were recovered; all had functioned perfectly for a year with no attendance. Two tilt components, the WE-Y and WW-Y, had not even drifted far enough (±3 ppm) during the year to activate the auto-zeroing system. (Y is NS tilt.) A major accomplishment was the removal of the former East tiltmeter, which had not been disturbed since 1979, and installing it as a third unit at the South site. A 1 meter diameter access hole in excess of 2 meters deep was made in solid (weathered) andesite with a gasoline powered jackhammer over several afternoons, and the borehole was installed in a 15 cm diameter hole in the bottom of this. It has stabilized very rapidly, which is typical of this installation method. Figure 1 shows the first week of data from this instrument. This is the deepest solid rock hole at Adak; we wanted to deepen the SE hole, but there was no time.

The Adak water tide gauge, a self-contained pressure sensor system that was to be used for vertical deformation sensing with regard to mean sea level, has continued to run well. It was broken loose from the piling by NOAA personnel in May as they repaired their gauge, and hung from the sturdy nylon cable conduit until it was re-fastened to the piling at low-low tide during the summer trip. It has operated for two years now without any problems; with a mm resolution out of a 3 meter range, the data exactly duplicate the NOAA float and bubbler data.

III: Task 3: The Digital Data System

<u>Objective</u>: To continue to develop and operate a digital data acquisition system to acquire geodetic data and to thoroughly monitor the environment of the instrument installations.

Accomplishments: The Adak digital data system continues to operate well, albeit not without occasional hardware problems with the acquisition microcomputer. Fortunately, these can be remedied by mailing replacement parts to our observer at Adak. The digital system has now run continuously for four years, having recorded 82 megabytes of data. A similar digital system has been prepared for the Mojave Desert program. It has an integral timing system rather than relying on the Datum clock.

A problem has arisen with the A.D. Data remote digitizers. They are no longer available. and some have been damaged beyond repair by lightning. In searching for a replacement, many similar systems were considered, but none was found that is both amenable to our low power requirements and compatible with the present data format. So a replacement system is being programmed into an RCA 1802 microcomputer board with a 16-bit digitizer sampling 14 channels. A prototype has been developed.

IV: Task 4: Data Interpretation

Objective: To process the digital data and make efforts to remove the environmental noise from the data, so as to establish the intrinsic long term stability of the tiltmeters. Various analysis techniques are then utilized to present the data in meaningful formats such that any precursory tilt events would become evident.

Accomplishments: The raw incoming data from Adak is routinely processed into 8-day plots, usually the day the floppy disk arrives. Cumulative plots are made periodically to look at months to years of the data. The latest continuous set runs from after the lightning strike damage was repaired in May of 1983 to the present, some 13,000 hours. Continuous files of the entire 4 year data set have also been used extensively for analysis of DC tilts and M2 tidal amplitude variations. However, significant gaps exist in some of the early data (a gap is any loss of more than 6 hours), and several weeks were lost after the lightning strike, and these have to be properly accomodated in any longterm analysis. All the data does exist in the form of Rustrak records from the on-site backup recorders running at 38 mm/day. A preliminary effort was made to provide time interval designations to the 1982-1983 data and then to digitize it to fill in the missing data. The time marking was not as precise as it should be for proper earth tide phase stability, so it will have to be re-done.

A major effort was made by Dr. Rene Rodriguez to analyze the data for any significant precursory indications. He devised a method to recover the net DC tilt over a given time interval by convolving the known noise sources (temperature. barometric pressure, etc.) with a linear ramp chosen empirically such that the synthesized result matches the original data. The results offer a strong suggestion of net tilt down to the northeast, at an average rate of 2.1 ppm/year down to the east and 0.4 ppm/year down to the north. A plausible explanation of this is offered in relation to the tectonics of the Adak canyon area of the subduction zone to the southwest of Adak, which is the suspected locale of a future large earthquake. The effort to determine DC tilts from the existing data needs much more work. There is strong evidence that the thermal noise is not "convolved" with the tilt, but merely added into the data, since the annual thermal cycles can be reduced by an order of magnitude by linear subtraction of the temperature profile, resulting in data from adjacent components that evidence good coherence.

25 October 1984
Sean-Thomas Morrissey

Figure 1: First week of data from newly installed Adak South site, North tiltmeter. Rapid stabilization to earth tide sensitivity is always achieved by this method.

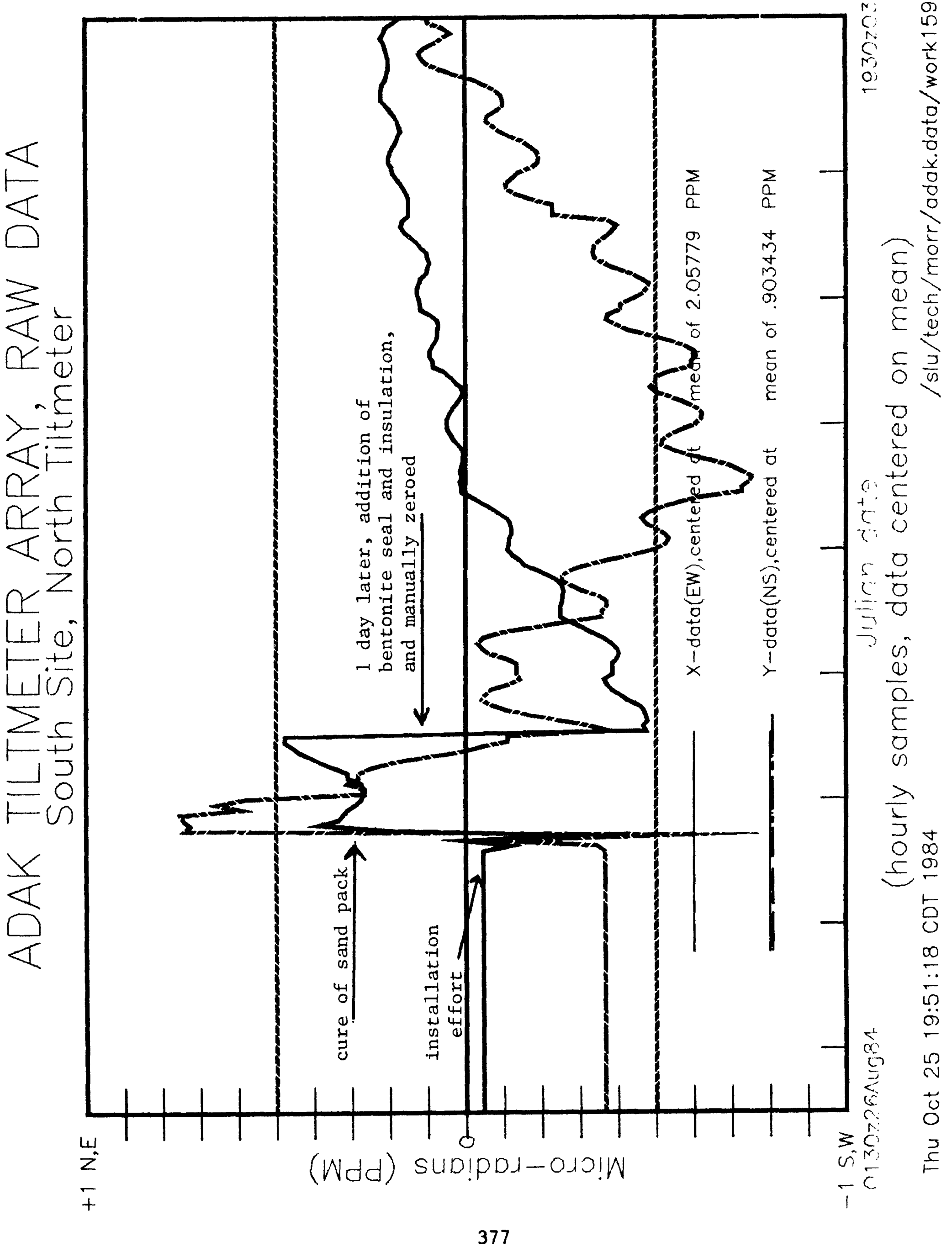

Figure 2: Sample of coherence of adjacent tiltmeter components after linear correction for annual thermal cycle. These instruments are about 1.5 meters deep in weathered rock.

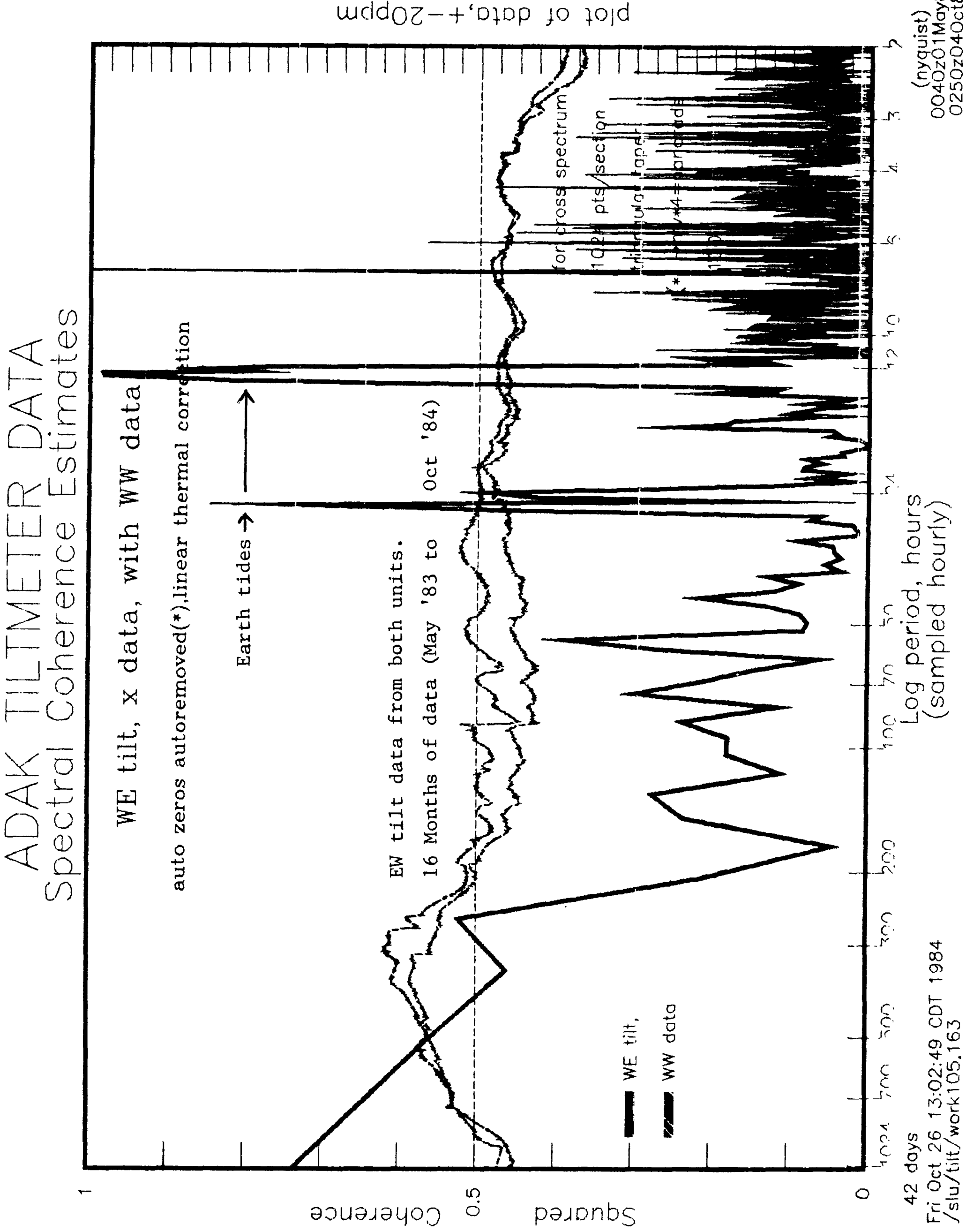

Crustal Deformation Observatory, Part (i):

Shallow Borehole Tiltmeters

14-08-0001-21939

Sean-Thomas Morrissey
Saint Louis University
Department of Earth and Atmospheric Sciences
P.O. Box 8099 - Laclede Station
St. Louis, MO 63156
(314) 658-3129

Objective: To apply the latest innovations and technology of instrumentation and installation methods to the shallow borehole tiltmeters at Pinon Flat such that their performance. particularly with regard to longterm stability, will compare more favorably with the data from the long baseline tiltmeters.

Accomplishments: The program began in June 1984, at which time long lead-time components were ordered. Prior to that, in December of 1983. the existing tiltmeters (Kinemetrics TM-1) and installation pits were inspected. The first part of the program is to provide all new electronics, cables, and bubble housings for the Autonetics bubble level sensors, and reinstall the four units in the existing 5 meter deep pits at PFO using the well-proven technique of tamping a special blend of foundry sand and hydraulic cement around the borehole housing. Toward this end, five new tiltmeter electronics systems are nearly completed, and the tapered cast-stainless borehole housings are being made. The current plan is to retro-fit and reinstall the four borehole units in December, after the AGU meeting. The four bubble sensors will be removed from the present units and re-used.

The second part of the program is to install the borehole sensors in 30 meter holes at PFO. We have demonstrated that this can be done in 10 meter holes, but new techniques are necessary for the 30 meter depth. Experiments are underway in investigating remote methods of tamping the sand pack. Current funding provides for drilling two 12" diameter holes to 30 meters. 30 meters is the depth of the "optical anchors" that are used for monitoring end pier stability of the present long-baseline instruments operated by UCSD and others.

25 October 1984
Sean-Thomas Morrissey

EXPERIMENTAL TILT AND STRAIN INSTRUMENTATION

9960-01801

C.E. Mortensen
Branch of Tectonophysics
U.S. Geological Survey
345 Middlefield Road, MS/977
Menlo Park, California 94025
(415) 323-8111, ext. 2583

Investigations

1. The Menlo Park GOES Data Collection System (DCS) is operational. Twenty-five Data Collection Platforms (DCPs), delivered in May, have been tested and 6 have been deployed. Of the 25 DCPs tested, 6 were returned for warranty repair. One more unit apparently failed after being installed in the field. Eight additional DCPs have been ordered; the new units will have a 16-bit A-to-D converter.

   Instrument sites with DCPs currently installed are as follows:

Location	Instrument type	No. of sensor inputs
Middle Mtn. (near Parkfield)	creepmeter/h2 gas	3
Gold Hill 1 (near Parkfield)	dilatometer	5
Gold Hill 2	tiltmeter cluster	6
Gold Hill 3	creepmeter/h2 gas	2
Adobe Mtn. (Mojavi)	dilatometer	5
Devils Postpile	dilatometer	5

In July imagery of the GOES East satellite failed. In order to provide coverage over the Gulf of Mexico and further east during the hurricane season, the GEOS West satellite was moved to the east and GOES 4, an older satellite serving as the spare, was activated for DCS functions. Unfortunately, the stability of the orbit of GOES 4 had deteriorated with age, causing daily excursions beyond the beamwidth of the 5m dish antenna at Menlo Park. During the most severe period, up to 70% of the data were lost each day. Adjustment of the antenna position did not seem to effect the temporal distribution or amount of data loss. Gradually, the positional stability of the satellite was improved. With careful adjustment of the antenna, data reception has been improved to nearly 100%. This experience with a problem beyond our control having such a severe effect on data reception caused us to consider various options for backup. A telephone modem at each DCP location appears to be the most attractive of these options.

2. In consultation with Mark Linker and John Langbein, a new collimating reflector for the two-color laser has been designed. Assembly of the prototype is awaiting the manufacture of parts.

3. Networks of tiltmeters, creepmeters and shallow strainmeters have been maintained in various regions of interest in California. A network of 14 tiltmeters located at seven sites monitor crustal deformation within the Long Valley caldera. Other tiltmeters are located in the San Juan Bautista and Parkfield regions. Creepmeters are located along the Hayward, Calaveras and San Andreas faults from Berkeley to Parkfield and shallow strainmeters are located in the Parkfield region. Observatory type tiltmeters and strainmeters are located at the Presidio in San Francisco and a tiltmeter in the Byerley Seismographic Vault at Berkeley. Data from all these instruments are telemetered using a 12-bit digital telemetry via phonelines and radio links to Menlo Park.

Results

1. The Kinemetrics tiltmeter at Casa Diablo (CA1), in the Long Valley caldera, recorded an apparent deformation, primarily on the EW component, coincident with the onset of an earthquake swarm in July. The deformation was probably very localized since the Westphal instrument (CA2) did not show a similar change at the same time. The two instruments are separated by about 100m. The CA2, NS component was not working during this period. The epicenters for the swarm were at the site of the tiltmeters, within the location error. There were reports of a blowout in a geothermal well that was being drilled nearby some 30 minutes before the onset of the swarm. Figure 1 shows the tiltmeter records spanning the time of the swarm onset. These signals are close to the noise level for these instruments.

2. Six DCPs are currently returning data via the GOES satellite to the Direct Readout Ground Station (DRGS) in Menlo Park. The DCPs digitize incoming analogue data with 13-bit resolution (12 bits plus sign). As a field test the

new satellite DCS is operating in parallel with the existing (12-bit) low-frequency, digital telemetry system. Some plots for comparison are shown in Figure 2. Interface problems with some types of sensors still exist and are being analized.

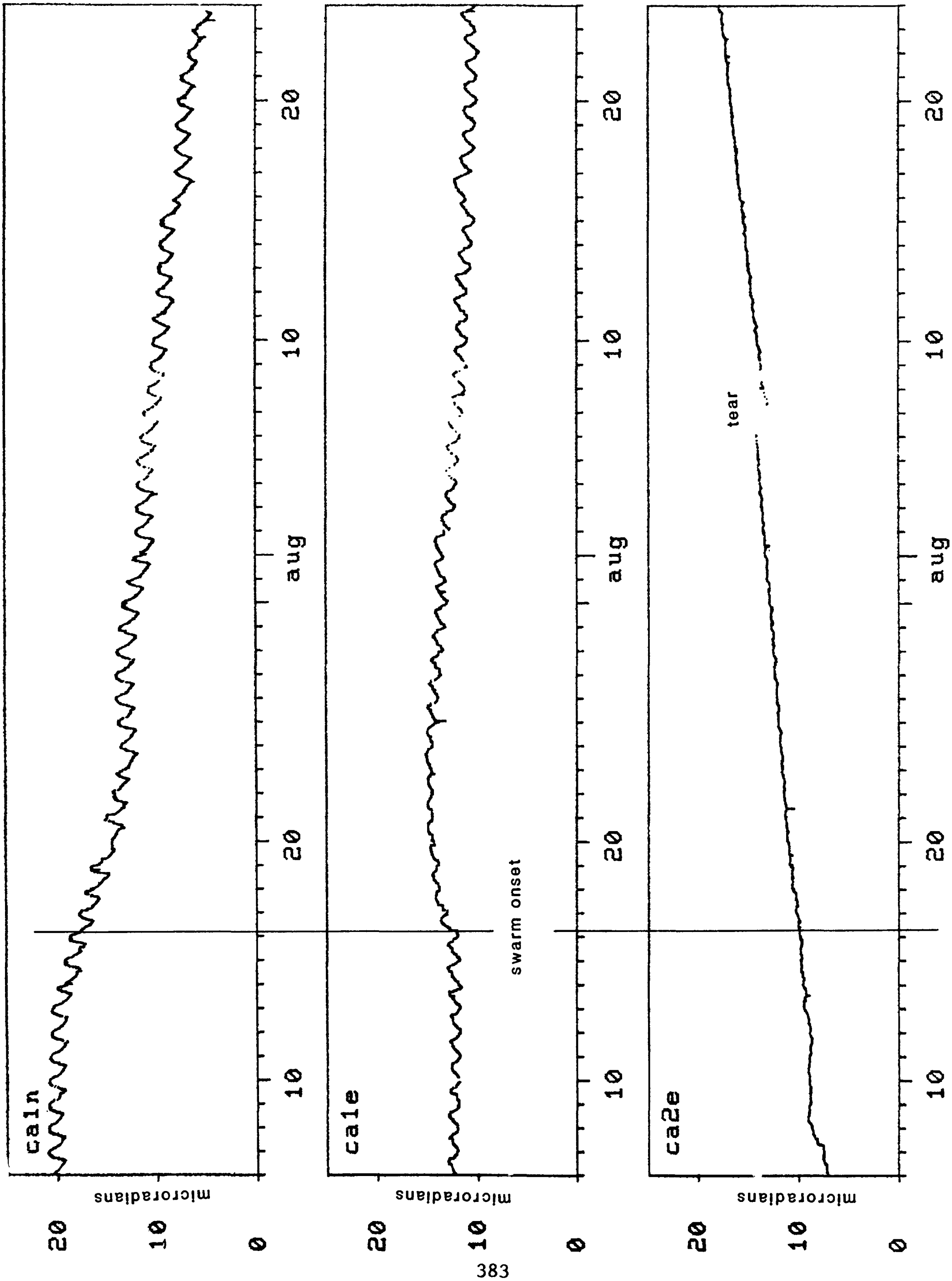
ca1n
ca1e
ca2e
microradians
microradians
microradians
20
10
0
20
10
0
20
10
0
10
20
aug
10
20
swarm onset
tear

FIGURE 1

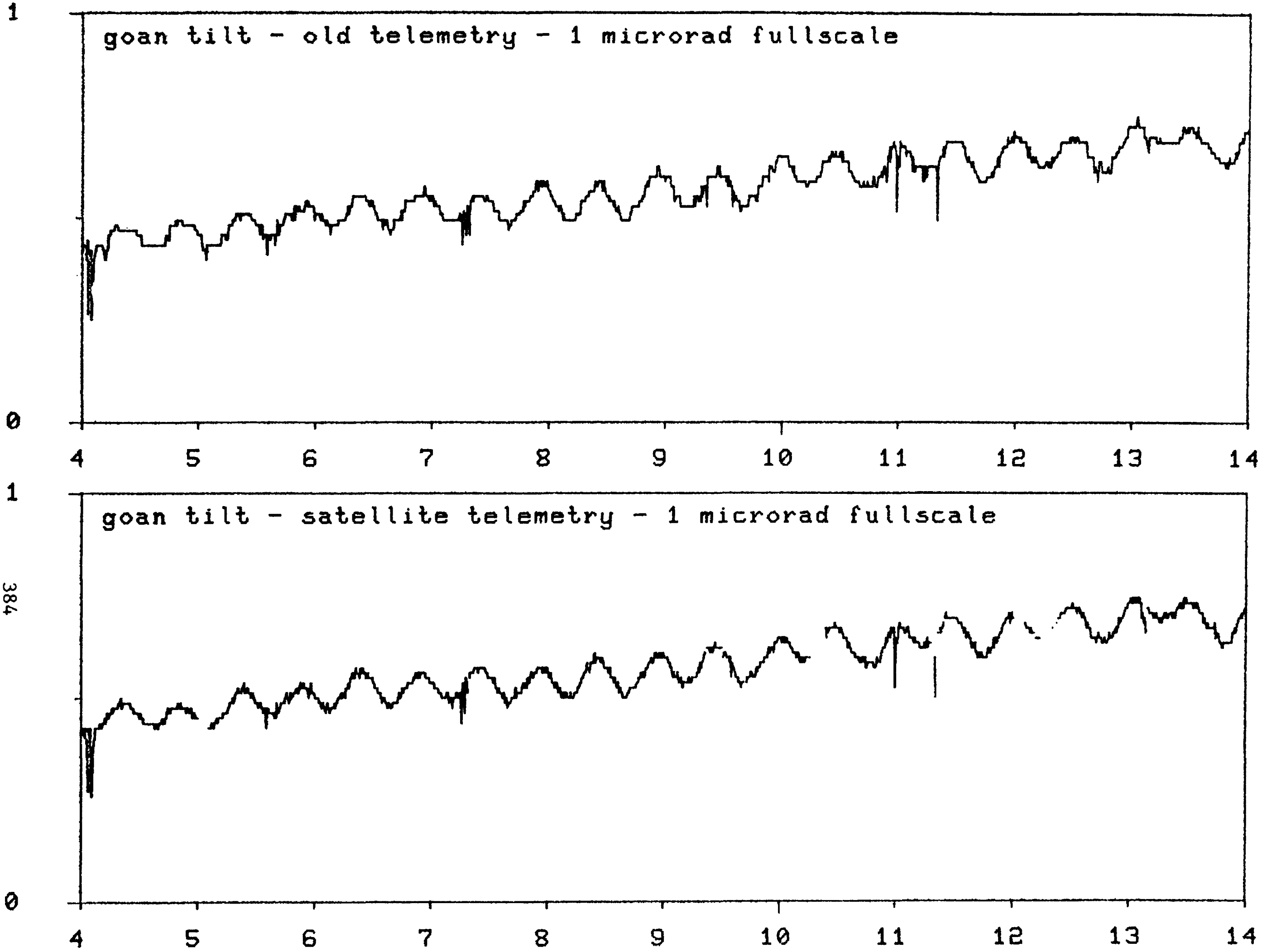
1
0
goan tilt - old telemetry - 1 microrad fullscale
4
5
6
7
8
9
10
11
12
13
14
1
0
goan tilt - satellite telemetry - 1 microrad fullscale
4
5
6
7
8
9
10
11
12
13
14

FIGURE 2

Dilatometer Operations

9960-03815

G. Douglas Myren
Branch of Tectonophysics
U.S. Geological Survey
345 Middlefield Road, MS/977
Menlo Park, California 94025
415-323-8111, ext. 2705

Investigations - Operations

The principal subject was operations of the dilatometer-strainmeter network in California.

1. Routine maintenance of instruments, paper changes, telemetry checks, and battery changes were accomplished. Barometric pressure transducers and temperature probe electronics were also maintained.

2. In June the road to Devils Postpile was opened for the summer and work was begun on a winter accessible enclosure for the strainmeter. This was completed and telephone hookup to digital telemetry by mid-August. Satellite telemetry was installed in late September.

3. In July and August sites were selected and permitted for 3 additional strainmeters and permitted for 3 additional strainmeters in the Parkfield area. Drilling was to begin by the end of September for installation later in October and November.

4. Satellite telemetry was also installed at Adobe Mountain in the Mojave Desert and one site at Gold Hill.

SEISMIC STUDIES OF FAULT MECHANICS

9930-02103

Paul Reasenberg
Branch of Seismology
U.S. Geological Srrvey
345 Middlefield Road, MS-977
Menlo Park, California 94025
(415) 323-8111, Ext. 2049

Investigations

1. A detailed analysis of the second-order moment (2-point correlation function) of earthquake catalogs.
2. Analysis of the hypocentral distribution and fault-plane solutions of aftershocks of the M 6.7 Coalinga, Ca. earthquake of May 2, 1983. The analysis utilizes solely automated data processing techniques.
3. Development of a clustering algorithm designed to efficiently identify aftershock clusters in a catalog based on a simple physical model of earthquake interaction.

Results

1. The second-order moment (cross-correllation function) of earthquakes in the U.S.G.S. central California catalog between 1969 and 1982 was calculated with respect to a magnitude threshold $M \geq 4.0$ over interevent distances up to 80 km and interevent times up to 320 days. The statistical procedures results in a representation of the spatial-temporal structure of the catalog associated with $M \geq 4.0$ earthquakes, and is capable of revealing patterns too weak to be detected in the space-time distribution of seismicity for individual earthquake sequences. A method is introduced for identifying aftershocks based on a physical 2-parameter model of the earthquake interaction process.

   The results show that the aftershock process dominates the second-order moment, and, surprisingly, may obscure the statistical expression of a precursory process. A concentration of foreshocks within 15 km and 3 days of $M \geq 4.0$ mainshocks exhibits an apparent migration toward the mainshock loci with velocity 2.6 to 5.3 km/day. This concentration may be related to an observed tendency for $M \geq 4.0$ events to cluster (autocorrellate) over this interevent range. The declustered catalog is Poissonion in space and time. When two $M \geq 4.0$ earthquakes occur within 80 km and 40 days of each other, aftershock productivity appears to be relatively enhanced in the earlier sequence, suggesting that aftershock populations are not solely dependent on their mainshocks, so that unusually productive ones may be predictors of future moderate earthquakes.

   Work was begun in preparing the U.S.G.S. - C.I.T. catalog for southern California for similar analysis.

2. The 1983 Coalinga, California earthquake consisted of a complex rupture

on two, or possibly three, planes of slip. These planes all strike approximately parallel to the axis of Coalinga Anticline, but vary widely in dip. The distribution of 2686 hypocenters, and the alinement of 682 nodal planes for aftershocks occurring between May 2 and June 30, 1983 enable this detailed inference of rupture geometry to be drawn. The identified planes dip 70-80 degrees NE, 45-55 degrees SW and 5-10 degrees SW. The two steeper planes intersect at the mainshock hypocentral depth (10 km), and define a wedge-shaped buried horst between 5 and 11 km depth that may have been uplifted during the earthquake by slip on both planes. The distribution of early aftershocks suggests that the first and largest mainshock displacement was probably on the SW dipping fault.

Co-seismic surface elevation changes are consistent with slip distributed on the multiple-plane structure proposed above. A teleseismic body-wave model portraying the mainshock as a double event is also consistent with the proposed structure. Evidence for secondary faulting in the form of bedding plane slip is found in the hypocentral distribution and nodal plane orientation of aftershocks at the north edge of the aftershock zone, along the northeast flank of the anticline. Considered together, these observations are consistent with a complex mainshock rupture between 5 and 11 km depth, with passive folding accomodating the seismic displacement in the overlying 5 km of rock.

This work was done solely with automated procedures. Notably, timing of p-phases and first motion polarities were obtained with a microprocessor, and all fault plane solutions were modeled, selected and plotted by computer programs.

3. A modification to the clustering algorithm used in the identification of aftershocks in central California (see (1) above) is being made. The problem is to model the change in minimum magnitude (for complete coverage) in a catalog during an aftershock sequence. It is well known that the minimum magnitude reported in a catalog rises during large sequences as the result of several factors including a) small events lost in the codas of other events, b) inability of network personnel to process events in the sequence to the usual level of completeness, c) inability of real-time miscrocomputer processors to keep up with the sequence. The clustering algorithm requires a realistic model of this network sensitivity change to reasonably model aftershock clusters.

Reports

Reasenberg, P., The second-order moment of central California seismicity, 1969-1982, submitted to J. Geophys. Res.

Eberhart-Phillips, D., and P. Reasenberg, Hypocenter locations and fault-plane solutions for Coalinga aftershocks, May 2-24, 1983: evidence for a complex rupture geometry, in Mechanics of the May 2, 1983 Coalinga, Ca. earthquake, U.S. Geological Survey Open-File Report 84- .

Reasenberg, P., D. Eberhart-Phillips and P. Segall, Preliminary views of the aftershock distribution: in the Coalinga earthquake sequence commencing May 2, 183, U.S. Geological Survey Open-File Report 83-511, 1983.

FAULT ZONE TECTONICS

9960-01188

Sandra S. Schulz, Beth D. Brown
Branch of Tectonophysics
U.S. Geological Survey
345 Middlefield Road, MS/977
Menlo Park, California 94025
(415) 323-8111 x 2763

Investigations

1. Directed maintenance and upgrading of creepmeter network in California.

2. Updated archived creep data on PDP 11/44 computer.

3. Continued to work on developing experimental procedures aimed at an operational prediction program.

4. Expanded, maintained and upgraded alinement array network on central and northern California faults.

5. Monitored effects of the April 24, 1984, Morgan Hill earthquake on creepmeters and alinement arrays along the Calaveras fault.

6. Submitted for publication results of study on the effects of the 1983 Coalinga earthquake on Parkfield creepmeters along the San Andreas fault, and results of study on the effects of the 1984 Morgan Hill earthquake on creepmeters and alinement arrays along the Calaveras fault in central California.

Results

1. Currently 28 extension creepmeters operate; 20 of the 28 have on-site strip recorders; and 17 of the 20 are telemetered to Menlo Park. Two Parkfield creepmeters (XMM1 and XPK1) were renovated and weatherized.

2. Fault creep data from all USGS creepmeter sites along the San Andreas, Hayward and Calaveras faults have been updated through July, 1984, and stored in digital form (1 sample/day). Telemetry data covering the period between July and the present is also stored in digital form (1 sample/hour) and updated every 10 minutes.

3. A computer program became operational that checks Parkfield telemetry data once each hour, and alerts Project personnel via 'beeper' whenever unusual fault movement occurs.

4. Currently 24 alinement arrays have been established or renovated and surveyed across five (5) active faults in California (San Andreas, Hayward, Calaveras, Nunez, Imperial). New arrays were installed or renovated at Coyote Reservoir and Ruby Canyon on the Calaveras fault, and at Taylor Ranch on the San Andreas fault near the two-color laser observatory in Parkfield, California. Each site will be remeasured every 90-120 days. Arrays typically cover 50-250 m, are placed across active fault zones and are used to guide emplacement of creepmeters, check creepmeter measurements, and monitor fault movement where creepmeters are logistically impractical.

5. Creepmeter SHR1 (Shore Road) is located on the Calaveras fault 10 km northwest of Hollister, California (Figure 1). Immediately following the April 24, 1984, Morgan Hill earthquake (magnitude = 6.2), SHR1 began recording triggered creep that totaled 12.9 mm after 18 hours. One month later, SHR1 recorded a 7.9 mm creep event. The creep activity at SHR1 is particularly interesting for several reasons:

    1. No unequivocal surface breakage was found in the epicentral area near Halls Valley. However, the day after the earthquake, surface fractures were found next to SHR1, located on the same fault but 50 km southeast of the epicenter.

    2. Although post-earthquake surface fractures were found 10 km northwest of SHR1 at Highway 152, no further surface disturbance was seen southeast of SHR1, or at any of the Hollister creepmeters.

    3. The 12.9 mm event immediately after the earthquake is the largest in the creepmeter's 13-year recording history. Previous events have not exceeded 9 mm.

    4. The 7.9 mm creep event one month after the earthquake is puzzling. It may represent acceleration due to aftershock activity, as was observed after the 1966 Parkfield earthquake, or it may only represent the creep event of about this size recorded nearly every summer by SHR1.

    5. In 1976, SHR1 began recording a three-year creep lag that ended only with the 1979 Coyote Lake earthquake (magnitude = 5.9), 15 km northwest on the same

fault. In addition, SHR1 recorded an 18-month creep lag just prior to the Morgan Hill earthquake (Figure 2). The station appears to be located on a part of the Calaveras fault sensitive to regional strain changes.

Reports

Brown, Beth D., 1984, Alinement array measurements following the 24 April 1984 Morgan Hill earthquake: in Hoose, S.N., ed., The Morgan Hill, California, earthquake of April 24, 1984 (A Preliminary Report): U.S. Geological Survey Open-File Report 84-498A, p. 60-63.

Brown, Beth D., 1984, Alinement array measurements in the San Felipe Valley: in U.S. Geological Survey Bulletin 1639 (in press).

Burford, R.O., and Schulz, S.S., 1984, Retardations in aseismic slip rate on the Calaveras fault at Shore Road: EOS (in press) (abstract).

Galehouse, Jon S., and Brown, Beth D., 1984, Southeastern limit of surface displacement on the Calaveras fault associated with the 24 April 1984 Morgan Hill earthquake: in Hoose, S.N., ed., The Morgan Hill, California, earthquake of April 24, 1984 (A Preliminary Report): U.S. Geological Survey Open-File Report 84-498A, p. 85-91.

Galehouse, Jon S., and Brown, Beth D., 1984, Surface Displacements near Hollister: in U.S. Geological Survey Bulletin 1639 (in press).

Schulz, Sandra S., Gerald M. Mavko, Beth D. Brown, Response of creepmeters on the San Andreas fault near Parkfield to the May 2, 1983, Coalinga earthquake (submitted to U.S. Geological Survey Professional Paper on Coalinga Earthquake, in press).

Schulz, Sandra S., 1984, Response of U.S.G.S creepmeters near Hollister to the April 24, 1984, Morgan Hill earthquake: in Hoose, S.N., ed., The Morgan Hill, California, earthquake of April 24, 1984 (A Preliminary Report): U.S. Geological Survey Open-File Report 84-498A, p. 64-71.

Schulz, Sandra S., 1984, Response of U.S.G.S. creepmeters near Hollister: in U.S. Geological Survey Bulletin 1639 (in press).

Schulz, Sandra S., 1984, Triggered creep near Hollister following the April 24, 1984, Morgan Hill earthquake: *in* The 1984 Morgan Hill, California earthquake: California Division of Mines and Geology Special Publication 68 (in press).

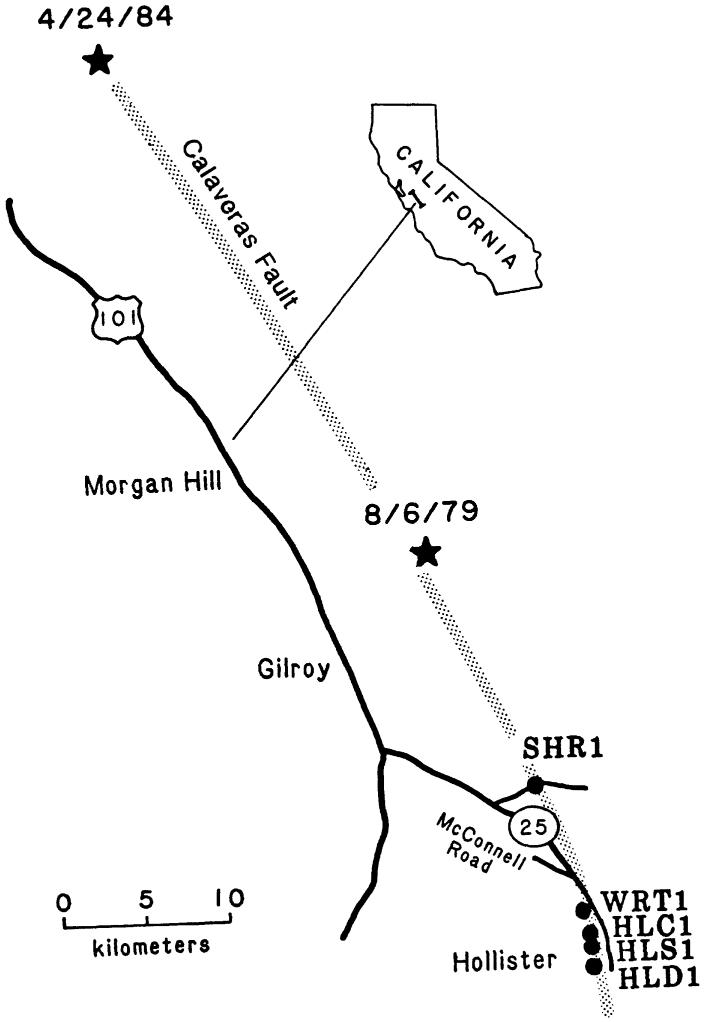

Figure 1. Map showing location of U.S.G.S. creepmeters near Hollister (circles), and epicenters of April 24, 1984, Morgan Hill and August 6, 1979, Coyote Lake earthquakes (stars).

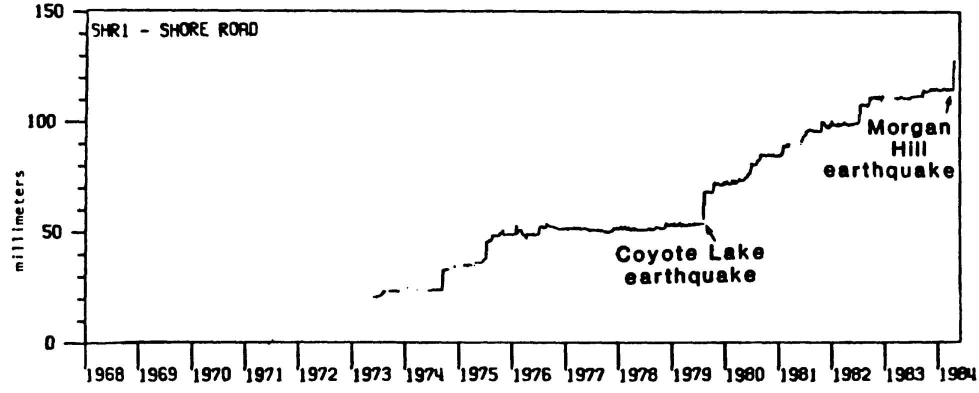

Figure 2. Long-term plot of fault creep recorded at SHR1 (Shore Road). A 3-year creep lag at SHR1 preceded the August 6, 1979, Coyote Lake earthquake 15 km distant, and an 18-month creep lag preceded the April 24, 1984 Morgan Hill earthquake 50 km distant. Both earthquakes occurred on the same fault on which SHR1 is located.

THE EXTENSION AND OPERATION OF A COMPUTER-CONTROLLED MONITORING NETWORK FOR RADON AND OTHER GEOCHEMICAL PRECURSORS, AND LABORATORY STUDIES ON SEISMO-GEOCHEMICAL PRECURSORS

14-08-0001-21268

M.H. Shapiro, A. Rice, J.D. Melvin, and T.A. Tombrello
Div. of Physics, Mathematics, and Astronomy - Caltech
Pasadena, CA 91125
(818) 356-4277

INVESTIGATIONS

Since the last reporting period we have continued to monitor radon, thoron, and environmental variables at all network sites except for Santa Anita where the borehole is dry. A new site at Acton was completed early this year to provide coverage of the San Andreas between existing stations at Lake Hughes and Lytle Creek. In addition to radon and thoron, carbon dioxide and hydrogen are monitored at several network stations. Borehole water level now is measured at all sites except for Anza and Ft. Tejon. (At these sites radon is monitored from pumped wells.) Water temperature is monitored at all sites.

RESULTS

In the past few months there has been some shift in the seismic patterns for southern California. Although the rate of background seismicity has not changed significantly, there have been more felt events in populated areas, mostly small to moderate earthquakes on offshore faults. Few of these, however, have been within the region monitored by our network. No unusual radon changes were observed before any of these events.

Most stations in our network have been recording normal levels of radon during the past six months. Exceptions include Lake Hughes, Lytle Creek, and Alandale which are undergoing carbon-dioxide driven radon spiking that is non-tectonic in origin. The Alandale spiking has been going on for most of the year, while the Lake Hughes and Lytle Creek episodes are more recent. Lake Hughes and Lytle Creek radon levels are strongly correlated. Lake Hughes radon also correlates with CO_2 while Lytle Creek radon is anti-correlated with the CO_2 level at that site. The reason for this is not fully understood at present.

Water levels at most stations are quite low at present, reflecting the relatively dry rainy season last winter. The Lytle Creek water level is particularly low at present.

The Sky Forest radon level has been climbing steadily over the past year; however, this may be related to the dropping water level at the site. A few radon spikes were observed recently at Kresge. These occurred immediately after a site visit, and are not believed to be significant. Radon and water level data from the network are presented in figures 1 and 2.

CALTECH ARCHIVE RADON DATA

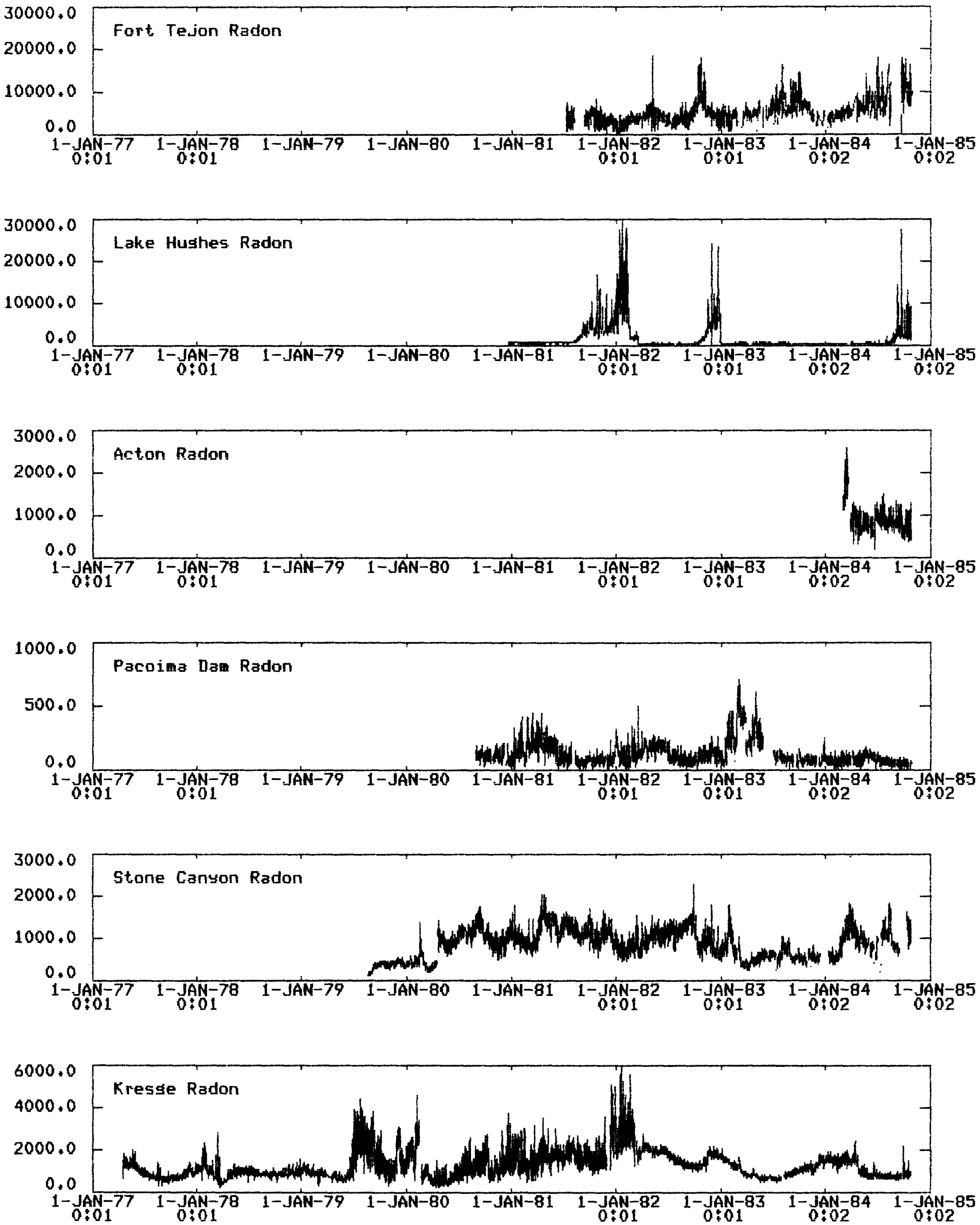

Fig. 1a

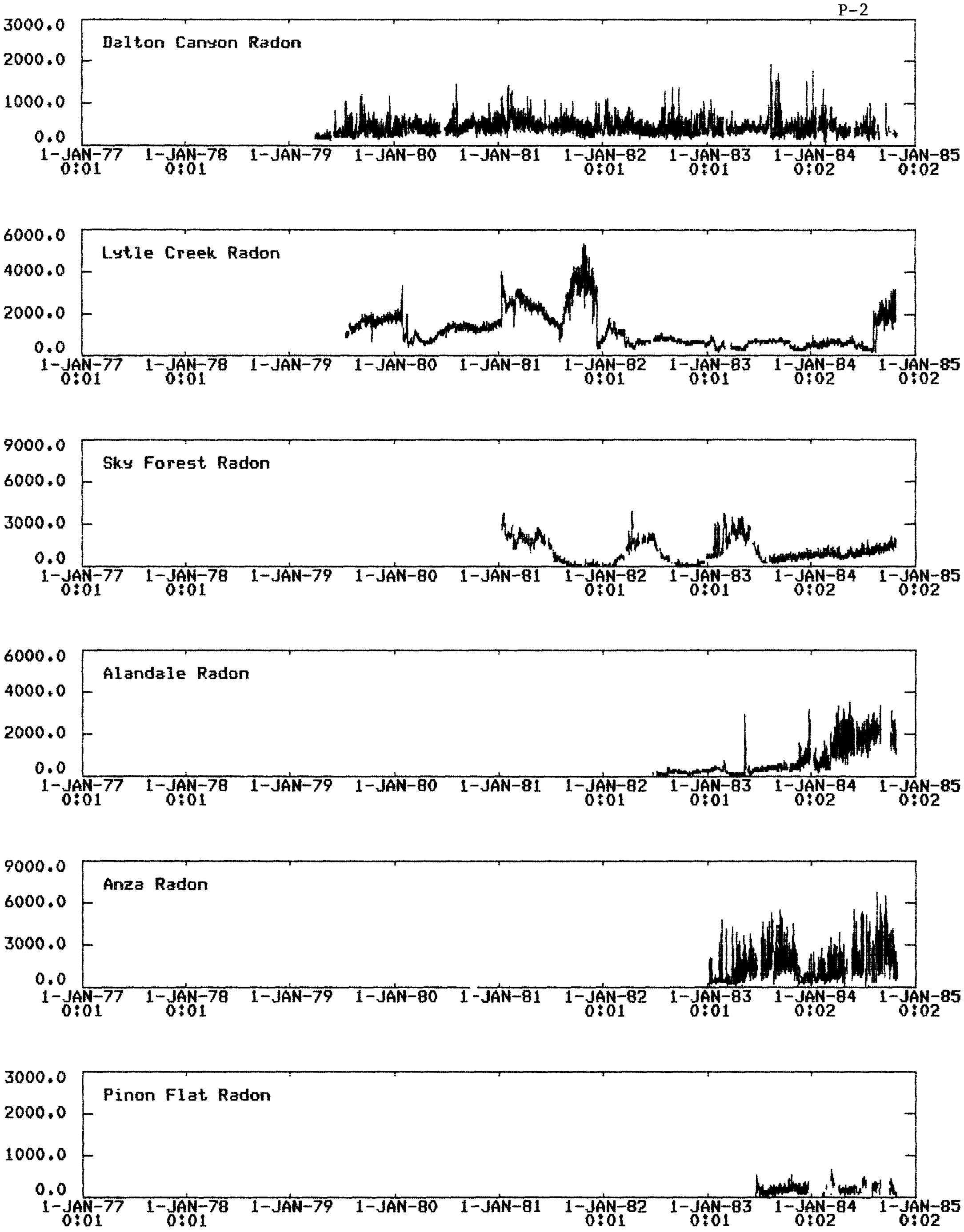
P-2
Dalton Canyon Radon
3000.0
2000.0
1000.0
0.0
Lytle Creek Radon
6000.0
4000.0
2000.0
0.0
Sky Forest Radon
9000.0
6000.0
3000.0
0.0
Alandale Radon
6000.0
4000.0
2000.0
0.0
Anza Radon
9000.0
6000.0
3000.0
0.0
Pinon Flat Radon
3000.0
2000.0
1000.0
0.0
1-JAN-77 0:01
1-JAN-78 0:01
1-JAN-79
1-JAN-80
1-JAN-81
1-JAN-82 0:01
1-JAN-83 0:01
1-JAN-84 0:02
1-JAN-85 0:02

Fig. 1b

CALTECH ARCHIVE WATER LEVEL DATA

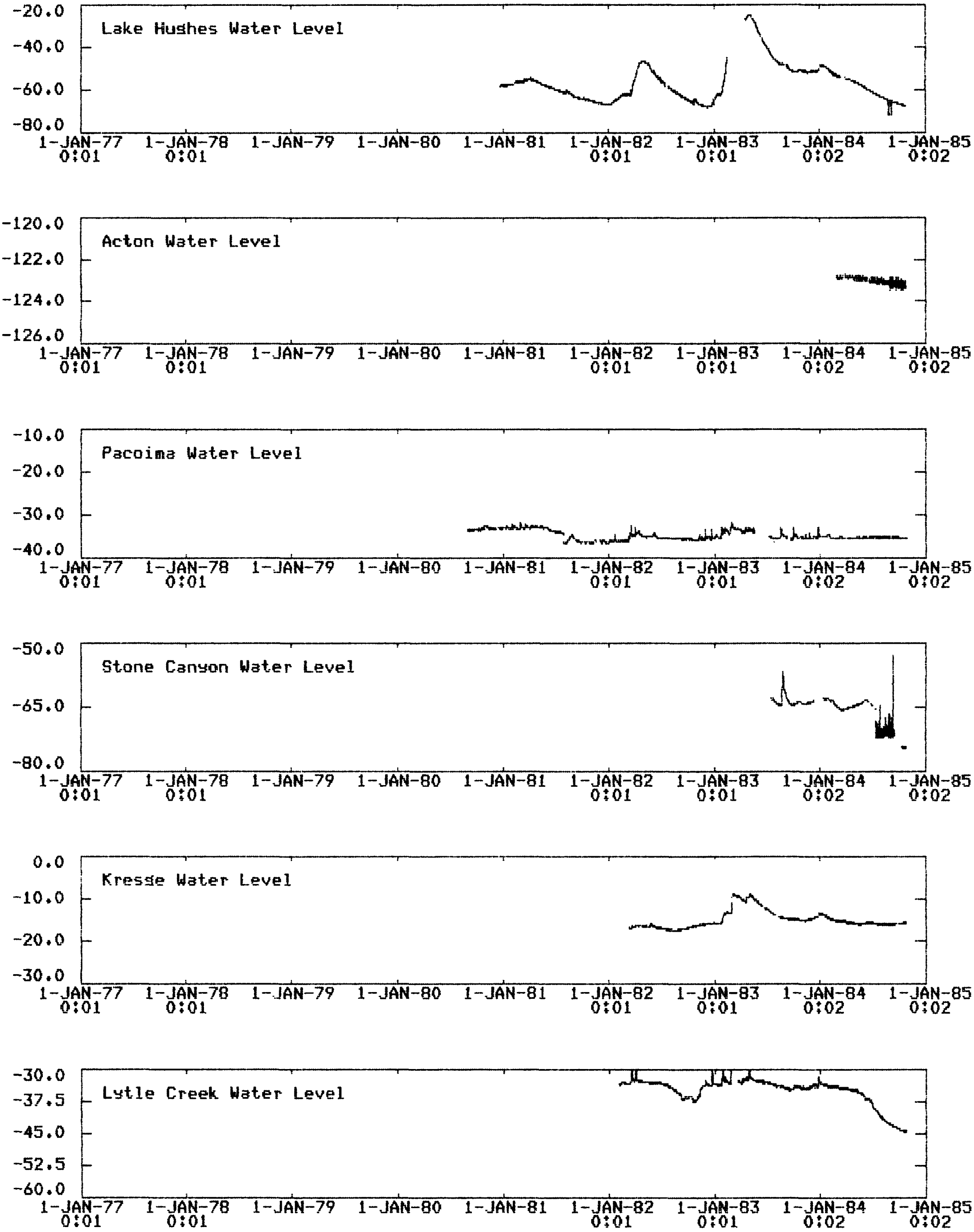

Fig. 2a

P-2

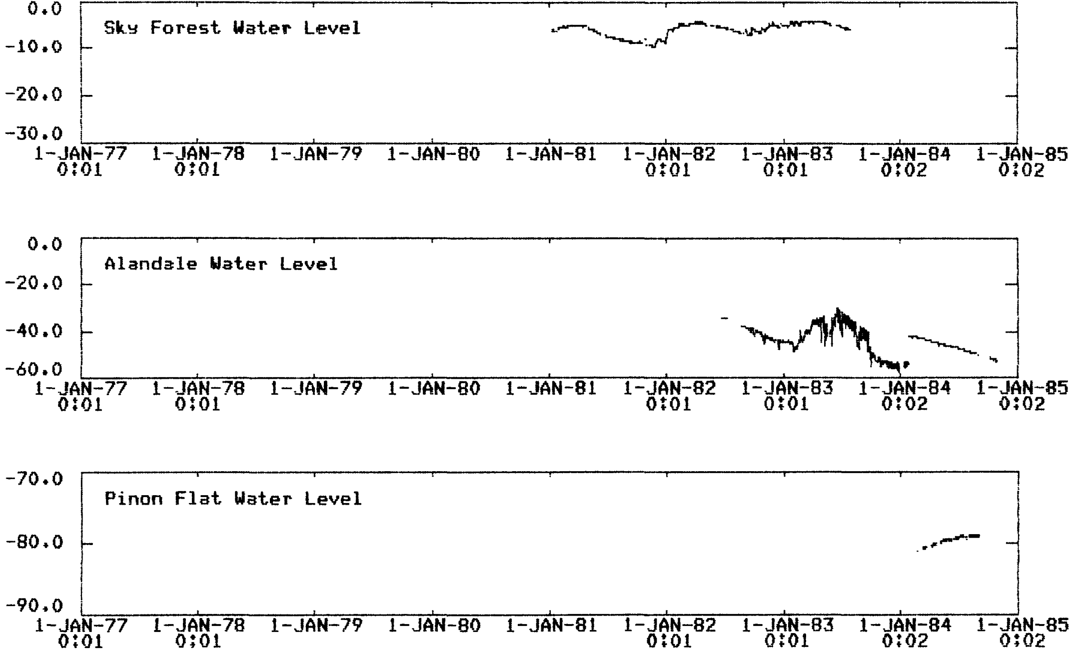
Sky Forest Water Level
0.0
-10.0
-20.0
-30.0
Alandale Water Level
0.0
-20.0
-40.0
-60.0
Pinon Flat Water Level
-70.0
-80.0
-90.0
1-JAN-77 0:01
1-JAN-78 0:01
1-JAN-79
1-JAN-80
1-JAN-81
1-JAN-82 0:01
1-JAN-83 0:01
1-JAN-84 0:02
1-JAN-85 0:02

Fig. 2b

A Crustal Deformation Observatory in Central California Near the San Andreas Fault

14-08-0001-21300

Larry E. Slater
CIRES
Campus Box 449
University of Colorado
Boulder, Colorado 80309
(303) 492-8028

Objective: A portion of the San Andreas fault in Central California near Parkfield has been subject to repeated earthquakes. These earthquakes are typically of magnitude 6 and occur approximately every 20 - 25 years. The last in the series of these earthquakes occurred in 1966. Several other researchers have suggested that a high probability exists that the next in the series will occur within 5 years. Because of those studies and the expectation that the location is also known we have installed a multiwavelength electronic distance measuring instrument (the C-meter) in the region. The instrument site is located near the center of the 1966 break and the array spans a considerable amount of the fault trace that showed ground breakage during the 1966 event.

Results: A radial geodetic array has been established near Parkfield, California. The array consists of approximately a dozen lines that are measured with a multiwavelength EDM instrument. The EDM instrument is located at the hub of the array and measures the lines several times each week. The instrument (the C-meter) has demonstrated a precision of approximately 1 part in 10 million in measurements of line lengths similar to the lines in this array.

The EDM instrument is located approximately 1 km south of Parkfield in a protective shelter on Carr Hill. At the other end of each of the lines is a smaller protective shelter housing the retro-reflectors. Each retroreflector is mounted on a special pier whose horizontal stability can be evaluated by independent measurements. Much of the installation of this array was completed during the summer and autumn of 1984.

Although some of the lines have exibited length changes consistant with the expected deformation patterns of the region we feel it is premature to attach any substantial interpretation to them at this time. Most of the lines have only been measured for a few weeks or months at this time and the changes are only now beginning to exceed the noise of the measurements.

The close proximity of other types of geophysical instrumentation such as creepmeters and alignment arrays will be of great assistance in evaluating the multiwavelength EDM data over the next few years.

Crustal Deformation Observatory - Part G

14-08-0001-21302

Larry E. Slater
CIRES
Campus Box 449
University of Colorado
Boulder, Colorado 80309
(303) 492-8028

Objective: Evidence of large scale crustal uplift in several regions prompted the design and development of several types of long-baseline fluid tiltmeters a few years ago. One of those, the 2-fluid tiltmeter, was conceived and designed in the late 1970's. Laboratory evaluation and short term tests verified the concept of the 2-fluid tiltmeter during the next few years but long-term stability tests were needed. A site in southern California, Pinon Flat Observatory, was selected because of the numerous other deformation studies ongoing there.

Results: The 2-fluid tiltmeter was installed along side 3 other long-baseline tiltmeters at Pinon Flat Observatory. The length of the fluid path was approximately 500 m and closely followed a contour across a gently sloping grade. The position of the fluid path proved to be a considerable problem, the nearly level path with gentle undulations and the small diameter of the fluid tubing (approx. 2 cm) provided many locations for bubbles to form and occlude the fluid along the path. The bubble problem has been reduced but not elimated. The earlier field tests were conducted across a gentle v-shaped valley where any bubbles that formed tended to migrate to one end or the other of the tiltmeter where they were easily vented.

Another major problem with the 2-fluid tiltmeter has been frequent, re-occurring problems with the electronics. The system was designed around early CMOS components that are now very difficult to find replacements for. These early CMOS components and design are not well protected and have been subject to frequent failure.

This effort has failed to produce the long-term stability test that was desired. We continue to be hopeful that the next 6 months will provide some of the evaluation needed for the 2-fluid tiltmeter since the concept is clearly valid.

MODELING AND MONITORING CRUSTAL DEFORMATION

9960-01488

Ross S. Stein, Wayne Thatcher
Branch of Tectonophysics
U.S. Geological Survey
345 Middlefield Road, MS/977
Menlo Park, California 94025
(415) 323-8111, ext. 2120

Investigations

Analysis and interpretation of repeated geodetic survey measurements relevant to earthquake-related deformation processes at or near major plate boundaries. Principal recent activities have been:

1. Reviews of the role of geodetic survey measurements in the study of active tectonic processes and earthquake repeat times, and the relation of these present-day measurements to geological measures of recent deformation.
2. Study of deformation associated with dip-slip faulting in regions of compressional tectonics (1983 M_s 6.7 Coalinga, CA, earthquake), and in regions of extensional tectonics (1983 M_s 7.3 Borah Peak, ID, earthquake).

Results

1. Geodetic Measurement of Active Tectonic Processes

Repeated geodetic observations are sufficiently precise to detect the growth of mountains, the relative movements of the great lithospheric plates, and present-day rates of fault slip and earthquake strain accumulation. The cyclic buildup and release of strain across major faults can be monitored over the short-term (~years or less) using ultra-precise modern techniques, and longer term movements can frequently be determined by utilizing the historic record of measurements, which in many active regions extend back into the late 19th century. Since about 1970, annual laser ranging surveys in the western U.S. and southern Alaska have delineated the pattern and current rates of deformation in these seismically active regions and begun to provide accurate fault slip rates to compare with late Holocene geological estimates. The imperfect balance between interseismic strain buildup and coseismic strain release introduces a component of permanent deformation into the earthquake cycle that under favorable conditions can be estimated geodetically, providing another link between present-day movements and those preserved in the recent geologic record. Examples include tectonically elevated former shore-lines related to great interplate thrust earthquakes and deformed river terraces observed in intraplate reverse faulting environments. Despite the relative uniformity of longer term deformation rates, accumulating evidence indicates considerable short-term irregularity, at least in some regions. Perhaps the best-documented example comes from southern California, where rapid, correlated changes among gravity, elevation, and horizontal strain measurements have recently been observed. (Thatcher)

2. Earthquake Deformation Cycle and the Time-Predictable Model

Geodetic and geologic observations from a handful of well-studied great plate boundary earthquakes provide a basis for exploring those features of the deformation cycle having the strongest influence on recurrence estimation. In ideal circumstances, the time-predictable model requires knowledge of only the seismic slip (and time) of the last earthquake and the rate of relative plate motion or fault slip. Practically, indirect measurements must usually suffice, local coseismic strain changes rather than seismic slip, and local deformation rate rather than slip rate. Permanent non-recoverable deformation, often roughly half the coseismic strain offset near great thrust earthquakes, complicates the inference of interplate seismic slip. Due to short- and long-term postseismic transients, commonly 20 to 40% of the coseismic strain drop, deformation rates are variable and not simply related to the plate motion rate. In rare instances these complications can be avoided and seismic slip and slip rate can be obtained more or less directly. When these favorable circumstances are absent and when knowledge of the deformation cycle is incomplete, recurrence accuracy can be improved by empirically correcting for unknown elements in the cycle. Systematic features in the spatial distribution of the transients and permanent deformation near subduction zones help identify the regions where these corrections are largest and where the shortcomings of the empirical approach are most severe. (Thatcher)

3. The Coalinga Earthquake: Concealed Reverse Faulting

The Coalinga earthquake ($M_L = 6.7$) uplifted Anticline Ridge 0.5 m, depressed adjacent Pleasant Valley syncline 0.25 m, but caused no fault rupture at the ground surface. A steeply dipping reverse fault is well fit by the geodetic and seismic data, whereas a gently dipping thrust fault is less compatible with the leveling and the location and depth of the mainshock. Using the N53°W strike and a 67°NE dip of the mainshock, the best-fit earthquake parameters are: 1.7 ± 0.5 m of dominantly reverse dip slip on a fault extending from a hypocentral depth of 12 ± 1.5 km to within 4 ± 1 km from the ground; $M_o = 6\text{-}7 \times 10^{25}$ dyne-cm. Because the geodetic and seismically determined moments are nearly equivalent, most of the slip was released seismically. The deformation caused by the 1983 earthquake strikingly resembles the structural contours of the Pleistocene Tulare Formation on Anticline Ridge. About 2 km of cumulative concealed fault slip would account for this similarity, yielding a slip rate of 1-4 mm/yr. Well documented examples of anticlinal uplift associated with larger thrust earthquakes, and similarities between Anticline Ridge and adjacent structures, argues that the earthquake potential along the eastern Coast Ranges is larger than previously recognized. (Stein)

4. Borah Peak, ID, Earthquake: Planar Normal Faulting

Geodetic elevation changes record surface deformation associated with the 28 October 1983 M_s 7.3 Borah Peak earthquake on the Lost River fault. Observational uncertainties sum to less than 20 mm over the 70 km length of the 1st Order leveling route. The coseismic elevation change across the surface rupture at Double Springs Pass Road was 1.56 m. We find no evidence to support an hypothesis of listric fault slip. A planar fault dipping 45 ± 2.5° to the SW and extending from the surface to a depth of 13 ± 1 km provides the best fit to the coseismic and postseismic data. The coseismic slip (through November 1983) is modeled to be 2.10 ± 0.10 m; the postseismic slip (November 1983 - July 1984) was 0.05 ± 0.01 m. The geodetic moment, M_o, of the Borah Peak event ($4 \pm 1 \times 10^{26}$ dyne-cm) is equivalent to that of the 1954 Fairview Peak, NV earthquake, but is one-third of the 1959 Hebgen Lake, MO, event. Despite the difference in moment, both the Borah Peak and Hebgen Lake earthquakes are consistent with steeply dipping planar faults extending to a depth of 12-13 km, possibly coincident with the brittle-ductile transition in the Intermountain Seismic Belt. (Stein and Barrientos)

5. Borah Peak Earthquake: Geodetic and Body Wave Inversion

Using elevation changes, we have resolved the fault orientation and fault dimensions together with slip direction and slip distribution associated with the 1983 Borah Peak earthquake. The fault model required a non-uniform moment distribution with larger amounts of slip occurring at depth than at the surface. The dip of the fault obtained from body wave modeling (53°) differs by four degrees from the solution obtained from the geodetic inversion (49°). Slip angles determined by the two methods differ by 38°. The geodetic estimate of the moment is 30% greater than that found by the body wave analysis. This is consistent with some fault slip occurring at periods in excess of 20 s, the limit of the body wave modeling detection. The body wave hypocenter corresponds to the southwestern corner of the fault. Since body wave analysis reveals the focal mechanism of the nucleation phase of rupture and geodetic analysis reveals the mechanism of rupture in its final state, an increase in the dip slip component of faulting is indicated as the dislocation moved upwards and toward the northwest. (Barrientos, Ward, Gonzalez-Ruiz, and Stein)

Reports

Barrientos, S., Steven N. Ward, Jaime R. Gonzalez-Ruiz, and R. S. Stein, 1984, Inversion for moment as a function of depth from geodetic observations and long period body waves of the 1983 Borah Peak, ID, earthquake, submitted to the U.S.G.S. Redbook Volume on the Borah Peak Earthquake, 22 pp.

Stein, R. S., 1984, Evidence for surface folding and subsurface fault slip from geodetic elevation changes associated with the 1983 Coalinga, California, Earthquake, submitted to the U.S.G.S. Professional Paper on the Coalinga Earthquake, 45 p.

Stein, R. S., and S. E. Barrientos, 1984, The 1983 Borah Peak, Idaho, earthquake: Geodetic evidence for deep rupture on a planar fault, submitted to the U.S.G.S. Redbook Volume on the Borah Peak Earthquake, 27 p.

Stein, R. S., and G. C. P. King, 1984, Seismic potential revealed by surface folding: 1983 Coalinga, California, Earthquake, Science, 224, p. 869-872.

Thatcher, W., and J. B. Rundle, 1984, A viscoelastic coupling model for the cyclic deformation due to periodically repeated earthquakes at suduction zones, J. Geophys. Res., 89, p. 7631-7640.

Thatcher, W. and N. Fujita, 1984, Deformation of the Mikita Rhombus: Strain buildup following the 1923 Kanto earthquake, Central Honshu, Japan, J. Geophys. Res., 89, p. 3102-3106.

Thatcher, W., 1984, The earthquake deformation cycle, recurrence, and the time predictable model, *J. Geophys. Res.*, *89*, p. 5674-5680.

Thatcher, W., 1984, The earthquake deformation cycle at the Nankai Trough, Southwest Japan, *J. Geophys. Res.*, *89*, p. 3087-3101.

Thatcher, W., 1984, Geodetic measurement of active tectonic processes, in *Active Tectonics - Impact on Society*, National Research Council, Washington, D.C., in press.

Thatcher, W., 1984, Cyclic deformation related to great earthquakes at plate boundaries: Models and observations, *Proc. Int'l Symp. on Recent Crustal Movements*, Wellington, New Zealand, in press.

Abstracts

Atwater, B. F., Tinsley, J. C., Stein, R. S., Trumm, D. A., and S. L. Wert, 1984, Late Holocene floodplains as structural datums across the Coalinga Nose-Guijarral Hills anticline, Fresno County, California, *U.S.G.S. Redbook Volume* on Coalinga earthquake.

Barrientos, S. E., Ward, S. N., Gonzalez-Ruiz, J. R., and Stein, R. S., 1984, Inversion of moment distribution with depth for the Lost River fault: 1983 Borah Peak, Idaho, earthquake, *EOS*, *65*, in press.

King, G. C. P., and R. S. Stein, 1984, Earthquake Potential of active faults, *EOS*, *65*, in press.

Stein, R. S., 1984, Strategies for modeling coseismic deformation, *AGU Chapman Conference* on Vertical Crustal Motion, 22-26 October 1984.

Stein, R. S., and S. E. Barrientos, 1984, Planar fault-slip associated with the Borah Peak, ID, earthquake, *EOS*, *65*, in press.

Thatcher, W., 1984, Cyclic deformation related to great earthquakes at plate boundaries, *21st Annual Mtg, Society of Engineering Science*, Blacksburg, VA, 15-17 October 1984.

GROUNDWATER RADON STUDIES FOR EARTHQUAKE PRECURSORS IN SOUTHERN CALIFORNIA

14-08-0001-21193

Ta-liang Teng
Center for Earth Science
University of Southern California
Los Angeles, CA 90089-0741

Investigations

We are investigating the relationship between groundwater radon content and earthquakes across the Central Tranverse Ranges of southern California.

Results

This is a six-month update of groundwater radon monitoring in the study area. The reporting period is from February to August, 1984. The most important accomplishments are:

A. Satisfactory operation of seven continuous radon monitors (CRMs) at six sites.

   1. Haskell Ranch - This is also a test site with two CRM units for calibration.
   2. Warm Springs
   3. Seminole Hotsprings
   4. Arrowhead #2
   5. Arrowhead #4
   6. Encino Park (warm spring)

B. Completion of an improved design and a second production run of ten CRM units. These new units have solid-state memories and microprocessor-controlled circuits capable of recording another four channels of slow sampling rate data.

C. Exploring more suitable sites for CRM installation in southern California and in the Long Valley areas.

Results of the past six-month CRM operation are given in data plots (Figures 1 through 6) with a standard time scale of 1 inch/month. Figure 1 shows a six month (February to August, 1984) calibration test of two CRM units which track each other within a few percent. Figures 2-4 record the background radon variations generally with a ±20% or less fluctuation. The slow decrease on radon data shown in Figure 5 (Arrowhead #4) beginning February, 1984 indicates a leakage developed in the plumbing system causing a minor amount of radon-rich gas to escape before reaching the counting cell. This problem is being corrected at the present. The leakage was due to the corrosion of hotspring water on the steel gas collector. The gas collector will be replaced by one which will less likely be subject to corrosion. The Encino Park CRM unit was installed in late January, 1984. Several data gaps were due to battery problems. The baseline shift in mid June, though minor, is real and the cause of this shift is under present investigation. Otherwise, the performance of this station is quite satisfactory. There does not seem to be anomalous readings over this six-month period.

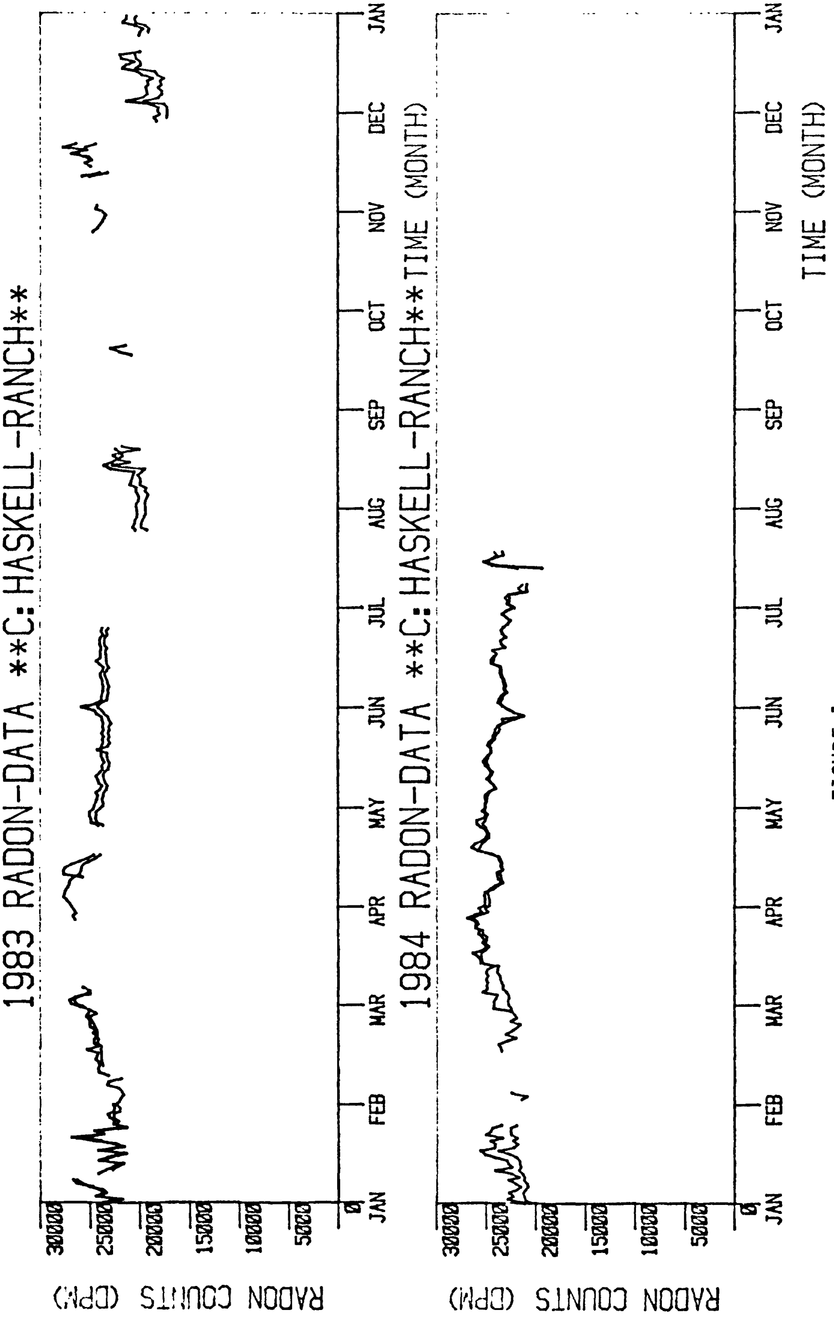

1983 RADON-DATA **C:HASKELL-RANCH**

1984 RADON-DATA **C:HASKELL-RANCH**

FIGURE 1

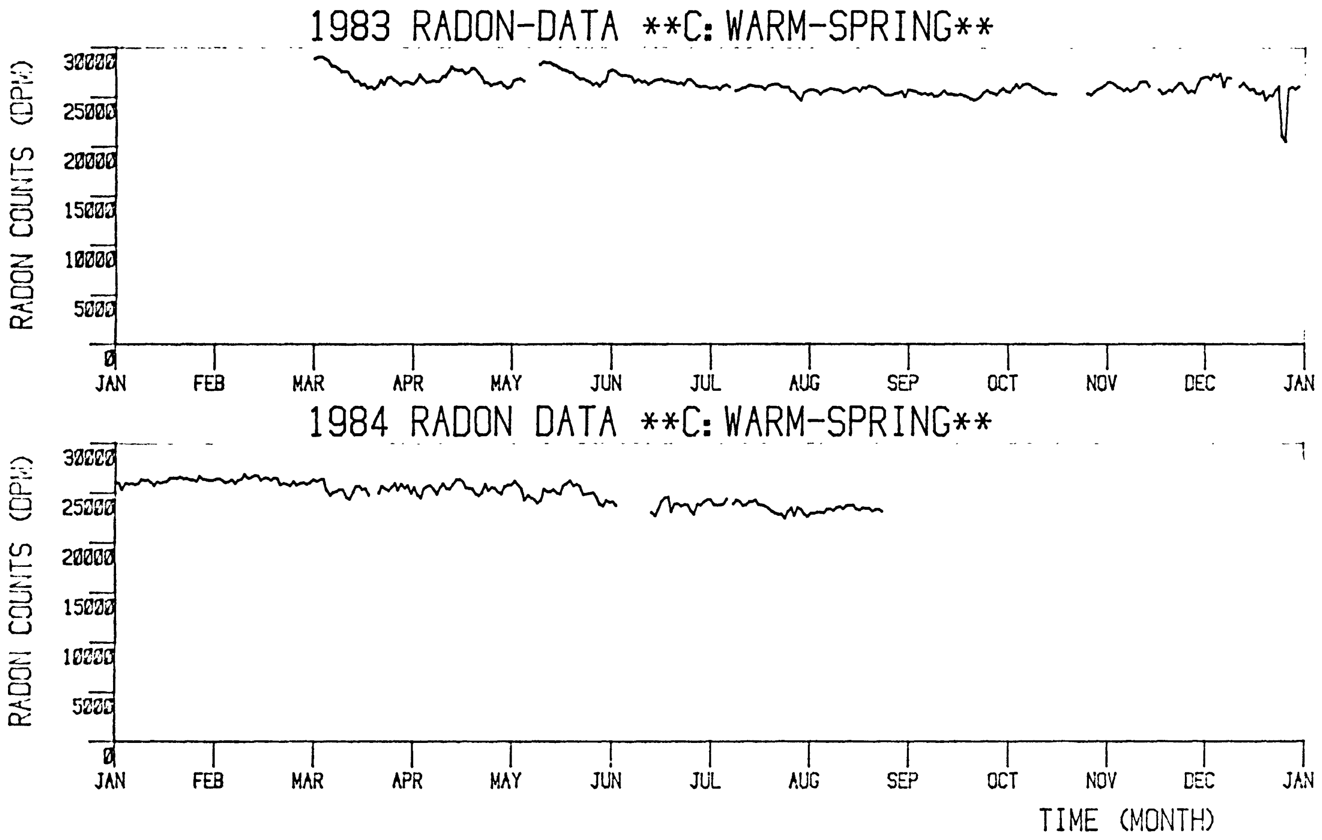
1983 RADON-DATA **C: WARM-SPRING**
RADON COUNTS (DPM)
30000
25000
20000
15000
10000
5000
0
JAN
FEB
MAR
APR
MAY
JUN
JUL
AUG
SEP
OCT
NOV
DEC
JAN
1984 RADON DATA **C: WARM-SPRING**
RADON COUNTS (DPM)
30000
25000
20000
15000
10000
5000
0
JAN
FEB
MAR
APR
MAY
JUN
JUL
AUG
SEP
OCT
NOV
DEC
JAN
TIME (MONTH)

FIGURE 2

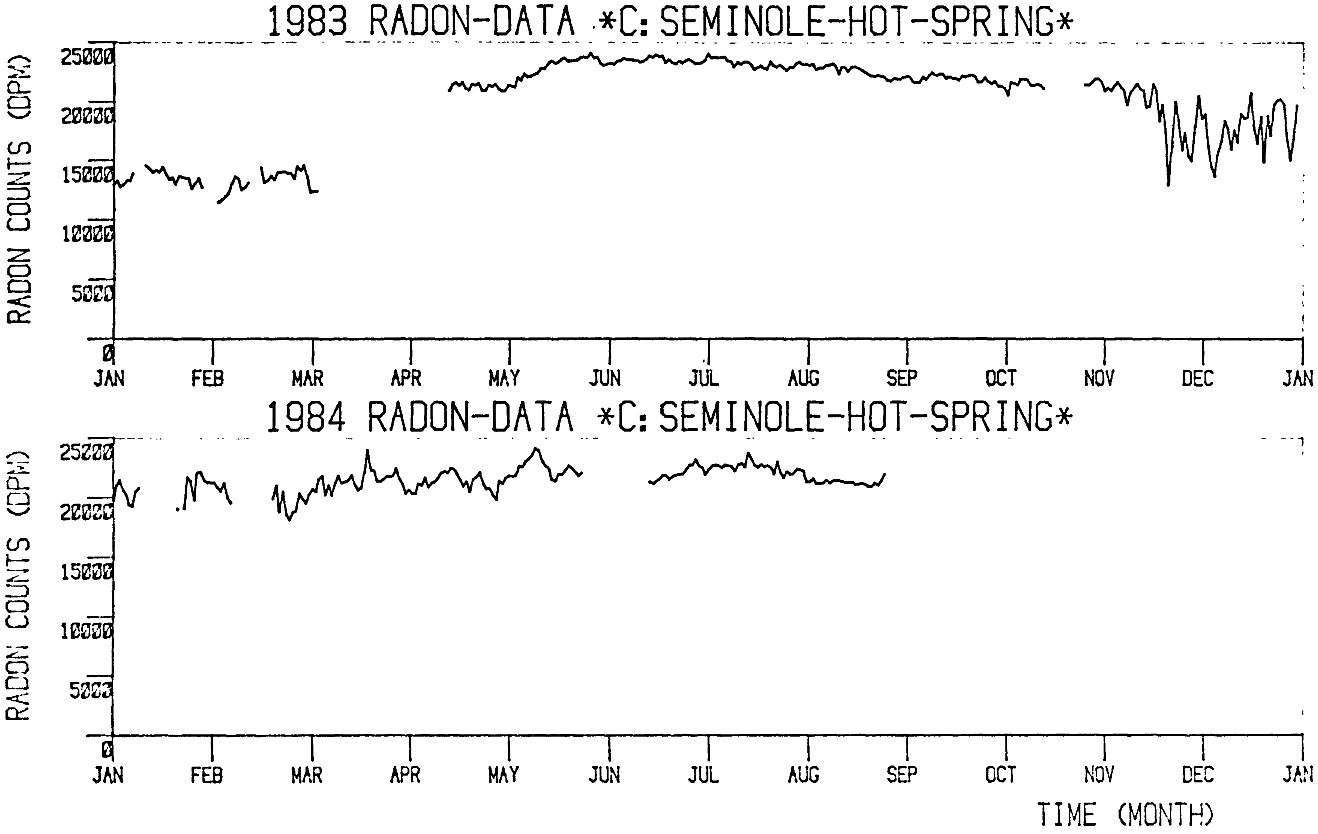

1983 RADON-DATA *C: SEMINOLE-HOT-SPRING*

1984 RADON-DATA *C: SEMINOLE-HOT-SPRING*

FIGURE 3

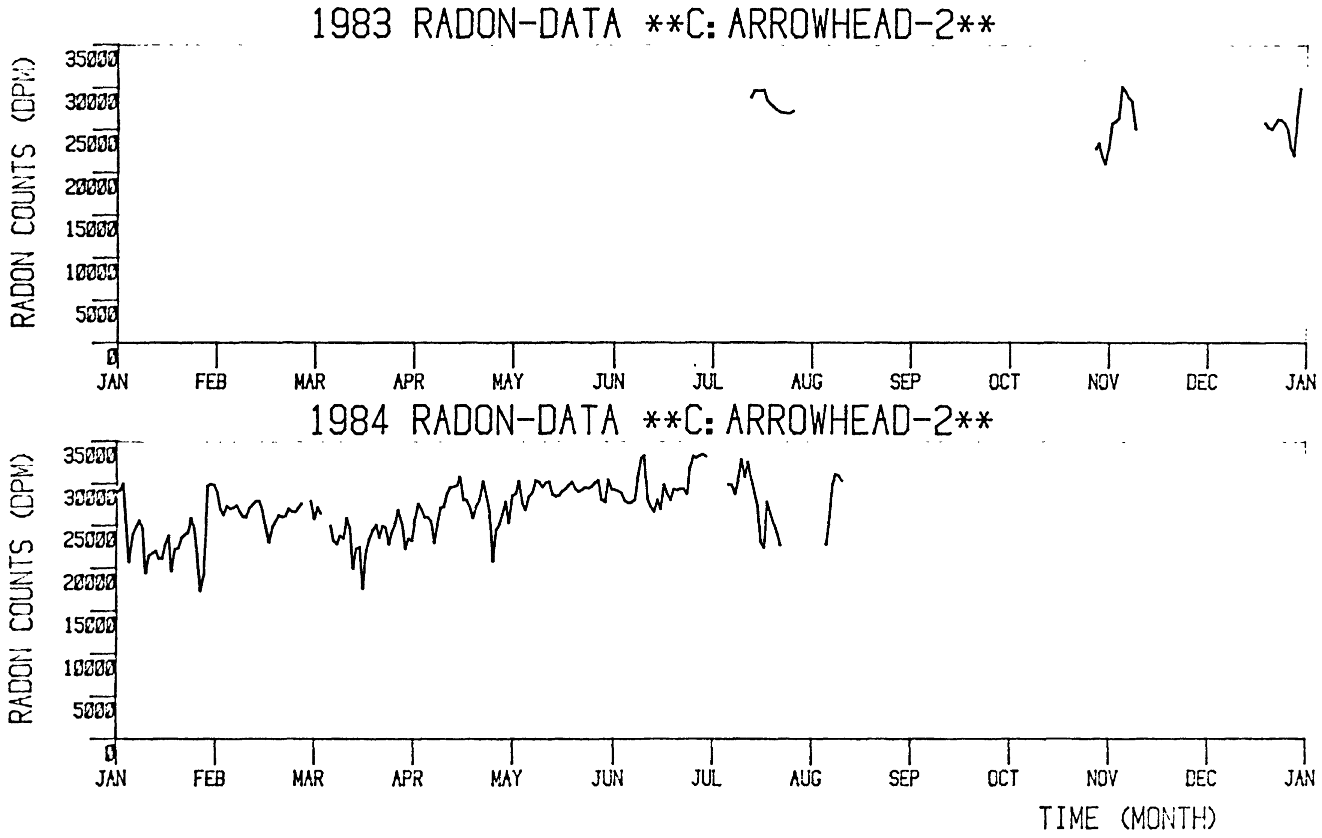

1983 RADON-DATA **C: ARROWHEAD-2**

1984 RADON-DATA **C: ARROWHEAD-2**

FIGURE 4

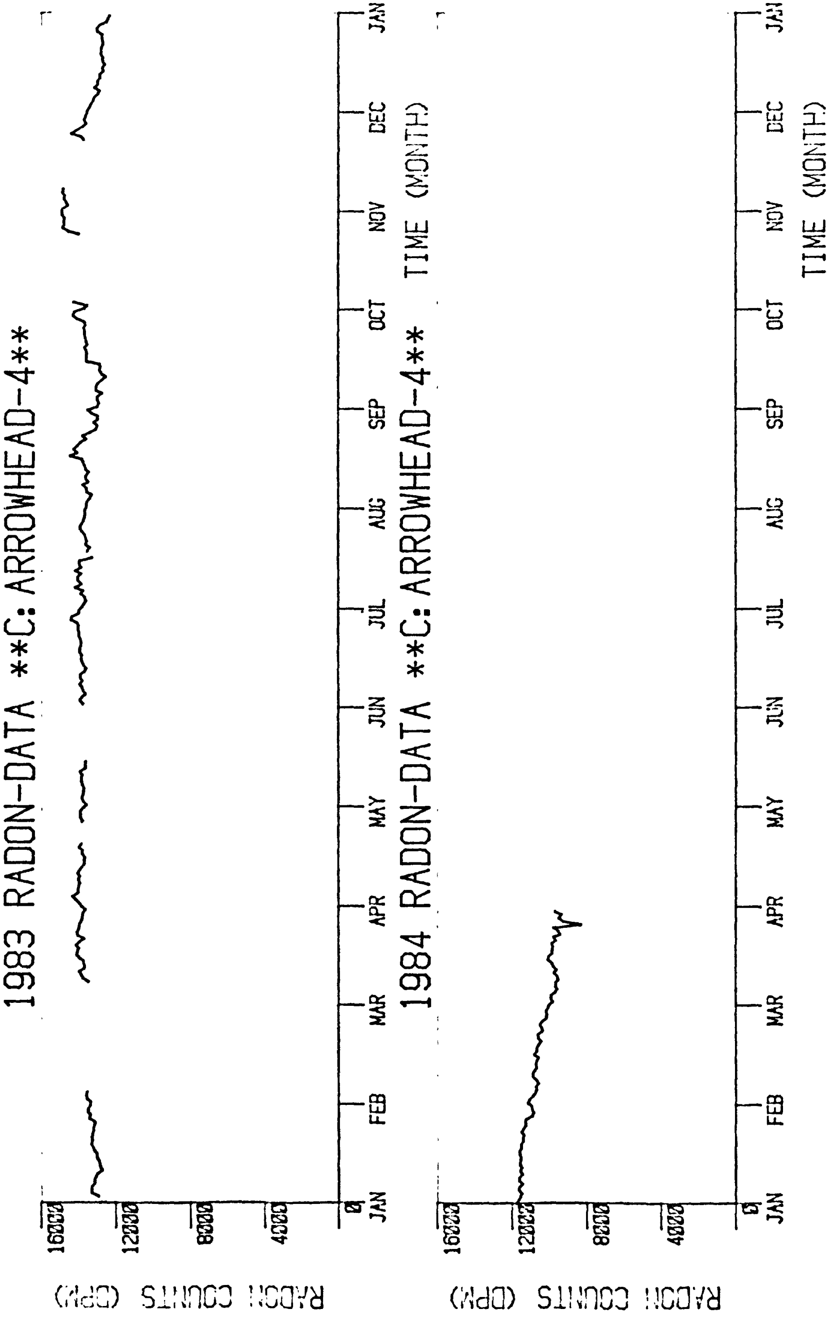
1983 RADON-DATA **C: ARROWHEAD-4**
RADON COUNTS (DPM)
16000
12000
8000
4000
0
JAN
FEB
MAR
APR
MAY
JUN
JUL
AUG
SEP
OCT
NOV
DEC
JAN
TIME (MONTH)
1984 RADON-DATA **C: ARROWHEAD-4**
RADON COUNTS (DPM)
16000
12000
8000
4000
0
JAN
FEB
MAR
APR
MAY
JUN
JUL
AUG
SEP
OCT
NOV
DEC
JAN
TIME (MONTH)

FIGURE 5

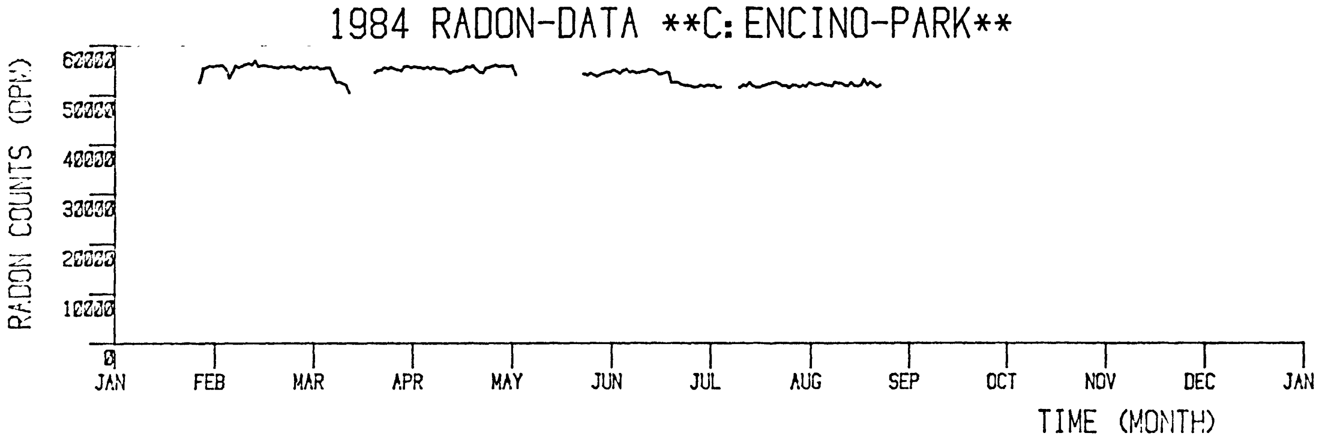
1984 RADON-DATA **C: ENCINO-PARK**
RADON COUNTS (DPM)
60000
50000
40000
30000
20000
10000
0
JAN
FEB
MAR
APR
MAY
JUN
JUL
AUG
SEP
OCT
NOV
DEC
JAN
TIME (MONTH)

FIGURE 6

Studies of the Seismic and Crustal Deformation Patterns of an Active Fault: Piñon Flat Observatory

14-08-0001-21270

Frank Wyatt, Duncan Carr Agnew, Jonathan Berger
Institute of Geophysics & Planetary Physics
Scripps Institution of Oceanography
University of California, San Diego
La Jolla, CA 92093
(619) 452-2019

Introduction

This contract supports the ongoing research program at Piñon Flat Observatory (PFO). The objectives of this program are: 1) To provide a common location with shared facilities for research on, and the development of, precision geophysical instruments; 2) To establish the accuracy with which each of these instruments measures different geophysical quantities by operating the best available reference standards; 3) To monitor reliably the state of strain in the lithosphere near the observatory, a region of imminent seismic activity.

Results: Laser Strainmeter Observations

The longest running instruments at (PFO) are the three 732 m laser strainmeters. Figure 1 (a and b) shows the results from all three components since 1974, when monitoring of tilting of the end monuments began. Figure 1(a) shows the components of strain measured by the three strainmeters (the continuous heavy lines), together with the geodetically determined strains measured on a subset of the USGS-Anza trilateration array surrounding PFO (data supplied by Dr. J.C. Savage). (Both techniques actually measure strain changes so these two series may be shifted vertically by arbitrary amounts.) This plot also shows the rainfall measured at PFO, and the larger earthquakes near PFO, labeled according to the rms coseismic deformation they could cause there.

The most obvious feature of Figure 1(a) is the large secular strain on the Northwest-Southeast (NW-SE) record through 1979. This does not agree with the geodetic measurements, and we are sure it is an instrumental artifact. While the end monuments of the North-South (NS) and East-West (EW) strainmeters are long gabbro columns sunk into pits, the end monuments of the NW-SE instrument were made from short gabbro piers installed just below floor level in underground vaults. The monument at the northwest end appears not to have been well constrained; we believe that the apparent secular strain prior to 1979 was caused by a downslope creep of this monument in response to wetting of the soil. To cure this problem, an optical anchor was installed at this end in 1979; the results from this instrument have improved considerably since this was done. A similar anchoring scheme for the southeast end was completed in December 1983.

Particularly over the earlier part of the record, the NS and EW strain records show much less secular change. We can recombine these two records to get changes in shear strain and dilatation; the results are shown, together with the equivalent geodetic measurements, in Figure 1(b). The agreement between the two measurements of dilatation is quite good, and provides strong evidence that neither technique is significantly contaminated by changing scale errors. The two measurements of shear also agree fairly well up to the beginning of 1979. After that time both show an increase in the shear rate. However, the strainmeter record also shows a large offset not evident in the trilateration data. Because it coincides with the onset of the wet winter of 1979, and an obviously rain induced response of both the NS and EW strainmeters, we do not believe this offset is real. Differences of this order might however be expected between the strainmeter and geodetic results because of spatial inhomogeneities in the strain field.

Our overall conclusion from the results presented in these two graphs would be that the true variations in the secular strain at PFO are unlikely to exceed a few hundred nanostrain in a year. While there are fluctuations on the PFO strain records, almost all of them can be attributed to the effects of local rainfall or other changes in the instrumentation.

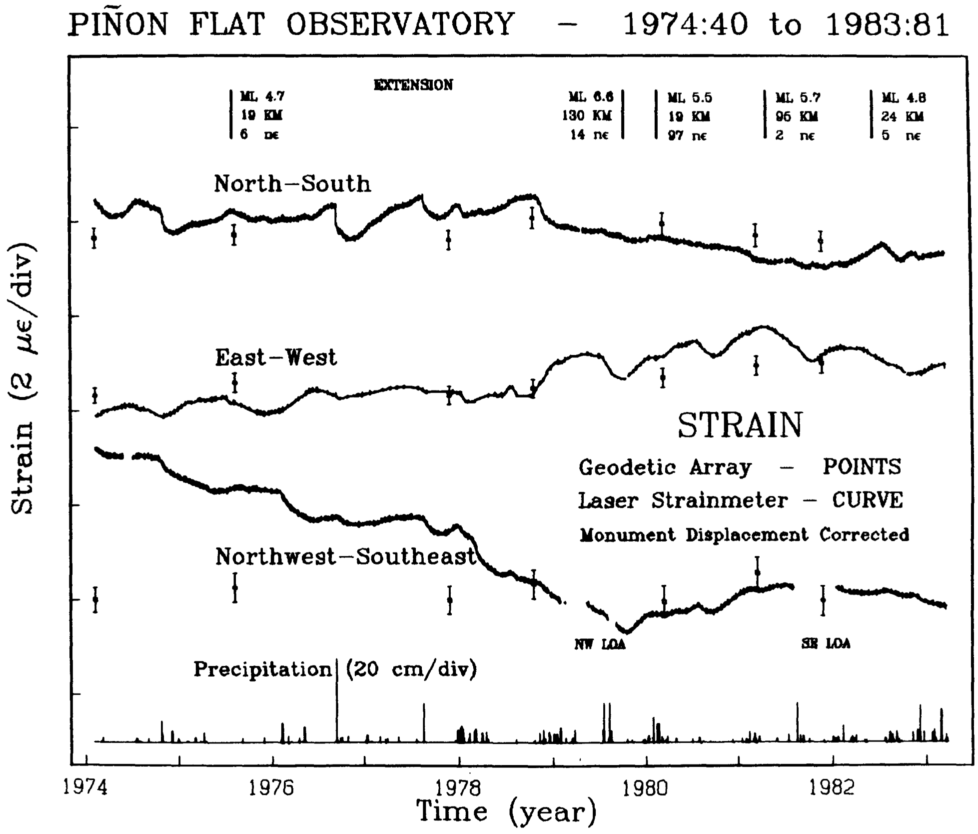
PIÑON FLAT OBSERVATORY - 1974:40 to 1983:81
EXTENSION
ML 4.7
19 KM
6 nε
ML 6.6
130 KM
14 nε
ML 5.5
19 KM
97 nε
ML 5.7
95 KM
2 nε
ML 4.8
24 KM
5 nε
North-South
East-West
Northwest-Southeast
STRAIN
Geodetic Array - POINTS
Laser Strainmeter - CURVE
Monument Displacement Corrected
NW LOA
SE LOA
Precipitation (20 cm/div)
Strain (2 με/div)
1974
1976
1978
1980
1982
Time (year)

Figure 1a.

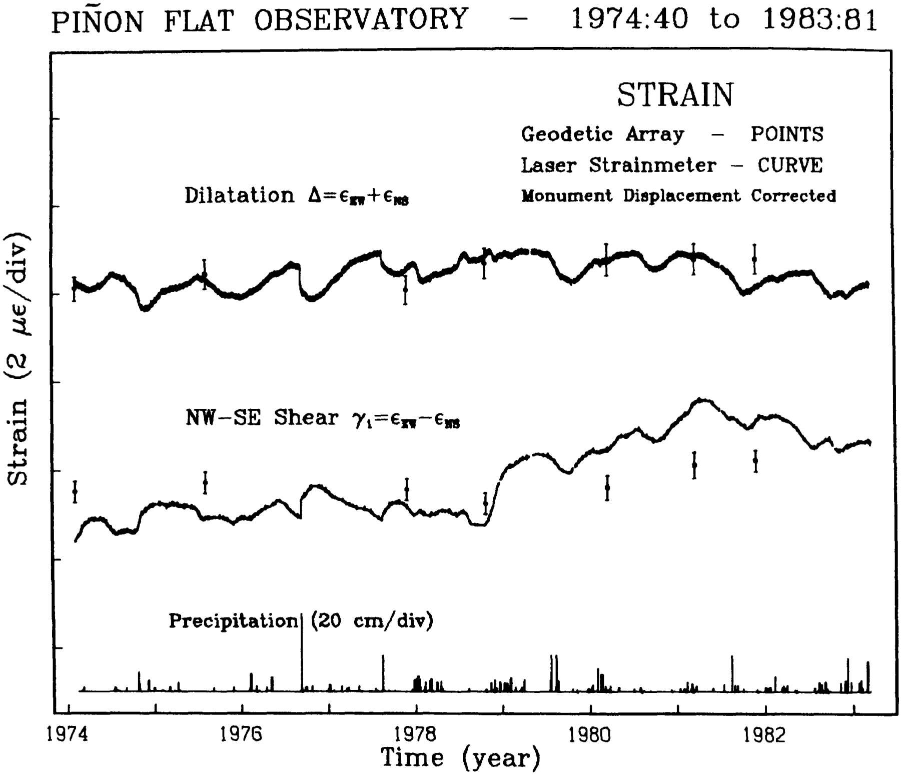
PIÑON FLAT OBSERVATORY – 1974:40 to 1983:81
STRAIN
Geodetic Array – POINTS
Laser Strainmeter – CURVE
Monument Displacement Corrected
Dilatation $\Delta=\epsilon_{EW}+\epsilon_{NS}$
NW–SE Shear $\gamma_1=\epsilon_{EW}-\epsilon_{NS}$
Precipitation (20 cm/div)
Strain (2 $\mu\epsilon$/div)
1974
1976
1978
1980
1982
Time (year)

Figure 1b.

Crustal Deformation Observatory, Part D

14-08-0001-21254

Frank Wyatt, Duncan Carr Agnew, Jonathan Berger
Institute of Geophysics & Planetary Physics
Scripps Institution of Oceanography
University of California, San Diego
La Jolla, CA 92093
(619) 452-2019

Introduction

This contract supports research coordination, operational support, data recording, and preliminary data reduction for investigators participating in the Crustal Deformation Observatory (CDO) program at Piñon Flat Observatory. The CDO program is a cooperative effort to evaluate existing and proposed instruments for measuring ground deformation in the period range of hours to years. Its fundamental principle is to operate instruments side-by-side, so that simple comparison techniques will allow problems to be isolated and progress to be made in reducing instrument noise and making the instruments more fieldworthy.

Since the beginning of 1984, the following changes have been made to instruments operated under the CDO program:

1. An "LED follower" system was added to the west end of the LDGO long-base tiltmeter, as a supplement to the laser interferometer.
2. The Cambridge center-pressure tiltmeter developed intermittant problems in June, and despite considerable work failed during the summer.
3. A group from the Air Force Geophysics Laboratory reinstalled an intermediate-depth borehole tiltmeter this spring, using an optical alignment technique.
4. The UCSB field crew made two further precise levellings of the benchmark array at PFO. Experimental stabilized monuments were added to this array in October.
5. Bruce Clark (Leighton Associates) installed two more prototype stressmeters in the northwest corner of the observatory.

6. Operation of the Carnegie borehole strainmeters has continued without problems, though the very frequent lightning storms this summer meant that the instruments were disconnected much of the time.

In addition, the usual work has been done of making adjustments on all the instruments, undertaking necessary repairs and construction, and maintaining the flow of data. This has been an especially arduous activity because the daily electrical storms greatly increased the failure rate of all the instruments.

A paper describing the results of a preliminary comparison of tiltmeters has been accepted for publication in Geophysical Research Letters (Wyatt et al 1984). The remainder of this report summarizes part of that paper.

The data are from October 1982 through November 1983, for four different tiltmeters. One is a Kinemetrics TM-1B, installed 4.5 m deep. The other three are long-base instruments, all running along the same azimuth and with the same length (535 m). In two of these the reference level is the surface of a liquid in a partially filled tube. In the Lamont-Doherty instrument (LDGO), the liquid level at each end is measured using a laser interferometer. In the UCSD instrument, the levels are measured using a white-light interferometer, one arm of which is mechanically controlled to follow the water surface. The University of Cambridge instrument (CAMB) uses a fluid-filled tube with a pressure transducer at the center; the differential pressure between the two sides gives the tilt. CAMB and LDGO share the same end vaults and air return pipe; the UCSD instrument is completely separate. To correct for near-surface motions, all instruments are referenced to the ground at 26 m depth. One anchoring system, shared by the Cambridge and Lamont instruments, uses an invar rod and inductive displacement sensor. The other, used by the UCSD instrument, is an unequal-arm vertical Michelson interferometer.

Figure 1 shows the signals from the long-base instruments after removing bad data (shown by gaps); for each instrument the data are shown both as recorded and with the earth tides removed. Except for the UCSD record and the latest part of the LDGO one, the offset across data gaps is arbitrary. While most gaps are so short (< 1 hr) that the offset can be easily determined by interpolation, choosing the offset for the longer gaps is somewhat subjective. If we use the UCSD data to align the sections of LDGO data we find that these two records differ by less than 120 nrad.

These records are so good thanks largely to the corrections for end-monument motions provided by the anchors. Intense storms in the fall and winter of 1982 flooded the UCSD east vault and caused the monument to move 0.7 mm up; the flooding and motion were less for the west monument. A-frame roofs have since been built over these vaults to keep the nearby ground dry. The LDGO monuments moved less, probably because A-frames had already been built over their vaults. The large offset in the tilt records in early 1983 reflects changes in the water table caused by drilling at borehole UQA, 90 m from the west end of the long-base tiltmeters. Earlier drilling nearby had shown a permeable horizontal joint at 103 m depth. Evacuating the water from borehole UQA during drilling reduced the pressure in this joint, causing the ground to subside by as much as 0.15 mm over a large area. Other water table fluctuations during this period have been much too small (< 5 m) and of the wrong sign to account for the long term tilt changes seen.

Fluctuations in the Cambridge tilt record correlate with the outdoor air temperature for periods from 50 to 5 days; at longer periods the tilt data show large drifts. If the air temperature is lowpassed at 0.1 cpd, delayed by 2 days, scaled by 20 nrad/K, and subtracted from the Cambridge tilt, the tilt fluctuations are greatly reduced, though the overall drift rate is increased.

Figure 2 summarizes the tiltmeter data in the frequency domain. The noise levels of the LDGO and UCSD instruments are about the same, although this may be an artifact of filling data gaps in the LDGO series by tidal interpolation. The coherence plot for these two records shows significant coherence at frequencies other than tidal and seismic. To our knowledge, this is the first time this has been observed at such low noise levels. The power spectra for the Cambridge and Kinemetrics tiltmeters are much higher, and the coherence outside the tidal bands is zero. The coherence we do find indicates only that the two coherent instruments are both responding to the same thing; we currently suspect temperature changes.

The two better instruments have required attention at least every week; the records are useful only because of this care. These instruments must be engineered for reliable field use before deploying them elsewhere.

Papers

F. Wyatt, R. Bilham, J. Beavan, A. G. Sylvester, T. Owen, A. Harvey, C. Macdonald, D. D. Jackson, D. C. Agnew, Comparing Tiltmeters for Crustal Deformation Measurement - A Preliminary Report. Geophys. Res. Lett., in press.

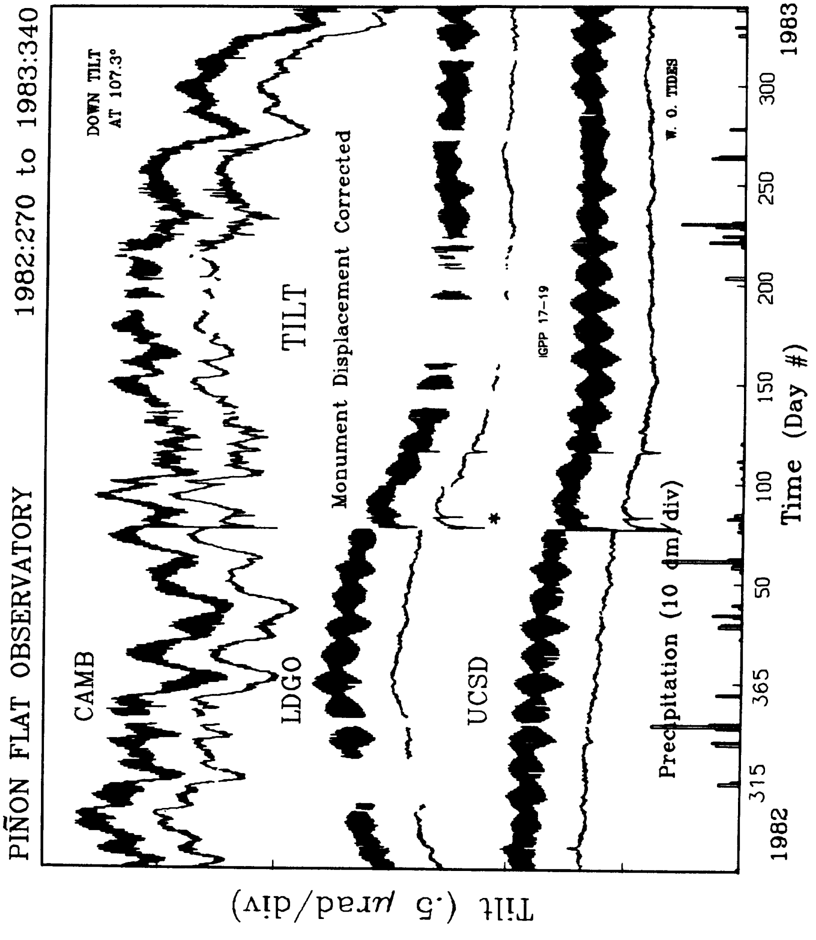
PIÑON FLAT OBSERVATORY
1982:270 to 1983:340
CAMB
LDGO
UCSD
TILT
Monument Displacement Corrected
DOWN TILT
AT 107.3°
IGPP 17-19
W. O. TIDES
*
Precipitation (10 cm/div)
Tilt (.5 μrad/div)
315
365
50
100
150
200
250
300
1982
1983
Time (Day #)

Figure 1.

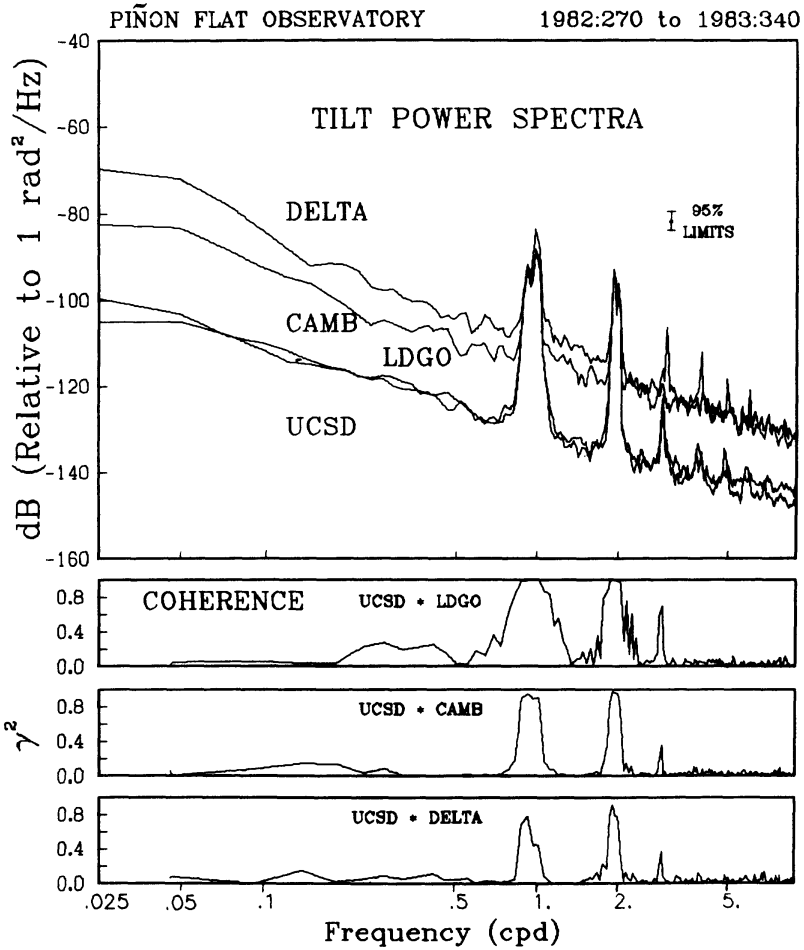
PIÑON FLAT OBSERVATORY
1982:270 to 1983:340
TILT POWER SPECTRA
dB (Relative to 1 rad^2/Hz)
-40
-60
-80
-100
-120
-140
-160
DELTA
CAMB
LDGO
UCSD
95% LIMITS
COHERENCE
UCSD * LDGO
UCSD * CAMB
UCSD * DELTA
γ^2
0.8
0.4
0.0
.025
.05
.1
.5
1.
2.
5.
Frequency (cpd)

Figure 2.

Thermal, Mechanical, and Chemical History of Wasatch Fault Cataclasite and Phyllonite, Traverse Mountains area, Salt Lake City, Utah

14-08-0001-G-886

R. L. Bruhn
W. T. Parry
Dept. of Geology and Geophysics
University of Utah
Salt Lake City, Utah 84112
(801) 581-6619

STATEMENT OF GOALS

The goals of this work are to investigate the geometry, mechanical and chemical characteristics of the Wasatch normal fault near Salt Lake City, Utah and use the results to infer the seismogenic properties of the fault zone. Particular points of interest are: 1) Documenting and modelling the rheological properties of the fault zone based on studies of fault rock material exposed in the footwall. 2) Establishing the geometrical and mechanical properties of the fault zone at a proposed fault segment boundary, which may mark the end of two independent earthquake rupture segments.

INTRODUCTION

The Wasatch normal fault zone extends for about 370 km from southern Idaho into central Utah. The fault zone has been divided into six major segments varying from 35 to 70 km in length by Schwartz and Coppersmith (1984). Characteristic earthquakes on these proposed segments are expected to be of magnitude 7 to 7.5. Segment boundaries are marked by offsets in the trace of the fault zone, bedrock salients and east-trending subsurface structures that are reflected in the gravity field (Schwartz and others, 1982; Zoback, 1983). The ends of normal fault zone segments correlate spatially with the positions of large, Precambrian and Phanerozoic structures that penetrated deep into the crust, to depths of at least 12-15 km, prior to development of the Wasatch fault zone in the Late Cenozoic (Smith and Bruhn, 1984).

Exposures of the Wasatch fault at Traverse Mountain near Salt Lake City provide an excellent opportunity to study the chemical and mechanical properties of the fault in crystalline rock, and to infer the nature of deformation currently occurring in the crystalline basement beneath Salt Lake Valley. A prominent salient in the Wasatch Fault occurs southeast of Salt Lake City in the Traverse Mountain-Corner Creek area where the fault curves around the Oligocene Little Cottonwood quartz monzonite stock. The quartz monzonite forms the footwall of the fault and Paleozoic sediments and Tertiary volcanic rocks form the hanging wall of the fault. Cataclasite and phyllonite formed from hydrothermal alteration and mechanical deformation of the Quartz monzonite comprise a partially preserved carapace up to 100 m thick on the southern and western margin of the stock. The objectives of this research project are to characterize the thermal, chemical, and mechanical history of the footwall rocks, estimate fluid pressure, temperature and composition from fluid inclusion and mineralogical charcteristics and develop a rheological model from mechanical characteristics of the fault rock.

Structural geometry of the Provo-Salt Lake segment boundary

The segment boundary between the Salt Lake and Provo segments of the Wasatch fault zone occurs along the southern margin of the Little Cottonwood stock, an Oligocene quartz monzonite stock located in the Traverse Mountain area south of Salt Lake City (Fig. 1). The segment boundary is marked by an east-trending fault zone that offsets the northern end of the Provo segment about 5 km eastward with respect to the Salt Lake segment on the northern side of the boundary. The Traverse Mountains form a prominent east-trending bedrock salient in the hanging wall of the Wasatch fault zone at the segment boundary. This salient is comprised of Paleozoic strata and Oligocene volcanic rock. These rocks are faulted against the southern margin of the Little Cottonwood stock along the segment boundary, which is comprised of an east-trending fault zone that dips 30°-40° south. The geometry of this latter fault zone is particularily important to developing a paradigm for normal fault segmentation. For example, continuous rupture propagation around the segment boundary during an earthquake would require a large rotation in the displacement vector during faulting; from an east plunging vector attitude along the Provo and Salt Lake segments to a south to southwestward plunge along the moderately dipping fault zone comprising the segment boundary.

Paleostress field

Changes in stress orientations and magnitudes in the vicinity of the segment boundary could also influence rupture propagation. We have begun testing this hypothesis by analyzing the geometry of fault populations in the footwall of the Wasatch fault zone, working from the central part of the Salt Lake segment into the segment boundary at Traverse Mountains. Paleo-stress orientations and ratios of principal stress magnitudes were calculated from the fault data using a linear inversion method. Our results indicate 1) that the paleostress field inferred from fault populations in the footwall was similar to the contemporary stress field, and 2) that the stress tensor varied from strongly triaxial in the central part of the fault segment to nearly uniaxial in the east-trending segment boundary.

Physical properties of the Wasatch fault zone

Excellent exposures of exhumed fault rock are preserved on the western and southern margins of the Little Cottonwood stock. Phyllonite, characterized by an ordered fabric defined by flattened and stretched quartz and aligned phyllosilicates, is preserved in outcrops along the southern margin of the stock. The phyllonite formed during an early period of dextral-normal slip in the east-trending segment boundary of the Wasatch fault zone. Ductile deformation and recrystallization probably occurred at depths of 9-10 km.

Cataclasite is preserved over large sections of the footwall along the eastern and southern margins of the Little Cottonwood stock. This cataclastic fabric is superimposed upon the phyllonite, indicating that large-scale cataclasis post-dated development of the phyllonite. Presumably, the transition from mesoscopically ductile to cataclistic flow occurred as the footwall was uplifted along the fault zone. Grain size in the cataclasite is markedly decreased relative to that of undeformed quartz monzonite. The equillibrium grain size of quartz and feldspar is 5 to 10 microns in the cataclasite. This finer grained material contains evidence of pressure solution, indicating that the prominent deformation mechanism may have changed from crack propagation to diffusive mass transfer as grain size was reduced during cataclasis. Mitra (1984) has suggested that such observations are consistent with a transition from mostly brittle to ductile flow in fault zones at temperatures well below those required for deformation of quartz by a dislocation mechanism. If correct, this concept has major implications for modelling frictional/quasi-plastic transitions in the Wasatch fault zone.

Geochemical Mapping and Analysis

Near the Wasatch Fault, footwall rock has been subjected to multiple alteration and deformation episodes with progressive displacement of the fault (Fig. 2). Successively younger, lower temperature, lower pressure mineral assemblages are superimposed upon older, higher temperature, higher pressure assemblages. Two distinct syndeformational alteration mineral assemblages are present in the footwall rock. A late, low-temperature assemblage of laumontite, prehnite, and clay minerals is superimposed on an earlier assemblage of chlorite, muscovite, and epidote. Mechanical deformation and hydrothermal alteration have produced striking textural changes. Igneous quartz grains show pronounced undulatory extinction, deformation lamellae, and healed fractures decorated with fluid and solid inclusions. Igneous biotite has kink bands, has recrystallized to an aggregate of smaller biotite grains, or has been replaced by chlorite. Sericite is disseminated throughout the feldspars which also contain veinlets of sericite, calcite, chlorite, and epidote.

Pore Fluid Pressure, Temperature and Composition

Igneous quartz which shows pronounced undulatory extinction and deformation lamellae contains abundant trains of secondary fluid inclusions that decorate healed fractures. In some cases solid inclusions of chlorite, sericite, or calcite accompany trains of fluid inclusions and sericite veinlets mark the extension of the fluid inclusion trains into surrounding feldspar. The fluid inclusions contain a carbon dioxide vapor bubble surrounded by liquid carbon dioxide and an aqueous salt solution. Melting of clatharate within the fluid inclusions indicates a mean salinity of the aqueous salt solution of 6.7 weight percent NaCl. Homogenization of liquid and vapor carbon dioxide takes place at 7.0 to 30.5^{o} C.

The mole fraction carbon dioxide, NaCl and H_2O in each inclusion were estimated from the density of the carbon dioxide phase, the density of the aqueous salt solution, and an estimate of the volume fraction of each inclusion occupied by carbon dioxide. The inclusions average 10 mole percent carbon dioxide. The temperature of homogenization of the aqueous salt solution with carbon dioxide represents the minimum temperature of entrapment of the inclusions and averages 295^{o} C. Interpretation of these data in terms of fluid pressures from the two phase boundary in the carbon dioxide-sodium chloride-water system suggests minimum fluid pressure of 1100 bars.

Geochronology Studies

The thermal and uplift history of the Little Cottonwood stock are being determined by fission track and potassium-argon dating. Samples have been collected from 11,000 foot elevation to the 5,000 foot elevation and from each of the hydrothermal alteration assemblages. Mineral separation is currently in progress.

REFERNECES

Crittenden, M. D., Jr., Stuckless, J. S., Kistler, R. W., and Stern, T. W., 1973, Radiometric dating of intrusive rocks in the Cottonwood area, Utah: Jour Research U. S. Geol. Survey 1, 173-178.

Schwartz, D. P. and Coppersmith, K. J., 1984, Fault behavior and characteristic earthquakes: J. Geophys. Research, v. 89, p. 5681-5698.

Slentz, L. W., 1955, Tertiary Salt Lake Group in the Great Salt Lake Basin, Utah,: Ph. D. thesis, University of Utah.

Smith, R. B. and Bruhn, R. L., 1984, Intraplate extensional tectonics of the eastern Basin-Range: Inferences on structural style from seismic reflection data, regional tectonics, and thermal-mechanical models of brittle-ductile deformation: J. Geophys. Res., v. 89, p. 5733-5762.

Zoback, M. L., 1983, Structure and Cenozoic tectonism along the Wasatch Fault zone, Utah: Mem. Geol. Soc. America, 157, p. 3-27.

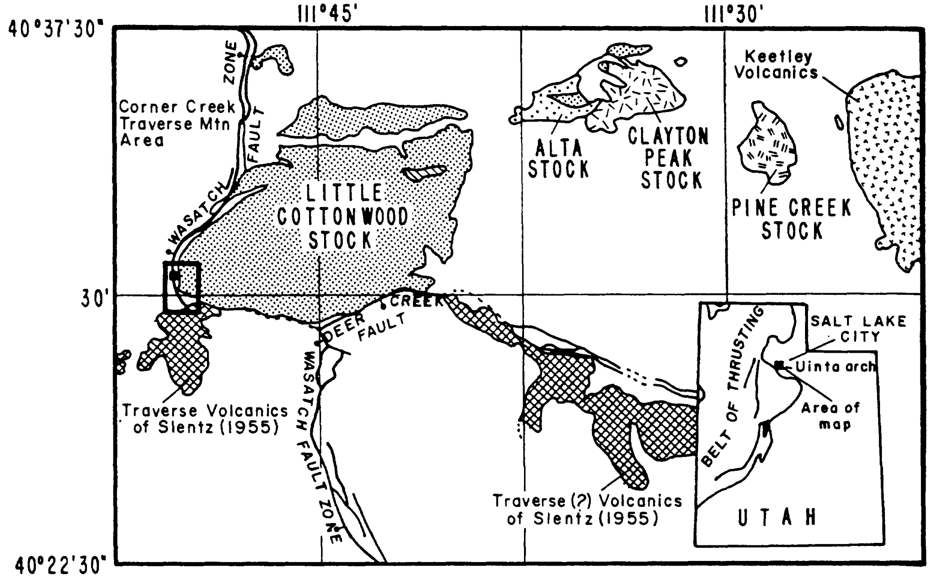

Figure 1. Index and geologic maps of the Corner Creek-Traverse Mountain area (modified from Crittenden et. al., 1973).

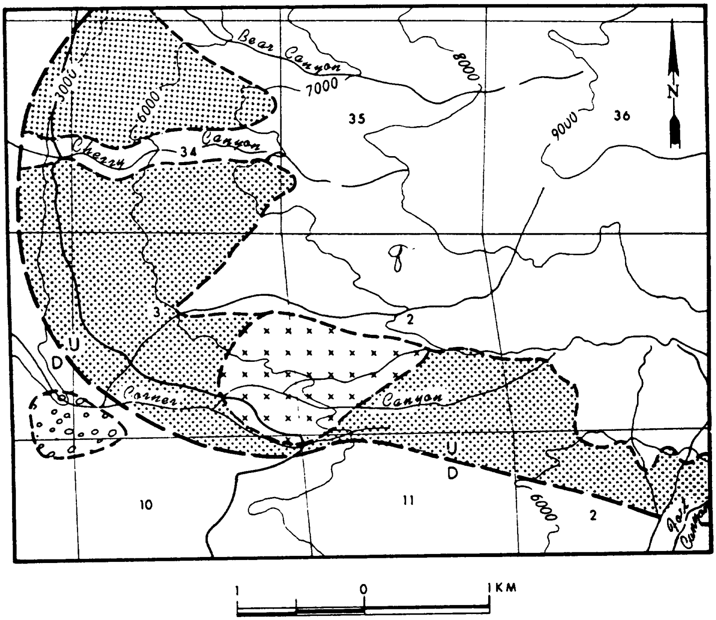

EXPLANATION

q Quartz monzonite of the Little Cottonwood stock

☐ Traverse volcanics and Oquirrh formation

× Laumontite, prehnite, and clay alteration in footwall quartz monzonite

▨ Chlorite, epidote, and sericite alteration in footwall quartz monzonite

○ Kaolinite, smectite, and sericite alteration in hanging wall volcanics and Oquirrh formation

—$\frac{U}{D}$— Wasatch Fault

Figure 2. Hydrothermal alteration zones in the Corner Creek-Traverse Mountain area.

ROCK MECHANICS

9960-01179

James Byerlee
U.S. Geological Survey
Branch of Tectonophysics
345 Middlefield Road, MS/77
Menlo Park, California 94025
(415) 323-8111, ext. 2453

Investigations

Laboratory experiments are being carried out to study the physical properties of rocks at elevated confining pressure, pore pressure and temperature. The goal is to obtain data that will help us to determine what causes earthquakes and whether we can predict or control them.

Results

We have measured complex resistivity of 2 saturated San Andreas fault gouges over a frequency of 10^{-2} to 10^{6} Hz and confining pressure from 0.2 to 200 MPa. Along with high conductivies (as large as 0.1 S/m) the samples exhibited strong low-frequency dispersion of permittivity. This large low-frequency permittivity, which is also observed in other geological materials, results in out-of-phase current of as much as 1 percent. It is often assumed that transient electrical currents in wet, conductive crustal rock decay on the order of microseconds. Yet induced polarization measurements commonly show background response, as well as response from some clays, in which 0.1 percent or more of the peak current is still flowing after many seconds. Inversion of our frequency response data into the time domain supports these findings of long decay times commonly found in 1P studies. Our results also have implications for earthquake-related phenomena.. If electrical charge were generated during an earthquake, a significant portion would persist for many seconds, allowing time for earthquake lights and other reported phenomena to be observed.

Reports

D. E. Moore, Ma Jin, R. Summers, J. Byerlee, 1984, The effect of pore pressure and heating time on the strength and sliding stability of a serpentine gouge, Rock Mechanics in Productivity and Protection, 24th Symposium on Rock Mechanics, p. 312-319.

C. Morrow, J. Byerlee, 1984, Frictional sliding and fracture behavior of some Nevada Test Site tuffs, Rock Mechanics in Productivity and Protection, 24th Symposium on Rock Mechanics, p. 467-474.

P. Solberg, J. Byerlee, 1984, A note on the rate sensitivity of frictional sliding of Westerly Granite, J. Geophys. Res., vol. 89, No. B6, p. 4203-4206.

Radiated Field from Circular Cracks and Asperities

USGS 14-08-0001-947

Shamita Das
Lamont-Doherty Geological Observatory
of Columbia University
Palisades, New York 10964
(914) 359-2900

Since it is now widely believed that earthquakes can be modelled as fracture of cracks or asperities, the radiated fields from circular cracks and asperities are compared to determine if these different physical cases can be differentiated from a study of observed seismic recordings. Using a 2-D antiplane shear fault model, Madariaga (1983) has suggested that cracks and asperities are indistinguishable from a high frequency point of view. An inherent property of such a model was that the edge of the crack and the asperity are of equal length. In reality, the perimeter length of cracks grow with time while that of asperities decreases with time in real 3-D situations. To investigate the effect of this, the radiated fields from circular cracks and asperities fracturing at a known constant velocity were compared.

The solid line in Figure 1 shows the S-wave particle velocity and acceleration due to a circular crack that grows from a point to a radius of 2a at a speed of $\alpha/2$, α being the compressional wave speed of the medium. The dotted line in Figure 1 shows the S-wave particle velocity and acceleration due to fracture at a speed of $\alpha/2$ of a pre-existing circular asperity of radius 2a, on a fault which as slipped everywhere except at this asperity. The average stress drop on the crack and asperity were the same, though it must be pointed out that the stress drop over the crack was uniform while for the asperity the stress drop was larger at the edges than at the centre (cf. e.g., Das and Kostrov, 1983). The particle velocity and acceleration for these two problems were calculated for a receiver situated along the normal to the crack or asperity as well as for receivers at an angle of 30°, 60° and 90° off the normal. Only the cases of the receiver along the normal and at 60° off the normal are shown. It is seen that along the normal the difference between the crack and asperity are significant both for particle velocity and acceleration but this difference decreases as one moves off the normal. For all cases studied, however, it was found that the initial slope of the particle velocity for the asperity was steeper than that for the crack, this difference being most pronounced along the normal and least along the fault plane (see figure caption for further discussion). Another major difference was that the acceleration was a 3-sided pulse (up-down-up or vice versa), depending on polarity for a crack and 2-sided (up-down or vice versa) for an asperity.

Radiation from a spontaneously fracturing crack and asperity is now under study.

P-3

Das, S. and Kostrov, B.V., Breaking of a single asperity: Rupture process and seismic radiation, *J. Geophys. Res., 88*, No. B5, 4277-4288, 1983.

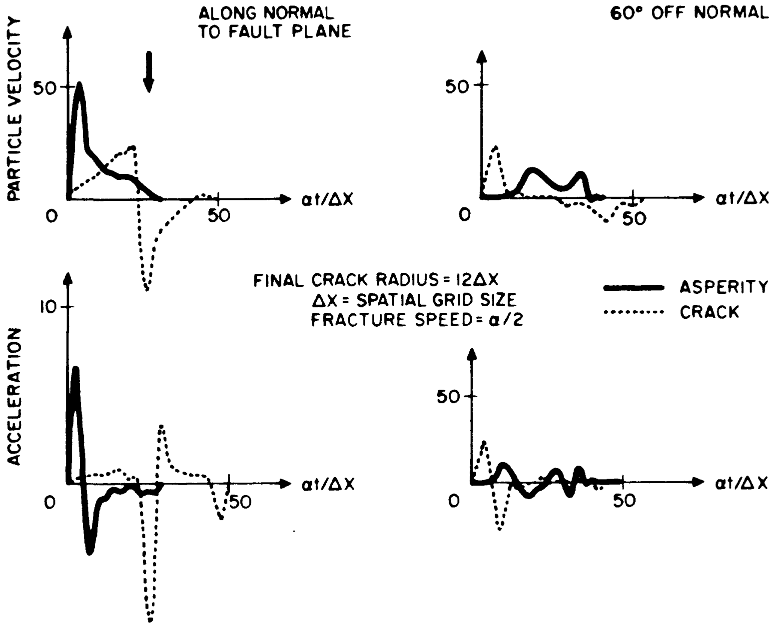

Figure 1. Particle velocity and accelerations for a circular crack and a circular asperity. Note that at first it may seem that for the case of a receiver located 60° off the fault normal, the crack particle velocity slope is much steeper. This is because when the asperity fracture commences, the slip propagates out into the previously broken zone. When the observer is off the normal, this slip in the broken region shows up as a small slip preceding the large slip due to the main fracture process. One should therefore measure the slope of the asperity pulse at the time of commencement of large slip. The arrow denotes approximate time of completion of fracture.

Mechanics of Earthquake Faulting

9960-01182

James H. Dieterich
U.S. Geological Survey
Branch of Tectonophysics
345 Middlefield Road, MS/977
Menlo Park, California 94025
415-323-8111, ext. 2573

Investigations

Constitutive Law for Dynamic Faulting Calculations

An analysis was completed that utilizes data from fault instability experiments to evaluate constitutive relations for dynamic fault slip.

Nucleation and Triggering of Earthquakes

Modeling continued of the processes associated with the nucleation and triggering of earthquake slip on a fault patch. Of particular interest in this investigation are the relationships between the occurrence of a stress step (such as might be caused by a fore-shock or mainshock) and time-delayed earthquake slip following the stress step.

Deformation Mechanics of Active Volcanoes

Detailed analysis was begun of the 1975 Kalapana, Hawaii earthquake and of related processes controlling the deformation of the south flank of Kilauea volcano.

Results

Constitutive Law for Dynamic Fault Calculations

Records of local fault stress and slip velocity from experiments in a large scale laboratory faulting experiment were analysed to evaluate fault constitutive laws prior to and during unstable rupture propagation. Parameters that were used in the evaluation include premonitory slip velocity, dynamic slip velocity, the magnitude of the stress increase ahead of the propagating rupture, the magnitude of the stress drop behind the rupture front and displacement weakening. Previous laboratory observations of quasistatic rock-on-rock frictional sliding led to the development of fault constitutive relations which incorporate effects of slip rate and slip history on frictional resistance. This type of friction model includes two competing velocity-dependent effects: (i) an instantaneous increase in frictional resistance with an increase in sliding speed and (ii) a decrease in friction with increasing sliding speed which occurs as a critical fault displacement is achieved. Local high-resolution records of fault displacements and shear stresses during stick-slip frictional instabilities produced on a simulated fault in a block of Sierra granite indicate that these models might also adequately describe the frictional response of the simulated fault under dynamic slip conditions. The maximum observed slip speeds during stick-slip are roughly three to four orders of magnitude larger than the speeds used in quasistatic tests. In addition, the velocity jumps observed during stick-slip are four to six orders of magnitude larger than those which typify the quasistatic tests. Slip weakening is observed during stick-slip which is similar to that predicted on the basis of the friction models. Stress changes, an increase from initial shear stress to peak shear stress and deceases from peak to residual and from initial to residual shear stress, are also in agreement with model predictions. The stick-slip data also suggest that an appropriate friction model must admit high-speed cutoffs to the velocity-dependent effects.

Deformation Mechanics of Active Volcanoes

Many deformation events on active volcanoes are associated with fault slip in addition to the effects of magma injection and withdrawal. The abundance of fault structures related to volcanoes and the common association of large earthquakes with volcanic centers attest to the possible importance of faulting in controlling volcano deformation. With A. Okamura of Hawaiian Volcano Observatory surface deformations due to coupled interactions between magma bodies and faulting are being analyzed using finite element calculations. The 1975 magnitude 7.2 Kalapana, Hawaii earthquake appears to have involved coupled interactions between fault slip and magma bodies beneath the summit and rift zones at Kilauea. Modeling of deformation data indicating slip on a nearly horizontal thrust fault accompanied by simultaneous draining of the summit magma reservoir and opening of rift reservoirs. Following previous studies, we interpret the driving force for the earthquake to be repeated injections of magma from the summit region into the southwest and east rift zones of Kilauea. The deformation data further suggest patterns of preseismic and postseismic fault creep similar to that reported for some tectonic earthquakes.

Nucleation and Triggering of Earthquakes

Delayed instability following application of a step in applied stress is characteristic of fault slip models utilizing laboratory derived state variable constitutive laws (see previous report for description of model and initial results). It is speculated that this delayed failure may be an important process in controlling the timing of a mainshock following a foreshock and aftershock sequence. Results obtained during the report period appear to satisfy the frequency vs. time statistics of foreshock occurrence aftershock decay.

Reports

Dieterich, J.H., 1984, History Dependent Failure Processes and Earthquake Prediction, Proceedings 4th Joint Meeting of UJNR Subcommittee Panel on Earthquake Prediction Technology (in press), 4 pp.

Dieterich, J.H., 1984, "Nucleation and Triggering of Earthquake Faulting (abstract), Program and Abstracts Society of Engineering Science, 21st Annual Meeting.

Dieterich, J.H. and Conrad, G., 1984, Effect of Humidity on Time- and Velocity-Dependent Friction, Jour. of Geophys. Res., vol. 89, p. 4196-4202.

Dieterich, J.H., and A. Okamura, 1984, Modeling Surface Deformations Due to Coupled Interactions Between Magma Bodies and Fault Slip (abstract), Am. Geophys. Union Chapman Conference on Vertical Crustal Motion: Measurement and Modeling, October 22-26, 1984.

Okubo, P.G., and Dieterich, J.H., 1984, Effect of Physical Fault Properties on Frictional Instabilities Produced on Simulated Faults, Jour. Geophys. Res., vol. 89, p. 5817-5827.

Okubo, P.G., and J.H. Dieterich, 1984, Constitutive Relations for Dynamic Fault Slip (abstract), EOS, Trans. Amer. Geophys. Union, 65, p. 280.

In Situ Stress Measurements

9960-01184

John Healy
Branch of Tectonophysics
U.S. Geological Survey
345 Middlefield Road MS 977
Menlo Park, CA 94025
415/323-8111, ext. 2535

Investigations and Results

The In Situ Stress Measurements project was closed down in July due to lack of funds. We have lost most of our key staff who are needed for data processing and analysis and project planning so that it has become impossible to continue our activities in their previous format. We have decided to reorganize this project and operate it in a different and more conservative mode. Our current activities are related to data analysis and the preparation of reports on previous work, and we anticipate that this will be the primary goal in the initial phases of a reorganized project.

Much of our time, effort, and expenditure of money during this reporting period were directed toward preparation for measurements in deep drill holes, to about 3 km. The system to accomplish these measurements is now essentially developed and completed, but the future of these measurements is at the moment uncertain because of the problems with money and staff as mentioned above.

Two important papers were prepared during this reporting period: "Report on televiewer log and stress measurements in holes USW G-3 and UE-25P#1, Yucca Mountain, Nevada Test Site," submitted to JGR for publication, and "In situ fluid pressure measurements for earthquake prediction: an example from a deep well at Hi Vista, California," by Healy and Urban, which indicates the feasibility of very stable and sensitive measurements of volumetric stress at depths of about 2,000'. Futher work is continuing on the latter data set because we believe it may be possible to achieve a stress sensitivity in this hole that exceeds the sensitivity of any other existing measurement of stress.

Reports

Gettings, M. E., Blank, H. R., Jr., Mooney, W. D., and Healy, J. H., 1984, Crustal structure of southwestern Saudi Arabia: submitted to Journal of Geophysical Research.

Healy, J. H. and Urban, T. C., 1984, In situ fluid pressure measurements for earthquake prediction: an example from a deep well at Hi Vista, California: submitted to Pure and Applied Geophysics.

Mooney, W. D., Gettings, M. E., Blank, H. R., and Healy, J. H., 1984, Saudi Arabian seismic-refraction profile: A traveltime interpretation of crustal and upper mantle structure: Tectonophysics, in press.

Stierman, D. J. and Healy, J. H., 1984, A study of the depth of weathering and its relationship to the mechanical properties of near-surface rocks in the Mohave Desert.

Stock, J. M. and Healy, J. H., 1984, Magnitudes and orientations of stress in an extensional regime, Yucca Mountain, Nevada: GSA Abstract with Programs, v. 16, no. 6.

Stock, J. M., Healy, J. H., Svitek, J., and Mastin, L., 1984, Report on televiewer log and stress measurements in holes USW G-3 and UE-25P#1, Yucca Mountain, Nevada Test Site: U.S. Geological Survey Open-File Report, in press.

Zoback, M. D. and Healy, J. H., 1984, Friction, faulting, and in-situ stress: Annales Geophysicae, in press.

CRUSTAL DEFORMATION OBSERVATORY

14-08-0001-21237

David D. Jackson & Michael Rogers
Department of Earth and Space Sciences
University of California
Los Angeles, California 90024
(213) 825-0421

OBJECTIVES

The Crustal Deformation Observatory is a cooperative project whose goal is to develop and test advanced methods for observing crustal deformation, and to compile an accurate record of such deformation at one site in southern California. The UCLA role is primarily data analysis. The site is at Pinon Flat Observatory (PFO), located between the San Andreas and San Jacinto faults near Palm Desert, CA. PFO is operated by UCSD.

We have measured tilt at PFO using both continuously recording tiltmeters and geodetic leveling. No tectonic tilt has occurred there since 1981, to within an uncertainty of about 100 nanorad/yr.

CONTINUOUS TILTMETER OBSERVATIONS

We have now analyzed 2.56 years of tilt data from three long baseline fluid tiltmeters at Pinon Flat Observatory, California. There are two fluid level tiltmeters using Michelson interferometers to measure water level at each end. These were built by UCSD and Lamont Doherty Geological Observatory, and will be referred to as 'UCSD' and 'LDGO' respectively. Cambridge University have built a fluid pressure tiltmeter (called 'CAMB') with a pressure transducer at the center. All three instruments are installed side by side with the LDGO and CAMB instruments sharing the same end piers.

The tiltmeter data are shown in Figure 1. The most stable tilt record (UCSD) shows a linear trend of 33 nanorad per year. This may be due to tilting or instrumental drift or a combination of both. The other tiltmeters are less stable and their records contain transients as large as a few hundred nanorads over a few months.

Figure 2 shows a subset of the data collected with the LDGO and UCSD instruments. The straight lines are least squares fit linear trends through both datasets. The estimated trends are -152 ± 2 and -35 ± 1 nanorad/yr, respectively. The error estimates are not very meaningful, because the data are far from being statistically independent, but they do serve as a guide to the deviations about linear trends. We do not associate the estimated trends with tectonic activity; rather we believe that the observed trends are approximate upper limits to the magnitude of secular tectonic tilting at Pinon Flat. The secular trends are of the same sign for both instruments suggesting that the variations are caused by true tilt, rather than by instrumental problems. However, these tilts might well be surficial effects rather than tectonic.

The spectrum of the UCSD tilt record for the entire 2.56 year time interval is red. Not only the daily and semidiurnal tilts, but also overtones and splitting can be clearly observed.

Temperature sensitivities for air temperature at 1 m below the surface as estimated by linear regression are 27.9 ± 3.3, 11.4 ± 0.8, and 1.9 ± 0.3 nanorad/deg for CAMB, LDGO, and UCSD, respectively. All are statistically significant at 95% confidence level.

Preliminary investigation shows rainfall to have an annual effect on the tilt data. Further analysis of this correlation is required, however.

LEVELING

UCSB has carried out more than 12 leveling surveys at PFO since 13 October 1979. Six of these surveys, from 25 January 1981 to 2 August 1983, have included the end points of the UCSD tiltmeter as monuments, random benchmark motions of up to 1 mm cause the dominant errors in the leveling data. Therefore, we established several special benchmarks anchored at about 10 m depth. Using these monuments we can estimate the tilt rate to within about 500 nanorad per year.

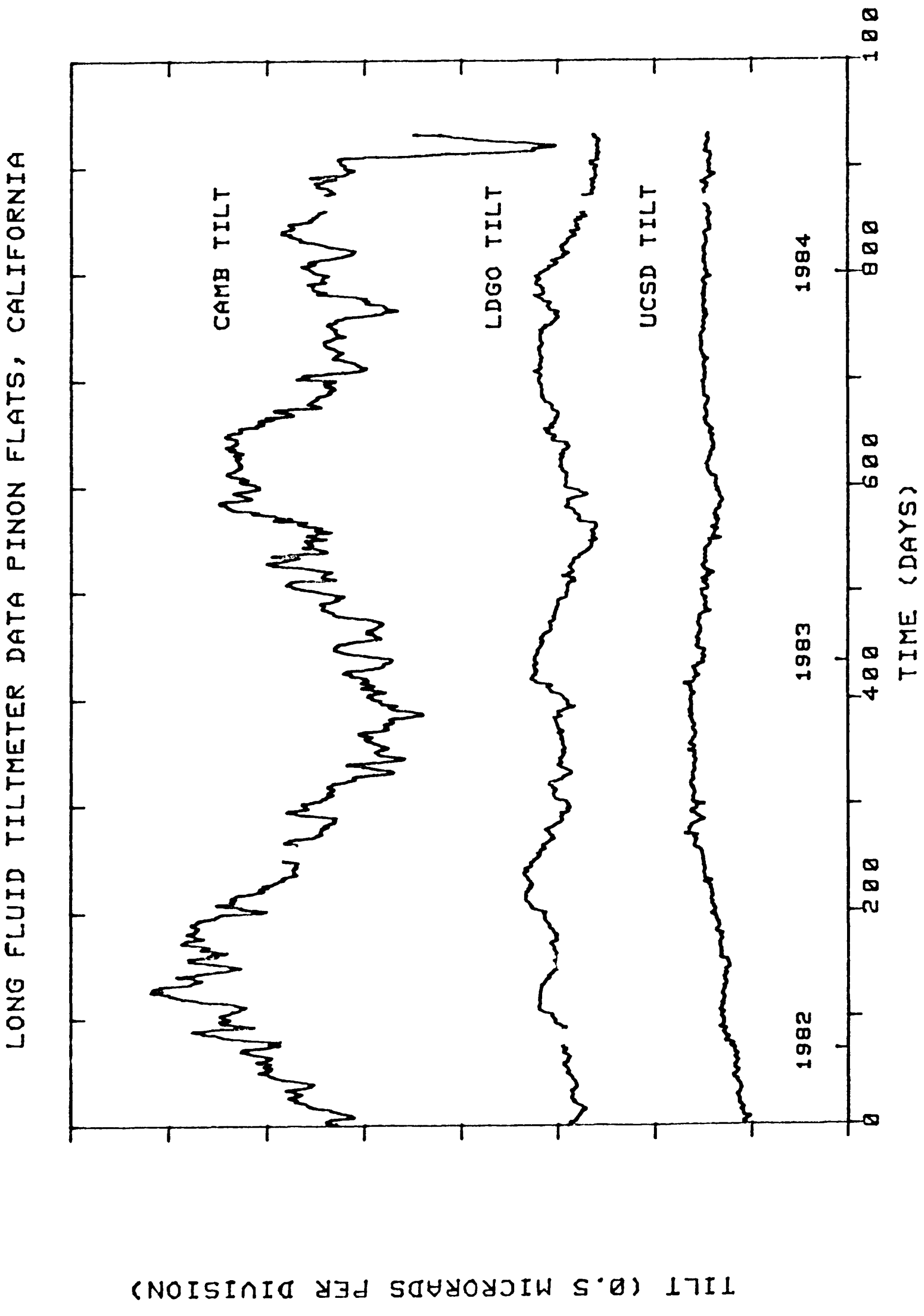
LONG FLUID TILTMETER DATA PINON FLATS, CALIFORNIA
CAMB TILT
LDGO TILT
UCSD TILT
1982
1983
1984
0
200
400
600
800
1000
TIME (DAYS)
TILT (0.5 MICRORADS PER DIVISION)

FIGURE 1.

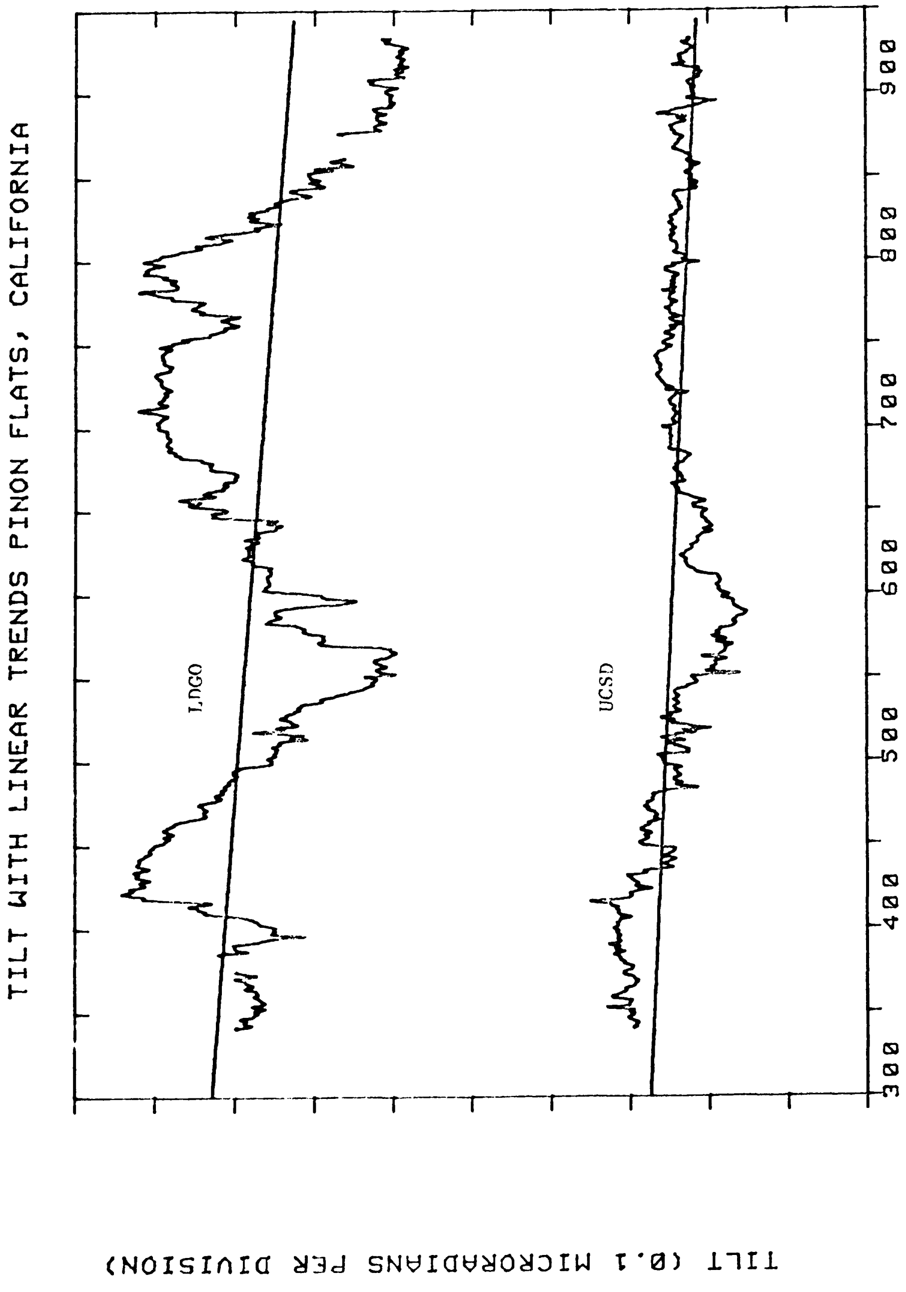
TILT WITH LINEAR TRENDS PINON FLATS, CALIFORNIA
LDGO
UCSD
300
400
500
600
700
800
900
TIME (DAYS)
TILT (0.1 MICRORADIANS PER DIVISION)

FIGURE 2.

Experimental Rock Mechanics

9960-01180

Stephen H. Kirby
Branch of Tectonophysics
U.S. Geological Survey, MS/977
345 Middlefield Road
Menlo Park, California 94025
(415) 323-8111, Ext. 2872

Investigations

We continue our research on the rheology of the lithosphere and the strength of rocks and minerals of the continental crust and upper mantle. This work focuses on establishing the laws governing flow and estimating the stress differences that can be supported within the earth.

Results

1. Water weakening and the rheology of the continental crust. We have made significant progress in our understanding in the plastic weakening of quartz by structural water, a phenomenon known as hydrolytic weakening. We reported in the Spring 1984 AGU Meeting and at an international symposium on quartz defects in Sweden last June the results of our systematic study of the effects of high pressure hydrothermal treatment of quartz crystals on their chemistry and plastic yield strength. This research has shown that the slow diffusive transport of water controls the time and temperature effect of the weakening process and that the classic discovery experiments published 20 years ago were misinterpreted. We have also studied the occurrence of intracrystalline water in naturally deformed quartz-bearing rocks in a mylonite zone in granitic rocks in the southern Sierra Nevada [Kronenberg and Wolf, 1984]. Using state-of-the-art Fourier Transform Infrared Spectroscopy, we see water-enriched quartz in the central shear zone, whereas the host granodiorite is relatively dry. This finding suggests that at least part of the strain localization and implied low strength is caused by hydrolytic weakening. This is the first solid evidence that hydrolytic weakening is effective governing stress differences in the continental crust.

2. Ductile strain localization in the continental lithosphere. Deep fault zones exhumed by uplift and erosion commonly display evidence for large plastic deformation, and deep aseismic slip is implied below the seismogenic zones of

many plate-scale faults. This phenomenon has important implications as to how intraplate seismogenic zones are tectonically loaded. In particular, plastic instabilities below the seismogenic zones along intraplate faults may control the recurrence time of great earthquakes, not necessarily the special material properties of the seismogenic zone or the nature of the far-field boundary conditions. This topic was explored in a resource paper written for the EPRI Workshop, "Criteria for Assessing Earthquake Potential," which Kirby attended in Washington, D.C. in July.

3. Xenolith studies of the deep continental lithosphere. Samples of the deep continental lithosphere brought up by alkali basalts, although to varying degrees chemically and physically modified during their ascent, are our best guide to the physical identity, conditions and processes occurring in the lower lithosphere. In June I served on a USGS committee to organize a Survey-wide Xenolith Consortium and Repository that coordinates direct observations on materials of the deep continental lithosphere, their physical properties and elucidation of the evolution of the continental lithosphere by understanding the *in situ* physical and chemical processes as revealed by the structures, textures and detailed geochemistry. This effort is designed to provide another class of earth-science constraints on geophysical investigations of the continental lithosphere. In late summer, Kirby also participated in a 5-week field campaign in northeastern China studying the ultramafic xenolith occurrences along the Tangcheng-Lujiang fault zone. This was a unique opportunity to study deformation in the mantle along a major plate-scale fault zone. Preliminary observations suggest that stresses and strain rates are unusually high in the mantle along this fault zone.

4. We were invited to contribute a resource paper on inelastic rock-water interactions at the DOE-sponsored workshop, "Fundamental Geochemistry Needs for Nuclear Waste Isolation," held in Los Alamos in June. The paper was presented at the meeting by Andreas Kronenberg who summarized the geochemical rock-water interactions that influence rock deformation and are pertinent to the waste isolation problem.

Reports

Kirby, S. H., Introduction and digest to the special issue on the chemical effects of water on the deformation and strengths of rocks, Jour. Geophys. Res., 89, 3991-3995, 1984.

Kirby, S. H., and Kronenberg, A. K., Hydrolytic weakening in quartz: uptake of molecular water and the role of microfracturing, Trans. Am. Geophys. Union, 65, 277, 1984.

Kirby, S. H., and McCormick, J. W., Inelastic properties of rocks and minerals: strength and rheology, in R. S. Carmichael, ed., Handbook of Physical Properties of Rocks, v. 3, 139-280, 1984.

Kronenberg, A. K., and Kirby, S. H., Electrical conductivity of quartz: time dependence and transition in ionic charge carriers, Trans. Am. Geophys. Union, 65, 277, 1984.

Lee, R. W., and Kirby, S. H., Experimental deformation of topaz crystals: possible embrittlement by intracrystalline water, Jour. Geophys. Res., 89, 4161-4166, 1984.

Linker, M. F., Kirby, S. H., Ord, A., and Christie, J. M., Effects of compression direction on the plasticity and rheology of hydrolytically-weakened synthetic quartz crystals, Jour. Geophys. Res., 89, 4241-4255, 1984.

LABORATORY EXPERIMENTS OF WAVE PROPAGATION IN ANELASTIC MEDIA

9910-02413

Hsi-Ping Liu and Louis Peselnick
Branch of Engineering Seismology and Geology
U.S. Geological Survey
345 Middlefield Road, Mail Stop 977
Menlo Park, CAlifornia 94025
(415) 323-8111, ext. 2731

Investigations

1. Data analysis for the effect of tidal stress on seismic traveltimes in a Massachusetts granite quarry.

2. Development of a modified phase-ellipse method for in-situ geophone calibration.

3. Model experiments investigating the effects of anelasticity on travel time and amplitude in seismic wave propagation.

Results

1. Conflicting results were obtained by previous investigators on the tidal variation of seismic traveltimes. In order to investigate possible site-dependence, we have conducted a seismic survey in a Massachusetts quarry where an experiment with positive results was made in 1971. The source for the present experiment was a cylindrical air-gun having four side ports fired in a mud-filled pit. Measurements were made along three baselines (BLs) radiating from the source. BL I was situated in nearly flat topography and paralleled closely with that of the 1971 experiment. BLs II and III ran along a cliff bounding the quarry pit and an excavated step outside of the pit, respectively. The survey was conducted in the time interval (230d23h, 231d11h) and 231d22h, 233d10h), 1983 (U.T.). Traveltimes for the 1st 10 extrema along BL I including the 1st p-arrival were analyzed. Nine of them showed $\Delta t/t$ variation having the same magnitude reported for the 1971 experiment (~0.75 percent). The traveltime data correlated with the theoretical solid-earth tidal strain which had a predominantly 24-hr periodicity. A second result is that tidal variations for two groups of body waves are 180° out-of-phase with each other. Because the horizontal and vertical tidal strains at the earth's surface are 180° out-of-phase, these traveltime variations are interpreted in terms of the different velocity sensitivities to the two sets of orthogonal joint systems observed in the granite.

2. The phase ellipse method is used in the in-situ determination of two parameters, f_0, the geophone natural frequencey and f_u, the geophone

upper resonance frequency, which are needed for a complete amplitude and phase response calibration of moving-coil electromagnetic geophones. For some commercial geophones the precision in the determination of f_u can be 16 times less than the precision in f_0. In such a case, the accuracy of determining f_u can be as low as ± 10 percent by the phase ellipse method. We have devised a modified phase ellipse method having increased precision: typical accuracy in the determination of f_0 and f_u is 0.1 percent and 0.7 percent, respectively, for the modified phase ellipse method.

3. The internal friction of several thixotropic and viscous materials have been determined in search of a suitable modeling material for anelastic wave propagation experiments at ~1 MHz. The quality factor, Q, of Castor Oil was found to be 146 at 1 MHz and 20°C. This is the lowest value of Q of the eight materials which we have investigated thus far and is a suitable material for anelastic model experiments.

Reports

Liu, H.-P., Sembera, E. D., Westerlund, R. E., Fletcher, J. B., and Reasenberg, P. A., 1984, Precise measurement of seismic traveltimes--investigation of tidal variation in shallow crust: abstract submitted to the American Geophysical Union 1984 Fall Meeting.

Fletcher, J. B., and Liu, H.-P., 1984, Precise measurement of seismic traveltimes from an air-gun source: submitted to Geophysical Journal of the Royal Astronomical Society.

Laboratory and Field Studies of Constitutive Relations of Fault Zones

G-820

John M. Logan
Center for Tectonophysics
Texas A&M University
College Station, TX 77843
(409) 845-3251

Objectives: The occurrence of major earthquakes along fault zones has made the physical and mechanical properties of such features of considerable interest. To this end we have continued our program of laboratory and field studies to attempt to determine constitutive relations that will accurately characterize the mechanical behavior of fault zones. The objective is to utilize such relations in theoretical models that will aid predictive efforts. It is our belief, that however appealing laboratory results of such investigations, they must be assessed through field studies before they can be utilized with confidence in any theoretical model.

Results. Our laboratory studies presently have five programs in progress, two of which are far enough along to have produced results. (1) Studies of normal stress and velocity dependence in wet and dry sandstone with and without quartz and halite gouge. A power law has been used to characterize the velocity dependence, and has been contrasted with previously used logarithmic forms. Both are found to be unsatisfactory when extended to seismically realistic times (i.e., $>$ 1 year). As these are empirical relations without an adequate physical insights of the present, we have argued to extend the laboratory tests to these more important times. A second important and unexpected result concerns the simulated gouge of halite. At confining pressures of 35 MPa, there is a change from positive velocity dependence and stable sliding at slow displacement rates to negative velocity dependence and stick-slip at intermediate displacement rates. Another transition to positive velocity dependence occurs at faster rates. But, contrary to all previous work, stick-slip still occurs, and only gradually changes to stable sliding at the very fastest rates. As the confining pressure measure to 250 MPa the range of negative dependence and stick-slip is gradually replaced by positive dependence and stable sliding. However, this change takes place over a pressure range that is wider than expected, with stick-slip extending well into the regime where halite should be pressure insensitive. Observational studies have yet to be completed.

Triaxial experiments at temperatures to 1000°C on simulated gouge of quartz have produced recrystallization when the specimen is saturated with water. Both the positive and negative velocity dependency has been found depending upon the degree of recrystallization, with brittle behavior characterized by negative dependency and stick-slip.

Three other projects are just in the initial stages: (1) the influence of ph and ionic strength of chemical solutions on the frictional behavior of quartzites and sandstones; (2) the velocity and time dependence of simulated gouges of mixtures of quartz and halite; (3) the mechanical response of dimineralogic mixtures of clay and quartz in simulated gouges.

Our field program has attempted to investigate the superposition of primarily brittle behavior superimposed upon ductile behavior along the Insobric-Tonale Fault Zone in northern Italy. Previous field studies have corroborated laboratory findings of the fabric of shear zones deformed in the brittle regime. The next important step is to utilize those fabric results to interpret more complex tectonic histories. Preliminary results indicate the feasibility of such an approach.

Publications

Shimamoto, T. and Logan, J. M., 1983, Unstable fault motion induced by the reduction in the normal stress (Abstract): EOS, Trans. Am. Geophysical Union, v. 64, p. 851.

Dula, W. F., Jr., Friedman, M., and Logan, J. M., 1983, High temperature deformation of artificial quartz gouge (Abstract): Trans. Am. Geophysical Union, v. 64, p. 839.

Logan, J. M. and Blackwell, M. I., 1983, The influence of chemically-active fluids on the frictional behavior of sandstones (Abstract): EOS, Trans. Am. Geophysical Union, v. 64, p. 835.

Shimamoto, T. and Logan, J. M., 1984, Laboratory friction experiments and natural earthquakes: An argument for long-term tests: Tectonophysics, in press.

Shimamoto, T, 1984 Journ. Geop. Research, in press.

Analysis of Reflection Survey Data on the San Andreas Fault Zone for Velocity and Attenuation Properties

14-08-0001-G-950

Thomas V. McEvilly and Jonathan E. Scheiner
Seismographic Station
Department of Geology & Geophysics
University of California, Berkeley
Berkeley, California 94720
(415) 642-3977

Methods to image crustal structure near and within the San Andreas Fault zone using seismic reflection data are under study using facilities of the Center for Computational Seismology at Lawrence Berkeley Laboratory. The data sets under investigation include the CGG line obtained by the University of California in 1978 at Bickmore Canyon, as well as a USGS line shot by Western near the Kettleman Hills (this latter data set has been provided by Carl Wentworth). The reflection technique offers potential for high resolution imaging and a variety of processing and analysis procedures for the study of velocity structure. In strongly heterogeneous media such as fault zones there is great difficulty in resolving features of interest; though not without its problems, the reflection technique is recognized as one of the most promising methods for understanding structure in such complex regimes. In addition to a parameterization in terms of velocity, it is believed that an understanding of the attenuation, (Q), profile will greatly enhance our knowledge of the material properties of the earth's crust, particularly in critically important areas such as this active segment of the San Andreas fault near Hollister. Based on the work of Sato (1977, 1978), Aki and Chouet (1975) and others we have developed a technique for analyzing the coda of a coherent seismic signal in terms of the scattering and attenuation properties of the sampled medium. (See next page for some examples of the preliminary results.) This weak scattering approach is to be contrasted with the results of the previously reported diffusion approach. In addition to the reflection data, a microearthquake study recorded data from a small local array in 1982; this data is being analyzed using the same coda method. Finally, conventional Q analyses are planned using the spectral ratio method along with forward modelling using a one-dimensional approximation. With such an enhanced parameterizion of crustal structure and well planned reflection profiling, the ultimate goal of improved seismic imaging of seismogenic zones appears within our grasp.

Envelopes of the coda energy decay over a particular window of an averaged seismogram are inverted for the apparent Q and a scaled mean free path; below are some examples of the energy envelopes and the least squares fits. The data on the left is taken from the Gabilan or west side of the fault; on the right are the corresponding plots from the Franciscan side. Q values are quite low and may reflect intensive scattering contributions.

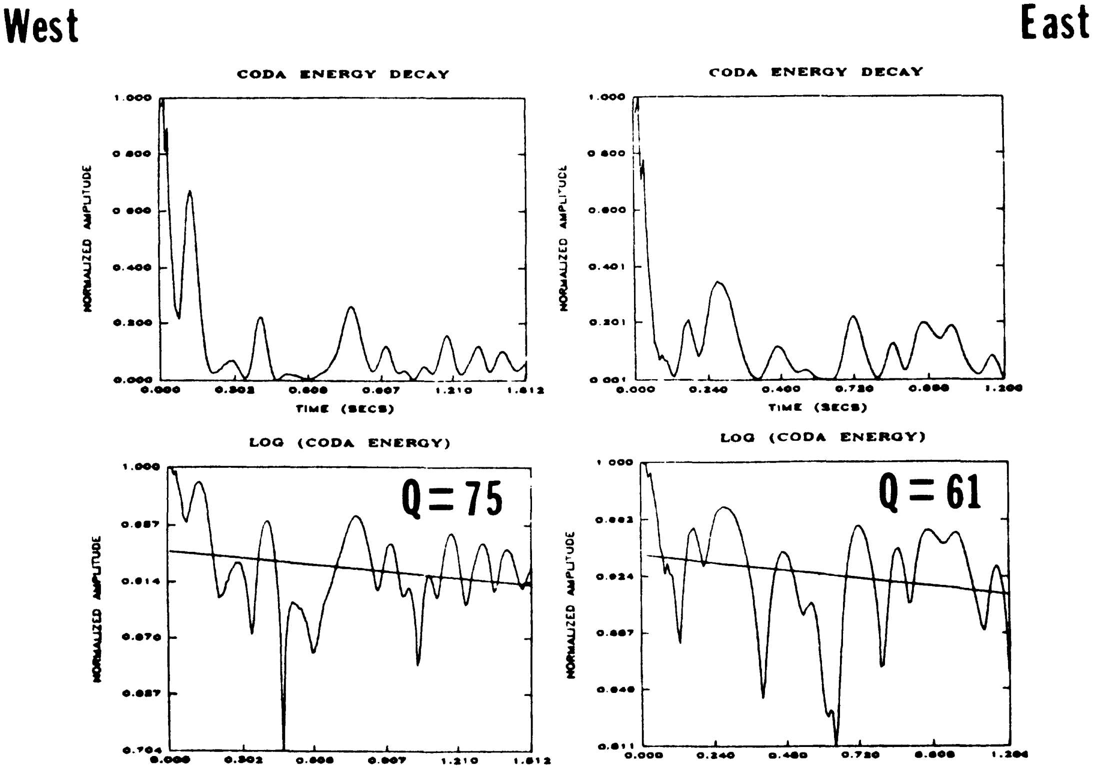

Active Seismology in Fault Zones

9930-02102

Walter D. Mooney
Gary S. Fuis
U.S. Geological Survey
Branch of Seismology
345 Middlefield Road, Mail Stop 977
Menlo Park, California 94025
(415) 323-8111, Ext. 2569

Investigations

1. Completion of a manuscript on a time-term study of Imperial Valley region (Kohler and Fuis) and continued study of the configuration of the subbasement (basaltic layer) in the same region (Fuis, Kohler, and McMechan).

2. Continued analysis of seismic refraction and reflection data from central California, including the region of the May 2, 1983, Coalinga earthquake (Walter); completion of a manuscript on tectonic wedging associated with emplacement of the Franciscan assemblage (Walter, C. Wentworth and others).

3. Completion of a manuscript on imaging of earthquake sources near Mammoth Lakes, California.

4. Completion of a manuscript on crustal structure in the Long Valley-Mono Craters, California, volcanic complex.

5. Completion of seismic-refraction experiment in southern Alaska (4 deployments, 29 shots). This experiment is part of the Trans-Alaska Crustal Transect (TACT) (Fuis, Mooney, Page).

6. Completion of seismic-refraction experiments at Newberry Crater, Oregon (1 deployment, 12 shots) (Stauber), and Hanford, Washington (2 deployments, 8 shots) (Mooney and Catchings).

7. Initiation of a seismic-refraction experiment in Maine (8 deployments, 41 shots) (Luetgert, Mooney, Fuis).

8. Continued cooperative work with the Peoples Republic of China (PRC) in building a seismic-refraction processing system for use by the PRC.

Results

1. In order to study the configuration of the subbasement in the Imperial Valley region, inferred to be intrusive basaltic rocks, all secondary arrivals in the Imperial Valley data set of 1979 that are interpretable as subbasement reflections were timed (Fuis) and will be analyzed using a method of intersecting hyperbolae (McMechan).

2. Structure along the eastern margin of the California Coast Ranges, where the Franciscan assemblage and Great Valley sequence are juxtaposed, seems to be marked by tectonic wedges. These are allochthonous masses thrust between underlying basement and overlying rocks peeled up by the wedge. Structure inferred from seismic reflection and refraction profiles in the southern Coast Ranges requires that the buried east boundary of Franciscan rocks is the tip of a tectonic wedge. In this interpretation, the Coast Range thrust, long interpreted to be a fossil subduction zone that juxtaposes Franciscan assemblage and Great Valley sequence, is the roof thrust of the Franciscan wedge.

   In the northern Coast Ranges, exposed structural relations can best be explained by several imbricate thrust wedges that have been driven eastward over Klamath-Sierran basement. The easternmost wedge tip is evident in reflection profiles. The inferred roof thrusts in the Great Valley sequence presumably merge northward into exposed, northwest trending strike-slip faults alined with the southern Klamath boundary. Eastward movement of the tectonic wedges has produced many tens of kilometers of offset on these tear faults. The Coast Range ophiolite has been thrust eastward far beneath the Great Valley sequence and onto Klamath-Sierran basement. Several terranes of Franciscan rocks have been thrust beneath the Coast Range ophiolite across the same basement. Subsequent east-directed reverse faulting in the late Cenozoic has offset the Coast Range thrust.

3. A finite difference technique by which an earthquake wavefield recorded at the Earth's surface could be extrapolated backward in time to produce an image of the source was presented by McMechan (1982). The resulting image is dynamic and reveals the temporal and spatial configuration of the acoustic equivalent of the source. The method was successfully tested on synthetic data, but no real earthquake data satisfying the prerequisites for processing were available in 1982. The data must be recorded close to the source and must be spatially dense. In January of 1983 a unique data set was recorded by the U.S. Geological Survey within Long Valley Caldera in eastern California. Three events were chosen from the aftershock sequence. Preprocessing of the data for each event includes construction of a true amplitude section, filtering, and interpolation to produce unaliased, equally spaced observations. Extrapolation of these data through a previously determined velocity structure produces coherent images in which both the source location and radiation pattern are visible. The images are also consistent with previously determined focal mechanisms. The results demonstrate the feasibility of imaging real earthquake sources.

4. Interpretations of four seismic refraction profiles in the tectonically active area between the eastern Sierra Nevada and the Basin and Range Province are presented. The four profiles sample the upper 7-10 km of the crust within the western half of Long Valley caldera, the Mono Craters ring fracture system and the "normal" crust north and northeast of Long Valley. The entire area observed shares a common crystalline basement consisting primarily of Mesozoic granitic rocks. At a depth of 2 km beneath the topographic surface, the P-wave velocity is uniformly 5.6 km/sec beneath which the velocity increases with a gradient of about 0.1 km/sec/km.

Clear secondary arrivals observed on a profile crossing the west part of the caldera provided further evidence for a reflecting boundary at a depth of 7 to 8 km beneath the west margin of the resurgent dome, which was initially identified and interpreted as the top of a magma chamber by Hill (1976).

Structural details resolved in the upper 2 km of the crust lead to the following conclusions.
1) P-wave velocities in the crystalline basement at depths shallower than 2 km vary from 3.6 km/sec to 5.0 km/sec. This variation reflects differences in the degree of fracturing of the upper portion of the basement.
2) An apparently homogeneous basement in the upper 7 to 10 km beneath the Mono Craters ring fracture system indicates that any extensive magma chamber must be at least 10 km deep there.
3) The down-dropped crystalline basement beneath the western half of Long Valley caldera dips gently (5 to 10 degrees) to the northeast. Apparent offsets along steeply-dipping caldera-bounding faults are 1.0 to 1.7 km along the northern, western and southern sides of the caldera with largest offsets in the north.
4) Rocks forming the caldera fill fall into essentially three P-wave velocity groups. From the surface downward these velocity groups are: 100 to 400 meters of 1.2 to 1.8 km/sec material corresponding to unconsolidated fluvial or lacustrine deposits or highly fractured rhyolite flows, 200 to 400 meters of 2.8-3.1 km/sec material corresponding to sparsely jointed post-caldera rhyolite, rhyodacite and basalt flows, and approximately 1000 meters of 3.9-4.4 km/sec material corresponding to deposits of Bishop tuff.

5. In June and July 1984, the USGS conducted a seismic refraction experiment in southern Alaska, as the first major project of the Trans-Alaska Crustal Transect (TACT) program. TACT is a multi-year, multi-disciplinary effort to investigate the crustal structure along a route paralleling the Alaska oil pipeline. The program includes many investigations including seismic refraction, seismic reflection, geologic mapping, and gravity and aeromagnetic studies. The 1984 seismic refraction experiment consisted of four deployments with 29 shots (fig. 1) designed to investigate in various ways the accreted terranes of southern Alaska and their sutures, including the current subduction zone(s) extending northwestward under the Kenai Peninsular and northward under the Wrangell volcanoes, and the active Denali fault zone.

All records were digitized and plotted in the field (120 instruments X 29 shots), and preliminary interpretations were made. Data quality was generally good (in terms of signal-to-noise ratio and instrument performance) and was exceptional on deployment 2, where instruments were deployed cross country by helicopter, away from highway noise, and where all shots were detonated in lakes. Basement velocities range from 5.8 to 6.2 km/s for most of the region of the experiment, but along deployment 2, along the structural grain in the Chugach terrane, a much higher velocity (6.8-7.0 km/s) is seen below a depth of a few km. One of the most striking features in the data is a clear reflection seen on deployment 1 from most shotpoints, at critical distances ranging from 25-55 km. Preliminary modeling of this feature indicates a reflecting layer with a velocity of 7.2-7.6 km/s that has an apparent dip of 6-9 degrees northward under the Chugach Mountains and Copper River Basin, reaching a depth of about 25 km near Glennallen. Data collected on deployment 2 reveal a series of strong reflections with critical distances ranging from 15 km to 120 km. One of these reflections is interpreted to come from the same reflecting layer as seen on deployment 1; along this line its depth is 11 km, and its dip is relatively small. Other reflections indicate deeper reflecting layers. Apparently there are low-velocity zones between these reflectors. No clear reflections are seen on deployment 3, but a couple of strong lateral velocity changes are seen, one at the inferred boundary between the Peninsular and Wrangellia terranes (see fig. 1).

The experiment plan for 1985 (fig. 2) includes a deployment parallel to the structural grain in the Prince William terrane and the strike of the seismically active Aleutian subduction zone (deployment 1). It is hoped that a reflecting layer will be seen on this deployment corresponding to the subducting oceanic crust, that can be traced via deployment 2 (fig. 2) into the region investigated by deployment 2 of 1984 (fig. 1). Perhaps it will be possible to identify such a layer with one of the reflecting layers discovered in this region in the 1984 experiment.

6. In August, 1984, the U.S.G.S., in conjunction with D.O.E./Rockwell Hanford Operations, conducted a seismic refraction experiment which extended from southeast Washington State to northeast Oregon. The 261 km long reversed profile, centered on the Columbia River within the Hanford Property, extended from 31 km southwest of the town of Biggs, Oregon, to approximately 51 km northeast of the town of Warden, Washington, along a N 51 E transect. The experiment consisted of 8 shots, ranging in size from 911 Kg to 2311 Kg, four shotpoints, and 241 stations with an average spatial sampling interval of 930 meters between end shotpoints and 1300 meters outside of those shotpoints. Preliminary interpetation suggests that the Columbia River Basalts range in velocity from approximately 5.1 km/sec to nearly 6.1 km/sec and may be 5 to 11 kilometers thick. Other prominent crustal refractors are present with velocities ranging from 6.1 km/sec to approximately 7.5 km/sec. Additionally, several low velocity layers and fault scraps are identifiable. Preliminary interpetation indicates that the crust may be about 41 km thick, in contrast to the earlier estimates of 25 to 31 km determined by earthquake data.

7. A major seismic refraction experiment was conducted in Maine and southern Quebec during September, October and November 1984 (fig. 3). The experiment consists of 8 deployments and 41 shots designed to investigate the crustal structure of the Appalachians both perpendicular to structural grain (deployments 1-3) and parallel to structural grain (deployments 4-8). Deployments 1-3, together 300 km long, coincide with a seismic reflection profile that is also currently being gathered. Data quality from the first deployment is exceptional (quiet sites, clear arrivals to 300 km). Basement velocity is generally less than 6 km/s. One clear reflection can be seen at a critical distance of 65-70 km. Clear Pn arrivals in the range 180-300 km along this line from a shotpoint in Quebec indicate an apparent velocity of 8.2 km/s. Lateral velocity variation is minimal.

Reports

Catchings, R. D., Mooney, W. D., and Hollbrook, W. S., Crustal structure of southeastern Washington from seismic refraction (abs): EOS Transactions American Geophysical Union, Fall 1984.

Colburn, R. H., and Walter, A. W., 1984, Data report for two seismic refraction profiles crossing the epicentral region of the Coalinga, California, earthquakes: U.S. Geological Survey Open-File Report 84-643.

Fuis, G. S., and Zucca, J. J., A geologic cross section of northeastern California from seismic refraction results, in, Nilsen, T. H., ed., Geology of the Upper Cretaceous Hornbrook Formation, Oregon and California: Society of Economic Paleontologists and Mineralogists, Pacific Section, v. 42.

Hill, D. P., Kissling, E., Luetgert, J. H., and Kradolfer, U., Constraints on the upper crustal structure of the Long Valley-Mono craters volcanic complex, eastern California, from seismic refraction measurements: submitted to Journal of Geophysical Research.

Kohler, W. M., and Fuis, G. S., Travel-time, time-term, and basement depth maps for the Imperial Valley region, California, from explosions: in review for Bulletin Seismological Society of America.

Luetgert, J. H., and Mooney, W. D., Earthquake profiling at Mammoth Lakes, California: Bulletin Seismological Society of America, in press.

McMechan, G. A., Luetgert, J. H., and Mooney, W. D., Imaging of earthquake sources in Long Valley caldera, California, 1983: submitted to Bulletin Seismological Society of America.

Mooney, W. D., Crustal structure in the vicinity of the Morgan Hill earthquake, in Tucker, B., ed., The 1984 Morgan Hill, California, earthquakes: California Division of Mines and Geology, in press.

Murphy, J. M., and Walter, A. W., 1984, Data report for a seismic refraction investigation: Morro Bay to the Sierra Nevada, California: U.S. Geological Survey Open-File Report 84-642.

Page, R. A., Fuis, G. S., Mooney, W. D., Nokleberg, W. J., and Plafker, G., Crustal transect of accreted tectonostratigraphic terranes in the Chugach Mountains and Copper River Basin, Alaska: initial results of TACT (abs.): EOS Transactions American Geophysical Union, Fall 1984.

Walter, A. W., Velocity Structure near Coalinga, California, in Rymer, M. J., and Ellsworth, W. L., eds., Mechanics of the May 2, 1983, Coalinga, California, earthquake: U. S. Geological Survey Open-File Report, in press.

Wentworth, C. M., Blake, M. C., Jones, D. L., Walter, A. W., and Zoback, M, D., Tectonic wedging associated with emplacement of the Franciscan assemblage, California Coast Ranges, in Blake, M. C., ed., Franciscan Geology of northern California: Society of Economic Paleontologists and Mineralogists, Pacific Section, in press.

Wentworth, C. M., Zoback, M. D., and Walter, A. W., Testing models of Franciscan and Nevadan obduction by scientific drilling in central California (abs.): EOS Transactions American Geophysical Union, Fall 1984.

Yerkes, R. F., McGarr A. F., Wentworth, C. M., and Walter, A. W., Abnormally high fluid pressures near the Coast Range-Great Valley boundary, CA, may aid northeast directed thrusting responsible for the 1983 Coalinga earthquakes (abs.): EOS, Transactions American Geophysical Union, Fall 1984.

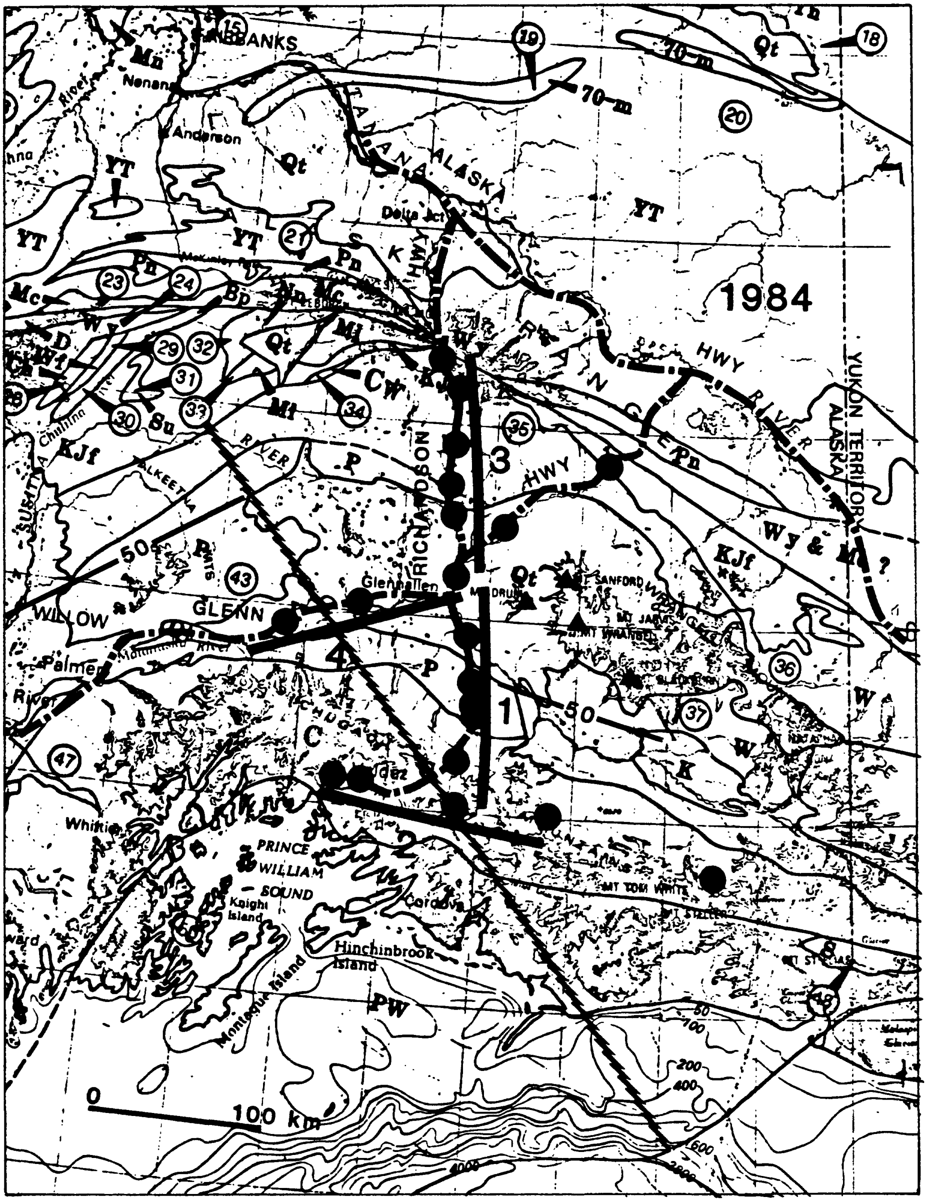

Fig. 1 Seismic refraction profiles for 1984 shown in relation to tectonostratigraphic terranes, 50-km depth contours on top of Aleutian and Wrangell Benioff zones (double lines), and the northeastern edge of Aleutian Benioff zone (jagged line). Dots are shotpoints; heavy lines show instrument deployments. Heavy dot-dash lines are highways. Triangles are the Quaternary Wrangell volcanoes. Major terranes are, from south to north: PW, Prince William; C, Chugach; P, Penisular; W, Wrangellia.

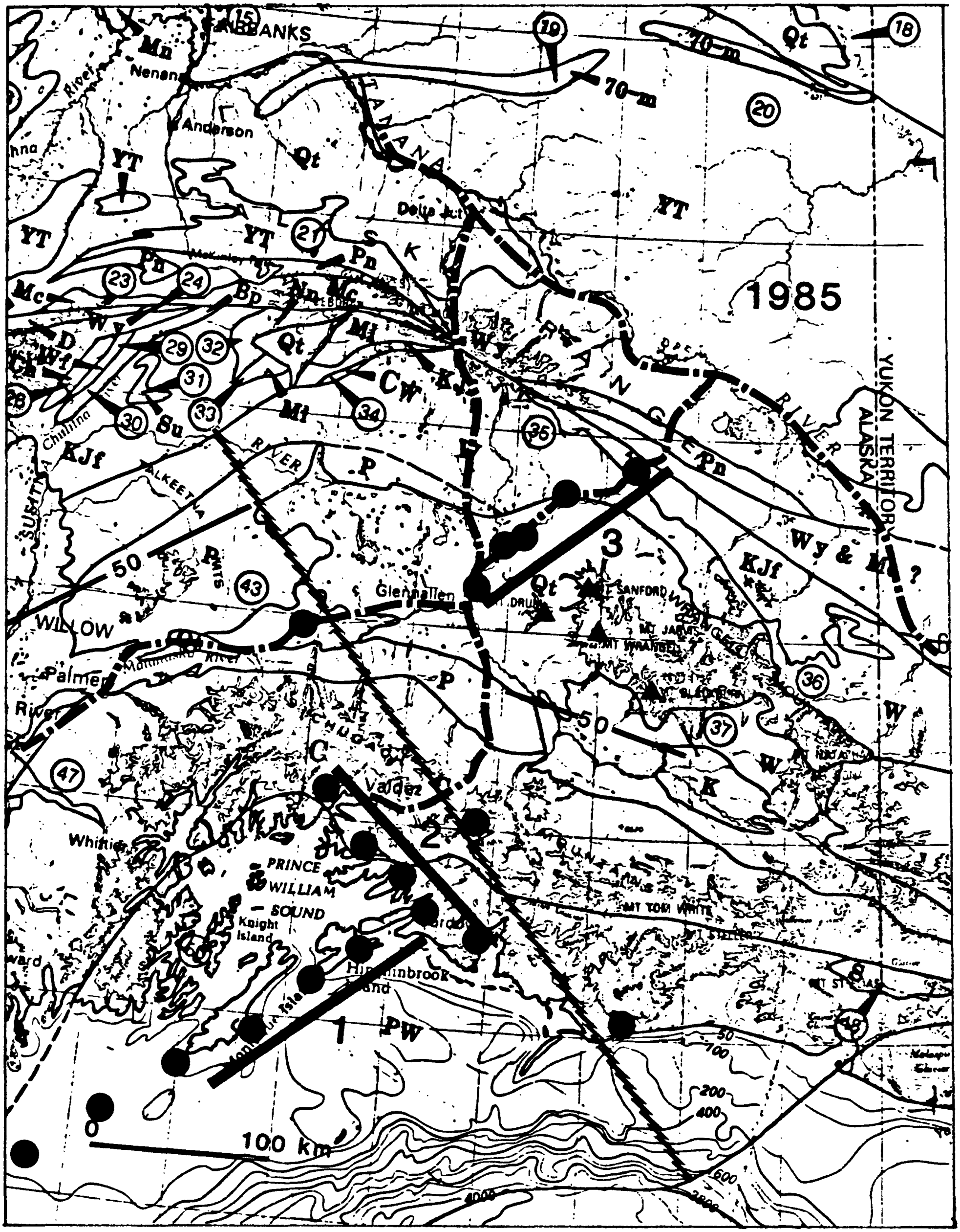

Fig. 2 Proposed seismic refraction profiles for 1985. For further explanation see Figure 1 caption.

Maine Seismic Refraction

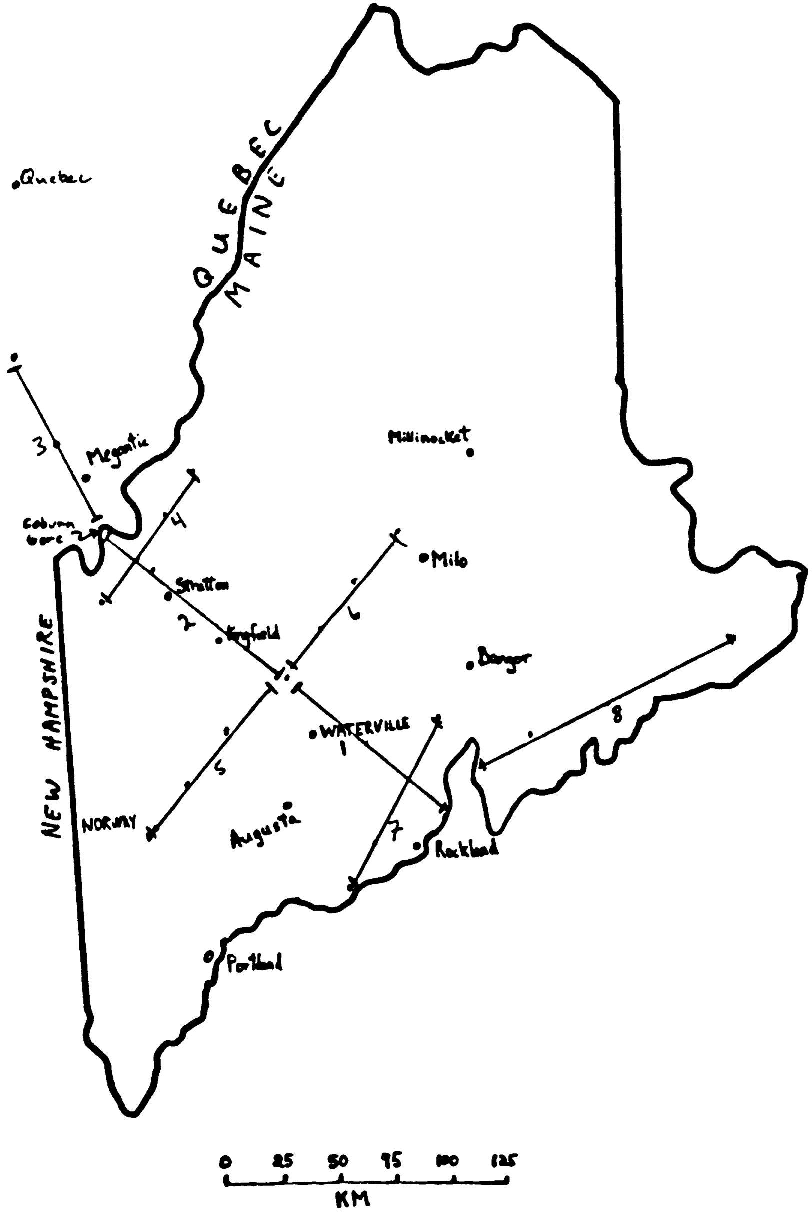

Fig. 3 Seismic refraction profiles in Maine and southern Quebec, 1984.

Rock Deformation

9950-00409

Eugene C. Robertson
Branch of Engineering Geology and Tectonics
U.S. Geological Survey
922 National Center
Reston, VA 22092
(703) 860-7404

Investigations

In following up earlier conclusions on the increasing production of gouge and breccia with increasing displacement of faults, the question of the effect of rock type, soft sedimentary rocks particularly, on the amount of crushing was studied by observations of faults in shale, sandstone, and coal in two coal mines and offsets of three veins of fluorspar in mines in southern Illinois. Comparisons of fault displacement to thickness of gouge plus breccia were to be made with results on faults in western mines and outcrops.

Results

Many steeply dipping faults have displaced Desmoinesian sedimentary rocks of middle Pennsylvanian age in south-central Illinois, and they were inspected underground recently in the Crown No. 2 and the Orient No. 4 mines which are working the Herrin No. 6 coal bed. Associated shale, sandstone, coal, and limestone beds were displaced a few millimeters to several hundred meters with dip-slip movement primarily, although three faults had predominantly strike-slip movements of 1-10 m.

The principal problem to be studied was the effect of faulting on the amount of brecciation of relatively soft shale to compare with observations of faults in harder rocks, granites, quartzites, and harder shales (argillites) in Montana and Idaho mines and outcrops. The latter is in an earlier published study which showed a correlation of fault displacement (d) with thickness (t) of gouge plus breccia on a log-log plot over 6 orders of magnitude (Robertson, 1983). Scatter of data around a trend line of $d/t = 100$ is considered to be due primarily to uncertainty in measurements of d and t, but rock type also is an important variable.

Data on soft sedimentary rocks on d and t from 8 faults in the coal mines and from 11 faults in the fluorspar mines of Illinois plot on the high t side of the trend line, as might be expected. Soft shale and coal would be more easily crushed, and thicker zones would be expected and were found in the faults observed; no observations could be made of sandstone or limestone. Previous data on faults in shales in Western States plot closer to the trend line, but the shales are more lithified, not as friable. At another occurrence of faulting of shale previously observed, the points plot on the low t side of the trend line; this difference may be explained by the low confining pressure (5 MPa) that probably prevailed and the greater hardness of the shale. Confining pressure on the Illinois shale may have been 30 MPa or more. Water conditions at faulting are not known.

The gouge and breccia of shale is easily confused with adjacent jointed, even shattered, but not displaced fragments. Measurements of t need to be carefully made, as wide jointing zones are produced adjacent to faults. A horse of jointed shale is usually found between fault branches.

In previous work on faults in the Illinois coal mines, the full length of many faults was mapped, from a few meters to 1 km. The extensive workings make such observations possible. In one fault in the 300-m-long central portion, $d = 1 \pm 0.1$ m, and d tapered to 10 cm for 50 m of length farther on the ends and then to zero beyond. Crushed rock was observed all along the fault zone to the ends.

Application of the correlation of d and t in faults may eventually be made to earthquakes and associated faults. Maximum earthquake magnitudes may become predictable from d and t measurements, although movement by creep would need to be considered as well. Information on rock type could be very important in such an evaluation.

Reference cited

Robertson, E. C., 1983, Relationship of fault displacement to gouge and breccia thickness: Mining Engineering, v. 35, no. 10, p. 1426-1432.

COUPLED DEFORMATION - PORE FLUID DIFFUSION EFFECTS IN FAULT RUPTURE

14-08-0001-21818

John W. Rudnicki
Department of Civil Engineering
Northwestern University
Evanston, Illinois 60201
(312)-492-3411

Investigations

1. Slip on impermeable fault zones.
2. Reservoir-induced seismicity.

Results

1. Previous solutions for slip in fluid-saturated rock masses [Booker, 1974; Rice and Cleary, 1976] impose the condition of no change in pore fluid pressure on the fault (slip) plane and, hence, are appropriate for a permeable fault. Faults in situ are, however, often barriers to fluid flow, possibly because the fault zone contains much clay or fine-grained gouge particles. The solution for a plane strain shear dislocation suddenly emplaced on an impermeable fault differs significantly from that for a permeable fault. The figure shows the shear stress, in nondimensional form, at a fixed position on the fault plane as a function of time for both a permeable and an impermeable fault. As indicated, the shear stress induced on the impermeable fault plane does not decay monotonically in time from the undrained (instantaneous) value to the drained (long-time) value. Before decaying, the shear stress for the impermeable fault rises to a peak in excess of the undrained value by about 20% of the difference between the drained and undrained values. This means that the effect of coupling between deformation and diffusion is initially destabilizing for the impermeable fault; that is, the coupling induces an increase of shear stress on the fault and promotes further slip. Also, although the shear stress on the impermeable fault decays with time, it remains higher than the shear stress on the permeable fault at any time.

Using two opposite signed dislocations to simulate a finite length fault suggests that this rise in shear stress occurs for 1.5 to 15 days for a fault 5 km. in length and diffusivities of $.1m^2/s$ to $1.m^2/s$. A characteristic time, defined as the time needed for the shear stress on the fault to decay to one-half of its long-time value, is $a^2/4c$ for the impermeable fault compared with $a^2/16c$ for the permeable fault where a is half the fault length and c is the diffusivity. Consequently, diffusive reloading of the fault, suggested by Nur and Booker [1972] as a contributor to aftershocks, does not begin immediately and occurs much more slowly for the impermeable fault.

The pore pressure induced on the fault plane is anti-symmetric and discontinuous; the value on one side is the negative of the value on the other side. If slip is inhibited by an increase in effective compressive stress, that is, the total compressive stress minus the pore fluid pressure, then slip would be promoted on the side with positive pore pressure and inhibited on the other side. The presence of transverse subsidiary faults on one side of a main fault but not on the other would be consistent with this prediction.

We have also obtained expressions for the pore pressure induced by a shear dislocation moving steadily at a speed V on an impermeable fault and used these to complement the work of Roeloffs and Rudnicki [1984] on fluctuations in water well levels associated with episodic creep. The pore pressure change near the fault is greater and sharper for the impermeable than for the permeable fault. More specifically, at a stationary observation point located at $Vy/2c = 0.1$, the peak value of the pore pressure is four to five times greater for the impermeable fault. At distances from the fault much less than one diffusion length, $2c/V$, the pore pressure for the impermeable fault falls to zero rapidly after the dislocation passes, but does not reverse sign as for the permeable fault. Because of this sign reversal for the permeable fault, positive and negative contributions tend to cancel when the dislocation solution is superposed to get a continuous slip distribution. Thus, the magnitude of the pore pressure change for a continuous slip distribution is very much less than for the dislocation. For the impermeable fault, the magnitude of the pore pressure change for a continuous distribution of slip is not so severely reduced compared with the dislocation response.

For the impermeable fault, the amplitude of the frequency spectrum is flat at low frequency. Consequently, water level changes may occur in wells with critical frequencies that are lower than the lowest frequencies present in the pore pressure field for the impermeable fault. Also, near the fault plane, the highest frequencies present in the solution for the impermeable fault are one to two orders of magnitude lower than for either the permeable fault solution or the "uncoupled" solution.

2. One possible cause of the observed correlation between peaks in seismic event frequency and annual water level changes in some reservoirs [Gupta et al., 1972; Simpson, 1976] is a phase lag between the peak mean compressive stress and the peak pore pressure. Such a phase lag could result in a temporary decrease of effective stress at some time during the annual cycle. To assess the importance of coupled deformation and pore fluid diffusion in producing effective stress changes, Roeloffs has calculated the stresses and pore pressures caused by a time varying two-dimensional reservoir load on the surface of a porous elastic half space. The reservoir load was assumed to vary harmonically in time with radian frequency ω and to be trapezoidal in shape with half-widths L_1 at the surface and $1.5\ L_1$ at the deepest point. The frequency and width enter in the nondimensional combination, $\Omega = \omega L_1^2/c$ where c is diffusivity. For an annual cycle, diffusivities in the range 10^3 to 10^6 cm^2/s and L_1 from 1 to 10 km., Ω ranges from .002 to 200.

For the highest diffusivity in the range considered, the pore pressure is nearly equal to the mean stress at depths several times L_1. As the diffusivity decreases, the peak pore pressure falls off more rapidly with depth, reaching a limiting value of 2/3 of the mean stress, which is the undrained value for the material properties assumed here. However, the amplitude of the mean stress at any given point is nearly the same over the entire diffusivity range. Furthermore, the peak compressive value of the mean stress is always within a few degrees of being in phase with the peak water level. For depths and diffusivities where undrained conditions prevail, the pore pressure is nearly in phase with the mean stress. However, the pore pressure lags the mean stress for the cases where appreciable diffusion occurs.

For the cases considered, the peak weakening is always less than 6% of the peak fluctuation in water level, and decreases with depth, except for the case $\Omega = 2.0$. For $\Omega = 2.0$, the peak effective stress is nearly constant down to twice the reservoir half-width. The phase lag between pore pressure and mean stress is not large enough to cause a peak weakening on the order of the sum of the peak pore pressure and mean stress. Thus, the predicted effective stress changes are small.

References

Booker, J.R., J. Geophys. Res., 79, 2037-2044, 1974.

Gupta, H.K., B.K. Rastogi and H. Narain, Bull. Seismol. Soc. Am., 62, 481-492, 1972.

Nur, A. and J.R. Booker, Science, 175, 885-887, 1972.

Rice, J.R. and M.P. Cleary, Rev. Geophys. Space Phys., 14, 227-241, 1976.

Roeloffs, E. and J.W. Rudnicki, PAGEOPH, to appear, 1984.

Simpson, D.W., Engineering Geology, 10, 123-150, 1976.

Publications

1. Rudnicki J.W., Effect of pore fluid diffusion on deformation and failure of rock, to appear in Mechanics of Geomaterials (edited by Z.P. Bazant), Proceedings of the IUTAM William Prager Symposium on Mechanics of Geomaterials: Rocks, Concretes, Soils, September 11-15, 1983, Northwestern University, Evanston, IL. Publication by John Wiley, Ltd., London, expected in 1984.

2. Roeloffs, E. and J.W. Rudnicki, Coupled Deformation-Diffusion Effects on Water Level Changes Due to Propagating Creep Events, (Abstract), EOS, Trans. Am. Geophys. Union, 64, 851, 1983.

3. Roeloffs, E. and J.W. Rudnicki, Coupled Deformation - Fluid Diffusion Effects on Pore Pressure Due to Propagating Creep Events, to appear in a special volume of PAGEOPH on Earthquake Hydrology and Chemistry, ed. by C.-Y. King, 1984.

4. Rudnicki J.W., Effects of dilatant hardening on the development of concentrated shear deformation in fissured rock masses, J. Geophys. Res., 89, 9259-9270, 1984.

5. Rudnicki, J.W., Slip on an impermeable fault in a fluid saturated rock mass (Abstract), submitted for presentation at the Fall AGU Meeting, 1984.

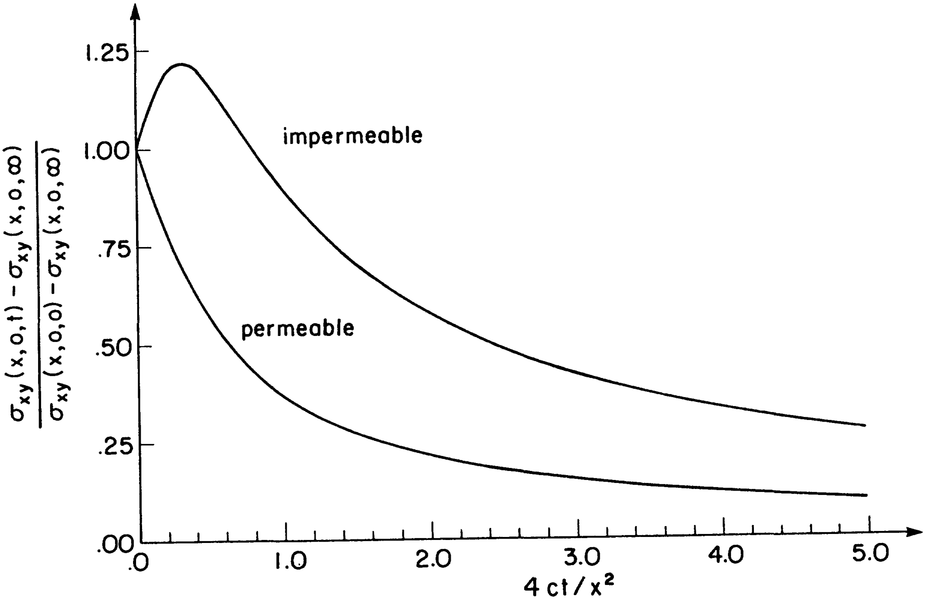

Heat Flow and Tectonic Studies

9960-01176

John H. Sass
Branch of Tectonophysics
U.S. Geological Survey
2255 North Gemini Drive
Flagstaff, AZ 86001
(602) 527-7726
FTS: 765-7226

Arthur H. Lachenbruch
Branch of Tectonophysics
U.S. Geological Survey
345 Middlefield Road
Menlo Park, CA 94025
(415) 323-8111, ext. 2272
FTS: 467-2272

Investigations:

1. Heat flow and tectonics of the Western United States: Temperature and thermal conductivity data from sites in the Mojave Block, Sonoran Desert, and the Colorado Plateau transition zone in Arizona are being reviewed, and heat-flow data revised. A preliminary interpretation of heat-flow data from the Brantley damsite near Carlsbad, New Mexico, was completed.

2. Heat flow and tectonics of Alaska: Interpretation of data from the National Petroleum Reserve, Alaska, is continuing with new measurements that now permit a reliable estimate of the undisturbed temperature. A dozen sites were selected along the Trans-Alaskan crustal transect for heat-flow determinations. Preliminary engineering work was begun regarding the long-term monitoring of permafrost temperatures as an aid in identifying local and global climatic changes in relatively early stages of development.

3. Thermal studies related to nuclear waste isolation: Numerous measurements of temperature were made in the unsaturated zone in all available wells near Yucca Mountain.

4. Instrumentation: A technique for measuring thermal properties at high temperatures was developed, and preliminary trials were performed.

Results:

1. Heat flow and tectonics of the Western United States: Analysis of heat flow along a broad region in southern California and southern Arizona reveals a complicated pattern of highs and lows corresponding to some degree with the major structures of the region. The heat flow along this zone is predominantly high (mean ∿80 mW m^{-2}) despite the fact that much of the region has been quiescent during the past 7 m.y. In western and central Arizona, the heat-flow pattern does not conform in detail to the published interpretations of Curie isotherms based on aeromagnetic data. Transient thermal models consistent with the observed heat-flow patterns are being refined.

Heat flow from seven shallow (less than 200 m) wells within an area of some 50 km^2 near Carlsbad, New Mexico, varies from 27 to 41 mW m^{-2} with a mean of about 34, somewhat lower than published estimates of about 42 to 45 mW m^{-2} from deep oil wells in the region. Some of the variability and the lower average might be ascribed to a slow downward percolation of ground water in the upper few hundred meters of this cavernous terrane. The lower mean might also reflect a more complete characterization of thermal conductivity in this instance relative to the previously published estimates. An analysis of heat-flow variations in individual wells indicates that vertical seepage of water within the cavernous zones is very slow (seepage velocity less than 1 ft/yr) and from this point of view, it might be reasonable to build a dam in this region.

2. Heat flow and tectonics of Alaska: Analysis of recently measured near-equilibrium temperatures from two dozen oil exploration wells on and near National Petroleum Reserve, Alaska, provides the first information on permafrost depth and recent climatic trends over most of the Alaskan Arctic Coastal Plain, foothills, and northern Brooks Range. The new data extend earlier project results from wells along the Arctic Coast which indicated a climatic warming of 1°C-3°C during the last century; with some important exceptions, the warming has generally been slower at inland sites. Over most of the Arctic slope, permafrost depth is in the range 200-400 m; along the Beaufort Sea Coast near Prudhoe Bay, it is 600 m. The depth is controlled primarily by lateral variations in the thermal conductivity of permafrost materials; variation in surface temperature and heat flow are relatively unimportant. The absence of thermal disturbance in coastal wells along the Beaufort Sea implies the shoreline there has been transgressing rapidly.

3. Thermal studies related to Nuclear Waste Isolation: Temperature profiles within the unsaturated zone suggest very little vertical water movement within that zone although some sharp changes in gradient might be related to phase changes from liquid to vapor or vice versa. Average gradients vary by a factor of 4 suggesting that convection at depths of 2.5 to 3.5 km might be controlling the local heat-flow pattern.

4. Instrumentation: Many determinations of thermal conductivity and diffusivity at high temperature published by DOE contractors disagree with previously published information, particularly for rock salt. These parameters are very important for engineering calculations related to nuclear waste isolation. We have adapted a technique originally proposed by J. C. Jaeger and J. H. Sass to available furnaces and have made some preliminary studies of lateral and radial temperature distribution preparatory to calibration runs of the technique.

Reports:

Bills, D. J., and Sass, J. H., 1984, Hydrologic and near-surface thermal regimes of the San Francisco volcanic field: U.S. Geological Survey Professional Paper, in press.

Lachenbruch, A. H., Sass, J. H., and Galanis, S. P., Jr., Heat flow in southernmost California and the origin of the Salton Trough: Approved - July 11, 1984.

Lachenbruch, A. H., Sass, J. H., Lawver, L. A., Brewer, M. C., and Moses, T. H., Jr., 1984, Depth and temperature of permafrost on the Alaskan Arctic Slope: U.S. Geological Survey Professional Paper, in press.

Morgan, P., and Sass, J. H., 1984, Thermal regime of the continental lithosphere: Journal of Geodynamics, v. 1, p. 143-166.

Pollack, H. N., and Sass, J. H., 1984, Thermal regime of the lithosphere, in Haenel, R., Rybach, L., and Stegena, L., eds., Handbook of Terrestrial Heat-flow Density Determination (Guidelines and recommendations of the International Heat Flow Commission), in press.

Sass, J. H., 1984, Thermal studies at the Brantley Damsite on the Pecos River near Carlsbad, New Mexico: U.S. Geological Survey Open-File Report 84-663, 25 p.

Sass, J. H., Galanis, S. P., Jr., Lachenbruch, A. H., Marshall, B. V., and Munroe, R. J., 1984, Temperature, thermal conductivity, heat flow, and radiogenic heat production from unconsolidated sediments of the Imperial Valley, California: U.S. Geological Survey Open-File Report 84-490, 38 p.

Sass, J. H., Lachenbruch, A. H., and Silver, L. T., 1984, Exploratory crustal drilling near the southern margin of the Colorado Plateau and in the San Francisco volcanic field (abstract), in press, 1984.

Sass, J. H., Lawver, L. A., and Munroe, R. J., A heat-flow reconnaissance of southeastern Alaska: Canadian Journal of Earth Sciences, in press, 1984.

Zoback, M. D., Healy, J., Lachenbruch, A. H., and Henyey, T., 1984, In situ stress, heat flow, and fault zone monitoring in a deep well near the San Andreas fault at Cajon Pass (abstract): in press, 1984.

Zoback, M. L., and Lachenbruch, A. H., 1984, Upper mantle structure beneath the Western U.S. (abstract): Geological Society of America, Annual Meeting, 97th, Reno, Nevada, 1984, Abstracts with Programs, v. 16, no. 6, p. 705.

Geophysical, Geological and Geochemical Characterization of Granitic Rocks Associated with the San Andreas Fault System

14-08-0001-G-945

Donald J. Stierman*
Alan E. Williams
Institute of Geophysics and Planetary Physics
The University of California
Riverside, California 92521
(714) 787-4611

Objective: Understanding the constitutive nature and rheological properties of seismically active regions in the crust is fundamental to scientific earthquake prediction. Important factors controlling the strength of rocks, and, hence, the failure process, include the confining pressure, temperature, and pore fluid pressure as well as the frictional behavior of the minerals. Petrologic and geochemical methods are used to study cataclastic rocks to determine the physical setting of their genesis. Calibration of the relationships between rock properties and geophysical signatures of fault zone rocks permit us to extrapolate data obtained from available boreholes downward into the seismic zone.

Investigations:

1. Gravity measurements across the San Andreas fault near Lake Hughes and Stone Canyon.

2. Petrographic, mineralogic and isotopic analysis of cataclastic quartz diorite from the 600 m deep Stone Canyon well.

3. Comprehensive analysis of engineering and geophysical information from the Stone Canyon well.

Data acquisition, analysis and results:

1. Gravity measurements were taken at 87 new stations on both sides and within the fault zone near Lake Hughes, on the locked segment of the San Andreas fault, and at 48 stations near Stone Canyon, on the creeping section of the fault. Elevation control in the rugged terrain characteristic of both study areas was made possible by loan of the HP-3810B laser distance and elevation meter from UCLA. These data are being interpreted in conjunction with underground gravity measurements made previously. This third dimension coverage provides control needed to discriminate between shallow and deep density contrasts. Preliminary modeling suggests that density changes associated with the fault zone near Lake Hughes are essentially restricted to the fault zone. Interpretation of the strong regional gradient suggests a deep crustal or upper mantle density contrast associated with the fault. Because the data base needed for outer zone terrain corrections at Stone Canyon had not been previously compiled for our computer, preliminary modeling of the Stone Canyon results has not begun. The data will be used to model the density structure of the fault zone, which will bear on the fault zone composition at depth. The data will determine the vertical extent of the rocks collected from the Stone Canyon well.

---

*Now at: Dept. of Geology, University of Toledo, Toledo, Ohio 43606
(419) 537-2046

2. Thin sections of six distinct deformation zones from the Stone Canyon cores are being studied. Although some hand samples appear mylonitic, microscopic examination shows the deformation was associated with brittle failure (see Figure 1A). Breccia in these deformation zones is usually, but not always, cemented by calcite or dolomite. There is a general tendency for the grain size of the carbonate cement to decrease with depth, and the cement in the deepest samples is fine-grained and discontinuous, which leaves the rocks friable. These rocks are mechanically weak and would not survive long in outcrop. Several generations of cement are found in deformation zones, showing reactivation of cemented failure planes. While the plagioclase and quartz grains in these deformation zones rupture in brittle failure, phylosilicate segregations appear to deform ductilely (see Figure 1B) and coalesce into thick, relatively planar bands of clay gouge along fracture surfaces. these rocks contain structures that appear to represent several stages in the development of fault gouge.

3. Bulk mineralogy was determined by the automated X-ray diffractometer for 30 samples distributed throughout the length of core. In addition to the plagioclase and quartz expected in quartz diorite, calcite and low-temperature hydrothermal alteration minerals were identified in all but the most pristine specimen. Fault gouge from depths of 44 m, 481 m and 553 m contain 59%, 32% and 37%, respectively, montmorillonite. This shows that development of low-friction montmorillonite in fault gouge is not restricted to the alteration of mafic rocks. The source of the ubiquitous calcite is not known.

4. Fluid inclusion analysis of the calcite cement of one breccia suggests a minimum deposition temperature of 200°C. This is equivalent to a depth, extrapolating the current temperature gradient, of 6 km. Other temperature indicators, such as quartz that appears to approach the ductile threshold (possible subgrain partitioning indicative of plastic recovery) in one breccia from 554 m, support the deep (or, at least, hot) environment associated with the development of these deformation zones. It is not clear how over 5 km of uplift and erosion would fit into the tectonic development of the San Andreas fault. An alternative source of these high temperatures could be coseismic upwelling of fluids originating at depth, frictional heating during faulting, or, an ancient geothermal event unrelated to the general framework of the San Andreas fault. Further work is needed to explore these possibilities.

5. Large deviations in $\delta^{18}O$ have been observed in seven preliminary whole-rock analyses. Significant ^{18}O depletion has occurred in some shallow rocks, and there is a hint of enrichment in a deeper sample (Table 1). Eight additional whole-rock analyses are currently being done. Such isotopic effects are most easily produced by circulation of fluids and probably reflect a complex history of fluids flowing through these rocks. Future isotopic studies will use a step-temperature furnace to control dehydration of phyllosilicates so that we can discriminate between water present at different stages in the development of fault gouge.

6. Analysis of the driller's notes, temperature gradient measurements, electrical logs and water levels in the Stone Canyon well show that the fluid pressure at the bottom on the well is about 4 bars above hydrostatic, and that several fractures intercepted during drilling contained fluids with pressures at least 10% above hydrostatic. Some mechanism, probably the cross-over of the least and intermediate principal stress directions, isolates the pressurized brine found at depth from the ground water.

Reports:

Stierman, Donald J., The relevance of measurements in deep boreholes to earthquakes prediction research (abstract); 1984 Fall Meeting, American Geophysical Union.

Marryott, Robert A., A. E. Williams and D. J. Stierman, Petrologic and geochemical studies of granitic rocks of the San Andreas fault: Stone Canyon (abstract); 1984 Fall Meeting, American Geophysical Union.

Stierman, Donald J. and A. E. Williams, Hydrologic and geochemical properties of the San Andreas faults at the Stone Canyon well; in press, *Pure & Applied Geophysics*, Special issue on the Hydrology and Chemistry of Earthquakes.

Stierman, Donald J., Geophysical and geological evidence for fracturing, water circulation and chemical alteration in granitic rocks adjacent to major strike-slip faults; *J. Geohpys. Res.*, *89*:5849-5857, 1984.

Stierman, Donald J. and A. E. Williams, Cover photo, *EOS*, July 24, 1984.

TABLE 1

OXYGEN ISOTOPIC ANALYSES OF WHOLE-ROCK SAMPLES FROM THE STONE CANYON WELL

Depth (m)	$\delta^{18}O$ (SMOW)
75	10.1%
102	10.9%
135	5.2%
158	7.1%
361	10.9%
552	10.2%
579	12.0%

FIGURE 1

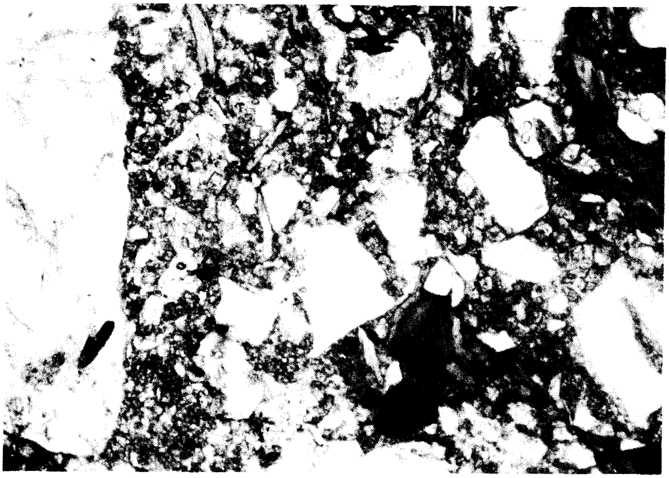

A. Microbreccia from approximately 1900' depth in the Stone Canyon Well. Angular clasts of quartz, feldspar and biotite from the granitic parent rock are cemented by a granular carbonate matrix. Field of view is approximately 1.8 mm.

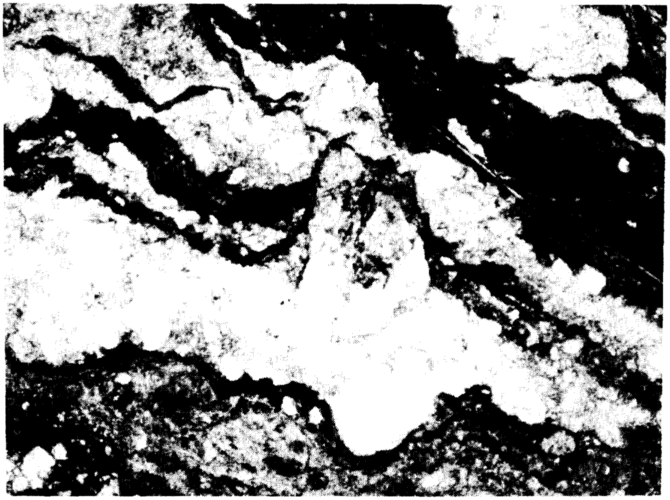

B. Shear induced segregations of medium to very fine grained biotite, chlorite and other phyllosilicates (dark bands) enclose pods of microbreccia composed of granitic material. Field of view is approximately 1.8 mm.

Earthquake Forecast Models

9960-03419

William D. Stuart
Branch of Tectonophysics
U.S. Geological Survey
Pasadena, California 91106
(818) 356-6883

Investigations

Research has concentrated on refining an earthquake instability model for large and great earthquakes on the San Andreas fault in southern California. The goal is to use model simulations and geodetic data to estimate locations, sizes, and times of future earthquakes. The assumption is that a model will be valid in the near future if it explains ground deformation and fault slip measurements associated with earthquakes in the past.

Results

The current model represents the San Andreas, Imperial, Cerro Prieto, and San Jacinto faults by flat vertical planes in an elastic half space. The fault is divided into 414 rectangular cells, each of uniform slip. In most of the cells, slip and stress are computed results and vary with position and time. In the remaining cells, which occupy steadily creeping areas, fault slip rate is imposed to approximate growing regional stress.

The main free parameter in the problem is the variation of brittle fault strength along strike. The fault is assumed to be brittle from the ground surface to about 12 km depth between Parkfield and the Salton Sea. Elsewhere, the fault slides freely or at a fixed rate. The strength of the brittle zone has been adjusted by trial until slips and times of instabilities (the earthquake analogs) agree with measured fault offsets since 1080 reported by Sieh and others. The brittle zone is found to be made of five contiguous sections of alternately low and high strength. The sections are : 1 - Parkfield to Bitterwater Valley, 2 - Bitterwater Valley to Lake Hughes, 3 - Lake Hughes to San Bernardino, 4 - San Bernardino to Palm Springs, and 5 - Palm Springs to the Salton Sea. Sections 1, 3, and 5 have low strength, and sections 2 and 4 have high strength.

The next future instability in the model occurs on section 5 within a decade or two. This result depends on several assumptions, the most important of which is that event X of Sieh and Jahns (G. S. A. Bull., 1984) extended from Lake Hughes to the Salton Sea.

Reports

Stuart, W. D., Earthquake instability model for southern California (abs.), 21st Annual Meeting of the Society of Engineering Science, 1984.

Stuart, W. D., Instability model for great earthquakes in southern California (abs.), EOS Trans. Am. Geophys. Un., 65, 284, 1984.

Stuart, W. D., R. J. Archuleta, and A. G. Lindh, Forecast model for moderate earthquakes near Parkfield, California, J. Geophys. Res., 1984, in press.

EXPERIMENTS OF ROCK FRICTION CONSTITUTIVE LAWS APPLIED TO EARTHQUAKE INSTABILITY ANALYSIS

USGS Contract 14-08-0001-6-821

Terry E. Tullis
John D. Weeks
Department of Geological Sciences
Brown University
Providence, Rhode Island 02912
(401) 863-3829

Investigations

1. We have investigated experimentally the dependence of friction of dolomite marble on velocity at normal stress of 75 MPa on samples having variable water content. We are attempting to relate the results of these experiments to stability of sliding of dolomite.

2. We are continuing our theoretical investigation of the stability of sliding of granite based on the theories developed by Gu, et al.(1984), and expanding the investigation to the case of two state variables which is required to completely describe our results on friction of granite.

3. We have continued our microscopic examination of fault gouge generated in these experiments in an attempt to determine the physical processes responsible for the observed frictional characteristics. We have been using optical interferometry to profile frictional sliding surfaces in order to investigate geometrical factors that may be involved.

Results

1. We have investigated the velocity dependence of the friction of dolomite marble over a velocity range covering 6 orders of magnitude: from .003 to 3000 microns per second. The experiments have been done at 75 MPa normal stress in a rotary shear configuration, with varying water content and zero pore pressure. The coefficient of friction ranges from .08 to .58 as shown in Figure 1, with the lowest curve representing the wettest sample and the next two being successively drier. The water content for the top curve is unknown, but because of its position on the figure, it is presumed to be the driest. These data do not follow a linear dependence of coefficient of friction on log velocity, but have a minimum point whose position shifts to higher velocity with increasing water content. The double curves for the lower three show nearly reversible response to increasing and decreasing velocity. According to theory, this velocity response implies that sliding will be less stable at low velocities than at high and that stability is reduced for higher water content in agreement with our observations. Similar changes of the slope of the friction-velocity curve have been reported for other rock types and could have important implications for stability of fault motion.

2. A numerical study of the stability of a spring and slider block system in which the frictional response of the sliding surface is described by two state variables, shows that the behavior can be represented on a three dimensional plot with axes of frictional resistance μ, log sliding velocity V, and the more slowly evolving state variable ψ_2. On this plot (Figure 2) a stability surface separates a region of stability below from a region of instability above. Steady state behavior is represented by the heavier diagonal line whereas constant state changes are represented by the lighter line in the $\psi_2 = 0$ plane. In contrast, a one state variable system requires only a two dimensional plot, and the stability boundary is a curve. Much more is known about one state

variable systems because it is more tractable mathematically than systems of two state variables. The surface illustrated uses the stiffness of our rotary shear apparatus and the constitutive parameters found experimentally to describe the behavior of granite. The predicted stability behavior matches experimental behavior: a 2x jump in load point velocity V* falls below the surface and was stable while a 3x jump falls above the surface and was unstable, agreement which is encouraging for earthquake prediction. Stability surfaces with shapes different from the one shown are produced by other combinations of stiffness and constitutive parameters.

3. In order to aid in scaling laboratory experimental results on friction to sliding on natural faults we have been trying to determine what determines the magnitude of the constitutive parameter L, which has dimensions of length and must therefore be scaled by some physical length of the sample or sliding surface or gouge layer. Our present investigation is into the possibility that some aspect of the surface roughness of the sliding surface determines L. Study of the topography of slickensided slip surfaces within the gouge generated on a dolomite sample has been done with optical interferometry using reflected light on a gold-coated surface. The interference fringes are photographed and digitized and the roughness is analyzed as a function of wavelength. The accompanying preliminary plot, Figure 3, shows that at long wavelengths the surface is smoother than would be predicted from study of its roughness at short wavelengths. At wavelengths shorter than 500 microns the slope is -2, indicating that the surface is geometrically self-similar. The topothesy, a number describing the roughness of a self-similar surface is 0.009 micron, indicating a very smooth surface. Although we need to extend our measurements to longer wavelengths, it appears that the surface has a corner wavelength and that it is even smoother at wavelengths longer than 500 microns. This suggests that autocorrelation distance for this surface is of the same order of magnitude as the corner wavelength and that this distance may be in some way related to the magnitude of the decay distance L for the constitutive law for sliding on this surface. The value of L for this dolomite sliding surface seems to depend on velocity of sliding, so that it is premature to draw any definite conclusions about the relation between the constitutive law and the surface topography.

Reference

Gu, J. C., Rice, J. R., Ruina, A. L., and Tse., S., Stability of frictional slip for a single degree of freedom elastic system with non-linear rate and state dependent friction, manuscript in preparation, 1984.

Reports

Weeks, John and Terry Tullis, Frictional behavior of dolomite, *Eos Trans. AGU, 65.*

Blanpied, Michael, Terry Tullis, and John Weeks, Stability and behavior of frictional sliding with a two state variable constitutive law, *Eos Trans. AGU, 65.*

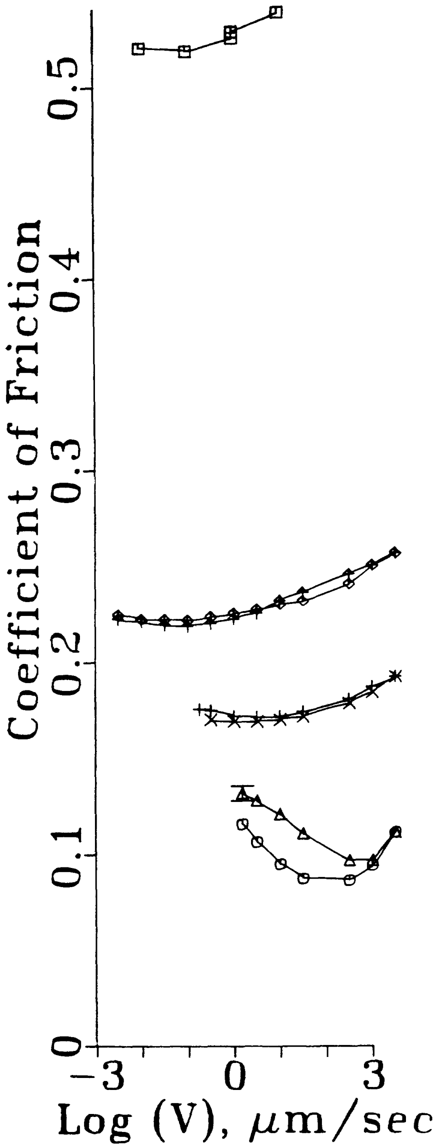

Figure 1. Results of velocity stepping experiments on dolomite. Each point represents steady state at the given velocity. The double curves illustrate the response for increasing and decreasing velocity. Three points should be noted: The coefficient of friction for the lowest three curves are extremely low; the lowest curve represents the wettest sample with the next two being successively drier; the minimum point shifts to higher velocity with increasing water content.

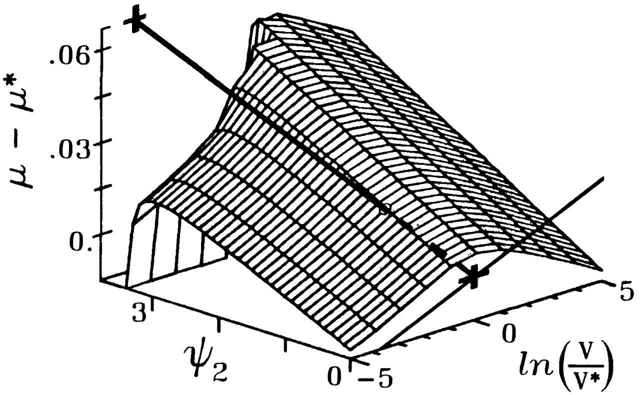

Figure 2. Stability for a frictional system described by a law having two state variables. The parameters of the frictional law were chosen to match those determined in our experiments on granite. Every point represents a possible condition of the sliding surface; those above the stability surface will evolve to instability whereas those below the surface will evolve to steady state represented by the cross. Conditions at steady state are represented by the heavy line, and the lighter line shows the result of sudden changes in stress.

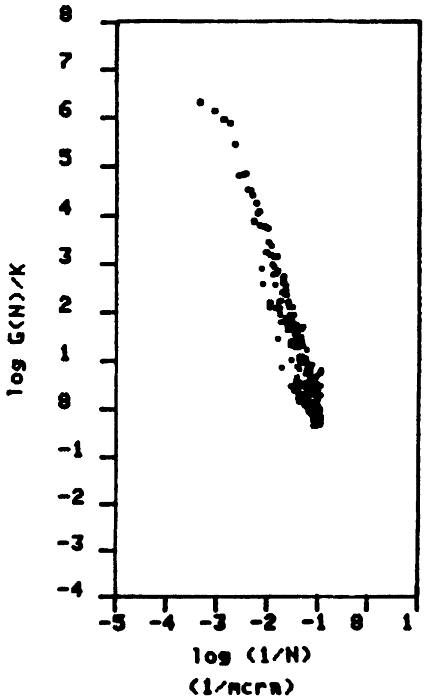

Figure 3. Normalized power spectrum of the surface of one of our dolomite samples. G(N) is the power spectral density, N is the wavelength, and K is the topothesy number, a measure of the smoothness of the sample. K is equal to 0.009. Below a wavelength of 500 microns, the slope is -2, indicating a self-similar topography. At longer wavelengths greater than 500 microns, the slope is -0.6, indicating a much smoother surface at longer wavelengths.

New Model of Earthquake Faulting

Contract No. 14-08-0001-21803

Joseph B. Walsh
Dept. of Earth, Atmospheric and Planetary Sciences
Victor C. Li
Dept. of Civil Engineering

Massachusetts Institute of Technology
Cambridge, Massachusetts 02139
617-253-5731

Investigations

We have been studying a model for faulting in which an earthquake is triggered by aseismic slip on a 'detachment zone' at the interface between the lithosphere and the underlying viscous strata. The detachment zone is a consequence of spatially and temporally non-uniform viscous forces as the lithosphere is dragged over the aesthenosphere. Slip on the detachment zone loads a fault in the elastic lithosphere, and, if frictional resistance on the fault is sufficiently low, an earthquake ensues.

Our studies so far have been directed toward calculating surface displacements, strains, and gravity changes associated with slip on the detachment zone. A graduate student, Steven C. Ho, developed a computer program which allowed him to find these parameters quickly for arbitrary dislocation distributions over the detachment zone, and he applied his results to uplift and strain data for the Palmdale (Cal.) region during an episode (1959-1977) of aseismic tectonic deformation. Preliminary results of the analysis were presented at the Fall Meeting of the AGU and at an informal meeting with R.O. Castle, J.C. Savage, and William Stuart at the U.S.G.S. Office of Earthquake Studies in Menlo Park, Cal.

Results

Ho found acceptable correlation between observed and calculated values of uplift and strain for his model. One difficulty with this tentative model is that the average slip rate over the detachment zone is about an order of magnitude larger than the estimated relative tectonic movement for this region. We examined two modifications of the model in an exploratory way: in one, the detachment zone is tilted 5° rather than horizontal, and in the other, slip on a vertical at depth plane is allowed, simulating aseismic creep on the San Andreas, the upper portion remaining fixed. Both modifications reduce the average slip required for agreement with observed values without changing the overall pattern.

Present Status

The principal investigators have completed a rough draft of a manuscript which summarizes the results of this research. We will complete this manuscript under the continuation contract and submit it for publication in the open literature.

Reports

Ho, S.C., V.C. Li, and J.B. Walsh, Surface deformation associated with aseismic slippages on detachment surfaces, EOS, Trans. Am. Geophys. Union, 64(45), 1983.

Ho, S.C., V.C. Li, and J.B. Walsh, Surface deformation associated with aseismic slippages on detachment surfaces, Research rept. R84-03, order no. 763, M.I.T. Department of Civil Eng., Feb. 1984.

Ho, S.C., Surface deformation associated with aseismic slippages on detachment surfaces, M.Sc. Thesis, M.I.T. Dept. Civil Eng., Cambridge Mass., Feb. 1984.

Aftershock Investigations and Geotechnical Studies

9910-02089

Richard E. Warrick
Eugene D. Sembera

Branch of Engineering Seismology and Geology
345 Middlefield Road, MS 977
Menlo Park, CA 94025
(415) 323-8111, ext. 2757

Investigations

1. The development of techniques for the improvement of field data acquisition, specifically in the application of triggered digital recording systems to aftershock studies.
2. Improvement in the methods used in generating recording, and interpreting shear waves in downhole surveys.

Results

1a. Field testing of the GEOS systems continue with these deployments:

Morgan Hill earthquake aftershocks, April - June (J. Fletcher, G. Sembera, C. Dietel, L. Beem).

Dam response studies (H.-P. Liu, G. Sembera, L. Beem).

Parkfield Array test (P. Spudich, G. Sembera, L. Beem).

Dilatometer tests (R. Borcherdt, M. Johnston, J. Sena, G. Sembera, L. Beem, C. Dietel, and G. Jensen).

High frequency experiment New England and eastern Canada (J. Boatwright, E. Cranswick, G. Sembera, C. Dietel, and T. MacDonald).

The DR-100 recorders were used in the New England and Dam Response projects and in New Mexico (K. King, G. Sembera).

1b. The maintenance facility for the GEOS systems was set up by J. Sena, who together with G. Jensen, R. McClearn, C. Dietel, G. Maxwell, and C. Criley are cooperatively proceeding with the building of new systems and the debugging of existing units.

1c. The instrumentation for the McGee Creek downhole experiment is being constructed and tested (R. Archuleta, E. Etheredge, M. Salsman, R. Forshee).

1d. Detailed lab tests to determine the characteristics of the GEOS systems was performed (G. Jensen).

2a. Plans for a power driven shear wave generator with H.-P. Liu and an improved sensor locking device were developed.

Reports

None.

PERMEABILITY OF FAULT ZONES

9960-02733

James Byerlee
Branch of Tectonophysics
U.S. Geological Survey
345 Middlefield Road, MS/77
Menlo Park, California 94025
(415) 323-8111, ext. 2453

Investigations

Laboratory studies of the permeability of fault gouges were carried out to provide information that will assist us in evaluating whether in a given region, fluid can migrate to a sufficient depth during the life-time of a reservoir to trigger a large destructive earthquake.

Results

The permeability of Westerly Granite was measured under cyclic loading for confining pressures, P_c, up to 96 MPa and pore pressures, P_p, to 86 MPa. This enabled us to test several aspects of the cubic root law for fractures relating permeability, k, to effective pressure P_e, $k^{1/3} = A + B \ln P_e$. A and B of this equation depend on geometric parameters of the cracks and $P_e = P_c - \alpha P_p$. The permeability of intact samples of Westerly Granite followed the cubic samples of Westerly Granite followed the cubic root law during each stress cycle. $\alpha = 1$ under all conditions of pressure and loading history. Permeability decreased significantly after each cycle. These reductions were recoverable with time due to stress relaxation in the sample.

Reports

C. A. Morrow, D. Moore, J. Byerlee, 1984, Permeability and pore fluid chemistry of the Topopah Spring member of the Paintbrush Tuff, Nevada Test Site, in a temperature gradient - Application to nuclear waste storage , Mat. Res. Soc. Symp. Proc., vol. 26, p. 883-890.

D. Moore, C. Morrow, J. Byerlee, 1984, Changes in permeability and fluid chemistry of the Topopah Spring member of the Paintbrush Tuff (Nevada Test Site) when held in a temperature gradient: Summary of Results, Open-File Report 84-273, p. 33.

DEVELOPMENT OF WIRELINE HYDROFRACTURING AND ITS USE AT THE MONTICELLO RESERVOIR SITE OF INDUCED SEISMICITY

14-08-0001-20537

Bezalel C. Haimson
University of Wisconsin, Madison
1509 University Ave.
Madison, Wisconsin 53706
(608) 262-2563

Investigations

1. Design and fabrication of a new hydrofracturing technique for in situ stress measurements using a 7-conductor wireline, geophysical logging truck and wellhead tripod.

2. Reenter testhole Mont-2, 1.1 km deep hole near the Monticello Reservoir, South Carolina, and utilize the new hydrofracturing technique to measure the in situ stresses. Attempt to correlate results to local induced seismicity.

Results

We have developed a new hydrofracturing field technique which renders the measurement of stress in deep holes significantly faster and less expensive. The major improvement is the conversion of hydrofracturing from a drillrod to a wireline method using separate flexible hydraulic lines for the packers and for the test interval. The newly designed fracturing tool can be moved from one depth to the next and reused indefinitely without retrieval to the surface. It accommodates downhole pressure transmitters and allows the attachment of other logging probes. The downhole electronic instrumentation is connected to surface power supplies and recorders through the 7 conductors in the wireline. The previously required drilling rig has been replaced by an easy-to-assemble wellhead tripod, and a hoist located in a geophysical logging truck. Hydrofracture delineation and orientation are determined by a wireline impression packer and orienting tool, or by a borehole televiewer. Figures 1 and 2 show schematically the new wireline hydrofracturing system.

We have employed the new system to carry out stress measurements in a 1.1 km hole near the Monticello Reservoir, South Carolina. The objectives of our tests were: (1) to evaluate the suitability of our newly designed wireline hydrofracturing system for conducting stress measurements in deep holes, and (2) to obtain principal stress magnitudes and directions at different depths in the hole and relate them to the local seismicity which was apparently induced by the reservoir impoundment. The wireline method of testing performed flawlessly, but proved to be considerably more sensitive than the drill-rod method to minor irregularities along the borehole wall.

The tests conducted in Mont-2 corresponded well with previous measurements (Zoback and Hickman, 1982). They reinforced the suggestion that shallow (100-200m) high horizontal stresses could have induced reverse faulting along existing fractures, thus triggering low magnitude earthquakes. In the 200-400m range stress relaxation, related to the local intense fracturing, appears to have occured (Fig. 3). Information on borehole breakouts, high hydrofracturing pressures and abundance of earthquake hypocenteres in the 500-1000m depth range suggests that the stress regime in the lower half of Mont-2 is again closely related to the induced seismicity. Additional stress measurements in that range should supply important information on stress-fault motion relationship.

Publications

1. Haimson, B. C. and M. Y. Lee, Additional stress measurement near the Monticello Reservoir, S. Carolina using wireline hydrofracturing, EOS, Trans. Am. Geophys. Un., 64, p. 856, 1983.

2. Haimson, B. C. and M. D. Zoback, A new look at the hydrofracturing stress measurements near the Monticello Reservoir, S. Carolina, EOS, Trans. Am. Geophys. Un., 65, p. 278, 1983.

3. Haimson, B. C. and M. Y. Lee, Development of a wireline hydrofracturing technique and its use at a site of induced seismicity, Proceedings of the 25th U.S. Rock Mechanics Symposium, Soc. Mining Engineers, New York, NY, p. 194-203, 1984.

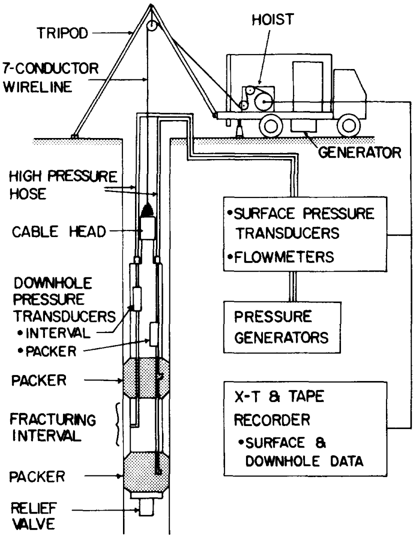

Fig. 1 - Schematic set-up of wireline hydrofracturing straddle packer system.

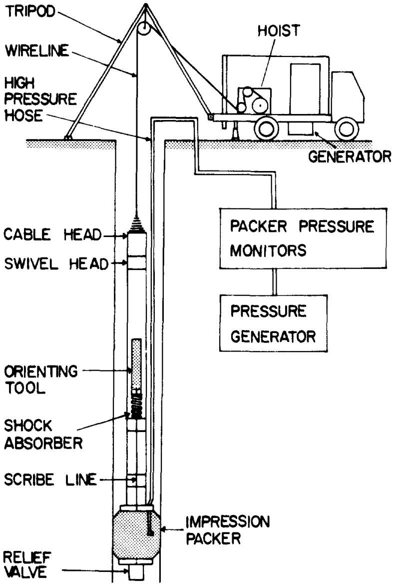

Fig. 2 - Schematic set-up of wireline impression - orienting tool systems.

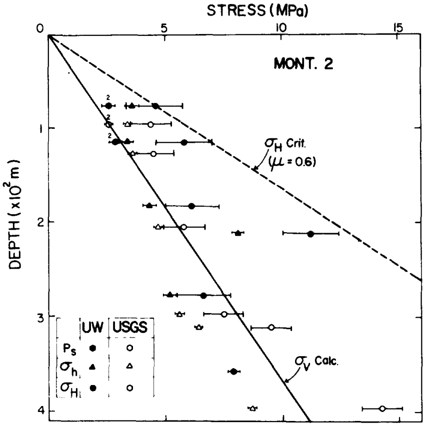

Fig. 3 - Hydrofracturing stresses near the Monticello Reservoir compared with the critical largest horizontal stress necessary for reverse faulting (using a minimum μ of 0.6). The second shut-in pressures in the top three tests (marked as 2) probably represent the magnitude of the vertical stress (solid line stands for the calculated vertical stress based on rock density). UW - University of Wisconsin measurements; USGS - Zoback and Hickman (1982) measurements.

Seismic Monitoring of the Richard B. Russell Dam Impoundment

14-08-0001-21241

Leland Timothy Long
School of Geophysical Sciences
Georgia Institute of Technology
Atlanta, Georgia 30332
(404) 894-2860

During the first six months of impoundment with water depths up to 30 meters, the Richard B. Russell Reservoir failed to induce observable seismicity. A lack of activity was unexpected since many neighboring reservoirs have exhibited reservoir induced seismicity. At this time, the reason for a lack of reservoir induced seismicity is unknown. However, the lack of seismicity could be explained by a delayed onset of seismicity, much like the delay in occurrence of larger events at the adjacent Clarks Hill Reservoir. Also, the geologic terrain and condition of ambient stress in the Richard B. Russell reservoir may differ substantially from adjacent areas.

Objective: The proposed work on this project had two objectives. The first was to assist in monitoring induced seismicity at the Richard B. Russell reservoir and thus permit a direct comparison with patterns of induced seismicity elsewhere. The observed patterns could also permit direct comparison with the surface geology. The second objective was to use high-frequency seismic recording systems to obtain detailed near-source data which would permit precision location of shallow reservoir induced earthquakes. The precision anticipated would be sufficient to document the progression of seismic activity as a function of depth and time. Hence, it was hoped that the detailed microseismicity would allow tracing of fluid movement to depth, and documentation of the growth in areal extent and magnitude of earthquakes in active zones.

Results: The monitoring of the Richard B. Russell area was achieved through a permanent four-station net. Three of these stations were converted to RF telemetry, and the fourth is located at the central RF receiving site. The mixed signals are transmitted via telephone to Georgia Tech for recording. The four-station net in the Richard B. Russell Reservoir area is augmented by three stations in the Clarks Hill Reservoir area.

The seismic monitoring net has allowed a complete documentation and location of all active quarries and most road construction sites requiring blasting. Travel times from the quarries indicate a P-wave velocity of 6.05 km/s (see Figure 1) measured in a northwest direction. Similarly, a P-wave velocity of 6.05 km/s was obtained from refraction data striking northeast. The velocity measurements in orthogonal directions show no evidence for anisotropy in the shallow crust.

The seismic net has detected no natural or induced activity in the area of the Richard B. Russell Reservoir (as of September 1984). Some

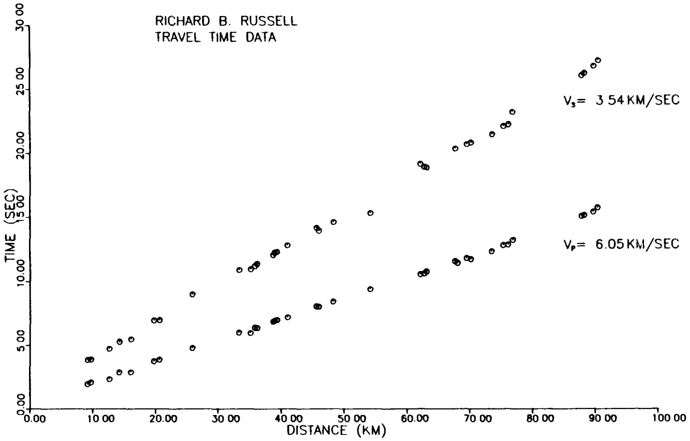

Figure 1. Travel times from blasts in the vicinity of the Richard B. Russell reservoir.

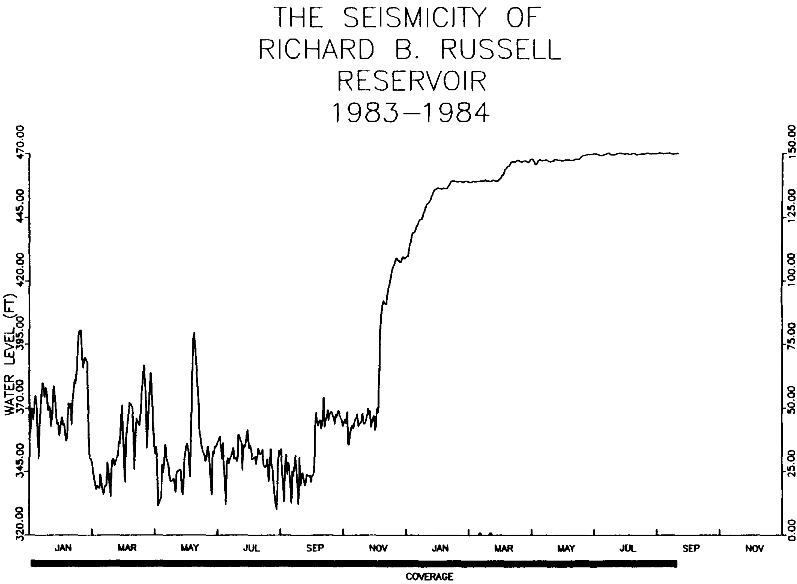

Figure 2. Water level history of filling of the Richard B. Russell Reservoir. Activity (none) and station coverage shown at bottom of the figure.

activity has continued in the McCormick area of the Clarks Hill Reservoir, but this area is outside the hydrologic influence of the Richard B. Russell reservoir. Figure 2 shows the water level versus time and the record of (non)activity.

Two explanations are offered for the present lack of seismicity. First, induced seismicity in this area may take longer to develop and the seismic data are documenting a delay in activity. The delay may relate to the rapid filling, which was accompanied by a disturbance of the soil and perhaps a sealing of joints and fractures by suspended clay. Thus, the downward penetration of water is limited or delayed. The time of year and perhaps water temperature may also contribute to effective permeability. Second, the geologic formations under the southern half of the Richard B. Russell Reservoir differ in average composition from formations under neighboring reservoirs. Much of the Richard B. Russell Reservoir below the Middleton-Lowndesville fault is underlain by mafic rocks which may be described as a melange. In contrast, the Clarks Hill Reservoir area is underlain by a mix of mafic volcanics and granitic intrusives. The stress release characteristics and permeability of these two types of units may differ, and this difference may be reflected in the existence of induced seismicity.

ARRAY STUDIES OF SEISMICITY

9930-02106

David H. Oppenheimer
Branch of Seismology
United States Geological Survey
345 Middlefield Road - MS 977
Menlo Park, CA 94025
(415) 323-8111, Ext 2791

Investigations

1. Invert microearthquake traveltime data collected at The Geysers geothermal field for 3-D velocity structure.
2. Relocate seismicity at The Geysers on weekly basis for new evidence of induced seismicity.
3. Analyze aftershock distribution of May 2, 1983 Coalinga earthquake.
4. Analyze teleseismic traveltime data recorded by CALNET for 3-D structure of the mantle.
5. Investigate frequency-wavenumber spectra of near-field strong motion array data to detect position of rupture front.

Results

1. A combined set of microearthquake and refraction traveltime data recorded on temporary and permanent seismic stations is used to model 3-D velocity variations in The Geysers-Clear Lake area. The analysis indicates low velocities along the Healdsburg-Rodgers Creek-Maacama fault system, and higher velocities between the Maacama and Bartlett Springs/Green Valley faults. A region of surficial low-velocity near Konocti Bay may be associated with either Clear Lake volcanics or Cache formation. No velocity anomaly is observed associated with The Geysers geothermal steam reservoir. A manuscript describing this work is currently in preparation.

2. Microearthquake activity continues to be induced adjacent to steam production and fluid injection wells at The Geysers. Subsequent to our previously published report on induced seismicity, six geothermal power plants have gone on-line. As of 1983, seismicity has been induced adjacent to units NCPA 2 and Unit 17, which both became operational 12/82. During the first six months of 1984, there is some indication of increased seismicity near SMUD 1 (12/83), but no seismicity above M=1.2 near units DWR (5/83), 18 (5/83), and Occidental 1 (5/84). We expect to observe seismicity induced at these latter units within a year, following trends documented in older regions of the steam field.

3. Coalinga earthquake traveltimes obtained from the permanent seismic network were augmented with data recorded by temporary 5-day analogue recorders during the May 2, 1983 aftershock sequence to derive station corrections and an improved velocity model by a joint hypocenter-velocity

inversion. The station corrections correlate well with the known geologic structure of Anticline Ridge. The velocity model was used to relocate over 2600 earthquakes for which automated fault plane solutions were calculated. The distribition of aftershock hypocenters and a select group of nodal planes appear to define three primary planes, dipping 70-80 degrees NE, 45-55 degrees SW, and 5-10 degrees SW. The two steeply dipping planes define a horst structure, and this complex model of rupture is consistent with modeling of both geodetic data and teleseismic body waves.

4. Programs to invert over 12,000 traveltimes from 65 teleseisms recorded by over 300 stations of the central California seismic network for 3-D velocity perturbations in the crust and mantle were modified to accomodate the large data set, correct the data for the crustal traveltime based upon a model for crustal thickening derived from Pn data, and incorporate both reading and ray-geometry weights. Preliminary inversion results show that mantle velocities at depths of 35-75 km are relatively high off-shore and beneath the Sierra Nevada. A similar pattern persists throughout the LVZ (Burdick and Helmburger, 1978) at depths of 75-150 km. At 150-225 km high velocity bodies are found beneath the southern and northern Sierra Nevada, and persisting to 300 km with lower amplitude. At 300-400 km no appreciable velocity perturbations are detected.

5. In a hypothetical test, synthetic ground velocity seismograms from an irregularly expanding rupture on a horizontal fault were calculated for a 21 element array. Frequency-wavenumber (f-k) spectra for sequential time windows were converted to the frequency-slowness (f-s) domain and projected back onto the fault plane via ray-tracing to yield an image of power radiated from the rupturing fault as a function of time. The expanding rupture can be seen in the sequence of f-s images. Testing of various array geometries shows that certain classes of arrays have unsuitable beam patterns which strongly contaminate the f-k spectra.

Reports

Spudich, P., and D. H. Oppenheimer, 1984, Imaging earthquake rupture by using dense accelerometer arrays, EOS, Trans. Am. Geophys. Union, in press.

Eberhart-Phillips, D., and P. Reasenberg, 1984, Hypocenter locations and fault-plane solutions for Coalinga aftershocks, May 2-24, 1983; evidence for a complex rupture geometry, in Mechanics of the May 2, 1983 Coalinga, Ca. earthquake, U.S. Geol. Surv. Open-File Report 84- .

Reasenberg, P., D. Eberhart-Phillips, and P. Segall, 1983, Preliminary views of the aftershock distribution in the Coalinga earthquake sequence commencing May 2, 1983, U.S. Geol. Surv. Open-File Rep. 83-511.

Mechanics of Faulting and Fracturing

9960-02112

Paul Segall
Branch of Tectonophysics
U.S. Geological Survey
345 Middlefield Road, MS/977
Menlo Park, California 94025

Investigations

1. Investigation of induced seismicity resulting from subsurface fluid extraction.
2. Analysis of the effect of free surface topography on vertical displacements from dip slip faults (with D. McTigue, Sandia).
3. Field and laboratory study of ductile shear zone formation in granitic rocks (with C. Simpson, V.P.I.)

Results

1. It is recognized that the extraction of fluids from the earth's crust may induce faulting and shallow seismicity. Extraction induced seismicity is usually associated with subsidence, and radially (inward) directed horizontal displacements. These displacements give rise to large horizontal contractions at the point of maximum subsidence and smaller extensions at the flanks of the subsiding region. A method for determining the stress and deformation associated with fluid extraction has been developed. The analysis assumes an elastically homogeneous fluid-infiltrated, poro-elastic half-space. Solutions are found by solving for the distribution of fluid mass, which in the coupled deformation-diffusion theory satisfies the homogeneous diffusion equation. The Biot constitutive equations for poro-elastic media relate alterations in fluid mass content at a point to the volumetric strain at that point. Thus, the stresses, strains, and displacements resulting from extraction can be represented by distributed centers of dilatation with strength proportional to the change in fluid mass. Calculated surface displacements and strains for the case of a single permeable layer embedded in an impermeable matrix agree quite well with observed profiles. The method predicts subsidence, inward directed horizontal displacements, a central zone of compression, and extension on the flanks of the subsiding region. The extraction induced stresses can be resolved into normal and shear components acting on potential fault planes to determine whether withdrawal enhances or inhibits

frictional slip. In general, extraction favors shallow thrust faulting in the central zone of contraction, and shallow normal faulting in the flanking zones of extension.

This approach has been used to assess the possibility that the 1983 Coalinga earthquake was induced by fluid extraction from overlying oil fields. The modeled extraction-induced stresses are found to be small (<0.5 bar) at hypocentral depths. Whether or not the induced shear stresses exceed the frictional resistance depends strongly on the dip of the fault plane, which is currently unresolved. The calculations have been tested by comparing predicted vertical displacements with results from repeated leveling surveys. The predicted average subsidence rate of 3 mm/yr is in excellent agreement with the measured displacement of three benchmarks within the oil field, which subsided at a rate of 3.3 ± 0.7 mm/yr prior to the 1983 earthquake. The theory is general and can be applied to other regions of extraction-induced deformation and seismicity.

2. Most models of fault deformation assume that the fault is embedded within an elastic half-space with a flat free surface. However, dimensional arguments indicate that topography can, in some cases, significantly influence the vertical displacement field. The first order correction to the displacement field is found using a perturbation scheme. The analysis assumes a two-dimensional dip-slip dislocation surface embedded within an elastic half-space with arbitrary free surface topography $h(x)$. The topography has characteristic height H and wavelength L. The displacements are expanded in powers of the characteristic slope H/L, where $H/L \ll 1$. The zero order solution is simply the solution to a dislocation beneath a flat free surface. The leading order correction (proportional to H/L) is the solution to the problem of a flat half-space with a distributed shear traction. We have found an exact solution for a single dislocation buried at depth D beneath an idealized fault scarp for the special case $L=D$. For a buried 60° dipping normal fault, the topographic correction reduces the uplift on the upthrown block and slightly increases the subsidence on the downthrown block. A straightforward numerical integration provides accurate solutions for general topographies. For a normal fault bounding a 1 km high range and a 10 km wide basin and breaking the ground surface, the topographic correction increases the uplift of the range approximately 10-20% over that predicted for a flat half-space. If the basin fill is elastically uncoupled, the surface deformation on the downthrown side of the fault is decreased by a like amount.

3. Small shear zones in granitic rock near Bear Creek, Sierra Nevada, CA, and Roses, NE Spain, display features which indicate that fracturing was an important process in the nucleation and propagation of these zones, many of which exhibit ductile textures and microstructures. Shear zones in the Bear Creek area range from "crack-like" faults to narrow mylonite zones. Field and petrographic evidence suggest that in all of these features, deformation was localized on earlier-formed, mineralized, dilatant fractures. Deformation within the zones, and in some cases within the adjacent granite, is accommodated in an apparently ductile fashion. This ductile deformation was accompanied by dilatant fractures that propagated into the two dilatational quadrants at the ends of the zones, consistent with their mode I character.

   Shear zones near Roses exhibit significant geometric and microstructural similarities to the Sierran zones. The terminations of apparently ductile shear zones are marked by splays which narrow to thin, apparently brittle cracks at their distal ends. However, unlike the Sierran examples, these splays branch symmetrically with respect to the main shear zones. Microstructural evidence for fracturing prior to ductile deformation in the Roses shear zones includes the presence of through-going, healed, dilatant microcracks in the feldspar and quartz adjacent to, and parallel to, the shear zone boundaries. In some cases quartz fillings within the microcracks show dynamic recrystallization textures which indicate ductile deformation post-dated the microcracking. The observation that several zones, within which all minerals appear ductilely deformed, have knife-sharp boundaries with relatively undeformed wall rocks support this interpretation. We suggest that fractures locally enhance the ductility of the granite by increasing local fluid fluxes, thereby promoting chemical alteration and/or hydrolitic weakening.

Reports

Segall, P., 1984, Rate-dependent extensional deformation resulting from crack growth in rock, Jour. Geophys. Res., v. 89, p. 4185-4195.

Segall, P., Stress and subsidence resulting from subsurface fluid withdrawal in the epicentral region of the 1983 Coalinga earthquake, submitted to Jour. Geophys. Res.

Segall, P. and R. F. Yerkes, Stress and fluid pressure changes associated with oil field operations: A critical assessment of effects in the focal region of the 1983 Coalinga earthquake, U.S.G.S. Prof. Paper on the Coalinga Earthquake, in press.

Induced Seismicity at Toktogul, Nurek and Aswan Reservoirs: Seismicity, Geology and Tectonics

14-08-0001-21869

David W. Simpson and William Leith
Lamont-Doherty Geological Observatory of Columbia University
Palisades, New York 10964
(914) 359-2900

Background

Our work is part of a continuing program of studies of induced seismicity at two large reservoirs in Soviet Central Asia, which began in 1975. In 1982, studies of induced seismicity at Aswan reservoir were added to the scope of work, following a magnitude 5 1/2 earthquake at Aswan in November 1981. In previous years, the work in Central Asia was concentrated at Nurek reservoir where, based on Soviet data and the results of our joint studies, there is an extremely well-documented case of induced seismicity. Since 1978, when the water level at Nurek approached its final depth of 300 m, the level of seismicity has decreased. While the Soviets continue to operate the network, we have turned to an integration of geological and seismological data, including broad-scale studied of the regional structural and seismological settings of these reservoirs within the tectonic framework of Central Asia, and to a comparison of our earlier results with the new data from Aswan.

Investigations

1. Nurek and Toktogul Regional Tectonics - Our work was directed at documenting the structure of the Vakhsh fold-and-thrust belt, within which Nurek reservoir sits, and at relating the seismicity of the belt to the shallow crustal structure. Working with the image-processing facility at the Environmental Research Institute of Michigan, a digitally enhanced Landsat image of the area around Nurek reservoir was constructed at a scale of 1:250,000. This image was then used as a base map for the compilation of structural and mapping data from previous years' studies. Upon completion of the mapping (see Leith and Alvarez, in prep.), work turned toward a detailed analysis of the seismicity of the same region. Using the Soviet earthquake catalogs for events from 1962-1980, the seismicity of the fold-and-thrust belt and adjacent authochthon were contrasted (Leith and Simpson, in prep.)

2. Central Asian Seismicity - Soviet catalogs for earthquakes in Central Asia (36°-45°N, 62°-80°E) -- an area encompassing the Tien Shan, Tadjik Depression, Pamir and Hindu Kush -- contain data on more than 20,000 earthquakes for 1964-1978. The ISC catalog for the same area and time period contains less than 4,000 events. The Soviet catalog, based on reports from local stations, allows for greater resolution of seismicity patterns than is possible from teleseismic observations alone. Major zones of seismicity (e.g., the Gissar-

Kokshal zone, the Talas-Fergana fault, and lineations within the Fergana Depression and northern Tien Shan) separate large crustal blocks which tend to be relatively aseismic (e.g., the Gissar ranges, the high Pamir, Issyk Kul Basin). The high levels of seismicity correlate with high gradients in topography, attesting to the importance of vertical crustal movements in this region.

For events common to both the Soviet and ISC catalogs, we have compared the two locations and, assuming the Soviet locations to be more accurate, determined the error and bias in the ISC locations. For ISC locations determined using less than 10 stations, relative differences in epicentral locations of up to 200 km are observed. When more than 50 stations are used, the differences are usually less than 20 km. Neither catalog provides sufficient resolution to compare depths for crustal earthquakes, but for intermediate-depth Pamir and Hindu Kush events, differences in focal depth similar in magnitude to those in epicentral locations are found. The Soviet locations tend to have shallower depths, compensated for by earlier origin times.

3. Aswan Induced Seismicity - Studies of induced seismicity at Aswan reservoir, Egypt have been partially supported by this project, the Government of Egypt and USAID (under subcontract to Woodward-Clyde Consultants). Because of numerous funding delays and contractural complications, the full extent of this project is only now (Fall, 1984) being officially started. Publications describing the work to date are now in preparation and will be included as part of the work in the successor to this contract.

4. Mechanism of Induced Seismicity - Data were collected on the seismicity associated with the filling of a dozen reservoirs worldwide. The common correlation between bursts of seismicity and reservoir filling cycles noted by us and other workers is being contrasted with the large earthquake seismicity that can be associated with reservoirs. Some simple diffusion equation formulations were experimented with, and it appears that, although the filling-cycle seismicity must be due to consolidation within the rock beneath the reservoir, the large events may alternatively reflect reservoir water diffusion (Simpson and Leith, 1984).

Publications

Leith, W., Stratigraphic evidence for the Mesozoic and Cenozoic development of crustal structure in the eastern Tadjik Depression, USSR, submitted to Nature, 1984.

Leith, W., and W. Alvarez, Structure of the Vakhsh fold and thrust belt, Tadjik SSR: an application of Landsat imagery to continuous-structure mapping, submitted to Geological Society of America Bulletin, 1984.

Leith, W., and D. W. Simpson, A comparsion of structure and seismicity along the western Gissar-Kohshal seismic zone, submitted to Journal of Geophysical Research, 1984.

Nicholson, C., D. W. Simpson, S. Singh, and J. E. Zollweg, Crustal Studies, velocity inversions and fault teconics: results from a microearthquake survey in the New Madrid seismic zone, Journal of Geoaphysical Research, v. 89, pp. 4545-4558, 1984.

Nicholson, C., and D. W. Simpson, Changes in V_p/V_s with depth: implications for appropriate velocity modelling, improved earthquake catalogs, and material properties of the upper crust, submitted to Journal of Geophysical Research, 1984.

Simpson, D. W., and R. M. Kebeasy, Induced seismicity at Aswan Reservoir, Egypt, Earthquake Notes, v. 54, pp. 32, 1983.

Simpson, D. W., and E. Kappel, Central Asian earthquakes, a comparison of ISC and Soviet catalogs, Earthquake Notes, v. 54, pp. 33, 1983.

Simpson, D. W., Intra- vs inter-plate tectonics in Soviet Central Asia, Joint Programme with Abstracts, 11th Annual Meeting Canadian Geophysical Union, Halifax, p. 44, 1984.

Simpson, D. W., S. Kh. Negmatullaev, and K. M. Mirzoev, Catalog of earthquakes 1955-1978 and water levels at Nurek Reservoir, to be published by Donish Press, Dushanbe, 1984.

Simpson, D. W. and W. Leith, Two types of reservoir induced seismicity, Proceedings of the Regional Assembly of IASPEI, Oct. 31-Nov. 7, 1984, Hyderabad, India, 1984.

Deep Hole Desalinization of the Dolores River

9920-03464

William Spence
Branch of Global Seismology and Geomagnetism
U.S. Geological Survey
Denver, Federal Center, MS 967
Denver, Colorado 80225
(303) 236-1506

Investigations

This project relates to monitoring of the seismicity of the region of the intersection of the Delores River and Paradox Valley, southwest Colorado. This project is a part of the Paradox Valley Unit of the Colorado River Basin Salinity Control Project and is being performed for the U.S. Bureau of Reclamation with support from the Induced Seismicity program of the USGS. In this desalinization project it is proposed to pump approximately 30,000 barrels/day from brine-saturated rocks beneath the Dolores River through a borehole to the Madison-Leadville limestone formation of Mississippian age, some 15,000 feet below the surface. There is a possibility of seismicity being induced, especially in the long term, by this desalinization procedure. The project objectives are to establish a pre-pumping seismicity baseline and, during the pumping phase, to closely monitor the discharge zone for possible induced seismicity. If induced seismicity does occur it should be possible to relate it to formation characteristics and to the pumping pressure and discharge rates.

Results

A ten-station seismograph network has been installed, centered on the location of the proposed injection well. This high-gain network has a diameter of about 80 kilometers. Final installation of the network was complete in September, 1983. Seismic data are presently being brought to Golden, Colorado, via microwave and phone line transmission. These data are fed through an A/D converter and then through an event detection algorithm. The network has operated at high quality, except for a period in Spring, 1984 when the network was decommissioned by a lighting strike. While 32 probable earthquakes have been identified in the region of the network there has been a general absence of earthquake activity within about 25 km of the network. Analysis procedures have been considerably complicated by a high rate of blasting activity in the region but means have been developed to distinguish the occurrence of natural earthquakes to good reliability. Notable regional earthquake activity occurred with a swarm of shallow events (maximum magnitude 3.2) near Carbondale, Colorado, a magnitude 3.4 shallow earthquake near Blue Mesa Reservoir, Colorado, and a 54-km-deep earthquake located about 25 km northwest of the network. These early results, combined with a lack of historical seismicity at the zone of the Paradox Valley seismic network, indicate that any seismicity induced by deep-well injection near Paradox Valley should be identifiable as such.

Report

Spence, W., and Jacobs, W., 1984, Seismic monitoring in the region of the Paradox Valley, Colorado (Annual report, July 1983 - June 1984, U.S. Bureau of Reclamation, Deep well injection site, Paradox Valley Unit, Colorado River Basin Salinity Control Project), 45 p.

Study of Reservoir Induced Seismicity and Earthquake Prediction in South Carolina

Contract No. 14-08-0001-21229

Pradeep Talwani
Geology Department
University of South Carolina
Columbia, S.C. 29208
(803) 777-6449

Investigations

1. Monitor seismicity near Monticello Reservoir, Newberry, S.C., and Lake Jocassee.

2. Develop a theoretical model for RIS.

Results

1. We have continued to monitor seismicity near Monticello Reservoir, Newberry, and Lake Jocassee, South Carolina. The level of activity at Monticello Reservoir was low for the first six months of 1984 when compared to previous years and was more confined beneath the Central part of the reservoir rather than the western side as in Previous years (Figure 1). Continued analyses of depths for Monticello Reservoir events shows a smaller percentage of deep activity (> 3.0 km) than in the last few years, but, due to the small sample size, these results may be inconclusive (Figure 2). We are acquiring analog tape data from the USGS to use in relocating earlier events and verifying the increase in activity at depth. We are also in the process of relocating all the stations in the network via satellite and recalibrating station polarities.

   Activity near Newberry, South Carolina has declined (< 1 event per month). We will continue to note Newberry seismicity but are no longer actively monitoring the area. We are working on a model for the swarms at Newberry based on geological, gravity and magnetic and seismic investigations.

   Seismicity at Lake Jocassee has been monitored since 1975, first with portable instruments, and now with three permanent stations. For the first six months of 1984, the level of activity was low and the magnitudes were small (< 2.0). Epicentral locations are shown in Figure 3 which includes blasts at Bad Creek, the proposed site of a new, large dam.

   We conducted a noise survey near Union, South Carolina, located roughly midway between Lake Jocassee and Monticello Reservoir, in preparation for installing a new permenent station. The station will be located in an area of historic seismicity, and will assist coverage in the northern section of the state, as well as be used as a relay in the telemetering of the permanent station SMT (near Lake Jocassee), which was disconnected in 1983, into Columbia.

2. A theoretical model for reservoir induced seismicity at Monticello Reservoir is not yet complete but involves the combined effects of pore pressure, lake load, and the mechanical properties of observed fracture gouge at depth.

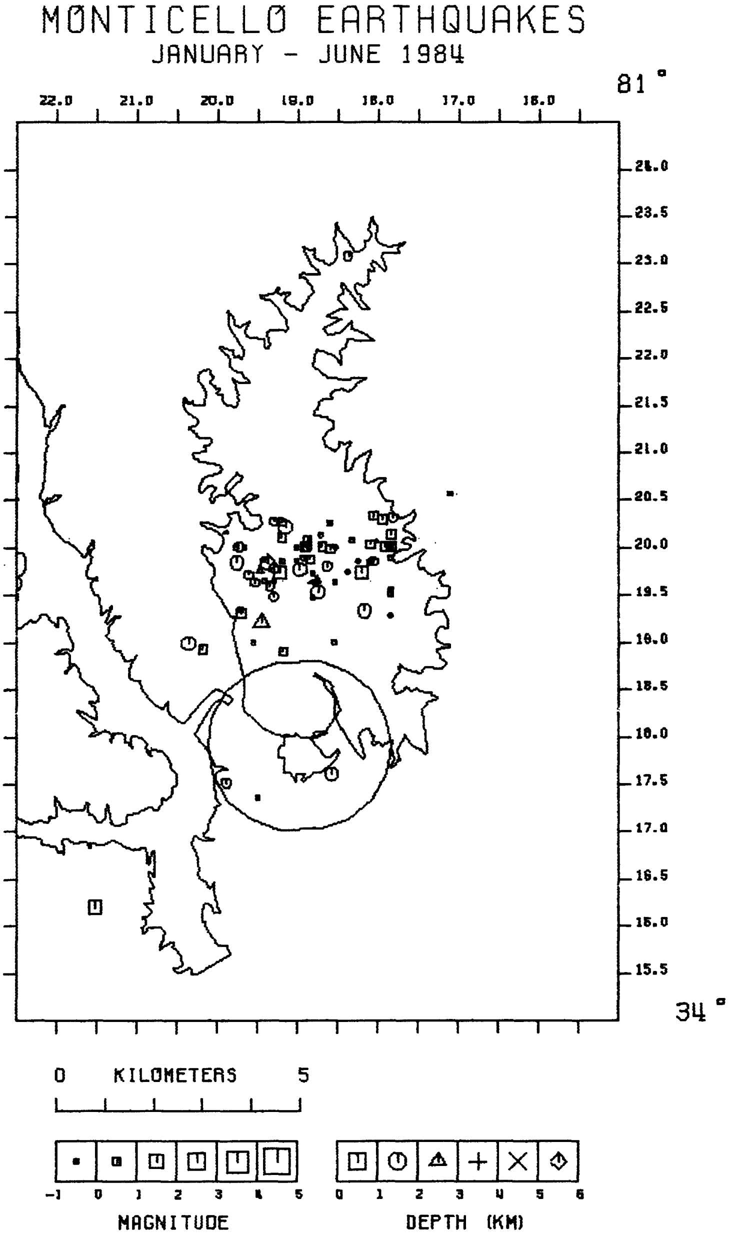
MONTICELLO EARTHQUAKES
JANUARY - JUNE 1984
81°
22.0
21.0
20.0
19.0
18.0
17.0
16.0
24.0
23.5
23.0
22.5
22.0
21.5
21.0
20.5
20.0
19.5
19.0
18.5
18.0
17.5
17.0
16.5
16.0
15.5
34°
0 KILOMETERS 5
-1
0
1
2
3
4
5
MAGNITUDE
0
1
2
3
4
5
6
DEPTH (KM)

Figure 1

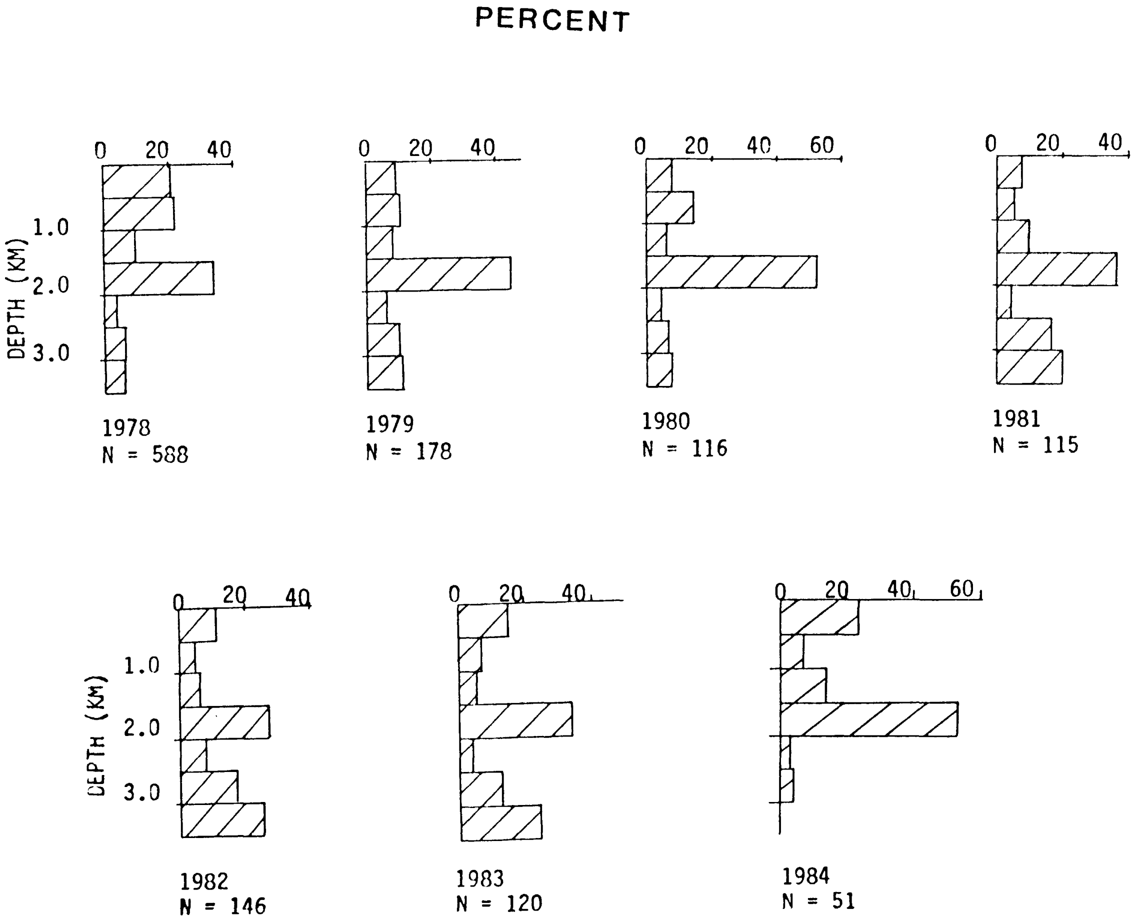
PERCENT
0
20
40
60
DEPTH (KM)
1.0
2.0
3.0
1978
N = 588
1979
N = 178
1980
N = 116
1981
N = 115
1982
N = 146
1983
N = 120
1984
N = 51

Figure 2

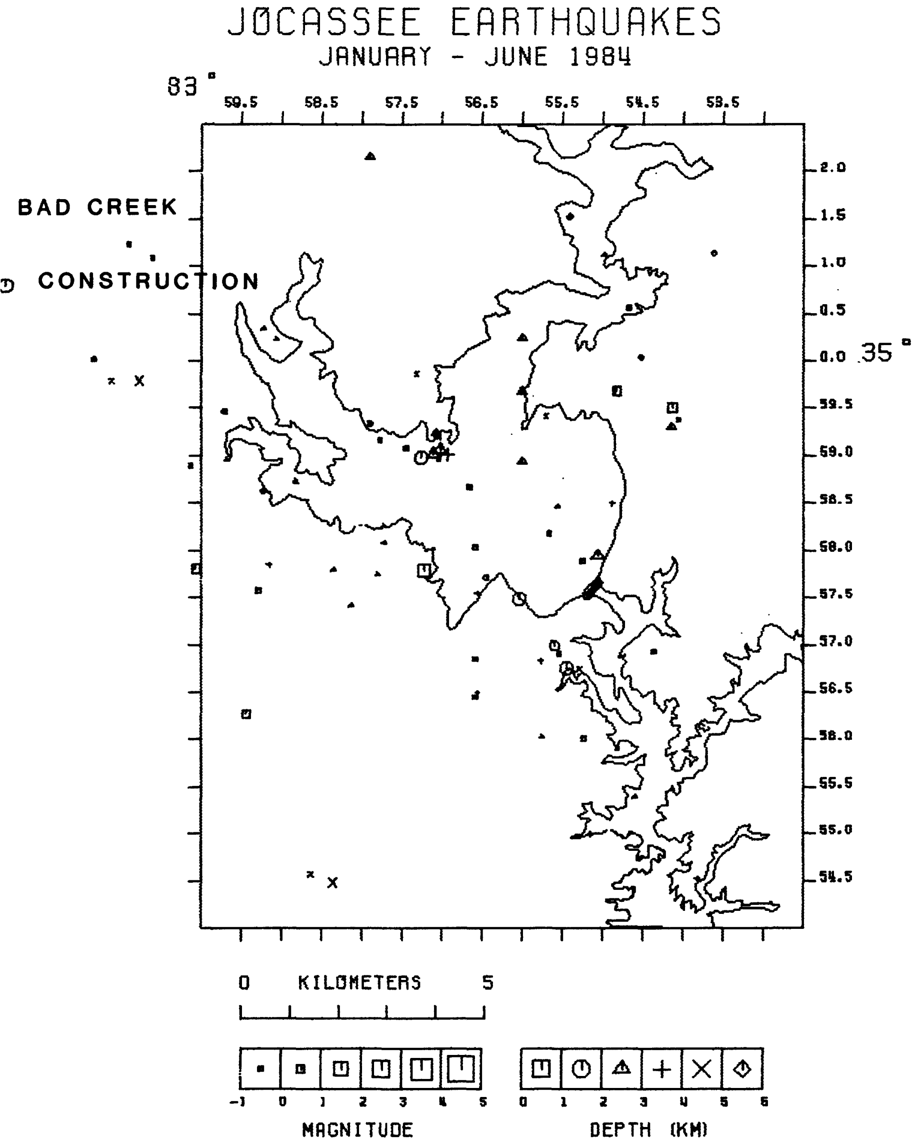
JOCASSEE EARTHQUAKES
JANUARY - JUNE 1984
83°
59.5
58.5
57.5
56.5
55.5
54.5
53.5
BAD CREEK
CONSTRUCTION
2.0
1.5
1.0
0.5
0.0
35°
59.5
59.0
58.5
58.0
57.5
57.0
56.5
56.0
55.5
55.0
54.5
0 KILOMETERS 5
-1
0
1
2
3
4
5
MAGNITUDE
0
1
2
3
4
5
6
DEPTH (KM)

Figure 3

Strong Motion Data Management

9910-02757

A. G. Brady

Branch of Engineering Seismology and Geology
U.S. Geological Survey
345 Middlefield Road, MS 977
Menlo Park, CA 94025
(415) 323-8111 X2881

Investigations

Research continues on the development of analytical test records for testing processing steps. This work is needed in order to make the tests required for verification of some of the more recent additional options in our processing procedures (see the USGS Open-File report 84-525: AGRAM, a series of computer programs for processing digitized strong-motion accelerograms, by April Converse). Two papers were presented at the 8th World Conference on Earthquake Engineering on these topics.

Routine digitizing (indicated by (D)) and computer processing (P) of strong motion earthquake recordings continues: 4 digital records (P) San Jose freeway bridge April 24, 1984; 13 records (P) Coalinga aftershock 7/22/84 0239; 8 records (D) explosive tests for soil/structure interaction, July 1984; 4 digital records (P) Hollister differential digital array April 24, 1984.

Reports

Brady, A. G., and Mork, P. N., 1984, Synthetic accelerograms for testing processing procedures, 8th World Conf. Eq. Eng., San Francisco.

Converse, A. M., Brady, A. G., Joyner, W. B., 1984, Improvements in strong-motion data processing procedures, 8th World Conf. Eq. Eng., San Francisco.

Brady, A. G., Porcella, R. L., Bycroft, G. N., Etheredge, E. C., Mork, P. N., Silverstein, B., and Shakal, A. F., 1984, Strong-motion results from the main shock of April 24, 1984, *in* The Morgan Hill, California, Earthquake of April 24, 1984, Seena Hoose (Compiler), USGS Open File-Report 84-498; submitted for USGS Bulletin.

Silverstein, B., and Brady, A. G., 1984, Data processing for the Coalinga aftershock of July 22, 1983, 0239 Oct, in preparation.

Worldwide Standardized Seismograph Network (WWSSN)

9920-01201

O. J. Britton
Branch of Global Seismology and Geomagnetism
U.S. Geological Survey
Albuquerque Seismological Laboratory
Building 10002, Kirtland AFB-East
Albuquerque, New Mexico 87115-5000
(505) 844-4637

Investigations

1. Technical and operational support were provided to each station in the Worldwide Standardized Seismograph Network (WWSSN) as needed and required.

2. Two hundred and thirty-six (236) modules and components were repaired, and four hundred and thirty-five (435) separate items were shipped to support the network during this period. Several shipments of photographic paper and chemicals were made to the stations requiring these supplies. All routine paper shipments have now been made. A minimum of emergency shipments should be required in the future.

3. Three WWSSN stations were visited by field enginners, Mr. Juan Nieto and Mr. Bob Pratt, during the month of August 1984. These stations were Arequipa, Peru (ARE), Nana, Peru (NNA), and Galapagos Islands, Ecuador (GIE). These stations were maintained and calibrated, and the station operators were given training in the equipment.

Results

A continuous flow of high quality seismic data from the cooperating stations within the network is provided to the users in the seismological community.

Digital Data Analysis

9920-01788

Ray Buland
Branch of Global Seismology and Geomagnetism
U.S. Geological Survey
Denver Federal Center, MS 967
Denver, Colorado 80225
(303) 236-1506

Investigations

1. Moment Tensor Inversion. Apply methods for inverting body phase waveforms for the best point source description to research problems.

2. Computation of Free Oscillations. Study the effects of anelasticity on free oscillation eigenfrequencies and eigenfunctions.

3. Earthquake Location Technology. Study techniques for improving the robustness, honesty, and portability of earthquake location algorithms.

4. Real Time Earthquake Location. Experiment with real time signal detection, arrival time estimation, and event location for regional earthquakes.

5. Detection Capabilities. Study the seismic event detection capability of each proposed station in the Southern Hemisphere Seismic Net (SHSN) now under development.

6. Network Day/Event Tapes. Support and enhance portable software for retrieving data from the Global Digital Seismograph "Network Day Tapes." Create and distribute Network "Event Tapes."

7. NEIS Monthly Listing. Contribute both fault plane solutions (using first-motion direction) and moment tensors (using long-period body-phase waveforms) for all events of magnitude 5.8 or greater when sufficient data exist. Contribute waveform/focal sphere figures of selected events.

Results

1. Moment Tensor Inversion. A study of the significance of the non-double-couple component of measured moment tensors has been completed. It has been concluded that this may be due to multiple ruptures, a non-planar fault surface, or tensile failure. Further, all possibilities seem to be observed in practice and under some conditions can be distinguished from one another. The catalogue of moment tensors for all sufficiently large events in 1981-1983 has been redone allowing for a source depth computed by the moment tensor algorithm.

2. Computation of Free Oscillations. First order perturbation theory was tested by computing anelastic toroidal free oscillations directly using simple Earth models and simple model rheologies. It was found that perturbation theory can result in 10% errors in Q for realistic Q models. This is

significant compared with reported fundamental toroidal mode observational errors. Also, the complete theory predicts an observable source phase which cannot be modeled by perturbation theory. This could result in the destructive interference of modes forming long period body phases which could be interpreted as an attenuation or a scattering effect.

3. Earthquake Location Technology. Probability density functions derived for NEIS travel-time and magnitude residuals have been refined. The PDF for travel-time residuals was found to vary systematically with source depth and magnitude. Further, it was possible to study biases as a function of distance and station. The most representative travel-time residual has been used to study robust earthquake location and to compare various methods. It appears that the robust R-estimator being studied has significant advantages over all other known methods for the teleseismic problem.

4. Real time Earthquake Location. In cooperation with the Istituto Nazionale di Geofisica (Italian government) a USGS developed frequency domain signal detection system was interfaced (in Rome) with the telemetered portion of the Italian national seismograph network. Software was developed (by the USGS) to manage the near real time flow of detection data allowing first arrival time estimation and event location (using algorithms developed by the Italians). Finally, waveforms, picks, association information, and hypocentral locations are saved in a data base (developed by the USGS).

5. Detection Capabilities. Each of the ten stations comprising the proposed SHSN network is to be studied in detail for ability to well record seismic events. The study of two more stations has been completed to bring the total to four.

6. Network Day/Event Tapes. Event tapes are being routinely produced and distributed to 11 data centers. Production and distribution is complete for the current (1984) tapes. Historical tapes have been produced for January 1980 - October 1982 and distributed for all of 1980. Eventually the tapes will cover 1980-present.

7. NEIS Monthly Listing. Since May 1981, fault plane solutions for large events have been contributed to the Monthly Listing. Beginning in November 1982, moment tensors and waveform/focal sphere plots are also being contributed. In the last six months the fault plane solutions and moment tensors of approximately 80 events were published. Catalogs of all fault plane solutions along with first motions data is being prepared for publication as a USGS circular.

Reports

Sipkin, S. A. and Needham, R. E., 1984, Kinematic source parameters of the 2 May 1983 Coalinga earthquake determined by time-dependent moment tensor inversion and an analysis of teleseismic first motions: *in* U.S. Geological Survey Professional Paper, in press.

Julian, B. R. and Sipkin, S. A., 1984, Earthquake processes in the Long Valley Caldera area, California: J. Geophys. Res., in press.

Needham, R. E., 1984, Preliminary report on the detection capabilities of SHSN stations: LPB-La Paz and ZOBO-Zonga Valley, Bolivia: U.S.G.S. Open-File Report 84-756.

Buland, R., 1984, Residual statistics: Terra Cognita, v. 4, p. 268.

Sipkin, S. A., 1984, Interpretation of non-double-couple earthquake mechanisms derived from moment tensor inversion: in preparation.

Systems Engineering

9920-01262

Harold E. Clark, Jr.
Branch of Global Seismology and Geomagnetism
U.S. Geological Survey
Albuquerque Seismological Laboratory
Building 10002, Kirtland AFB-East
Albuquerque, New Mexico 87115-5000
(505) 844-4637

Investigations

1. Design, develop, and test microprocessor based seismic instrumentation.

2. Design, develop, procure, and test special electronic systems required by seismic facilities.

3. Design, develop, and test microprocessor/computer software programs for seismic instrumentation and seismic recording systems.

Results

1. The major effort during this time period was devoted to training and checkout of the China Digital Seismic Network (CDSN) field recording systems and the Beijing depot repair facility instrumentation for three visiting People's Republic of China scientist and engineers. The People's Republic of China personnel spent part of June, July, August, and most of September at the Albuquerque Seismological Laboratory Engineering Section. Training consisted of technical subjects, individual equipment units, depot repair systems, power system operation, and field recorder systems.

2. After training on specialized engineering design systems, the People's Republic of China personnel were assigned and completed four of the engineering tasks required by the CDSN system.

3. With the training and experience received by the People's Republic of China scientists and engineers, they will be able to start the training of other personnel in China and finish the facility work for the CDSN field recording systems installations. The training they received on the depot repair facility equipment is one year ahead of the initial schedule. The depot repair facility should be operational in the early stages of CDSN field recording system installations and will be very beneficial if trouble arises from damaged or inoperative units.

4. The initial shipments of equipment to China have begun. The majority of the remaining equipment will be shipped in the next four to six months.

Seismic Observatories

9920-01193

Leonard Kerry
Branch of Global Seismology and Geomagnetism
U.S. Geological Survey
Albuquerque Seismological Laboratory
Building 10002, Kirtland, AFB-East
Albuquerque, New Mexico 87115-5000
(505) 844-4637

Investigations

Recorded seismological data at Albuquerque ASL, New Mexico on a continuing basis. Recorded and provisionally interpreted seismological and geomagnetic data at observatories operated at Newport, Washington; Cayey, Puerto Rico; and Agana, Guam. Assisted in the operation of the Puerto Rican Seismic Telemetry Network from the main base located in Cayey, Puerto Rico. Operated advanced equipment for gathering research data for universities and other agencies at Cayey, Puerto Rico and Agna, Guam. At Agana, Guam, a 24-hour standby duty was maintained to provide input to the Tsunami Warning Service operated at Honolulu Observatory by NOAA and to support the Early Earthquake Reporting function of the National Earthquake Information Service.

Results

Provided data on an immediate basis to the National Earthquake Information Service and the Tsunami Warning Service. Continued to send seismograms obtained from the WWSSN Systems to NEIS for use in the ongoing USGS programs. Analog seismic records and digital seismic tape records were obtained from the SRO system and forwarded to ASL for use in ongoing USGS and other users' programs. Data from advanced research equipment was forwarded to universities or other agencies working in conjunction with USGS. Seismic data from the Puerto Rican net was provided on a continuing basis to the University of Puerto Rico for their use in studying and research of the seismicity of the Puerto Rican area.

Responded to requests from the public, interested scientists, universities, state, and Federal agencies regarding geophysical data and phenomena.

Seismic Data Library

9930-01501

W. H. K. Lee
U. S. Geological Survey
Branch of Seismology
345 Middlefield Road, Mail Stop 977
Menlo Park, California 94025
(415) 323-8111, ext. 2630

This is a non-research project and its main objective is to provide access of seismic data to the seismological community. This Seismic Data Library was started by Jack Pfluke at the Earthquake Mechanism Laboratory before they joined the Geological Survey. Over the past ten years, we have built up one of the world's largest collections of seismograms (almost all on microfilm) and related materials. Our collection includes approximately 4.5 million WWNSS seismograms (1962 - present), 1 million USGS local earthquake seismograms (1966-1979), 0.5 million historical seismograms (1900-1962), and 20,000 earthquake bulletins, reports and reprints.

During the past six months (April - September, 1984), about 60 users from 15 different institutions have visited our Seismic Data Library for over 120 times in total.

Seismic Review and Data Services

9920-01204

R. P. McCarthy
Branch of Global Seismology and Geomagnetism
U.S. Geological Survey
Denver Federal Center, MS 969
Denver, Colorado 80225
(303) 236-1513

Investigations and Results

Technical review and quality control were carried out on 528 station-months of seismograms from the World-Wide Standardized Seismograph Network (WWSSN). Seventy-four station-months of Seismic Research Observatory (SRO & ASRO) seismograms were provided to the National Earthquake Information Service (NEIS) for their PDE programs on a current basis. An average of thirty-six WWSSN current station-months were supplied monthly for the NEIS fault plane solution program. Under the cooperative WDC-A International Data Exchange (IDE), seismograms from the WWSSN sent for this program outside normal schedules were forwarded to the WDC-A covering six separate events.

The annual Station Performance Report(s) sent to each WWSSN director are in preparation. These cover instrumental and operational details including timing precision, calibrations, damping, noise patterns and intensities, recording quality, label data, seismogram backlogs, and any unusual problems that may have occurred. Overall standards in the WWSSN remain at high levels. Timing accuracies are generally maintained at under 50 milliseconds daily error. Temporary paper shortages occurred at a few stations due to delivery problems from Kodak. The instruments from Natal (NAT) are now relocated at Caico, Brazil (CAI) but no recordings have been received since the installation in July 1983. The Galapagos Islands (GIE) station has been put back into operation this past September after being down for over two years. There are 98 operational WWSSN stations plus 8 of questionable status.

Monthly reports covering the analog and digital records received from the WWSSN, SRO, and ASRO were distributed to officials and researchers in the USGS, NOAA and DOD. Information and consultations regarding station data and operations were provided to government officials, researchers and private parties as needed.

National Earthquake Information Center

9920-01194

Waverly J. Person
Branch of Global Seismology and Geomagnetism
U.S. Geological Survey
Denver Federal Center, MS 967
Denver, Colorado 80225
(303) 236-1500

Investigations and Results

The weekly publication, Preliminary Determination of Epicenters (PDE), continues to be published on a weekly basis, averaging about 70 earthquakes. The PDE monthly listing, and Earthquake Data Report (EDR) continue to work very well on the VAX, with very little down time encountered. Programs for data entry have been modified and transferred from the 1170 to the VAX and operting smoothly.

The personal contacts with many of our foreign visitors, explaning the need for faster reporting of data, have been the most productive way for receiving data. We continue to receive telegraphic data from the U.S.S.R. in a very timely manner on magnitude 6.5 or greater earthquakes and some smaller damaging quakes in the U.S.S.R. and bordering countries. Data from the PR of China via American Embassy are being received in a very timely manner and in time for the PDE Publication. We are now receiving 4 stations on a weekly basis from the PR of China and about 22 from SSB by mail, which in most cases are in time for the monthly. We now have rapid data exchange (alarm quakes) with Centre Seismologique European-Mediterranean (CSEM), Strasbourg France; Instituto Nazionale d: Geofisica, Rome, Italy; data by telephone from Mundaring Geophysical Observatory, Mundaring, W.A.; and routine telegraphic data from Seismological Geophysical Institue of Montenegro, Titograd, Yugoslovia.

The monthly listing of earthquakes are up to date. As of September 30, 1984, monthly listing and Earthquake Data Reports (EDR) were completed through May 1984. A total of 4,985 events were published; for the calendar year 1983, 9,842 events were published. During 1983, we received 581,453 readings groups from 1,736 stations throughout the world, this compares with 500,192 groups from 1,457 stations during 1982. Fault Plane Solutions continue to be determined, when possible, and published in the monthly listing and EDR for any earthquake having Mb magnitude ≥ 5.8. Centroid Moment Tensor Solutions from Harvard University continue to be published in the monthly listing and EDR. Moment Tensor Solutions are being computed by the U.S. Geological Survey and are also published in the above publications. Waveform plots are being published for selected events having Mb magnitudes ≥ 5.8.

The earthquake Early Alerting Service continue to provide information on recent earthquakes on a 24-hour basis to scientists, news media, and the increasing general public. Sixty-four releases were made from April 1, 1984, through September 30, 1984. The largest earthquakes released during this time period were in Japan. A 6.9 MS in Kyushu, Japan on August 6 and 6.9 MS off the east coast of Honshu, Japan on September 18. In the United States, the largest was a magnitude 6.7 MS off the coast of Northern California on September 10, 1984.

Reports

Preliminary Determination of Epicenters (PDE) 26 weekly publications April 5, 1984, to September 26, 1984--Numbers 11-84 through 36-84. Compilers: W. L. Irby, Willis Jacobs, John Minsch, W. Person, B. Presgrave, William Schmieder.

Monthly Listing of Earthquakes and Earthquake Data Reports (EDR 6 publications--December, 1983, through May, 1984). Compilers: W. Irby, Willis Jacobs, John Minsch, R. Needham, W. Person, B. Presgrave, W. Schmieder.

Seismological Notes, BSSA: Waverly J. Person vol. 74 no. 3--July-August 1983; vol. 74 no. 4--September-October 1983.

Earthquake Information Bulletin: vol. 16, no. 1, Earthquakes, Waverly J. Person July-August 1983; vol. 16, no. 2, Earthquakes, Waverly J. Person September-October 1983; vol. 16, no. 3, Earthquakes, Waverly J. Person November-December 1983.

Source Properties of Great Basin Earthquakes

9950-03835

Arthur C.Tarr

Branch of Engineering Geology and Tectonics
U.S. Geological Survey
Box 25046, MS 966, Denver Federal Center
Denver, CO 80225
(303) 236-1605

Investigations

One new principal investigation was begun and two principal investigations of last report period were continued in the last two quarters of FY 1984. These investigations are:

1. Information systems element of the Wasatch Front Regional and Urban Hazards Evaluation.

2. Development of software to analyze digital data recorded by portable seismic systems.

3. Analysis of digital data recorded by portable seismic systems at Nevada Test Site in 1981.

One of the elements of the new Wasatch Front Regional and Urban Hazards Evaluation study is Information Systems. One of the goals of the study is to get hazards information rapidly and efficiently into the hands of those geologists, geophysicists, engineers, planners, and consultants who will need the information. The form of the information ranges from newly published reports and maps to original data sets to bibliographies of existing reports and maps. The Information Systems element was created to facilitate geotechnical information transfer during and after the completion of the study. The Utah Geological and Mineral Survey (UGMS) and the USGS are partners in the Wasatch Front effort; hence, one UGMS person (Don Mabey) and one USGS person (I) were selected to co-manage the design and the implementation of the element.

One objective of the second investigation was to locate existing software, written in FORTRAN, that would perform spectral analyses on digital data recorded by seismic systems used in the field by investigators from Golden. Another objective was to modify such software once it was located and converted to the Golden VAX 11/780 computer. The modifications were intended to expand the number of field systems whose data could be analyzed and to improve the efficiency of data processing of large quantities of digital data, such as are acquired in aftershock monitoring following large earthquakes. A final objective was to evaluate the feasibility of implementing the data analysis software on a powerful microcomputer for field data processing.

The objective of the third investigation was to analyze digital seismic data that had been recorded in 1981 at Jackass Flats on the Nevada Test Site (NTS). The intention was to compare source parameters of earthquakes in areas near Yucca Mountain, a proposed site of a nuclear waste repository, with source parameters of earthquakes elsewhere on the NTS and on Pahute Mesa. In addition, the spectra were expected to provide data that could be used for testing a newly-recalibrated ML magnitude scale for the Southern Great Basin Seismic Network (SGBSN).

Results

Don Mabey and I proposed an information systems strategy that included the elements:

1. Vehicles for timely dissemination of information.

2. Identification and inventory of existing information resources.

3. Creation, where necessary, or upgrade of information resources.

Implementation of strategy elements during the reporting period were:

1. Establishment of the Wasatch Forum, a quarterly newletter edited by Wendy Hassibe of USGS's Salt Lake City Public Information Office, to communicate newsy information and progress reports to program participants and associates between the annual workshops. Establishment of an Information Directory which lists project participants, locations, and telephone numbers, provides guidelines to accessing various information resources, and contains descriptions of data set and software resources.

2. Solicited recommendations for data sets and software to be included in the inventorys.

3. Initiated the upgrade of a computerized geotechnical bibliography at the UGMS. Recommended upgrades to the UGMS computer center to permit data exchange with program participants and interested users.

The seismic data analysis system was expanded during the reporting period to include digital data recorded by Geotech MCR-600 and Bison field systems. The addition of a high-speed cassette tape reader to the system is currently underway and is intended to speed the processing of the voluminous amount of MCR-600 data recorded near Borah Peak, Idaho in September 1984. Five new utility programs were added to the analysis package to further automate some of the more tedious aspects of maintaining large data masses. The draft of a User's Guide was circulated for internal review by users of the data analysis software; eventually it will be published as an Open-File Report.

Analysis of the seismic data recorded by the Jackass Flats field stations has essentially been completed, with Pahute Mesa events recorded by the SGBSN remaining for analysis. A draft report describing the preliminary results of the data analysis is currently in internal review. One significant result, of course, was that Golden researchers now have a new tool for the analysis of digital seismic data from field systems. Several projects have been awaiting such a system and are expected to be heavy users of this new tool in the future.

Another result of the Jackass Flats study was a set of phase arrival and first-motion data which complemented existing SGBSN data sets of relatively low-magnitude earthquakes. The digital data provided additional depth and azimuthal control on hypocenter determinations and essentially verified several fault-plane solutions determined from network data only. The digital data demonstrated that SGBSN determinations are already quite good. Although the hypocenters and focal mechanisms did not change in a substantive way, the addition of new data should inspire confidence in results of the ongoing Network. With regard to determination of magnitude, moment, and source parameters such as stress drop, the digital data were exceptionally useful.

Local magnitudes <ML> determined from measurements of asymptotic spectral level Ω_0 independently confirmed that ML determined from coda length measurements (using California constants) is strongly overestimated, by perhaps as much as 1.4 magnitude units. Spectral estimates of <ML> were, on the average, 1.1 magnitude units smaller than ML coda length magnitudes published in the SGBSN Bulletin. Revised estimates of coda length ML for NTS earthquakes are consistent with the values calculated from spectral levels.

Seismic moment, source radius, and stress drop were determined for nine well-recorded southern NTS earthquakes ranging in <ML> magnitude (determined from seismic moment) from 0.3 to 1.9; stress drops were small, ranging from about 0.05 bars to 0.9 bars. Stress drop seems to increase with depth, as Fletcher and others have noted in studying Oroville, California earthquakes. Individual measurements of asymptotic spectral level and corner frequency are subject to considerable uncertainty, however; stress drop is particularly sensitive to uncertainty in corner frequency. Further study of the reasons for scatter are prerequisite to more definitive conclusions about spatial variation of stress drop at NTS.

Data Processing Center Operations

9930-01499

John Van Schaack
Branch of Seismology
U. S. Geological Survey
345 Middlefield Road MS/77
Menlo Park, California 94025
(415) 323-8111, ext. 2584

Investigations

This project has the general housekeeping, maintenance and management authority over the Earthquake Prediction Data Processing Center. Its specific responsibilities include:

1. Day to day operation and performance quality assurance of 5 network magnetic tape recorders.
2. Day to day management, operation, maintenance, and performance quality assurance of 2 analog tape playback stations.
3. Day to day management, operation, maintenance and performance quality assurance of the U.S.G.S. telemetered seismic network event library tape dubbing facility (for California, Alaska, Hawaii, and Oregon).
4. Projection of usage of critical supplies, replacement parts, etc., maintenance of accurate inventories of supplies and parts on hand, uninterrupted operation of the Data Processing Center.

Results

Procedures and staff for fulfilling assigned responsibilities have been developed and the Data Processing Center is operating smoothly and serving a large variety of scientific user projects.

National Strong Motion Data Center

9910-02085

Joanne Vinton
Branch of Engineering Seismology and Geology
U.S. Geological Survey
345 Middlefield Road, MS 977
Menlo Park, California 94025
(415) 323-8111, ext. 2982

Investigations

The goals of the National Strong Motion Data Center are to:

1) Maintain a strong capability for processing, analyzing, and disseminating all strong motion data collected on the National Strong Motion Network and portable arrays;
2) Support research projects in the Branch of Engineering Seismology and Geology by providing programming and computer support for computation of numerical models;
3) Provide digitizing and processing capabilities rapidly in the event of an earthquake as an aid to earthquake investigations.

Results

The National Strong Motion Data Center consists of a Digital Equipment Corporation VAX-11/750 computer running the VMS operating system, and a PDP-11/70 and two LSI-11/23 computers running the RSX operating system. The VAX has been installed since February 1984, and programs are being transferred to it from the PDP-11/70, to take advantage of the large address space. The LSI-11/23's are for use in the field, to locate and plot aftershocks on site.

All four computers are connected to the Office VAX-11/780 and to each other to allow file transfers and remote logons. These computers are also connected to ISD's VAX 11/780 and Marine Geology's VAX 11/780.

Data collected during this six month period were from the strong motion experiment in the Anza desert in southern California, and from the Morgan Hill aftershock sequence.

Reports

None.

Regional and National Seismic Hazard and Risk Assessment

9950-01207

S. T. Algermissen
Branch of Engineering Geology and Tectonics
U.S. Geological survey
Denver Federal Center, MS 966
Denver, CO 80225
(303) 236-1611

Investigations

1. Investigations of a number of large historical earthquakes is continuing with particular emphasis on 1) the 1811-12 New Madrid earthquakes and other large shocks in the New Madrid region; 2) the 1872 Chelan Lake, Washington, earthquake; and 3) the November 7, 1881, Colorado earthquake. Intensity information is currently being gathered and analysed on the October 18, 1984, Laramie Mountains, Wyoming earthquake (M = 5.5) for possible insights to the enigmatic source of the 1882 Colorado earthquake. Evaluation of damage data collected following the May 2, 1983, Coalinga, California, earthquake and the October 28, 1983, Mount Borah Peak, Idaho, earthquake is in progress.

2. A procedure for incorporating uncertainty of seismic source zone boundaries into regional probabilistic seismic hazard evaluations has been developed and documented.

3. Investigations for the empirical prediction of strong earthquake ground motion in the eastern United States based on site-specific analyses, semi-theoretical scaling relations, and Modified Mercalli intensities are in progress.

4. Interim assessments of the probabilistic ground motion hazard for southern Nevada, including the National Test Site, have been completed.

5. Earthquake hazard maps are being compiled for Salt Lake County, Utah, describing potential liquefaction, landslides, fault movement, and expected regional patterns of intensity for application in seismic risk investigations.

6. A draft of a multi-chapter professional paper entitled, "Seismic Hazard Studies in the United States," S. T. Algermissen, ed., has been completed.

Results

1. The October 18, 1984, Laramie, Wyoming, earthquake was strongly felt in parts of the Denver, Colorado, area as was the 1882 earthquake. Sites in the Denver area for which 1882 earthquake reports exist have been canvassed and the effects of the 1984 and 1882 earthquakes are being compared for these specific locations. Information to date makes the "two-shock" hypothesis for the 1882 earthquake appear less likely. Two miscellaneous field study maps have been published that estimate possible effects resulting from the recurrence of great earthquakes in the New Madrid seismic zone. A draft of a multi-chapter U.S. Geological Survey circular dealing with the same topic is near completion.

2. The acceleration level calculated for a given return period may increase from 50-80 percent when a site is moved from 10 km outside a discrete source zone boundary to 10 km within the boundary. In regions where seismotectonic features are unknown, such large differences in ground motion values across short distances is an artificial requirement of discrete source zone boundaries. A Gaussian smoothing technique is one way of minimizing this effect and is documented in a manuscript currently in review for journal publication.

3. In the near-field, all three methods of predicting strong ground motion are found to yield consistent results once adjustments are made to consistently base peak acceleration estimates on fault-distance models. In addition to the reports dealing with strong ground motion cited here, two other journal papers are currently in review.

4. Significant differences in estimated probabilistic ground motion hazard for southern Nevada and the Nevada test site region are obtained using earthquake recurrence estimates derived from either 1) recent, contemporary seismicity, 2) pre-atomic testing historic seismicity, or 3) geological information. The results indicate a need for significant catalog work to investigate and remove the effects of nuclear explosions and the need for a reliable, contemporary seismotectonic model.

5. An open-fle report detailing potential hazards to the Salt Lake County domestic water system is currently in review.

6. Professional paper chapters concerning the national seismic hazard maps (O.F. 82-1033), seismic source zones, parameter variability, attenuation functions, and seismic hazard estimates in Alaska are currently in internal review.

Reports

Bender, B., 1984, A two state model for seismic hazard estimation: Seismological Society of America Bulletin, v. 74, p. 1463-1468.

______1984, Seismic hazard estimation using a finite fault rupture model: Seismological Society of America Bulletin, v. 74, p. 1899-1923.

______1984, Incorporating acceleration variability into seismic hazard analysis: Seismological Society of America Bulletin, v. 74, p. 1451-1462.

Campbell, K. W., 1984, Observed structural modification of recorded strong gound motion _in_ Seminar on Earthquake Ground Motion and Building Damage Potential, San Francisco, 1984, Proceedings, 10 p. (in press).

______1984, The selection and development of strong motion scaling relationships for seismic hazard stuides, _in_ Course on Geologic and Hydrologic Hazards, Denver, 1984 Proceedings: U.S. Geological Survey Open-File Report, 57 p. (in press).

______1984, Near-source attenuation of strong ground motion for moderate to large earthquakes--an update and suggested application to the Wasatch fault zone of north-central Utah, in Evaluation of Regional and Urban Earthquake Hazards and Risk in Utah, National Earthquake Hazards Reduction Program Workshop, 23rd, Salt Lake City, 1984, Proceedings: U.S. Geological Survey Open-File Report, 17 p. (in press)

______1984, Strong ground motion data and its use in earthquake engineering, in Pathways and Future Directions for Environmental Data and Information Users, Denver, 1984, Proceedings, 22 p. (in press).

______1984, Strong motion scaling relations: a ten year perspective: Bulletin of the Seismological Society of America, 57 p. (in press).

Hopper, M. G. and Algermissen, S. T., 1984, Estimated maximum regional seismic intensities associated with an ensemble of great earthquakes that might occur along the New Madrid seismic zone, east-central United States: U.S. Geological Survey Miscellaneous Field Studies Map MF-1712.

______1984, Types of damage that could result from a great earthquake in the New Madrid, Missouri, seismic zone: U.S. Geological Survey Miscellaneous Field Studies Map MF-1713.

Perkins, David M. and Thenhaus, Paul C., 1984, Earthquake recurrences estimated by calibrating qualitative geological rate estimates, in Conference on evaluation of regional and urban earthquake hazards and risk in Utah, August 14-16, 1984, Salt Lake City, Utah: U.S. Geological Survey Open-File Report (in press).

Seismic Hazards of the Hilo 7 1/2' Quadrangle

9950-02430

Jane M. Buchanan-Banks
Branch of Engineering Geology and Tectonics
U.S. Geological Survey
Hawaiian Volcano Observatory, Box 51
Hawaii Volcanoes National Park
Hawaii, 96718
(808) 967-7982

Investigations

1. Completed draft of contribution to circular on structural damage and ground failures resulting from November 16, 1983, M 6.6, Kooiki earthquake, and began writing professional paper chapter on same topic.

2. Continued to learn computer programs and to input geologic data from the Hilo quadrangle. Geologic mapping continues.

3. Assisted with geologic observations during the March 25-April 15, 1984, eruption of Mauna Loa Volcano.

Results

1. Prepared a paper describing results of preliminary studies of the structural damage and ground failures that resulted from the Kooiki earthquake and forwarded this contribution to co-author for inclusion in a circular on the earthquake. This circular contribution is being rewritten and expanded, and will be submitted for publication as a professional paper chapter.

2. Data on chemistry of rock samples, paleomagnetic orientations and radiocarbon dates of lava flows, have been entered into the computer and can be retrieved in a variety of formats. Data entered under one key, such as sample number, can have a new key assigned and be resorted. This ability to manipulate the data greatly enhances the cross referencing and checking of the information.

   Geologic mapping in the Hilo quadrangle is nearly completed and field checking is underway. Thus far 28 lava flows from Mauna Loa have been mapped, 2 from Kilauea, and 8 from Mauna Kea. The flows range in age from 103 years (the 1881 flow from Mauna Loa) to >24,000 years old.

3. The eruption of Mauna Loa Volcano which began on March 25, 1984, continued until April 15. The flows produced from this eruption traveled about 26 km downslope from the vent stopping about 8 km above the outskirts of Hilo.

Continuous daytime geologic observations were made of the activity and lava production at the vents. Posteruption involvement included transcribing of field notes, annotation of photos, and interpretation of processes.

During June 1, I moved my office from a trailer adjacent to the Hawaiian Volcano Observatory building to a house in the park residential area devoted to the Hawaii Geologic Mapping Project. The new phone number is listed in the heading of this report.

Analytical Investigation of Soil Liquefaction

9910-03390

Albert T. F. Chen
Branch of Engineering Seismology and Geology
U.S. Geological Survey, MS-974
345 Middlefield Road
Menlo Park, CA 94025
(415) 323-8111, Ext. 2605

Investigations

(1). Updated computer programs on liquefaction potential assessment and seismic site response analysis.

(2). Continued to study the liquefaction and slope failure hazards of the debris dams north of Mt. St. Helens, Washington.

(3). Participated in the study of the liquefaction potential in the Los Angeles region.

Reports

Chen, A.T.F., 1984, MULAP4 -- A multi-linear analysis program for ground motion studies of horizontally layered systems: Report No. USGS-GD-84-002, NTIS-PB84-182815, National Technical Information Service, Springfield, VA 22161, 46p.

Liquefaction Investigations

9910-01629

Thomas L. Holzer
Branch of Engineering Seismology and Geology
U.S. Geological Survey
345 Middlefield Road, MS 977
Menlo Park, California 94025
(415) 323-8111 ext. 2760

Investigations

1. Completed compilation of liquefaction maps for the Los Angeles basin area.

2. Conducted additional subsurface investigations near the San Fernando Valley Juvenile Hall in Sylmar, California where a liquefaction induced lateral spread developed during the 1971 San Fernando earthquake. Began the preparation of a report on our findings at that site.

Results

A complete set of liquefaction susceptibility and liquefaction opportunity maps were prepared for the Los Angeles Basin area. Factors that were considered in compiling the maps include type and age of sedimentary deposits, depth to free ground water, penetration resistance of the sediments, and a seismogenic model of the region. Areas most likely to contain liquefiable sediments are those where deposition has occurred recently (with in the last 1000 years) and where ground water lies within 10 m of ground surface. Recurrence intervals for earthquake ground shaking strong enough to generate liquefaction at localities within the Los Angeles Basin area range from 30 to 40 years.

Reports

Youd, T.L. and Wieczorek, G.F., 1984, Liquefaction during the 1981 Westmorland and previous earthquakes near Westmorland, California: U.S. Geological Survey Open-File Report 84-680, 36 p.

Prediction of Strong Ground Motion in the Puget Sound Region: The 1965 Seattle Earthquake

14-08-0001-21306

S.M. Ihnen and D.M. Hadley
Sierra Geophysics, Inc.
15446 Bell-Red Road, Suite 400
Redmond, Washington 98052
(206) 881-8833

Seismic intensity patterns in the Puget Sound region show large spatial variations which cannot be attributed to surface geology. The purpose of this project is to use seismic raytracing techniques on a three-dimensional model of the subsurface structure to determine if this spatial variation can be predicted, and if so, to incorporate knowledge of subsurface structures into seismic risk maps for this area.

Model Construction: The digital velocity model constructed for the crust and upper mantle beneath Puget Sound contains seven layers. They are, from the surface downward: (1) a water layer for modeling ray interactions with Puget Sound and related water bodies; (2) a layer of variable depth and laterally varying velocities representing unconsolidated sediments near the surface; (3,4) upper- and lower-crustal layers; (5,6) the top and bottom of the subducted Juan de Fuca plate; and (7) the upper mantle. Considerable care was used to assure that the model incorporates the best available geological, geotechnical, and geophysical information. In particular, the shape of the sediment-bedrock interface was reconstructed from echo-sounding and well information and wave speeds were assigned by correlating surface geology with lithologic descriptions of rocks whose seismic velocities are known. Q values for each layer are computed using standard relations between the wave speed and attenuation. A location map of the study area and a contour map of the sediment layer are shown in Figures 1 and 2, respectively.

Raytracing: Synthetic accelerograms were computed at 1600 stations spread over the 8000 km^2 surface of the study area. Source and attenuation effects were included by convolving each arrival with an appropriately Q-filtered acceleration source time function. The source time function used was a segment of an accelerogram recorded on rock in the near-field of one of the 1980 Mammoth Lakes earthquakes. The computations assumed a point source at the hypocenter of the 1965 (m=6.5) Seattle earthquake and the published focal mechanism. Peak horizontal accelerations and durations were computed for each synthetic. Accelerations are scaled such that the observed and predicted peak accelerations match at the Tacoma strong motion station, which had a PGA of 0.067g.

Results: Figure 3 shows the logarithm of the predicted peak horizontal ground acceleration in the 1965 event. The largest predicted acceleration is nearly 0.6 g in a small area SW of downtown Seattle called Harbor Island. Analysis of the results suggest that most of this large value arises from focusing of rays in the deep sedimentary basin beneath Seattle, amplified by low velocity sediments near the surface. Interestingly, Harbor Island was the site of the most severe building damage and highest seismic intensity in the 1965 earthquake.

In general the predicted PGA's are in excellent agreement with the observed seismic intensity patterns and also with the small number of strong-motion accelerograph records from this event. In Figure 4 we show the predicted variation of PGA with distance for this 60 km deep event. Also shown are data points from comparable Japanese earthquakes.

Additional simulations are being performed for other epicenters and the results will be incorporated into a set of seismic risk maps for the Puget Sound region.

Reports:

Ihnen, S.M. and D.M. Hadley, 1984, Prediction of strong ground motion in the Puget Sound region: the 1965 Seattle earthquake, SGI-R-84-113, submitted for publication in Bulletin of the Seismological Society of America.

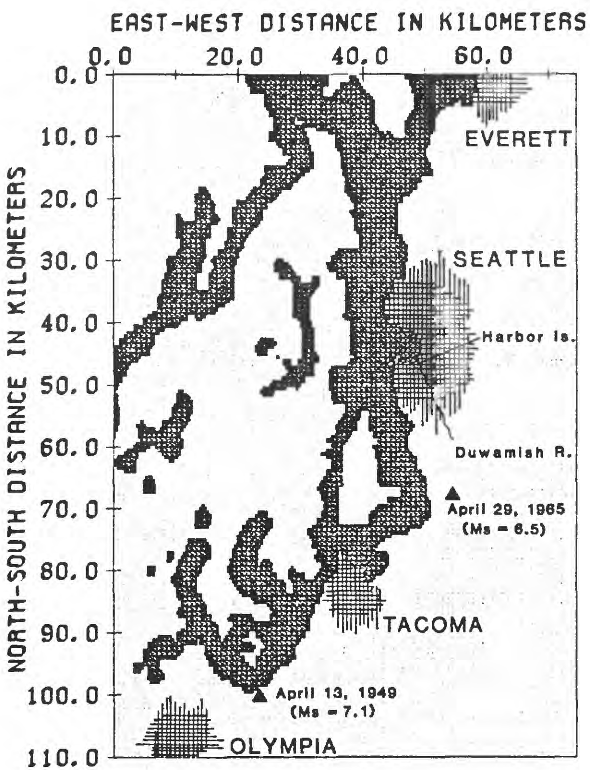

Figure 1. Reference map of study area. Origin of coordinates at NW corner is located at 48N latitude, 123W longitude. Epicenters of 1965 and 1949 earthquakes are shown by triangles.

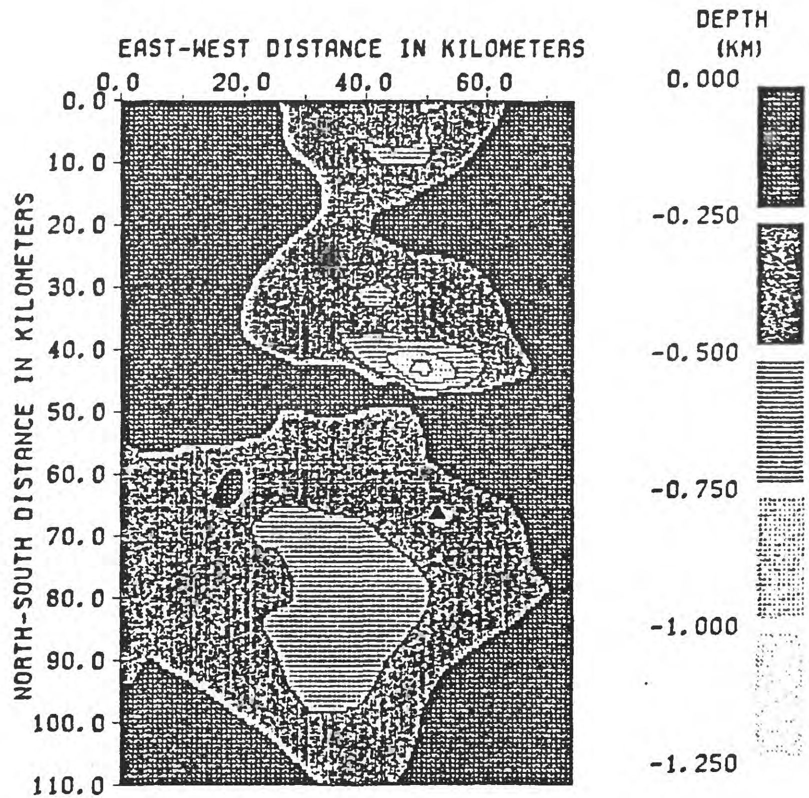

Figure 2. Contoured depth of sediments (Layer 2). Triangle is epicenter of 1965 event.

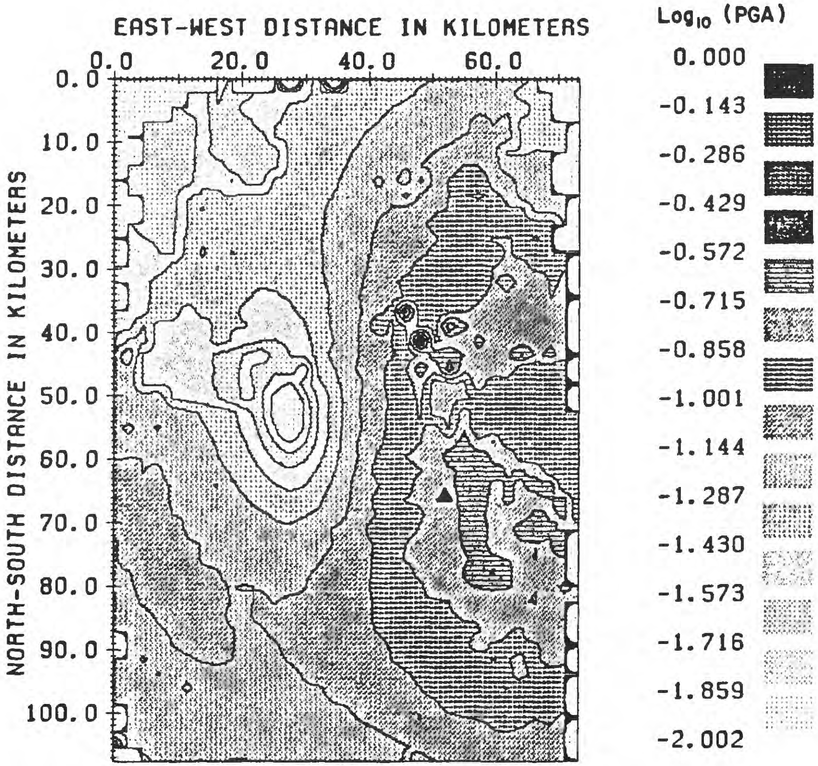

Figure 3. Contoured peak horizontal accelerations, 1965 earthquake, ISC epicenter. Note that the quantity contoured is the base ten log of acceleration, expressed as a fraction of g. Every change of 0.33 units is crudely equivalent to one seismic intensity unit. Low values of acceleration within 2-4 km of the edge of the model are artifacts of the modeling procedure and should be ignored. Triangle is epicenter of 1965 earthquake.

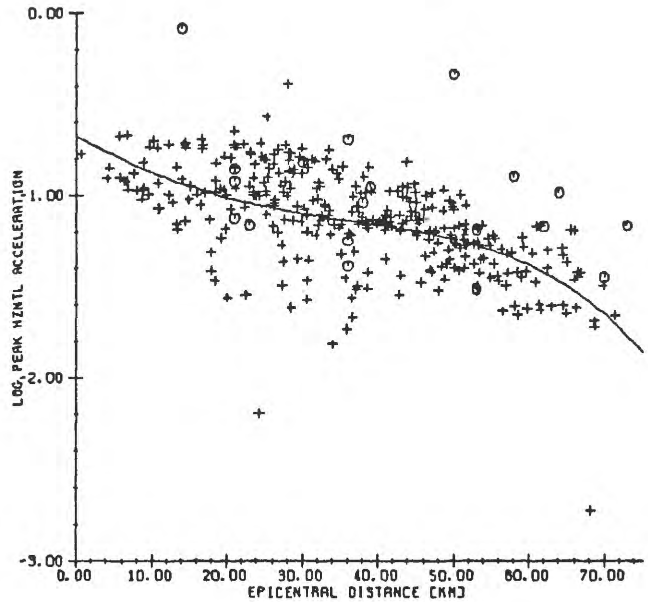

Figure 4. Plot of logarithm of peak ground acceleration (as fraction of g) vs. epicentral distance. Pluses (+) are predicted values from raytrace simulation of 1965 event. Circles are data from comparable Japanese earthquakes.

Seismic Slope Stability

9950-03391

David K. Keefer
Branch of Engineering Geology and Tectonics
U.S. Geological Survey
345 Middlefield Road, MS 998
Menlo Park, CA 94025
(415) 856-7115

Investigations

1. Continued development of quantitative methods for predicting earthquake-induced landslides on a regional scale.

2. Continued development of refined susceptibility criteria for predicting failure of rock slopes during earthquakes.

3. Conducted field studies following the Morgan Hill, California, earthquake of April 24, 1984.

4. Performed airphoto studies of landslides caused by the Coalinga, California, earthquake of May 2, 1983.

5. Conducted statistical and analytical studies of landslides along the Mississippi River bluffs to determine factors causing landslides and relation to the 1811-12 New Madrid, Missouri, earthquakes.

Results

1. Using both theoretical and historic/empirical studies, we have delineated three zones surrounding a seismic event: (1) a zone within which there is a high probability of failure of susceptible slopes, (2) a zone with a less than even, but still finite, probability of failure of susceptible slopes, and (3) a zone, beyond the outer limit defined by data from worldwide historical events, which is so far from the seismic source that the probability of landslides is very small, even on susceptible slopes. Three maps have been prepared, showing these zones for each major category of landslides for a postulated M 6.5 event in the Los Angeles area.

2. The April 24, 1984, Morgan Hill earthquake was felt strongly throughout the San Francisco Peninsula and the Santa Cruz Mountains. A large landslide near La Honda, California, was observed soon after the earthquake and was probably triggered by the earthquake. This landslide had an area of approximately 6.5 hectares (16 acres). Although no nearby strong-motion records are available, the shaking intensity near the landslide was so strong that one resident ran from a house; this suggests an intensity of Modified Mercalli (MMI) VI.

3. From field and statistical evidence it appears probable that most coherent slides and earthflows along the Mississippi River bluffs are related to

the 1811-12 earthquakes. From this we conclude that the bluffs in the study area are susceptible to large-scale landsliding in future major earthquakes. At present we cannot accurately evaluate the susceptibility of specific portions of the bluffs to earthquake-induced landsliding because we lack quantitative information about the effects of variation in geology, hydrology, and material properties. Our best indices of the potential for earthquake-induced landsliding along the bluffs are slope height and proximity to seismic sources. These factors can be used to predict the relative severity of landsliding along the bluffs in a future major earthquake.

Reports

Bailey, R. A., Harp, E. L., Keefer, D. K., Bennett, M. J., Miller, C. D., Wood, S. H., and Stine, Scott, 1984, Mono Craters, Long Valley caldera--seismicity, volcanism, and engineering geology (field trip 11) roadlog, *in* Lintz, Joseph, Jr., ed., Western geological excursions, V. 2; Geological Society of America Annual Meeting, Reno, Nevada, November 5-8, 1984: Reno, Nev., Mackay School of Mines, Department of Geological Sciences, p. 36-56.

Harp, E. L., and Keefer, D. K., 1985 (in press), Landsliding [Section] *in* Predicted geologic effects of a postulated earthquake along the northern part of the Newport-Inglewood zone, Chapter, *in* Ziony, J. I., ed., Earthquake hazards in the Los Angeles region: U.S. Geological Survey Professional Paper.

Harp, E. L., Sarmiento, John, and Cranswick, Edward, 1984, Seismic-induced pore-water pressure records from the Mammoth Lakes, California, earthquake sequence of May 25-27, 1980: Seismological Society of America Bulletin, v. 74, no. 4, p. 1381-1393.

______1984, Seismic-induced pore-water pressure records from the Mammoth Lakes, California, earthquake sequence of May 25-27, 1980 [abs.]: Earthquake Notes, v. 55, no. 1, p. 26.

Harp, E. L., Tanaka, Kohei, Sarmiento, John, and Keefer, D. K., 1984, Landslides from the May 25-27, 1980, Mammoth Lakes, California, earthquake sequence: U.S. Geological Survey Miscellaneous Investigations Series Map I-1612, scale 1:62,500.

Jibson, R. W., 1984, Earthquake-induced landslides in the New Madrid seismic zone [abs.]: Earthquake Notes, v. 55, no. 1, p. 19-20.

Keefer, D. K., 1984, Landslides caused by earthquakes: Geological Society of America Bulletin, v. 95, no. 4, p. 406-421.

______1984 (in press), Reply to discussion *of* Landslides caused by earthquakes, by D. K. Keefer, 1984 (*in* Geological Society of America Bulletin, v. 95, no. 4, p. 406-421): Geological Society of America Bulletin.

______1984 (in press), Review *of* An outline of soil and rock mechanics, by Pierre Habib, 1982 (Cambridge University Press, 149 p.): Engineering Geology.

Keefer, D. K., Harp, E. L., and Wilson, R. C., 1984, Landslides and related ground failures, *in* Scholl, R. E., and Stratta, J. L., eds., Coalinga, California, earthquake of May 2, 1983: Earthquake Engineering Research Institute Report 84-03, p. 99-105.

Mavko, G. M., and Harp, E. L., 1984, Analysis of wave-induced pore-pressure changes: Seismological Society of America Bulletin, v. 74, no. 4, p. 1395-1407.

Wieczorek, G. F., and Keefer, D. K., 1984, Landslide at La Honda, California probably triggered by the April 24, 1984, Morgan Hill earthquake, in Hoose, S. N., compiler, The Morgan Hill, California earthquake of April 24, 1984; a preliminary report: U.S. Geological Survey Open-File Report 84-498-A, v. 1, p. 109-115.

Wilson, R. C., 1984 (in press), Review of Numerical methods in geomechanics, by J. B. Martins, ed., 1982 (D. Reidel Publishing Company, Dordrecht, The Netherlands): Engineering Geology.

Wilson, R. C., and Keefer, D. K., 1985 (in press), Predicting earthquake-induced landslides, in Ziony, J. I., ed., Earthquake hazards in the Los Angeles region: U.S. Geological Survey Professional Paper.

Effect of Lateral Heterogenieties on Strong Ground Motion

14-08-0001-21257

C.A. Langston
440 Deike Building
Department of Geosciences
The Pennsylvania State University
University Park, PA 16802
(814) 865-0083

Investigations

1. Simulation of high-frequency strong ground motions over plausible three-dimensional geologic structure. Synthetic seismograms are calculated for responses from arbitrary point sources in or near the structure of interest.
2. Calculation of strong ground motions over models of geologic structures in the Puget sound area.
3. Study of anomalous site effects in the Pasadena, California area for strong ground shaking from the 1971 San Fernando earthquake.

Results

1. The study of anomalous site effects in the Pasadena, California area has been submitted to the B.S.S.A. for review.
2. Strong ground motions from the 13 April 1949 magnitude 7.1 Puget Sound earthquake are being investigated to examine the relative contributions of source and near-receiver structure. The source properties of the 1949 event are being determined by the analysis of teleseismic P and S waveforms recorded for the earthquake. Using a variety of modeling techniques Eli Baker of the U.S.G.S. and the P.I. are in the process of determining the focal mechanism, depth and time function of the event.

Reports

Langston, C.A. (1984). The influence of alluvium geometry on strong ground motions during the 1971 San Fernando earthquake, submitted to Bull. Seism. Soc. Am.

A Study of Source Parameters of Large Northeastern Earthquakes
14-08-0001-21295

John E. Ebel
Weston Observatory
Dept. of Geology and Geophysics
Boston College
381 Concord Road
Weston, Massachusetts 02193
(617) 899-0950

Objective: During the first half of the 20th century, several relatively large earthquakes took place in northeastern North America. The events, which occurred in 1925 near La Malbaie, Quebec (M=6.8), in 1935 near Timiskaming, Quebec (M=6.3), in 1939 near La Malbaie, Quebec (M=5.2), in 1940 near Ossipee, New Hampshire (M=5.6), and in 1944 near Massena, New York (M=6.0), were recorded widely by seismographs in North America, South America and Europe. The purpose of this study is to use synthetic seismogram analysis techniques to determine the source parameters (focal mechanism, depth, source time function, stress drop and seismic moment) for each event. This information can then be used to help investigate the cause of moderately-large earthquakes in northeastern North America.

Summary of Results:

1925 Earthquake: A number of source parameters have been estimated for the 1925 earthquake. Magnitudes have been measured from a number of seismograms from stations located in Europe and North America. The values which are shown in Table 1, indicate that this event had m_b = 6.9 and M_s = 6.6. The m_b reading is not very well resolved since the traces at both stations where m_b was determined were low amplitude. The teleseismic body waves at several stations in Europe have been synthesized to extract additional source parameters. The depth of the earthquake has been determined to have been between 7 and 10 km depth, the seismic moment from the body waves to be approximately 3 x 10^{26} dyne-cm, and the time function to have a duration of about 3 or 4 seconds. From these measurements, the fault length is found to be about 5 to 10 km, and the stress drop to lie in the 100 to 200 bars range. All of these numbers are preliminary and are being checked as part of the analysis. The earthquake focal mechanism is clearly thrust, but the strikes of the nodal planes cannot be well constrained since all of the high-quality observations lie within a very small distance and azimuth range from the source. It has been determined, however, that nodal plane strikes parallel with the seismicity trends mapped by Anglin (1984) are not inconsistent with the teleseismic body waveforms.

1935 Earthquake: While this earthquake was not as large as that in 1925, it was of sufficient size to yield a fair collection of seismograms for analysis. Magnitudes for the event for both body waves and surface waves (Table 1), are low compared to those expected from the body wave moment (Table 1). Moments and magnitudes for the 1982 Miramichi, New Brunswick main shock and the 1978 Santa Barbara, California earthquake highlight this apparent discrepancy. The short-period body waves from California are quite emergent in character, perhaps indicating a complex source time history. All of the M_s measurements are from one azimuth and could be biased by the source radiation pattern or propagation effects. One measurement of M_L using the method of Ebel (1982) yields $M_L \geq 5.5$. The body wave moment is reasonably well determined from the synthetic seismogram analysis, and it is consistent with a moment of 5×10^{25} dyne-cm estimated from the surface waves. The time function for this earthquake is about 3 seconds duration and the source depth was about 8 km. A stress drop of 50 to 200 bars is consistent with these data. Like the 1925 earthquake, this event had a thrust mechanism, but the strikes of the nodal planes would either be northwest or northeast. This ambiguity is due to the limited azimuthal range of body-wave data.

1939 Earthquake: This event had m_b estimated to be about 5.0 and relatively few observations of either body waves or surface waves at teleseismic distances. No analysis has yet been attempted on this earthquake.

1940 Earthquakes: A short-period record from Mt. Wilson, California indicates that the December 20 earthquake had m_b about 5.2. The short-period record from the December 24 event is missing, so no direct measurement of m_b for that earthquake can be made. However, at the surface waves from the December 24 event appear to be about a factor of 2 larger than those for the December 20 shock, so the former is judged to be about a .3 of a magnitude unit larger than the latter. No waveform modeling has been performed for either of these events.

1944 Earthquake: Only a cursory examination of the waveforms from this earthquake have been made. The body waves on the several records at hand are very low amplitude and not well-suited for analysis. The surface waves from this shock are somewhat larger than those for the December 24, 1940 earthquake. This event also has not yet been analyzed.

References:

F.M. Anglin, Seismicity and Faulting in the Charlevoix Zone of the St. Lawrence Valley, Bull. Seism. Soc. Am., 74, 595-604, 1984.

G.L. Choy, J. Boatwright, J.W. Dewey and S.A. Sipkin, A Teleseismic Analysis of the New Brunswick Earthquake of January 9, 1982. J. Geophys. Res., 86, 2199-2212, 1983.

J.E. Ebel, M_L Measurements for Northeastern United States Earthquakes. Bull. Seism. Soc. Am., 72, 1367-1378, 1982.

R.L. Street and F.T. Turcotte, A Study of Northeastern North American Spectral Moments, Magnitudes and Intensities, Bull Seism. Soc. Am., 67, 599-614, 1977.

T.C. Wallace, D.V. Helmberger and J.E. Ebel, A Broadband Study of the 13 August 1978 Santa Barbara Earthquake, Bull. Seism. Soc. Am., 71, 1701-1718, 1981.

TABLE 1

Earthquake Sizes

	Magnitude		Moment (dyne-cm)	
	M_B	M_S	Body Waves	Lg Waves*
			1925 La Malbaie, Quebec	
VIE	7.0	6.4	3×10^{26}	2.3×10^{25}
UCC		6.5		
DBN		6.8		
ZUR		6.8		
PAS	6.8	7.0		
RAV		6.4		
HOH		6.4		
HLW		6.3		
AVE.	6.9	6.6		
			1935 Timiskaming, Quebec	
DBN		5.2	2×10^{25}	2.9×10^{24}
COP		5.3		
SCO		5.1		
MWC	5.5			
PAS	5.1			
AVE.	5.3	5.2		
			1982 Miramichi, New Brunswick	
NEIS	5.8	5.1	5.3×10^{24} (A)	1.9×10^{24} (B)
			1978 Santa Barbara, California	
NEIS	5.5	5.6	1.1×10^{25} (C)	

* From Street and Turcotte (1977)
(A) From Choy *et.al.* (1983)
(B) From HRVD long-period moment-tensor solution
(C) From Wallace *et.al.* (1981)

Whole Waveform Inversion of Regional Digitial Seismic Data
Estimation of Anelastic Attenuation in Surficial Layers

14-08-0001-20640

Robert B. Herrmann
Department of Earth and Atmospheric Sciences
Saint Louis University
P.O. Box 8099 Laclede Station
St. Louis, MO 63156
(314) 658-3131

Goals

1. Investigate the possibility of using high frequency regional network data for the direct inversion for focal mechanism and seismic moment by waveform inversion.

2. Use short period surface waves recorded as part of refraction surveys to determine shallow shear wave velocity and shear wave Q structure.

Investigations

1. Waveform studies are progressing well. The systematics of how to approach the inversion process are being discerned. Basically, the object is to match observed digital data waveforms with synthetics. Rather than starting first with a complete waveform matching procedure. the following steps are used:

   a) use P-wave first motion data to estimate free surface angle in incidence, which is used to check the appropriateness of the earth model used;

   b) find all focal mechanisms that satisfy P-wave first motion data;

   c) find the subset of the solutions of b) which satisfy S/P amplitude ratios and intratrace amplitude ratios;

   d) find the subset of c) which matches the observed waveforms.

   We have had considerable success with some of the New Brunswick aftershocks, and are still examining the Arkansas and Monticello data sets. The work is still developmental in that the processing steps are still not a series of simple steps and because the effect of shallow earth structure. upper hundreds of meters, is known to be important but is not well constrained.

2. An interactive surface wave inversion package has been developed and is being thoroughly tested. The package contains programs for spectral analysis, phase matched filtering, phase and group velocity inversion for shear-wave structure. inversion for shear wave Q, and generation of synthetic seismograms for comparison. These programs are designed for use on 16 bit minicomputers, but will of course function well on larger machines.

   The programs developed will be one Volume in the multi-volume Computer Programs in Seismology being compiled now.

   There are many ways of combining dense surface wave data to obtain data for Q inversions. Unfortunately, such data sets are not that available. There has been some success in estimating Q-models using single station data. The idea is very simple. First, an observed surface, from a blast recorded by a regional network, is analyzed to obtain group velocity dispersion and hence a path average shallow shear-wave structure. Using this earth model, synthetic seismograms are generated interactively, using different Q-models. The effect of the Q-model on the waveform is substantial, and a crude, but important, idea can be obtained of the appropriate shallow Q-structure.

Reports

Russell. D., H. J. Hwang and R. B. Herrmann (1984). SURF: An interactive set of surface wave dispersion programs for analyzing crustal structure. 56 th Annual Meeting Eastern Section, Seismological Society fo America, Saint Louis University, October 10-12 (Abstract).

Saikia. C. K. and R. B. Herrmann (1984). Source mechanism of the aftershocks of the New Brunswick earthquake, 1982, 56 th Annual Meeting Eastern Section, Seismological Society fo America, Saint Louis University. October 10-12 (Abstract).

ESTIMATION OF NEAR-SOURCE HIGH-FREQUENCY GROUND MOTION FOR LARGE MAGNITUDE EARTHQUAKES

14-08-0001-21349

Robin K. McGuire

Dames & Moore
1626 Cole Boulevard
Golden, Colorado 80401
(303) 232-6262

Investigations

A stochastic model is developed for the prediction of high-frequency near-field ground motions during large-magnitude earthquakes (6 $1/2<\mathbf{M}<8$) in the western United States. The finite thickness of the seismogenic zone--which causes the rupture areas of large earthquakes to have elongated shapes--is taken into account by adopting Joyner's (1983) generalization of the Hanks-McGuire (1981) source spectrum. This model contains two corner frequencies: one associated with the total faulting duration and another associated with the rise time. The source spectrum is then interpreted in terms of a separable kinematic model of faulting. This kinematic model determines the space-time distribution of energy release, as well as directivity effects.

For the determination of model parameters, it is assumed that fault width is limited by the thickness of the seismogenic zone, that average slip scales with rupture length, and that the high-frequency level of acceleration scales with the square root of rupture length. In addition, it is assumed that the postulated source spectrum agrees with the Hanks-McGuire spectrum for earthquakes with equal rupture length and width. These assumptions leave one free spectral parameter, which controls the scaling of rise time, the smoothness of slip along the fault, and the smoothness of the dislocation time function. Two attractive choices of that parameter are discussed, including their physical significance and quantitative consequences. An alternate form of the model is also identified; this form combines the features of the above two choices of the parameter and agrees with Das' (1982) findings on the kinematics of earthquakes with long rupture areas.

Based on the source spectrum and the equivalent kinematic model, a stochastic-process model of ground acceleration is constructed. The model is made nonstationary to account for the effect of time-varying distance and azimuth. These effects are important for sites where the minimum distance to the fault is of the same order as the rupture length. The stochastic model is used to evaluate the variation in time of the instantaneous rms and central frequency of ground acceleration; these are then used to compute the probability distribution of peak ground acceleration. In addition, the effect of spatial variation of the (local-average) stress drop (i.e., the variation of energy release along the rupture) is modeled by means of a random process of stress drop along the fault. This is accomplished through an efficient Monte Carlo simulation, in which only sample functions of stress drop are simulated.

Results

The model is used to compute expected values and variances of ln [peak acceleration] for moment magnitudes up to 8 1/2 and for distances of 1 through 100 km; several values of the model parameters are considered. Results are compared with the available strong-motion data, finding reasonable agreement. The only serious discrepancy occurs with the Kern County data, which constitute a large portion of the available $M \geq 7$ data; they exceed model predictions by a factor of 2. Some possible explanations for these differences are discussed.

REFERENCES

Hanks, T.C., and R.K. McGuire, 1981. "The Character of High-Frequency Strong Ground Motion," Bull. Seis. Soc. Am., Vol. 71, pp. 2071-2095.

Joyner, W.B., 1983. "A Scaling Law for the Spectra of Large Earthquakes," submitted to the Bull. Seis. Soc. Am.

Analysis of Earthquake Ground-Shaking Hazard for the Salt Lake City-Ogden-Provo Region

21914

M.S. Power, F.H. Swan, III, D.P. Schwartz, R.R. Youngs
Woodward-Clyde Consultants
100 Pringle Avenue
Walnut Creek, California 94596
(415) 945-3000

Objectives: We have recently initiated an assessment of ground motion hazard for the Ogden-Salt Lake City-Provo urban corridor using a probabilistic approach, often termed a seismic exposure or a seismic hazard analysis. The seismic exposure or seismic hazard is expressed as levels of a ground motion parameter, such as peak ground acceleration, having certain probabilities of being exceeded during a specified time period. The results of this study will be shown on regional maps as contours of peak ground acceleration for selected probabilities of exceedance. Also, acceleration response spectra corresponding to selected probabilities of exceedance will be developed for representative locations in the study region for use in further establishing the damage potential of ground motions to buildings.

The seismic exposure at any particular site location in the region depends on:

1. The location and geometry of earthquake sources relative to the site.

2. The frequency of occurrence (i.e., recurrence) of earthquakes of various magnitudes on the sources, up to the maximum magnitude for each source.

3. The attenuation of ground motions from the sources to the site.

In the basic seismic exposure analysis, these factors are incorporated in three probability functions:

1. The probability that the earthquake rupture surface is a specified distance from the site is assessed by considering both fault location and geometry and the relationship between earthquake magnitude and rupture area.

2. The recurrence rate is used to calculate the probability that an earthquake of a particular magnitude will occur during a specified time period. The magnitude range is limited by the maximum magnitude possible on the source.

3. The probability that the ground motions from an earthquake of a certain magnitude occurring at a certain distance will exceed a specified level at the site is based on the selected attenuation relationship.

By combining the three probability functions, the probability of exceeding a specified level of ground motion at a site within the specified time period is computed. A relationship between ground-motion level and probability of exceedance is obtained by repeating the exposure computation for several levels of ground motion. The ground-motion level corresponding to a specified probability of exceedance (or return period) is then obtained from this relationship. A schematic diagram of the basic seismic exposure analysis model is shown in Figure 1.

In a basic seismic exposure analysis, it is assumed that certain source characterization parameters, including fault segment length, fault dip, fault width, maximum earthquake magnitude, and earthquake recurrence rate, are known with certainty. In fact, there usually is uncertainty in these parameters, which can significantly affect estimates of the seismic exposure. In the present study, these uncertainties in source characterization parameters are being incorporated through an extended seismic exposure model using logic trees.

Results: Work conducted to date has focused on the selection and characterization of the seismic sources that contribute to the seismic exposure of the study area. Two different types of sources are being examined: known faults that can produce moderate to large magnitude earthquakes and a "floating" source that accounts for smaller magnitude earthquakes that cannot be associated with known geologic structures. The selected sources are shown in Figure 2. These are: segments of the Wasatch fault (sources 1-6), the East Cache fault (source 7), the Strawberry Valley fault (source 8), the Oquirrh-Boulter-Tintic fault (source 9), the Oquirrh Marginal fault (source 10), and a fault zone in Great Salt Lake (source 11). Sources 1 through 10 are each defined by lake Pleistocene and/or Holocene fault scarps; source 11 is interpreted from seismic reflection profiles.

For each fault data are being obtained that characterize it in space (geometry) and time. These data include potential fault rupture length, fault width (based on dip and down dip extent), displacement per event, slip rate, average recurrence intervals, deviation from mean recurrence, and elapsed time since the most recent event. These data from the Wasatch and East Cache faults are summarized in Table 1.

Reports: Power, M.S., Schwartz, D.P., Youngs, R.R., and Swan, F.H., III, Analysis of earthquake ground-shaking hazard for the Salt Lake City-Ogden-Provo region: Paper presented at the Workshop on Evaluation of Regional and Urban Earthquake Hazards and Risk in Utah, Salt Lake City, August 14-16, 1984.

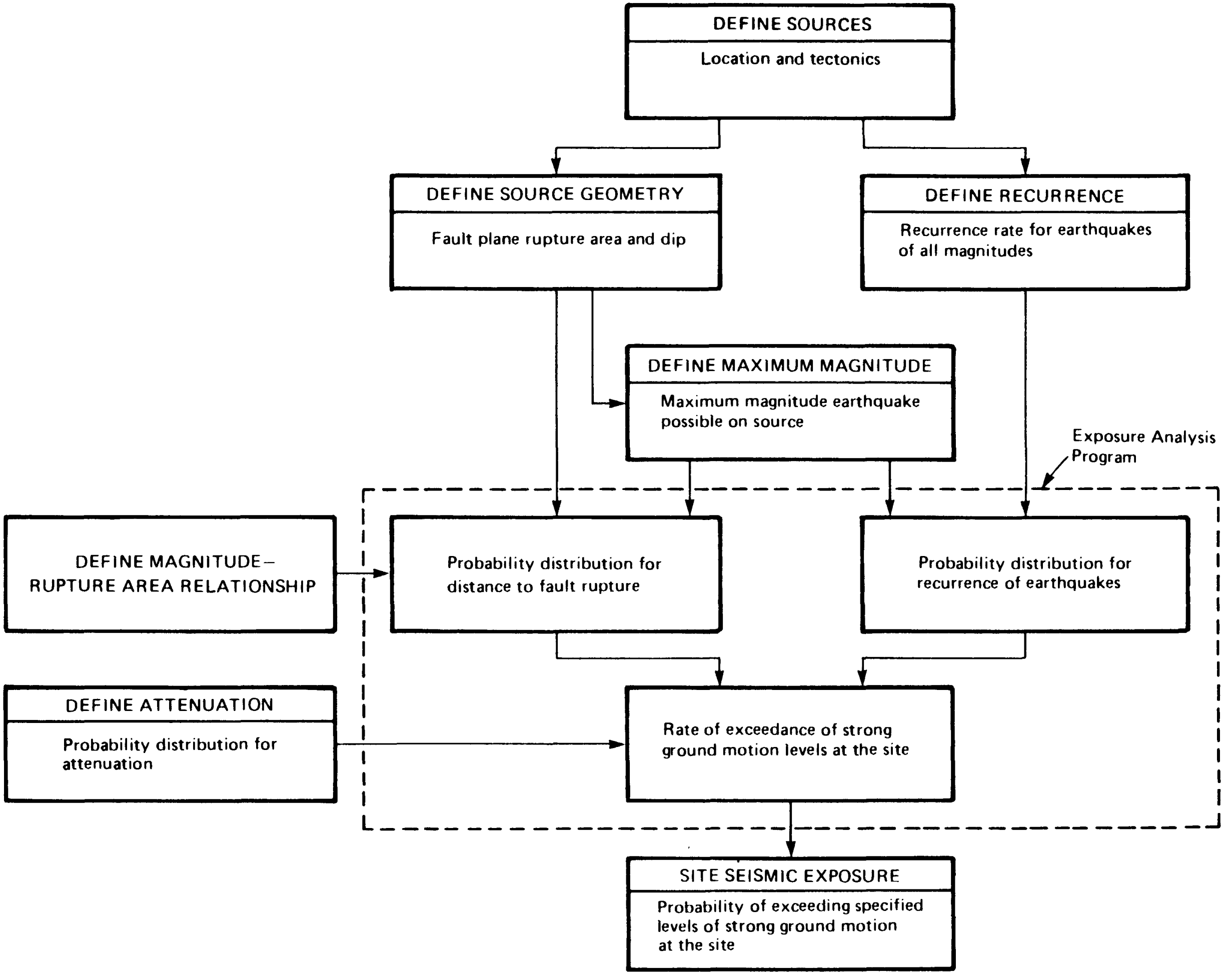

Figure 1. Schematic Diagram of Seismic Exposure Model

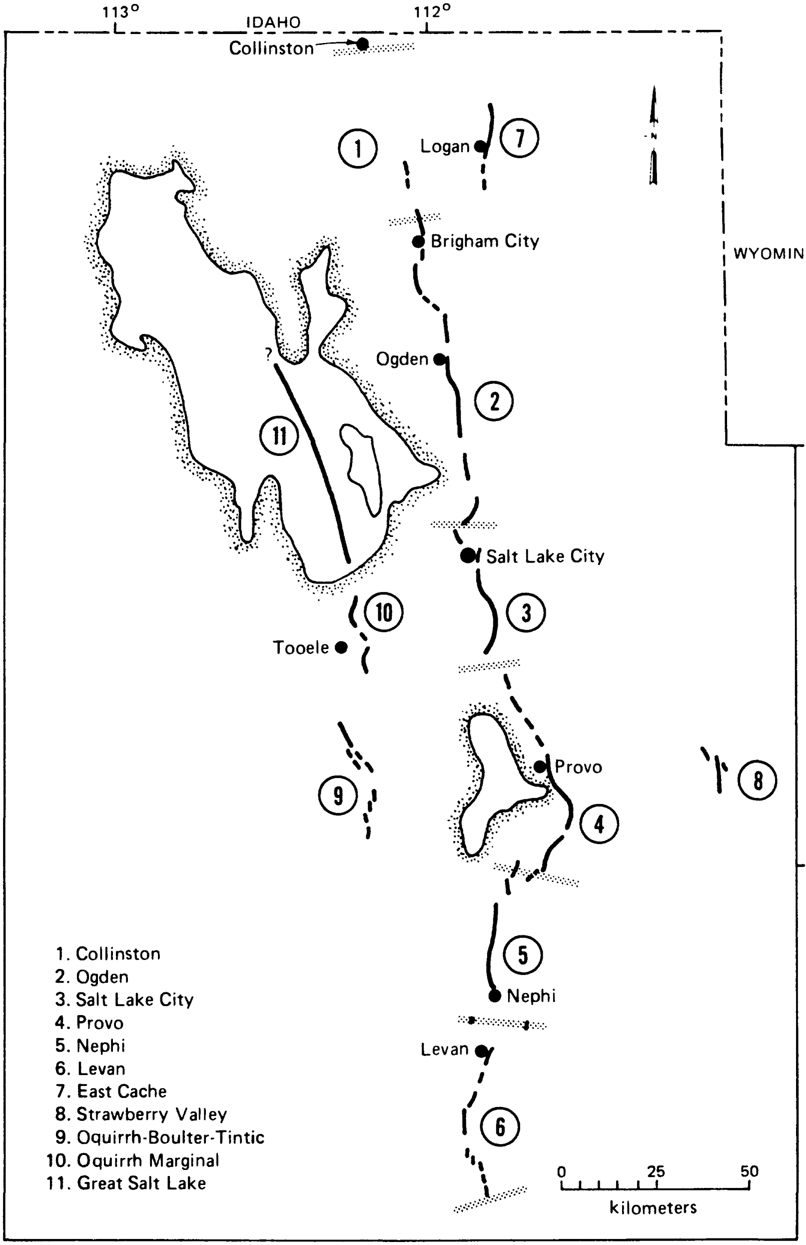

Figure 2. Map of Proposed Sources (faults and fault segments) for Seismic Exposure Analysis of Ogden-Salt Lake-Provo Corridor. Wasatch Fault Zone Segments Are from Schwartz and Coppersmith (1984)

TABLE 1

FAULT BEHAVIOR DATA
WASATCH FAULT ZONE

Segment	Site	Slip Rate (mm a^{-1})^{a}	Displacement per Event (m) Measured	Displacement per Event (m) Average^{b}	Recurrence Interval	Recurrence Average (yr)	Elapsed Time (yr)^{c}	Reference
Collinston	-	$\geq$ 0 (13,500)	-	-	-	-	$\geq$ 13,500	Schwartz and others (1983)
Ogden	Kaysville	1.3 (+0.5, -0.2)^{e} (8,000; +1000, -2000)	1.6 1.7	- -	2 (after 1580)^{d}	2000	$\leq$ 500	Swan and others (1980)
Salt Lake City	Little Cottonwood Canyon	0.76 (+0.6, -0.2) (19,000 ± 2000)	-	2 (2)	-	2400-3000	-	Swan and others (1981); Schwartz and Coppersmith (1984)
Provo	Hobble Creek	0.85 - 1.0^{e} (13,500)	2.7	1.6-2.3 (6-7)	6-7 (after 13,500)	1700-2600	> 1000	Swan and others (1980)
Nephi	North Creek	1.27-1.36 (± 0.1) (4580)^{d}	2.0-2.2 2.0-2.5 2.6	2.3 (3) -	2 (between 4580 and 3640)^{d} 1 (after 1100)^{d}	1700-2700	300-500	Schwartz and Coppersmith (1984)
Levan	Deep Creek	$\leq$ 0.35 ± 0.05 (7300)^{d}	2.5	-	1 (after 7300)^{d}	-	<1750^{d}	Schwartz and Coppersmith (1984)
East Cache	Logan	0.1-0.2 (14,000-15,000)	1.35 1.4	- -	1 (between 15,000 and 13,500) 1 (after 13,500)	-	6000-10,000	Swan and others (1982)

a Age of displaced datum (years B.P.) on which slip rate is based is shown in parentheses.
b Number of events on which average is based is shown in parentheses.
c Time in years since the most recent surface faulting earthquake.
d Age in ^{14}C yr B.P.
e Modified from Swan et al. (1980).

Detailed Geologic Studies, Central San Andreas Fault Zone

9910-01294

John D. Sims
Branch of Engineering Seismology and Geology
U.S. Geological Survey
345 Middlefield Road, MS 977
Menlo Park, California 94025
(415) 323-8111, ext. 2252

Investigations

Detailed geologic field investigations of structure, and surficial and bedrock deposits in and adjacent to the central section of the San Andreas fault zone (San Juan Bautista to Wallace Creek, Carrizo Plain) were conducted to determine horizontal and vertical slip rates and the detailed tectonic environment of the zone. Investigations are conducted through detailed geologic mapping, trenching studies, and geomorphic study of offset terraces and stream courses.

Results

1. Studies of rates of slip along the San Andreas and Calaveras-Paicines faults continue. Results of trench studies along the San Andreas fault at Melendy Ranch indicate an average slip rate of ~ 22 mm/yr during the last 800 years. This geologically determined rate is in good agreement with geodetically determined rates of 20-22 mm/yr recorded by creepmeters and alinement arrays. These data strongly suggest the San Andreas fault at Melendy Ranch has had uniform slip for the last 800 years. Field studies along the Calaveras-Paicines fault is complete and charcoal samples have been submitted for ^{14}c analysis.

2. Mapping of the fault zone continues (fig. 1). Analysis of interpretation of the tectonic and stratigraphic data in the Parkfield area shows that the Gold Hill fault may be traced into the Stockdale Mountain quadrangle. Mapping in the Parkfield-Cholame Hills and Cholame Valley quadrangles is now complete. Mapping is in progress in the Stockdale Mountain, Cholame, and Orchard Peak quadrangles. Completed mapping now covers nearly all of the area expected to contain ruptures in the next Parkfield earthquake.

Reports

Harms, K. K., Clark, M. M., Rymer, M. J., Bonilla, M. G., Harp, E. L., Herd, D. G., Lajoie, K. R., Lienkaemper, J. J., Mathieson, S. A., Perkins, J. A., Wallace, R. E., and Ziony, J. I., 1984, The April 24, 1984 Morgan Hill, California earthquake: The search for surface faulting, in Hoose, S. N., ed., The Morgan Hill, California earthquake of April 24, 1984: U. S. Geological Survey, Open-File Report 84-498A, p. 92-108.

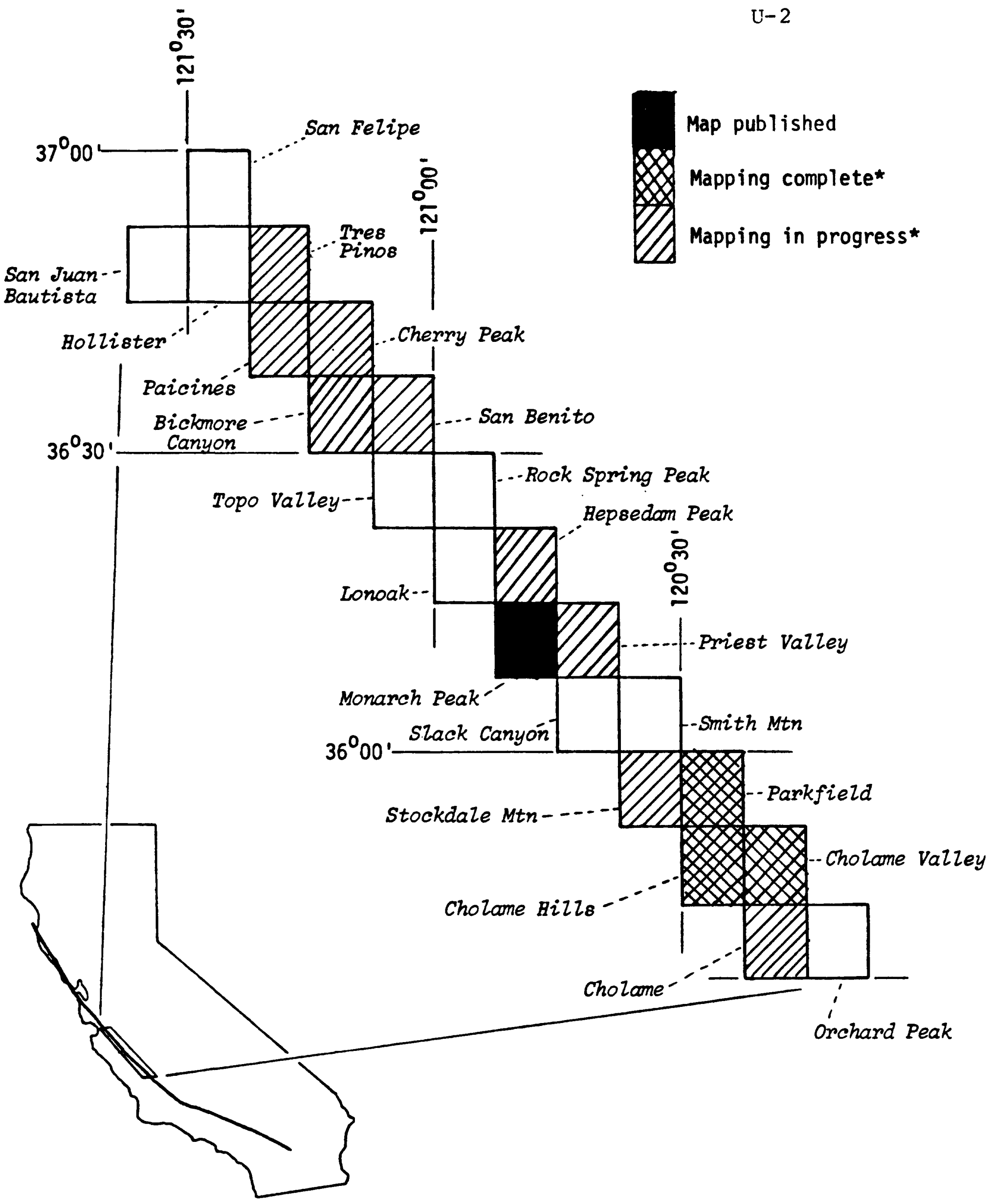

Figure 1 . **Index map of 7 1/2-minute quadrangles to be studied** in the detailed mapping part of the project. A part of each quadrangle is to be mapped in detail. The mapped part is a srtip varying from 3 to 10 km wide that includes the San Andreas Fault Zone. The fault zone is approximately located in the middle of the mapped strip.

Source and Path Effects for Northeastern US Earthquakes - Implications for Earthquake Hazards

Contract No. 14-08-0001-21284

M. Nafi Toksöz and Jay J. Pulli
Earth Resources Laboratory, M.I.T.
42 Carleton St., Cambridge, MA 02142
(617) 253-7852

Investigations:

1) Determination of the source mechanism of the January 11, 1982 aftershock of the New Brunswick earthquake using body wave inversions.

2) Determination of the source mechanism of the October 7, 1983 Adirondack, NY (Goodnow) earthquake using body wave inversions.

3) Examination of the intensity data for the October 7, 1983 Adirondack, NY earthquake.

Results:

1) The January 11, 1982 aftershock of the New Brunswick earthquake was the largest aftershock of this series (m_b=5.4). This earthquake was too small to produce clear long period P-waves at teleseismic distances, so we have studied the short period waveforms using the waveform inversion technique[1]. Figure 1 shows the data and synthetics for the best solution. The source depth was 5.3 km with a scalar seismic moment of $4.1(10)^{23}$ dyne-cm. The fault plane has a strike of 345°, a dip of 53°, and a rake of 98°. The duration of the source time function was 0.92 sec. This event has a similar mechanism as the main shock, but is simpler and shallower. One reason we have studied this event is that it helps us distinguish source effects from structural effects in the observed waveforms of the January 9 main shock (m_b=5.7). By comparing these two events, we find that the initial oscillation in the waveforms of the January 9 event that was identified as the first of two subevents [2] was indeed a source effect, because it was not observed for the aftershock.

2) The October 7, 1983 earthquake in the Adirondack Mountains of NY (near Goodnow) was the largest earthquake in NY during the last 40 years (m_b=5.2). Excellent recordings were obtained for this event at both regional and teleseismic distances. The source mechanism for this event has been studied using the waveform inversion technique for short period data (Figure 2) [3]. The source depth was 7 km and the scalar seismic moment was $2.5(10)^{23}$ dyne-cm. Using a source radius of 0.75 km from the aftershock distribution [5], a value of 140 bars is obtained for

the stress drop. This is a relatively high value and provides additional support for the hypothesis that earthquakes in the northeastern US are of high stress drop.

3) With the assistance of the Lamont-Doherty Geological Observatory and Weston Observatory of Boston College, we have collected approximately 1300 intensity datapoints for the October 7, 1983 Adirondack earthquake. This project is part of our continuing study of seismic wave and intensity attenuation in the northeastern US [4]. This new data significantly increases our database and provides better coverage for areas west of the Appalachians where the attenuation of seismic waves is lower. Intensity attenuation models are now being recalculated by areally separating the datsets. Figure 3 shows the modal site intensity values obtained in this study as well as the theoretical intensity distribution for an $m_b=5.2$ earthquake [4,6]. The figure shows that this event was generally felt at one intensity level higher than predicted by the model. We are currently investigating whether or not this is a problem with the intensity interpretations. Also, the event was widely felt to the east and west, but not to the north and south. This may be a source effect, indicating that the intensity was mainly a response to S-waves or surface waves radiating perpindicular to the fault planes.

Reports and References:

1. Nabelek, J.L. (1984), Determination of Earthquake Source Parameters from Inversion of Body Waves, *PhD Thesis*, Massachusetts Institute of Technology, Cambridge, MA, 361 pp.

2. Nabelek, J.L., Suarez, G., and Toksöz, M.N. (1982), Source parameters of the New Brunswick earthquake of January 9, 1982 from inversion of teleseismic body and surface waves, *(abstract)*, *Earthquake Notes*, *53*, No. 3, 28.

3. Suarez, G., Seeber, L., Aviles, C., Schlessinger-Miller, E., and Nabelek, J.L. (1984), The Goodnow, NY earthquake: results from a broadband teleseismic analysis, *(abstract)*, *EOS*, *65*, 239-240.

4. Pulli (1984), Attenuation of coda waves in New England, *Bull. Seis. Soc. Amer.*, *74*, 1149-1166.

5. Seeber, L., Cranswick, E., Armbruster, J., and Barstow, N. (1984), The October 1983 Goodnow aftershock sequence, regional seismicity, and structural features in the Adirondacks, *(abstract)*, *EOS*, *65*, 240.

6. Klimkiewicz, G.C. (1982), Reassessment of ground motion attenuation models for the northeast, *(abstract)*, *Earthquake Notes*, *53*, No. 3, 23-24.

New Brunswick
aftershock 11 January 1982
mb = 5.4

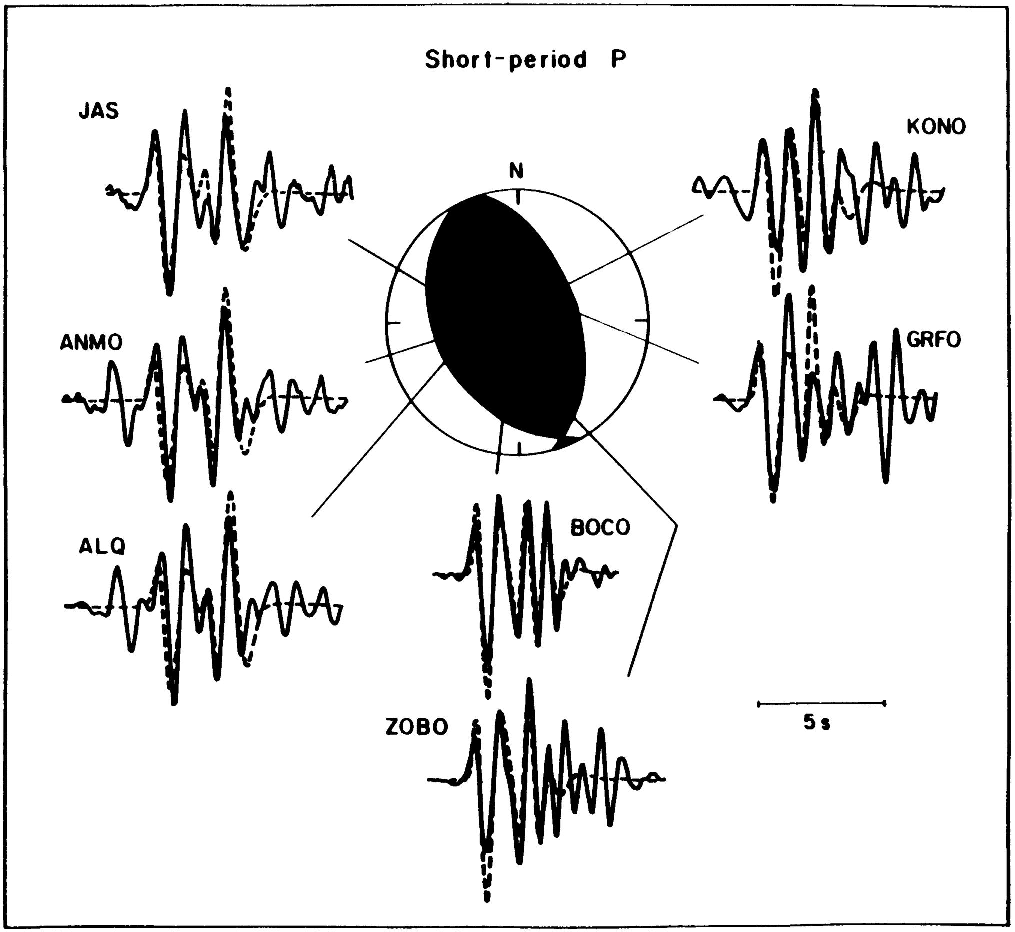

Figure 1

GOODNOW, N.Y.

MAIN EVENT 10/07/83

$m_b = 5.2$

INVERSION OF SHORT-PERIOD P-WAVES

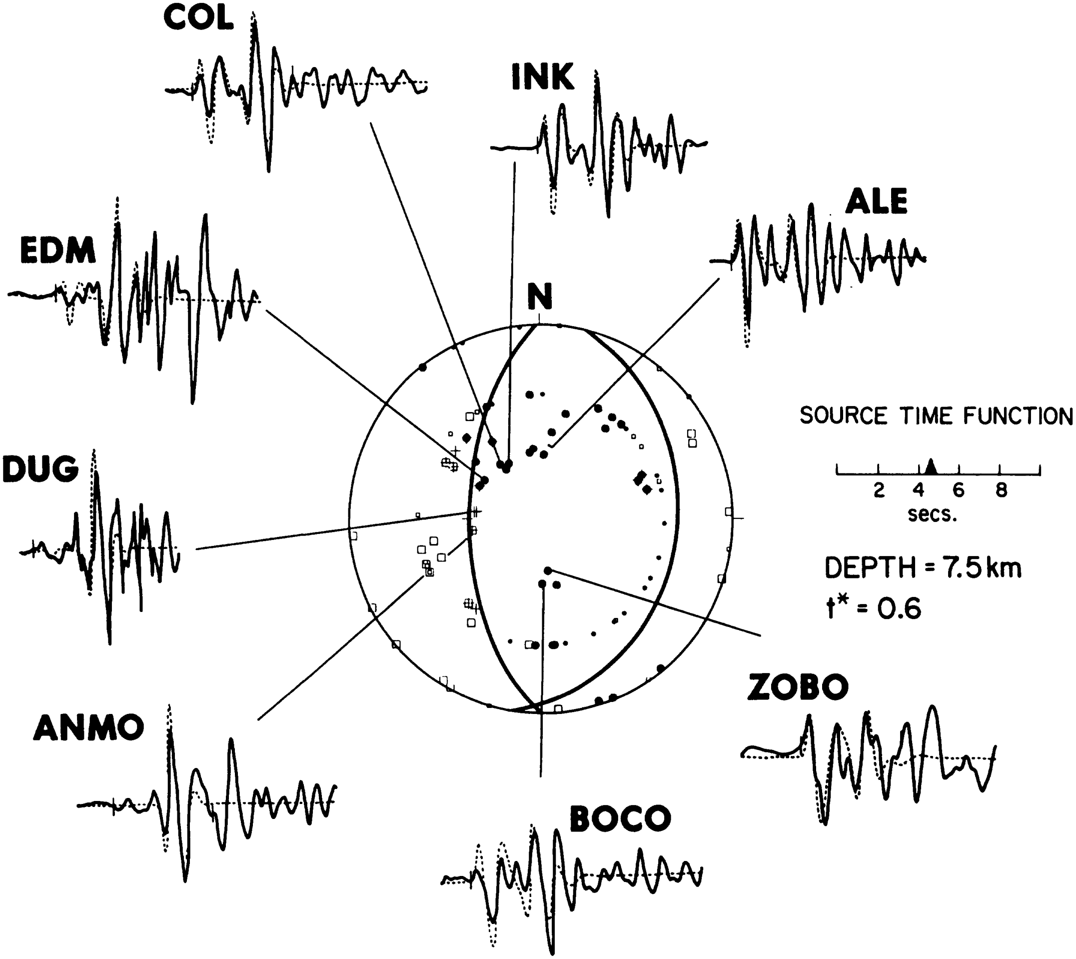

Figure 2

Observed intensity points for the Goodnow, NY earthquake with theoretical isoseismals using the equation by Klimkiewicz (1982)

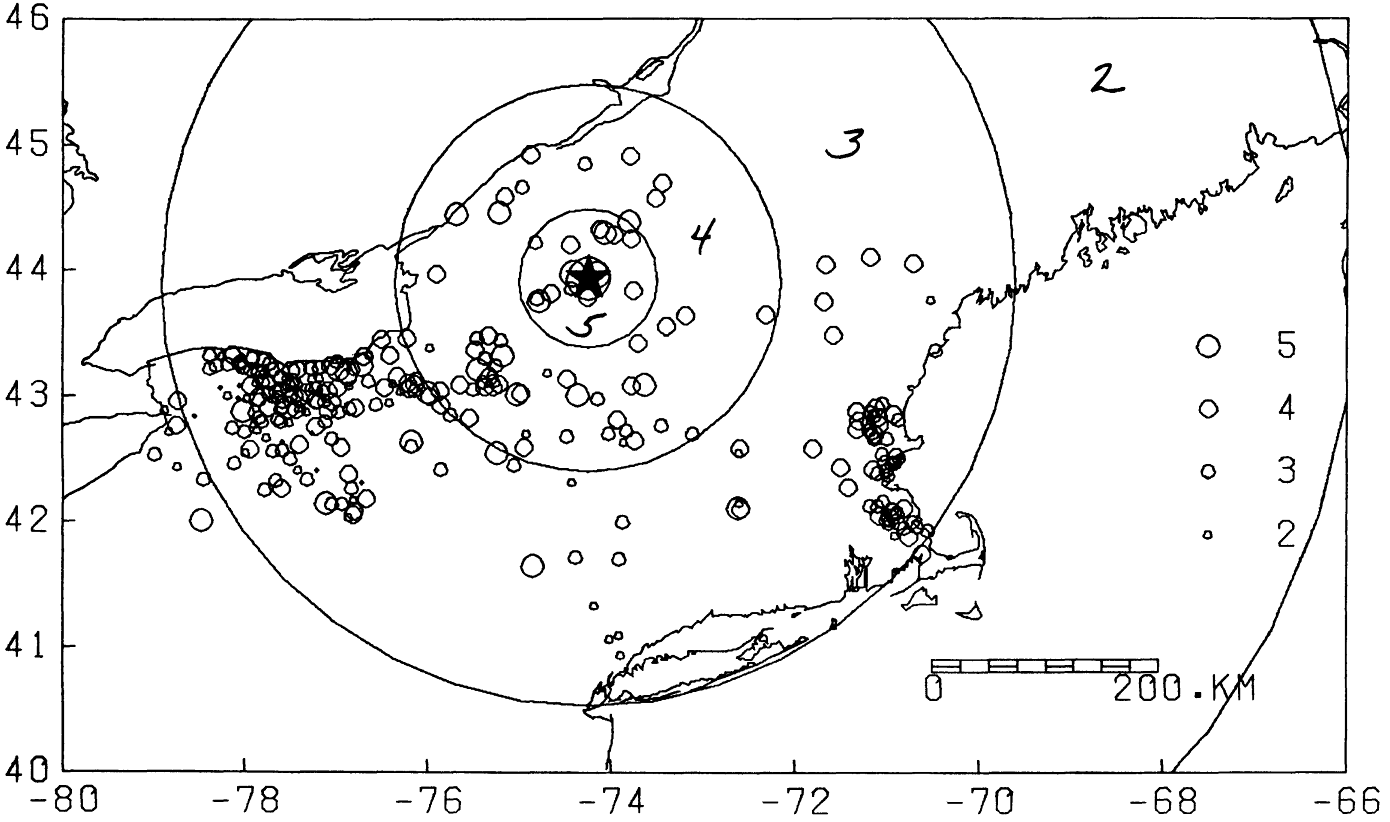

Figure 3

Physical Constraints on Source of Ground Motion

9910-01915

D. J. Andrews
Branch of Engineering Seismology and Geology
U.S. Geological Survey
345 Middlefield Road, MS 9-77
Menlo Park, California 94025
(415) 323 8111 ext. 2752

Investigations

Application of the diffusion equation to scarp degradation.

Results

For a change of pace I have pursued Tom Hanks' idea that fault scarp profiles evolve according to the diffusion equation. The second moment of a localized disturbance governed by the linear diffusion equation grows linearly in time. The zeroth, first, and second moments of slope of an observed scarp profile can provide an inverse solution for scarp age, if the initial second moment is provided by some model assumption, such as a given initial slope.

A program has been written to accept an observed profile, find the product of diffusivity times age, and plot the fitted solution together with the data.

The inverse program has been tested with synthetic data calculated by both analytic and finite difference methods. Dependence of the age determination and profile shape has been investigated for varying initial profiles, multiple fault traces, multiple events, and non-linear dependence of mass flux on slope.

Report

Andrews, D. J., 1984, Mixed-Mode Shear Crack Propagating Between Rayleigh and S-Wave Velocities [abs.]: AGU Fall Meeting.

Strong-Motion Interpretation for Structural Engineering

9910-02759

Joseph J. Fedock/ Hsi-Ping Liu
Branch of Engineering Seismology and Geology
U.S. Geological Survey
345 Middlefield Road, MS 977
Menlo Park, CA 94025
(415) 323-8111 x 2024

Investigations

The focal points of investigations continue to center around three separate areas related to the earthquake response of engineering structures:

1) The development of a new testing technique that can be used to determine the in-place dynamic properties of dam structures. Continued research and development in this area will provide a better understanding of the seismic behavior of large concrete and earth dams since many of the limitations of existing forced vibration techniques can be circumvented by this new methodology.

2) The design of strong-motion instrumentation schemes for engineering structures such as buildings, dams, and bridges. The coordination and implementation of this instrumentation program continues to constitute a major portion of the research effort.

3) Analysis of strong-motion records that have been obtained from structures instrumented by the USGS and other agencies. These analyses are used to improve the state-of-the-art in the earthquake-resistant design procedures, and to provide feedback for the selection of structures and the type and extent of strong-motion instrumentation to be employed at new and existing structures.

Results

A successfull experiment was conducted during late August 1984 at Monticello Dam, a concrete arch structure located near Vacaville, California. This dynamic test utilized a high-pressure air gun as the source of excitation in which nine seismometers were located at three separate crest locations on the dam to record structural responses. The air gun was suspended from a pontoon boat in the reservoir behind the dam approximately 30 ft from the dam face. Measurements of the dam's motions were obtained for various depths of the air gun in the reservoir and for several pressure values of the air.

Preliminary observations of the recorded data show that some vibrational modes of the dam were noticeabley excited by the air gun test. More extensive analyses of these records are being initiated.

During the second half of FY 1984 the strong-motion instrumentation network at the Transamerica Building, San Francisco, was completed and is now operational. Instrumentation schemes at Pacific Park Plaza, Emeryville, and Great Western Bank, Berkeley, have been initiated in which both free-field and structure accelerographs are to be employed. Additional instrumentation designs are underway.

An investigation of structures suitable for strong-motion instrumentation in the San Francisco Bay Region has been completed and a similar study of dams in California is being initiated.

The Mammoth Lakes earthquake sequence of May 1980 has provided some of the most extensive acceleration records available for studying the seismic response of an earth dam subjected to strong ground shaking. Long Valley Dam, located near Bishop, California, was instrumented with 22 accelerometers on its embankment and in the immediate vicinity, and over 60 high-quality, long-duration accelerograms were recorded for the three largest earthquakes of the sequence. The time-history motions from these three events were analyzed to determine the main features of the dam's motions. Comparisons of free-field and embankment responses were made to help establish the amplification of the structural motions and identify modes of vibration of the structure. Finally, representative material properties were estimated using existing theories of earth dam behavior and comparisons of observed natural periods with those predicted by the various theories were performed.

Reports

Fedock, J., "Strong-Motion Instrumentation of Earth Dams", Proceedings of the Eighth World Conference on Earthquake Engineering, Vol. 7, pp. 367-374, July 1984.

U.S. Geological Survey San Francisco Bay Region Instrumentation Advisory Committee, "Report on Recommended List of Structures for Seismic Instrumentation in the San Francisco Bay Region", U.S. Geological Survey Open-File Report, 84-488, June 1984.

Estimating Strong Ground Motion for Engineering Design and Seismic Zonation

9910-01168

W. B. Joyner
D. M. Boore

Branch of Engineering Seismology and Geology
U. S. Geological Survey
345 Middlefield Road, MS 977
Menlo Park, California 94025
(415) 323-8111, Ext. 2754, 2698

Investigations

1. Analysis of strong-motion data leading to the development of predictive equations for strong-motion parameters and development of methodology for making predictive maps of strong ground motion.
2. Cooperation with professional groups in the development of code provisions for earthquake resistance.
3. Study of the scaling of earthquake spectra.

Results

Recommendations have been prepared for revisions in the seismic zoning of California as used in building codes. These recommendations are under study by the Structural Engineers Association of California.

Reports

Bakun, W.H., and Joyner, W.B., 1984, The M_L scale in central California: Bulletin Seismological Society of America, scheduled for the October issue.

The Effects of Site Geology on Ground Shaking on the Wasatch Front

9950-03788

A. M. Rogers
Branch of Engineering Geology and Tectonics
U.S. Geological Survey
Box 25046, MS 966, Denver Federal Center
Denver, CO 80225
(303) 236-1585

Investigations

This study builds upon the work of several previous studies in the Wasatch Front urban area. Hays and King (1982) and King and others (1983) published a study of seismic response based on recorded ground motions at 42 sites in the Wasatch Front region induced by distant explosions and an earthquake. The sites were chosen to sample a variety of geologic conditions. Response spectra and alluvium-to-rock spectral ratios were computed from the horizontal-component data recorded at each location. Generalized descriptions of the lithology underlying each recording site were obtained from R. D. Miller's (written commun., 1984) maps of unconsolidated surficial deposits. The lithologic descriptions were categorized into three groups: silt and clay, sand and gravel, and rubble. The log-normal mean of the spectral ratios was then computed for each of the lithologic groups for two period bands (0.2 to 0.7 s for the short-period band and 0.7 to 1.0 s for the long-period band).

Results

In the short-period band, the mean spectral ratios vary from 2.7 (rubble sites) to 6.2 (silt and clay sites), while in the long-period band, they vary from 3.2 to 7.2, respectively (fig. 1). Ninety-percent confidence intervals about the mean spectral ratios indicate that stations underlain by silt and clay have significantly higher short-period response than those underlain by sand and gravel. There are too few sites underlain by rubble to obtain statistically meaningful results. The results for the long-period data also are not statistically significant using this categorization. Based on this analysis, we have produced maps (figs. 2, 3, and 4) for the urban areas of Brigham City, Ogden, Salt Lake City, and Provo, showing expected relative ground-shaking response for the short-period band.

References cited

Hays, W. W., and King, K. W., 1982, Zoning of the earthquake ground-shaking hazard along the Wasatch Fault zone, Utah: Third International Earthquake Microzonation Conference, Seattle, 1982, Proceedings, v. 3, p. 1307-1318.

King, K. W., Hays, W. W., and McDermott, P. J., 1983, Wasatch Front urban area seismic response data report: U.S. Geological Survey Open-File Report 83-452, 68 p.

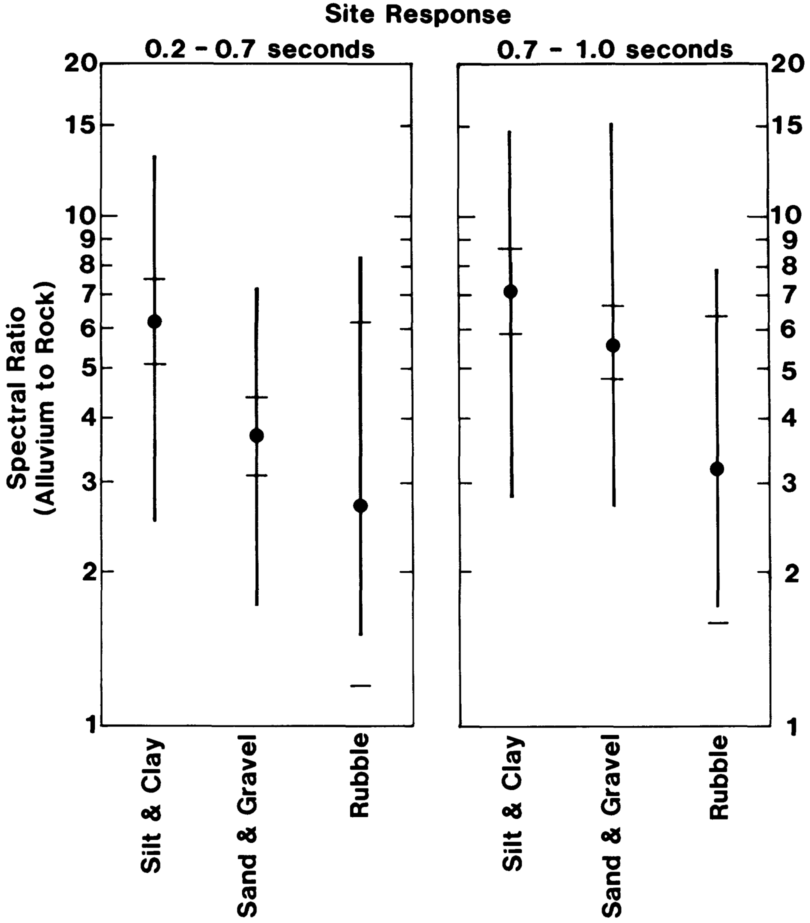

Figure 1.--Response relative to bedrock of sites underlain by three categories of surface deposit: silt and clay, sand and gravel, and rubble. Solid dots indicate the log-normal mean of the spectral ratio for each category. Vertical bars indicate the range of individual sites' spectral ratios in the category. Horizontal bars show the 90-percent confidence intervals for each category.

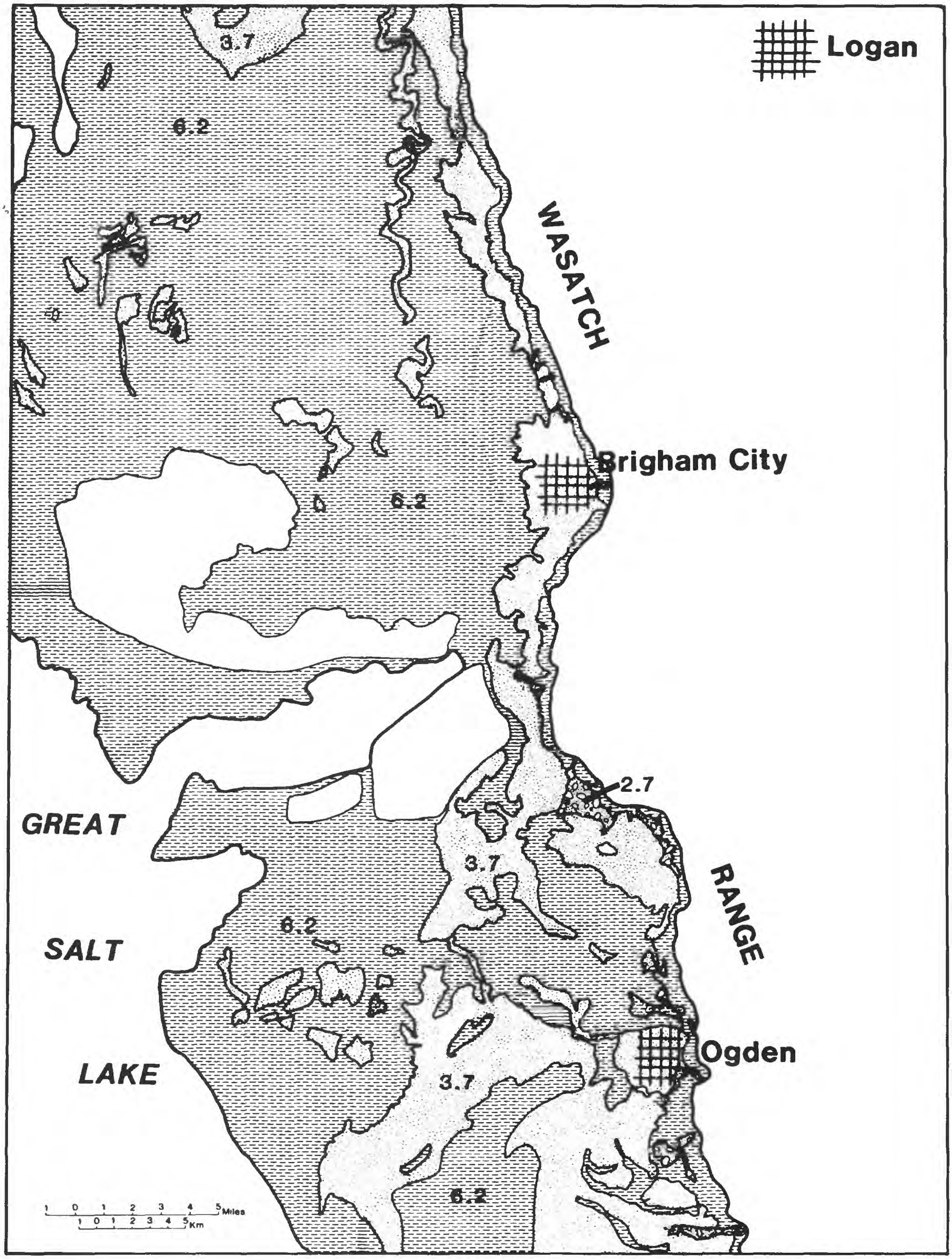

Figure 2.--Map of expected relative ground-shaking response in the north part of the Wasatch Front urban area. Numbers indicate mean ground response relative to bedrock locations.

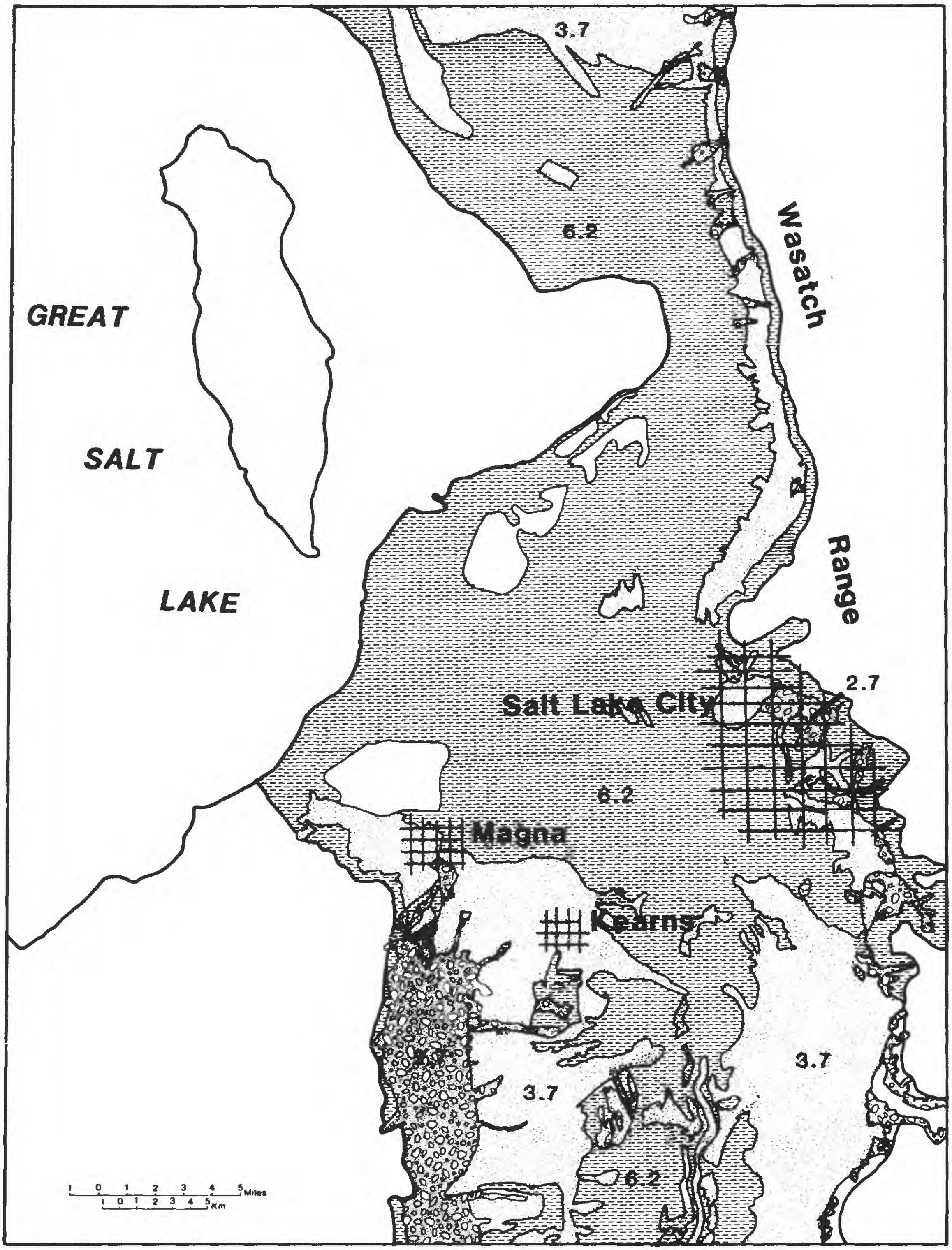

Figure 3.--Map of expected relative ground-shaking response in the central part of the Wasatch Front urban area. Numbers indicate mean ground response relative to bedrock locations.

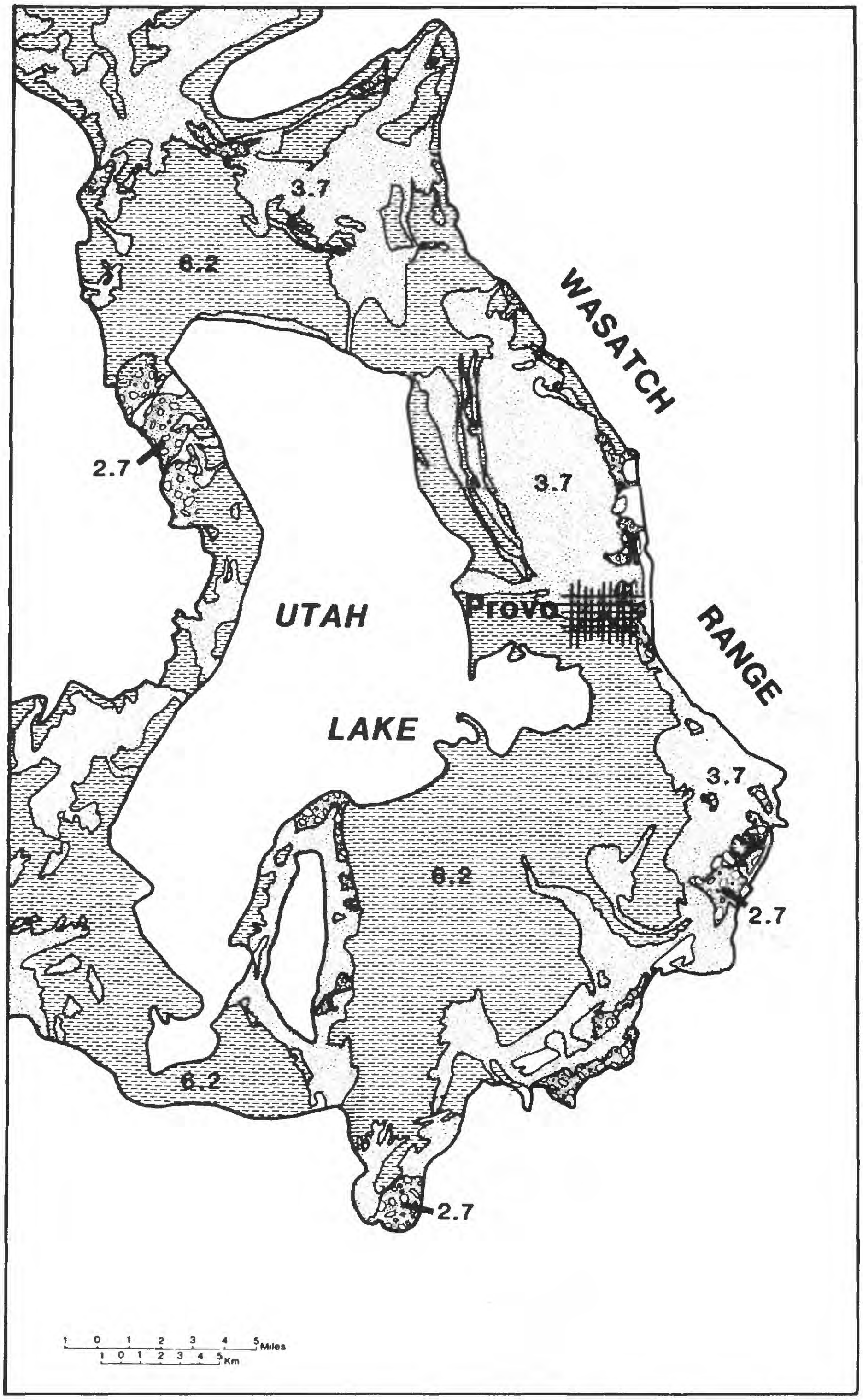

Figure 4.--Map of expected relative ground-shaking response in the south part of the Wasatch Front area. Numbers indicate mean ground response relative to bedrock locations.

Strong Ground Motion Prediction in Realistic Earth Structures

9910-03010

P. Spudich
Branch of Engineering Seismology and Geology
U.S. Geological Survey
345 Middlefield Road, MS 977
Menlo Park, California 94025
(415) 323-8111, ext. 2395

Investigations

1. Analysis of the strong motion records from the 1984 Morgan Hill earthquake.

2. Improvement of the isochron method for calculating high frequency synthetic seismograms for extended earthquake sources.

3. Preliminary design of a short-baseline two-dimensional accelerometer array for installation at Parkfield, California, for the observation of earthquake rupture dynamics.

Results

1. In collaboration with Greg Beroza of MIT, we are using the isochron method to model the ground accelerations caused by the 1984 Morgan Hill earthquake. Preliminary analysis of the data indicates that little energy was liberated while the rupture progressed from the hypocenter to Anderson Lake. Strong shaking at Coyote Creek initiated with a stopping phase (sic) generated near Anderson Lake. The strong shaking following the stopping phase may be caused by the subsequent propagation of the rupture past the barrier (?) that impeded its progress at Anderson Lake.

2. In collaboration with Greg Beroza, we have made further improvements to the speed and generality of the isochron method. Ability to handle wave attenuation was aided by the use of a Futterman Q operator, and the method was improved to remove the restriction that the slip time-funtion be position independent. The method can now accomodate completely arbitrary and general rupture behavior.

3. In collaboration with David Oppenheimer, we have initiated design of a two-dimensional array of accelerometers to be installed at Parkfield, California. We hope to use this array to record the next Parkfield earthquake. The array will consist of about 25 digital, 3-component accelerometers, located within a 2 km^2 area. The array design is being optimized to observe the rupture front in two dimensions as it propagates down the fault, although it will also be of use for studies of transient soil strain during the earthquake. To design the array, we are synthesizing ground motions at each proposed array element site, using the method discussed in investigation 2, above. The motions are analyzed by a moving window frequency-wavenumber analysis method. We break the ground motion into short time slices (1-2 seconds), and do f-k analysis

on each time slice. For each slice we thus determine the directions from which energy impinges on the array. We then raytrace this energy back to its source on the fault plane.

Reports

Bakun, W.H., Clark, M., Cockerham, R., Ellsworth, W., Lindh, A., Prescott, W., Shakal, A., and Spudich, P., 1984, The 1984 Morgan Hill, California, earthquake, *Science*, **225**, 288-291.

Cormier, V., and Spudich, P., 1984, Amplification of ground motion and waveform complexity in fault zones: examples from the San Andreas and Calaveras faults, *Geophys. J. Roy. Astr. Soc.*, in press.

Spudich, P., and Frazer, L.N., 1984, Use of ray theory to calculate high frequency radiation from earthquake sources having spatially variable rupture velocity and stress drop, *Bull. Seism. Soc. Am.*, in press.

INVESTIGATION OF AREAS OF RECURRING LIQUEFACTION IN THE VICINITY OF THE NEW AND ALAMO RIVERS, IMPERIAL VALLEY, CALIFORNIA

Contract No. 14-08-0001-21232

Kenneth H. Stokoe, II
Civil Engineering Department
The University of Texas at Austin
Austin, Texas 78712 (512) 471-4929

INVESTIGATIONS

On April 26, 1981 an earthquake of magnitude 5.6 occurred in the northwestern part of the Imperial Valley. Damage due to this earthquake is estimated at 1 to 3 million dollars, mainly due to structural damage in the towns of Westmorland and Calipatria. In addition, liquefaction and other secondary ground effects occurred over a large area.

Field personnel were deployed in January, 1983 to investigate sand deposits in this area which have liquefied in past earthquakes. The locations of five study sites investigated are shown in Figure 1. The Wildlife site was of most interest because it has been instrumented to monitor ground motions and porewater pressure buildup in the soil in order to monitor soil behavior during future earthquakes. At each of the study sites investigated a sand or silt layer liquefied during the 1979 Imperial Valley earthquake and/or the 1981 Westmorland earthquake.

Field tests performed at the sites included: Standard Penetration Tests (SPT), Electrical Cone Penetration Tests (CPT), Crosshole Seismic Tests, and Spectral-Analysis-of-Surface-Waves Tests (SASW). The last two tests listed were used to determine the shear wave velocity versus depth profiles. A composite profile of the Wildlife site is shown in Figure 2.

Soil samples of the liquefiable sands and silts were taken at four of the sites. These samples were drained in the field to prevent excessive disturbance and transported to the laboratory. Resonant column tests were then performed on trimmed specimens. The resonant column tests were used to obtain the relationship between shear modulus and material damping ratio as a function of duration of confinement, magnitude of confining pressure, and shearing strain amplitude. The resonant column test results as well as the field test results were then used in the liquefaction analyses described below.

ANALYSES

In terms of the analytical study, the main objective is to evaluate the predictive capabilities of the methods which are in use at the present time (empirical correlations with SPT and CPT, Seed's simplified procedure, and the cyclic stress approach). In addition, a recently developed method (the cyclic strain approach) is also being evaluated. These predictive methods are being compared through the use of the study sites. The case histories derived from these sites are unusual in that there was much recorded seismic data from two recent earthquakes which occurred in the Imperial Valley region (1979 and 1981 earthquakes). In addition, field observations of surface manifestations of liquefaction are very detailed and thorough.

The empirical correlations used in this study consist of relating the SPT resistance and CPT resistance with the cyclic stress ratio occurring at a site at the time of a given earthquake. This relationship is then compared to other case histories to give an estimate of the liquefaction susceptability of the site. In the simplified procedure, the shear stresses occurring in the field are correlated with shear stresses causing liquefaction in the laboratory (usually determined by cyclic triaxial tests) to estimate whether or not liquefaction should have occurred during that earthquake.

In the cyclic stress approach, stresses occurring in the field are estimated by computer analyses (SHAKE and DESRA are being used) which take digitized earthquake records and propogate them numerically through a soil profile. In this study, the earthquake records are being scaled (multiplied by a certain factor to increase or decrease the peak horizontal ground surface acceleration (a_{max}) of the motion) and then the stresses correlated with these scaled motions are compared to the laboratory results to estimate the a_{max} at which a given site will liquefy (see Figure 3). The earthquake records used for the computer analyses were taken from the 1979 and 1981 earthquakes.

Finally, the newly developed cyclic strain approach is also being used to estimate site behavior. This method is employed in much the same way as the cyclic stress approach, except that strains occurring at a site during an earthquake (estimated by SHAKE and DESRA) are compared to strains causing liquefaction in laboratory tests. For the cyclic strain method, the laboratory tests are strain controlled, whereas the stress approach employs stress-controlled testing.

This study is in progress, and the results are preliminary. However, the cyclic strain approach is proving to be very promising towards estimating liquefaction, while the stress approach and the simplified procedure seem to be somewhat conservative. Predictions of liquefaction at the study sites for the 1981 Westmoreland Earthquake using the cyclic stress and cyclic strain methods are summarized in Table 1. The table shows that both methods predicted the liquefaction behavior of the study sites correctly, however, the cyclic stress approach tends to be more conservative.

REPORTS

Three reports in progress.

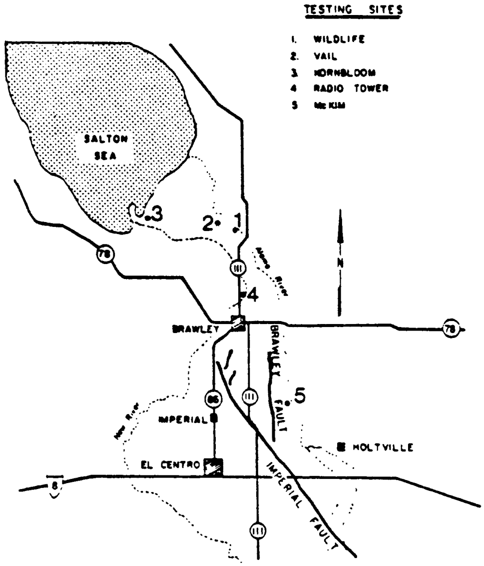

Figure 1 - Map showing locations of Imperial Valley study site.

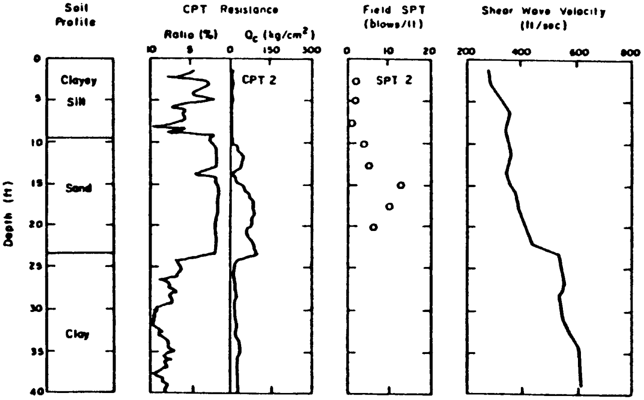

Figure 2 - Composite profile of Wildlife site.

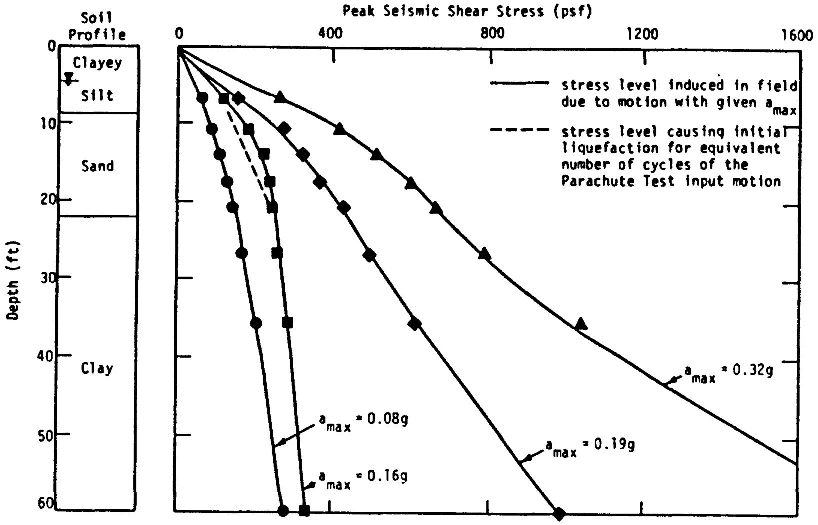

Figure 3 - Variation in cyclic shear stress with depth for Wildlife site using program SHAKE.

Site	estimated a_{max} for 1981 earthquake	a_{max} causing liquefaction		estimation of liquefaction		Observed Liquefaction
		cyclic strain approach	cyclic stress approach	cyclic strain approach	cyclic stress approach	
Wildlife	0.26g	0.23g	0.15g	yes	yes	yes
Radio Tower	0.18	0.17	0.14	yes	yes	yes
McKim	0.12	0.35	0.15	no	no	no
Vail Canal	0.26	0.22	0.14	yes	yes	yes
Kornbloom	0.28	0.25	0.15	yes	yes	yes

Table 1 - Summary of predictions of liquefaction of study sites during the 1981 Westmorland earthquake using program SHAKE.

Late Pleistocene-Holocene Soil Chronology for Evaluating Tectonic Framework and Events

14-08-0001-21829

Edward A. Keller
Department of Geological Sciences
University of California
Santa Barbara, California 93106
(805) 961-4207

D. L. Johnson
Department of Geography
University of Illinois
Urbana, Illinois
(217) 333-0589

T. K. Rockwell
Department of Geological Sciences
California State University
San Diego, California 92182
(619) 265-4441

Objective: 1) Develop a chronology for Holocene and late Pleistocene deposits based upon relative development of soils; and 2) apply the chronology to evaluate late Pleistocene and Holocene tectonic framework and events in three study areas: 1) Wheeler Ridge south of Bakersfield, California; 2) the northern front of the San Emigdio Mountains west of Wheeler Ridge and 3) Frazier Mountain near Gorman, California.

Investigations: The primary task during the summer of 1984 was to describe and sample soils on the major geomorphic surfaces in each of the study areas. A secondary activity was formulation of initial hypotheses concerning the tectonic framework in the study areas based on the preliminary soils work.

Results and Discussion: Fifty soil profiles in the study areas were described and sampled. Soil samples have been sent to a laboratory at the University of New Mexico for particle size analysis and determination of carbonate content.

Soils in the Frazier Mountain area vary from young A-C profiles with minimum development to well developed soils with argillic B horizons; 5YR 5/6, pebbly clay loam, moderate angular blocky structure, and many medium, continuous clay films. These B horizons extend to a depth of several meters and overlie a horizon with calcium carbonate coated pebbles. High geomorphic surfaces on the southeast side of Frazier Mountain have apparent anomalously weakly developed soils compared to the soils on the high surfaces on the northwest side of the mountain.

Soils on the north flank of the San Emigdio Mountains also vary from weak A-C profiles to soils with well developed argillic B horizons with up to Stage IV calcic horizons (Table 1).

Soils on Wheeler Ridge are similar to those of the San Emigdio Mountains, varying from A-C profiles to soils with well developed argillic B horizons and carbonate (K) horizons. The stage of carbonate development in K horizons is one of the most distinguishing characteristics of the soils at Wheeler Ridge. The youngest soils are A-C profiles and as the soil development becomes stronger the carbonates increase from Stages I through IV.

Age control for the youngest A-C profiles in the three study areas will come from ^{14}C dates on charcoal. We are also attempting ^{14}C dates on carbonate rinds from clasts in the calcic horizons. Absolute dates on the late Pleistocene and older soils are critical to the tectonic interpretation and will be difficult to obtain. We hope to use carbonate rinds on clasts to obtain uranium-thorium (U series) dates. The presence of abundant high-quality carbonate coatings on many of the clasts is encouraging and we believe that an attempt to date them will be successful.

Interpretation of the tectonic framework based on limited soil chronology in the San Emigdio Mountains and Wheeler Ridge suggests several hypotheses. First, Wheeler Ridge is an active anticline probably growing at a measurable rate to the east. Uplift, tilting and faulting associated with the growth of Wheeler Ridge is denoted by soils on geomorphic surfaces that are higher and older to the west of the eastern terminus of the anticlinal structure. Absolute dates on these soils will help determine the rates of deformation. Second, mountain fronts of the San Emigdio Mountains have migrated north during the Pleistocene, thrusting the mountains over the piedmont (alluvial fans) at the southern end of the San Joaquin Valley, as suggested by Davis (1983). Soil chronology is useful in identification of old mountain fronts and style of deformation associated with their tectonic migration over the San Joaquin Valley. Absolute dating of the soils will provide rates of the uplift tilt, and folding associated with the formation of new mountain fronts produced by the active tectonics of blind thrust faults such as the Wheeler Ridge and White Wolf faults.

Reference Cited

Davis, T. L., 1983. Late Cenozoic structure and tectonic history of the western "Big Bend" of the San Andreas fault and adjacent San Emigdio Mountains. Unpublished Ph.D. dissertation, University of California, Santa Barbara.

Table 1. Generalized soil characteristics for the north front of the San Emigdio Mountains.

Designation	Soil Thickness (cm)	B horizon					Carbonates
		Type	Color	Texture	Structure	Clay Films	
Q_1	50-68	A-C Profile, primary fluvial stratification					Weak Stage I
Q_2	100-191 +	A-C Profile, primary fluvial stratification					Stage I
Q_3	130 +	Cambic	10YR 3/3 m	loamy sand-silty clay loam	massive-strong coarse, prismatic	none	Stage II
Q_4	250 +	Argillic	7.5YR 4/6 m	Sandy clay loam	coarse, angular blocky	many, thick, continuous	Stage IV

FAULT ACTIVITY AND RECURRENCE INTERVALS
OF THE WESTERN SEGMENT OF THE WHITTIER FAULT, CALIFORNIA

Contract #14-08-0001-21368

F. BEACH LEIGHTON, LAWRENCE R. CANN,
ERNEST R. ARTIM AND MARK C. BERGMANN
Leighton and Associates, Inc.
1151 Duryea Avenue
Irvine, California 92714
(714) 250-1421

Investigations

The primary objective of this investigation was to extend knowledge of the Whittier fault, focusing on the 31-kilometer segment west of Brea Canyon. Specifically, the study is intended to locate, more accurately, the active fault traces, establish their recency of activity and, if possible, estimate the recurrence interval of significant earthquakes. Specific tasks of this project have included the following:

1. Selected locations for trenching based on existing knowledge and additional onsite surface observations.

2. Excavate and log nine (9) trenches across the apparently active traces of the fault (Trenches 1A and 1B, 2, 3A and 3B, and 4A, 4B, 4C and 4D), totalling 978 lineal feet, to a maximum depth of 18 feet. All trenches were geologically logged at a scale of 1" = 5', with localized areas logged at 1" = 2'.

3. Evaluate existing tools for estimating earthquake recurrence intervals for their application to the Whittier fault.

Results

1. A main trace and/or splays of the western segment of the Whittier fault were found to exist in eight (8) of the nine (9) trenches excavated in four sites of the study area.

2. Carbonaceous materials suitable for age-dating were not found to exist in the exploratory trenches. Bone fragments were encountered in one location in faulted mudflow/older alluvial material. Amino acid, uranium, or other dating techniques of these bone fragments are being evaluated.

3. A splay of the Whittier fault associated with the main trace was encountered in Trench 4-D and produced a vertical displacement of the walls of a krotovina (animal burrow) of 1/4 to 3/4 inches. The infilled material is believed to be of less than 1,000 years old. However, datable detrital carbonaceous material was not found in the infilled material.

4. Faulted, older alluvium was encountered in Trench 3A. Visual evaluations indicate this older alluvial material to be in excess of 11,000 years old.

5. The bedrock units of the Puente Formation exposed during trenching dip steeply (36 degrees to 87 degrees) toward the north and south. These units were locally folded. The majority of the fault traces that were exposed are parallel or subparallel to the orientation of the bedding, and therefore are at least locally bedding plane faults.

6. The fault traces encountered vary from 1 to 3 inches in width, but one trace expressed by extensively sheared and brecciated material was 25 feet in width. The zone of fault traces in the study area varies from 250 to 300 feet in width.

7. Slickensides observed along one of the main faults suggest the slip along this fault is right-reverse oblique. Locally, striations were found to plunge 12 degrees west, as measured from the horizontal. The orientation of this fault is N52-54°W, dipping 77 to 86 degrees north.

8. The faults exposed during this investigation in the study area suggest that the western segment of the Whittier fault has displaced earth materials that appear to be at least of Holocene age.

- ① BG N45°W, 66°S
- ② B N66°W, 73° N
- ③ B N57°W, 62°S
- ④ F N65°W, 62°S
- ⑤ B N67°W, 88°N
- ⑥ BG N81°W, 73°N
- ⑦ B N81°W, 61°S
- ⑧ F N82°W, 85°S
- ⑨ F N56°W, 88°N
- ⑩ B N48°W, 87°S
- ⑪ F N62°W, 42°S
- ⑫ B N62°W, 79°N
- ⑬ B N82°W, 83°N
- ⑭ B N46°W, 85°N
- ⑮ B N79°E, 79°N
- ⑯ B N49°W, 89°N
- ⑰ B N56°W, 90
- ⑱ B N52°W, 88°N
- ⑲ B N88°E, 44°S
- ⑳ B N70°E, 88°S

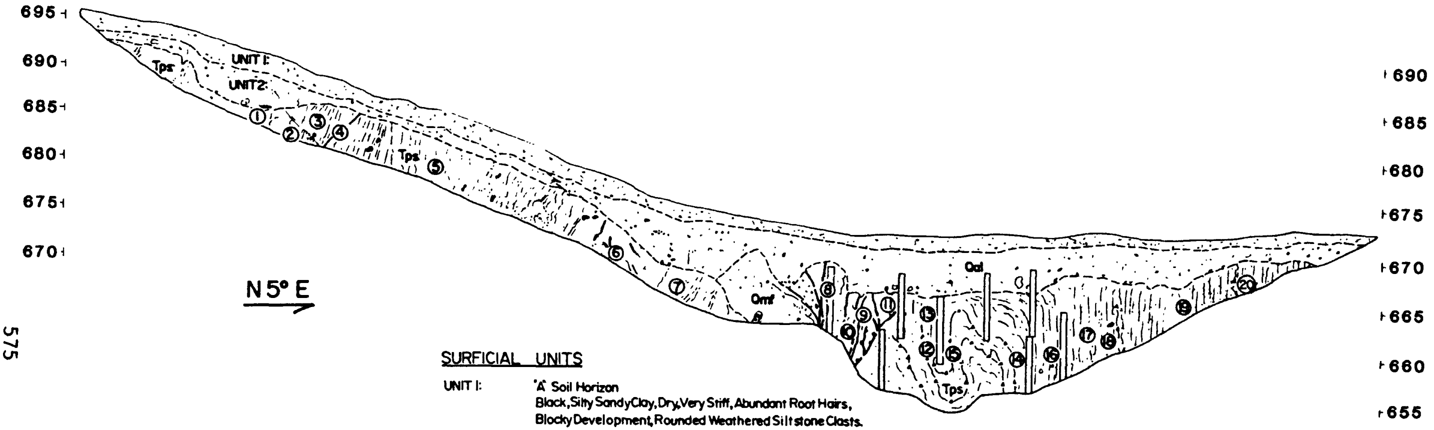

SURFICIAL UNITS

UNIT 1:	'A' Soil Horizon Black, Silty Sandy Clay, Dry, Very Stiff, Abundant Root Hairs, Blocky Development, Rounded Weathered Siltstone Clasts.
UNIT2:	'C' Soil Horizon Yellow Tan Silty Sand, Dry to Damp, Stiff, Abundant Decayed Roots, Angular Fragments of Sandstone and Siltstone, Occasional Burrows, Moderately Porous Throughout.
Qal:	Alluvium Med. Brown to Black Clayey Silt to Clayey Sand, Dry to Damp, very Stiff to Hard, Rounded Pebble Lenses, Occasional Black Clay Blebs, Occasional Tiny Bits of Charcoal, Scattered Subangular Pebbles, Crude Stratification, Gravel Lenses.
Qmf:	Mud Flow Lt. Orange Brown to Yellow Tan Silty Sand, Damp, Very Stiff, Angular Fragments of Siltstone, Slightly Porous.

BEDROCK UNIT

Tps:	Soquel Member, Puente Formation Gray and Orange Fine Sandstone and Olive Gray Siltstone, Damp, Hard, Abundant Diatomaceous Beds, Occasional Oval Concretions, Finely Laminated.

GEOLOGIC LOG
WEST WALL TRENCH - 4B
WHITTIER FAULT
ARROYO SAN MIGUEL AREA
LA HABRA HEIGHTS CALIFORNIA

Proj.	1820084-01	Scale	1" = 5'	Date	10/26/84
Engineer/Geologist	LC/MB	Drafting By	LM		
LEIGHTON and ASSOCIATES, INC.					

STUDY OF SEISMIC ACTIVITY BY SELECTIVE TRENCHING ALONG THE ELSINORE FAULT ZONE, SOUTHERN CALIFORNIA

Contract No. 14-08-0001-21376

T. K. Rockwell
Geology Department
San Diego State University
San Diego, CA 92182

and

D. L. Lamar
Lamar-Merifield Geologists, Inc.
1318 Second Street, Suite 25
Santa Monica, California 90401
Telephone: (213) 395-4528

Investigations

A trench was dug and logged at a previously studied site across the Glen Ivy North fault, a strand of the Elsinore fault zone between Corona and Lake Elsinore (Lamar and Swanson, 1981, 1982).

Results

Additional analysis of exposures in the trench wall and radiocarbon dating of organic-rich layers has revealed the following events:

Number of events	Age
1 or 2	post-1660 A.D.
1	between 1275 and 1660 A.D.
1	between 1260 and 1275 A.D.
2	pre-1260 A.D., undated

These are dendrochronologically corrected (Stuiver, 1982) Carbon 14 dates; the errors range from ± 40 to ± 100 years for these corrected dates. These results suggest an average earthquake recurrence interval of 200 to 300 years.

References

Lamar, D. L. and S. C. Swanson, 1981, Study of seismic activity by selective trenching along the Elsinore fault zone, southern California: Lamar-Merifield Technical Report 81-4, Final Report U.S.G.S. Contract 14-08-0001-19144, 50 p.

Lamar, D. L. and S. C. Swanson, 1982, Ages of displaced strata in trenches along Elsinore fault zone, southern California: Geol. Soc. Amer. Abstracts with Programs, v. 14, p. 179.

Stuiver, Minze, 1982, A high-precision calibration of the AD radiocarbon time scale: Radiocarbon, v. 24, p. 1-26.

Subsurface Velocity and Attenuation Measurements at a Strong Motion Site

Contract No. 14-08-0001-21823

Bruce Redpath, Reuben Hale and Richard Lee
formerly with
URS/Blume Engineers

Berkeley, California 94705
415-849-2700

Objectives: If the subsurface velocity structure and anelastic properties of a site can be acquired with borehole geophysical techniques, then surface motion at that site can be calculated by propagating bedrock motion up through the attenuating overburden layers. Downhole measurements of compression- and shear-wave velocities are now a routine procedure. Measurement of **in situ** material damping using downhole methods is not routine, but it is straightforward and should become an accepted procedure for site characterization and response calculation. The site of the subsurface accelerometer array at the Richmond Field Station [RFS] of the University of California, Berkeley, offered an ideal location to test the use of **in situ** measurements coupled with a theoretical approach to obtain the subsurface-to-surface transfer function. The concept is very similar to the work reported by Johnson and Silva (1981). Several earthquakes have been recorded at the RFS by accelerometers on the surface, in bedrock at a depth of 131 ft, and in the alluvium at a depth of 49 ft. Transfer functions obtained from recorded earthquakes can be compared with the predicted transfer functions. Our specific objectives were: 1) to measure the **in situ** shear-wave velocity and **Q** at the RFS; 2) to compare the **in situ** value of **Q** with damping values obtained from resonant-column laboratory tests of soil samples; and 3) to compare bedrock-to-surface transfer functions from strong motion records with those predicted on the basis of the measured anelastic structure of the site.

Results: The results of the geophysical field measurements of velocity and damping were reported in the previous volume (**XVIII**) of this series of Technical Report Summaries.

Strong motion records from the RFS were transferred to a Hewlett-Packard 5451 computer from the original analog tapes at the U.C. Berkeley Seismograph Station, and a number of transfer functions have been computed. As a representative example, Fig.1 shows the average of four surface-to-bedrock amplitude ratios obtained from the two horizontal components recorded during two of the Briones earthquakes of 8 January 1977 (M4.0 at 08:58:13 and M3.8 at 09:39:41). A comparison of Fig.1 with the shear-wave transfer function calculated by Johnson and Silva (their Fig.10) confirms that the calculated and observed fundamental modal frequencies are in good agreement. The shear-wave amplification factor of about 25 at 2Hz calculated by Johnson and Silva, although in accord with some of the observed single-component, single-event amplitude ratios, is larger than the corresponding average value in Fig.1. Some of this difference may be attributed to the bedrock shear-wave velocity of about 2950 ft/sec used in their calculations, compared with a velocity of about 2150 ft/sec that we measured. The lower velocity implies less amplification at the surface because of the smaller change in acoustic impedance and lower reflection coefficient at the alluvium-bedrock interface.

Johnson and Silva estimated that **Q** varied from a value of 6 at shallow depths to a value of 20 for the deeper alluvial materials; their estimates were based on ultrasonic attenuation tests on drill cores. Their reported velocities and **Q** estimates are equivalent to a average **Q** of 12.3 for the entire section from the surface to bedrock. It is interesting to note that our **in situ** attenuation measurements resulted in a **Q** value of 12.5 for this same section.

Work remaining in this program consists of using our measured values of **in situ** properties to recompute the bedrock-to-surface transfer function.

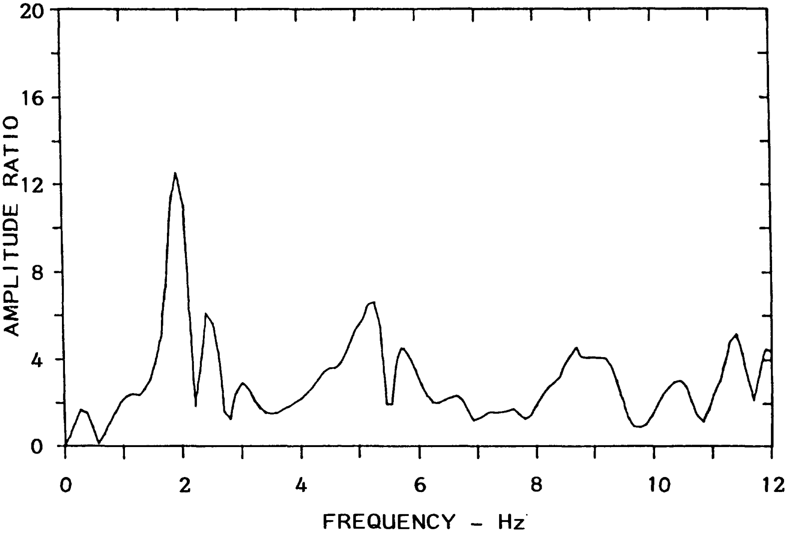

Fig.1 Average surface-to-bedrock amplitude ratio at Richmond Field Station for the two horizontal components recorded during two Briones earthquakes of 8 January 1977.

Reference:

Johnson, L.R. and Silva, W., 1981, The effect of unconsolidated sediments upon the ground motion during local earthquakes, Bull. Seis. Soc. Am., vol.71, pp.127-142.

Prediction and Other Studies of Earthquakes in the Beijing Area

14-08-0001-21341

Francis T. Wu
Department of Geological Sciences
State University of New York
Binghamton, New York 13901
(607) 798-2512

Ta-liang Teng
Department of Geological Sciences
University of Southern California
Los Angeles, California 90008

Objectives: Large and moderate earthquakes have occurred in Northeastern China in the recent as well as historical past. For studying earthquake prediction and seismicity in general and the understanding of seismic environment of the Eastern United States through a comparison of earthquakes in these two regions, we are conducting several studies in the Beijing-Tangshan-Tianjin area. We have placed water well level measurement systems of our own desing alongside the Chinese instruments in deep wells to monitor wells that have responded to possible precursory changes previously; we hope to see whether future earthquakes would generate similar signals and to understand what are the conditions of the wells that make a particular well sensitive to such precursory changes. While the telemetering equipment purchased by us and a PDP11/44 computer for the regional network are coming online, we have recorded a series of aftershocks in the Tangshan area (site of the disastrous 1976 M=7.8 event); seismic parameters (focal mechanism, moment, corner frequency etc.) for these events have been obtained and we intend to compare them to those of earthquakes in the United States and calibrate the magnitude scale used in China against moment magnitudes.

Data Acquisition and Analysis: The activities in the past six months include the following:

1. Effort to put the PDP11/44 computer on-line. Due to hardware problems the Institute of Geophysics has not been able to input the 36 or so telemetered stations on-line. USGS is currently arranging for DEC service from the Far East to rectify the problems.

2. Make modifications in the clock systems for the digital calculator/printer water well level recording systems. The clocks will be accurate to within a few hundredth of second/day, accurate enough to study the phase variations of long period diurnal and atmospheric tides.

3. Data analysis of aftershocks recorded on digital event

recorders in the Lulong area 30 km northeast of Tangshan city. M>6 earthquakes occurred here after the 1976 Tangshan earthquake. The five recording sites are within 15 km of the events. We have found that the frequency content of these events is comparable to those of the Eastern United States, with corner frequencies ranging from 8-20 Hz for magnitude 2 to 4.5 earthquakes. The computed stress drops are also comparable. Some of the larger events were located by the Beijing telemetered network and given magnitudes; we shall calibrate the magnitudes against the moment. Interestingly enough, the relatively high frequency spectral content of the Eastern Chinese events in comparison to events in Western China (Figs. 1 and 2) seems to bear an inverse relation to the level of seismicity, in very much the same manner as shown by earthquake records in United States.

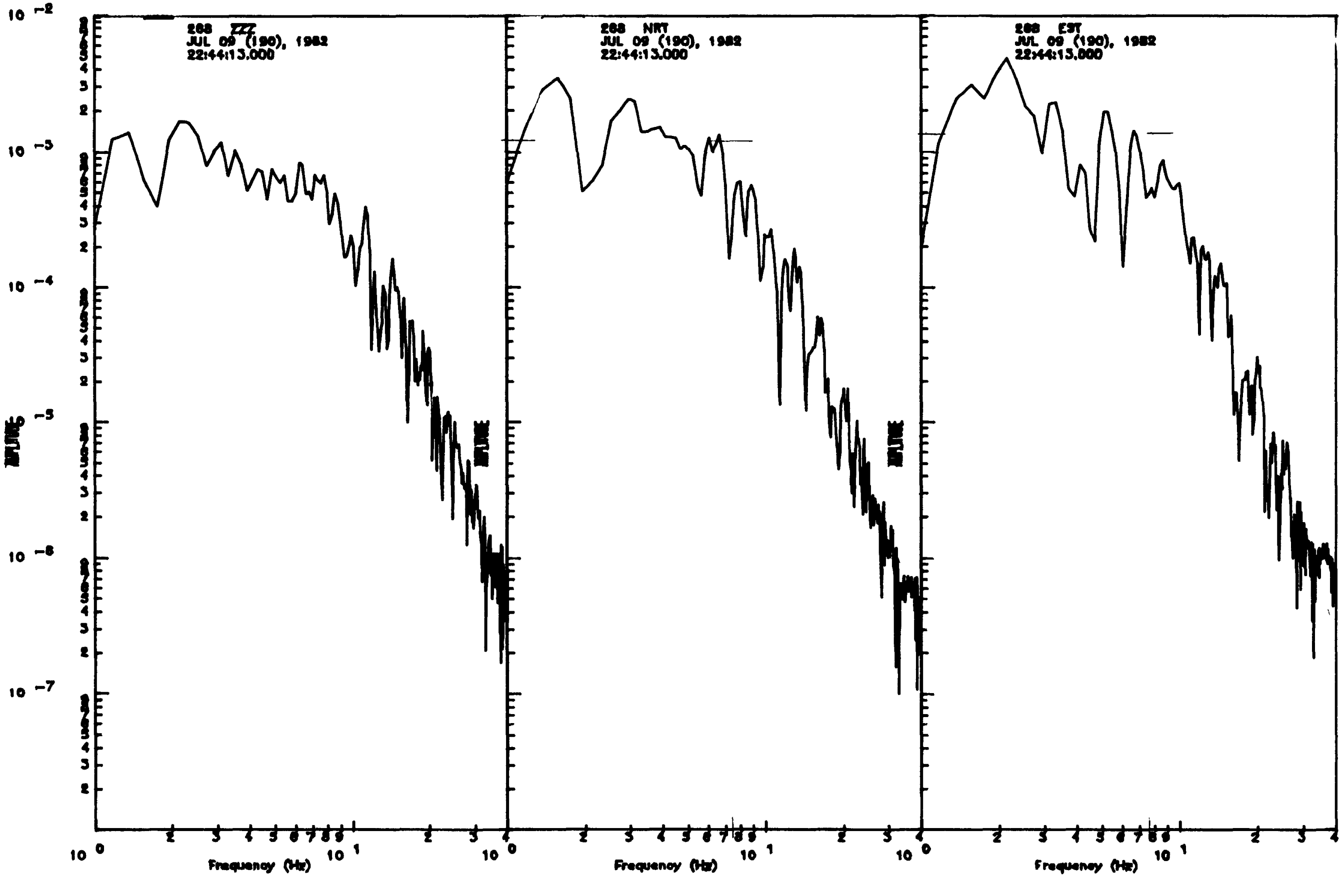

Figure 2. Spectra for a Western Chinese earthquake.

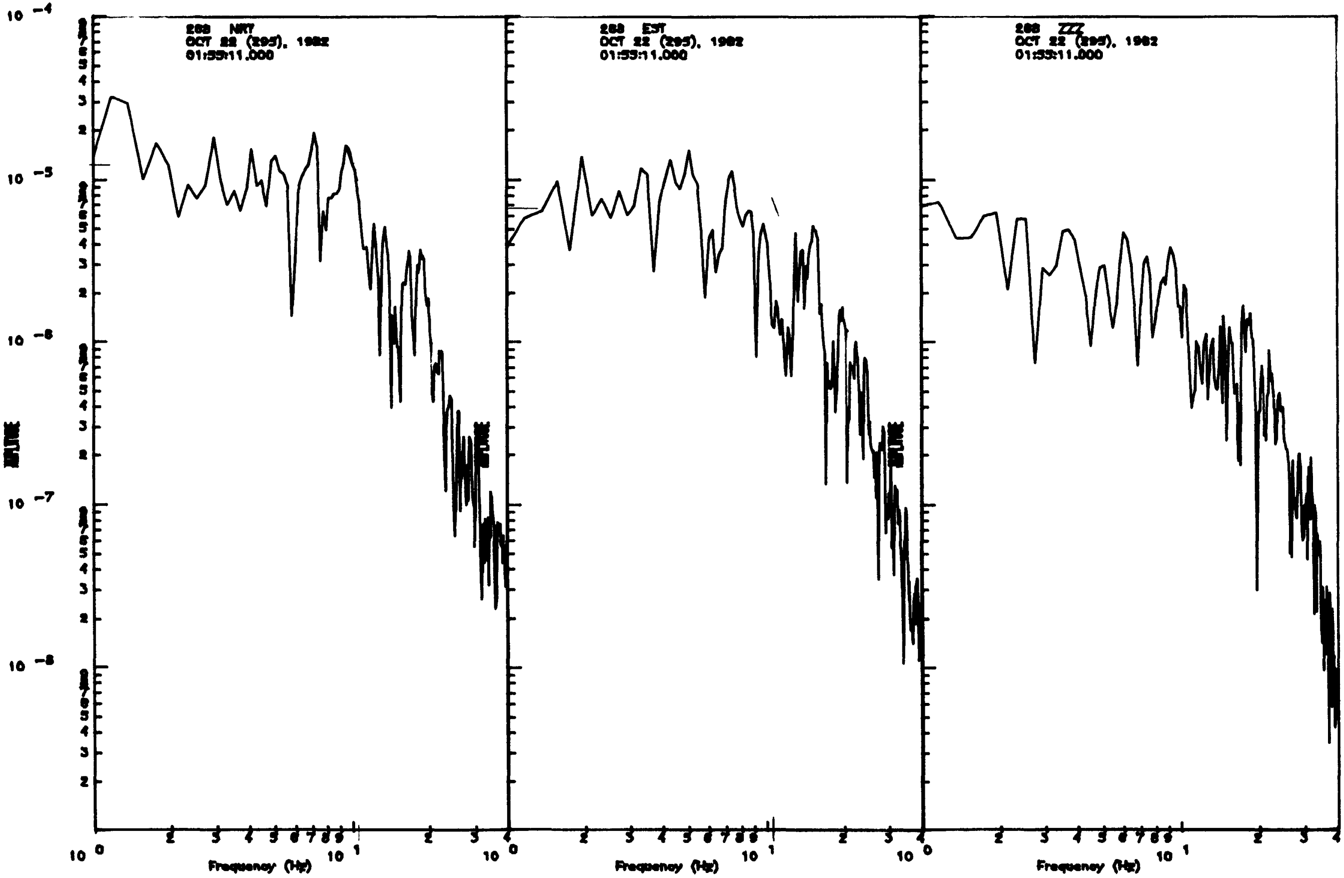

Figure 1. Spectra for an Eastern Chinese earthquake.

Earthquake Prediction Based on Seismicity Patterns

14-08-0001-21324

M. Wyss and R. E. Habermann
CIRES, Box 449
University of Colorado
Boulder, Colorado 80309
(303) 492-8028

The emphasis of our recent work has shifted from large, thrust type events at subduction zones to moderate strike-slip events in the United States, primarily Hawaii and California. We have quantitatively recognized significant seismicity rate decreases prior to several such events. In this summary we briefly describe these anomalies.

We have used several statistical approaches to anomaly recognition in order to quantitatively define the anomalies we have observed. These definitions consist of four parts: The spatial and temporal extent of the anomaly, the z value which results from the comparison of the anomalous rate to the background rate, and the magnitude band in which the anomaly is observed. These definitions are then used in searches of entire fault systems for similar anomalies. This technique of anomaly evaluation allows one to empirically determine false alarm rates as well as to recognize possible precursors to future events.

The detection history of events in central California is interesting because of possible changes in the magnitudes discovered by Bakun (personal communication) and reported by Reasenberg and Ellsworth (JGR, 87, 10637-10655, 1982). Our techniques for recognizing detection or reporting changes are capable of recognizing such changes. Preliminary study of the detection history for the region of the Calaveras fault indicates that the proposed magnitude changes are not a large effect. We do, however, see enough indication of such changes so that the final word is not in. In contrast, the magnitude changes appear clearly in the Parkfield area. The anomalies discussed here for California were identified in a data set in which the magnitudes after April 1977 were increased by 0.1 unit.

The Coyote Lake Earthquake; August 6, 1979; Calaveras Fault, California; M = 5.9.

This event was examined with magnitude cutoffs of 1.5+, 1.7+, 2.0+, 2.2+, and 2.5+. Significant decreases in seismicity rate occurred in all of these magnitude bands near the rupture zone prior to the mainshock. Nineteen different anomalies with durations of between 22 and 161 weeks (depending on the magnitude band and the region examined) were recognized prior to this event. All of the anomalies were significant at the 99%+ level according to the z test for a difference between two means. A search of all data between January 1969 and July 1984 for nine segments of the Calaveras fault with the same dimensions as the anomalies revealed no false alarms for 42% of these anomalies. This strongly suggests that the quiet periods reflect a unique phenomena related to the preparation for this mainshock. All of the quiet periods ended during early 1979, some eight months prior to the mainshock, when the seismicity returned to a normal rate. The events which occurred in this region during

1979 prior to the mainshock probably contain important information concerning the preparation process.

The Morgan Hill Earthquake; April 24, 1984; Calaveras Fault, California; M = 6.1.

This event was examined for the same magnitude bands as the Coyote Lake event described above. Again, significant rate decreases were identified in all magnitude bands. Eleven anomalies were defined with durations varying from 25 to 158 weeks. Six of these could be recognized with no false alarms in a search of the entire Calaveras fault. The quiet periods in this case again ended roughly one year prior to the mainshock.

The Kaoiki Earthquake; November 16, 1983; Kaoiki Fault, Hawaii; M = 6.6.

This event occurred on a strike-slip fault between the volcanoes Mauna Loa and Kilauea. The aftershocks covered an area of about 10 km radius, suggesting significant failure throughout a volume surrounding the main fault. We examined the seismicity in the area of this event using a magnitude cutoff of 1.9+. A strong decrease in the rate of occurrence of those events occurred during mid-1981, about 2.5 years prior to the mainshock. This decrease is particularly noteworthy because it showed the highest z-value of any of the precursors we have identified during six years of work on this problem (z = 10). The probability of observing such a decrease is the same as that of observing a data point ten standard deviations from the mean of a normal distribution. An important point evident even from a preliminary examination of the precursor to this event is that the quiescence is weak in the immediate epicentral area. This is similar to the pattern observed prior to the 1975 Kalapana, Hawaii event and may indicate the presence of an asperity in that region.

Conclusion: The anomalies we have recognized in California are very encouraging for prediction of moderate events on strike-slip faults in that region. The anomaly evaluation technique we have developed and tested on the Calaveras fault provides empirical determinations of false alarm rates and, therefore, probabilities of occurrence of a mainshock given an observation of seismic quiescence. The observation of similar anomalies in Hawaii, and in many subduction zones, suggests that the process responsible for precursory seismic quiescence can occur in varied tectonic situations.

The identification of significant quiescence-type precursors prior to numerous mainshocks in different tectonic situations indicates that such observations can be a powerful tool for earthquake prediction. We are presently examining the details of the precursors described above. This examination includes careful attention to the relationships of these precursors to tectonic and geologic features in the regions of the mainshocks. Such relationships are clearly important in any case, particularly, however, in the interpretation of presently occurring anomalies (should they be recognized).

Recent Publications:

Habermann, R. E., Spatial seismicity variations and asperities in the New Hebrides seismic zone, Journ. Geophys. Res., 89, 5891-5904, 1984.

Habermann, R.E. and M. Wyss, Background seismicity rates and precursory seismic quiescence: Imperial Valley, California, B.S.S.A., 74, 1743-1756, 1984.

Wyss, M., R.E. Habermann, and J.C. Griesser, Seismic quiescence and asperities in the Tonga-Kermadec arc, Journ. Geophys. Res., 89, 9293-9304, 1984.

Wyss, M. and R.E. Habermann, Seismic quiescence in California and Hawaii: A tool for prediction of $M > 5.5$ earthquakes, submitted to Science.

Habermann, R.E. and M. Wyss, Recognition and evaluation of precursory quiescence on the Calaveras fault, California, in progress.

Time-dependent Constitutive Relation for the San Andreas and Hayward Fault Gouges

14-08-001-21352

Chi-yuen Wang
Dept. of Geology and Geophysics
University of California, Berkeley
Berkeley, California 94720
(415) 642-2288

Investigations

I. Investigation of the time-dependent constitutive relation for the San Andreas and Hayward fault gouges and several clays.

II. Study of the constitution of the San Andreas fault zone to seismogenic depths.

III. Gravity survey across the San Andreas fault zone near Bear Valley, San Benito County, California.

Results

I. Systematic and extensive experimental studies on the mechanical properties of fault gouges collected from the San Andreas and the Hayward fault zones and on a few kinds of clays were carried out at various pressures and strain rates. Each material was studied at three different confining pressures and, at each confining pressure, three different strain rates. From the results of these experiments we have made the following observations.

(1) The strengths at the yield points of most samples, such as the Hayward fault gouge, kaolinite and chlorite, and some San Andreas fault gouge and illite, are not significantly affected by the rate of deformation, but they increase with confining pressure. Figure 1 gives an example for this observation.

(2) Experimental results for gouge layers of different thicknesses but sheared at the same speed show that the strengths of gouge layers with different thicknesses for the same gouge material are almost identical. (Figure 2).

(3) Under "drained" condition, fault gouges generally show significant strengthening with continued deformation (Figures 1 and 2). Microscopic examination of the sheared samples shows that severe granulation occurred during the shearing process. (Pictures are not provided here because of the poor quality in the reproduction.) This granulation may be an important mechanism for the observed work-hardening.

(4) An important exception to the above general observation is the strength of fault gouge rich in expandable clays (i.e. montmorillonite). For these materials, there is an apparent dependence of strength on deformation rate (Figure 3, for example). Samples sheared at slower rate usually become stronger. By using the data for the rate of flow of water expelled from the sample, we calculated the pore pressures in the sample during the shearing process. Results of the calculation are in close agreement with those calculated from using the permeability data of Morrow et al. (1984) for the same materials at similar conditions, and show that the differences in pore pressure in the samples sheared at different rates are too small to explain the differences in strength of the samples. Examination of the sheared samples using X-ray diffraction technique shows that samples shear at different rate have different hydration states; this difference in the hydration states may be an important

cause for the difference in the strength of the samples.

(5) If the drainage of the fault gouge is poor either due to extremely low permeability or due to fast shearing rate, the strength of fault gouge may decrease with increasing deformation, resulting in an apparent "displacement weakening" of the gouge layer (Figure 3).

(6) Based upon a detailed analysis of our experimental data, we constructed constitutive relations capable of predicting the change of void ratio that develop with time in saturated clayey fault gouges subjected to known stress changes. Since porosity affects many properties of clayey materials, such as their strength and permeability, these relations are believed to be important, particularly for quantitative modeling of the deformation of fault gouge under tectonic loading. The constitutive relations are phenomenological in nature and have been developed by incorporating ideas from soil mechanics. These are discussed below in the order of different stress and deformation regimes:

Under confining pressure (Pc), the void ratio (e) of saturated clayey materials is found to be linearly related to the logarithmic effective confining pressure (Figure 4), similar to that developed in soil mechanics at much lower pressures. The relation is:

$$e = B_0 \ln P_c + C_0 \qquad (1)$$

where B_0 and C_0 are empirical constants determined from experimental data.

As deviatoric stress is applied two deformation regimes are recognized. Before yielding, deformation involves rearrangement of solid particles but there is no apparent reduction of grain size. The relationship between stress and displacement, for most samples, is independent of the shearing rate. The difference in the calculated pore pressures (P_w) of the samples is too small to significantly affect this relationship. In this regime, the following equation adequately describes the reduction in void ratio of the sample as a function of shear stress (τ) and effective normal stress, i.e.

$$e = A_1 \tau + B_1 \ln(\sigma_n - P_w) + C_1 \qquad (2)$$

Empirical constants B_1 and C_1 for each specimen turns out to be nearly equal to B_0 and C_0, respectively, for the same specimen. Such similarity in material constants suggests strongly that the decrease in the void ratio during shearing may be caused by the superposition of two independent mechanisms, one due to the effective normal stress (σ_n) and the other due to shear stress. In a recent study by Carrol et al. (1984), a similar separation of the effects of normal and shear stresses is assumed to describe the reduction of porosity in sandstone.

After yielding, the constitutive relation becomes

$$e = A_2 \ln \tau + B_2 \ln(\sigma_N - p_w) + C_2 + E_2 \ln t \qquad (3)$$

Figure 5 shows an example for the fit of this equation to the experimental data. Microscopic examination of the sheared specimens show clear evidence that granulation is an important process in this deformation regime and the reduction of grain size is a function of the magnitude of the shear stress experienced by the sample.

Additional tests of these consitutive models have been successfully carried out by using clayey samples of different thickness.

II. Inferences on the constitution of the San Andreas fault zone in central California is made based upon interpretation of existing geophysical data for the fault zone, in light of laboratory data for material properties at elevated pressures. Through this procedure we arrive at a viable model that the San Andreas fault zone in central California throughout the seismogenic regime is composed of saturated fault gouge rich in clays (Wang, 1984). Although this model was proposed before (Wu et al., 1975; Wang et al., 1978), the present study is much more tightly constained not only because a large amount of new geophysical data for the San Andreas fault zone in central California has been included but also because, for the first time, all the relevant geophysical data (seismic velocities, electrical resistivity, magnetic and gravity anomalies) and geochemical data (e.g., chemistry of the aqueous fluids in the fault zone and the stability fields of clays at high pressures and high temperatures) are taken together in a unified interpretation.

The results of the above investigation strongly suggest that a comprehensive constitutive relation for clay-rich fault gouge may be important for modeling the behaviors of the San Andreas fault in central California.

III. A detailed gravity survey was carried out near Bear Valley in San Benito County, California, along a route which transects the San Andreas fault at a high angle. This route follows the one used in a seismic reflection survey by McEvilly (1981). A total of 160 locations, each with a height determination accurate to about 1 ft were occupied with two calibrated LaCoste-Romberg gravimeters. Gravity measurements were corrected for tides, instrumental drift, and height above the mean sea level. Further data reduction due to topography will be needed before the data can be used for modeling the density of the fault zone.

Publications (copies attached)

Wang, C.Y., On the constitution of the San Andreas fault zone in central California, **J. Geophys. Res., 89**, 5858-5866, 1984.

Ph.D. Thesis Completed

Chu, C.L., **Constitutive Relations of Clays and Clayey Fault Gouge at High Pressures**, University of California, Berkeley, 1984.

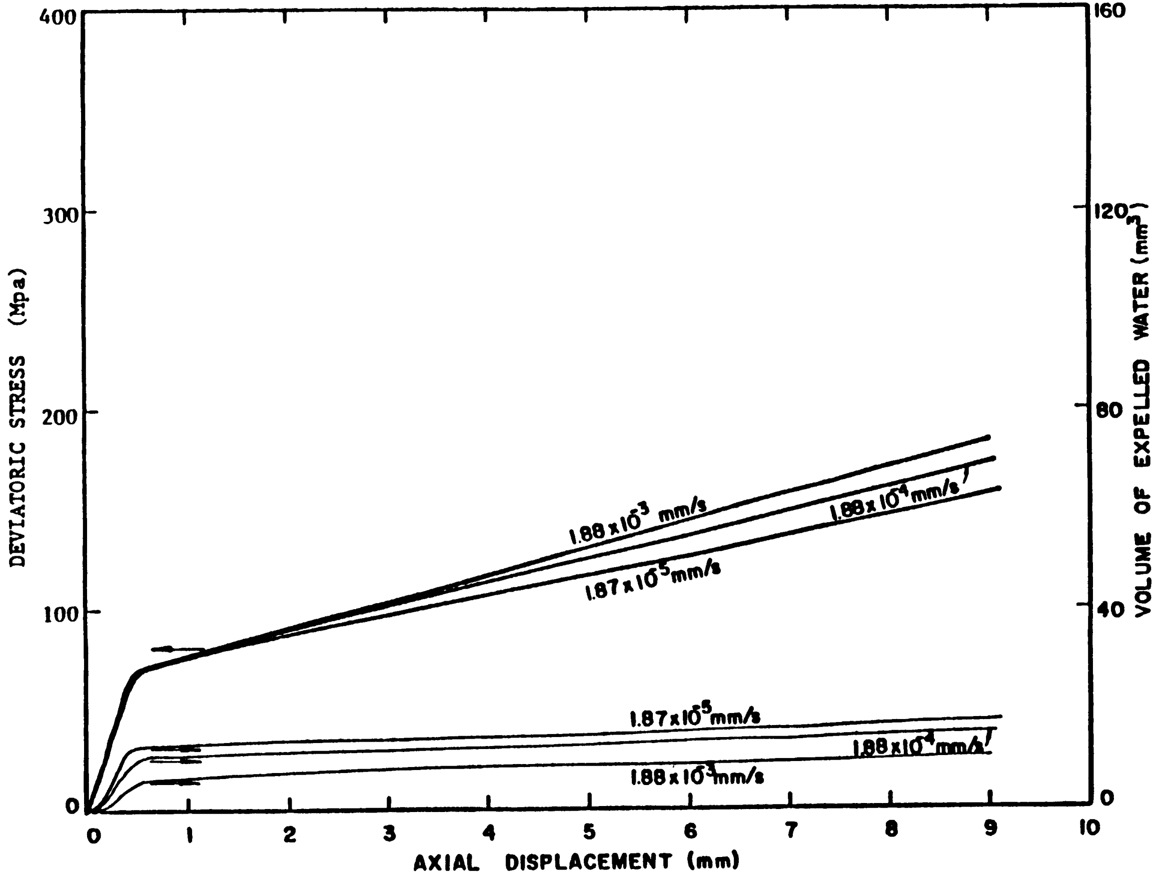

Figure 1.

Experimental results for the Hayward fault gouge sheared at three different rates of 10^{-3}, 10^{-4} and 10^{-5} mm/sec, under a constant confining pressure of 200 Mpa. Shear stress and the volume of expelled water are plotted against shear displacement. Note that for all the rates, the strengths of the samples at the yield point remains the same.

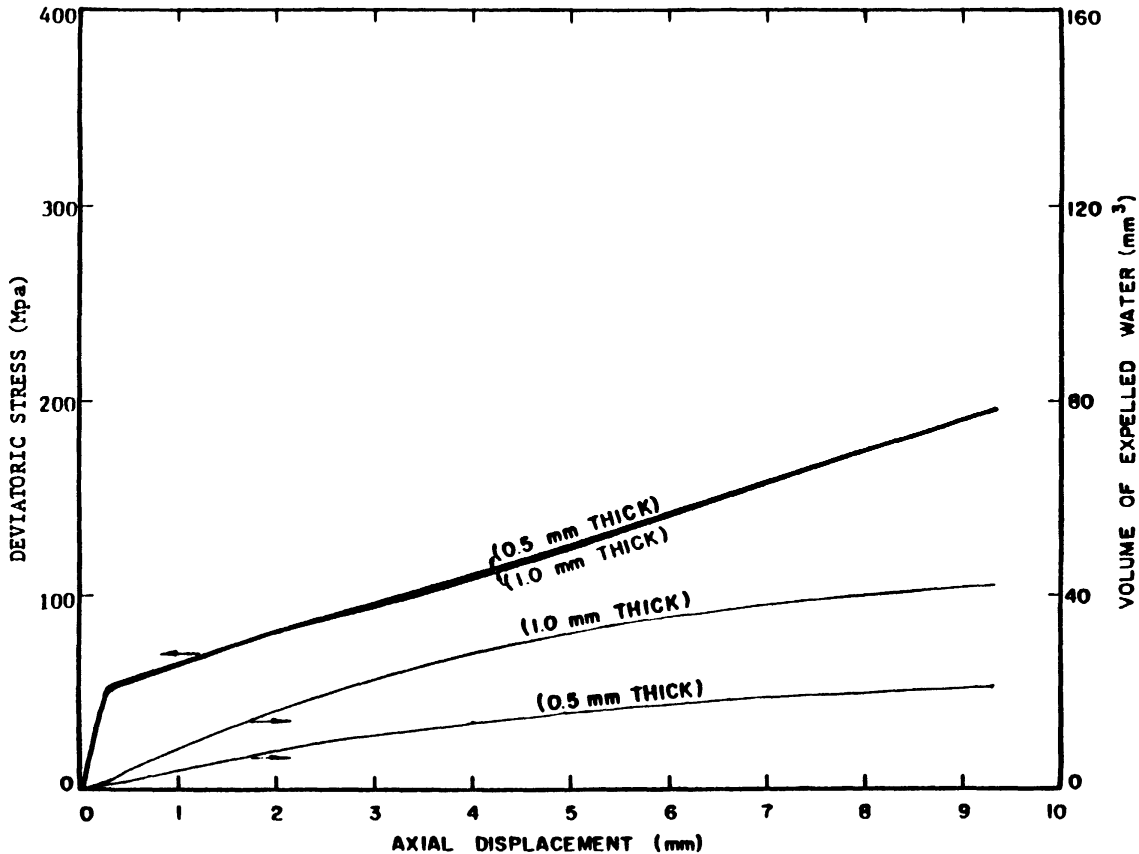

Figure 2.

Experimental result for the San Andreas fault gouge sheared at a rate of 10^{-3} mm/sec and a confining pressure of 100 Mpa. Two samples with different thicknesses were studied. Note that stress-displacement relations for the two samples are nearly identical.

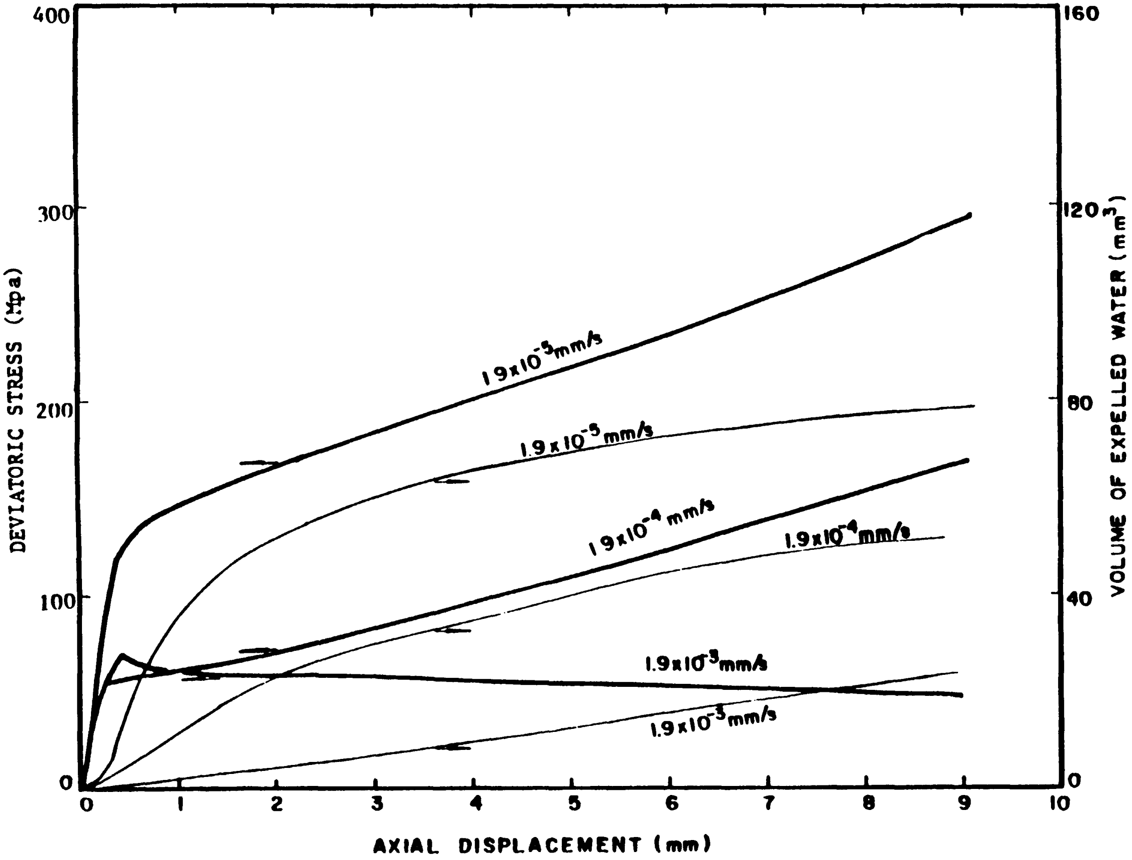

Figure 3.

Experimental results for montmorillonite gouge sheared at three different rates of 10^{-3}, 10^{-4} and 10^{-5} mm/sec, under a constant confining pressure of 200 Mpa. Note that the sample sheared at the slowest rate (10^{-5} mm/sec) is much stronger than the other samples. The sample sheared at the highest rate (10^{-3} mm/sec) shows displacement weakening.

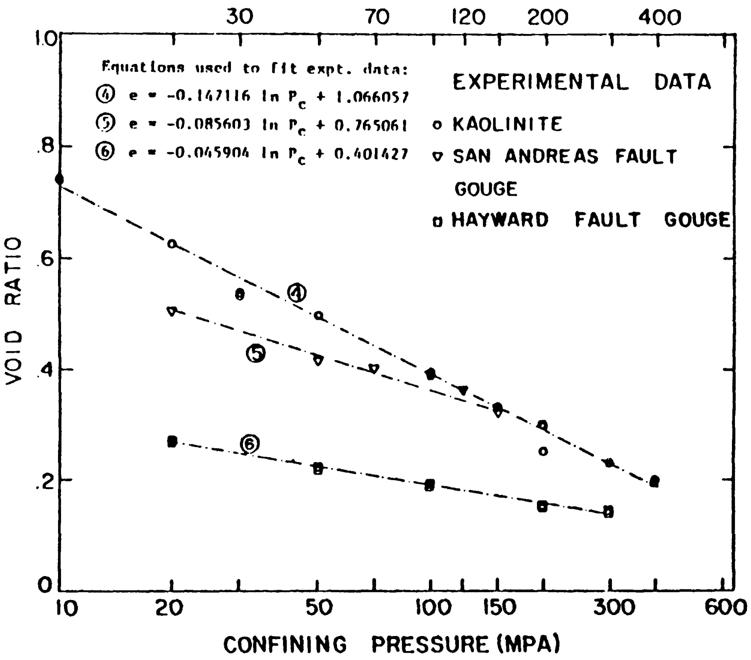

Figure 4 (a) VOID RATIO VERSUS CONFINING PRESSURE OF CONSOLIDATED KAOLINITE, SAN ANDREAS FAULT GOUGE AND HAYWARD FAULT GOUGE SAMPLES.

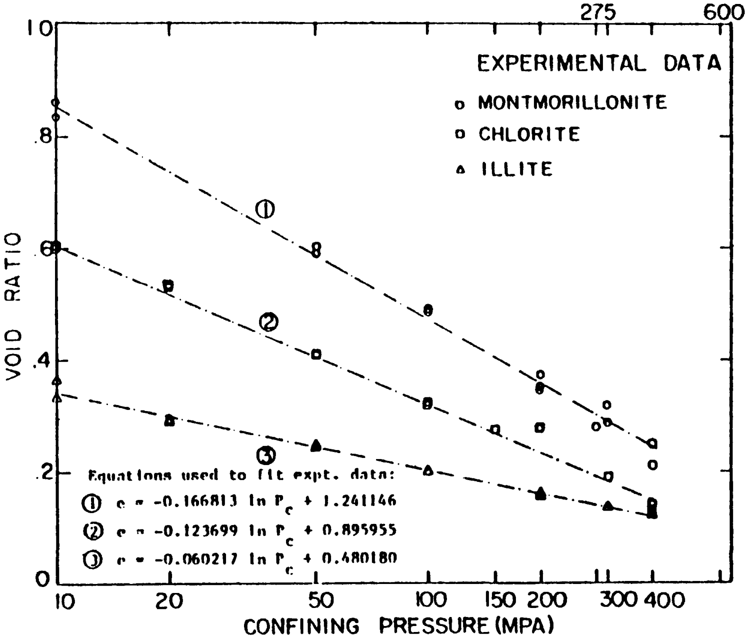

Figure 4 (b) VOID RATIO VERSUS CONFINING PRESSURE OF CHLORITE, MONTMORILLONITE AND ILLITE SAMPLES.

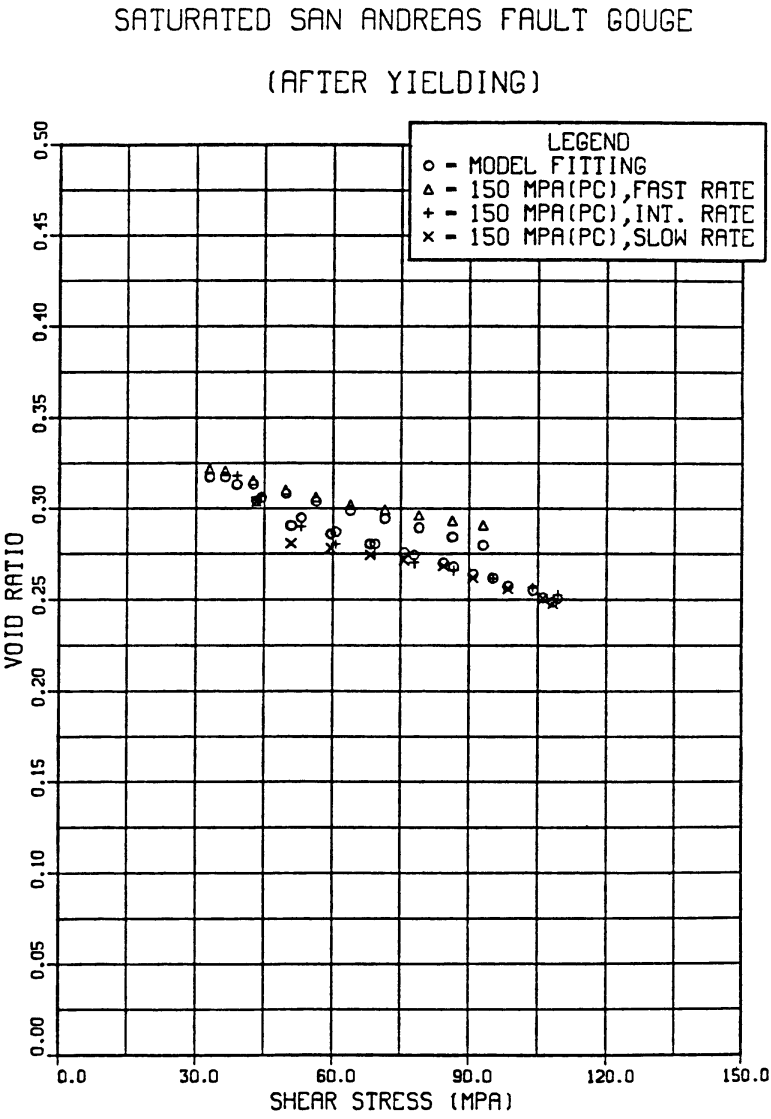

Figure 5.

Comparison of void ratio versus shear stress between laboratory results and model fitting using equation 3, for saturated San Andreas fault gouge subjected to shear deformation after yielding has occurred.

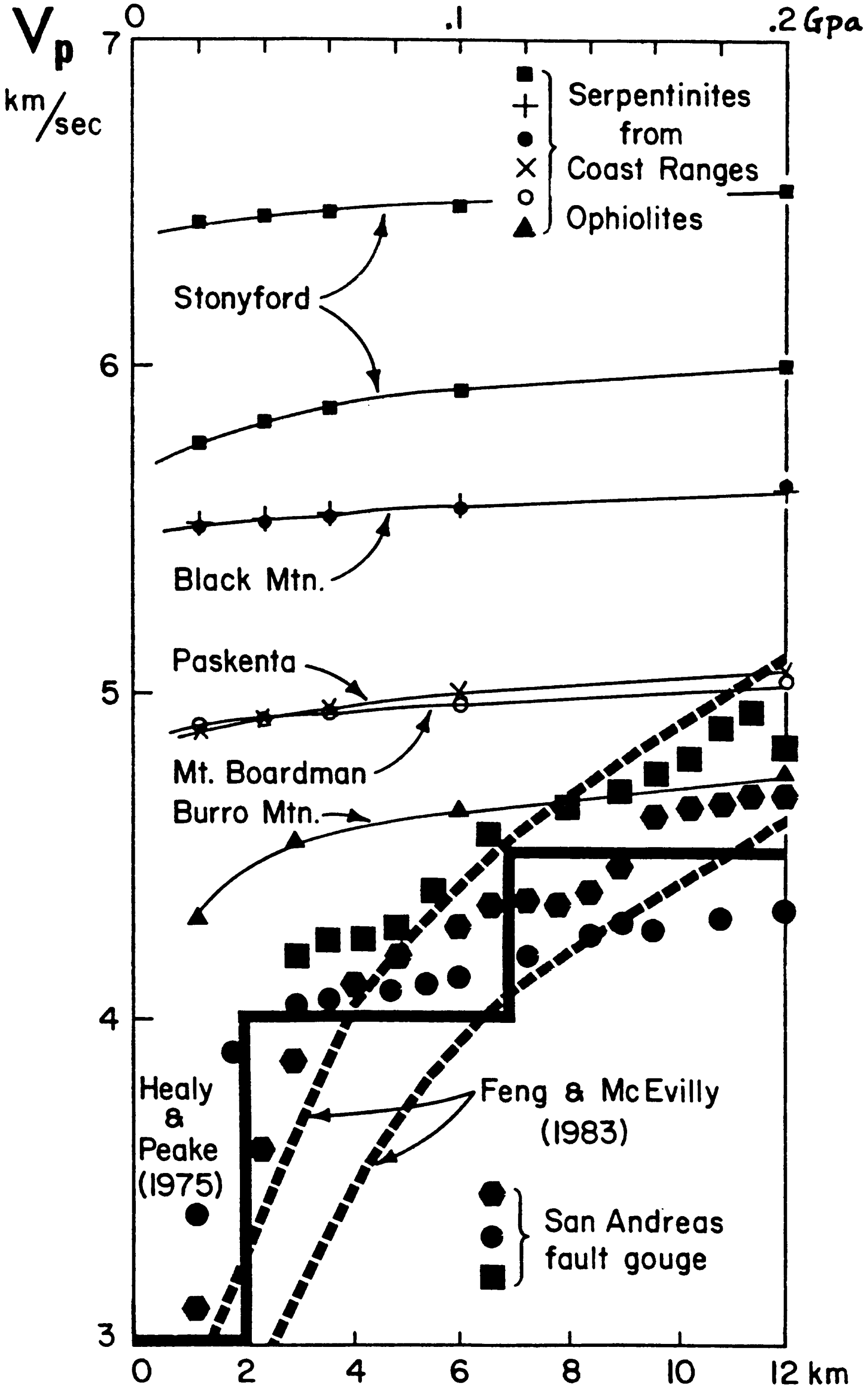

Figure 6.
Seismic P-velocity structures of the San Andreas fault zone in central California by Healy and Peake (1975) and Feng and McEvilly (1983), plotted together with the velocities of compressional waves in several saturated San Andreas fault gouges (Wang et al., 1978, 1984) and California serpentinites (Christensen, 1966, 1978) determined in laboratory at elevated effective confining pressures.

Figure 6.

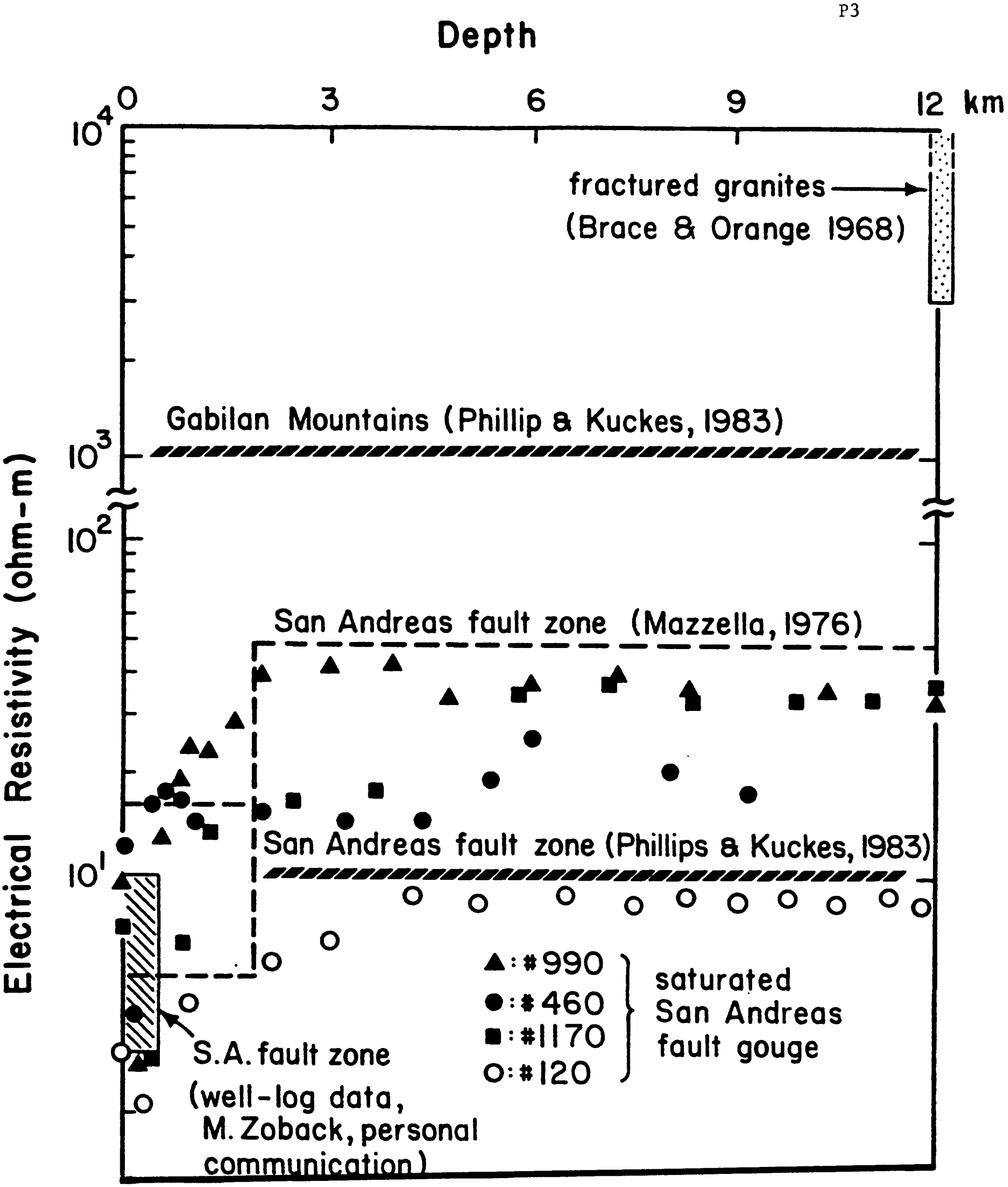

Figure 7.

Electrical resistivity structures of the San Andreas fault zone by Mazzella (1976) and Phillips and Kuckes (1983) and well log resistivity data within the fault zone (M. Zoback, personal communication), plotted together with the electrical resistivity in several San Andreas fault gouges determined at elevated pressures (Wang, 1984) and in saturated granites compressed to fracture at 0.2 GPa confining pressure and 0.05 GPa pore pressure (Brace and Orange, 1968). Also shown is the resistivity structure of the Gabilan Range (Phillips and Kuckes, 1983).

Two-Color Laser Geodimeter

14-08-0001-21852

Larry E. Slater
CIRES
Campus Box 449
University of Colorado
Boulder, Colorado 80309
(303) 492-8028

Objective: A multiwavelength electronic distance measuring instrument has been utilized at several locations in California over the last 9 years. The results of these previous efforts encouraged additional studies using similar instruments. The purpose of this effort is to construct 2 additional instruments similar to the CIRES instrument. These new instruments will be used in an observatory mode similar to that used by the CIRES instrument. These new instruments will provide a considerable increase in the amount of crustal deformation data that can be collected at the various sites.

Results: The new instruments will, in large part, be similar to the CIRES instrument. Newer, more advanced, computer hardware will allow more detailed real-time data evaluation. Most of the analog and digital electronic components and modules have been reduced in size and packaged in a more durable configuration than the prototype CIRES instrument. The status of specific subsystems is outlined below:

1) The new systems will contain an HP 150 computer that will provide a considerable increase in computing power and data handling capabilities over the existing CIRES instrument. All hardware has been delivered and most of the software is in place.

2) The mechanical design of the optical head is complete and machine parts are expected to be complete by December 1984. Assembly of optical head should be completed within a month of the delivery of machine parts. The optical head will be very similar to CIRES instrument optical head.

3) All off-the-shelf items (He-Ne lasers, He-Cd lasers, travelling wave tube amplifiers, photomultiplier tubes, etc.) have been delivered.

4) The analog and digital modules have been completed and tested.

5) The microwave module is progressing well. The new electro-optic modulators appear to function as well, if not better, than the existing modulator in the CIRES instrument.

The initial testing and evaluation of the completed instruments is expected to be complete by the early months of 1985. The new instruments will then be transported to California for side-by-side evaluation with the CIRES instrument. It is anticipated that the new instruments will be ready for field use at the other California sites by the summer of 1985.

INDEX 1

INDEX ALPHABETIZED BY PRINCIPAL INVESTIGATOR

INDEX 2

INDEX ALPHABETIZED BY INSTITUTION

Foothill-De Anza Community College	Cotton, W. R.	104
Foothill-De Anza Community College	Hall, N. T.	112
Georgia Institute of Technology	Long, L. T.	486
Kentucky, University of	Street, R. L.	35
Lamar-Merifield Geologists, Inc.	Lamar, D. L.	342
Lamont-Doherty Geological Observatory	Beavan, J.	170
Lamont-Doherty Geological Observatory	Beavan, J.	290
Lamont-Doherty Geological Observatory	Bilham, R.	47
Lamont-Doherty Geological Observatory	Bilham, R.	295
Lamont-Doherty Geological Observatory	Das, S.	430
Lamont-Doherty Geological Observatory	McCann, W. R.	226
Lamont-Doherty Geological Observatory	Simpson, D. W.	494
Lamont-Doherty Geological Observatory	Seeber, L.	26
Lamont-Doherty Geological Observatory	Sykes, L. R.	249
Lamont-Doherty Geological Observatory	Taber, J.	39
Lamont-Doherty Geological Observatory	Taber, J.	252
Lawrence Livermore National Laboratory	Daily, W. D.	178
Leighton and Associates, Inc.	Clark, B. R.	303
Leighton and Associates, Inc.	Leighton, F. B.	573
Massachusetts Institute of Technology	Aki, K.	158
Massachusetts Institute of Technology	Aki, K.	160
Massachusetts Institute of Technology	Madden, T. R.	366
Massachusetts Institute of Technology	Toksoz, M. N.	550
Massachusetts Institute of Technology	Walsh, J. B.	478
Memphis State University	Reinbold, D. J.	133
Nevada, University of	Ryall, A. S.	23
Nevada, University of	Ryall, A. S.	134
New York, State University of, Binghamton	Wu, F. T.	580
Northwestern University	Rudnicki, J. W.	461
Oregon State University	Levi, S.	122A
Oregon State University	Yeats, R. S.	152
Oregon State University	Yeats, R. S.	276
Pennsylvania State University	Langston, C. A.	534
Queensland, University of	Gladwin, M. J.	315
Redwood Research, Inc.	Kelleher, J.	200
Saint Louis University	Herrmann, R. B.	66
Saint Louis University	Herrmann, R. B.	539
Saint Louis University	Morrissey, S-T.	373
Saint Louis University	Morrissey, S-T	379
Saint Louis University	Stauder, W.	31

GPO 588-571/38134